ISIRR 2003

VIIth INTERNATIONAL SYMPOSIUM INTERDISCIPLINARY REGIONAL RESEARCH - ISIRR 2003
HUNGARY – SERBIA & MONTENEGRO – ROMANIA
Hunedoara, ROMANIA
25th – 26th, September, 2003

Section V
- TECHNICAL SCIENCE -

25th September, 2003
11^{00} - 13^{00}

25th September, 2003
15^{00} - 19^{00}

26th September, 2003
11^{00} - 13^{00}

"SIDERURGISTUL" CLUB - AMPHITHEATER No.2 – HUNEDOARA

Teodor HEPUŢ – President & Chairman
Caius PĂNOIU - Member
Imre MIKLOS - Member

	Name of the Authors		Title of Presented Papers
0501.	*Gyula MESTER, Tibor MESTER*	- HUNGARY	*Building Applications Of XML Web Services*
0502.	*Liviu BRÎNDEU, Radu ILEA*	– ROMANIA	*Dynamics of the Displacements by Vibrations on Plane Sieves*
0503.	*Iosif HAJDU Pavel TRIPA Ovidiu BRÂNZAN*	– ROMANIA	*The Influence of the Fracture Surface Orientation to the Rolling Direction About the Fracture Toughness of a Steel Belonging to a Pressure Vessel*
0504.	*PĂUNESCU Dan, VLĂDUŢ Valentin*	– ROMANIA	*Researches Regarding the Computer-Aided Test of a Hauling Eye, Using the Data Acquisition System Dap 2400*
0505.	*VLĂDUŢ Valentin, BIRIŞ Sorin, BUNGESCU Sorin, PĂUNESCU Dan, DIMA Ion*	– ROMANIA	*Computer-Aided Test of the Disk Harrow Gd 3.2 in Simulated and Accelerated Regime on the Hydropulse Installation and the Stress States Analysis*

0550.	*Isidor PREJBAN, Stefan MAKSAY*	*– ROMANIA*	*The Influence of the Thermal Treated Semi-Finished Products Thickness on the Technological and Operational Characteristics*
0551.	*HEPUŢ Teodor, SOCALICI Ana Virginia, PUŢAN Vasile, POPA Erika*	*– ROMANIA*	*Researches Concerning Dephosphorization Process at Electric Furnace EBT*
0552.	*Vasile BACRIA*	*– ROMANIA*	*Considerations Upon the Motion of the Porous Materials with Elastic Skeleton*
0553.	*TIRIAN Gelu Ovidiu*	*– ROMANIA*	*Digital Interface Board with Four 8-Byte Output Ports*
0554.	*Gilbert-Rainer GILLICH Nadia POTOCEANU Constantin MARTA*	*– ROMANIA*	*Study of Machine Dynamics Phenomena with Java Applets*
0555.	*Imre KISS Vasile George CIOATA; Vasile ALEXA; Maria SCURTU*	*– ROMANIA*	*Industrial Study Upon the Basic Chemical Composition of the Nodular Cast Iron Rolls*
0556.	*Imre KISS Sorin RATIU; Ana JOSAN; Maria SCURTU*	*– ROMANIA*	*Alloyed Elements for the Nodular Cast Iron Semihard Rolls*
0557.	*Imre DÉKÁNY, Szilvia PAPP, Rita PATAKFALVI, László KÖRÖSI*	*- HUNGARY*	*Noble Metal and Semiconductor Nanoparticles Stabilized in Layer Structured Materials – Abstract*
0558.	*Endre FORGÁCS, László SZERI*	*- HUNGARY*	*Diagnostic Test of Food Industry Machines – Abstract*
0559.	*DEMIAN Doru, RUSU Nicolae, ANGHEL Stela,* *FÜLE Antal, TAKÁCS Imre*	*– ROMANIA* *- HUNGARY*	*Computerised System for a More Fluid Cross-border Railroad Traffic*
0560.	*Ioan RUJA, Ştefan SZABO, Ion VELA*	*– ROMANIA*	*The Using of Computing Technology in Acquisition and Interpretation of Mechanical Construction Vibrations*

ISIRR 2003

BUILDING APPLICATIONS OF XML WEB SERVICES

Professor Gyula MESTER D. Sc.
Tibor MESTER M. Sc.
Szegedi Tudományegyetem, Szegedi Élelmiszeripari Főikolai Kar
Műszaki Informatika Tanszék, *gmester@szef.u-szeged.hu*
Geomant Kft., Budapest, *tmester@geomant.com*

Abstract:
The paper presents the development and application of XML Web Services using .NET technologies. The development of the XML Web Services will be presented in ASP.NET Web Matrix Project environment.

Keywords:
XML Web Services, ASP.NET Web Matrix Project, moving process

1. INTRODUCTION

This paper presents the development and application of XML Web Services using .NET technologies. The computing industry is converging on a new model for building software, this model enables a standard way of connecting software applications and exchanging information using the Internet. This new Internet-based integration methodology, called XML Web services enables applications, machines, and business processes to work together in ways never previously possible [1].

The development of the XML Web Services will be presented in ASP.NET Web Matrix Project environment. The design of the XML Web Services of moving process is illustrated. Through the use of a Web Service, we can easily create a solution of a moving process.

The paper is organized as follows:

- Section 1, Introduction.
- In Section 2, the general architecture of the ASP.NET XML Web Services is illustrated.
- Building ASP.NET Web Service using ASP.NET Web Matrix Project is given in Section 3.
- Conclusions are given in Section 4.

2. THE GENERAL ARCHITECTURE OF THE ASP.NET XML WEB SERVICES

The Internet is quickly evolving from today's Web sites to a next generation of programmable Web sites. These programmable Web sites become more than passively accessed sites - they become intelligent Web Services.

The CLR (Common Language Runtime) provides built-in support for creating Web Services. We build Web Services using open standards that allow client developers to create and interact with Web services from variety of sources. Using the XML, the data generated to and from your service is formatted in a standard way. Web Services provide the ability to share data with large variety of clients.

Web services and clients use the SOAP (Simple Object Access Protocol) when communicating with one another. SOAP allows a client to make a request to registered object on a server via standard internet protocols, such as HTTP.

With the advent of .NET, support for ASP.NET development has been fully integrated into Visual Studio .NET. It provides an extremely powerful and usable environment for ASP.NET development in the guise of Web Forms. The structure of the Visual Studio.NET environment is shown in Fig. 1.

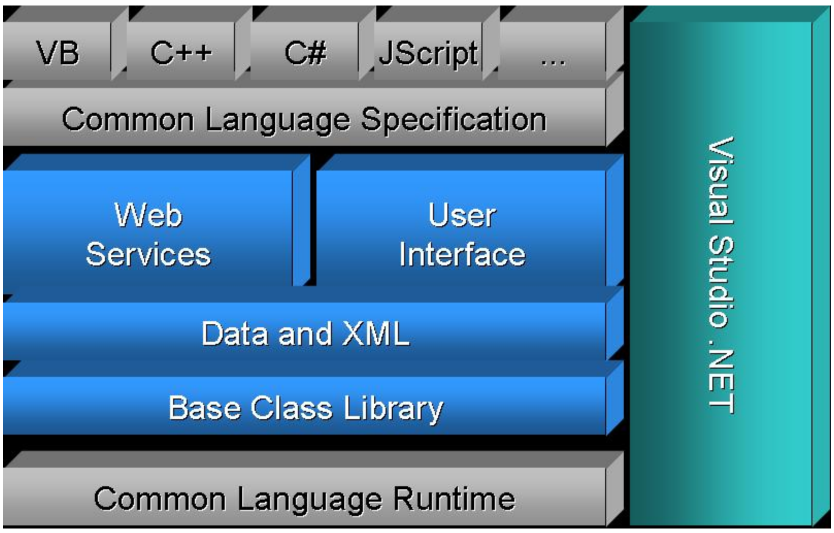

Fig. 1. *The structure of the Visual Studio.NET environment*

When we use Visual Studio.NET to create a XML Web Service, all components are built into a single Web Service project. Today Visual Studio.NET is joined by another MS product: ASP.NET Web Matrix Project.

ASP.NET Web Matrix Project is just a simplified development environment for building ASP.NET applications, such as XML Web Services.

3. BUILDING XML WEB SERVICE USING ASP.NET WEB MATRIX PROJECT

ASP.NET provides support for XML Web Services with the .asmx file. This file (v_sz.asmx) starts with an ASP.NET directive <@**WebService>** using the language Visual Basic.NET. It imports the namespace System.Web.Services. We must include this namespace. Next, the class Sample is declared. Finally, any methods that will be accessible as part of the service have the attribute **<WebMethod()>** in Visual Basic. The following code in Figure 2.

C:\ASP_NET_Source_WebMatrix\v_sz.asmx *

```
<%@ WebService language="VB" class="Sample" %>

Imports System
Imports System.Web.Services
Imports System.Xml.Serialization

Public Class Sample

    <WebMethod> Public Function v(b As Single, t3 As Single,
    skn As Single, snz As Single, vd As Single) As Single

     v = (0.5 * b * t3) + (2 * (skn + snz)* b + vd ^ 2) ^ 0.5

        Return v
    End Function

 <WebMethod> Public Function sz(t1 As Single, t2 As Single,
 t3 As Single, v As Single, b As Single) As Single

     sz = (t1 + t2 + 0.5 * t3) * v + (v - 0.5 * b * t3) ^ 2 / (2 * b)

        Return sz
    End Function
End Class
```

shows a very simple v_sz.asmx file.

***Fig. 2** The code view of the v_sz.asmx file*

To make this service available we place the file v_sz.asmx on a server: http://localhost:8080/

inside a virtual directory. Then we save and run the XML Web Service. A dynamically generated page describing our XML Web Service will automatically appear in a new instance of our Web browser.

The resulting page would show the public methods for this Web service (Fig. 3), as well as which protocols (SOAP) we can use to invoke these methods (Fig. 4).

In Fig. 3 we will see the XML Web Service's HTML description file, containing two methods: sz and v. When we tested these methods, the XML Web Service will return an XML response of the solution of moving process in a new instance of our Web browser (Fig. 5).

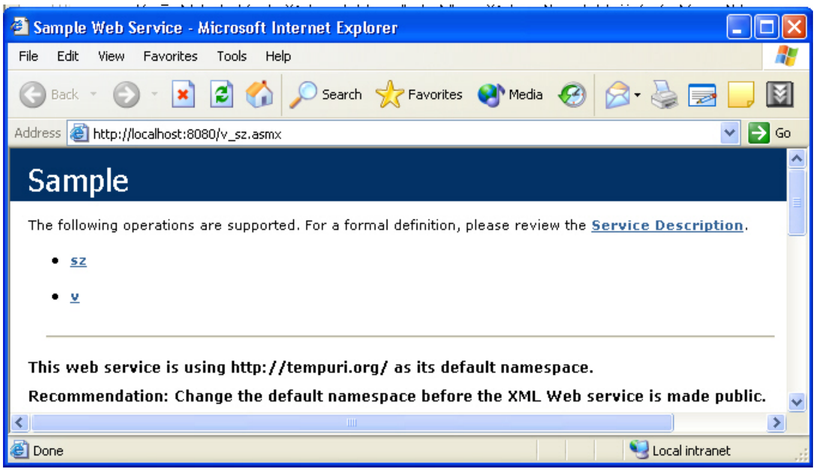

Fig. 3 *The XML Web Service methods*

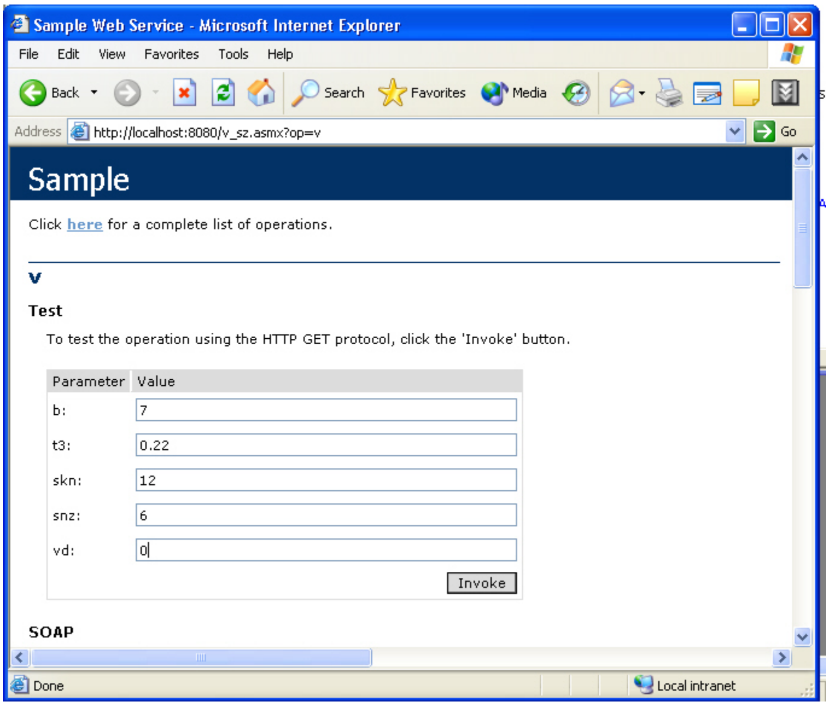

Fig. 4 *The test form*

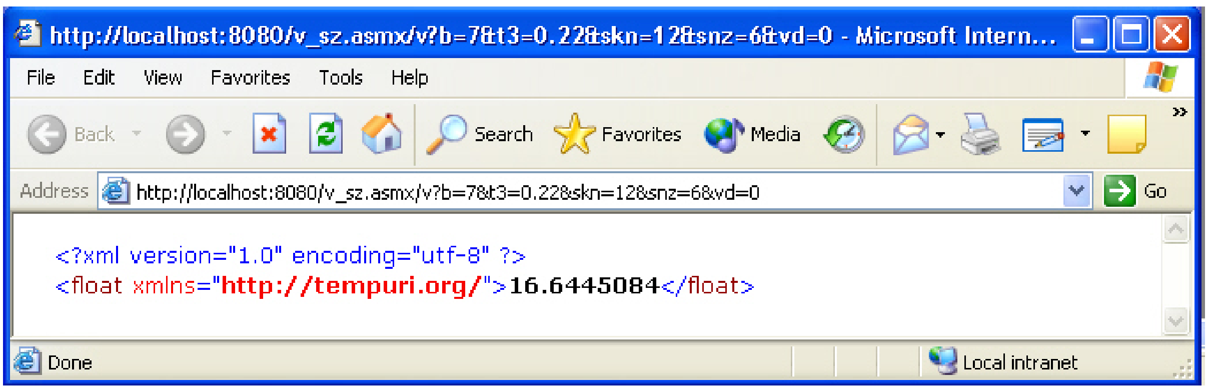

Fig. 5 *The first solution of the moving process*

4. CONCLUSIONS

The paper presents the development and application of XML Web Services of the moving process using .NET technologies. The development of the XML Web Services will be presented in ASP.NET Web Matrix Project environment.

Web Matrix a powerful, intuitive, and extremely useful tool for creating web sites and web pages and provides support for developers to easily expose a SOAP-based XML Web Service.

5. REFERENCES

[1] Gyula Mester, "*Internet technologiák*", Subotica, 2002.

[2] Gyula Mester, "*Web alkalmazásfejlesztés*", Szeged, HU, 2002.

[3] Platt, David S., *"Introducing Microsoft.NET"*, Microsoft Press, 2001.

[4] *http://www.asp.net*

[5] *http://www.microsoft.com*

[6] *http://www.developer.hu*

DYNAMICS OF THE DISPLACEMENTS BY VIBRATIONS ON PLANE SIEVES

Liviu BRÎNDEU[1], Radu ILEA[2]

[1]Politehnica University of Timisoara, e-mail: brindeu@mec.utt.ro
[2]Banat Agricultural University of Timisoara, e-mail: ilearn@k.ro

Abstract:

The separation operation of different materials at a large range of machines is effected thanks to the vibration of the working element. The separation operation is analyzed with the help of the model of particle what executes displacements by vibrations on a rough plane. Displacement regimes of the particle are studied, by forward and backsliding and by detachment. Because of the velocity discontinuity what appears as a result of the friction between the particle and plane or of the fall on the plane in the case of detachment, vibro-impacting motion regimes appear. In consequence, for the motion study, the well-known methods are applied, concerning the study of vibro-impacting regimes.

The obtained results are in concordance with the experimental data, obtained on the machines what generate displacements by vibrations. At each machine, series of measurements were performed, in different points and different working conditions.

Keywords:

motion, plane sieves, sliding regimes, vibrations

1. INTRODUCTION

The dynamic study of the separation processes, effected by the material displacement, in the presence of friction on the surfaces of plane sieves, is developed on the basis of the two mass model in contact with friction [1] - [3].

It must underline that in a lot of processes, based on vibrational displacements, can also appear, motions with detachments and falls of the particle on the vibrating plane. This kind of regimes are vibro-impacting phenomena and form an up-to-date field [4] - [5]. Initially, only vibrational displacements with sliding on the vibrating plane are taken into account; these ones have vibro-impacting character, because of the discontinuity of the friction force.

In a series of anterior papers [6] - [7], new models and study methods were conceived for the determination of motion regimes with impacts and important conclusions were established. This paper represents a trial of solution of the problem of the vibrational displacements in the presence only of the sliding with friction.

2. SLIDING REGIMES

In the study of the plane sieves, driven by a generated kinematic drive, the motion of the particle on the plane in the presence of friction and also the motion with detachments and impacts at fall were analysed. It is important to underline that in both the situations, motions with velocity discontinuities appear; for these motions, the general methods of vibration theory are not applicable.

As example it is in detail treated the case of the motion of the particle on an inclined plane of angle α in relation to the horizontal, what executes a translation motion, $u(t)=r \sin\omega t$, on the direction making the angle β with the horizontal. It is supposed that the particle executes a relative sliding motion on the plane, forward in relation to the plane.

As a rule, at a certain moment, the particle begins to slide on the plane, from the repose position, forward or back. The moment when the forward sliding begins is noted by t_1 and, consequently, $\psi_1=\omega t_1$, and for the beginning of the back sliding, by t_2 and, consequently, $\psi_2=\omega t_2$. It is specified that these moments correspond to the condition that the acceleration $\ddot{x}$ to be null. If the expression of the acceleration is annulled, for the initial moments of the sliding motion are obtained the equations

$$\sin\psi_{1,2} = \frac{g}{r\omega^2}\cdot\frac{\sin(\alpha \pm \varphi)}{\cos(\beta \mp \varphi)} \tag{1}$$

where the first sign corresponds to the forward sliding and the other one, to the back sliding.

From these relations, there are determined the parameters ψ_1 and ψ_2, respectively t_1 and t_2 what determine the beginning moments of the sliding motions, from the repose position.

Because that for the determination of the angles ψ'_1 and ψ'_2, the equation has the same form, the solution can be simultaneously made. As consequence, in order to describe the initial and final moments of sliding, the variables $\psi'=\omega t'$, can be considered.

Taking into account that the sliding regime ceases at the moment $t=t'$ what corresponds to the annulment of the relative velocity, that is to say $\dot{x}=0$, it is deduced the equation.

$$\sin\psi = \frac{\cos\psi' - \cos\psi}{\psi' - \psi} \tag{2}$$

Diagram from fig.1 illustrates the dependence $\psi' = \psi'(\psi)$ according to the relation (2).

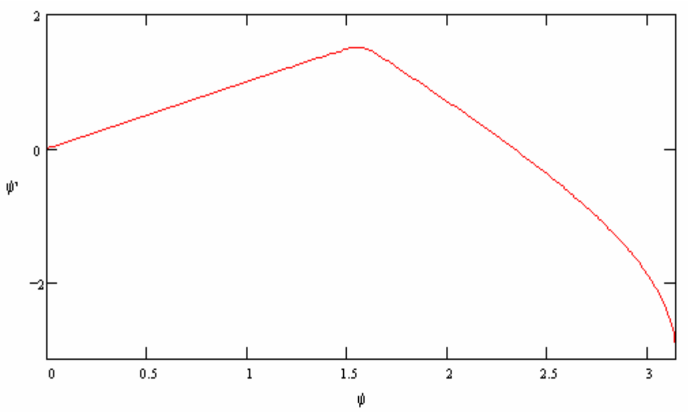

Fig.1

This equation permits the calculus of the quantity ψ', consequently of the moment t=t', corresponding to the ceasing of sliding.

Taking account of the equations (2) for the calculus of ψ', the displacement is

$$s = \frac{r\cos(\beta \mp \varphi)}{\cos\varphi}\Phi(\psi) \qquad (3)$$

where it is used the notation

$$\Phi(\psi) = \sin\psi - \sin\psi' + \frac{\psi' - \psi}{2}(\cos\psi + \cos\psi') \qquad (4)$$

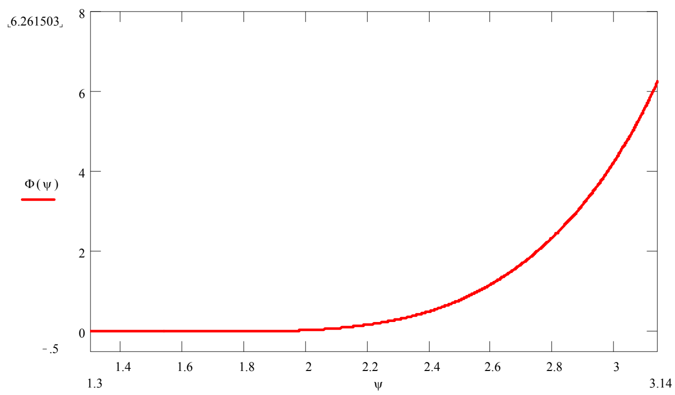

Fig.2

The function Φ(ψ) given by (4) is represented in fig.2 for ψ∈(0,π).

The plotting of absolute velocity v and velocity of transport v_1 and, also, of the displacement $s_1 u \cos\beta$, along the plane, together with the sliding s can be easily watched in the plotting of a cycle of the plane vibration.

3. DETERMINATION OF SLIDING MOTIONS

It is important to notice that the determination of regimes of sliding motions consists in the solution of the equation (2) and calculus of the function (4). This remark makes that the problem to be reduced oneself to the study of the function (4) of variable ψ, the variable ψ' being linked to ψ by the equation (2).

Concerning the equation (2), it can also make an important remark which simplifies the study; if ψ and ψ' are replaced by $\pi - \psi$ and $\pi - \psi'$ the equation (2) is also, verified. It means that the backsliding takes place in the same way as the forward sliding, that is to say it is necessary to resolve only one time this equation.

Evidently, the equation (2) has the trivial solution $\psi' = \psi$ what corresponds to the beginning of sliding.

In fact, it is of interest only the solution $\psi' \neq \psi$ $(\psi' > \psi)$ what determines the end of sliding.

Without resolving the equation (2), it can consider the implicit function ψ'(ψ), which, by differentiation, conducts to the expression

$$\frac{d\psi'}{d\psi} = \frac{(\psi' - \psi)\cos\psi}{\sin\psi' - \sin\psi} \tag{5}$$

derivative whose sign depends of cos ψ.

A special importance has the function (4) for the calculus of relative displacements. Taking account of the equation (2), after a simple calculus, the function ϕ(ψ) can be written as

$$\Phi(\psi) = \frac{1}{2\sin\psi}(\sin\psi' - \sin\psi)^2 \tag{6}$$

what shows that the displacement given by the relation (3) is always positive.

The study of the function Φ(ψ) necessitates, also, the calculus of derivative, in order to define the mode of variation. If the equation (2) and derivative (5) are considered, it is obtained, by the differentiation of the function (6), the expression

$$\frac{d\Phi}{d\psi} = -\frac{1}{2}(\psi' - \psi)^2 \cos\psi \tag{7}$$

The sign of this derivative is determined by the quantity cos ψ. As consequence, the function Φ(ψ) is increasing for cos ψ >0 and decreasing for cos ψ < 0.

The characteristics, established for the functions ψ'(ψ) and Φ(ψ) permit the discussion of all possible situations, using the corresponding graphic plotting, too.

The determination of sliding motion regimes can be simply made, starting with the equation (1), from which it is deduced, and then, from the relations (1) and (4) or the corresponding diagrams, the quantities ψ' and then Φ(ψ) are deduced. In this way, for a motion cycle, the moments of sliding beginning and end are deduced and, also the value of the sliding displacement, in accordance with the relation (3).

After the determination of these quantities, it is easy to calculate the characteristic elements for the duration and velocity of the displacement on the vibrating sieves and the degree of separation or the productivity of vibrating sieves.

4. EXPERIMENTAL RESULTS CONCERNING THE WORK OF VIBRATING SIEVES

The separations of seeds from the heap on the sieves of the cleaning systems of the cereal-picker-combines or machines for seed cleaning and sorting, takes place thanks to the phenomenon of material stratification in its components what are separated according to the density, as well thanks to the sieving state of the material on the separation surface, produced by the sieve motion.

In order to verify the results obtained by theoretical study, experimental measurements were effected for the duration and velocity of displacement of the material on the surface of vibrating sieve, the degree of separation of the components from the mixture what is conditioned and the sieve productivity, as function of the kinematic parameters of the motion of cleaning system, respectively the number of rotations of the driving mechanism, the amplitude and frequency of vibrations.

In order to obtain edifying results, the experimental tests were effected in working conditions at self-driven cereal-picker-combines and machines for seed cleaning and sorting.

For the experimental tests, it was used the selector S-5 (fig.3 – where: 1-sieve frame, 2-top sieve, 3-bottom sieve, 4-springs, 5-shift with eccentric, 6-crank, 7-collecting trough) of the seed cleaning machine MCS-5/2,5, where the supply discharge and sieve inclination angle were modified.

The tests were effected with identical samples of wheat, resulted from the direct harvesting in field with the combines of the Didactic Station of Timişoara.

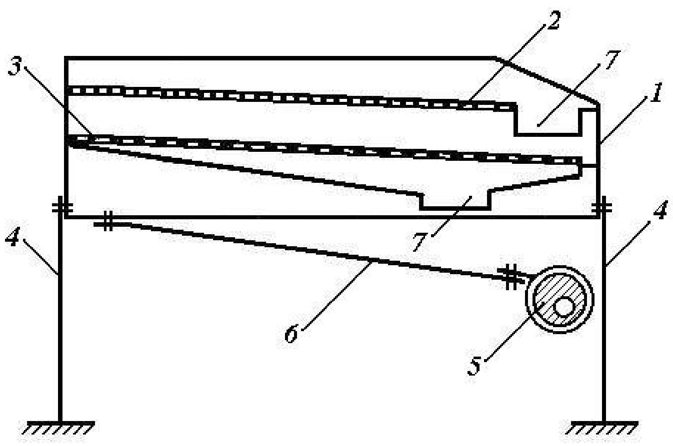

Fig.3. Driving mechanism of sieves

The material for an experimental test, having the mass of 25 Kg, was uniformly distributed on the supply sieve.

The results concerning the duration of displacement of the material sample and, also, the productivity and the separation degree of the material on the sieves, at the number of rotations of the shaft with eccentric of 410 rot/min, are centralized in the table 1.

Analysing the values, centralized in the table, the following remarks can be made:

- the duration of displacement of the seeds on the surface of the vibrating plane decreases with the increasing of the inclination angle of sieves and increases with the increasing of the supply discharge;
- the velocity of displacement of the seeds on the vibrating plane is so much bigger as the duration of displacement is more little and inversely;
- the purity of the cleaned material, given by the degree of separation of the mixture components is so much higher as the supply discharge is more little. The purity of selected material decreases with the increasing of inclination of the sieves. It must also mention the fact that the degree of separation inversely proportionally varies with the velocity of flowing, that is to say the purity of the selected material is so much more little as the velocity of displacement of seeds on the sieves is bigger;
- the productivity of sieves increases with the increasing of the velocity of displacement of the seeds on the sieves, the angle of inclination of sieves and, also, the supply discharge with material. It must notice that the purity of the selected material decreases with the increasing of productivity of the sieves.

The analysed situations are in concordance with the calculus, effected on the basis of the proposed dynamic model.

Table 1

Nr. crt.	Angle of inclination (degrees)	Supply descharge (Kg/s)	Number of rotations of driving shaft 410 rot/min			
			Duration of displacement (s)	Velocity of displacement (m/s)	Degree of separation (%)	Productivity (g/m^2s)
1	2	0,83	17,68	0,77	95,65	432
		1,11	23,11	0,59	93,70	540
		1,40	28,89	0,47	88,30	704
2	4	0,83	16,11	0,84	95,00	464
		1,11	21,36	0,63	91,80	584
		1,40	26,79	0,51	87,60	776
3	6	0,83	14,88	0,91	94,40	500
		1,11	19,96	0,68	90,10	624
		1,40	24,86	0,55	84,30	840
4	8	0,83	14,00	0,97	94,00	536
		1,11	18,73	0,72	87,50	664
		1,40	23,29	0,58	78,40	892

5. REFERENCES

1. Brîndeu L., Roşca G., Ilea R., “Deplasări vibraționale cu alunecare pe plan”, Analele Univ. Oradea, Fasc. Mecanică, 45-50, 1998.
2. Brîndeu L., Hegedus A., Biro I., Deak F., “A magok halado mozgasa egy rezgo sikon”, Conference on R&D in Agricultural Engineering, Godollo Hungary, 1999.
3. Biro I., Deak F., Ilea R., Brîndeu L., Hegedus A., Toader M., “A magok mozgasanak viszgalata vibracios szalitogepen”, Conference on R&D in Agricultural Engineering, Godollo, Hungary, 1999.
4. Silaş GH., Brîndeu L., “Sisteme vibropercutante”, Ed. Tehnică, Bucureşti, 1986.
5. Brîndeu L., Fenchea M., “Working process of mills with hammers”, Bul. Şt. Şi Tehn. Al Univ. “Politehnica” din Timişoara, Tom 43(57), Mecanica, 1998.
6. Brîndeu L., Hegedus A., Biro I., Deak F., “Computer simulation of Horizontal Cylindrical Riddle”, 3rd International Symposium Interdisciplinary Regional Research (Hungary, Romania, Yugoslavia), Novi Sad, Yugoslavia, 1998.
7. Brîndeu L., Toader M., Hegedus A., “Dynamics of the Vehicle Under the Action of the Road Discontinuity, Conference on Vehicle System Dynamics, Identification and Anomalies, VSDIA’98, Budapest, Hungary, 1998.
8. Brîndeu L., Hegedus A., Orgovici I., Ilea R., Biro I., Deak L., “The dynamics of the moving grain using vibrational plane sieves”, Kutatasi es fejlesztesi tanacskozas, Nr.25, Godollo, Hungary, 2001.

THE INFLUENCE OF THE FRACTURE SURFACE ORIENTATION TO THE ROLLING DIRECTION ABOUT THE FRACTURE TOUGHNESS OF A STEEL BELONGING TO A PRESSURE VESSEL

Iosif HAJDU, Pavel TRIPA, Ovidiu BRÂNZAN

Universitatea "Politehnica" Timişoara, Facultatea de Mecanică
Universitatea "Politehnica" Timişoara, Facultatea de Mecanică
CIMVEST ARAD

Abstract

For a steel plate meant for pressure vessels we have determined the fracture toughness on Chevron type specimens, with the longitudinal axes oriented on six different directions, shifted with 30^{o}.

The tests have been performed with constant loading speed of different values at normal temperature. We had in view to determinate the direction, after which the fracture toughness is maximum. But the primary results have not emphasized the existence of such a direction.

Key words: *fracture toughness, fracture mechanics, Chevron specimen, normal temperature, steel for boilers, rolling direction*

1. INTRODUCTION

The steel machine parts includes a lot of microscopic cracks which can not be eliminated and diminish the strength capacity. The strength capacity is estimated be the mechanical characteristics of the material which are influenced by a lot of factors. In the case of steel plates, one of the factors may be the fracture surface orientation to the rolling direction.

In the framework of the paper, as a mechanical characteristic, in order to evaluate the strength capacity, the fracture toughness has been considered. As influence elements, the fracture surface orientation to the rolling direction and the loading rate have been taken into consideration.

The analysis has been performed for a pressure vessel steel STAS 2883/3-88, brand R 360 , cutted from a thick rolling steel plate.

After a laboratory study, the following static and dynamic mechanical characteristics have been obtained: R_e = 256.2 MPa; R_m = 381.2 MPa, $A_{10}(\delta_{10})$ = 26.6%; Z = 65.9%. KV = 13.3 [J]

2. SPECIMENS AND EXPERIMENTAL INSTALATION

In order to estimate the fracture toughness, the Chevron specimens have been used. The option for these specimens is based on the fact that the thickness of the rolling plate (22 mm) is too small to manufacture specimens according to the standard STAS 9760-84. Moreover, for these range of specimens, it is not important to respect the plane state of deformation.

In the same time, the tests performed on these range of specimens are easy to be carried out, and these are not necessary special experimental installations. The obtained results may be considered as acceptable for an experimental investigation.

The manufacturing process in order to obtain the Chevron specimens, according to different directions reported to the rolling direction, is presented in Fig.1.

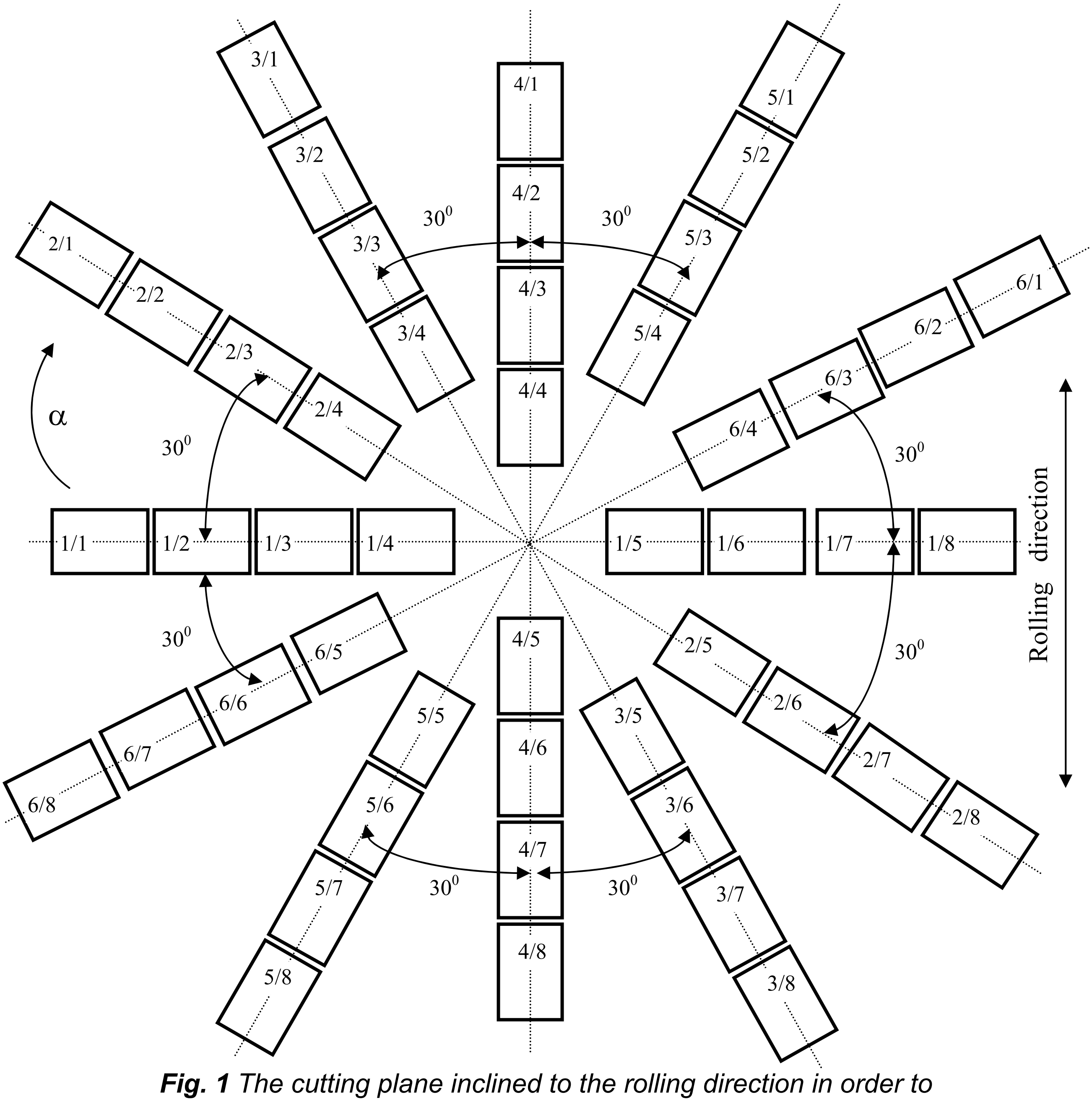

Fig. 1 *The cutting plane inclined to the rolling direction in order to manufacture the specimens*

The shape and the dimensions of the Chevron specimens, in order to estimate the fracture toughness, is presented in Fig.2 [1,2].

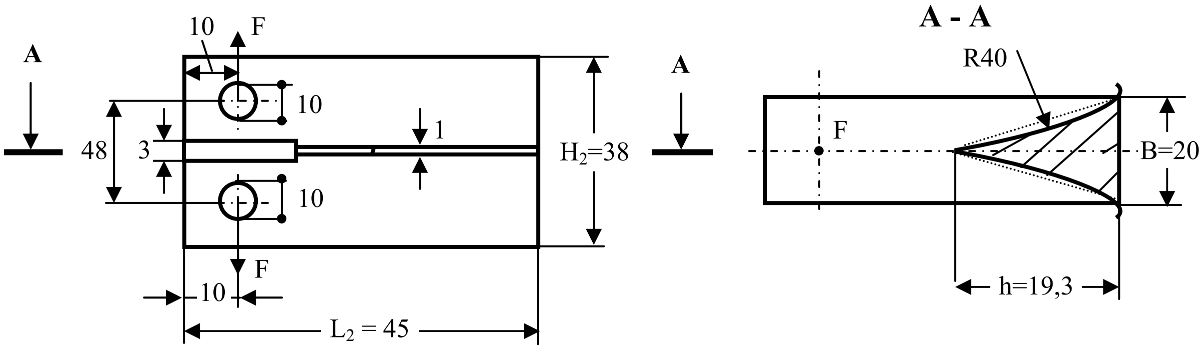

Fig.2 *The test specimen*

The Chevron specimens have to present a triangular shape of the fracture surface. Because of the machanical manufacturing process, the real specimens not present such a shape of the fracture surface, but a surface with curved lateral lines, R = 40 mm (the continuous line in Fig.2). Taking into account the above mentioned aspects, in order to calculate the fracture toughness, the both shape of the fracture surface have been taken into account. The shape of the fracture surface, in direct relationship with the fracture toughness has an influence about the maximum force recorded during the test process.

The tests have been performed at the standard temperature and on an experimental installation, proper conception and implementation [3], (Prof. dr. eng. I. Hajdu). The installation is able to obtain different loading rates. The test may be performed both at standard and high temperatures.

3. THE FRACTURE TOUGHNESS

As a result of the Chevron specimens analysis, the fracture toughness, expressed by the stress intensity factor K_{IV}, may be estimated according to the relation [1,2]:

$$K_{IV} = A \cdot \frac{F_{max}}{B^{\frac{3}{2}}} \tag{1}$$

where:

A – a coefficient in function of the sharpeed angle of the fracture surface. For the used specimens, the coefficient value of A = 22 has been considered

F_{max} – the maximum recorded force during the test

B – the specimen thickness (Fig.2).

The results, for different loading rates which are different to the rolling surrface orientation, as well for the effective and corrected fracture surface, are presented in Fig.3a,b,c,d,e,f.

a)

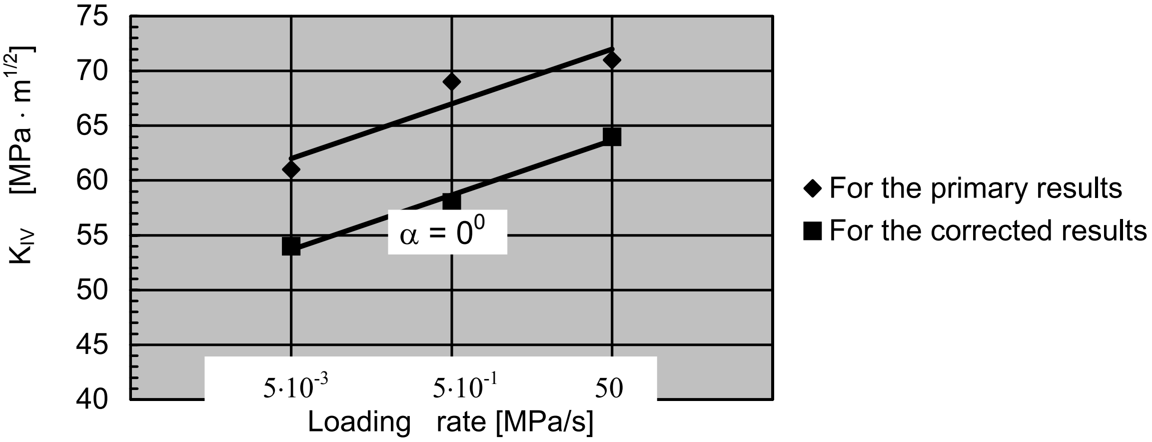

b)

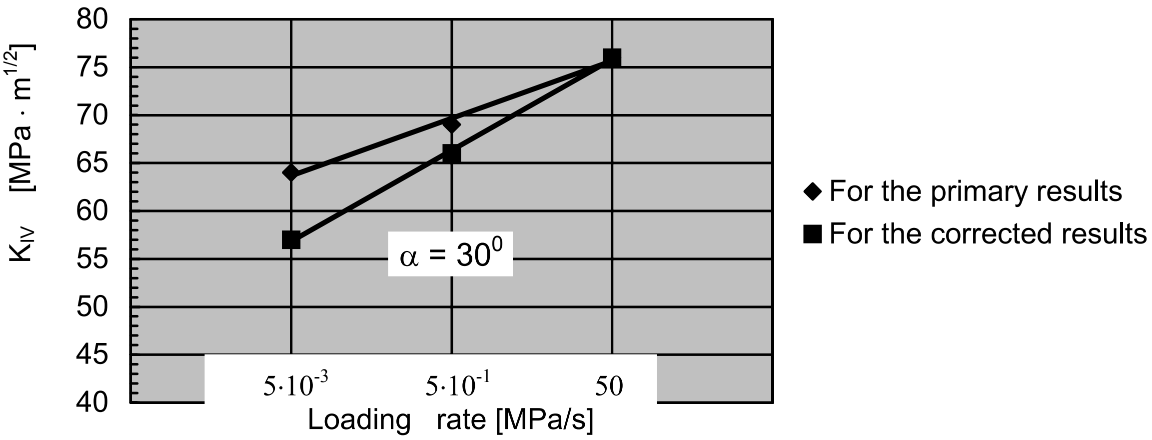

c)

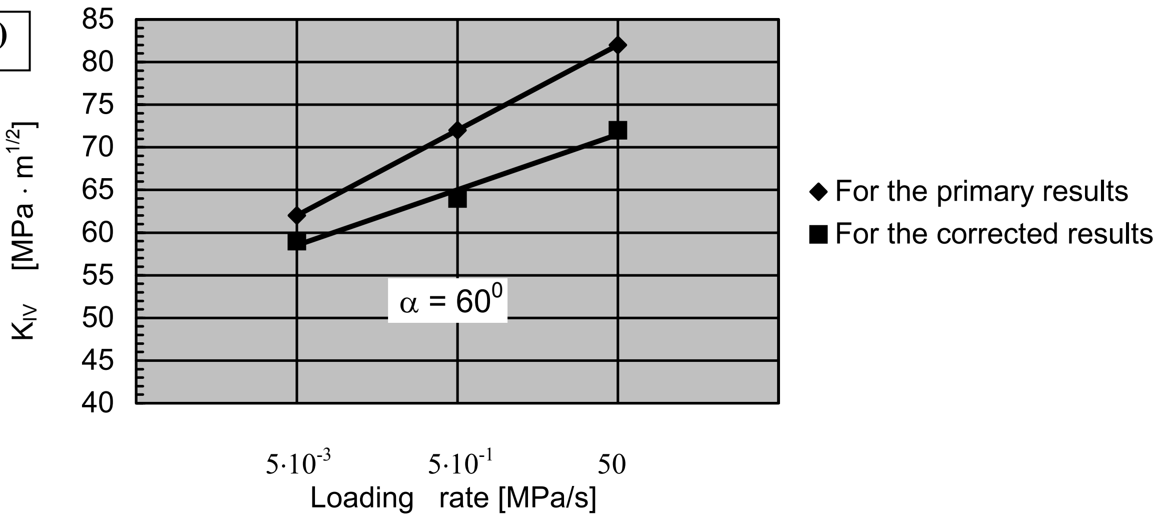

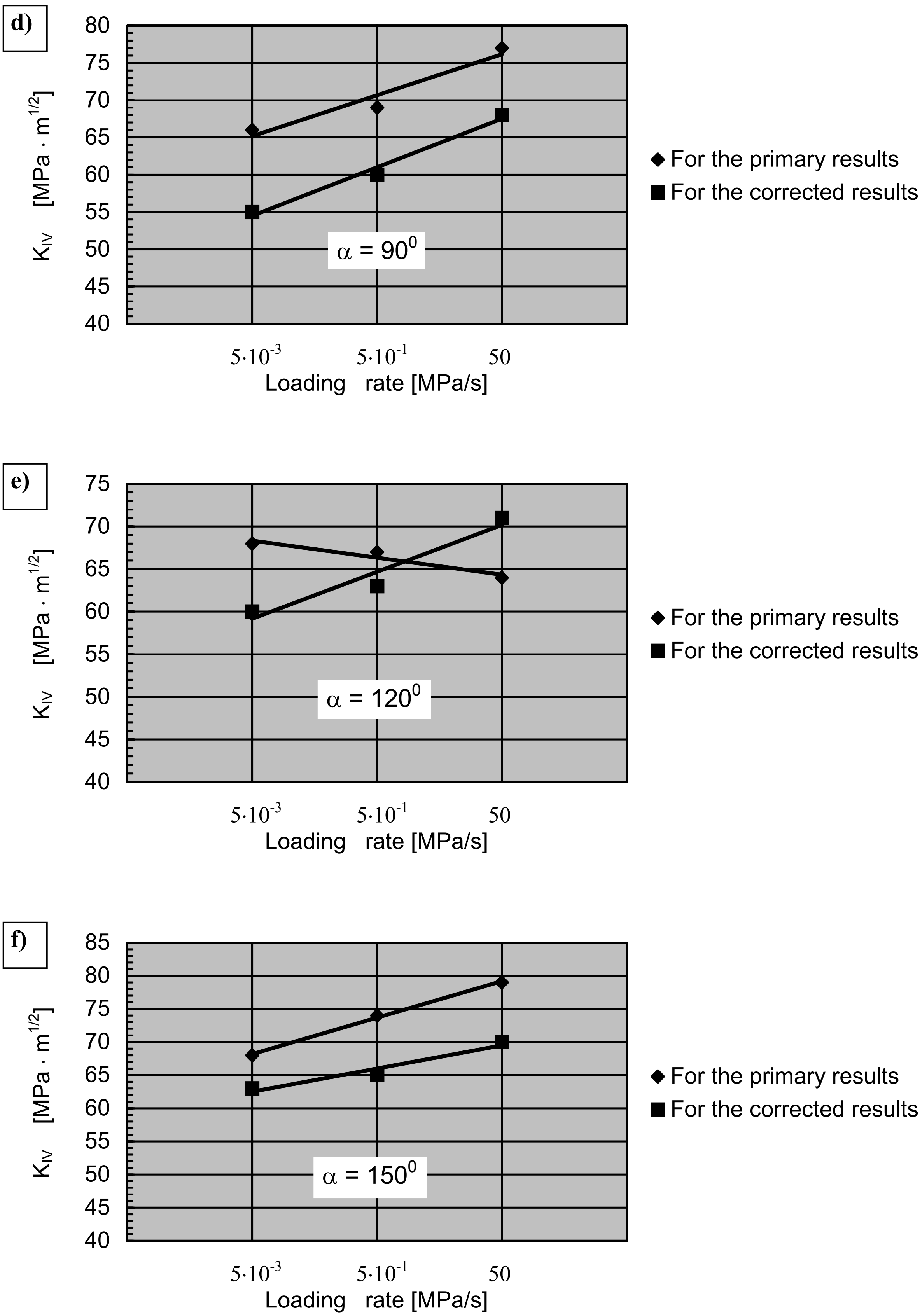

Fig.3 *The fracture toughness*

4. CONCLUSIONS

As a consequance of the results in Fig.3, it may be concluded:

- The fracture toughness K_{IV} (except a single primary direction) with the loading rate, afteh all the other directions of the longitudinal axys of the tested specimens.
- The fracture toughness estimated on Chevron specimens, considered as primary specimens with the same shape of the fracture cross-section, has high values (closely to the superior limit in comporison with the fracture toughness re-calculeted for the corrected maximum fracture force value.
- For the analysed steel, the fracture toughness is relatively less influenced by the rolling direction orientation of the longitudinal axys of the tested specimens.
- As a relativ small influence, it may be obsrved an increasing of the K_{IV} for the specimens orientated in directions 2, 3 and 6 in comparison with the direction a and 5 presented in Fig.1
- It may be considered that the rolling process of the steel plate has no influence about the promoting of a special direction for fracture propagation.

5. REFERENCES

1. Brown, K. R., *The Chevron Notched Fracture toughness test,* ASTM Standardization News, November 1988
2. Sherman, D. H., *Fracture Toughness Testing Using Chevron Notched Specimens,* Metals Handbook, Nineth Sdition, Vol. 8, Mechanical Testing ASM, Ohio, 1985
3. Hajdu, I., *Contribuții la studiul influenței temperaturii şi vitezei de încărcare asupra limitei de curgere al unui oțel moale,* Teză de doctorat, Timişoara, 1964
4. Barsom, J. M., Rolfe, S. T., *Fracture and fatigue Control in Structures. Application of fracture Mechanics,* Prentice Hall Inc. New Jersey, 1987
5. Tripa, P., *Mecanica ruperii cu aplicații la conducte,* REZMAT 4, Editura MIRTON, Timişoara, 1998

RESEARCHES REGARDING THE COMPUTER-AIDED TEST OF A HAULING EYE, USING THE DATA ACQUISITION SYSTEM DAP 2400

[1)]PAUNESCU Dan, [2)]VLADUT Valentin

[1,2)]INMA Bucureşti

Abstract

In order to determine the mechanical resistance of certain subassemblies as component parts of agricultural machines, motor-vehicles, trailers, etc., it is necessary to test them in order to see the way they behave from the point of view of breaking resistance.

As for exactly determining the behaviour of these subassemblies at field stresses it would be necessary a long period of time, most of the manufacturers choose the solution of testing them in a simulated and accelerated duty on the "hydropulse" installation.

In the case of the present paper it is shown the mecahanical resistance testing in a simulated and accelerated duty of a hauling eye (let) belonging to the hitch of an agricultural dumping trailer RAB 4 and the conclusions drawn after performing these determinations.

Key words: *mechanical resistance, hydropulse, hauling eye, accelerated duty*

1. INTRODUCTION

The hauling eye, manufactured by S.C. Autonova S.A. belongs to the hitch assembley and is used in order to haul the agricultural dumping trailer RAB 4.

The eye is mounted at the end of the hitch, into a welded socket and is attached with a horned nut M30 and with a bolt of 6.3 x 30.

The Main dimensions of the eye are presented in tables 1 and 2.

Table 1 - Ensuring The Mobility Degrees

Crt. Nr.	Name	Values acc. to SR ISO 5692:1996	Values acc. to the techn. docum.	Values measured before the test	Values measured after the test	Remarks
1.	Steering angle	min. $\pm 60^{o}$	-	$\pm 65^{o}$	$\pm 65^{o}$	
2.	Pitch angle	min. $\pm 20^{o}$	-	$\pm 23^{o}$	$\pm 23^{o}$	
3.	Roll angle	min. $\pm 20^{o}$	-	$\pm 22^{o}$	$\pm 22^{o}$	

Table 2 - Dimensional And Angular Measurements

Crt. Nr.	Dimensions according to SR ISO 5692:1996	Dimensions accord to the draw no. RM 2,5 - 1.6/N rev. b.	Dimensions measured before the test	Dimensions measured the test	Remarks
1.	$\Phi\ 50_0^{+0,8}$	$\Phi\ 50^{+0,8}$	Φ 50,1	Φ 50,1	
2.	A-A: 30±0,5 30_0^{+1}	B-B: 30±0,5 30_0^{+1}	30.1÷30,5 30.1÷30,8	30.0÷30.6 30.1÷30.8	
3.	Section B-B: max. 50 min. 30	Section C-C: 40±1	40.3	40.3	
4.	120°	120°	120°	120°	
5.	-	448±1	449.3	449.3	
6.	110 min. 112 max.	110	112	112	
7.	min. 15 max. 20	R 16	R 17	R 17	
8.	-	M 30	M 30	M 30	
9.	-	R 5	R 5.2	R 5.2	
10.	-	R 4	R 4	R 4	
11.	-	R 10	R 10	R 10	
12.	-	Φ 27±0,5	Φ 27.22	Φ 27.22	
13.	-	$\Phi\ 38_0^{-0,25}$	Φ 37.85	Φ 37.85	
14.	-	$\Phi\ 54_{-0,25}^{-0,1}$	Φ 53.84	Φ 53.83	

2. TESTING CONDITIONS

The test of the hauling eye has been performed - mounted on the device mentioned at 5 and that represents a simulation of the extremity of the hitch on a 550 m length, ended with a squared flange, having a side of 330 m and a thickness of 15 mm, with 8 attachement holes, figure 1.

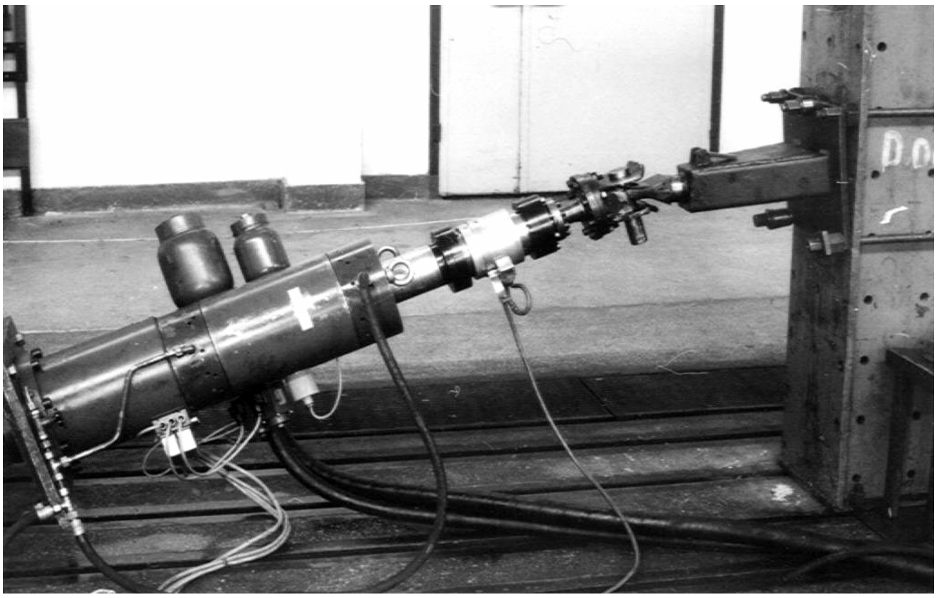

Figure 1 - **Assembly performed on the "HYDROPULSE" installation, in order to test the hauling eye**

During the attaching of the eye to the testing stand pillar it has been considered that the longitudinal axe of the eye should be horizontal. A hydraulic cylinder of 100 kN has been used for the tests. The Chains of force and stroke measuring, of the cylinder have been framed within the 1st precision classe (force measuring chain - LMF 08/± 100 kN; stroke measuring chain - LMC 04/± 100 mm; switch cabinet of the hydraulic cylinder - DCCCH - 08/.

The testing parameters and their values are presented in table 3 and have been established according to the technical documentation of the product and to annex IV of the Directive 89/173/EEC.

Table no. 3

Crt. Nr.	Parameter Name	Value
1.	Maximum towing mass	6000 kg
2.	Maximum mass of the tractor vehicle	3500 kg
3.	Maximum vertical load on the coupling point	500 kg
4.	Dynamic test load, D	21,7 kN
5.	Horizontal force, F_h	21,7 kN
6.	Vertical force, F_v	7,36 kN
7.	Testing force, F	23 kN
8.	Maximum force, F_{max}	23 kN
9.	Resultant, F_{med}	12,1 kN
10.	Minimum force, F_{min}	1,15 kN
11.	Testing angle reporting to the horizontal	18° 44'
12.	Testing frequency, f	12÷14 Hz
13.	Number of cycles of pulsatory strain	2.000.000

After being performed the fatigue tests, has been also performed the endurance test regarding the eye ability to connect with coupling devices mounted on the tractors according to SF no. 42 - 96, p. 2.4.

3. RESULTS OF THE TESTS

The effective values of the applied force and the appropriate displacement measured on the direction of the hydraulic cylinder axe, during the test, are presented in table 4.

Tabelul nr. 4

Crt. Nr.	Nr. of performed cycles	Maximum force [kN]	Maximum displacement [mm]
1.	2500	23.1	1.53
2.	620000	23.15	1.56
3.	1350000	23.08	1.58
4.	2000600	23.15	1.60

The diagrams force - time are represented in figure 2.

After having performed 2000600 cycles, there haven't found any breakages, cracks, remanent deformations, or other visible external damages.

The control of the eye coupling ability consisted in the performing of 500 successive couplings according to 2,4. from S.F. no. 42 - 96; the check finished, there haven't found any damages or deformations of the contact surfaces.

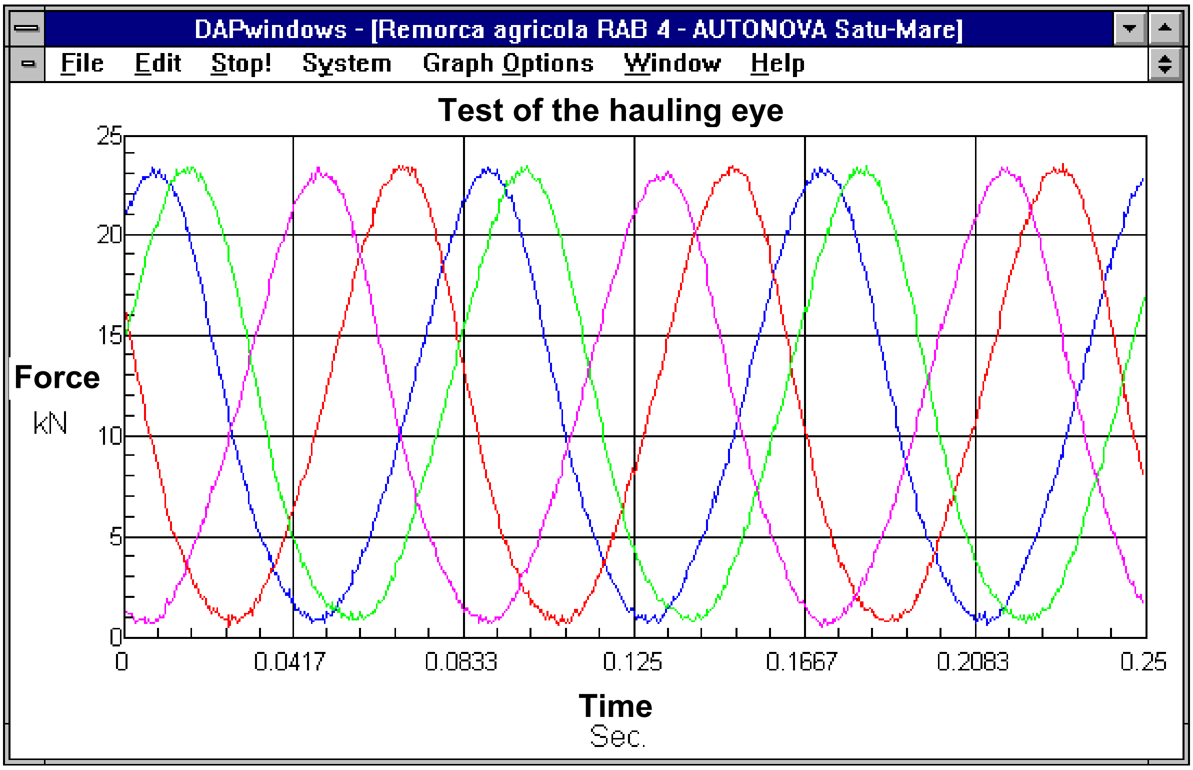

Figure 2 **- Force-time diagram for the hauling eye**

Au n = 2,500 cycles;
At n = 620,000 cycles;
At n = 1350,000 cycles;
At n = 2000,600 cycles.

4. CONCLUSIONS

The hauling eye forming the hitch assembly, equipies the agricultural dumping trailer RAB 4.

The eye has been appropriate as for the fatigue test and for the coupling ability to the complementary coupling devices (500 successive couplings).

The necessary data in order to determinate the dynamic stress at which the product has been subdued, have been transmitted to the beneficiary, for supplementing those belonging to the technical documentation. The tests have been performed on the hydropulse installation of dynamic tests, and after having performed 2000600 cycles, there haven't found any breakages, cracks, remanent deformations or other visible external damages of the hauling eye.

BIBLIOGRAPHY

[1]. Popa C., Păunescu D., a.o. - *Mechanical Test of the hauling Eye - Drawing nr. RM 2.5 - 1.6/B according to the Directive 89/173/EEC, Testing Report, INMA Bucharest, 2002.*

[2]. Popa C., Păunescu D., a.o. - *Mechanical test of the resistance frame of tractor CEAHLĂU 4601, in compliance with Directive 86/298/EEC, Testing Report, Bucharest, 2002.*

COMPUTER-AIDED TEST OF THE DISK HARROW GD 3.2 IN SIMULATED AND ACCELERATED REGIME ON THE HYDROPULSE INSTALLATION AND THE STRESS STATES ANALYSIS

[1)]VLĂDUŢ Valentin, [2)]BIRIŞ Sorin, [3)]BUNGESCU Sorin,
[4)]PĂUNESCU Dan, [5)]DIMA Ion

[1)]INMA Bucharest, [2)] P.U. Bucharest, [3)]U.S.A.M.V. of Banat Timişoara,
[4)]INMA Bucharest, [5)] -

Abstract

For simulating the field stresses during the working process of agricultural machines they are tested in laboratory in a simulated and accelerated duty on the "hydropulse" installation.

This solution was chosen by most of the manufacturers for exactly determining the machines and their subassemblies behaviour without testing them in the field for a long period of time.

In the case of the present paper it is presented the testing in a simulated and accelerated regime of the disc harrow GD 3.2., the analysis of the stress states for determining the critical zones and the conclusions which are drawn after performing these stresses.

Key words: *hydropulse, disc harrow, the stress states, simulated and accelerated regime*

1. INTRODUCTION

The disk harrow GD 3.2 comprises four sets of disks, arranged in V, with possibility of varying the angle of sets between the interval 12÷24° and the overall dimensions: length: 3,300 mm; width: 3,200 mm; mass: 950 kg.

The determination of the harrow stress in transport conditions has been performed at a rate of speed of 15 km/h, the running surface being a gravel road. In order to record the displacements in the harrow transport position, there have been utilized, two acceleration moving-coil transducers, mounted on the axle, in front of the left and right wheels.

For simulating the field stresses, in transport position, under the harrow wheels there have been mounted two hydraulic cylinders left/right, of 2.5 tf capacity, the hitch being hinged by the attaching device to the testing stand (figure 1).

The hydraulic cylinders have been commanded, through the driving board, to perform the testing program previously settled.

There has been established at every normal working shift in the field (of 8 hours) that the main transport from the station to the field and viceversa should be performed within a hour term. The conclusion is that at 1000 worked ha there are necessary 69 hours of transport, a stress program of 10^6 cycles being equal to 152,887 sec. (42.5 hours) of transport.

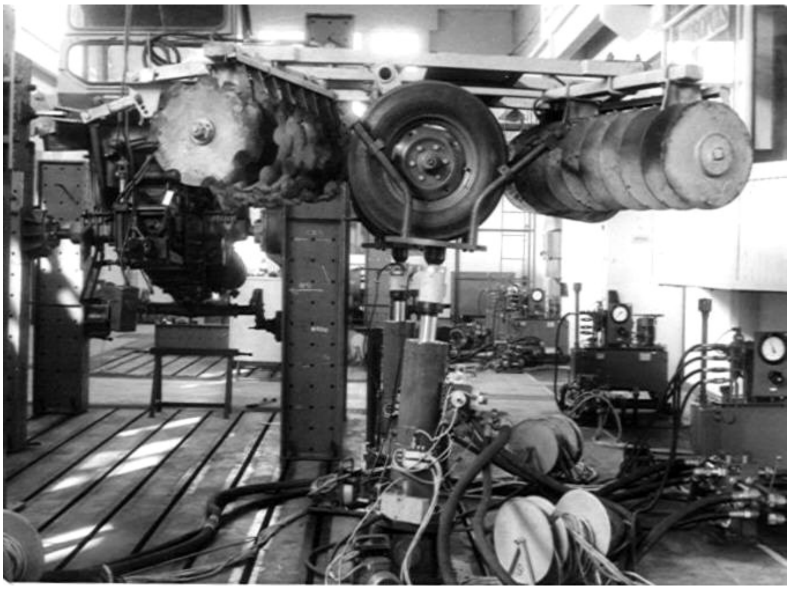

Figure 1*- Simulated and accelerated test of the disk harrow GD 3.2, in the transport*

2. RESULTS OF THE TESTS

- **The necessity of the analysis**

The usual evaluation criteria of the resistance, for the component parts of an unit/equipment/aggregate employ the effective stress in all the operating situations, beginning with the design stage for the checked hypothesis or through the measuring/control during the product working.

We can determine the effective stress by its calculus, or it can be measured, when we dispose of the appropiate apparata and processing devices, the admissible stress being presented alongside with the material specifications. The results of the resistance analysis can give useful information, even for the test its self.

For the present analysis it has been used a computer P I 133 MHz, 32 Mb RAM, 1,2 Gb HD and a specialized program of structural analysis ANSYS 2.0A.

- **Input Data**

The performance of the resistance analysis comprises the following input data: 2 general drawings of the harrow GD 3.2; the material of what is made the harrow; the curve SMITH of the fatigue resistance; the real stress, measured in the field, given in "ASCII" from (F45.ASC, F55.ASC, F65.ASC, F75.ASC) including the significant records during the work, respectively the aleatory traction force and (T13D.ASC, T15D. ASC, T1A3D.ASC, T1A5D.ASC0 the significant records in transport regime, respectively the accidental displacement to the wheel axle. The usual load of the advancement direction: $FY = 5 \cdot FX$,
where: FX - is the traction force distributed on a bearing battery;

FY - the force on a lateral direction distributed on a bearing respecting to the approach angle of the harrow disk ($\alpha = 15°$).

- **Analysis of the stress during the transport**

In order to analyse the stress in transport regime, connected to the procedure of the dynamic response analysis, the program ANSYS, the model of the static analysis has been supplied, in order to analyse the dynamic response.

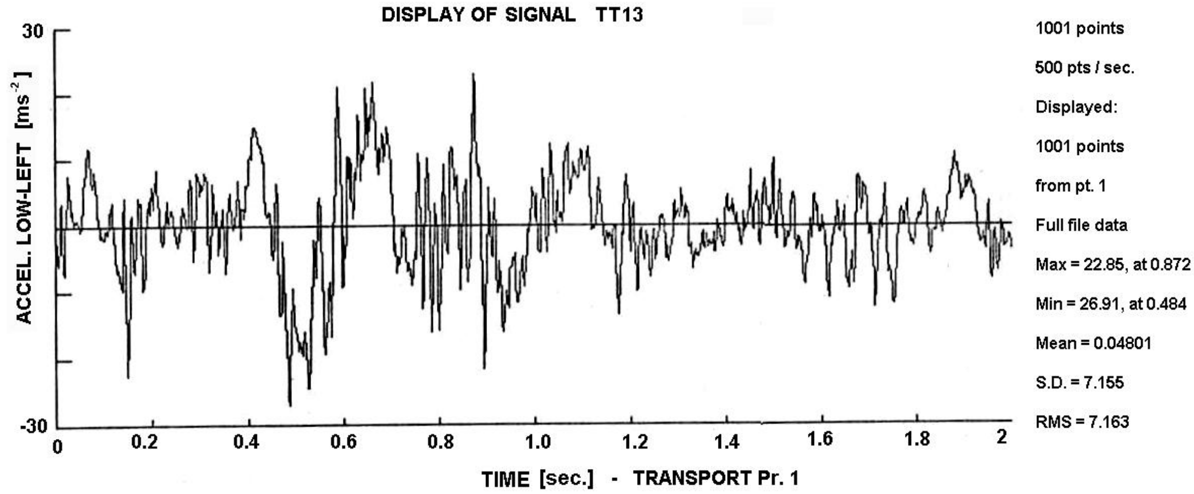

Figure 2 *- Zone 6÷8 sec. (Brought to 0) comprising the peaks*

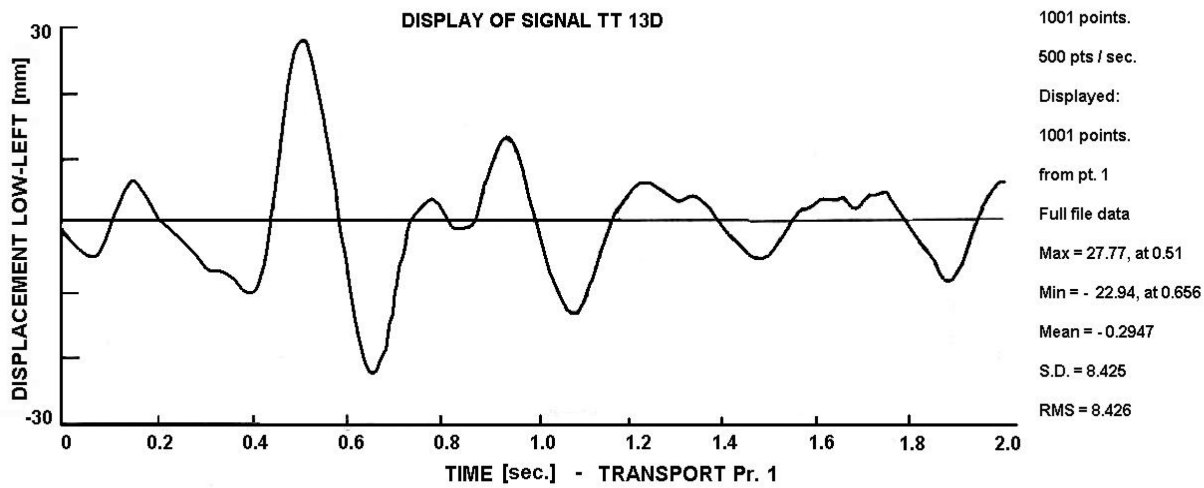

Figure 3 *- Zone 6÷8 sec. (Brought to 0) comprising the peaks*

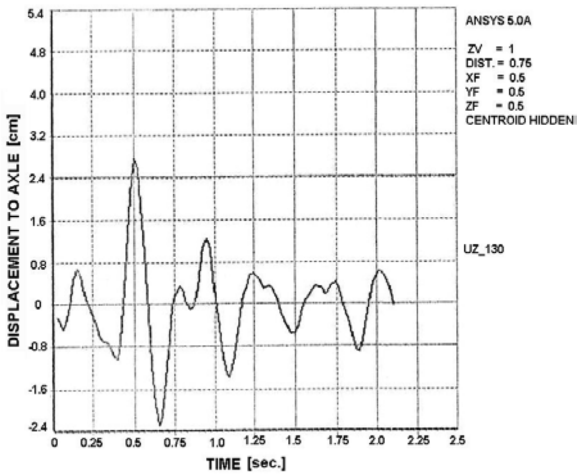

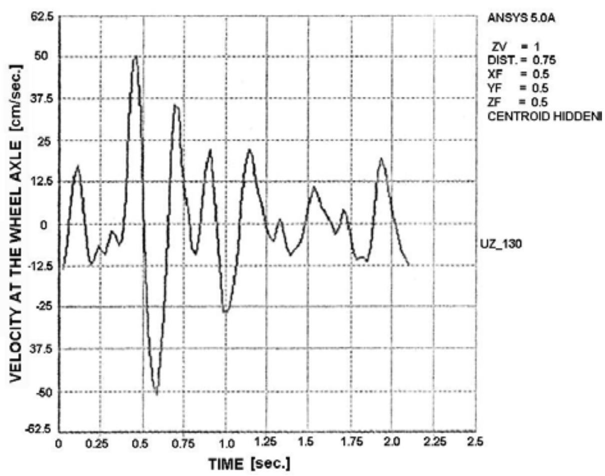

Figure 4 *- The wheel axle displacement* ***Figure 5*** *- Velocity at the wheel axle*
(Disk harrow GD 3.2 during the transport)

In order to reproduce the real stress generated during the harrow transport, due especially to the forces of inertia has been applied as an impulse the displacement to the wheel axle.

The displacemnt signal has been introduced exactly as it has been provided by the measurements, in order to avoid the unnecessary ambiguites. Because of the external memory restrictions, the interval has been considered 6 until 8 seconds, comprising the maximum displacement: 2.77 cm. The signal has been applied into the point 130 on the wheel axle, the soil reaction in time being presented in figure 7.

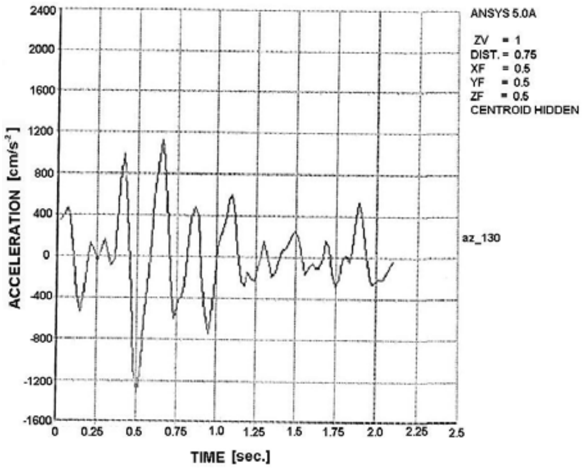

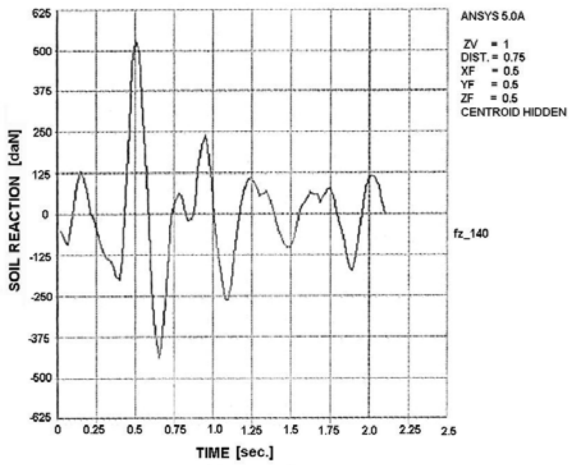

Figure 6 *- Acceleration at the whee axle* ***Figure 7*** *- Soil reaction during the transport*
(Disk harrow GD 3.2 during the transport)

- **Stress analysis in transport regime**

There have been extracted in order to be shown following areas:

a) Rear battery joint - internal frame, for which it has been represented in time the stress (figures 8 and 9), from which it results:

$$\sigma_{max\_din} < 140 \text{ daN/cm}^2$$

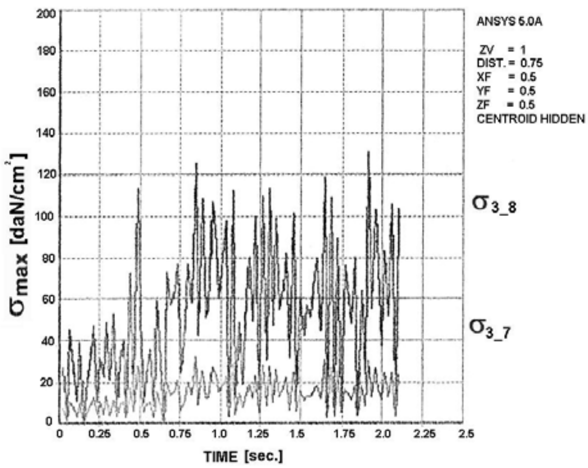

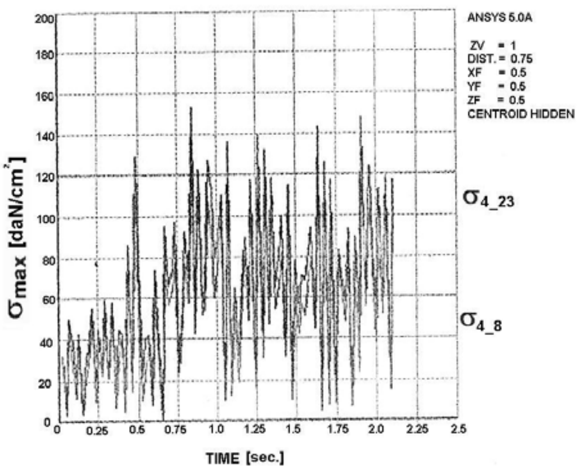

Figure 8 *- Stress in element 3* ***Figure 9*** *- Stress in element 4*

b) Rear battery attaching - external frame, for which the stress of the adjacent elements is presented in figures 10 and 11, resulting in:

$$\sigma_{max\_din} < 225 \text{ daN/cm}^2$$

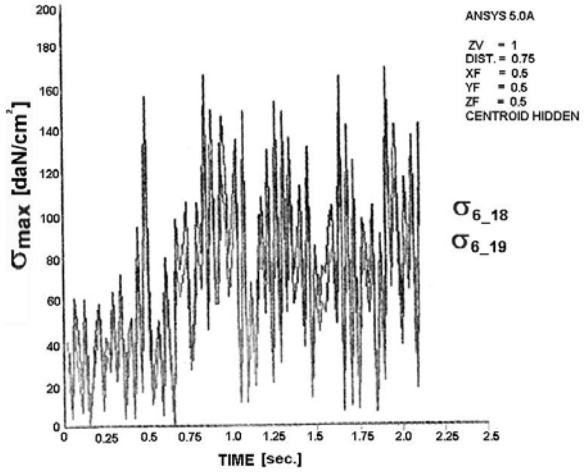

Figure 10 *- Stress in element 6*

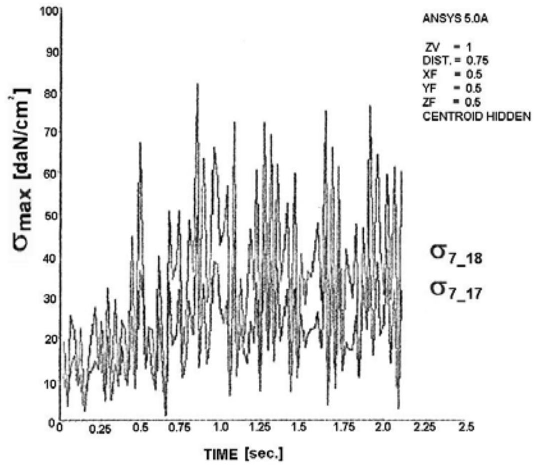

Figure 11 *- Stress in element 7*

c) Joint between the train axle - external frame, for which the dynamic stress is presented in figures 12 and 13, resulting in:

$$\sigma_{max\_din} < 170 \text{ daN/cm}^2$$

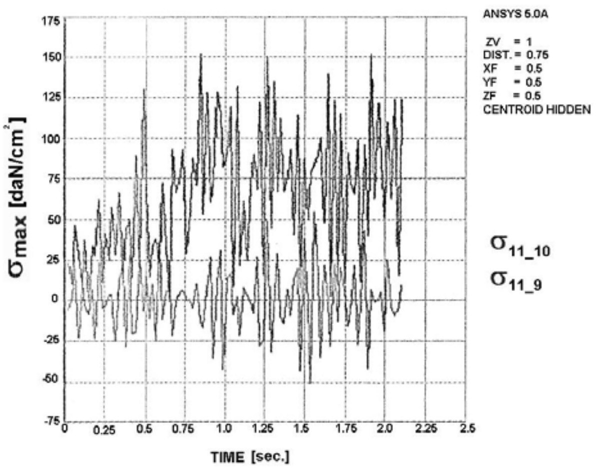

Figure 12 *- Stress în element 11*

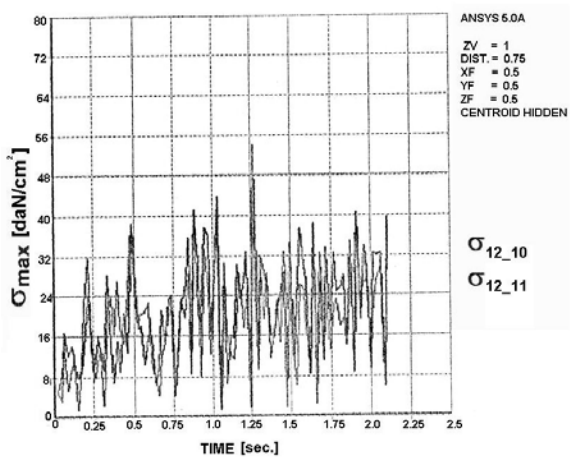

Figure 13 *- Stress in element 12*

d) Joint between the train-axle and the external frame, for which the dynamic stress is presented in figures 14 and 15, resulting in:

$$\sigma_{max\_din} < 113 \text{ daN/cm}^2$$

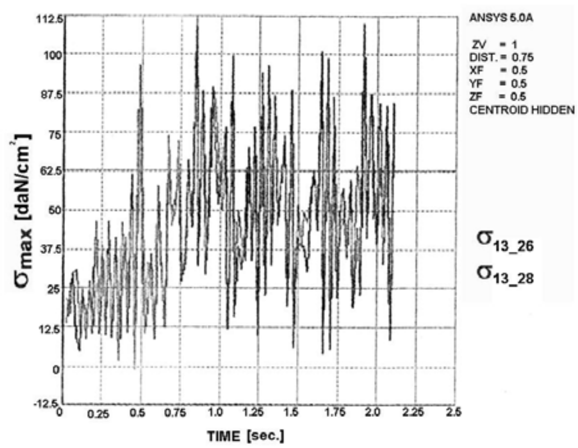

Figure 14 *- Stress in element 13*

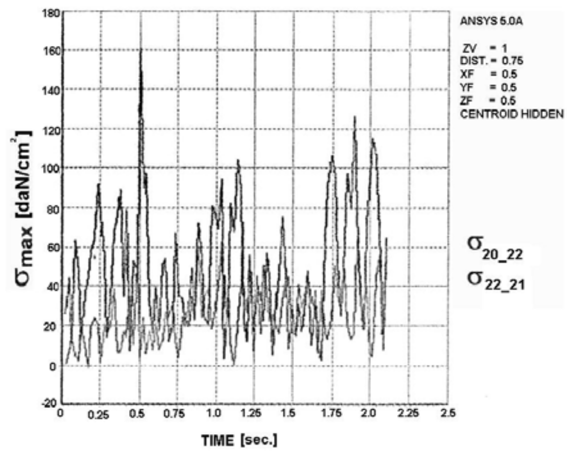

Figure 15 *- Stress in element 14*

e) Front battery articulation - internal frame, for which has been represented in time the stress for figure 13, resulting in: $\sigma_{max\_din} < 60$ daN/cm^2.

f) Front battery attachement - external frame for which the strss in the adjacent elements presented in figures 15 and 16, resulting in: $\sigma_{max\_din} < 160$ daN/cm^2.

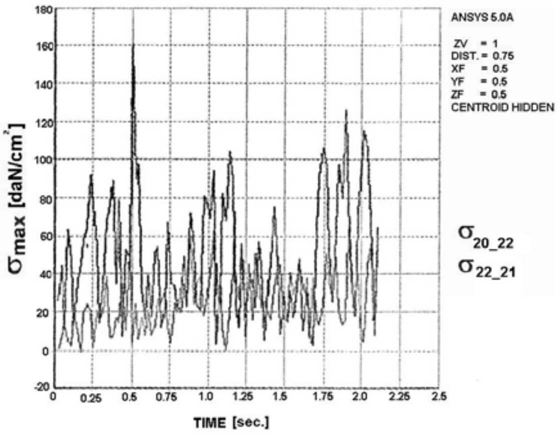

Figure 15 - *Stress in element 14*

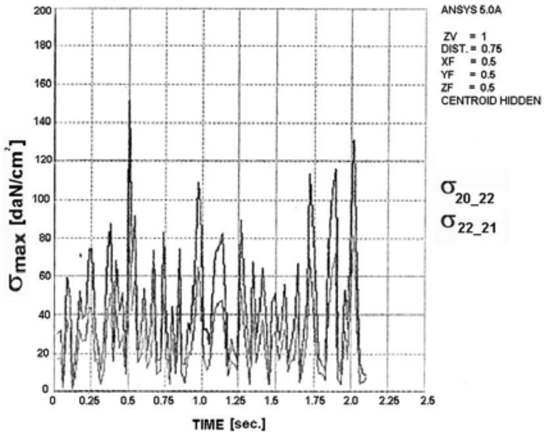

Figure 16 - *Stress in element 20*

As is results from above, the dynamic stress doesn't surpass the value of 225 daN/cm^2, calculated for the signal that was considered as significant for the analysis. It is also possible that in transport position should obtain accidentally a resonance situation, but testing the aggregate in such regime is impossible because that regime can not be approximated.

- **Results of the tests in simulated and accelerated regime on the Hidropuls instalation**

After having covered the whole volume of tests there has been found that, in case of stress in the transport position of the harrow GD 3.2, having run 1.5x10^6 cycles of stress there haven't been any remanent deformations or cracks into the harroe structure.

3. CONCLUSIONS

Following the analysis of the displacements, deformations and stress in the harrow structure through the method of finite elements ANSYS and on the hidropulse it has been found that:

- for the transport loading has been performed the analysis of the induced stress in critical areas through the method of the dynamic response of the program ANSYS, taking into consideration as a critical case - the recording T13D.ASC (figure 17), the values of this stress being presented in the diagrams from figures 7÷16; the maximum value of the dynamic loadings is of 225 daN/cm^2;
- after having covered the whole cycle of loadings, in transport position, there haven't been found any remanent deformations, breakings or cracks in the harrow structure.

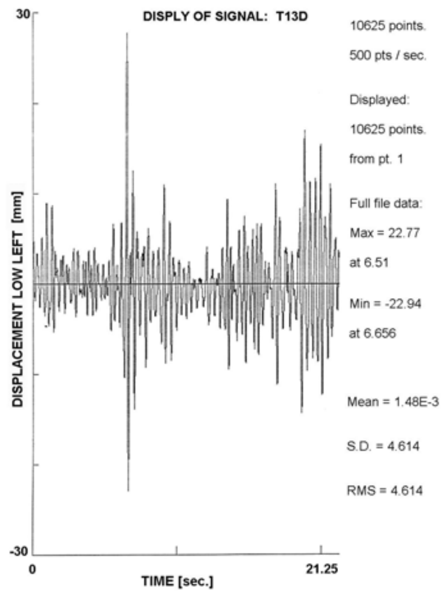

Figure 17 - Critical case

4. BIBLIOGRAFIE

[1]. Dima I., Bondar Gh., Fransua A. - *Test of the disk harrow GD 3.2 M in simulated and accelerated regime on Hidropulse*, Testing Report, INMA Bucharest, 1995;

[2]. Popa C., Păunescu D., ş.a. - *Mechanical test of the resistance frame of the tractor CEAHLĂU 4601 in compliance with the Directive 86/298/CEE*, Testing Report, Bucharest, 2002.

THE FUNCTIONING SIMULATION OF AN ELECTRICAL INSTALLATION AFFERENT TO A CRUCIBLE INDUCTION FURNACE, BY USING THE PSCAD - EMTDC PROGRAM

[1]IAGĂR Angela, PĂNOIU Caius, ABRUDEAN Cristian

[1] University „POLITEHNICA" TIMIŞOARA, Faculty of Engineering HUNEDOARA

ABSTRACT

The paper presents the simulation of the functioning process of an electrical installation afferent to a crucible induction furnace, supplied to an industrial frequency. The simulation being presented by using the PSCAD-EMTDC program.

KEYWORDS: *induction furnace, industrial frequency, simulation*

1. INTRODUCTION

In this paper the electrical installation of an electromagnetic induction furnace, with crucible, is being analysed. The capacity of the furnace being 12.5 tones cast iron.

The furnace is supplied by using a three-phase transformer (f = 50 Hz). The transformer has the rated output Sn = 2625 kVA, the connexion Δ/Δ, $3\times6/1.2$ kV, and the voltage control in steps (4 primary steps and 8 secondary ones). The balancing of the three-phased network is made through a Steinmetz symmetry diagram, with coil and capacitors, while the compensation of the power factor of the furnace is made through a battery of capacitors.

The purpose of the paper is the simulation of the functioning process of an electrical installation afferent to a crucible induction furnace, by using the PSCAD-EMTDC program. The simulation results have been compared with the experimental data obtained by measurements made in the lower voltage part of the electrical installation of the furnace.

2. EXPERIMENTAL RESULTS

For measuring the electrical quantities of the studied installation, there has been used a data acquisition system.

The measured electrical quantities (high voltages and currents) have been transformed, by using an adapting block, into voltages that have a compatible range with the used acquisition board (ADA 3100). The acquisition data frequency had the value 12.5 kHz. The acquisition time has been 400 ms, each signal having 20 periods which can be selected by the program. The time between the two consecutive data windows has the value 5 s.

The measured electrical quantities (the secondary voltages, the currents absorbed by the installation of the furnace from the three-phased network and the currents that pass through the inductor) are presented in Fig. 1.

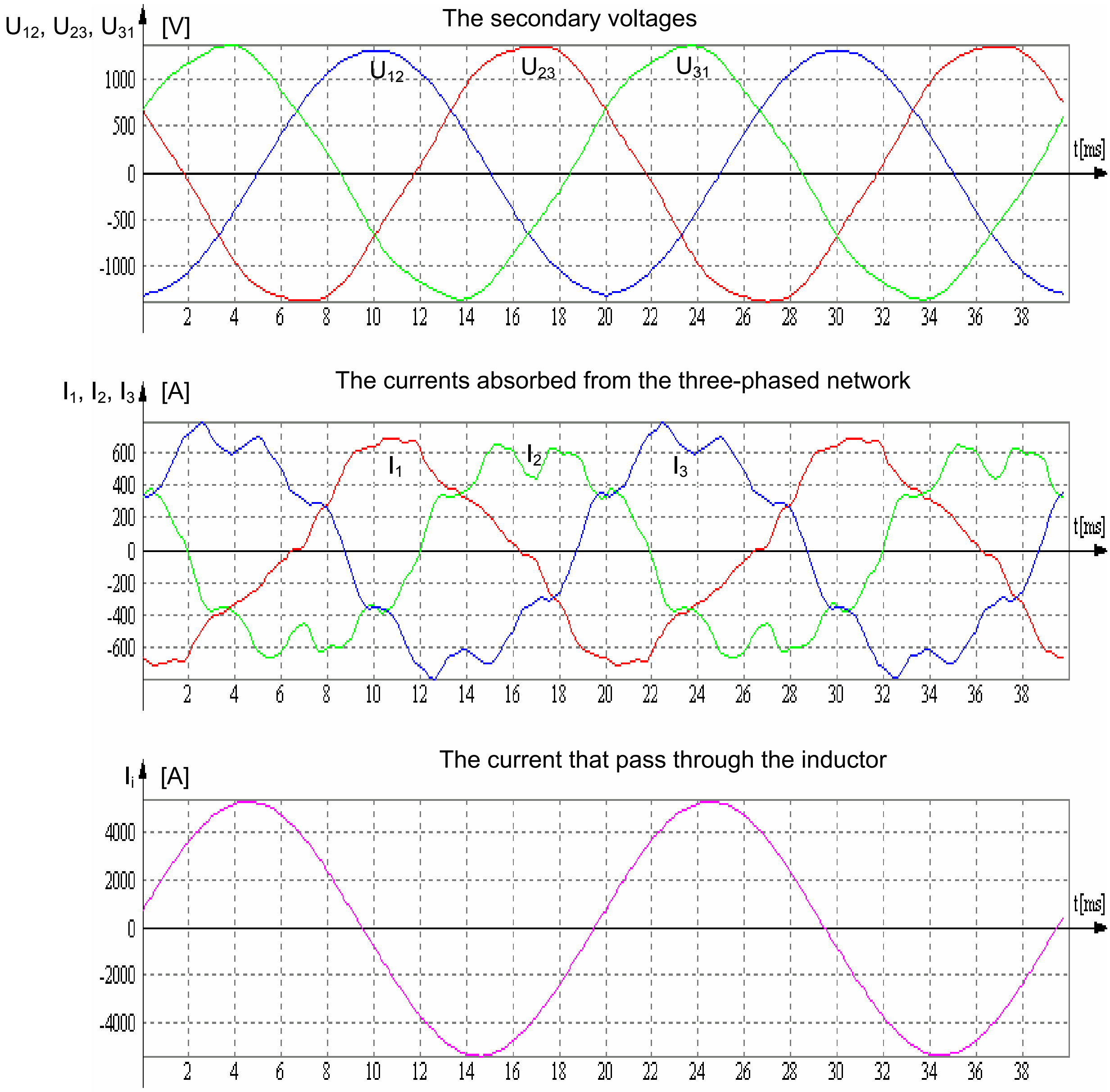

Fig. 1. *The electrical quantities measured in the lower voltage part of the studied electrical installation*.

There have been ascertained some electromagnetic disturbances in the currents absorbed by the installation of the furnace from the three-phased network; this indicates the non-linear characteristic of the components from the electrical installation of the analysed induction furnace.

Having this remark as a starting point, supposing, as well, that the coil (with magnetic core) from the symmetry installation is saturated, by using the PSCAD-EMTDC program, a simulation of the functioning process of the electrical installation has been obtained.

3. THE SIMULATION OF THE FUNCTIONING PROCESS OF THE ELECTRICAL INSTALLATION AFFERENT TO AN INDUCTION FURNACE OF INDUSTRIAL FREQUENCY BY USING THE PSCAD-EMTDC PROGRAM.

3.1. The modelling of the changing inductance of a symmetry coil

The saturation of the magnetic core of the symmetry coil can be mathematically modelled by using the relation (1). Formula (1) expresses the non-linear dependence of the magnetic induction from the coil, on the magnetic field strength and on temperature:

$$B = \mu_0 \cdot H + B_{s0} \cdot \frac{H_a + 1 - \sqrt{(H_a + 1)^2 - 4H_a(1-a)}}{2(1-a)} \cdot \left(1 - e^{\frac{T-T_c}{c}}\right), \qquad (1)$$

where $H_a = \dfrac{\mu_0 \cdot H(\mu_{ro} - 1)}{B_{s0}}$. (2)

In relations (1) and (2):

$\mu_0 = 4\pi \cdot 10^{-7}$ H/m represent the vacuum absolute permeability;

H [A/m] – is the magnetic field strength (the magnetic field is generated by the current from the symmetry coil);

T [°C] – is the temperature of the magnetic circuit of the coil;

$T_c = 800°C$ is the Curie temperature characteristic to the material of the electrical steel, from which the magnetic circuit of the coil is made.

$a \in (0; 0,5)$; $c \in (20; 100)$

B_{s0} [T] – represent the saturation magnetic induction of the electrical steel at the temperature of T = 0°C;

μ_{r0} – is the initial relative magnetic permeability (T = 0°C).

Therefore the induction of the coil can be determined by the expression:

$$L = \frac{\Phi}{i} = \frac{B \cdot S}{i}, \text{ [H]} \qquad (3)$$

where: S [m^2] – is the quadrate section of the symmetry coil;
i [A] – the current through the coil.

Let a = 0,01 ; 0,49 and c = 100; 500; μ_{r0} = 1400; B_{s0} = 2T; T = 30°C; H = 1....10000 A/m, a MATLAB program has been created to implement the relations (1) and (2) in order to determine the curve B(H) for the magnetic circuit of the symmetry coil. In the Fig. 2 is presented the obtained curves B(H).

3.2. The simulation results

In order to present the simulation of the functioning process of an electrical installation afferent to a crucible induction furnace, there has been used a PSCAD-EMTDC program. In the expressions (1) and (2) we notes:

$$c_{11} = \frac{T - T_c}{c}; \qquad (4)$$

$$c_1 = 1 - e^{\frac{T - T_c}{c}}; \tag{5}$$

$$c_2 = \frac{\mu_0(\mu_{r0} - 1)}{B_{s0}}; \tag{6}$$

$$H_a = H \cdot c_2 = N \cdot I \cdot c_2, \tag{7}$$

where N denotes the number of turns of the symmetry coil (N=72) and I denotes the current that passes through the symmetry coil;

$$H_{a1} = H_a + 1; \tag{8}$$

$$H_{a2} = 4H_a(1 - a); \tag{9}$$

$$H_{a3} = \sqrt{(H_{a1})^2 - H_{a2}}; \tag{10}$$

$$H_{a4} = \frac{H_{a1} - H_{a3}}{2(1 - a)}; \tag{11}$$

$$B_1 = \mu_0 \cdot H = \mu_0 \cdot N \cdot I; \tag{12}$$

$$B_2 = B_{s0} \cdot H_{a4} \cdot c_1; \tag{13}$$

$$B = B_1 + B_2. \tag{14}$$

The simulation results are shown in Fig. 3.

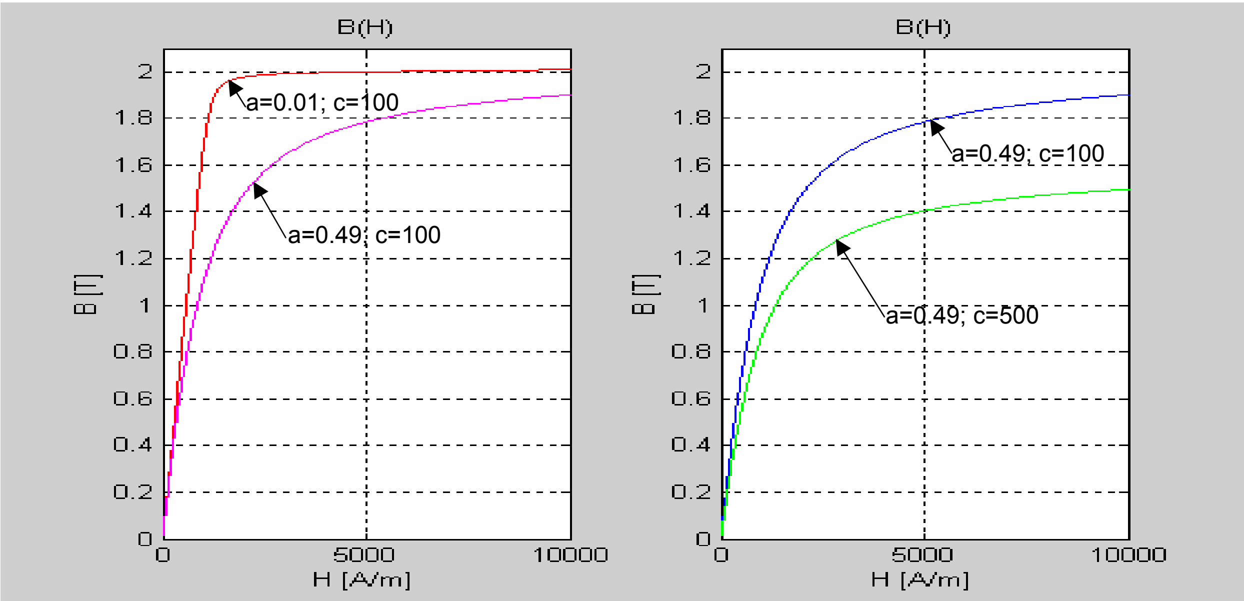

Fig. 2 *The dependence B(H) for the magnetic circuit of the symmetry coil.*

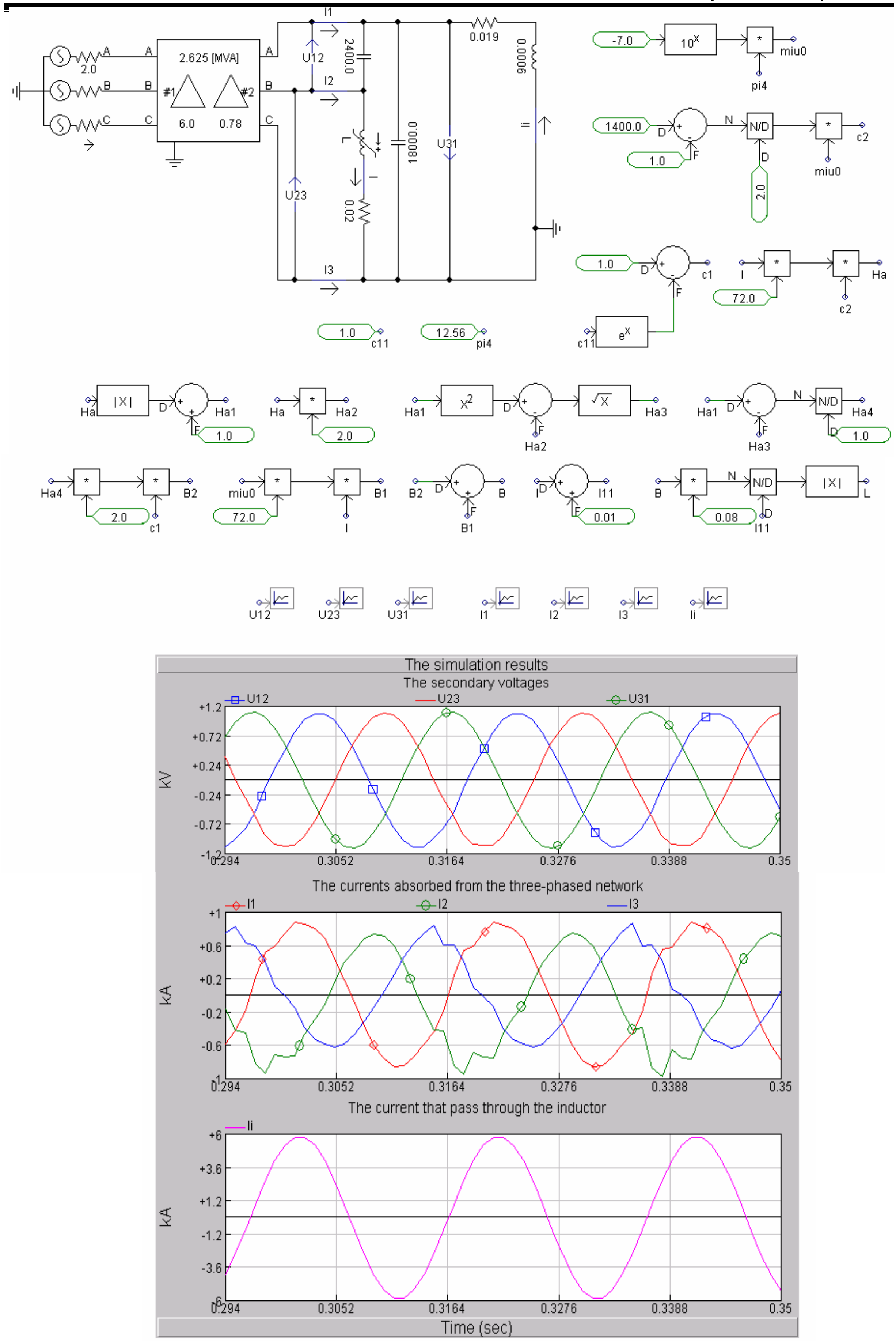

Fig. 3 *The simulation results by using PSCAD-EMTDC.*

4. CONCLUSIONS

The experimental measurements have proved the existence of some electromagnetic disturbances in the currents absorbed by the installation of the induction furnace (f = 50 Hz) from the three-phased network.

By using the PSCAD-EMTDC program and supposing that the coil (with magnetic core) from the symmetry installation is saturated, a simulation of the functioning process of the electrical installation has been obtained.

A good concordance between the experimental results and the simulation results obtained by using the PSCAD-EMTDC program can be observed; this indicates the that the saturation of the coil, from the symmetry installation, can be represent an explanation for the existence of the electromagnetic disturbances in the currents absorbed by the installation of the furnace from the three-phased network.

5. BIBLIOGRAPHY

1. A. Buta , A. Pană – *Simetrizarea sarcinii rețelelor electrice de distribuție,* Editura Orizonturi universitare, Timişoara, 2000.
2. Marilena Ungureanu, M. Chindris, I. Lungu – *Utilizari ale energiei electrice*, Editura Didactică şi Pedagogică, R.A. Bucureşti, 1999.
3. *** PSCAD-EMTDC – *User's guide, 2001.*

ISIRR 2003

STUDY OF THE LOW-PASS AND HIGH-PASS, FIRST- AND SECOND ORDER ACTIVES FILTERS

Eugen RĂDUCA

prof. eng of University „Eftimie Murgu” Reşiţa

Abstract

The author has realized studies of the low-pass, high-pass, band-pass and band-rejection active filter with operational amplifiers. The studies has included building and simulation on PC this circuits realized with operational amplifiers. This paper presented the work above low-pass and high-pass first- and second order filters. Those are presented electrical schemes of the filters and the graphical results of the simulation and the conclusions after the comparison between the simulation and the physical circuits.

Keywords

low-pass high-pass first- and second order filters, operational amplifier

1. Above active filters theory

1.1 Low-pass filter

The general transfer function of a low-pass filter is:

$$A(s) = \frac{A_0}{\prod_i \left(1 + a_i s + b_i s^2\right)}; \qquad (1)$$

with A_0 being the pass band gain.

The filter coefficients distinguish between types and order filters [1].

For a first-order filter, $b_i = 0$:

$$A(s) = \frac{A_0}{1 + a_i s}; \qquad (2)$$

and for a second-order filter :

$$A_i(s) = \frac{A_0}{\left(1 + a_i s + b_i s^2\right)}; \qquad (3)$$

The higher- order filter is building with cascading connection of first-order and/or second-order filters.

The transfer function of the First-Order Noninverting Low-Pass Filter (fig.1) is:

$$A(s) = \frac{1+\frac{R_2}{R_3}}{1+\omega_0 R_1 C_1 s}; \qquad (4)$$

with the relations between the parameters:

$$A_0 = 1+\frac{R_2}{R_3}; \qquad (5)$$

$$a_1 = \omega_0 R_1 C_1; \qquad (6)$$

The coefficient a_1 is taken from the tables [1].

To dimension the circuit, specify the corner frequency f_c, the DC gain A_0 and capacitor C_1 and then solve for resistor R_1 and R_2:

$$R_1 = \frac{a_1}{2\pi f_C C_1}; \qquad (7)$$

$$R_2 = R_3(A_0-1); \qquad (8)$$

The transfer function of Second Order Unity-Gain Sallen-Kay Low-Pass Filter (fig.3) is:

$$A(s) = \frac{1}{1+\omega_C C_1(R_1+R_2)s+\omega_C{}^2 R_1 R_2 C_1 C_2 s^2}; \qquad (9)$$

with the relations between the parameters:

$$A_0 = 1$$

$$a_1 = \omega_C C_1(R_1+R_2); \qquad (10)$$

$$b_1 = \omega_C{}^2 R_1 R_2 C_1 C_2; \qquad (11)$$

Given C_1, C_2 with the condition:

$$C_2 \geq C_1 \frac{4b_1}{a_1{}^2}; \qquad (12)$$

The resistor values for R_1 and R_2 are calculated through:

$$R_{1,2} = \frac{a_1 C_2 \pm \sqrt{a_1{}^2 C_2{}^2 - 4b_1 C_1 C_2}}{4\pi f_C C_1 C_2}; \qquad (13)$$

1.2 High-pass Filter

By replacing the resistors of the low-pass filter with capacitors and the capacitors with resistors a high-pass filters created.

The general transfer function of a high-pass filter is then:

$$A(s) = \frac{A_0}{\prod_i \left(1 + \frac{a_i}{s} + \frac{b_i}{s^2}\right)} ; \qquad (14)$$

The transfer function of a single stage is:

$$A(s) = \frac{A_0}{1 + \frac{a_i}{s}} ; \qquad (15)$$

for a First-Order Noninverting High-Pass Filter, and:

$$A_i(s) = \frac{A_0}{\left(1 + \frac{a_i}{s} + \frac{b_i}{s^2}\right)} ; \qquad (16)$$

for a Second Order Sallen-Kay Unity-Gain High-Pass Filter

The transfer function of the First-Order Noninverting High-Pass Filter (fig.5) is:

$$A(s) = \frac{1 + \frac{R_2}{R_3}}{1 + \omega_C R_1 C_1 \frac{1}{s}} \qquad (17)$$

with the relations between the parameters:

$$A_\infty = 1 + \frac{R_2}{R_3} ; \qquad (18)$$

$$a_1 = \frac{1}{\omega_C R_1 C_1} ; \qquad (19)$$

To dimension the circuit, specify the corner frequency f_c , the DC gain A_0 and capacitor C_1 and then solve for resistor R_1 and R_2 :

$$R_1 = \frac{1}{2\pi f_C a_1 C_1} ; \qquad (20)$$

$$R_2 = R_3(A_\infty - 1) ; \qquad (21)$$

The transfer function of Second Order Unity-Gain Sallen-Kay High-Pass Filter (fig.7) is:

$$A(s) = \frac{1}{1+\frac{2}{\omega_C R_1 C}\cdot\frac{1}{s}+\frac{1}{\omega_C^2 R_1 R_2 C^2}\cdot\frac{1}{s^2}}; \qquad (22)$$

with the relations between the parameters

$$a_1 = \frac{2}{\omega_C R_1 C}; \qquad (23)$$

$$b_1 = \frac{1}{\omega_C^2 R_1 R_2 C^2}; \qquad (24)$$

Given C, The resistor values for R_1 and R_2 are calculated through:

$$R_1 = \frac{1}{\pi f_C C a_1}; \qquad (25)$$

$$R_2 = \frac{a_1}{4\pi f_C C b_1}; \qquad (26)$$

2. CONCLUSIONS

Electrical schemas are presented in fig.1, fig.3, fig.5, fig.7. For the simulated schemas the solutions can be visualized in fig.3, fig.5, fig.7, respectively fig.8. For real schemas the graphical characteristics was be obtained from point by point method.

The conclusions presented has be obtained in conditions when the values of the real components differed with maximal 2% of the values from simulated circuits.

Four principal conclusions are:

- characteristics gain-frequency are very appropriate for the two cases
- real filter can presented some suprarise or decrease and oscillates amortized on the front an high-pass filter and an low-pass filter (which not appear through the simulated program). This excluding to be difficulty.
- for any situation gain value has sensible differed for the two cases.
- Electronics Workbench program can bee utilized simple with successful in the study of active filters.

3. REFERENCES

1. Thomas Kugelstadt - Active Filter Design Techniques, 2001, SUA
2. Amplifiers and Comparators – Data Book , Texas Instruments, 2001, SUA

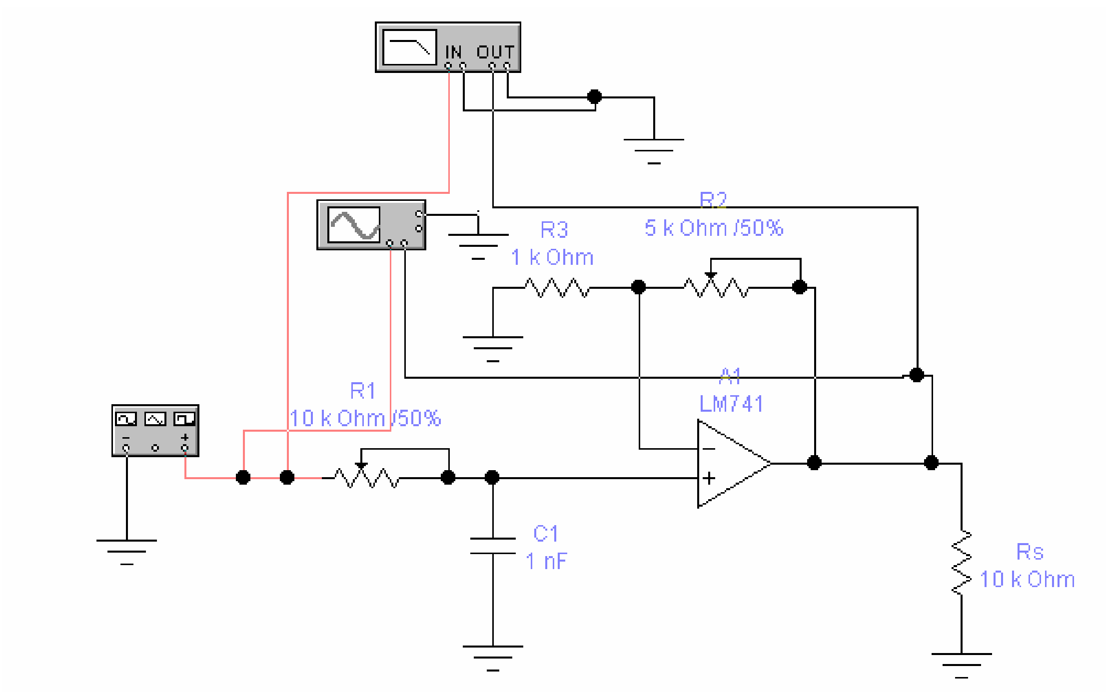

Fig.1 First-Order Noninverting Low-Pass Filter

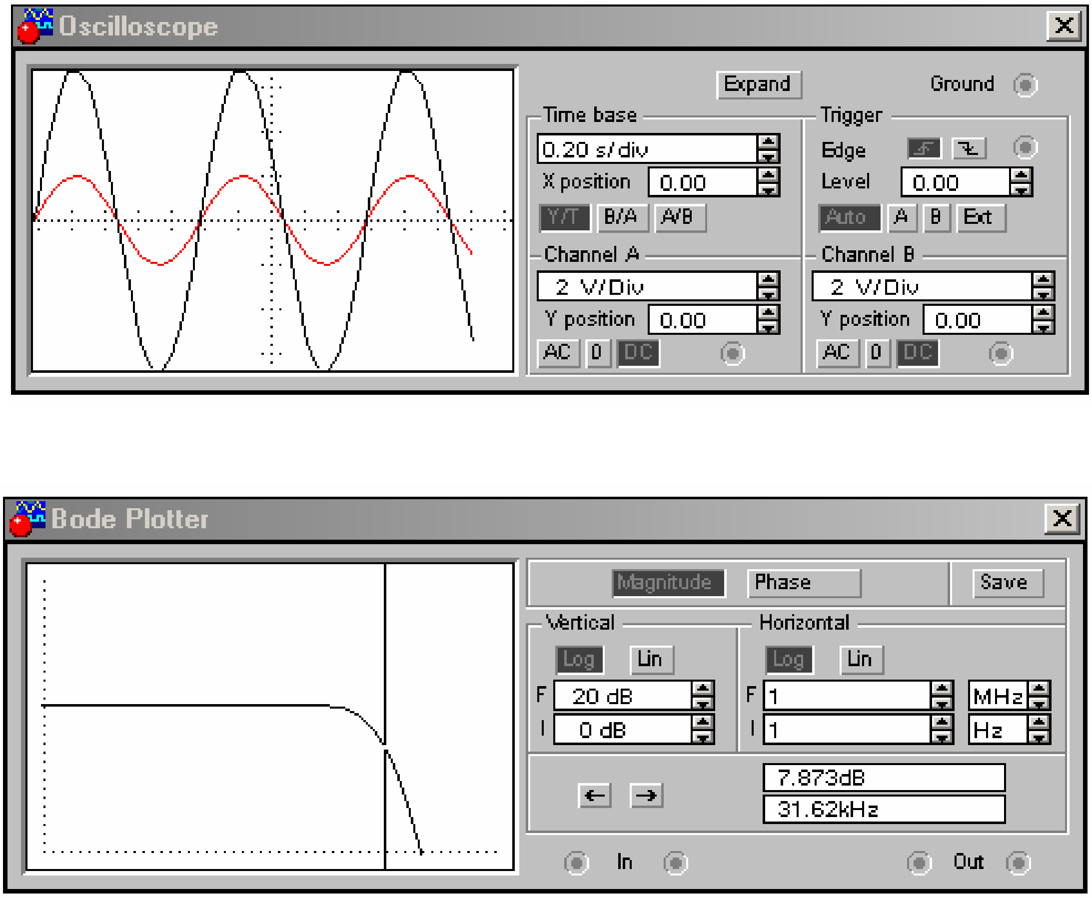

Fig.2 Graphical solutions after the circuit's from fig1 simulation on PC

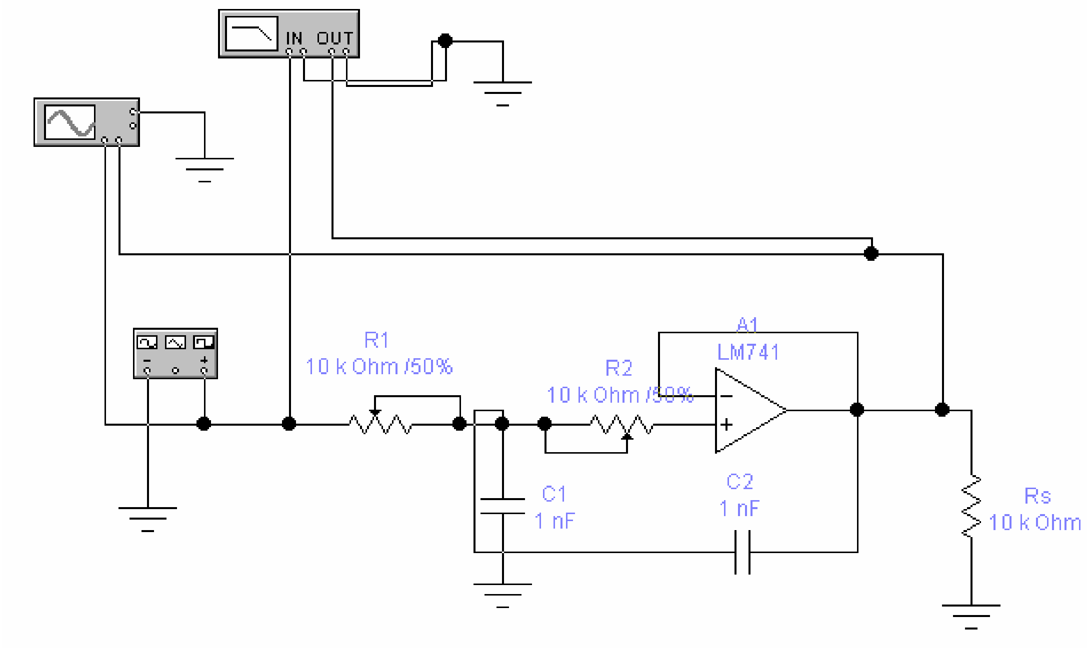

Fig.3 Second Order Unity-Gain Low-Pass Filter

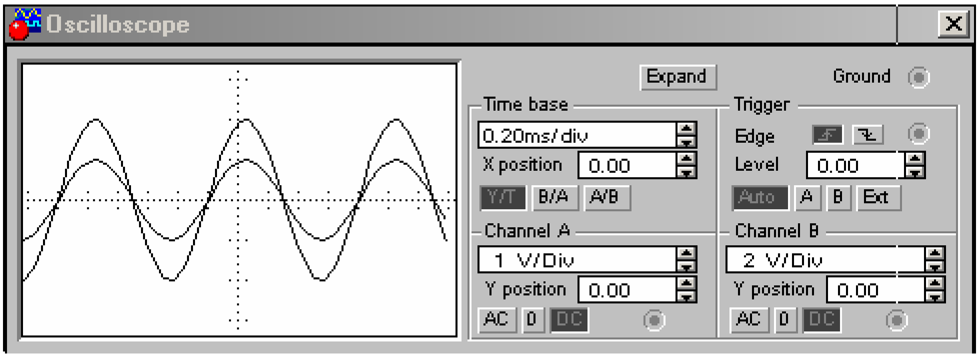

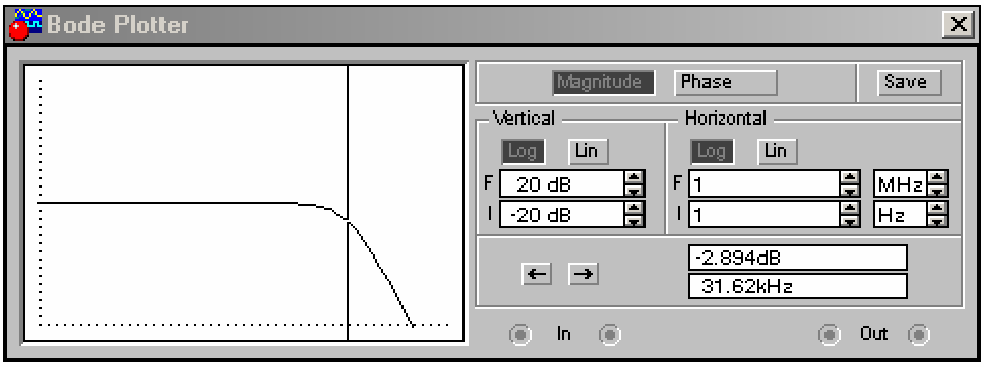

Fig. 4 Graphical solutions after the circuit's from fig.3 simulation on PC

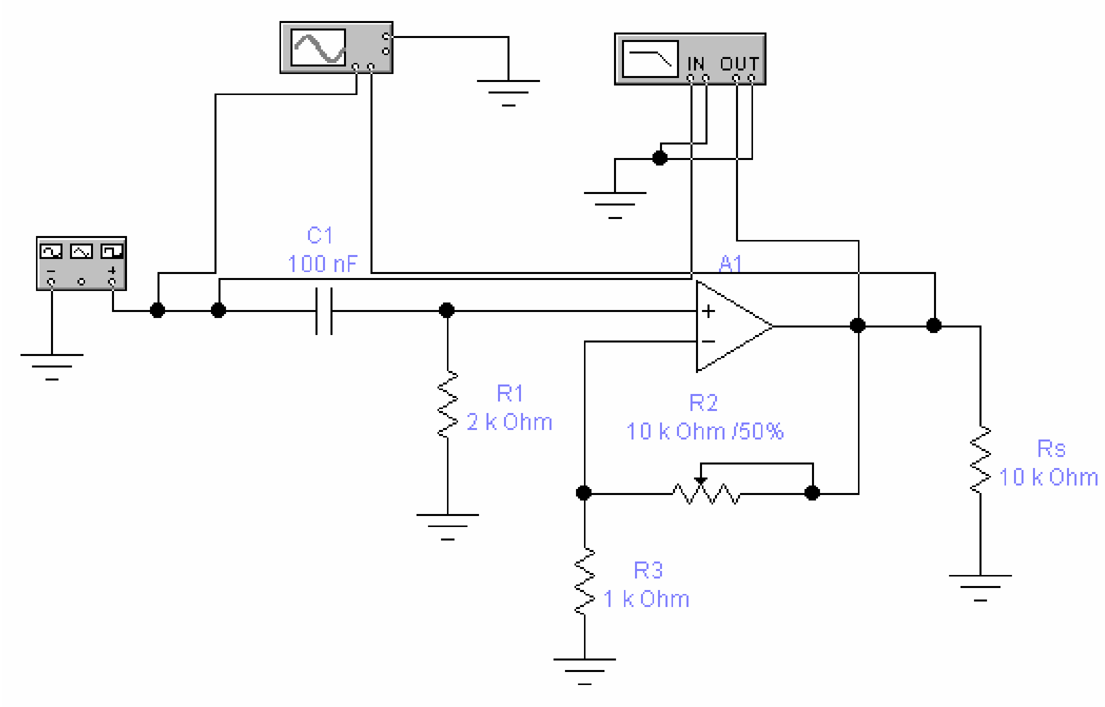

Fig.5 First-Order Noninverting High-Pass Filter

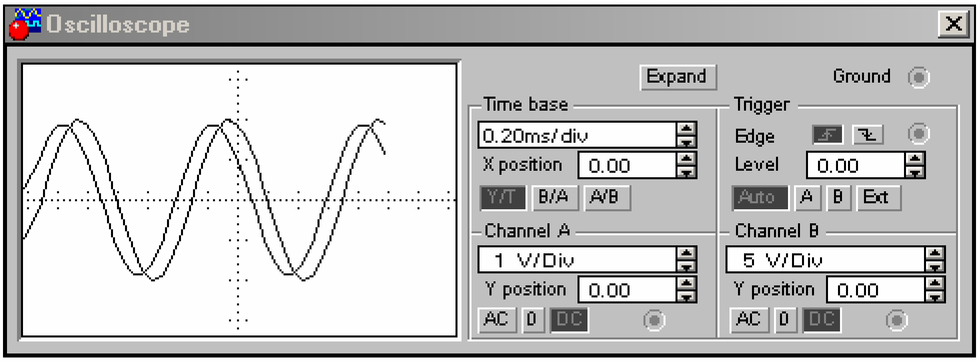

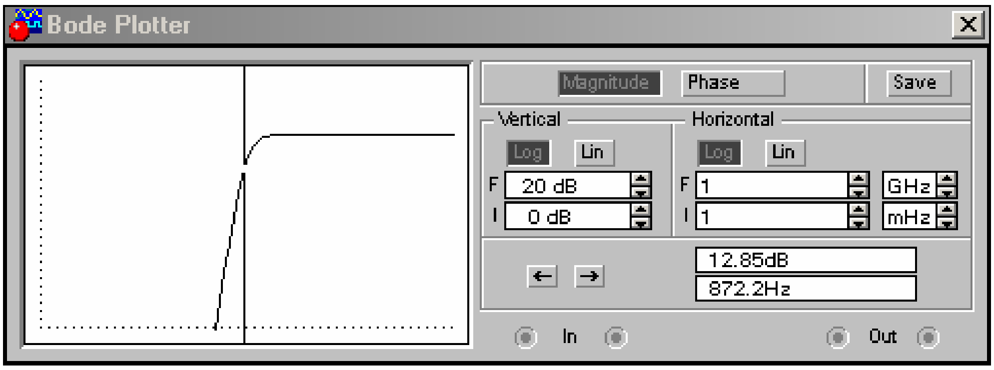

Fig.6 Graphical solutions after the circuit's from fig.5 simulation on PC

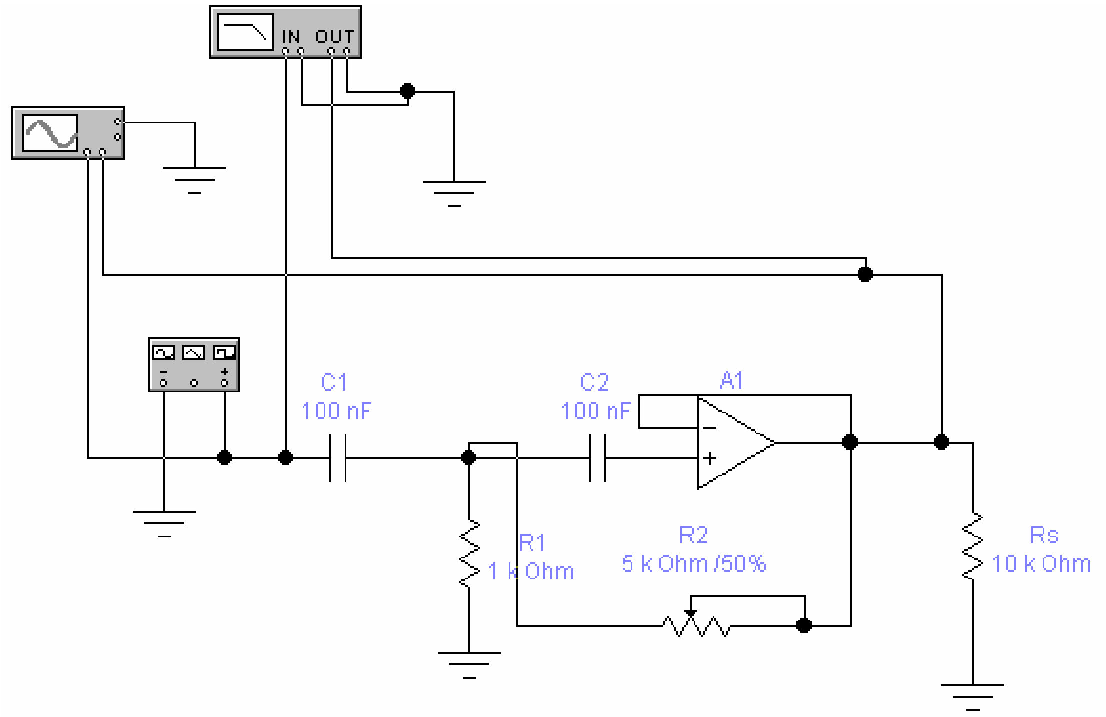

Fig.7 Second Order Unity-Gain High-Pass Filter

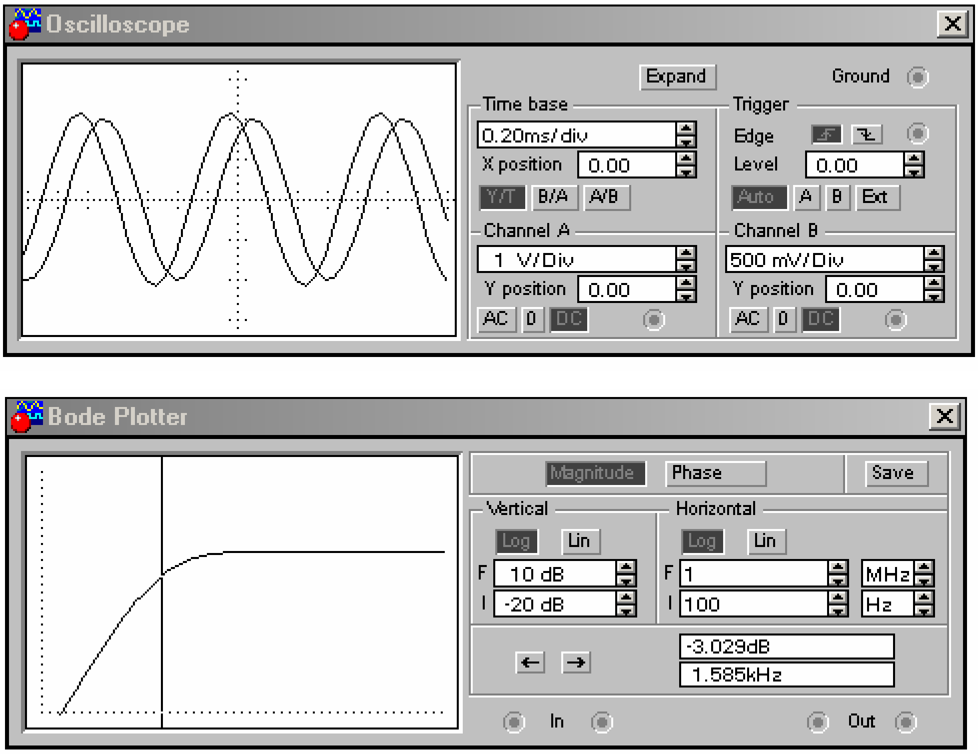

Fig.8 Graphical solutions after the circuit's from fig.7 simulation on PC

CONSIDERATION ON THE RELATION CAUSE – EFFECT AT THE MEASUREMENT DEVICE FOR MECHANICAL SIZES BASED ON THE ELASTIC ELEMENTS

CARDEI Petru, Ing. JERCALEANU Chiriac,
INMA Bucharest, E-mail icsit@sunu.rnc.ro

Abstract

This paper propose some reflection about the measuring of the mechanical sizes process (strength, moments, ...), using elastic elements (flexors) in the measuring devices. For a good measurement, generally, is theoretically required a certain type of dependence between the state physical sizes of the elastic element and the loads of the system, which we try to measure. There is possible as the dependence between the state physical sizes of the elastic element and the loads of the system to be a one - to - one function? If not, there is a restriction of the function between the loads and the state physical size, where this function is a one - valued function? How is implicate in this problem the principle of Saint - Venant and the equation of the elastic continuous media? These are only few questions at the paper try to find some partial answers.

Keywords: *cause, effect, measurement*

Introduction

In the direct problem of the elasticity there are given the body geometry and material properties, the limit conditions, the initial conditions (if the problem is dynamic) and the loads. The equation of the linear elasticity gives the solution: the displacements vector and the strain and stress tensors. In the case of this paper we have the inverse problem. On the elastic system is measured the strain (and by calculus, the stress) in a certain number of system locations. The question is if there is some relation between the physical and geometrical characteristics of the elastic system and the stress calculated (on the basis of the measured strain in certain locations) which can gives the interaction components.

The device for the measurement of the interaction

The geometry of the device for the measurement of the interaction parameters (forces and moments) is shown in the figure 1.

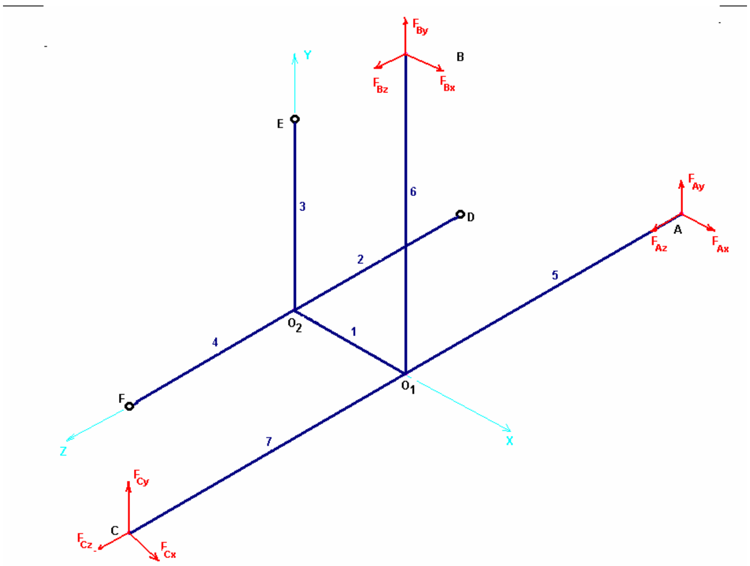

Fig. 1 *The scheme of the interaction measurement device.*

The points where the device is coupled at the tractor are D, E, F and the points where the device is coupled at the farm machinery are A, B, C. Be *L* the length of the beams AO_1, BO_1 and CO_1, *l* the length of the beams DO_2, EO_2 and FO_2, *d*, the length of the beam O_1O_2. I suppose that in the points A, B, C action the strength:

$$\vec{F}_A = F_{Ax}\vec{i} + F_{Ay}\vec{j} + F_{Az}\vec{k},\ \vec{F}_B = F_{Bx}\vec{i} + F_{By}\vec{j} + F_{Bz}\vec{k},\ \vec{F}_C = F_{Cx}\vec{i} + F_{Cy}\vec{j} + F_{Cz}\vec{k}\ , \tag{1}$$

where $\vec{i}, \vec{j}, \vec{k}$, are the unit vectors of the axes O_2x, O_2y, O_2z. The point O_2 is the origin of the axes system. In these conditions, the components of the resultant strength and resultant moment are (according to [3] or [4]) :

$$F_x = F_{Ax} + F_{Bx} + F_{Cx},\ F_y = F_{Ay} + F_{By} + F_{Cy},\ F_z = F_{Az} + F_{Bz} + F_{Cz},. \tag{2}$$

Then the longitudinal stress (see [1]) has the next expression:

$$\sigma(x,y,z) = \frac{F_x}{A} + \frac{y(d-x)F_y}{I_z} - \frac{z(d-x)F_z}{I_y} + \frac{zL(F_{Cx}-F_{Ax})}{I_z} - \frac{yLF_{Bx}}{I_y} + \frac{L(F_{Ay}+F_{Bz}-F_{Cy})}{I_p}r\ , \tag{3}$$

where *x* is the coordinate along the beam and *y* and *z* are the coordinates in the plane of the cross section of the beam (see figure 2) and $r=(y^2+z^2)^{1/2}$, I_y and I_z are the moment of inertia of the beam cross section and I_p is the polar moment of the beam cross section. Between the moments of inertia there is the relation $I_p=I_y+I_z$. For simplicity I suppose that $I_y = I_z = I$.

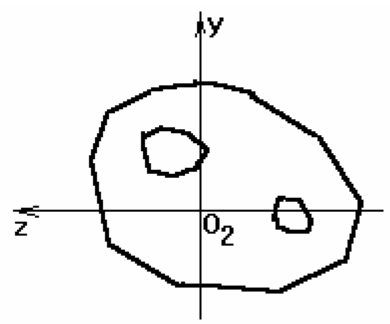

Fig. 2 *The coordinates in the beam cross section.*

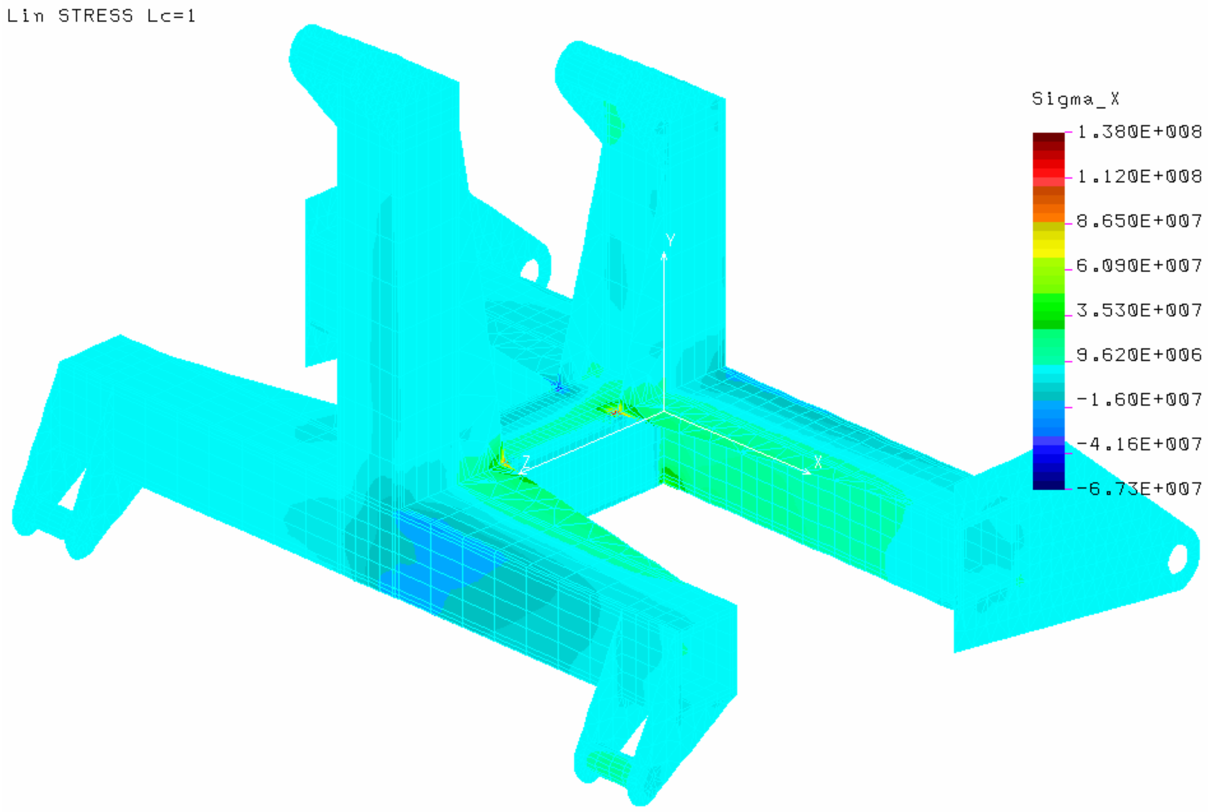

Fig. 3 *The measurement system and the location of the six strain gauge.*

The 3-dimensional real geometry of the measurement device is shown in the figure 3. We suppose placed six strain gauges in the six measurement points on the central beam . If we write down the variables:

$$u_1 = \frac{F_x}{A}, u_2 = \frac{F_y}{I}, u_3 = \frac{F_z}{I}, u_4 = \frac{L(F_{Ax} - F_{Cx})}{I}, u_5 = \frac{L}{I} F_{Bx}, u_6 = \frac{LF_{Ay} + LF_{Bz} - LF_{Cy}}{I_p}, \tag{4}$$

and we write the relation (3) for each measurement point, *i*= 1,… ,6, then is obtaining next system of linear equations:

$$u_1 + (d - x_i) y_i u_2 - (d - x_i) z_i u_3 + z_i u_4 - y_i u_5 + \sqrt{y_i^2 + z_i^2}\, u_6 = \sigma_{mi}, \quad i = 1, \ldots, 6, \tag{5}$$

where σ_{mi} is the stress calculated starting from the measured strain (with the strain gauge) in the point *i* (*i*= 1,… ,6). The matrix form of the system (5) is:

$$Tu = \sigma_m, \tag{6}$$

where:

$$T = \begin{pmatrix} 1 & (d - x_1) y_1 & -(d - x_1) z_1 & z_1 & -y_1 & \sqrt{y_1^2 + z_1^2} \\ 1 & (d - x_2) y_2 & -(d - x_2) z_2 & z_2 & -y_2 & \sqrt{y_2^2 + z_2^2} \\ 1 & (d - x_3) y_3 & -(d - x_3) z_3 & z_3 & -y_3 & \sqrt{y_3^2 + z_3^2} \\ 1 & (d - x_4) y_4 & -(d - x_4) z_4 & z_4 & -y_4 & \sqrt{y_4^2 + z_4^2} \\ 1 & (d - x_5) y_5 & -(d - x_5) z_5 & z_5 & -y_5 & \sqrt{y_5^2 + z_5^2} \\ 1 & (d - x_6) y_6 & -(d - x_6) z_6 & z_6 & -y_6 & \sqrt{y_6^2 + z_6^2} \end{pmatrix}, \; u = \begin{pmatrix} u_1 \\ u_2 \\ u_3 \\ u_4 \\ u_5 \\ u_6 \end{pmatrix}, \; \sigma_m = \begin{pmatrix} \sigma_1 \\ \sigma_2 \\ \sigma_3 \\ \sigma_4 \\ \sigma_5 \\ \sigma_6 \end{pmatrix}. \tag{7}$$

Then the solution there is and is unique if and only if det T $\neq$0. In this case the solution is:

$$u = T^{-1}\sigma_m . \tag{8}$$

Using the relations (4) is obtained :

$$F_x = u_1 A, F_y = u_2 I, F_z = u_3 I, F_{Cx} - F_{Ax} = u_4 \frac{I}{L}, F_{Bx} = u_5 \frac{I}{L}, F_{Ay} + F_{Bz} - F_{Cy} = u_6 \frac{I_p}{L}. \tag{9}$$

and finally, with (2):

$$F_{Ax} = \frac{Au_1 - \frac{I}{L}(u_5 + u_4)}{2}, F_{Cx} = \frac{Au_1 - \frac{I}{L}(u_5 - u_4)}{2}. \tag{10}$$

The formula (3) is valid only for the central zone of the beam O_1O_2 (see figure 1 and 3), thus we try to locate the measurement points in this zone, where the boundary effects are slow .

The main disadvantage of this procedure for the calculus of the interaction between the tractor and the farm machinery is the high sensibility of the linear operator at the errors of the experimental strain (or stress). The experimental error has a component which results from the difference between the simple solution (3) and the real solution (the real solution obtained solving the elasticity equations). It is possible to consider that these errors are equal for any measurement location. In this case, the numerical study shows that the strength error is equal with the measured stress error. But, if, for example, at least one of measured stresses errors differs from the others and even only by sign, not necessarily so in absolute value, then the strength errors increase very much. For example, if the errors of the measured strain give the calculated stress value error for all location, 0.1 % then the strength error is, also, 0.1 %, but if the errors of the measured strain are 0.1% for five of the strain gauges and -0.1% for the sixth strain gauge, then the strength error is 12.85%. These aspects are in study for the moment. We know that, for multiple connected domains and concentrated strengths there is theorems of oneness for the solution (see [2] and [5]).In certain conditions results if that the strength fields are slowly modified, then the stress state is also slowly modified. Unfortunately we cannot obtain an analytical solution for our problem and then the numerical solution is the unique solution that we can obtain. This solution is the reference solution. With this solution we can simulate the process of measurement of the interaction between the tractor and farm machinery.

In this conditions we use for the calculus a method based on the experimental (simulation) results. Using the experimental results is possible to obtain functions which give the loads if we know the longitudinal stresses on the beam O_1O_2 .

Simulation of the measuring. Results, precision

For example we consider a measurement device like this plotted in the figure 1, with next characteristics: *d*= 0.3 m, *L*= 0.5 m, *l*= 0.3 m, *S*= 0.1 m, all the beams of the measurement device are square pipe with the 0.39 m side and 0.008 m thickness (see figure 3). The coordinates of the strain gauge location on the beam O_1O_2, are given in the table 1.

Table 1 *Measurement location coordinates and the theoretical longitudinal stresses.*

Element level	**x, m**	**y, m**	**z, m**
1540	0.175000	0.024000	-0.04000
987	0.182714	-0.008000	0.04000
986	0.182714	0.008000	0.04000
1539	0.175000	0.008000	-0.04000
988	0.182714	-0.024000	0.04000
1537	0.175000	-0.024000	-0.04000
985	0.182714	0.024000	0.04000
699	0.175000	0.040000	0.04000

Using the simulation data, is obtain next linear function for the loads:

$$
\begin{aligned}
&F_x(\sigma_{z1540},\sigma_{z987},\sigma_{z986},\sigma_{z1539},\sigma_{z988},\sigma_{z1537},\sigma_{z985},\sigma_{z699}) = 0.0566\cdot\sigma_{z1540} - \\
&35.8466\cdot\sigma_{z987} - 55.5556\cdot\sigma_{z986} - 32.066\cdot\sigma_{z1539} - 0.8866\cdot\sigma_{z988} + 0.1981\cdot\sigma_{z1537} + \\
&63.8283\cdot\sigma_{z985} - 61.1098\cdot\sigma_{z699}; \\
&F_y(\sigma_{z1540},\sigma_{z987},\sigma_{z986},\sigma_{z1539},\sigma_{z988},\sigma_{z1537},\sigma_{z985},\sigma_{z699}) = 0.0257\cdot\sigma_{z1540} - \\
&16.3015\cdot\sigma_{z987} + 25.2643\cdot\sigma_{z986} + 14.5822\cdot\sigma_{z1539} + 0.4032\cdot\sigma_{z988} - 0.0901\cdot\sigma_{z1537} - \\
&29.0263\cdot\sigma_{z985} + 27.7901\cdot\sigma_{z699}; \\
&F_z(\sigma_{z1540},\sigma_{z987},\sigma_{z986},\sigma_{z1539},\sigma_{z988},\sigma_{z1537},\sigma_{z985},\sigma_{z699}) = 0.6187\cdot\sigma_{z1540} + \\
&894.0309\cdot\sigma_{z987} + 651.8893\cdot\sigma_{z986} + 1180.6579\cdot\sigma_{z1539} + 8.6551\cdot\sigma_{z988} + 0.8084\cdot\sigma_{z1537} - \\
&199.5535\cdot\sigma_{z985} - 139.5446\cdot\sigma_{z699}
\end{aligned} \tag{11}
$$

The functions (11) are calculated using the least – squares method with experimental (numerical experiments) data. The performance of this method can be estimated using the table 2.

***Table 2**. Some results of the (11) formula.*

The real resultant loads, N			The calculated resultant loads, N		
F_x	F_y	F_z	F_x	F_y	F_z
431	-196	925	433	-197	943
431	-196	1735	431	-196	1781
431	-196	2235	429	-195	2234
431	-196	1475	433	-197	1452

Conclusions

The main conclusion of this stage of the research is that the dependence between the loads and the body (the measurement device) stresses is not a globally one – valued function.

Then we try to find a local one – valued dependence between the loads and the body stresses and the local three dimensional interval will be theoretically estimated. The experimental data processing will made using the result of this estimation (function like (11)).

REFERENCES

[1] Hute,Engineer's Handbook, Technical Printing House, Bucharest, 1995;

[2] Lazăr Dragoş, Principles of Mechanics of the Continuous Media, Technical Printing House, Bucharest, 1983;

[3] Nicolae Posea, Material Strength, Didactic and Pedagogical Printing House, Bucharest, 1979;

[4] Victor Drobota, Material Strength, Didactic and Pedagogical Printing House, Bucharest, 1982;

[5] W. Kecs, P.P. Teodorescu, Introduction into the Theory of Distributions with Applications in Technique, 1975;

THE INFLUENCE OF THE TECHNOLOGICAL PARAMETERS ON THE PRIMARY COOLING AT THE CONTINUOUS CASTING

Erika ARDELEAN[1], Marius ARDELEAN[2], Ana SOCALICI[2]

[1] Facultatea de Inginerie Hunedoara, Universitatea Politehnica Timişoara
[2] Facultatea de Inginerie Hunedoara, Universitatea Politehnica Timişoara

Abstract

The primary cooling – inside the mould – has a high importance in what concerns the thickness of the solidified steel scum. If the scum is too thin when coming out of the mould, under the action of the ferro-static pressure generated by the liquid steel from inside and due to the own weight of the strand, the scum can force through, thus resulting the strand breaking.

The paper presents a series of correlation between the different technological parameters (the steel temperature inside the tundish, the casting speed, etc.) and the cooling conditions inside the mould for the section 240x270 mm and for the 150 mm round.

Keywords

Continuous casting, primary cooling, steel temperature, parameters

1. INTRODUCTION

When starting the continuous casting, the steel is cast until the mould is filled up (Figure 1). After that, without stopping the steel casting, the dummy bar, that was previously mounted on the bottom of the mould, together with the semi-finished product that is already developed, comes out from the mould and continues its line in the continuous casting installation up to the secondary cooling area. From here, the line continues further, through the drawing and straightening rolls, towards the cutting equipment and cooling bed.

Before the semi-finished product leaves the mould, a high heat exchange between the outer surface of the semi-finished product and the inner walls of the mould takes place. These walls are strongly water-cooled. The cooling that takes place inside the mould as a result of the heat exchange has to ensure the building up of a steel scum, thick enough to resist to the longitudinal tensile stresses (when the semi-finished product moves relating to the mould walls). After the semi-finished product comes out from the mould, the scum has to resist also to the transversal tensile stresses (generated by the pressure inside the steel).

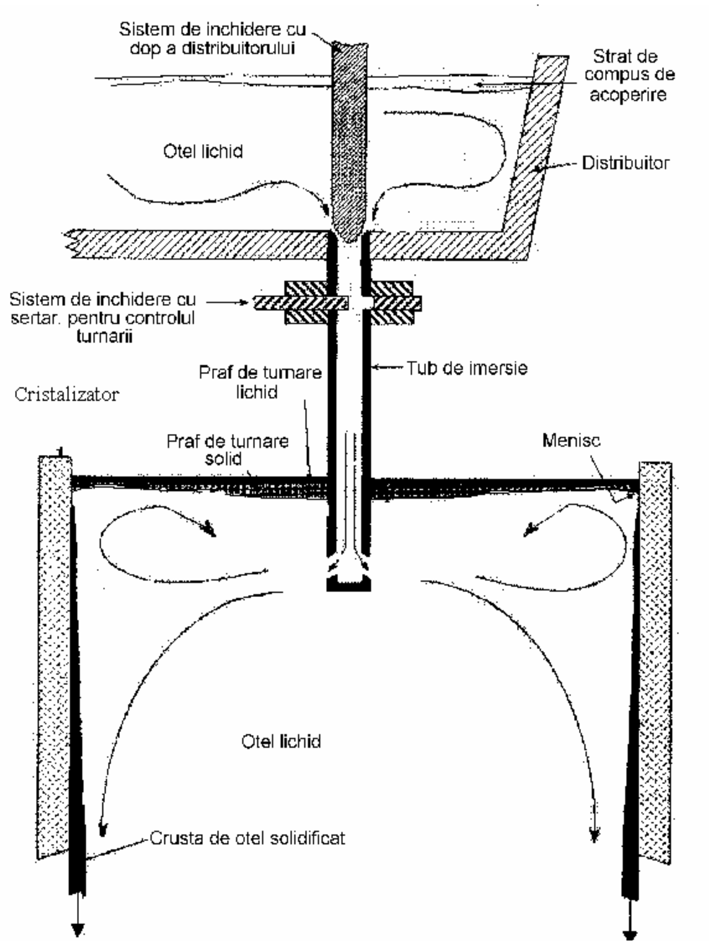

Fig.1 Continuous casting of the steel true the mould

The necessary thickness of the solidified scum when the semi-finished product comes out from the mould, highly depends on the product section. For the small billets, a thin scum is sufficient, while the big sections require a thicker and more resistant scum, due to the higher ferro-static pressure that acts on the semi-finished product when this comes out from the mould. For this reason, the cast speed decreases together with the increasing of the cross section of the semi-finished product.

2. EXPERIMENTS AND RESULTS

In order to study the solidification of the steel when continuously casting, we have tested a number of 55 heats, OL 37-2k grade, cast as 240x270 mm bloom and 55 heats, OLT 35 grade, cast as Ø 150 mm billets.

We have analyzed a series of parameters that influence the primary solidification, as follows: the steel temperature inside the tundish, the casting speed and also the parameters of the cooling water inside the mould (temperature, pressure, flow), all measured at certain time periods. The data were processed in the Matlab programme and the results are shown both graphically and analytically.

Figure 2 presents the casting speed depending on the steell temperature in the tundish and respectively the water temperature in the mould for 150 mm round, all these being measured initially and then at different time periods since beginning the casting. We have considered the sequential cast heats as being individual cast heats, taking into consideration the fact that only the temperatures and the casting speeds at beginning the casting are different. It can be noticed that at low steel temperatures in the tundish the casting speed is higher and the temperature of the water in the tundish has higher values.

The global correlation coefficient: ryx1x2 = 0.7390

The equation of the regression surface are:

$$z = -630.6283+ 0.8531*u -0.7280*v+0.0006*u.*v-0.0003*u.^2-0.0038*v.^2 \qquad (1)$$

In comparison, Figure 3 shows the same relation for the 240x270 mm bloom. Excepting the different temperatures of the steel inside the tundish, there can be noticed more lower values for the casting speed. We must take into consideration the bigger section in the second case. The global correlation coefficient together with the equation of the regression surface is

- the global correlation coefficient: ryx1x2 = 0.5915
- the equation of the regression surface

$$z = -33.3665 + 0.0525*u + 0.0466*v - 0.0014*v.^2 \qquad (2)$$

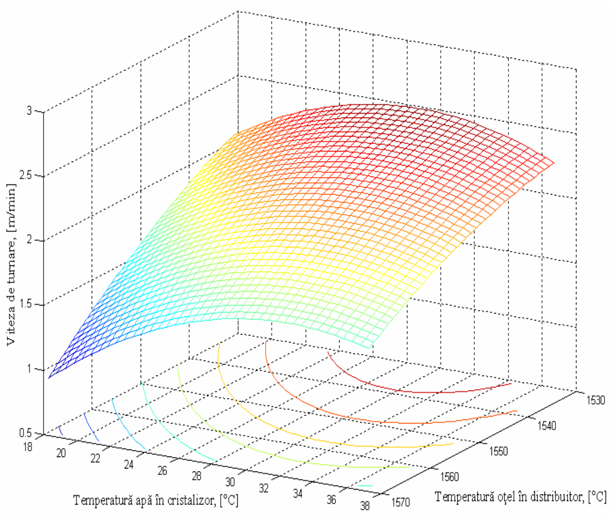

Fig.2 The dependence between casting speed, the steell temperature in the tundish and the water temperature in the mould for Φ150mm

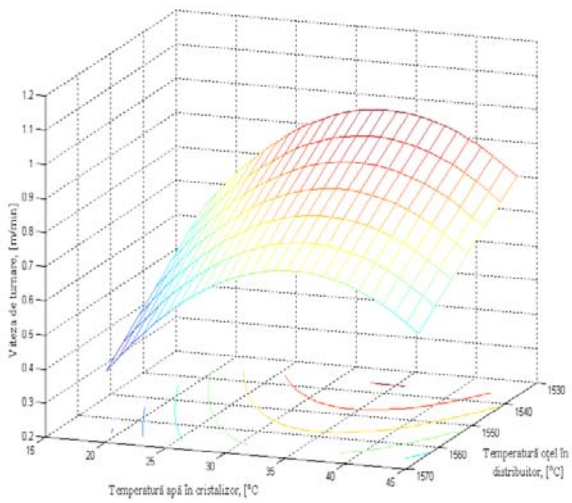

Fig.3 The dependence between casting speed, the steell temperature in the tundish and the water temperature in the mould for bloom 240x270mm

In what concerns the other parameters of the mould, as: water flow and respectively the water pressure in the mould, they have a high importance for the building of the semi-finished product scum. When coming out from the mould, the scum is thick enough in order to resist to the outer and inner stresses, without breaking.

From this point of view, in case of the Ø150 mm profile (Figure 4), for a certain casting speed, the pressure and the cooling water flow in the mould can be chosen. There is an inversely proportional dependence between these parameters.

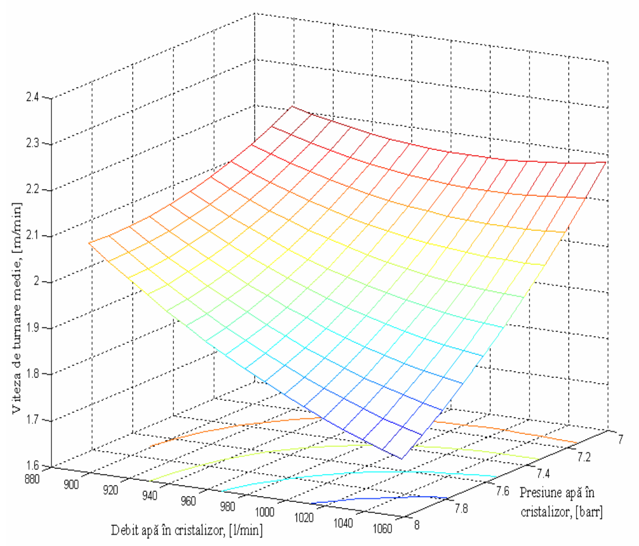

Fig.4 The dependence between the speed casting, pressure and the cooling water flow for the Ø150 mm profile

The global correlation coefficient: ryx1x2 = 0.6975

The equation of the regression surface

$$z = 3.3405 - 0.3328*u + 0.0032*v - 0.0022*u.*v + 0.1446*u.^2 \quad (3)$$

In what concerns the bloom, by taking into consideration its section, the cooling is performed differently on the two sides, as follows:

- in Figure 5, the directly proportional variation of the average casting speed depending on the cooling water parameters for the small side of the mould (240 mm) with the global correlation coefficient:

ryx1x2 = 0.7589 and the equation of the regression surface

$$z = -212.6674 - 8.4313*u + 0.4495*v + 0.0113*u.*v - 0.2633*u.^2 - 0.0002.*v.^2 \quad (4)$$

- in Figure 6, the interdependence of the same characteristics for the big side of the mould (270 mm), with the global correlation coefficient: ryx1x2 = 0.850 and the equation of the regression surface

$$z = 804.8152 - 136.3525*u - 0.6430*v + 0.1386*u.*v + 0.1582*u.^2 - 0.0002*v.^2 \quad (5)$$

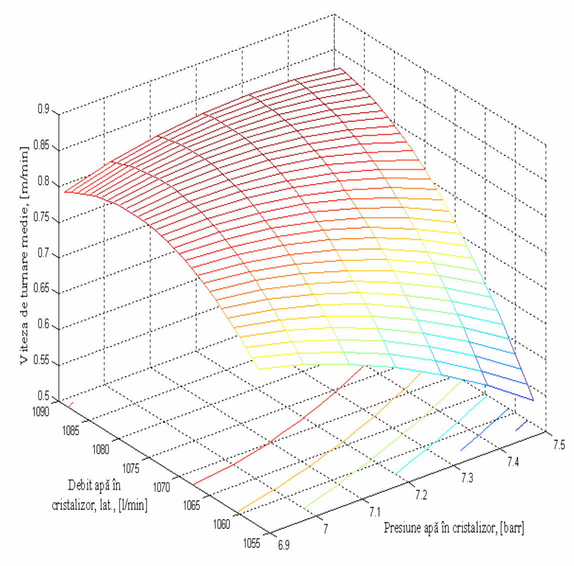

Fig.5 Variation of the average casting speed depending on the cooling water parameters for the small side of the mould (240 mm)

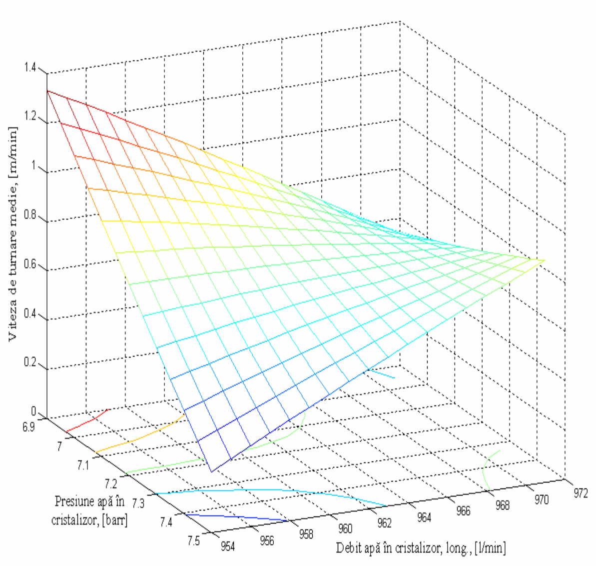

Fig.6 Variation of the average casting speed depending on the cooling water parameters for the big side of the mould (270 mm)

In this case there exists a variation that is similar to that of the round for low values of the casting speed, and respectively a directly proportional variation for higher values of the casting speed.

3. CONCLUSIONS

Based on the performed study and on the shown graphical and analytical dependence, a series of conclusions result, as follows:

- the solidification of the steel in the mould is very important. The thickness of the semi-finished scum when coming out from the mould and the integrity of the continuously cast strand depend on this;
- the steel temperature in the tundish has to be within the technological limits required for the continuously steel grade, in order to perform a proper cooling;
- in order to obtain a thick enough scum when coming out from the mould, the cooling water parameters (temperature, flow, pressure) are to be correlated with the technological parameters, such as casting speed;
- both the regression surfaces and the reached equations can be used in practice in order to reach a parameter, when the other two are already known.

4. REFERENCES

1. ARDELEAN, E., HEPUT, T, ARDELEAN, M. - Turnarea continua a otelului, Editura Politehnica Timisoara, 2001.
2. THOMAS, B.G. - Heat flow model of the continuous slab casting mold, interface and shall, Metallurgical Transactions, 1993.

THE INFLUENCE OF THE TECHNOLOGICAL PARAMETERS ON THE SECONDARY COOLING AT THE CONTINUOUS CASTING

Marius ARDELEAN[1], Erika ARDELEAN[2]

[1] Facultatea de Inginerie Hunedoara, Universitatea Politehnica Timişoara
[2] Facultatea de Inginerie Hunedoara, Universitatea Politehnica Timişoara

ABSTRACT

When cooling the semi-finished product in the mould, the secondary cooling takes place. During this, the solidification has to be performed on the entire cross section of the strand. In order to achieve this, beside a proper primary cooling, the factors that influence the secondary cooling have to be also correlated: the water flow on the three areas of the installation, the water pressure in the secondary line, etc.

All these have in view a proper solidification length; an intense cooling can generate cracks due to the thermal stresses, while a too slow cooling can generate a partial solidification of the strand up to the cutting machine area.

The paper shows also the differences that appear when continuously casting two different sections: 240x270 mm bloom and Ø 150 mm billet.

Keywords
Continuous casting, secondary cooling, water flow

1. INTRODUCTION

The purpose of the secondary casting is to continue the cooling of the strand after it has come out from the mould and to solidify completely the cross section of the strand. However, the developing of the solidification is limited by certain natural restrains, as: thermal conduction in the strand scum, cooling efficiency of the cooling agent, and last but not least, quality considerations regarding the semi-finished product.

The scum built in the mould ensures the shape of the cast section. In most cases, the scum does not present enough mechanical strength under the action of ferro-static pressure. In order to achieve a proper solidification and to lead the strand under proper conditions, the secondary area is arranged.

Spraying directly water under pressure through nozzles performs this cooling. This water is able to penetrate the steam layer built by vaporization and to ensure the continuously and permanent water – metal contact.

The end of the secondary area is located in the point of balancing the inner heat of the metal that has reached its surface by conductivity with the heat exhausted by radiation from this surface.

The efficiency of the cooling in the secondary area is determined both by the water flow (proportional to the casting speed) and by the water distribution on the metal surface. The spraying has to ensure the continuously cooling, corresponding to a constant temperature decrease from 1200-1300°C when coming out from the mould, to 700-900°C at the end of the secondary area. The temperature decreasing is easily reached in the case of square or round sections, where the liquid area decreases quickly. The heat content in case of slabs is high for a longer time, fact that explains the existence of the solidification cone also in the extraction equipment.

The secondary cooling area is next to the mould. In generally, it lays on over 30 up to 50% of the liquid core length. This area is divided in under-areas, which are individually controlled. The cooling agent, water or water-air mixture, is sprayed through nozzles on the surface of the strand, and it is controlled in a manner that the temperature of the strand surface decreases steadily in casting direction. The temperature is to be steadily on the periphery of the strand. The spraying nozzles, the spraying angle, the distances between the nozzles and the water presure are to be regulated so that around the periphery of the strand, a steady or almost steady temperature at a certain level is achieved. Several cooling areas are sequentially arranged and controlled along the strand, in order to ensure the decreasing of the spraying flows and the cooling efficiency according to the speed and the liquid core of the strand.

2. EXPERIMENTS AND RESULTS

For studying the steel solidification when continuously casting, we have tested a number of 55 heats, OL 37-2k grade, cast as 240x270 mm bloom and respectively 55 heats, OLT 35 grade, cast as Ø150 mm billet.

Taking into consideration the issues that were mentioned in the introduction part of this paper, we have studied the interdependence between the average casting speed and the parameters of the secondary cooling water on all the three areas. So, Figure 1, 2 and 3 show this interdependence for the 240x270 mm profile.

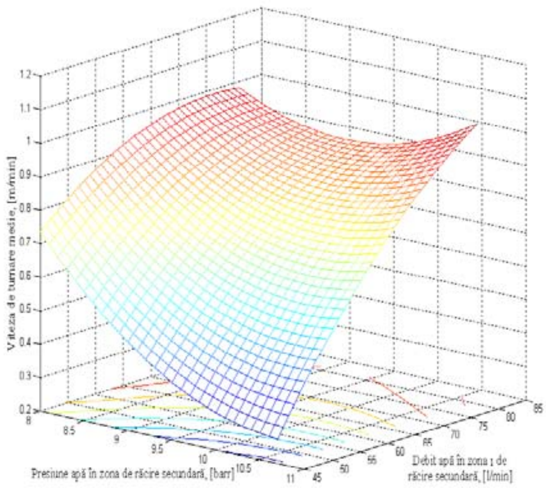

Fig.1 The interdependence between the average casting speed and the parameters of the secondary cooling water on first area

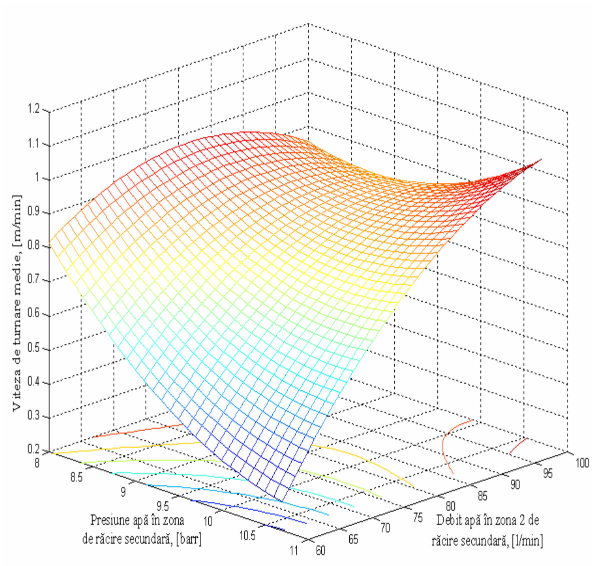

Fig.2 The interdependence between the average casting speed and the parameters of the secondary cooling water on the second area

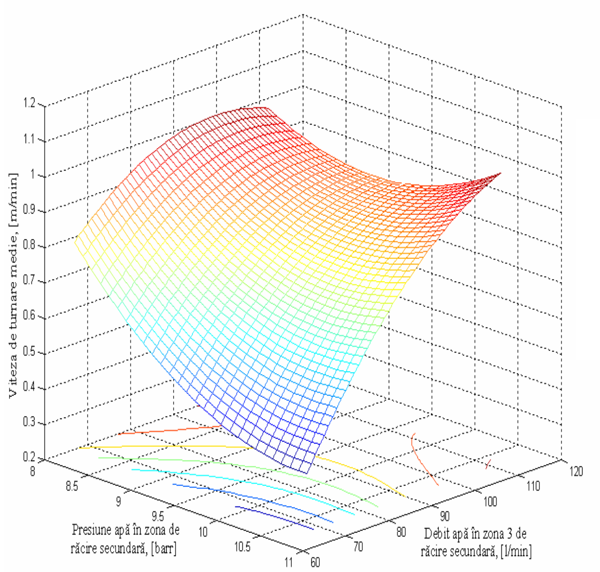

Fig.3 The interdependence between the average casting speed and the parameters of the secondary cooling water on the three area

By analyzing the previous presented surfaces, it can be noticed a similar dependence: at low casting speeds, the cooling water pressure admits relatively high values but also minimal values for water flow. But, together with the increasing of the casting speed, the flow increases and the cooling water pressure decreases slowly (a certain cooling programme), or both flow and cooling water pressure increase. If the pressure admits relatively constant values for the three cooling areas (8,6 – 10,7 bar), then the flows admit values as follows: 54 – 81 l/min for the first cooling area, 63 – 100 l/min for the second cooling area and 73 – 112 l/min for the third area, hence higher and higher flows in order to solidify the continuously cast semi-finished product on its entire cross section. All the three obtained surfaces show a saddle point in the technological field, being easy to notice graphically.

For the three surfaces the global correlation coefficient together with the equation of the regression surface is:

- for Figure 1: the global correlation coefficient: ryx1x2 = 0.8531 and the equation of the regression surface

$$z = 7.7904 - 1.5080*u - 0.0029*v + 0.0053*u.*v + 0.0588*u.^2 - 0.0003*v.^2 \quad (1)$$

- for Figure 2: the global correlation coefficient: ryx1x2 = 0.8122 and the equation of the regression surface

$$z = 8.0186 - 1.5857*u + 0.0022*v + 0.0065*u.*v + 0.0533*u.^2 - 0.0003*v.^2 \quad (2)$$

- for Figure 3: the global correlation coefficient: ryx1x2 = 0.8205 and the equation of the regression surface

$$z = 7.4566 - 1.5436*u + 0.0099*v + 0.0039*u.*v + 0.0603*u.^2 - 0.0002*v.^2 \quad (3)$$

In case of the Ø150 mm billet, the diagrams have the shape presented in Figure 4, 5 and 6, also for all the three cooling areas. It can be noticed that in case of the round profile, the cooling programme is changed – taking also into consideration the smaller section of the strand. In this case, for a pressure of 8,2 – 8,6 bar, the flows in the area 1 and 3 have similar values: 41 – 60 l/min and respectively 44 – 73 l/min and they increase for the area 2 at 53 – 84 l/min. The dependence for the analyzed parameters is directly proportional: if the casting speed increases, the flow increases and the cooling water pressure also increases, but slowly.

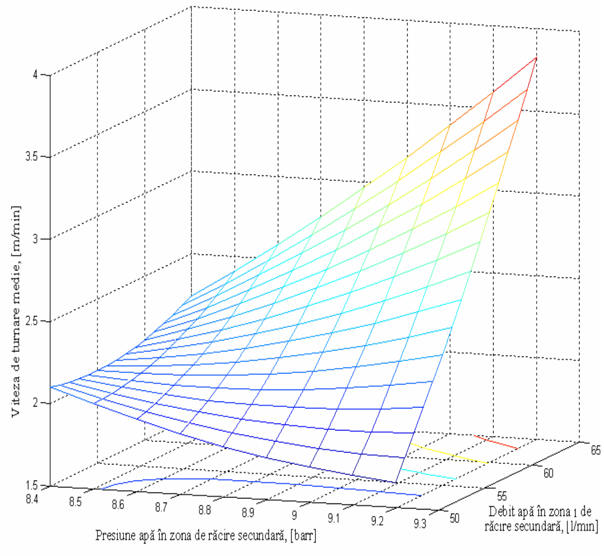

Fig.4 First cooling area for Ø150 mm billet

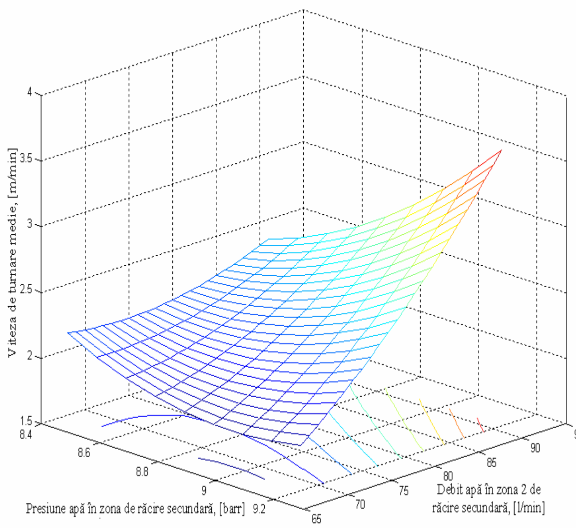

Fig.5 Second cooling area for Ø150 mm billet

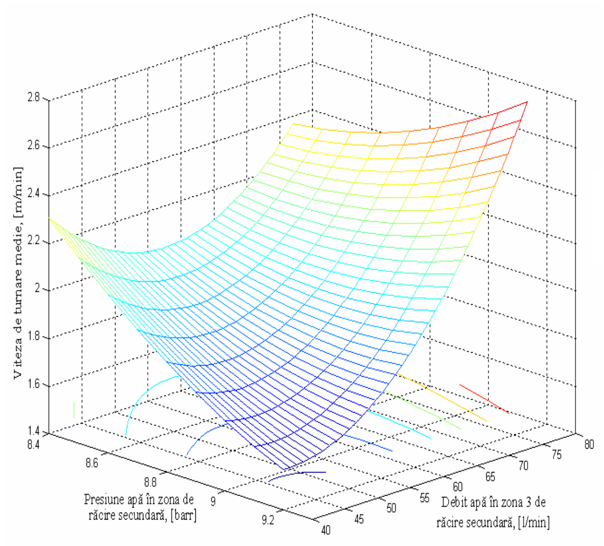

Fig.6 Three cooling area for Ø150 mm billet

For the next three surfaces the global correlation coefficient together with the equation of the regression surface is:

- for Figure 4: the global correlation coefficient: ryx1x2 = 0.7922 and the equation of the regression surface

$$z = 117.4840 - 16.8878*u - 1.6084*v + 0.1694*u.*v + 0.4466*u.^2 + 0.0017*v.^2 \qquad (4)$$

- for Figure 5: the global correlation coefficient: ryx1x2 = 0.7424 and the equation of the regression surface

$$z = 142.0105 - 25.2259*u - 0.8354*v + 0.0833*u.*v + 1.0917*u.^2 + 0.0009*v.^2 \qquad (5)$$

- for Figure 6: the global correlation coefficient: ryx1x2 = 0.5080 and the equation of the regression surface

$$z = 62.8048 - 10.8913*u - 0.4316*v + 0.0388*u.*v + 0.4782*u.^2 + 0.0009*v.^2 \qquad (6)$$

3. CONCLUSIONS

The following conclusions result by analyzing the previously presented data:

- the secondary cooling programme has to be chosen depending on the section of the profile that is to be cast, on the continuously cast steel grade and last, but not least, it has to be correlated with the technological parameters of the casting process. This fact requires in certain cases the correction and the using of another cooling programme, exactly during the casting process, fact that is performed by the process computer;
- for the 240x270 mm profile, the tendency was that of gradually increasing of the colling water flow on the three secondary cooling areas;

- for the 150 mm round, the second area has admitted 30 – 40% higher values in what concerns the cooling water flow comparing to the other two cooling areas;
- the global correlation coefficients have relatively high values, that means a lower dispersion grade and thus the surface equations are possible to be applied with small errors in the industrial practice.

4. REFERENCES

1. ARDELEAN, E., HEPUT, T, ARDELEAN, M. - Turnarea continua a otelului, Editura Politehnica Timisoara, 2001.
2. THOMAS, B.G. - Heat flow model of the continuous slab casting mold, interface and shall, Metallurgical Transactions, 1993.
3. *** Documentatia tehnica a firmei Mannesmann, 1995.

ISIRR 2003

CONSIDERATIONS CONCERNING THE IMPACT OF THERMAL FATIGUE UPON THE HOT ROLLING CYLINDERS

PINCA-BRETOTEAN Camelia*, TOADER Ştefan*
PLEŞA Dorin**

*UNIVERSITY „POLITEHNICA" TIMIŞOARA,
FACULTY OF ENGINEERING HUNEDOARA, ROMÂNIA
** S.C. SIDERURGICA S.A. HUNEDOARA, ROMÂNIA

ABSTRACT:

The paper propose rolling cylinder analysis by Utilization of electronic calculation technique to study the hot rolling cylinders thermal regime is a novelty from scientific and experimental viewpoint.

This research of thermal fatigue strength of hot rolling cylinders is a novelty and it's an original concept in this field and the damage survey of these cylinders is one of the most interesting issues from economical and scientific viewpoint.

KEYWORDS:
thermal fatigue strength, rolling cylinder

1. INTRODUCTION

The research of thermal fatigue strength of hot rolling cylinders is a novelty and it's an original concept in this field and the damage survey of these cylinders is one of the most interesting issues from economical and scientific viewpoint.

Many aspects of the hot rolling thermal regime are still less studied and currently there are no efficient methods to determine and adjust the rolling cylinders temperature.

The purpose of this work is to present few directions concerning the quality improvement of rolling cylinders, aiming the increasing of durability and safety in operation.

The hot rolling cylinders work in composed variable stress conditions, that are due to the rolling process carried-on in a cyclic succession.

Repeating of heating and cooling to each rotation produces cyclic temperature variations both on the surface and in the cylinders' section, causing thermal stresses that exceed in many cases the strength limit of the cylinder's material, leading to specific cracks in the surface layer according to the pictures from fig.1.

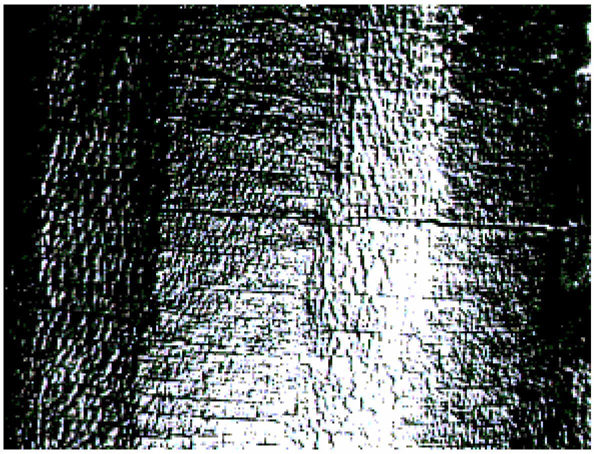

***Fig. 1** The aspect of the caliber surface of a rough rolling cylinder with nuances of circular cracks and longitudinal cracks*

It is known that during the hot rolling process the surface of the work cylinders is heated and cooled periodically at each cylinder's rotation. In fig. 2 is shown the plastic deformation and temperature variation principle diagram on the cylinders surface, resulted from the logical rolling process analysis [1].

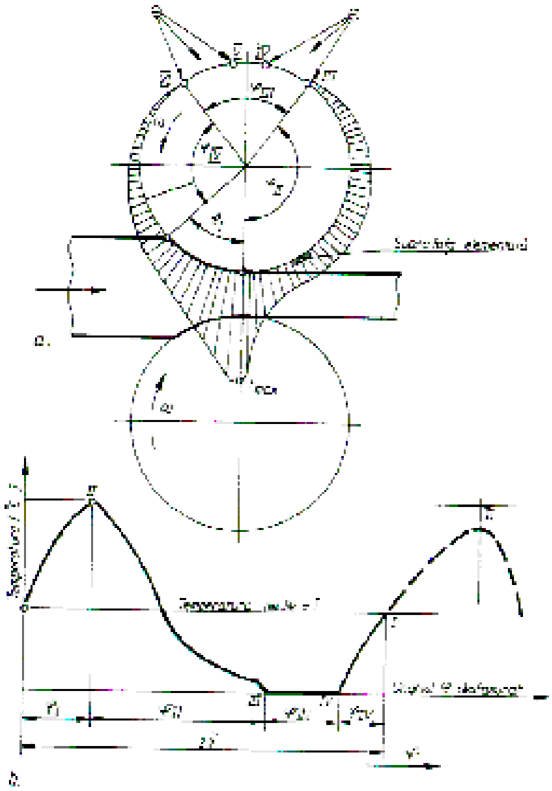

***Fig. 2** The hot rolling process diagram and the temperature variation on the rolling cylinders surface*

2. UTILIZATION OF ELECTRONIC CALCULATION TECHNIQUE AT THE STUDY OF THERMAL REGIME OF THE HOT ROLLING CYLINDERS

The study of hot rolling cylinders thermal regime by electronic calculation technique is a novelty both from scientific and experimental viewpoint. This study has been achieved on an experimental rolling mill, using an installation adapted in this purpose, shown in fig. 3.

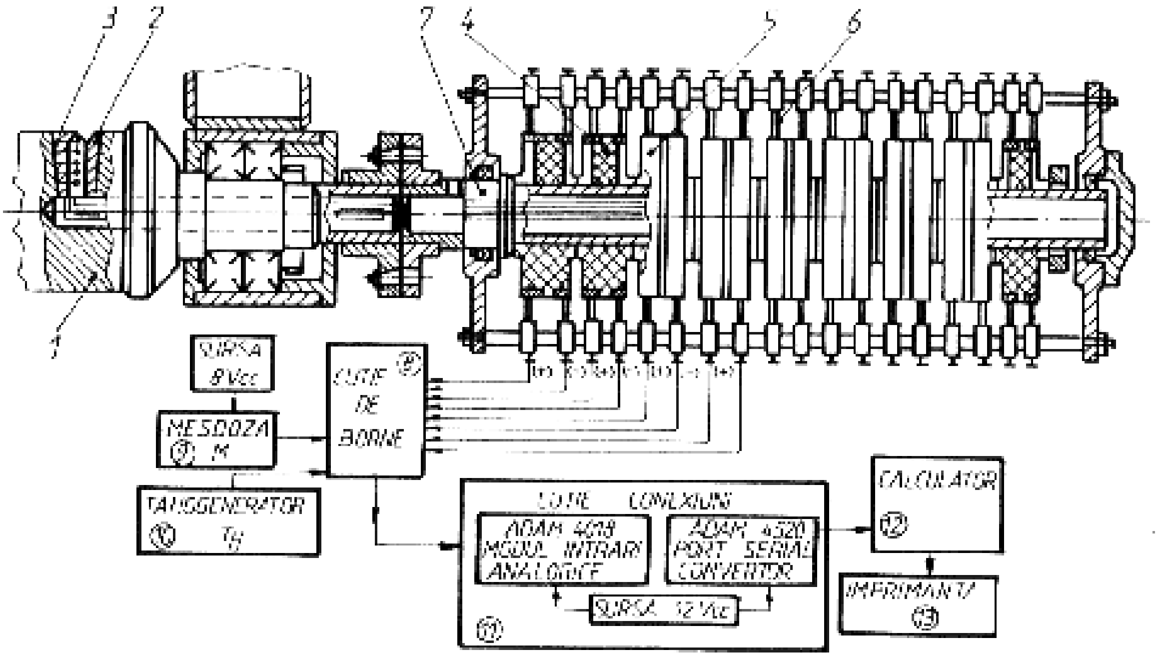

***Fig. 3** Experimental installation for the study of the rolling cylinders thermal regime by electronic calculation technique*

The collecting principle of thermal stresses from cylinder no. 1 has been achieved in classical mode, by the tapered bolt 2, in which were initially implanted the thermocouples 3, connected to the graphite brushes 4, having the copper rings 5 and graphite brushes 6.

The thermal stresses produced by the thermocouples were transmitted through the cables to the terminal box 8, to which were also connected the signals in mV from the dose 9 and tachogenerator 10. By a connection plug, the signals from the terminal box were transmitted in the switch box (fig. 4) with analogue modules of ADAM 11 type and further were undertaken by the electronic calculation system 12 and 13.

From the analysis of the characteristic parameters of more work cylinders from the stands of semis, profiles and wire rolling mills within a steel works company, resulted that, inside the rough stands, the cylinders' rotations number is between n_{1min}=30,2 rot/min and n_{5max}=182,3 rot/min.

Meantime were studied also the middle values from the range of the analyzed rotation number, being established that the most cylinders have rotation speeds between n_2=61,2 rot/min, n_3=87 rot/min and n_4=129 rot/min.

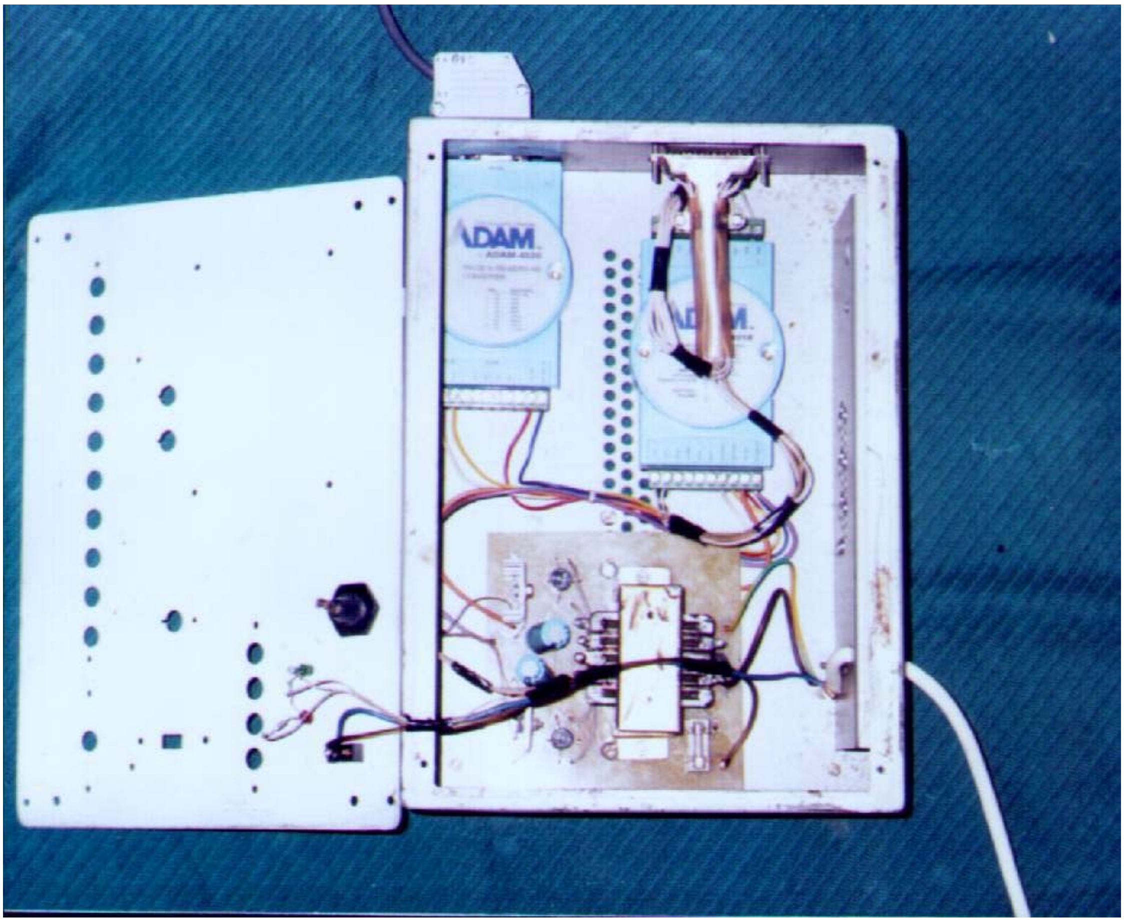

Fig. 4 *The terminal box unit with ADAM-type analogue modules*

Thus, our research on the rolling cylinders thermal regime was performed after five isochrones conditions for which were rolled 50 pcs. of OLC 45 steel bars, having the dimensions of 50x50x300 mm and a rolling temperature of 1150^0C.

In order to obtain measurements of the temperature variations given by bolt-implanted thermocouples was necessary to draw-up a calculation program with the following components:

ADAMTH.CPP file – contains program enter data (“main 0” function). This is interpreting the control line, initializes the acquisition module and reads the data at a given interval by pressing the ESC key (code 27).

ADAM.H file – contains declarations of functions from ADAM.CPP and other types of used data.

ADAM.CPP file – contains functions to initialize and transmit controls, as well as to receive data from the acquisition module.

COMMON.H file – contains declarations for COMMON.CPP module.

COMMON.CPP file – contains functions necessary to display data on the screen.

For the five isochrones experimental conditions were registered five files, for each of them being established the pitch number within a rotation interval of 2π radians, being registered the surface and section temperatures of the cylinders, at depths of Δr = 0.2; 1.5; 3; 6 mm, as well as the related rotation number n[rot/min] and rolling forces F[kN].

Table 1 *Extract from file IV for experimental rolling with n = 129 rot/min*

No.crt./division		V_0=TC_1 Δr = 0,2mm	V_1=TC_5 Δr = 1,5mm	V_2=TC_2 Δr = 3mm	V_3=TC_3 Δr = 6mm	n [rot/min]	Dose F[kN]
	0	1	2	3	4	5	6
0	0,00	115,6	82,3	70,5	65,2	131	11
1	1,00	169,3	88,6	73,4	68,4	129,2	11,7
2	2,00	315,5	102,9	75,4	69,4	129,7	11,8
3	3,00	372,9	119,5	78,4	70,9	129,9	11,8
4	4,00	386	139,7	80,1	73,4	129,5	11,9
5	5,00	388,6	164,5	84,3	76,6	130,1	12
6	6,00	370	178,2	95,7	79,4	131,2	11,9
7	7,00	320,2	187,7	104,5	80,5	129,3	11,9
8	8,00	271,8	190,4	110,4	86,2	129,1	11,9
9	9,00	240,5	199,3	114,6	90,2	128,7	12
10	10,00	230,2	206,7	123,3	99,6	128,5	12
11	11,00	216,4	210,2	127,6	105,3	128,2	11,9
12	12,00	214,1	206,9	130,1	112,2	128	12
13	13,00	210,5	202,7	133,7	115,1	128,3	12
14	14,00	209,1	198,5	134,4	120,3	128,5	12
15	15,00	203,4	186,7	135,5	124,6	129	12,1
16	16,00	194,7	183,5	129,4	125,3	129,3	12,1
17	17,00	186,1	177,6	119,4	120,4	129,4	12
18	18,00	177,3	172,5	113,3	115,5	129	12,1
19	19,00	165,9	166,4	110,5	109,2	128,6	11,9
20	20,00	163,8	163,2	107,1	106,5	128,5	11,9
21	21,00	159,8	158,6	106,3	102,4	128,7	11,9
22	22,00	156,1	151,3	103,9	92,3	128,9	12
23	23,00	151,4	147,5	102,2	83,4	129,3	11,9
24	24,00	148,7	142,8	100,8	72,6	129,2	11,9
25	25,00	147,2	137,3	94	72	128,7	11,9
26	26,00	146,1	132,1	88	71,6	128,6	12
27	27,00	139,2	129,3	84,6	72,1	128,9	12

In table 1 is shown the file IV obtained at the experimental rolling with n = 129 rot/min and in fig. 5 is shown the diagram of rolling cylinders temperature variation, resulted from the experimental rolling with n = 129 rot/min.

From a careful analysis of the five isochrones diagrams of registered temperatures, the maximum temperature variations on the cylinders surface and in section are produced at low rolling speeds. For example, in the diagram achieved with n = 30.6 rot/min the maximum temperature was 481^0C. Also in this diagram we can see high temperature values also in the cylinders section, at depths of Δr = 1.5; 3; 6 mm respectively. The peaks of temperature variation curves have a certain horizontal movement, this being the heat transfer time in cylinder's section depth. Characteristic to the temperature variation curves is also the fact that at relatively low speeds, in the area of cylinder's cooling water jets angles, the temperature on the cylinder surface decreases substantially, being lower than the temperature of the superficial layer at the depth of Δr = 1.5 mm.

But this situation is not appearing anymore at high rolling speeds, when the rotation number exceeds the value of n = 129 rot/min, the curves Δr = 0.2 mm and Δr = 1.5 mm are almost tangent and when n = 182.3 rot/min, these curves stay spread and the sub-cooling phenomenon of the cylinder's surface is not appearing anymore.

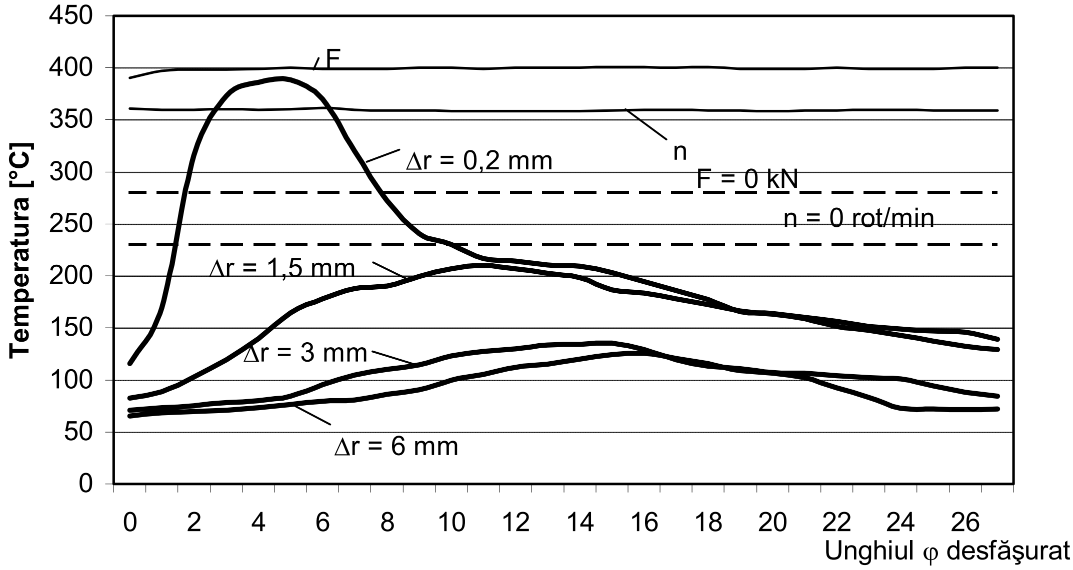

Fig. 6 *The diagram of rolling cylinders temperature variation, resulted further the experimental rolling with n = 129 rot/min.*

3.CONCLUSIONS

The thermal fatigue phenomenon of the hot rolling cylinders is produced more deeply at low rolling speeds, when the circular and longitudinal cracks network is pronounced.

Utilization of electronic calculation technique to study the hot rolling cylinders thermal regime is a novelty from scientific and experimental viewpoint.

BIBLIOGRAPHY

1. TOADER ŞT., BRETOTEAN C. – *Research upon thermal fatigue strength of hot rolling cylinders*, Scientific research contract, Bucharest, 1996.
2. PLEŞA D. - *Research concerning the hot rolling process temperature variation on rolling cylinders*, Ph. D. Work, Petrosani, 2002.

ISIRR 2003

A VANE ANALYSIS BY FINITE ELEMENT METHOD

Prof. univ. dr.eur. eng. Tiberiu Stefan Mănescu
Prof. univ. dr. eng.Viorel Câmpian
Conf. univ. dr. eng. Dorian Nedelcu
Ş.l. dr. eng. Camelia Bretotean – Pinca

"Eftimie Murgu" University Reşiţa, Romania

Abstract: *The paper propose a vane analysis by the finite element method, from mechanical conduct point of sight, as response to exterior forces action. The analysis will be made using a projection and assisted by calculator analysis program: Microstation Modeler – for 3D model generation and COSMOS/DesignSTAR – for analysis by the finite element method.*

Key words: vane, finite element, deformations, tension state.

1. INTRODUCTION

The vane has 1620 kg, disc diameter of 1470 mm and is made of T20Mn14N material, fig. 1, having the next characteristics: $R_{p0,2}$ = 295 N/mm^2, R_m = 600 N/mm^2, A_5 = 18 %, Z = 25 % respective $KCU_{300/2}$ = 49 J/cm^2.

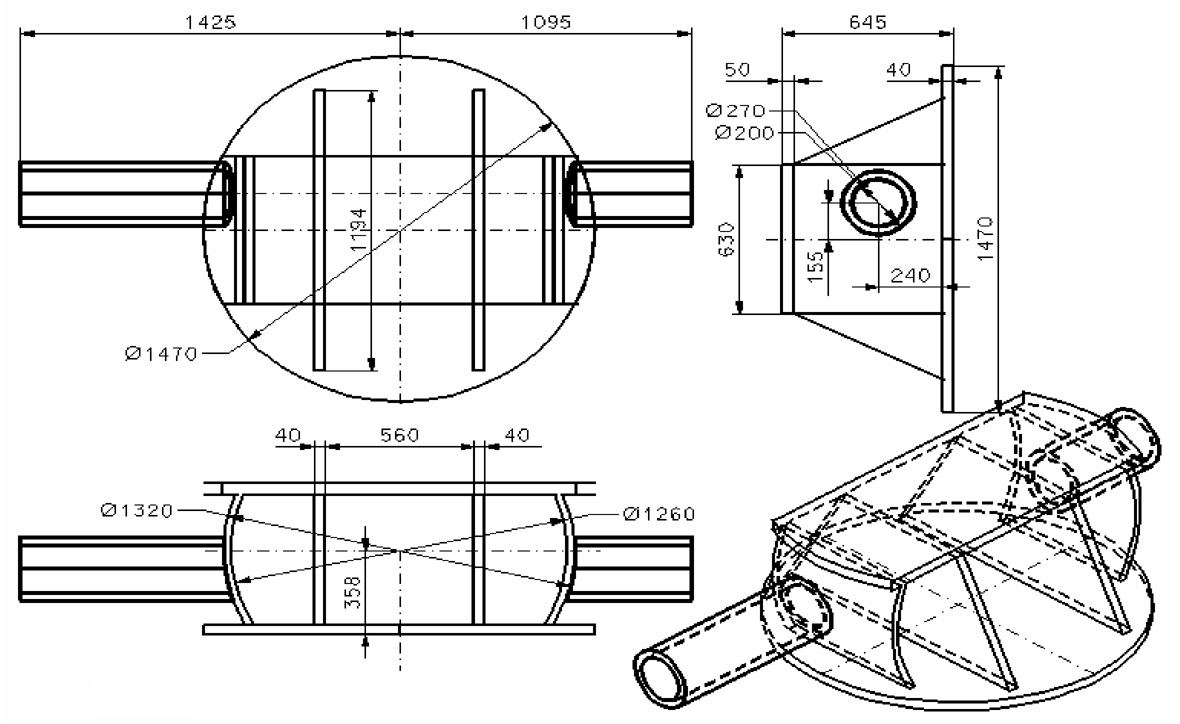

Fig.1. *The vane's structural description*

2. WORK METHODOLOGIE

The piece was modeled 3D by Microstation Modeler, fig. 1 and exported in Parasolid format to the finite element analysis program finit COSMOS/DesignSTAR, version 3.0/2001, fig. 2, having available the next analysis types:

- static linear and nonlinear analysis;
- modal: own frequencies and vibrating modes;
- buckling calculus;
- linear and nonlinear heat transfer in permanent and transitory regime;
- fluids flowing;
- electromagnetic analyze.

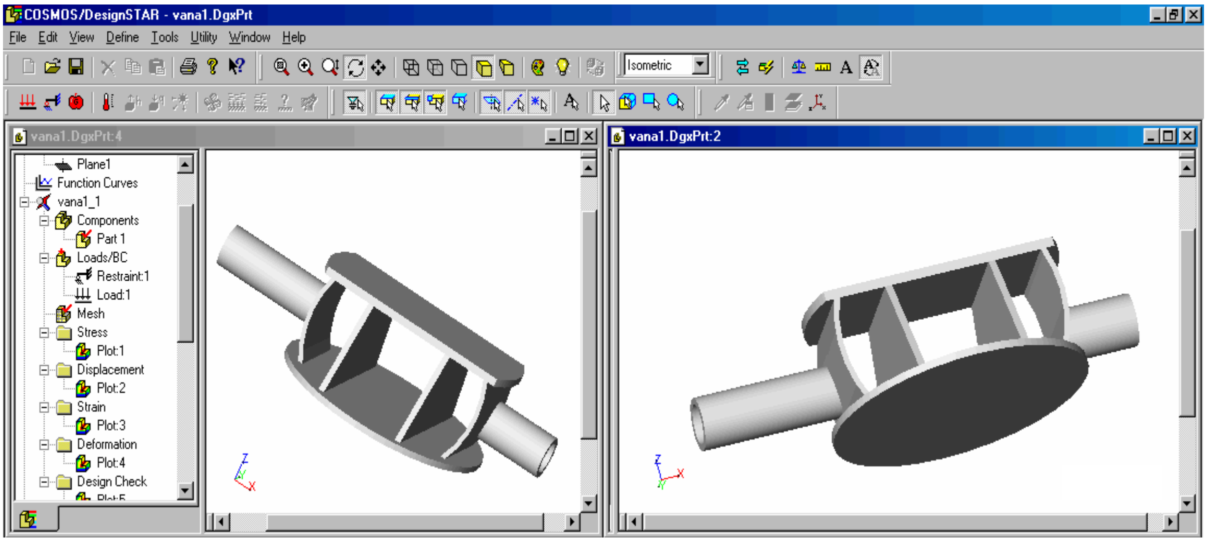

Fig.2. *The vane's geometrical model*

In the present paper it will be made a static linear analyze, having the followings periods:

- *3D model import* –3D generation vane was realized by Microstation Modeler, an assisted by calculator analysis program projection, what offers strog posibilities of geometric modulation.
- *Defining study of case* – part from which are defined analyze characteristics (the name, the type of the analyze: static linear and discretisation type, respective **Solid** (for moderated parts through solids) or **Shell** (for moderated parts trough surfaces); for vane model was chosen discretisation of type **Solid**;
- *defining material* – materials can be selected from the library of materials, provided with the program (fig. 3), which includes materials organized on categories: steel, iron, aluminum, copper, etc., each

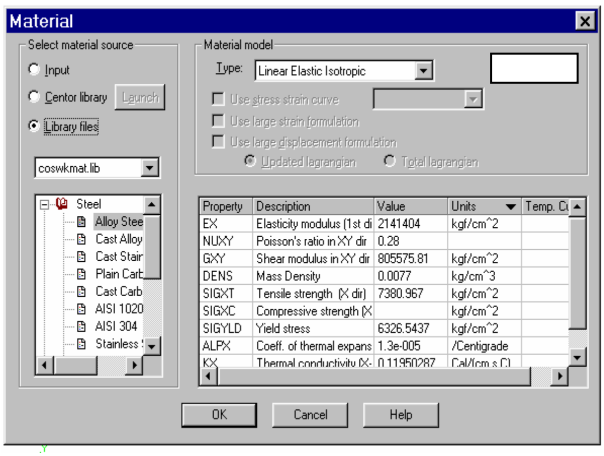

Fig.3. *The library of materials, provided with the program*

category containing a set of materials with predefined proprieties. Can be made usual operations: to create categories, to

❑ introduce new materials, to modify the existing ones, to rename, to erase, etc.; from the library of materials was selected a steel having the modulus of elasticity E = 2141404 Kgf/cm^2 and the value of the Poisson's coefficient □ = 0,28;

❑ *defining loadings* – the applicable types of loadings are:

- "<u>Force</u>" – allows to apply a total force on one or many selected entities: vertex, edge or face;
- "<u>Torque</u>" – allows to apply a torsional moment on one or many selected faces;
- "<u>Moment</u>" – allows to apply a moment on one or many selected entities: vertex, edge or face;
- "<u>Uniform pressure</u>" – allows to apply a distributed pressure on the selected face.

The applying direction of the loading can be normal or directional, by the specification of the components value on the 3 axes, and for every type of loading can be selected the measure unit.

The piece is embed on cylindrical surfaces, and over the circular disc is applied a uniform distributed pressure, having the value of 1x10^6 N/m^2, fig. 4;

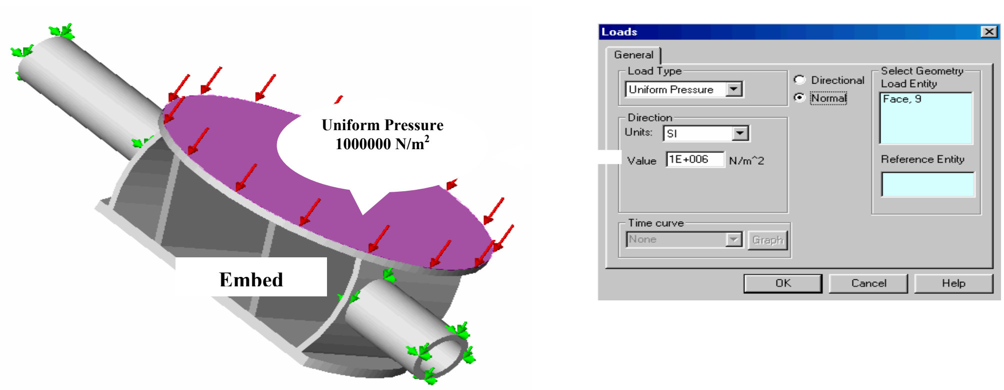

Fig.4. *The calculation model of the vane*

❑ *model discretisation* – COSMOS/DesignSTAR offers the possibility to automatic generation of the discretisation, initially proposing a global digital quantity of discretisation, calculated in function of model volume, its surface and information of geometrical type; the discretisation size (number of nods and elements) are depending of the model geometry and dimensions, of the selected quality: caddish - "*Draft*" or fine - "*High*" , tolerations, the imposed discretisation type and specifications referring to contact. Therewith, DesignSTAR permits local specification by the user of the element sizes, having different value from the global one, at the side of the vertexes, edges and faces, for a precise discretisation of the delicate zones from geometrical point of view "*User-defined Mesh Control*".

The discretisation with elements of "*solid*" type, offers two alternatives:

• "<u>draft quality mesh</u>" – by solid linear tetrahedral elements generation, defined by 4 nods connected by 6 linear edges;

• "<u>high quality mesh</u>" – by solid parabolic tetrahedral elements generation, defined by 4 nods, 6 median semi nods, respective 6 edges.

• The discretisation control offers 3 possibilities:

• "<u>Automatic Transition</u>" – impose appliance of details, holes, geometrical sections of small dimension compared with the whole model discretisation; it is recommended to deactivate this option to large models discretisation, having a lot of small geometrical dimensions portions, to avoid the generation of a useless number of finite elements;

• "<u>User Defined Controls</u>" – when this option is activated, the program applies the discretisation specifications over all explicit by the user defined zones (vertex, edges, faces), others than the ones resulted from the global discretisation applied in the left-over of the model.

• "<u>Smooth Surface</u>" – activating this option, the program refines discretisation, in reallocating frontier nods, to improve the initial discretisation quality.

For the analyzed model was generated 10205 finite elements with 20366 nods,

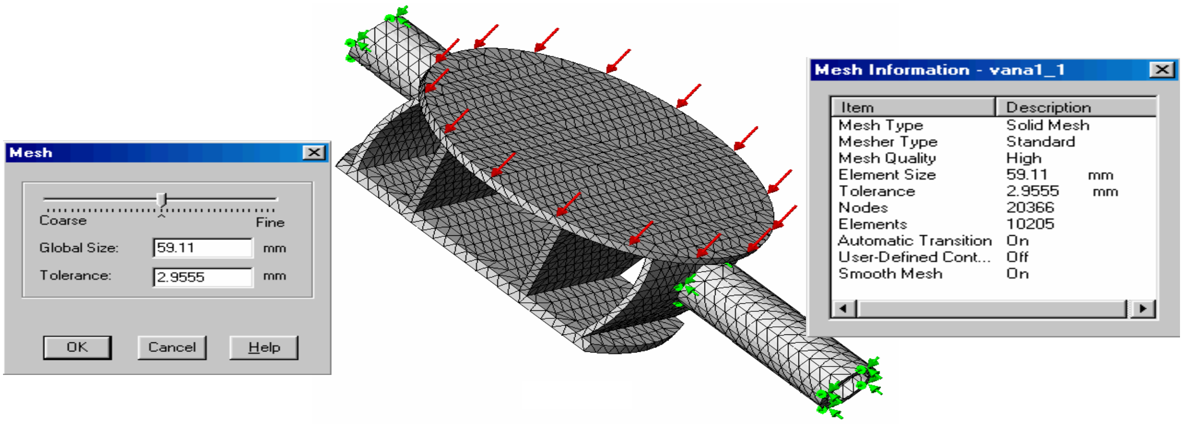

Fig.5. *The discretization for the analyzed model*

❑ *analyze calculus* – for the anterior defined conditions and on a calculator having an updated configuration, the calculus did not presented any problems from the consumed time point of view;

❑ *visualizing results* – COSMOS/Design Star offers strong instruments for the results visualization on graphical form (color maps and diagrams) respective numerical value: tensions and stresses, displacements, deformations, relative verification having imposed admissibility criterions

3. RESULTS

The color map corresponding to deformations is presented in fig. 6. The maximal resultant displacement is 3.441 mm, and the displacement zone is bigger than 2.7 mm, being presented in fig. 7, where we can observe the displacement asymmetry generated by the asymmetrical disposal of the cylinders.

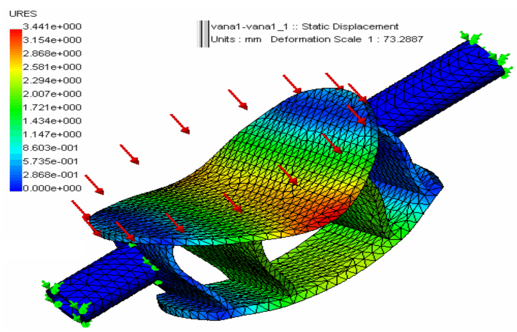

Fig.6. *Deformation of the vane*

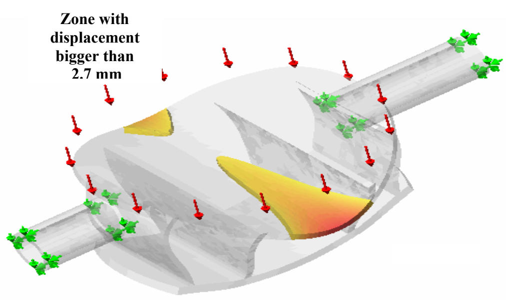

Fig.7*. Zone with displacement bigger than 2,7 mm*

The displacement variation in the long of the piece is numerical presented in fig. 8, and graphical in fig. 9. The maximal displacement zone is positioned on the central portion of the disc, opposed to the cylinders, fig. 10.

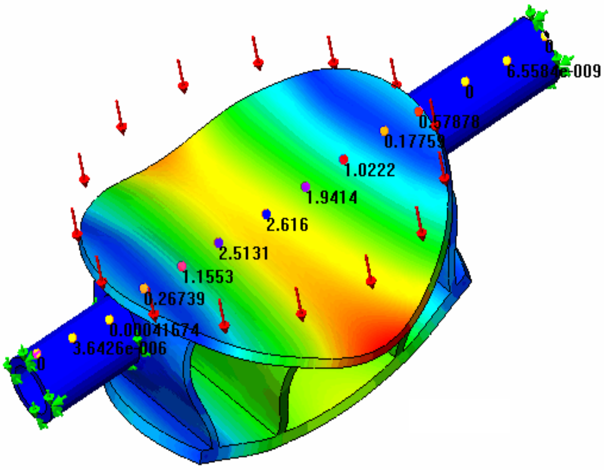

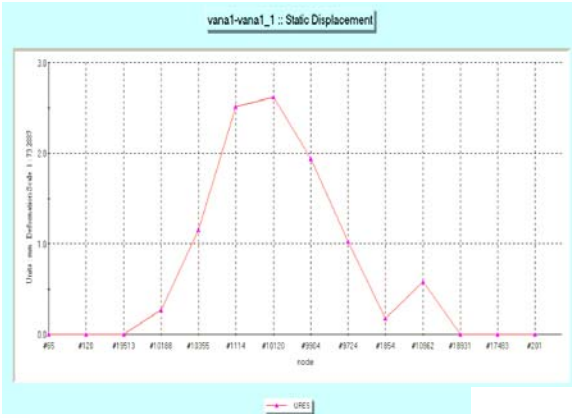

Fig.8*. The displacement variation in long of the vane*

Fig.9*. The graphical displacement the variation*

The corresponding color map to the Von Mises tension is presented in fig. 11; the tension variation in the long of the piece is presented numerical in fig. 11, and graphical in fig. 12. The maximal tension is 400 Mpa.

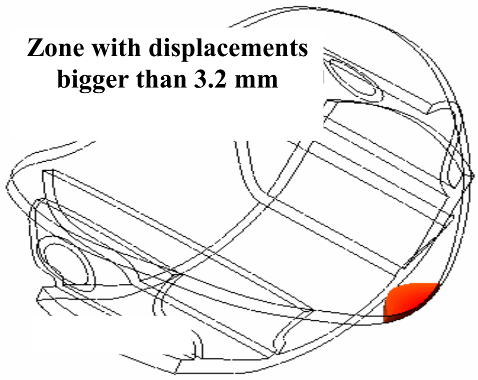

Fig.10. *Zone with displacements bigger than 3.2 mm*

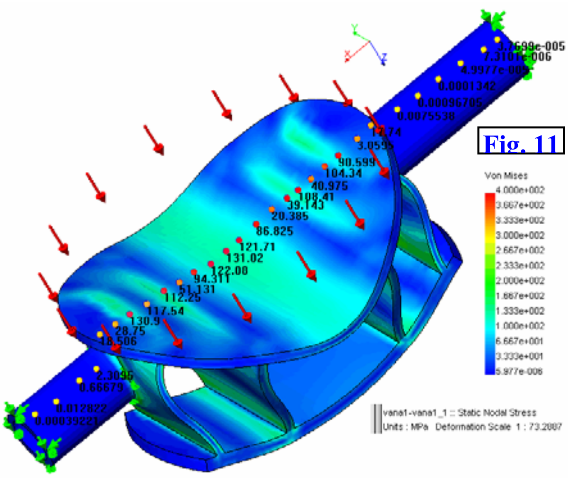

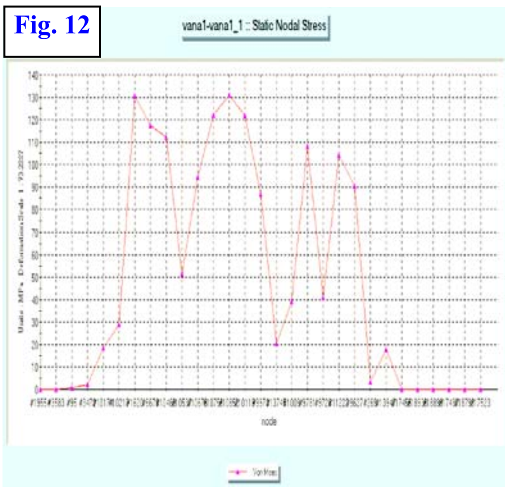

Fig.11*. The tension variation in long of the vane*

Fig 12. *The graphical tension variation*

Fig. 13, a,b,c presents tension zone having a bigger value than 135 MPa, 200 MPa respective 250 MPa, resulting the substantial reduce of the zone with tension increment and their localization to the superior part of the lateral ribs. The maximal value for the tension of 400 MPa generated by the program can be considered as a local value, applied on a very reduced zone, similar to the effect of a local concentrator.

The calculus was relapsed for the same piece, on which was modified the thickness of the two central vertical ribs, from 40 mm to 50 mm. In these conditions, the maximal displacement was reduced to 2.882 mm, and the Von Mises tension to 354 MPa.

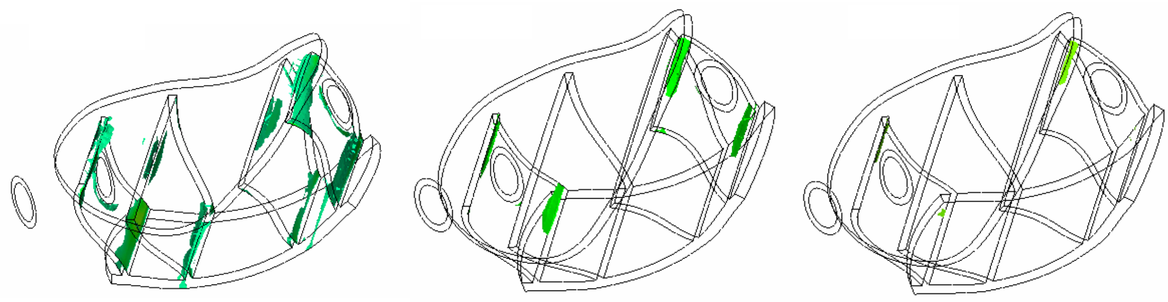

a b c

Fig.13. *The maximal value for the tension:*
a) Zone with tensions bigger than 135 MPa; b) Zone with tensions bigger than 200 MPa; c)Zone with tensions bigger than 250 MPa

4. CONCLUSIONS

The paper exemplifies the obtained results by the method of finite element over a vane, using both programs Microstation Modeler and COSMOS/Design Star. The analyze results are presented graphical and numerical, with the prominence of the sensitive zone, from deformations and tension point of view. Also analyze a variant of the vane, generated by the increasing the thickness of the two central ribs.

The modeling of piece behavior by the method of finite element offers digital and qualitatively results, which allow the knowledge of mechanical behavior of the piece and the analyze of the possible variants, offering in this way to the engineer a projecting instrument especially efficient.

Bibliography

1. MĂNESCU, T. – *Analiza deformaţiilor ce apar la obturatoare de tip vană fluture biplană*, Analele Universităţii Eftimie Murgu Reşiţa, 2002.

2. BOLEANŢU, L., MĂNESCU, T. – *Aspecte referitoare la calculul tensiunilor şi deformaţiilor clapetei vană fluture biplane, în regim static de acţionare*, Construcţia de Maşini, Nr. 3, Bucureşti, 1981.

3. NEDELCU, D. - *Cosmos/Design Star, analiza funcţională a structurilor*, Rev. T & T- Tehnică şi Tehnologie, Bucureşti, ISSN 1453 8423, Nr. 3/2002.

4. NEDELCU D. – *Proiectarea asistata de calculator prin Microstation*, Editura EUROSTAMPA, Aprilie, Timisoara, 2001, ISBN 973-8244-03-X

RESEARCH AND EXPERIMENTS REGARDING THE STRUCTURE IMPROVEMENT OF STEEL INGOTS

Ana Virginia SOCALICI

Universitatea POLITEHNICA TIMIŞOARA, Facultatea de Inginerie HUNEDOARA

ABSTRACT

The paper present the experiment made with the purpose of improving the structure of steel ingots undergoing smiting by adding microcoolers in the central part of the liquid ingot, to create a new crystallization and solidifying front. Application of this technology allowed the substantial increase in the homogeneity and spreading degree of the dendrite structure, the decrease in the stretch and width of the chemical in homogenates development area and that of the air holes placed at the edge of the primary grains, the reduction of segregation and gas content. It has also been ascertained the increase in the plasticity characteristics of the metallic material (at the same resistance) with 30-50%.

***KEYWORDS**: steel, ingot, microcoolers, improvement, characteristics.*

1. INTRODUCTION

The solidifying of steel ingots is associated with important contractions, independent of the purity degree, fact that leads to a certain deterioration of the structure and the appearance of chemical and structural in homogeneity. The mechanism of the solidifying process in these ingots is determined a great degree by thermal phenomena that occur while transmitting the heat from the liquid steel to the environment [1]. These phenomena depend especially on the ratio between the ingot volume and surface, ratio that adjust the speed of heat evacuation from the liquid steel.

The problem that has to be saved to attenuate the deficiencies of classic solidifying is the adaptation of the efficient method of heat evacuation from the solidifying steel. An efficient influent technology upon the solidifying process consists of introduction in the liquid ally of the microcollers [2].

2. EXPERIMENTAL RESULTS

The researches concerning the possibilities of leading the solidifying process have been done on industrial charges of OLC 45 steel on this purpose it has been experimented the introduction in the cast-iron, of different types of microcoolers.

This, it has been administered grains obtained by cutting rolled wire of the same brand as the casted iron. The effect of the microcoolers has been studied in many versions depending on wire diameter and quantity added, at each version with grains experimenting on 20 ingots studied in parallel with ingots of the same charge casted classically.

According to the data from the specialty literature and the results of preliminary trials, it has been established as best the experimenting with the following quantities of added microcoolers: 2-4kg/t with diameters 2-6 mm. The introduction of grains in the cast-iron has been administered in filling percents of 30%, 60% and 90%. In order to study the behaving of the microcoolers in the melted mass there have been introduced wire bands of the mentioned diameters, studying after solidifying their influence on the local solidifying phenomena and the manner of orientation of the solidifying front the melting-time difference (for bars 4 – 5 sec, for grains 3 sec, both from 6 mm wire) is determined by the fact that the specific surface of heat absorption is much bigger for grains than bars.

From these presented above it results that low-diameter grains will melt in a shorter time, which means that in all experimented versions the grains reached the liquid phase. This phenomenon allows a chemical homogenization and in the same time produces a local deep-freezing, accelerating the crystallization process.

To clarify the real behaving of microcoolers in the mass of liquid steel undergoing solidifying, it has been experimented the introduction in probe moulds of microcoolers in the form of bars of steel wire of 3,5 mm ϕ, the same time with the casting in the moulds of witness ingots. Following the macro and microscopic analysis of taken samples it has been noticed that on a certain area around the microcooler finer crystals have been formed, which shoos that in this region the deep-freezing was more intense (fig. 1).

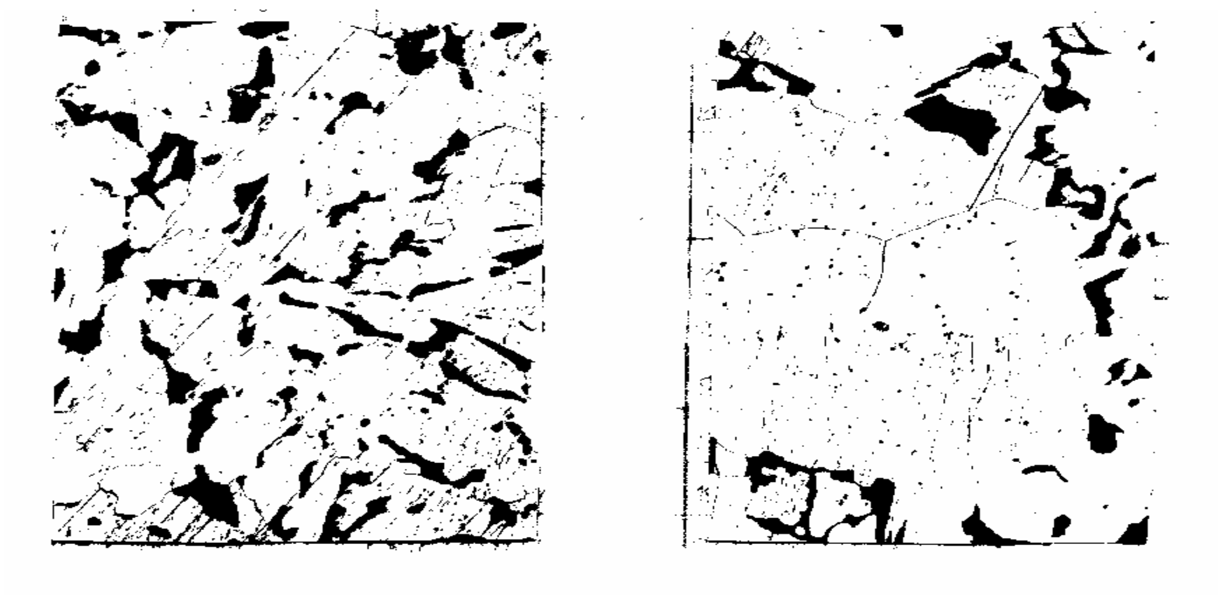

a. b.

Fig. 1. Sample microstructure:
a – with microcoolers; b – without microcoolers.

The ingots casted this was underwent smiting and from the resulted semiproducts samples have been taken to determine their mechanical characteristics. After the microscope study of metallographic samples collected, there was noticed that in the ingots with added microcoolers a grain refinement is obtained, which leads to chemical homogeneity (fig. 2). There is also obtained an increase in metal extraction, of about 90% in grains-casted ingots compared to 82% in the classical casted ones.

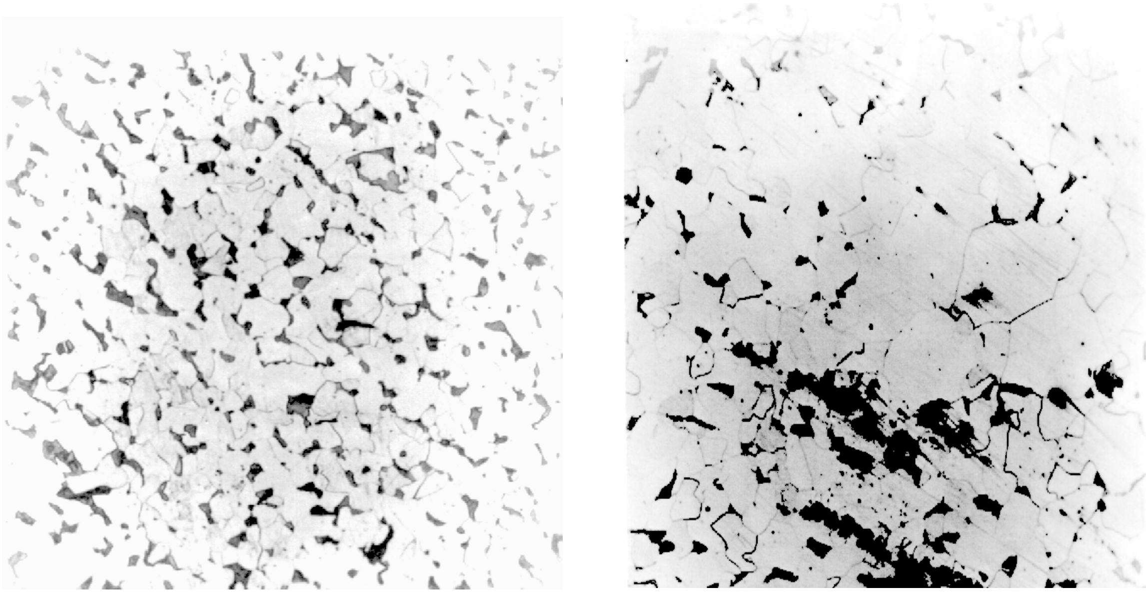

a. b.

Fig. 2. Microstructure:
a – with microcoolers; b – without microcoolers.

The charges have been studied on in the manufacturing flow, samples being taken from each ingot to determine the comparative physic-mechanical properties between the steel classically casted and that with microcoolers. It is noticed an increase in the resistance properties and the plasticity represented by stretching and striction is increased by 20%. Therefore the increase in the plasticity properties is determined by the effect of the microcoolers on the structure in the solidifying phase by stopping the formation of gross-dendrites and the formation still from this phase of a finer structure.

The data concerning the mechanical trials have been processed using the MATLAB and SIDHD 5 program and the results obtained showed in figures 3, 4, 5, and 6.

Equation of regression surface is:

$R_{p0,2} = 3{,}578 \cdot m^3 + 0{,}231 \cdot d^3 + 0{,}908 \cdot m^2d - 0{,}541 \cdot md^2 - 25{,}903 \cdot m^2 - 8{,}868 \cdot d^2 + 5{,}806 \cdot md + 85{,}360 \cdot m - 22{,}75 \cdot d + 391{,}137$

$R_m = -0{,}407 \cdot m^3 + 0{,}998 \cdot d^3 + 0{,}336 \cdot m^2d - 0{,}055 \cdot md^2 - 5{,}351 \cdot m^2 - 7{,}8 \cdot d^2 + 0{,}033 \cdot md + 61{,}6 \cdot m + 4{,}97 \cdot d + 599{,}10$

$A_5 = 0{,}230 \cdot m^3 + 0{,}220 \cdot d^3 - 0{,}032 \cdot m^2d + 0{,}041 \cdot md^2 - 2{,}789 \cdot m^2 - 1{,}22 \cdot d^2 - 0{,}379 \cdot md + 12{,}650 \cdot m + 1{,}88 \cdot d + 19{,}828$

$Z = 0{,}602 \cdot m^3 + 0{,}415 \cdot d^3 - 0{,}029 \cdot m^2d - 0{,}013 \cdot md^2 - 6{,}822 \cdot m^2 - 2{,}06 \cdot d^2 + 0{,}0198 \cdot md + 24{,}720 \cdot m + 0{,}757 \cdot d + 43{,}709$

$R_{p0,2}$, R_m, A_5, and Z - mechanical characteristics;
m – specific quantity of microcoolers;
d – diametre of microcoolers.

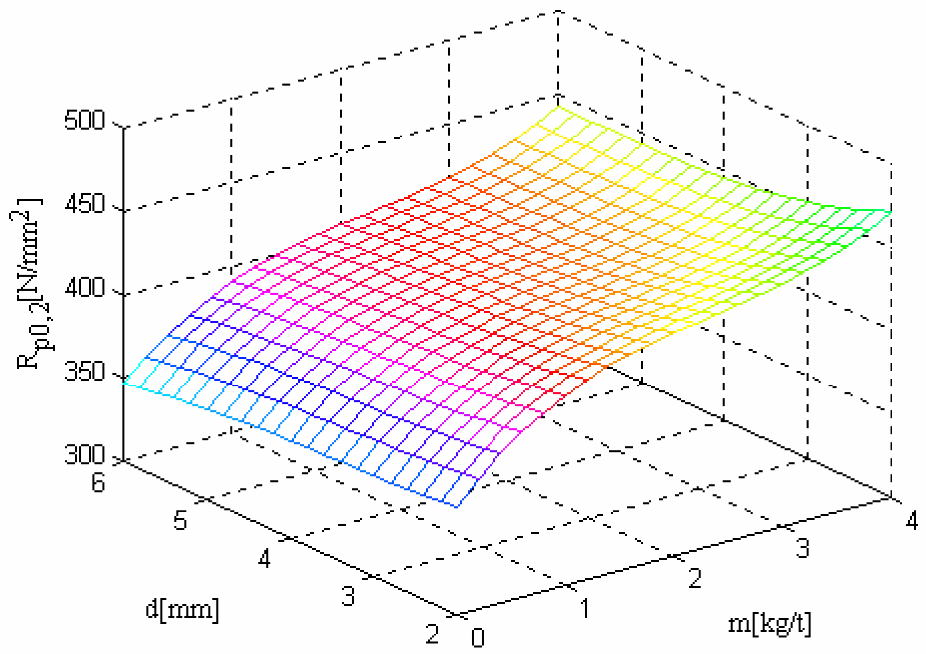

Fig. 3. Regression surface $R_{p0,2}$.

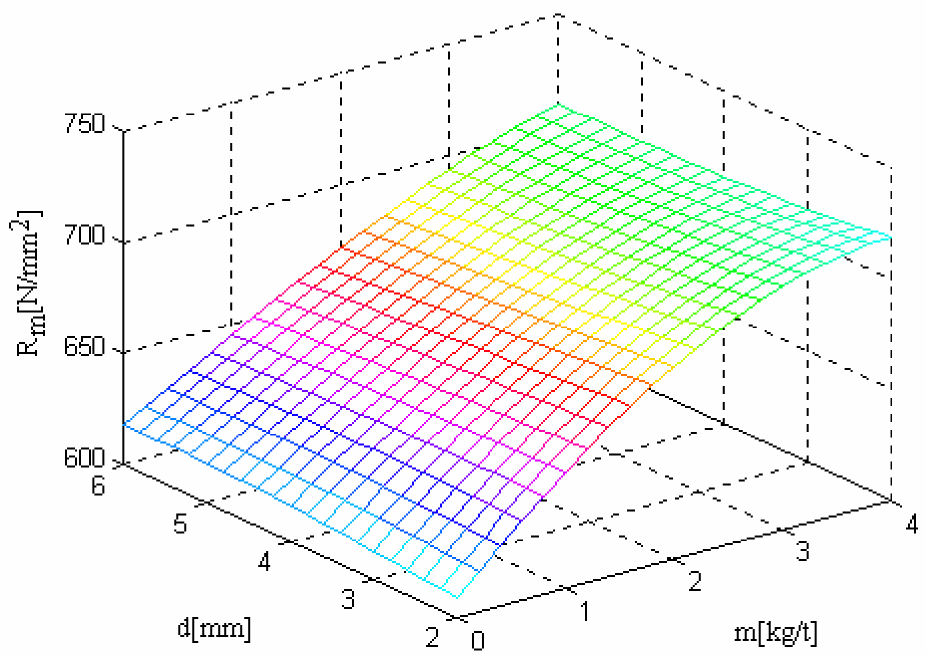

Fig. 4. Regression surface R_m.

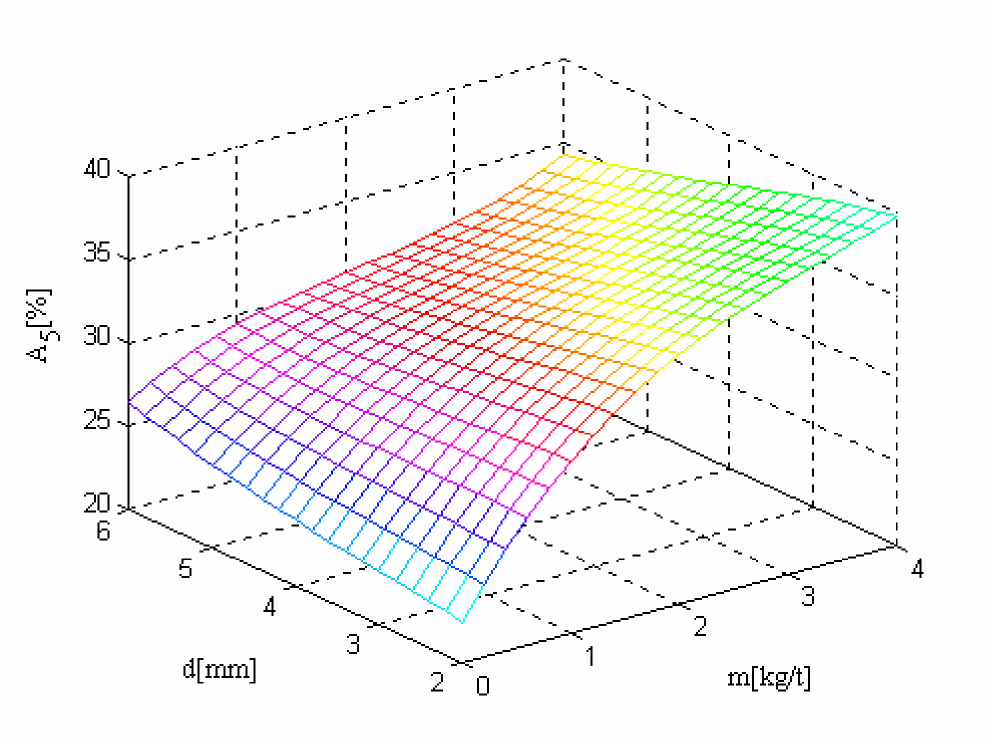

Fig. 5. Regression surface A_5.

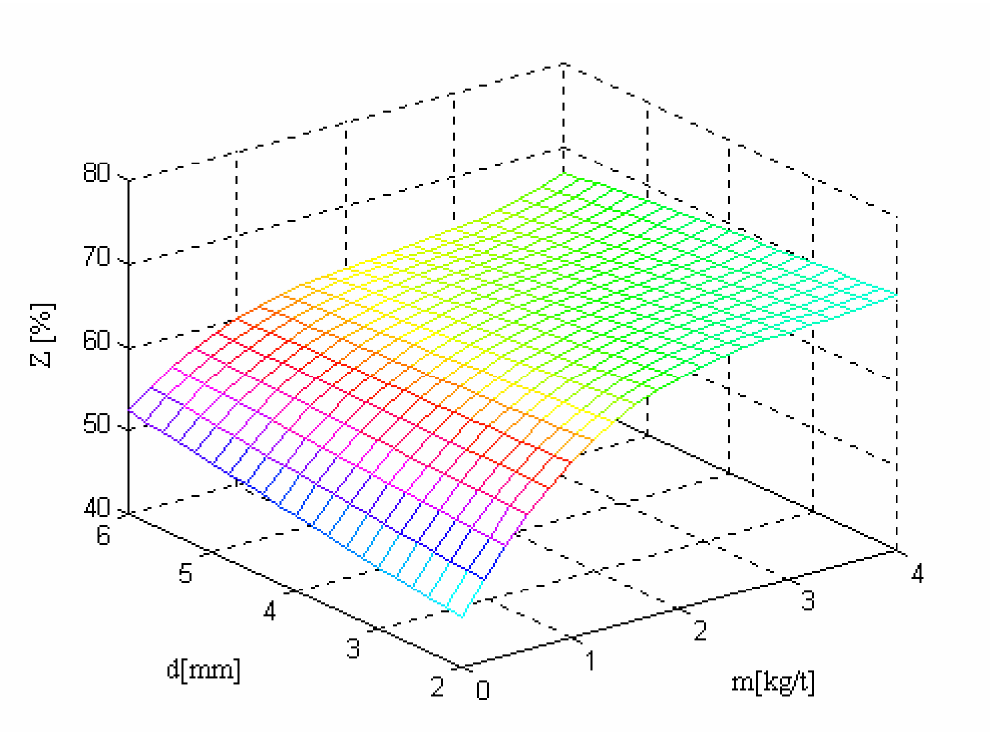

Fig. 6. Regression surface Z.

It has been remarked, after studying the curves variations for the determined mechanical characteristics, a certain increase in all mechanical ($R_{p0,2}$, R_m, A_5, and Z) characteristics and a significant homogeneity of their values.

3. CONCLUSIONS

Following these experiments, the following conclusions have been drawn:

- the modification of marginal air holes zone meaning their migration to the interior of the ingot;
- the microblisters from the head of the ingot stretch on a smaller surface compared to the classically casted ones;
- it has been obtained a flattening of the blisters format in the ingots casted with microcoolers and the reduction, this way, of their volume, resulting in a substantial increase of metal extraction, this effect of increase being proved to be direct proportional with the reduction of casting temperature and the increase in the quantity of added microcoolers;
- it has also been obtained a reduction of the temperature gradient in the steel crystallization interval of 1,5 – 2 times and a more rapid uniformization of it on the ingot's cross-section;
- a substantial increase in the structural homogeneity and the qualitative properties represented by resistance and plasticity;
- a refinement of the casting structure;
- an increase in extraction, an average of 88 – 90%.

4. REFERENCES

1. Efimov, V.A. – Steel casting and cristalisation, Ed.Tehnică, Bucureşti, 1976.
2. Bratu, C., Sofroni, L. – Researches concerning leading steel proces of cristalisation using microcoolers, Metalurgia, Nr.6, 1981, pag.281.
3. Ilca, I., Socalici, A. - Researches on leading the ingot solidification of steel for forging, Buletinul Ştiinţific al U.P.T. Tom 42(56), Fascicola 2, Timişoara, 1997, pag. 226.
4. Ilca, I., Socalici, A. - Research on the Quality Improvement of Some Forged Pieces, Buletinul Ştiinţific al U.P.T. Tom 45(59), Fascicola 2, Timişoara, 2000, pag. 299.
5. Ilca, I., Socalici, A. – Micro-cooler Used In Improving The Quality Of Large Ingots Meant For Forging, Buletinul Ştiinţific al U.P.T. Tom 46(60), Fascicola 2, Timişoara, 2001, pag. 147.

SOFTWARE FOR THE OPTIMISATION OF THE CUTTING APPARATUS KINEMATICAL PARAMETERS FOR AGRICULTURAL HARVESTING MACHINES

BIRIŞ Sorin-Ştefan[1]
VLĂDUŢ Valentin[2], BUNGESCU Sorin-Tiberiu[3]

[1]„Politehnica” University of Bucharest
[2]I.N.M.A. Bucharest, [3]U.S.A.M.V.B Timişoara

Abstract:

In this paper it is presented a specialized software written in AutoLISP language, for the optimisation of the cutting apparatus kinematical parameters which, on the basis of some improved mathematical models, allows the analytical plotting of these trajectories in a very short time and with maximum precision, making possible the easy optimisation of some kinematical parameters of the working process, as: the machine rate of travel (travel speed), the bladed-rotor rotation speed or the operating crank rotation speed.

Keywords:
software, optimisation, cutting apparatus, kinematical parameter, agricultural harvesting machines, AutoLISP

1. INTRODUCTION

For the optimisation of the cutting apparatus kinematical parameters first it is necessary the parameterised generating on the basis of same constructive and functional parameters, the blades trajectories focussing the areas no covered by knives or the overlapping areas.

The trajectories of the cutting blades represent, for the straight reciprocating motion apparatus, the result of composing two translation motions (on due to the agricultural machine displacement and another one due to the straight reciprocating motion of the blades driven by a "reciprocating rod-crank" - type mechanism). For rotary apparatus the trajectories are of cycloid-shaped, resulting from the composing of two motions a translation one (due to the agricultural machine displacement) and a rotational one (due to the rotary motion of the cutting blade on the horizontal plane).

For the optimisation of some kinematical parameters of the cutting apparatus, as: the machine rate of travel (travel speed), the bladed-rotor rotary speed or the operating crank rotary speed, in this paper is presented an AutoLISP software, which allows the analytical plotting of the blade trajectories with maximum precision.

2. THE CUTTING DIAGRAM GENERATION FOR THE STRAIGHT RECIPROCATING MOTION CUTTING APPARATUS FOR HARVESTER MACHINE

The straight reciprocating motion cutting apparatus can be with knife and counter-knife or with double-knife. The most utilised cutting apparatus for all cultures of the cereals are the one with knife and counter-knife, with normal cutting (Fig. 1).

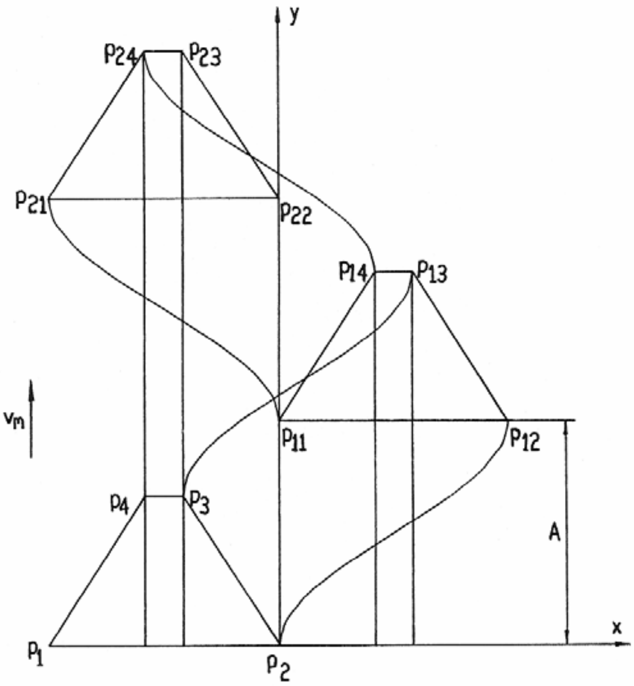

Fig. 1. *The cutting diagram of a conventional sickle bar mower with countershear*

The space passed through by the knife of the cutting apparatus in lateral directions, dependent on connecting rod-crank mechanism used for drive, is calculated with following equation [1,4,6]:

$$x = r \cdot (1 - \cos \omega t) \qquad (1)$$

where: r –is the radius of the drive mechanism crank, [m];

ω –the crank angular speed, [rad/s].

The space passed through by the harvester machine (A [m]) (Fig. 1) in concordance with machine speed (v_m [m/s]) and with rod-crank mechanism rotation speed for the cutting apparatus drive (n [rev/min]), respectively:

$$A = \frac{30 \cdot v_m}{n} \qquad (2)$$

The motion equations of the straight reciprocating motion cutting apparatus dependent on space passed through by the machine (A) and the drive mechanism crank length (r), are:

$$\begin{cases} x = r \cdot (1 - \cos \frac{\pi \cdot x}{A}) \\ y = \frac{A}{\pi} \cdot \arccos(1 - \frac{x}{r}) \end{cases} \tag{3}$$

In order to draw the cutting diagram on the computer, according to the mathematical pattern described before, an AutoLISP software was developed and used. The table 1 contain the values which can be considered as working dates, and the figure 2 show as the cutting diagrams for each of these working dates.

Table 1. *The working dates for cutting diagram from figure 2*

Parameters	*Figure 2*			
	a)	*b)*	*c)*	*d)*
The machine speed, v_m [m/s]	2	2.5	3	3.5
The crank rotation speed, *n* [rev/min]	1000	1000	1000	1000
The crank length, *r* [cm]	3.8	3.8	3.8	3.8

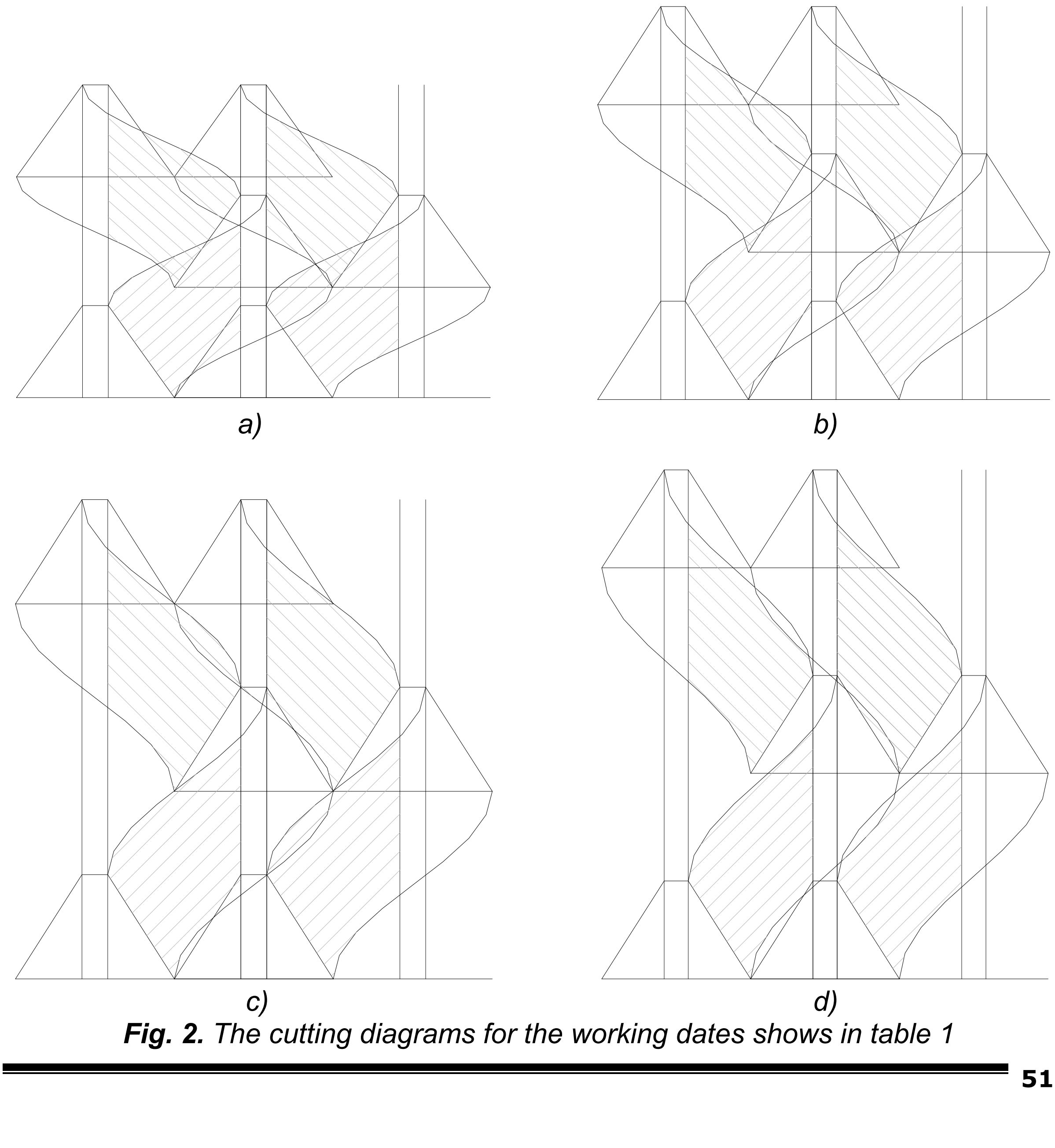

a) *b)* *c)* *d)*

Fig. 2. *The cutting diagrams for the working dates shows in table 1*

3. THE CUTTING DIAGRAM GENERATION FOR ROTARY APPARATUS FOR MOWING MACHINES

The rotary motion cutting apparatus can be: with horizontal plane motion or with vertical plane motion. There is, all over the world, a tendency in using the rotary cutting apparatus with horizontal plane motion, used especially for cutting grass and brush, which cutting diagram is represented in Fig. 3.

The space passed through by the machine (*S*) in the time of knife action (*t*), dependent on its speed (v_m), must be in concordance with cutting apparatus length (*h*), which the expression is [1]:

$$S = v_m \cdot t = h \quad (4)$$

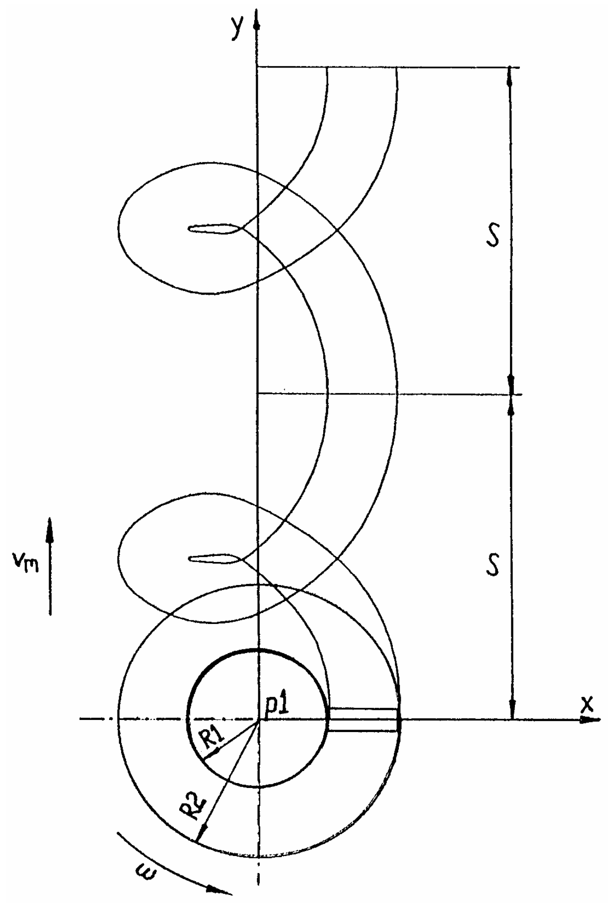

Fig. 3. *The cutting diagram for the rotary cutting apparatus with horizontal plane motion*

The time which a knife drive in a complete revolution is calculated with expression:

$$t = \frac{60}{z \cdot n} \quad (5)$$

where: z –is the number of the rotor blades;
n –the disk rotation speed, [rev/min].

The space passed through by the machine (S) in a full rotation of the cutting apparatus rotor, dependent on machine travel speed (v_m [m/s]) and on the disk rotation speed (n [rev/min]), has the expression:

$$S = \frac{v_m \cdot 60}{n} \qquad (6)$$

The x,y-coordinates of the blade path can be calculated using the following equations:

$$\begin{cases} x = R \cdot cos(\omega \cdot t) \\ y = v_m \cdot t + R \cdot sin(\omega \cdot t) \end{cases} \qquad (7)$$

where: R is the disposal radius of whichever point on the blade.

In order to plot the cutting diagram on the computer, according to the mathematical model described before, an AutoLISP software was developed, and the results of the running of this software is presented in figure 4. The table 2 contain the values which can be considered as working dates.

Table 2. *The working dates for cutting diagram from figure 4*

Parameters	*Figure 4*		
	a)	*b)*	*c)*
The machine travel speed, v_m [m/s]	2	3	4
The disk rotation speed, n [rev/min]	500	500	500
The disk radius, R_1 [m]	0.2	0.2	0.2
The blade length, h [m]	0.1	0.1	0.1

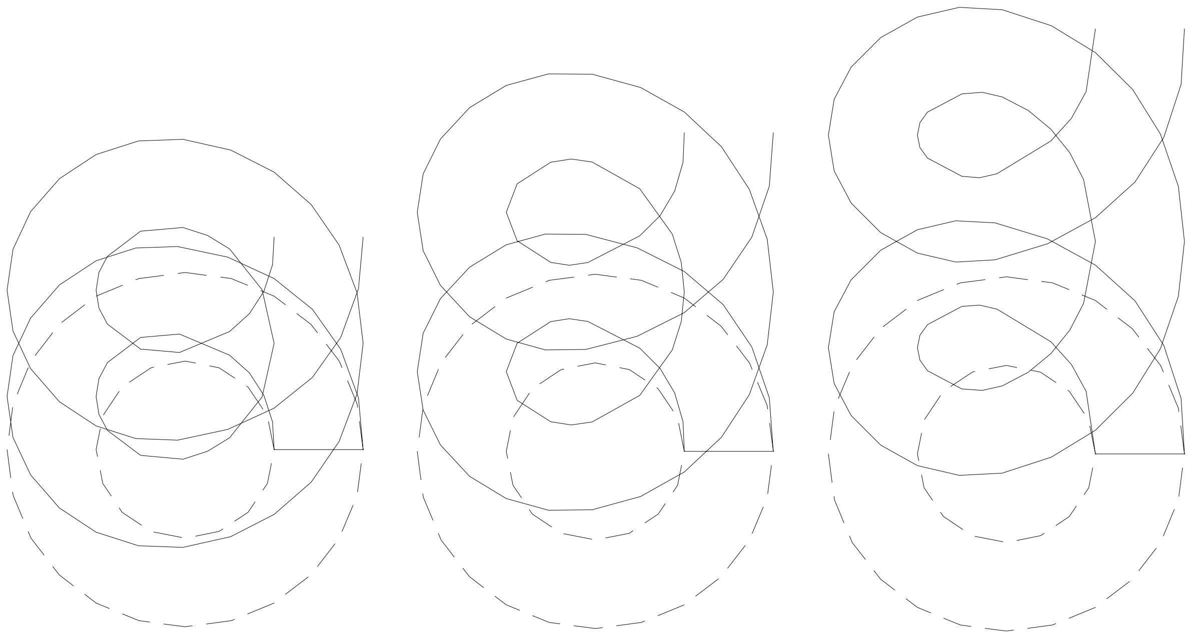

a) *b)* *c)*

Fig. 4. *The cutting diagrams for the rotary cutting apparatus with horizontal plane motion, results from running of AutoLISP software*

4. CONCLUSIONS

The software written in AutoLISP language allows the parametrical computer aided generation of the cutting diagram in a very short time and with maximum precision, on the basis of some kinematical and functional parameters given by the keyboard.

With a minimum effort, this software can be developed to determine the optimum travel speed, on the basis of optimum paths of the knives.

Because of necessary knowledge from several domain such as: harvesting machines, analytical geometry, computer programming, computer aided design, etc., this paper has a pronounced interdisciplinary character.

This paper presents a new concept concerning the optimisation of the cutting apparatus kinematical parameters for agricultural harvesting machines, based on the mathematical description of the knifes motion and their parameterized computer aided generating, using AutoLISP and AutoCAD.

5. REFERENCES

[1] **Babiciu P., Biriş S.Şt., Paraschiv G.,** Programe de inițiere în AutoLISP cu aplicații în construcția de maşini agricole, Editura PRINTECH, 1998.
[2] **Biriş S.Şt.,** Computer-aided design of the complex parts in the machines building field, Modelling and optimization in the machines building field (MOCM-3), Romanian Academy, Branch office of Iaşi, 1997, pag. 1-7.
[3] **Modenov P.S.,** Geometrie analitică, Editura Tehnică, Bucureşti, 1957.
[4] **Scripnic V.,Babiciu P.,** Maşini agricole, Editura Ceres, Bucureşti, 1979.
[5] **Stăncescu C.,** AutoLISP - Manual de programare, Editura FAST 2000, Bucureşti, 1996.
[6] **Strivastava A., Goering C., Rohrbach R.,** Engineering Principles of Agricultural Machines, ASAE Textbook Number 6, 1993.

THE COMPUTERISED CALCULUS IN THE PROGNOSIS OF THE PHASE EQUILIBRIUM DIAGRAM OF THE TERNARY SYSTEM AL-CU-SI

Florentina Adriana CZIPLE

Eftimie Murgu University, REŞIŢA

ABSTRACT

The paper presents a model for establishing the mathematical functions of the liquidus and solidus curves, from the binary diagrams Al-Si, Si-Cu, Cu-Al and their use in the prognosis of the phase equilibrium diagram from the ternary system Al-Cu-Si. We have studied the model of the non-ideal liquid solution of the regular type. The calculus and graphic plotting of the equations for the binary systems has been performed on the computer with the software programmes MathCad 2000 Professional, Statistica 5, Curve Expert, and for the ternary system Al-Cu-Si, with the 3D StudioMax software.

Keywords: *computerised modelling, spline surface*

1. INTRODUCTION

The present-day technical activities utilise a various range of materials, most of them being binary, ternary or polynary alloys. The general trend, intensely manifested these past decades, is the progressive mathematisation in the research of materials, the wider and wider use of mathematical methods and of computerised calculus in:

- Physical-chemical-mathematical modelling;
- Planning of the physical-chemical experiment;
- Processing experimental data;
- Optimisation of the physical-chemical properties;
- The prognosis of the equilibrium diagrams.

As nowadays there is no possibility to completely and accurately solve the issue of the prognosis of equilibrium diagrams, many researchers confer great attention to searching and elaborating qualitative and quantitative laws.

The main method of such works is the analysis of the known equilibrium diagrams as they englobe and contain all the laws and correlations we must find. The statistical method for the prognosis of a phase equilibrium diagram in a ternary system is a theoretical method for assessing the character of the components' interaction in the binary systems. The prognosis of the general aspect of binary equilibrium diagrams and of their fragments is performed with the help of criteria and statistical processing of data from the known diagrams, plotting statistical graphs, obtained thorough the use of the main characteristics of the atomic-crystalline structure of the components. The reliability of such a prognosis may well go over 90% [1].

The mathematical computerised modelling of the ternary phases diagram of equilibrium Al-Cu-Si was realised by generating the liquidus and solidus surfaces from the liquidus and solidus curves of the binary phase diagrams Al-Si, Si-Cu, Cu-Al (Fig.1). The liquidus and solidus curves of the binary diagrams lead to the graphic plots of curves forming the perimeter of the liquidus and solidus surfaces of the ternary system Al-Cu-Si (Fig. 2a, 3a).

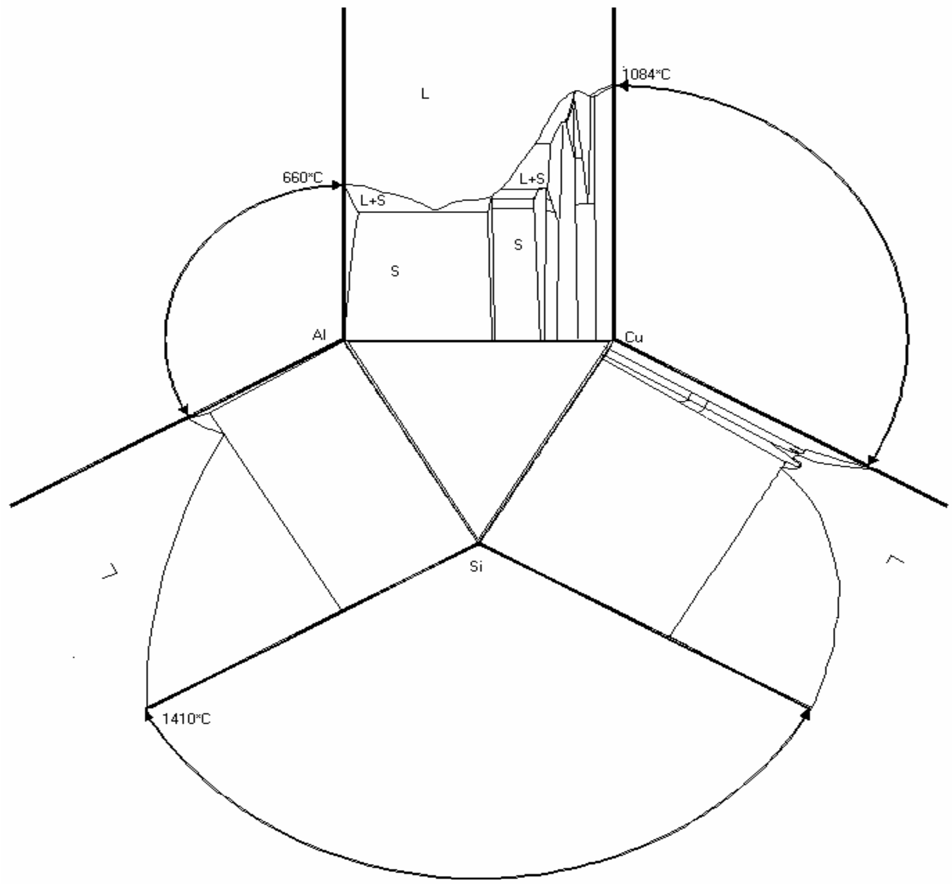

***Fig. 1**. The three binary diagrams (Si-Al), (Al-Cu), (Cu-Si), which are swung over in the plane of the Gibbs compositional triangle of the system Al-Cu-Si*

The construction of the mathematical model of the ternary phases diagram Al-Cu-Si was performed on a computer with the software *3D StudioMax Version 5.0* [7], which analyses the concatenated functions of the liquidus and solidus curves [6] form the binary diagrams Al-Si [1], Al-

Cu [4], Cu-Si [5], as well as B-spline functions. In the terminology of the mechanical drawing the term „spline” indicates an elastic band for drawing smooth curves along a set of control points (the NURBS <*Non Uniform Rational B-Spline*> *concept*). Mathematically, such curves may be described by portions as approximations of polynomial functions of the third grade, with all three orders of continuity (continuity of the zero, first and second order) in the control points [2].

2. THE COMPUTERISED PLOTTING OF THE LIQUIDUS AND SOLIDUS SURFACES

The definition of the spline surface obtained for the liquidus and solidus surfaces is made through the topological product of the mixture functions of the three B-spline functions representing the liquidus and solidus curves form the diagrams Al-Si, Si-Cu, Cu-Al, used for the computation of the vector of each point of the spline surface, expressed in the relations [2]:

$$P_{(u,v,z)} = \sum_{i=0}^{l} \sum_{j=0}^{m} \sum_{k=0}^{n} p_{i,j,k} \cdot N_{i,s}(u) \cdot N_{j,t}(v) \cdot N_{k,w}(z) \tag{1}$$

where:

u,v,z – the parameters of variation of the mixture functions;
$p_{i,j,k}$ – the vector of one of the (l+1)(m+1)(n+1) control points on the surface;
$N_{i,s}(u)$, $N_{j,t}(v)$, $N_{k,w}(z)$ – mixture functions, mixture polynomials;
l, m, n – number of control points of the respective polynomials;
s, t, w – points of the (l+1), (m+1), (n+1) control points;

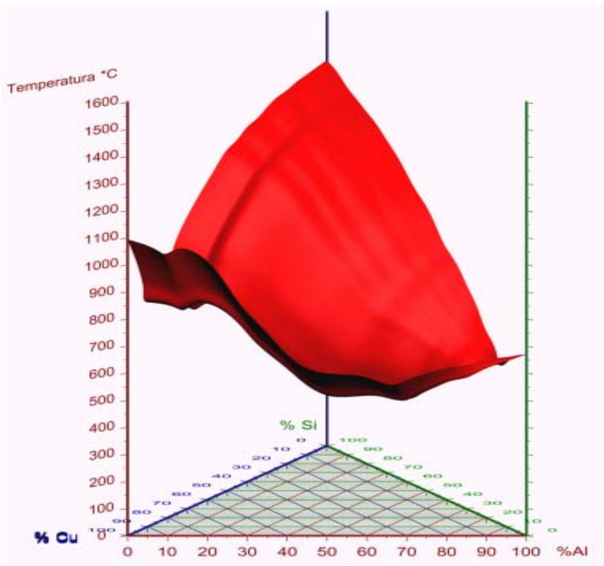

(a)

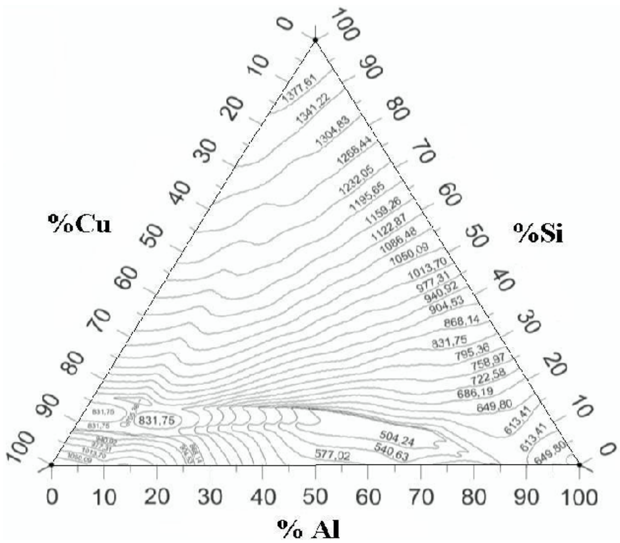

(b)

Fig. 2 *The liquidus surface of the system Al-Cu-Si.*
(a) space plotting; (b) projection of the liquidus surface on the plane of the Gibbs triangle (at. %) Al, Cu, Si.

The projection of the liquidus and solidus surfaces on the plane of the Gibbs triangle (fig.3b-4b) allows the positioning of the isotherms in the plane, which offers information on the physical shape and thermal characteristics of the surface.

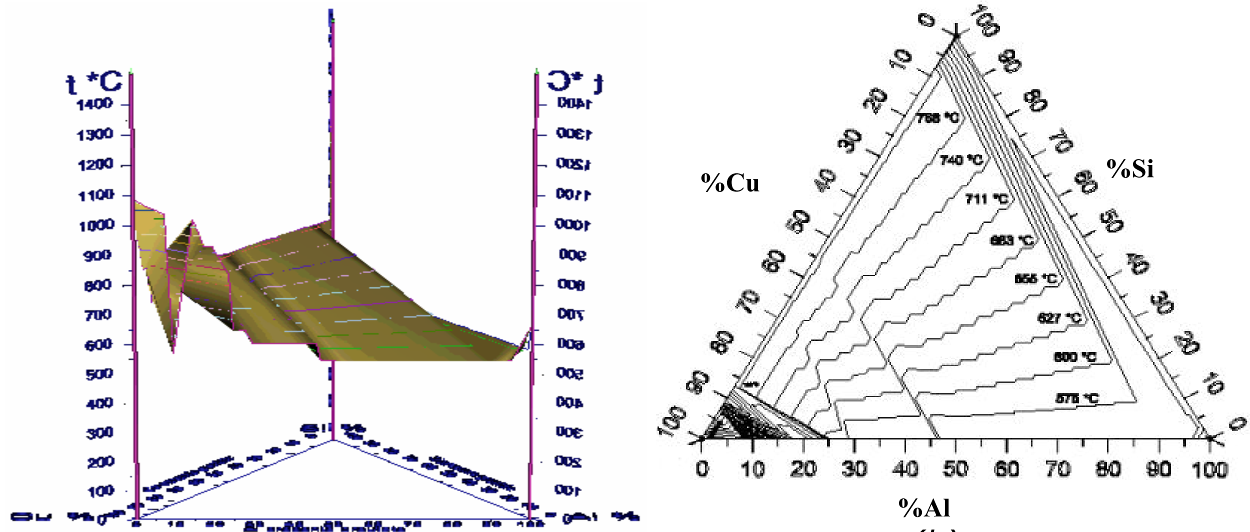

(a) *(b)*

***Fig. 3** The solidus surfaces of the ternary phases diagram Al-Cu-Si.*
(a) Perspective view. Vertical close-up view:the solidus curve(Cu-Al)
(b)) projection of the liquidus surface on the plane of the Gibbs triangle
(%) Al, Cu, Si.

The surfaces thus plotted are smooth, but in reality, at the solid-liquid interface, at the microscopic level, the surfaces contain a series of prominences due to the preferential concentration of different species of atoms, following the modification of the concentration of phases when the temperature drops.

3. Testing the mathematical model

The testing of the mathematical model of the liquidus and solidus surface was performed by determining the correlation coefficient ***r*** [8] of the mathematical model against the real model made of alloys from the system Al-Cu-Si [3]:

$$r \equiv \sqrt{\frac{S_t - S_r}{S_t}} \tag{2}$$

where **- S_t** is **the standard deviation,** quantifying the spreading of data around the medium experimental value $\overline{y}$, according to the relation [8]:

$$S_t = \sum_{i=1}^{n} \left(\overline{y} - y_i\right)^2 \tag{3}$$

where - S_r is defined as the **deviation of the model compared to the experiment** calculated (4), $S_r = \sigma^2$ [8]:

$$\sigma^2 = \frac{\sum_{i=1}^{n}\left(y_{i,\exp} - y_{i,calc}\right)^2}{2n} \qquad (4)$$

The data resulted form the experiment [3] are presented in Table 1.

Table 1 *The values of temperatures from the database of the mathematical model (calculated value) and the real model (experimental value)*

Sample alloys	Beginning of solidification (°C)		End of solidification (°C)		Solidification range (°C)	
	Computed value	Experimental value	Computed value	Experimental value	Computed value	Experimental value
AlSi6Cu4	**628**	**y_1: 615**	**576**	**y_1: 540**	**52**	**y_1: 75**
		y_2: 610		**y_2: 530**		**y_2: 80**
		$\bar{y}$: 612,5		**$\bar{y}$: 535**		**$\bar{y}$: 77,5**
AlSi9Cu3	**618**	**y_1: 580**	**555**	**y_1: 490**	**63**	**y_1: 90**
		y_2: 578		**y_2: 479**		**y_2: 99**
		$\bar{y}$: 579		**$\bar{y}$: 484,5**		**$\bar{y}$: 94,5**
AlSi12Cu	**630**	**y_1: 580**	**558**	**y_1: 515**	**72**	**y_1: 65**
		y_2: 570		**y_2: 529**		**y_2: 41**
		$\bar{y}$: 575		**$\bar{y}$: 522**		**$\bar{y}$: 53**

After the statistical analysis performed by comparison with the real model [3], the mathematical model of the liquidus and solidus surfaces determined theoretically (Fig. 2a, 3a) exhibit a correlation coefficient of **r=0,91**.

4. Conclusions

- The ternary diagram of phase equilibrium modelled thorough mathematical and thermodynamic calculus (Fig.4), delimits the domains of phase transformation (the liquid monophase domain, the bi-phase liquid-solid domain, the domain of solid phases), without indicating the number and nature of phases from the domains.
- The correlation coefficient *r=0,91* of the liquidus and solidus surfaces leads to the conclusion that the mathematical model conceived has a rather satisfying reliability degree.
- the mathematical model of the liquidus surface plotted through the projection of isotherms on the plane of the basic Gibbs triangle allows the placement of the ternary eutectice area within the perimeter of the isotherm of 504,24°C (Fig. 2b).

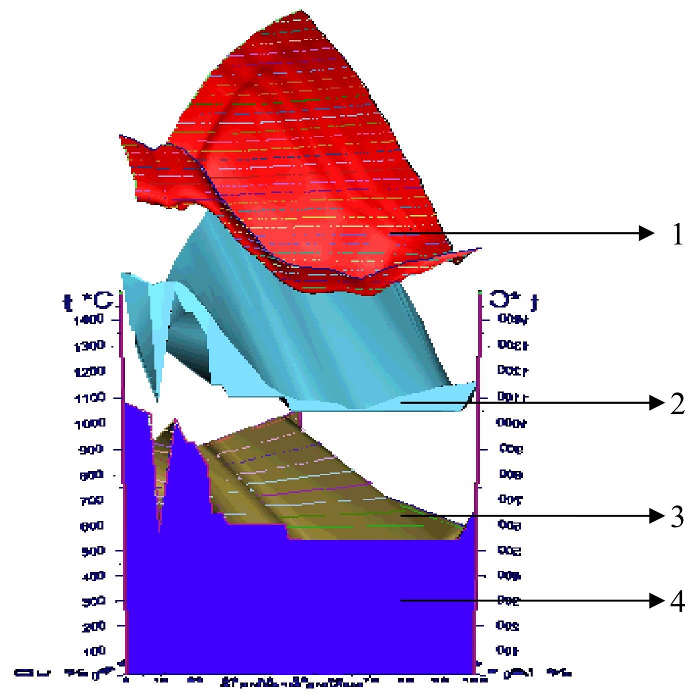

Fig. 4 *The theoretical ternary phase diagram Al-Cu-Si, the liquidus surface (1), the liquid-solid interval (2), the solidus surface (3), the solid phases space (4).*

- The practical applicability of the model consists in the fact that with the help of the database one may approximate the melting temperature of any type of alloy from the system Al-Cu-Si.

Bibliography

1. ALOMAN, A, - Theory of equilibrium diagrams, Romanian Academy Publishing House, Bucharest, 1999
2. BAICU, R., VOLOVICI, D.- Systems of graphic processing, the Blue Publishing House, 1999
3. CZIPLE, F.,- Organisation and computerised monitoring of an experiment of thermal analysis of alloys from the system Al-Cu-Si, Academic Days - The 8th Edition, Timisoara 2003, p.142
4. MURRAY, J.L, -Al-Cu (Aluminium-Cooper), *Int.Met.Rev*., 30(5), 1985
5. OLESINSKI R.W, ABBASCHIAN, G.J. -The Cu-Si System, *Bulletin of Alloy Phase Diagram,* v7, Nr.2, 1986
6. STEINBACH, I., B. KAUERAUF, C. BECKERMANN, J. GUO, Q. LI, - Three-Dimensional Modeling of Equiaxed Dendritic Growth on a Mesoscopic Scale. *Modeling of Casting, Welding and Advanced Solidification* v. VIII, edited by B. G. Thomas, C. Beckermann, Warrendale: TMS 1998
7. *** 3D StudioMax, 5.0 Portions Copyrighted © 1989–2002 mental images GmbH & Co. KG Berlin, Germany.
8. ****Collection STAS (STAS 7122-65) Mathematical statistics in technics; The Technical Series A, 59, State Publishing House for Publications Bucharest 1966, p.33

THE ESTABLISHMENT, PLOTTING AND STATISTIC–MATHEMATICAL INTERPRETATION OF THE LIQUIDUS SURFACE FROM THE PHASE EQUILIBRIUM DIAGRAM OF THE TERNARY SYSTEM Al-Cu-Si

Florentina Adriana CZIPLE

Eftimie Murgu University, REŞIŢA

ABSTRACT

The paper forwards the conclusions of a survey performed on a mathematical model of the phase equilibrium from the ternary system Al-Cu-Si. The author presents the calculus of the statistic equation of the liquidus surface model from this diagram, the plotting and statistical-mathematical interpretation of the results obtained.

***Keywords**: liquidus surface, ternary phase diagram*

1. INTRODUCTION

The model of obtaining a liquidus surface through thermodynamic-mathematical computerised modelling consists of a thermodynamic analysis and a mathematical complex treatment of the pure components and of their interaction in the binary systems and in the ternary system. The phase equilibriums liquid-solid from the binary diagram Al-Si [1], Al-Cu [6], Cu-Si [7] were treated analytically, rigorously deducing he equations of the phase transformation curves delimiting the monophase liquid domain form the biphase liquid-solid domain based on the models of the regular un-ideal solutions.

2. THE COMPUTERISED GENERATION OF THE LIQUIDUS SURFACE

In order to establish the liquidus curve that forms the perimeter of the liquidus surface of the ternary system Al-Cu-Si, we mathematically processed - through concatenation - the following functions (Table 1) inferred from the phase equilibrium of the binary systems Si-Al, Al-Cu, Si-Cu, valid in the specified sub-intervals of the x variable (% atomic) [4]:

Table 1 *The mathematical functions of the fragments of liquidus curve from the binary diagrams Al-Si, Si-Cu, Cu-Al*

Binary system	Interval	Equation	Coefficients
Al-Si	$x_{Al} \in [0 \div 89]$	$T = \dfrac{12100 - 3000\left(x_{Al}^{L}\right)^2}{7{,}189 - 1.987 \cdot \ln\left(1 - x_{Al}^{L}\right)}$	
	$x_{Al} \in (89 \div 100]$	$T = \dfrac{2570 - 3000\left(1 - x_{Al}^{L}\right)^2}{7{,}189 - 1.987 \cdot \ln\left(x_{Al}^{L}\right)}$	
Al-Cu	$x_{Cu} \in [0 \div 17]$	$y = a + b \cdot x + c \cdot x^2 + d \cdot x^3$ y=Temp (K) x=atomic fraction Cu	$a = 933.54386$ $b = -612.93$ $c = 58.049536$ $d = -2407.9807$
	$x_{Cu} \in (17 \div 32]$	$y = a + b \cdot x + c \cdot x^2 + d \cdot x^3$	$a = 582.7285$ $b = 2329.2222$ $c = -6472.7855$ $d = 6053.0285$
	$x_{Cu} \in (32 \div 36]$	$y = a + b \cdot x + c \cdot x^2 + d \cdot x^3$	$a = 21163.327$ $b = -178178.43$ $c = 518571.02$ $d = -499999.6$
	$x_{Cu} \in (36 \div 52]$	$y = a + b \cdot x + c \cdot x^2 + d \cdot x^3$	a =607.53922 b =350.58049 c =1289.9897 d =-128.99897
	$x_{Cu} \in (52 \div 60]$	$y = a + b \cdot x + c \cdot x^2 + d \cdot x^3$	a =10908.29 b =-57118.803 c =108281.59 d =-66600.059
	$x_{Cu} \in (60 \div 66]$	$y = a + b \cdot x + c \cdot x^2 + d \cdot x^3$	$a = 17156.008$ $b = -84609.564$ $c = 146785.78$ $d = -83333.367$
	$x_{Cu} \in (66 \div 83]$	$y = a + b \cdot \cos(c \cdot x + d)$	$a = 1301.3147$ $b = 22.765299$ $c = 19.183136$ $d = -1.7903553$
	$x_{Cu} \in (83 \div 100]$	$y = a + b \cdot x + c \cdot x^2 + d \cdot x^3$	$a = -7916.6496$ $b = 28158.738$ $c = -28631.32$ $d = 9746.5882$
Si-Cu	$x_{Cu} \in [0 \div 7]$	$y = a + b \cdot x + c \cdot x^2 + d \cdot x^3 + e \cdot x^4$ y=Temp (K) x=atomic fraction Cu	$a = 1682.8106$ $b = -262.72908$ $c = -1658.5227$ $d = 3296.7172$ $e = -3087.1212$
	$x_{Cu} \in (7 \div 8]$	$y = a + b \cdot x + c \cdot x^2$	a =-8649.5116 b =25778.253 c = -16990.83
	$x_{Cu} \in (8 \div 8{,}2]$	$y = \dfrac{1}{a + bx^c}$	$a = 0.0010221998$ $b = -0.0001547649\ 5$ $c = 1.4769895$
	$x_{Cu} \in (8{,}2 \div 8{,}6]$	$y = ax + b$	$a = 693$
	$x_{Cu} \in (8{,}6 \div 100]$	$y = \dfrac{a}{1 + b \cdot e^{-cx}}$	$a = 1376.8063$ $b = 1038913.7$ $c = 17.978334$

We studied the binary diagrams Si-Al, Al-Cu, Cu-Si, determining the analytical equations and the optimised empirical statistical functions of the liquidus curves, with the experimental data from the literature [1],[6],[7].

In order to establish the analytical equations of the liquidus curves separating the liquid monophase domain from the bi-phase domain where the solid component has known thermal and thermodynamic properties, we applied three computation models for: the ideal liquid solution ($\Delta C_p=0$ and $\Delta C_p \neq 0$) and for the non-ideal solution of the regular type [1], [4]. The empirical equations of the liquidus curves were established for the cases where there were no thermal and thermodynamic data of the solid phases [4],[3],[6], [7].

The selection of the optimum equations of the equilibrium curves was performed with the help of the computer, based on the *correlation coefficient r* and on the *estimated standard error S*, by statistically-mathematically processing the experimental data from the literature, using the statistic software *CurveExpert*

The liquidus surface form the system Al-Cu-Si modelled on the computer with the 3D software StudioMax, using the concatenation of functions (table 1), is presented in fig.1 .

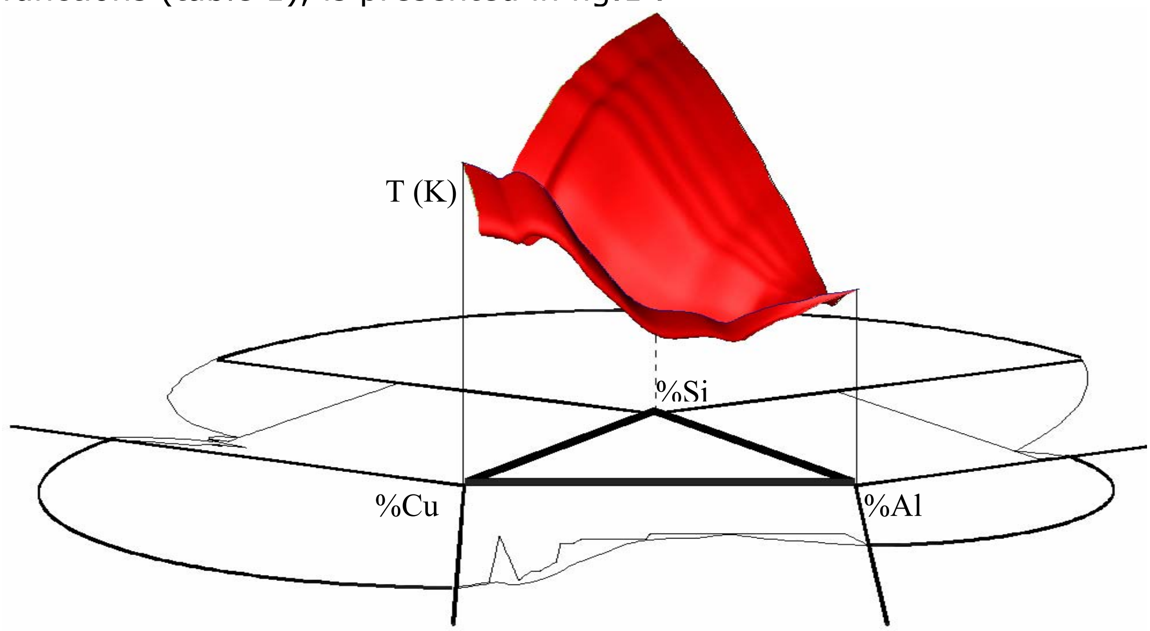

Fig. 1 The computerised generation of the liquidus surface from the ternary diagram Al-Cu-Si

The generation of the liquidus curved surface from the spatial diagram of phase equilibrium of the ternary system Al-Cu-Si was performed on a computer using the mathematical instruments that utilise sets of complex mathematical functions which define the surface through a set of control points specified by the user (Fig.2). These points resulted through the mathematical processing of the liquidus and solidus curves of the binary systems Si-Al, Al-Cu, Cu-Si, with the graphic software *3D Studio Max*.

The plotting (Fig.2) starts from the Gibbs triangle with the concentration expressed in atomic %, and the axis perpendicular on the triangle plane represents the temperature in Kelvin degrees. The acknowledged term for discretisation is „mesh".

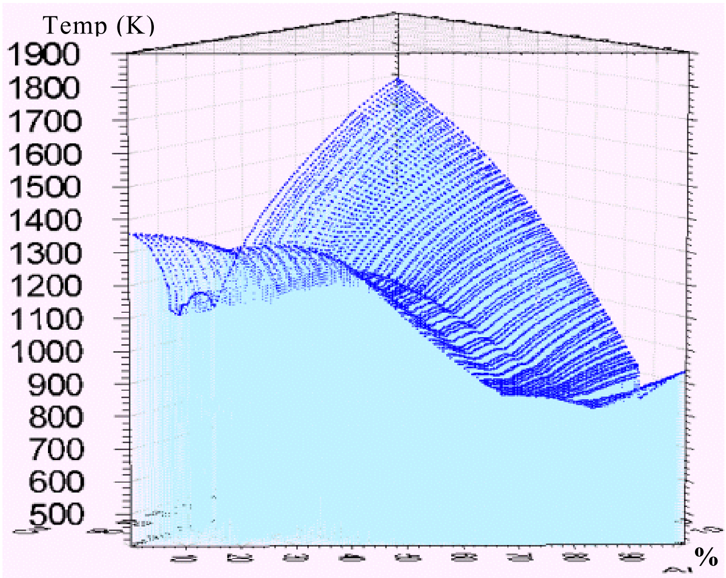

Fig.2 The liquidus surface mathematically modelled, in the ternary system Al-Cu-Si.

The projection of isotherms of the liquidus surface (Fig.3) on the plane of the Gibbs triangle, obtained through the computerised slicing of the surface with horizontal parallel planes offers information on the physical shape and thermal characteristics of each point on these surfaces.

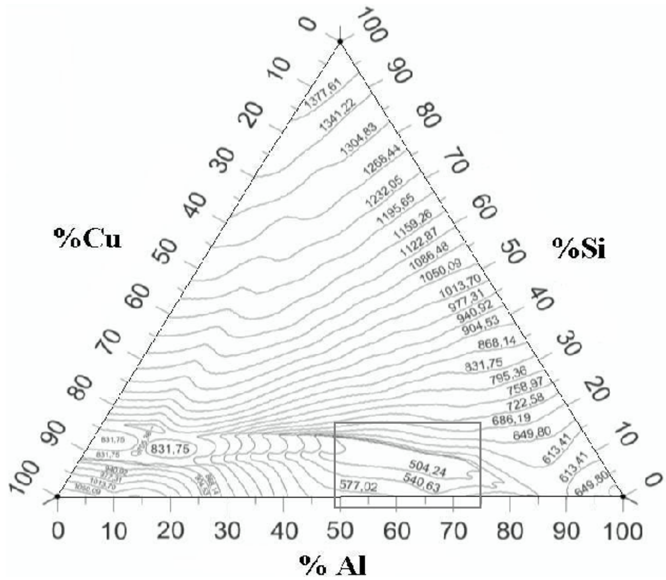

Fig.3 The projection of the liquidus surface on the plane of the Gibbs triangle and the delimitation of the ternary eutectic area.

The study of the mathematically modelled diagram under the temperature of 504°C (Fig.4) leads us to the conclusion that the ternary system Al-Cu-Si has four zones of composition where there may exist ternary eutecticle, at the temperature of 476,4°C [4].

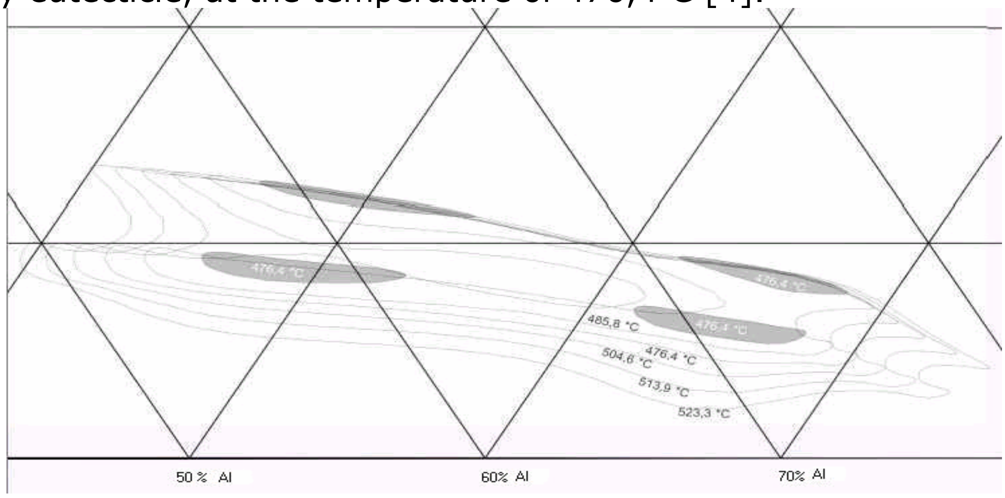

Fig.4 The projection on the Gibbs triangle of the isotherms form the zone of the ternary eutecticles. The area delimited by the isotherm of 476,4°C.

3. The statistical-mathematical equation of the surface

From the database of the mathematical model of the liquidus surface (Fig.2) we selected with the help of the computer 15467 points on the surface having the co-ordinates : *concentrations* x_{Al}, x_{Si}, x_{Cu}, *(atomic %) and temperature (K)*. With these data [4], with the *Statistica 5* software, we established the approximation equation (1) of the liquidus surface through non-linear multiple regression with the full-cubic approximation model [5].

The specific graph offered is a scatterplot with a 95% confidence interval, after a correlation analysis is run [4].

$$T = 918{,}959 \cdot x + 1491{,}086 \cdot y + 1355{,}557 \cdot z + 409{,}962 \cdot x \cdot y - 249{,}939 \cdot x \cdot z - 811{,}233 \cdot y \cdot z - 1354{,}968 \cdot x \cdot y(x-y) - 1396{,}364 \cdot x \cdot z(x-z) + 2416{,}135 \cdot y \cdot z(y-z) + 2564{,}369 \cdot x \cdot y \cdot z \quad (1)$$

where, T- temperature (K); x- at.% Al; y- at.% Si; z- at.% Cu

3. Conclusions

The practical applicability of the equation of the *statistical model* (1) presented in this paper and of the plotting (Fig. 2, Fig. 3) is that it allows the approximation of the melting temperature of any alloy of the (Al-Cu-Si) type, provided we know its chemical composition (at.%). Furthermore we may approximate the alloy’s composition knowing only the melting temperature and the concentration of one of the components.

The theoretical calculus of the diagrams of phase equilibrium has the advantage of using a small amount of thermo-dynamic data and the possibility of utilising computation techniques, with appropriate software. This considerably reduces the research time and expenses. It is necessary to create mathematical methods, software and even special languages that could simplify the computerised calculus of the phase equilibrium diagrams and in general the calculus in the domain of the thermodynamics of the physical-chemical systems. [1],[2].

The theoretical thermodynamic computations of the equilibrium diagrams, based on the physical and chemical properties of substances and using the new technique, adequate mathematical and graphic software, allow [2]:

- The tentative, expected construction of the equilibrium diagrams which haven't been experimentally determined yet;
- The completion of the partially plotted equilibrium diagrams;
- The correction of the experimental equilibrium diagrams;
- The qualitative analysis and systematic classification of the possible type of equilibrium diagrams;

Each theoretical study must nevertheless be sustained by the experimental confirmation through appropriate methods.

Bibliography

1. ALOMAN, A, Theory of equilibrium diagrams, Romanian Academy Publishing House, Bucharest, 1999, p.22, 64-66. 141, 591, 796-798, 843.
2. ALOMAN, A, Thermodynamic-mathematical modelling of phase binary equilibriums, Bren PH, Bucharest, 2001, p.32.
3. CHANG, A, Y. YAN, -Calculated phase diagrams of Aluminium alloys from binary Al-Cu to multicomponent commercial alloys, *Journal Alloy Compounds*, 2001, p.151,320
4. CZIPLE, F, Doctorship Dissertation, Timişoara, 2003
5. MULLER, A, Mathematical description of solidification cooling curves of pure metals, Materials research, Vol. I, Nr.1, Porto Alegre, 1998, Brazilia, p.29-38
6. MURRAY, J.L, -Al-Cu (Aluminium-Cooper), *Int.Met.Rev*., 30(5), 1985, p.17
7. OLESINSKI R.W, ABBASCHIAN, G.J. -The Cu-Si System, *Bulletin of Alloy Phase Diagram,* v7, Nr.2, 1986, p170-178

EXPERIMENTAL INVESTIGATIONS ON A PROCEDURE FOR WELDING THE MEMBRANE WALLS OF THE BOILERS WITHIN THE THERMOELECTRIC POWER STATIONS, IN ORDER TO INCREASE THE LIFETIME OF THE COMPONENTS

LĂPUŞAN Amalia*, POPESCU Bogdan**

*University « Politehnica » Timisoara,
Faculty of Engineering Hunedoara, Romania
** S.C.Termorep S.A. Hunedoara, Romania

Abstract: *Due to the high necessity to increase the lifetime of the thermoelectric equipment, many welding technologies have been adjusted in order to re-commission the installations, being successfully applied when executing the maintenance operations.*

The work presents a process for welding the membrane walls of the boilers or of the over-heated water vessels.

There are shown the results of the tests made on the welded joints in order to homologate the welding procedure and also the possibilities for the applying this method for other energetic vessels tubes.

Keywords: *welding procedure, boilers, lifetime*

1.INTRODUCTION

Replacing the used components is not seen today as an ultimate technical solution within the maintenance of the thermoelectric power stations anymore, because the using field of welding has highly developed. The reasons that support the decision taken for repairing an used component, as an alternative of its replacement, are not just of technical nature, but they present important economical aspects, like: increasing the availability of the installation, avoiding the unplanned breaking due to the damaging of the components, increasing the security of operation, prolonging the lifetime of the component, reducing the maintenance costs and the time necessary for replacing the component.

The damaging process by corrosion and erosion of the vessels tubes are seen as being important processes within a thermal station, and the causes that lead to the occurring of such damaging mechanisms are multiple (fuel quality, burning system, etc.). Because of the implementation of the systems for cleaning the waste gases, imposed by the environment protection legislation and because of the chemical burning processes that take place, a porous and non-adherent sulfide film is built on the outer surface of the tubes. This finally leads to the beginning of an accelerated corrosion process and to a strong damaging by erosion. The result is the premature ending of their lifetime, with serious effects in what concerns the installation efficiency.

The welding technologies, as reparation / prevention methods, represent a solution of high interest for the new components but also for the damaged ones, thanks to the advantages they have: they do not need the replacement of the existent tubes; they can be applied as on-site reparation methods without dismantling the component; they do not need thermal treatment before and after welding; the lifetime of the component is increased with approximately 10 years under normal operation conditions of the vessel; the method combines the high corrosion resistance of the outer surface of the welding coated tube with the advantage of using of a cheap and non-pretentious steel.

2. UTILIZED MATERIALS

The membrane walls subject to the welding are part of the CR 16 vessel, destined to the Paroseni thermal station.

The basis materials subjected to the welding procedure are: the OLT 45 K steel STAS 8184-87 under the form of tube having the dimensions Ø 38 x 4 mm, delivered by S.C. Silcotub S.A. Zalau, respectively the steel OL 37.2k STAS 395-88 made by S.C. Siderurgica S.A. Hunedoara, delivered under the form of strip steel having the dimensions 20 x 5 x 6 m.

Table 1 shows the chemical composition of the two steels.

Table 1. *The chemical compositions of the basis materials*

Material	C [%]	Mn [%]	Si [%]	P [%]	S [%]	Al [%]
OLT 45 K	0,18	0,68	0,26	0,31	0,17	0,24
OL 37.2k	0,15	0,64	0,26	0,024	0,025	-

The thermal treatment applied to the tube made of OLT 45 is normalizing.

The mechanical characteristics guaranteed by the producers are:

- *for OLT 45 K steel* – $R_{p0,2/350/450}$ = 217 N/mm^2; $R_{p0,2}$ = 366 N/mm^2; R = 508 N/mm^2; A = 29,4%. There are also guaranteed the toughness characteristic and the one reached as a result of the tube enlargement test.
- *for OL 37.2k steel* – $R_{p0,2}$ = 320 N/mm^2; R_m = 420 N/mm^2; A_5 = 34%.

The utilized addition material is welding steel wire, having ϕ1,2 mm, SG2 grade, delivered by Industria Sarmei S.A. Campia Turzii, that has the chemical composition shown in Table 2.

Table 2. *Chemical composition of the welding wire*

Material	C [%]	Mn [%]	Si [%]	P [%]	S [%]	Cr [%]	Ni [%]	Cu [%]
Welding steel wire	0,09	1,42	0,98	0,012	0,012	0,08	0,14	0,17

The welding wire has been delivered as *bright coppery,* having the breaking resistance minimum 900 Nmm.

3. SHAPE AND DIMENSIONS OF THE SAMPLES

The sample for homologation is to be made of a 6-tube register, having the length of 3000 mm, according to Figure 1a. Figure 1b shows the way of sampling the specimens, by indicating the areas of sampling.

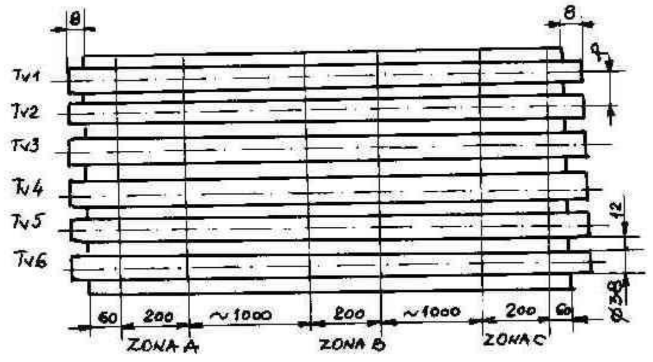

Figure 1a. *Shape and dimensions of the sample*

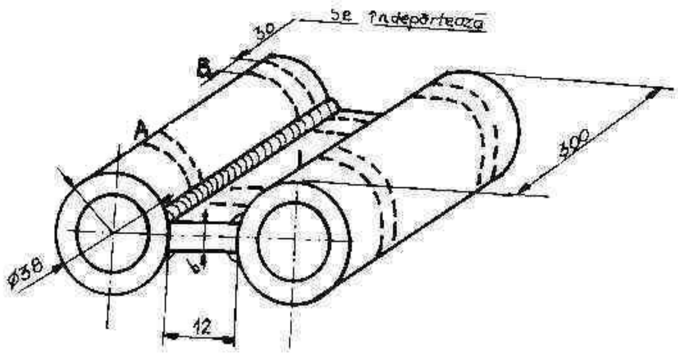

Figure 1b. *The way of sampling the specimens for lab tests*

The preparing and the welding of the sample is to be made accordingly to WPS and under the general welding conditions used in practice.

The preparing of the table and tube edges in the welding area is made by mean of a wire brush, or if necessary, by polishing. The sample does not require neither preheating nor thermal treatment.

4. RESULTS

The control of the membrane wall quality is performed as follows: visual and dimensional control of the weldings, dimensional control of the wall with checking the pitch, the width, the register length, checking the length for each tube of the register, checking the deflection in the register plane and in a plane that is perpendicular on the register plane, checking the strip steel movement as comparing to the middle axis of the register, respectively checking the surfaces of the welded joints by mean of 100 % penetration liquids.

The lab tests performed on samples taken from the areas A, B, C of the welding, according to Figure 1b, were as follows:

- tensile test on a specimen under the form of a strip having the dimensions 20 x 5 mm and the initial cross section of S_0 = 100 mm^2.
- bending test in the wing plane on each strip steel, the bending angle being 50°.
- rod enlargement test of each tube ring up to a deformation value of 10% of the tube diameter.
- twisting test of the strip steel at an angle of 90°.
- flattening test in wing plane, respectively in a plane that is perpendicular on the wing plane, at different distances.

Out of the sample register, i.e. out of each of the three areas marked with A, B, C, there were sampled specimens by mechanical cutting (mill cutting) on the entire width of the register, parallel side samples, as follows:

- all one 20 mm wide strip on which the flattening test is performed perpendicular on the wing plane (the pressure force has a direction that is perpendicular on the wing plane); before testing, each tube from each strip is to be separated by mechanical cutting on the middle of the strip steel.
- all one 20 mm wide strip for performing the transversal tensile test on the wing plane; before testing, steel disks are to be mounted inside each tube, in order to prevent the tube deformation during the test.
- all one 20 mm wide strip on which the flattening test in the wing plane is to be performed (the pressure force is located in the wing plane); before testing, each tube from each strip is to be separated by mechanical cutting on the middle of the strip steel.
- all one 10 mm wide strip that is to be subjected to the bending test in the wing plane (the bending axis is parallel to the longitudinal axes of the tubes).
- all one 10 mm wide strip that is to be subjected to the bending test perpendicular on the wing plane (the bending axis is perpendicular on the longitudinal axes of the tubes).
- all one 10 mm wide strip that is to be subjected to the twisting test of the strip steel, around an axis located in the wing plane.
- all one 15 mm wide strip on which the rod enlargement test of each tube ring is to be performed. The test is to be performed according to STAS 1111-79, by mean of a taper chuck, with 1:10 tapering.

There were also performed Vickers and HV5 hardness tests for the welded joints, i.e. for each welding seam according to SR EN 1043-1/1997.

Before measuring the hardness on one sample made of two tubes, from each of A, B, C groups there are performed the **macroscopic and microscopic analysis**, and the results are shown as follows.

At the macroscopic analyze of the area A, there was determined that the welding seams are made of a single layer, and a seam of the sample in the Figure 2b has an elongated pore. Figures 2a and 2b show the micro-fractographies of the samples.

At the macroscopic analyze of the area B, there was determined that the welding seams are made of a single layer, the sample in Figure 2c does not show any defects, but the sample in Figure 2d shows a pore in one seam and a melting deficiency in another one.

At the macroscopic analyze of the area C, there was determined that the welding seams are made of a single layer and do not show any defects, and Figure 2e and 2f show the micro-fractographies of the samples.

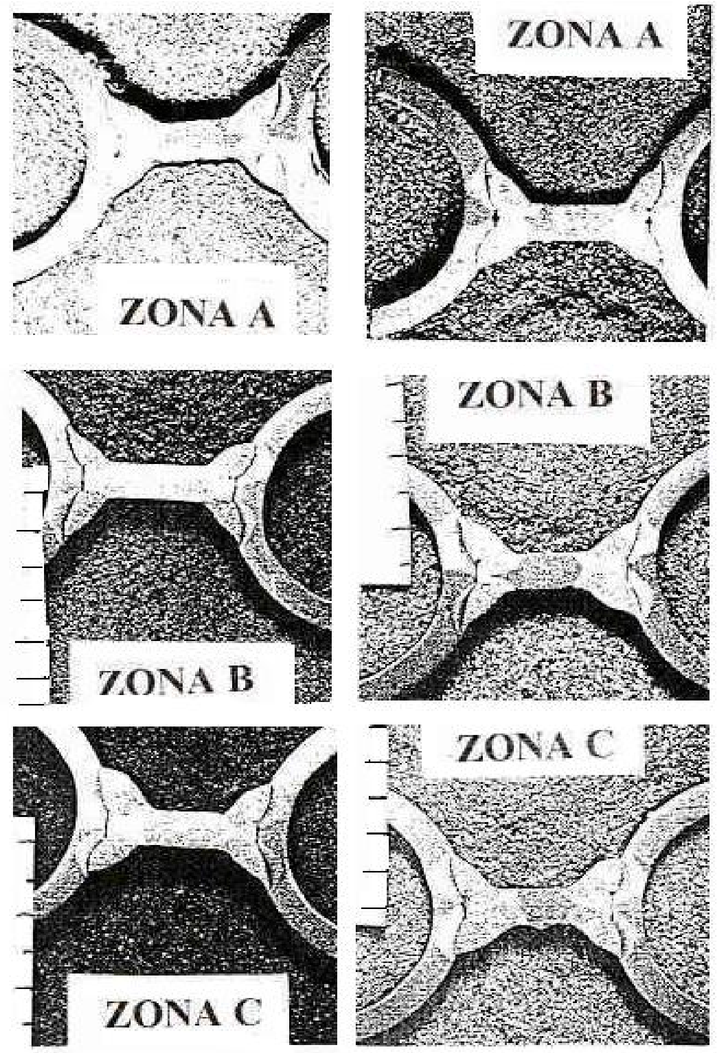

Figure 2. *The samples for lab tests – Nital 4% etching*

The microscopic analyze of the samples leads to the conclusion that all the samples from the three areas A, B, C show the same metallographical characteristics, i.e.:
Welding: casting structure; ZIT: normalizing structure; MB1-tube: pearlitic-ferrite structure; MB2-strip steel: pearlitic-ferrite structure and tertiary cementite, and also ferrite grain of 8 points.

After testing the welding with Helling Bid 1 type penetration liquids and after a previous abrasive and chemical cleaning of the welding there were not detected any surface defects, like: pores, cracks, craters and edge notches.

As a result of these tests, no defects of the welding joint or of the welding seams were detected.

5. CONCLUSIONS

The checking carried on in order to homologate the welding procedure performed on a steel within the group 1 according to CR 7/96, leads to the homologation of the welding procedure on any other lower alloyed steels from this group or steels from this group having a lower yield point, under the condition that the welding materials used for the homologation of the procedure can be also used for steels from other groups.

The homologation is valid even if other adding metals are used, if these have an equivalent chemical composition and if they are part of the same class of tensile strength. The homologation for the protection gase is limited at the type of the gas used when checking in order to homologate the welding procedure is performed.

In what concerns the thickness of the basis material, the thickness of the homologated sample represents the minimal wall thickness that can be used. In what concerns the diameter, the validity field of the procedure is 0,8 D … 2D.

The welding process has multiple potential possibilities to modify the initial characteristics of the basis material and of the adding material, to perform in welded joint the non-homogenity of the chemical composition, of the structure and of the mechanical characteristics, and also to create residual strains and plastic deformations, with effects on the quality of the welded joint and on the operational security, that can be diversified thanks to the welding capacity factors.

Hence, the influence of welding is that demonstrated more pronounced and diversified when manual welding with adding material is performed in enclosure. In this case interferes the recognized easiness for generating technological deviations and welding defects.

REFERENCES

[1]. Aldea, M., ş.a. - *Cazane de abur şi recipiente sub presiune - îndrumător*, Editura Tehnică, Bucureşti, 1982.

[2]. Babeu, T.D., Ciubotariu, N. - *Comentarii asupra aspectelor globale din examinarea unor conducte în exploatare,* Proc.of the Sc. Com. Meeting of „Aurel Vlaicu” Univerity, Third Ed. Vol.4, Arad, 1996.

[3]. Budău, V., Liță, M., Crăciunescu, M.- *Aspecte ale comportării în exploatare a materialului supraîncălzitorului de abur de la un cazan de 19 t/h*, Conferința de tratamente termice şi termochimice, 17-19 sept.1992, Cluj-Napoca, pag.120…125

[4]. Burducea, C.,Leca, A.- *Conducte şi rețele termice*, Editura Tehnică, Bucureşti, 1974.

[5]. Delamarian, C.- *Manual pentru mentenanța şi retehnologizarea instalațiilor termoenergetice industriale*, Editura Sudura, Timişoara, 1999.

[6]. Nădăşan, Şt.,ş.a.- *Încercări şi analize de metale*, Editura Tehnică, Bucureşti, 1965.

STUDY REGARDING THE WAYS FOR PRACTICAL EXECUTION OF SOME ENCLOSURES FOR HEATING THE SPECIMENS AND THEIR ADJUSTMENT FOR THE TESTING MACHINES IN ORDER TO PERFORM HIGH TEMPERATURE MECHANICAL TESTS

LĂPUŞAN Amalia Ana

UNIVERSITY „POLITEHNICA "TIMISOARA,
FACULTY OF ENGINEERING HUNEDOARA, ROMANIA

Abstract: *This work presents a critical study on the possibilities of practical execution of some rooms, resp. furnaces, with relatively small sizes, in view of their future adjustment for the tensile testing machine, Brinell hardness tester, Charpy friction pendulum, existing in the Material Resistance Lab inside the Engineering Faculty of Hunedoara.*

By executing these rooms it is desired to carry on some strength and toughness mechanical tests for the steels that operate at high temperature, in order to increase the lifetime of the components made of such steels.

Keywords*: the tensile test, high temperature, hardness test, shock bending test*

1. INTRODUCTION

The ordinary test performed at high temperatures within the industrial labs is the tensile test, but at beneficiary's request, there can be also performed the hardness and the shock bending test.

The temperature at which the tests on materials are generally performed and at which tests on metallic materials are specially performed, is stipulated by the standards corresponding to the type of the test performed and/or to the product standards, respectively to the specification agreed between the parties (the material producer and the beneficiary).

2.ENCLOSURES FOR HEATING THE SPECIMENS FOR PERFORMING THE HIGH TEMPERATURE TENSILE TEST

In principle, the tensile test under high temperature conditions is performed in the same way as at the ambient temperature. The difference consists in the fact that the specimen is previously heated at the desired temperature and it is held at this temperature, in certain prescribed limits, during the test.

In order to perform the mechanical tensile tests at high temperatures, the possibility to adjust a furnace-enclosure, which is to be connected to a temperature measuring system, was studied for the universal machine for tensile testing. Figure 1 shows the constructive elements.

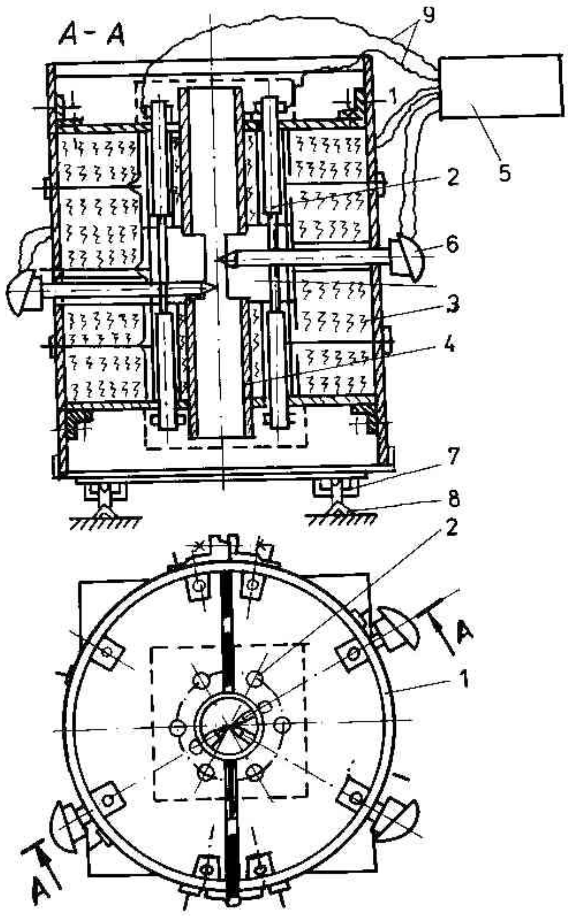

Fig.1. *Furnace-enclosure for heating the specimens: 1-cylindrical wall; 2-resistors; 3-thermal insulating;4-refractory steel tube; 5-electrical installation; 6-PtRh-Pt thermocouples;7-mobile carrier; 8-guidings*

The constructive version of a furnace enclosure presented in Figure 1 consists of a cylindrical vertical electric furnace, having the following main parts: the resistors (2) made of silicon carbide bars (6 pieces), the thermal insulating (3) made of ceramic fiber, the central tube (4) made of refractory steel for protecting the bars (2) and the semi-covers 5 (upper and lower) between which the other components of the furnace are located (2, 3, 4).

The electrical installation for switching and controlling the heating (9), the thermocouples (6) Pt-RhPt 10% (3 pieces) and the carrier (7) for supporting the furnace are elements that are attached to the furnace in order to operate it during the lab tests.

For an easier maintenance of the lower part of the furnace, this is made of two semi-cylindrical half (with a vertical separation plane that passes through the cylinder shaft) that are connected by hinges and screw tightening elements. Between the ceramic fiber insulating (that resists up to 1250°C) and the outer metallic walls, a 6 mm thick asbestos layer was mounted. The thermocouples (6) are guided towards the specimen through tubes made of refractory metallic pipes that are fastened with distance pieces on the semi-covers (5).

The ceramic fiber is fastened on the inner walls of the furnace by means of some refractory anchors with 5mm diameter. The silicon carbide bars (2) are inserted in tubes made of fire clay, that are cut-out only against the chamber for heating the specimen.

The central tube (4) made of refractory steel is cutout on two opposite sides on the length of the chamber for heating the specimen. This length is equal with the gauged length.

The mobile carrier (7) moves on the guides (8) together with the furnace (1), on which it is fastened by screws (M6) after each breaking of a specimen, in order to replace it with another one, for a new test.

The three thermocouples Pt-RhPt are connected (after their pairing) as follows: the first one for regulating the electric supplying installation at the temperature required for measurement, the second one is connected to a installation for digital measurement of the specimen temperature and the third one is mounted on a device for recording the temperature during the practical measurements.

3.ENCLOSURES FOR PERFORMING HARDNESS TESTS AT HIGH TEMPERATURES

The hardness tests performed at high temperatures have gained more and more importance, as the resistance elements of the vessels, of the gas and steam turbines, of the reactors, etc. work long time at high temperatures, being stressed by high mechanical loads. As comparing to the tensile tests, the high temperature hardness test has the advantage that it is performed very quickly and with much more simple devices.

The corresponding testing methods are the Brinell and Vickers procedures. In order to perform these, there can be used normal construction devices, at which a heating furnace is adjusted.

The specimen that is to be tested is brought into the furnace heated at the required temperature and it is held there until the furnace temperature is reached. The temperature is automatically adjusted within ±3°C. There is to be made vacuum (0,01 mm Hg) inside the furnace in order to avoid the oxidizing of the specimen surface.

When the temperature of the specimen has reached the prescribed temperature, the penetration tester is pressed with a corresponding force, just like when determining the hardness at ordinary temperatures. The measuring of the print dimension is performed after the specimen is taken out of the furnace and its temperature has reached the ambient temperature. The time during which the penetration tester is kept in contact with the specimen has a decisive influence on the measurement result. This time can vary from a few minutes up to a few hours and is to be chosen depending on the nature of the material.

The penetration testers used when performing these tests have to be temperature resistant. For temperatures under 300°C, there are to be used alloyed steel balls, for temperatures between 300-600°C there are to be used diamond penetration testers and at temperatures over 600°C, there are to be used synthetic carborundum penetration testers.

In order to avoid a too intense heating of the penetration tester, it is very advantageous to use the dynamic methods, at which the contact between the penetration tester and the heated specimen is kept only during the shock.

Two possibilities for execution the enclosures that are used for performing the high temperature hardness tests are presented. At the lower end of the rod 1 (Figure 2) the holder 4 is mounted with the hole under the penetration tester 2. The upper end of the rod is to be brought into the hole made at the end of the device and it is fastened into it by means of a tightening screw 7. A rod having a penetrating tester with a 120° acute-angled tip can replace the rod on which the detachable penetration testers 2 are mounted. On the working table of the device, the holder (console) 3 made of high temperature resistant steel that is used as a holder for the studied specimen, is to be simple fastened or screwed on.

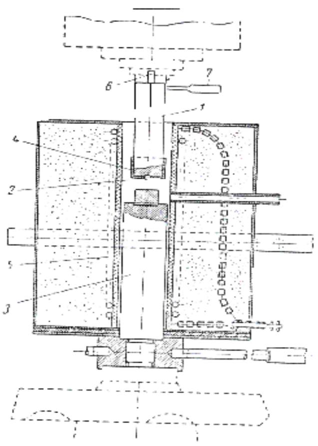

Fig.2. *Constructive version of an enclosure that can be adjusted to the Brinell hardness device*

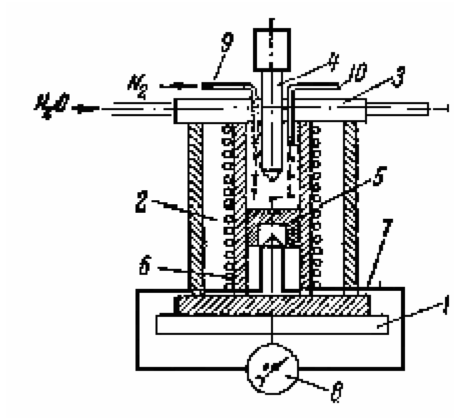

Fig. 3. *Constructive version of an enclosure used for heating the specimens that are to be subjected to the high temperature hardness test*

The main request for a proper performing of the high temperature hardness test is the equality between the temperature of the tested specimen and that of the penetration tester. The shape of the enclosures used when performing the hot hardness tests do not cause difficulties in what concerns the heating of the specimen and of the penetration tester at the required testing temperature, as long as the furnace is isolated from the device working table by asbestos packing or by any other material which is not heat conductive.

In order to prevent the furnace muffle from being rusty, this can be protected inner and outer by an inert gas, for example nitrogen (Figure 3). This protection can be also made in order to reduce the effect of the scale layer, even if very thin, that is generated on the surface of the specimens subjected at high testing temperatures. In case of the constructive version from Figure 3, the gas from the bulb passes through the pipe 9, and the spare gas passes through the pipe 10.

4.WAYS OF HEATING THE SPECIMENS FOR PERFORMING HIGH TEMPERATURE SHOCK BENDING TEST

The equipment used for performing the high temperature shock-bending test is the Charpy friction pendulum that has a simple and robust construction, and which has to fulfil all the conditions imposed by the standard *SR EN 10045-2:1994 Shock-bending test on Charpy specimens, Vol. 2: Checking the testing equipment (friction pendulum).*

The experiments within the high temperature field are more difficult to be performed because, as comparing to other mechanical tests, in case of shock-bending test, the temperature of the specimen could strongly change during the manipulation of the specimen from the furnace to the testing equipment.

For a more thoroughly study of the phenomenon that occur during this dynamic shock test, friction pendulums endowed with special equipment that allow the recording of the strains during the test are used.

The heating of the specimens up to the testing temperature can be performed inside different types of enclosures that differ depending on their position inside the testing machine.

An analyzed constructive version is that in which the detachable electric furnace is mounted on a supporting pole near the ram fastened in the upper position. The furnace shell is to be made of two parts, connected by hinges. For lining, the fire clay is used. On the front and on the back walls of the furnace, there are holes for bringing the specimens inside the furnace-working chamber.

After the required temperature is reached, the specimen is kept 10-15 minutes inside the furnace, and then, by switching on the test, the furnace opens and the ram falls together with the specimen.

The high precision can be reached by the rapidity of opening the furnace and of performing the test (a few seconds).

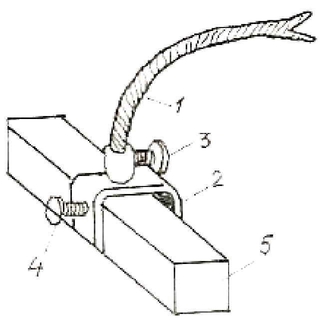

Fig.4. *Way of fastening the thermocouple on the specimen for performing the shock bending test*

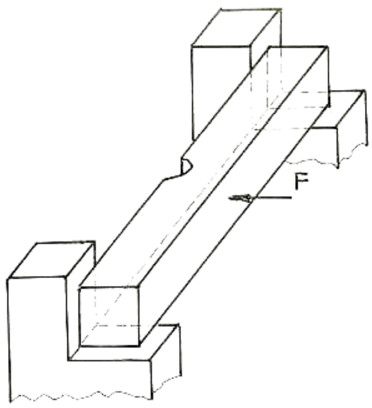

Fig. 5. *Performing the test on the heated specimen*

A special issue during this test is that of measuring the specimen temperature until it breaks. This can be performed as follows: on the opposite side of the specimen notch, at 10 mm from the front side or even on the front side, a 1,2 mm diameter and 5 mm depth hole is to be executed. In this hole the high spot of the thermocouple is brought and it is fastened by means of a thin Ni-Cr wire. Between the thermocouple and the Ni-Cr wire, an asbestos plate for electrical insulating is placed.

Some of the advantages of this method could be the fact that the high spot of the thermocouple is located on the side opposite the specimen notch, at 10 mm distance from the front side or even on the front side. The conditions for cooling the middle part of the specimen and its front part are different. That is why their temperature must not be the same. The asbestos packing that protects the specimen not to be strongly cooled in case it comes into contact with the walls of the impact machine attenuates a little the shock.

The thermocouple is fastened as follows: the thermocouple 1, insulated with an asbestos string is fixed on the specimen O by means of some special clamps, so that the high spot is to be found on the notch. The screw 3 fastens the thermocouple in clamps, and the screws 4 are to be strongly tightened in order to hold the specimen properly. When a certain desired temperature is reached, the thermocouple together with the clamps is taken out from the specimen and then the test is performed. In this way, the temperature control can be performed until the specimen breaks.

5.CONCLUSIONS

When performing the high temperature tensile test it is not recommended to heat individually each sample because of the very high time wastes and that is why more productive methods are to be developed. They have to be oriented on the reducing of the heating period, excluding the influence generated by the heating acceleration on the test results.

The main request for a proper performing the high temperature hardness test is the equality between the temperature of the tested sample and that of the penetration tester. The shape of the enclosures that are used when performing the warm hardness tests does not generate difficulties concerning the heating of the sample and of the penetration tester at the prescribed testing temperature, as long as the furnace is isolated from the table of the device by asbestos packing or by any other material that is not heat conductive.

Bibliography

[1]. Borzdîk, A.M.- *Metodî goriaceh mehaniceschih ispîtanii metallov*, Moscova, 1962.

[2]. Caţarschi, V.- *Contribuţii privind modernizarea tehnologiilor de încălzire a unor oţeluri susceptibile la fisurare în vederea deformării plastice ulterioare*, Teză de doctorat, Universitatea Tehnică „Gheorghe Asachi”, Iaşi, 1996.

[3]. Lăpuşan, A.- *Studiu privind modalităţile de realizare a unor incinte pentru încălzirea epruvetelor în vederea încercărilor mecanice de duritate la temperaturi ridicate*, A Treia Conf. Naţ. „Prof. Dorin Pavel-fondatorul hidroenergeticii româneşti”, Sebeş, 2003, pg. 89-92.

STUDIES AND RESEARCHES REGARDING THE ANALYZE OF CHEMICAL COMPOSITION AND THE REASONS FOR TAKING OUT OF OPERATION THE MILL ROLLS CAST AT S.C. SIDERMET S.A. CALAN

Ana JOSAN[1], Ion SPOREA[2], Doina Elena PETRE[1], Adrian GAVANESCU[1]

[1]Universitatea "Politehnica" din Timişoara, Facultatea de Inginerie Hunedoara
[2]Universitatea "Politehnica" din Timişoara, Facultatea de Mecanică Timisoara

Abstract: *The paper presents a critical analyze of the rolls cast out of nodular iron at S.C. Sidermet S.A.. Călan and inspected in operation at S.C. Siderurgica S.A. Hunedoara. The chemical compositions for 15 inspected rolls, the casting temperatures and the characteristics recorded when put into operation are shown. With these data, there were performed a series of correlation, the specific graphics, the equations and the regression coefficients were shown. The reasons for putting out of operation the inspected rolls were analyzed and the hardness and durability histograms were drawn.*

Keywords: *rolls, hardness, durability*

I. INTRODUCTION

The economical efficiency of the rolled products manufacturing highly depends on the quality of the roll, whose durability is determined both by the characteristics of the material the rolls are manufactured out of and by the operating conditions.

When selecting the material, the mill type, the sizes of the roll (diameter), the rolling speeds, the stands of the rolling mill train the rolls are manufactured for, the working temperature of the panel within the rolling process, the way of cooling during the operation and the pass sizes are to be taken into consideration.

Depending on these factors, not only the material, but also the roll manufacturing technology is different in order to ensure the characteristics imposed by the operating conditions.

Usually, the nodular iron rolls are designated for rolling the small sections with the diameter of 300÷600 mm on pre-finishing stands.

2. ANALYZE THE TECHNOLOGY FOR CASTING THE MILL ROLLS OUT OF NODULAR IRON

In order to analyze and to optimize the technology for casting the mill rolls al S.C. CILINDRUL S.A. Călan, there were taken into study 15 rolls cast out of nodular iron, FNS2. These rolls were also inspected during the operation at S.C. Siderurgica S.A. Hunedoara, within the 650 mm Rolling Mill.

Table 1 shows the chemical composition of these rolls and also the data recorded during operation.

Table 1. Chemical composition and the characteristics of the mill rolls cast out of nodular iron

Roll no.	Chemical composition, %								Cast. temp. °C	Casting time	Brinell hardness		Dura-bility t/mm
	C_{total}	Mn	Si	S	P	Cr	Ni	Mo			Panel	Neck	
1	2,98	0,64	1,87	0,06	0,165	0,29	1,15	0,75	1265	110"	366	280	29
2	2,9	0,79	1,7	0,09	0,29	0,33	1,51	0,24	1270	100"	419	288	28
3	3,1	0,6	1,74	0,09	0,162	0,33	1,92	0,31	1280	130"	450	273	68
4	3,03	0,63	1,88	0,021	0,181	0,37	1,75	0,37	1260	145"	340	300	55
5	3,14	0,62	1,74	0,09	0,249	0,3	1,36	0,26	1280	140"	375	303	58
6	3,09	0,68	1,94	0,044	0,248	0,31	1,47	0,28	1275	120"	385	275	41
7	3,08	0,61	1,73	0,018	0,187	0,28	1,31	0,26	1260	155"	381	252	40
8	3,17	0,6	1,74	0,09	0,162	0,33	1,92	0,31	1280	130"	388	276	61
9	3,06	0,69	0,68	0,01	0,163	0,4	1,69	0,41	1270	160"	412	287	42
10	3,2	0,63	1,75	0,02	0,164	0,3	1,45	0,25	1275	135"	390	280	10
11	3,08	0,68	1,94	0,044	0,248	0,31	1,51	0,42	1270	140"	386	275	71
12	2,72	0,79	1,7	0,06	0,116	0,33	1,51	0,24	1265	100"	380	262	72
13	3,2	0,63	1,75	0,02	0,164	0,3	1,35	0,25	1270	140"	381	264	67
14	2,98	0,64	1,87	0,06	0,165	0,29	1,28	0,34	1280	100"	352	260	26
15	3,15	0,6	1,74	0,09	0,162	0,33	1,92	0,31	1280	130"	387	276	27

Table 2. Chemical composition (STAS 9432-85)

Type rolls	Chemical composition, %									Brinell hardness
	C	Mn	Si	S_{max}	P_{max}	Cr_{max}	Ni	Mo	Mg	
FNS2	3,0-3,5	0,1-0,7	1,2-2,5	0,02	0,15	0,6	1,5-2,5	0,3-0,5	0,02-0,04	354-441

Regarding the 15 analyzed rolls, the followings were established:

- only one roll could be framed within the limits admitted by the reception Standard, regarding the chemical composition;
- the elements that have a negative influence on the quality of the rolls in what concerns the S and the P content can be presented as follows: at 5 rolls the S content is exceeded and at 3 rolls the P content is exceeded;
- the elements that have a positive influence on the quality of the rolls with Ni, Mn and Mo can be presented as follows: at some rolls, the content is below the admissible limit;
- the casting temperature at one roll was 1230°C instead of 1250°C, which is the minimum temperature required by the technological process;
- because of these deviations in what concerns the chemical composition and because of other elements within the manufacturing process, the hardness required by STAS: 354–441 HB could not be obtained for all the rolls.

By using the recorded data, a series of correlation was performed, and the equations and the regression coefficients were shown. Following this analyze, some deviations from the STAS 9432-85 requirements regarding the chemical composition were established (see fig. 1, 2, 3).

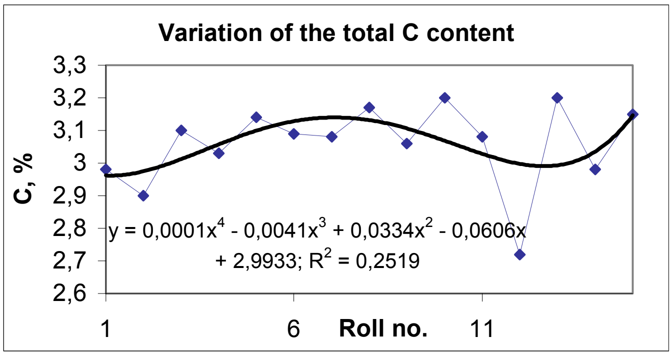

Fig.1. Variation of the C content.

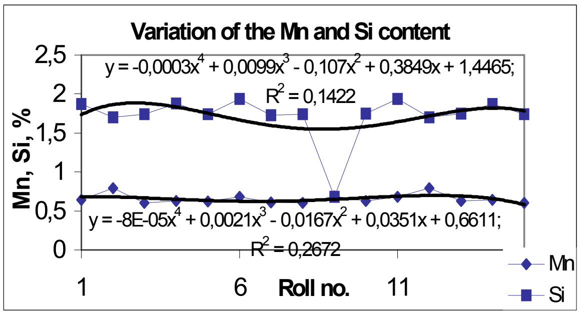

Fig.2. Variation of the Mn and Si conent.

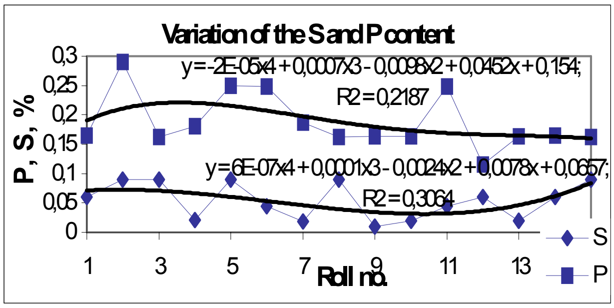

Fig.3. Variation of the S and P content.

Figure 4 shows the hardness recorded depending on the carbon content, and figure 5 shows the hardness histogram. It can be noticed that in general, almost all the hardness values are located with in the STAS 9432-85 and STAS 4596-87 limits (excluding the rolls no. 4 and 14, that have a lower hardness than required by STAS, i.e. 354…441 HB).

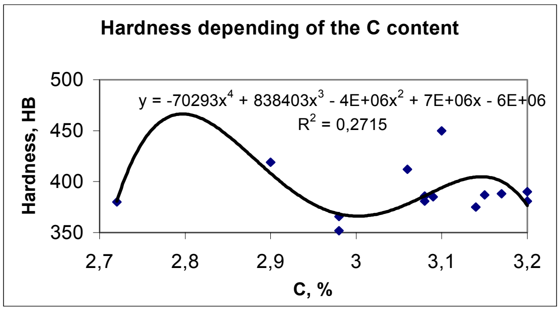

Fig.4. Variation of the hardness depending on the C content.

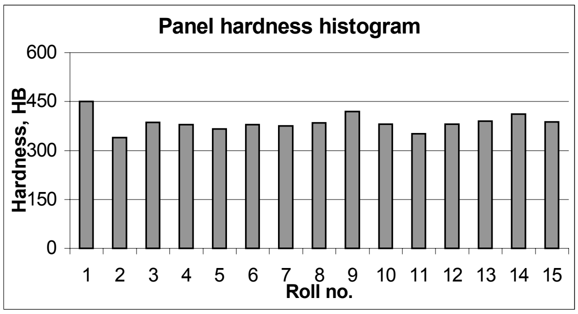

Fig.5. Panel hardness histogram

Figure 6 shows the deviation of the roll durability depending on the hardness, and figure 7 the durability histogram.

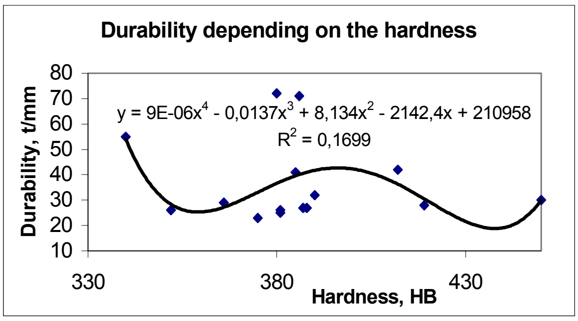

Fig.6. Variation of the durability depending on the hardness.

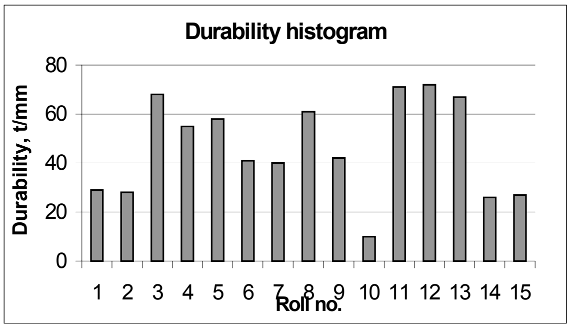

Fig.7. Durability histogram.

The reasons for taking out of operation the mill rolls are in generally the followings:

- occurring the cracks in the roll shell, because of the thermal fatigue;
- thermal wear that could be in principle explained by the different behavior of the components that form the basic metallic mass under temperature deviations. The main components within the structure of the nodular irons

used when manufacturing the mill rolls are: pearlite, cementite and nodular graphite. Cementite is the component with the highest volume variation depending on the temperature, it is strongly strained and cracks. During the rolling process, the more coarsely the cementite separations are, the more the cracks increase.

- the presence of the graphite separations leads to the increasing of the working area heat conductance, phenomenon that reduces somehow the stresses between the cold and warm areas, thus reducing the thermal wear;
- the mechanical-thermal wear, due to the passing of the warm rolled product through the roll in the austenitic field, is directly influenced by the fineness of the basic metallic mass structure and also by the form and the size of the graphite separations. In order to obtain a proper durability, a fine, homogenous structure with high pearlite dispersion degree is required.

3. CONCLUSIONS

By analyzing the 15 mill rolls cast out of nodular irons at S.C. Cilindrul S.A. Călan and tested in operation at S.C. Siderurgica S.A. Hunedoara, one can say that:

- 9 rolls (i.e. rolls no.3, 4, 5, 6, 8, 9, 11, 12, 13) went naturally out of using, and according to figure 7, they had the highest hardness values;
- 5 rolls (i.e. rolls no. 1, 2, 7, 9, 15) showed exfoliation, and the recorded durability was lower;
- 1 roll (roll no. 10) broke when driving, because of the mechanical shock.

Figure 8 shows this recorded situation as percentages.

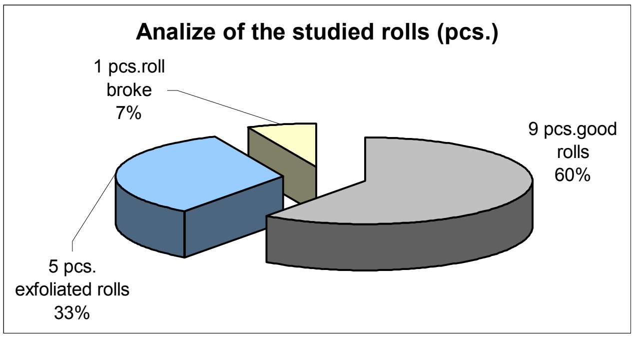

Fig.8. Analyze of the studied rolls.

BIBLIOGRAPHY

1. *Budaghianț, N. A., Karsski, V.E - Cilindri de laminor turnați, E.T., București 1986;*
2. ** * * - Studiul posibilităților fabricării cilindrilor de laminor din fonte cu grafit nodular la S.C.Siderurgica S.A.Hunedoara, Contr.Cercet, ICP, Hunedoara,1996;*
3. *Sofroni, L. ş.a. - Fonta cu grafit nodular, Editura tehnică, Bucuresti, 1978*
4. ** * * - Mică Enciclopedie de metalurgie, Ed. Ştiinţifică şi Enciclopedică, Bucureşti, 1980.*

SIMULATIONS OF THE PLATE-TYPE ELECTROSTATIC PRECIPITATORS HIGH FREQUENCY POWER SUPPLIES USING PSCAD/EMTDC 3.0.8 SOFTWARE

Gabriel Nicolae POPA[1], IOSIF POPA[1], Viorel TITIHĂZAN[2]

[1] Faculty of Engineering Hunedoara, "Politehnica" University of Timişoara, Romania
[2] Faculty of Electrical Engineering, "Politehnica" University of Timişoara, Romania

Abstract:

The globalization of the environmental pollution problems caused by the increse of industrial production will lead in the cleaning of the waste gases. The structures and control of power supplies of the plate-type electrostatic precipitators is one of the most important factor to diminish the pollution. The plate-type electrostatic precipitators must operate in its electromagnetic environment without interfering with the operation of other equipments (radios, televisions and mobil communications systems). The power supplies and the electrical model of electrostatic precipitators has non-linear elements that cause distorsions of the power supplies currents.

The paper presents the simulations of the primary and secondary currents and voltages, the total harmonic distorsion and the apparent power depending on frequency (between 4 and 24 kHz) of the plate-type electrostatic precipitators high frequency power supplies using PSCAD/EMTDC 3.0.8 software.

Keywords:
plate-type electrostatic precipitators, power supply, current harmonics

1.INTRODUCTION

In thermal power stations, the gas particles from boilers are passed through a Corona charging field where they receive an electric charge, usually negative for the plate-type electrostatic precipitators, and then as charged particles are deflected by the electric field. Then the charge particles are moved from the negative electrodes (discharge electrodes) to positive electrodes (plate electrodes) where will be deposited. The positive electrode is normally earthed. The particles are remove from the positive electrodes into receiving hoppers by mechanical shock impulse rapping in a dry application (the case of plate-type electrostatic precipitators). The plate-type electrostatic precipitators are made from a number (three or four for thermal power station) of series sections (fields), each section is energized by its own transformer rectifier set and has it own hopper [2,6].

The electric power system is very complex. EMTDC is a simulator of electric networks with the capability of modelling complex power electronics and controls of the non-linear networks. When run under the PSCAD graphical user interface, the PSCAD/EMTDC combination becomes a powerful means of visualizing the enormous complexity of portions of the electric power systems. It is widely used by electrical engineers from industries and academic institutions world wide.

For a maximum collection efficiency is important that the voltages in the sections of plate-type electrostatic precipitator (ESP) to be close by electrical discharges. This condition is carry out if the voltages in the sections of ESP are continuous adjustable in the range of Corona voltages [3]. The change of gas parameters at the entrance of ESP causes more electrical discharges and the collection efficiency slows down. The sections of ESP must have a power supply, that assure a continuous voltage, and an automat voltage regulator, with proper tuning [5].

2.HIGH FREQUENCY POWER SUPPLIES FOR PLATE-TYPE ELECTROSTATIC PRECIPITATOR

In the last two decades, the development of fast electronic switching devices (fast-thyristors, IGBT and so on) have cause the development of power supplies of ESP [1].

The main circuit of a.c.-c.c. convertor for a section of ESP is presented in fig.1.

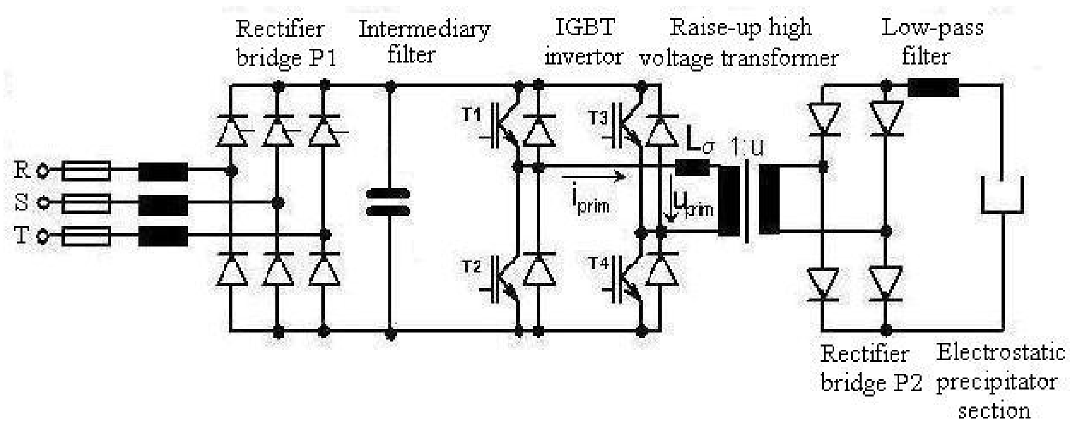

Fig.1. *A.c.-c.c. convertor for a section of ESP*

The circuit from fig.1 has the main components:

- the primary three-phase rectifier bridge P_1 without control;
- the c.c. intermediary filter to slow down the voltage ripples that is an electrolytic capacitor with small disipation;
- the primary invertor, with different configuration and components, with switching frequency in the range from kHz to 50 kHz;
- the raise-up single phase transformer at high voltage and frequency (380V/65kV) for the section of ESP; is made from ferrite toroidal core for minimize disipation;
- the secondary high voltage and frequency rectifier bridge P_2 that is used to obtain the continuous voltage in section of ESP;
- the low-pass filter to reduce the current harmonics that appears from electrical and Corona discharges; is made from R-L components.

3.SIMULATIONS OF THE PLATE-TYPE ELECTROSTATIC PRECIPITATORS HIGH FREQUENCY POWER SUPPLIES

With the PSCAD/EMTDC 3.0.8 software was simulated a high frequency power supply unit of ESP section presented in fig.2. This power supply unit may be energized a section of a large plate-type ESP (the gas flow Q=650000 m^3/h, distance between the same electrodes s=0.350 m) from the Thermal Power Station Mintia-Deva from Romania. The plate-type ESP has four identical sections. In fig.2 is presents the electrical installation of one ESP section using in simulations.

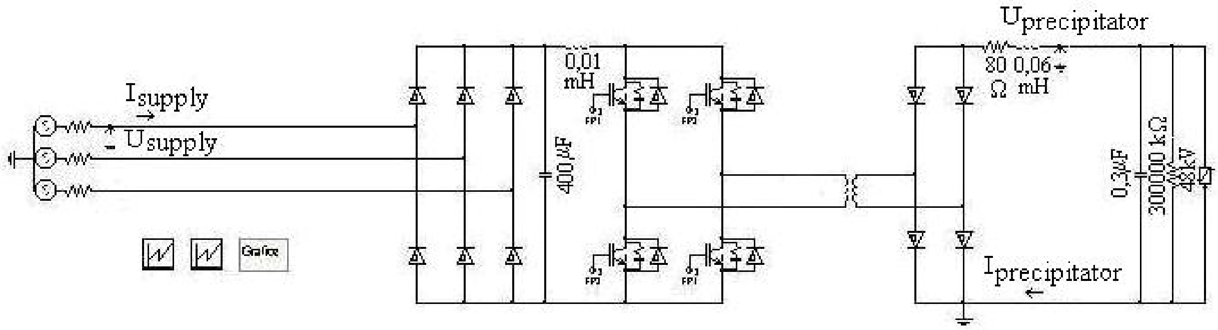

***Fig.2.** The electrical installation of the ESP section using in simulations*

The control of firing angle of transistors is presented in fig.3.

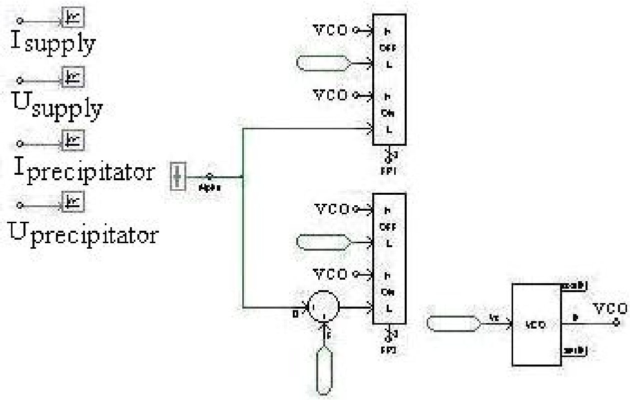

***Fig.3.** The control of firing angle of transistors*

The main parameters there are used in simulations are (fig.2): U_{supply}=380V (50Hz, 3~), C_1=400μF, L_1=10 mH (the c.c. intermediary filter); invertor with IGBT bridge; a raise up single-phase transformer 380V/65kV; R_1=80Ω and L_2=60mH (filter to reduce the current harmonics).

The section of electrostatic precipitator was approximate with a capacitor, a resistor and a varistor in parallel connection [1]. The capacitor (C=0,3μF) is the electrical capacitance of the precipitator depends on the geometrical and dimensions of the sections and the dielectric proprieties of the process gaz. The resistance (R=300kΩ) depends on the particle transport in the electrical field. The varistor (U_z=48kV) is given by electrical discharge in the section of electrostatic precipitator.

It were simulated the primary voltage and current, the secondary voltage and current for a firing angle by 30^0, at switching frequency by 16kHz.

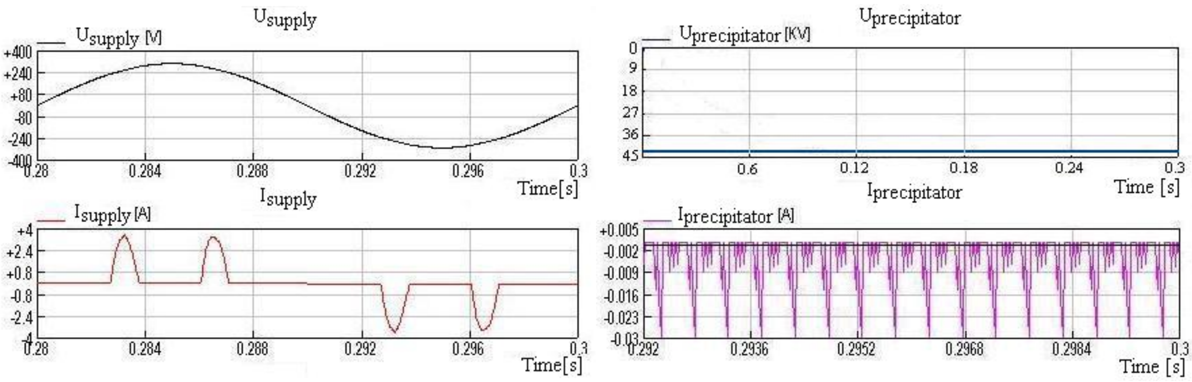

Fig.4. *The primary voltage (U_{supply}) and current (I_{supply}), secondary voltage ($U_{precipitator}$) and current ($I_{precipitator}$) for a firing angle by 30^0, at switching frequency by 16kHz*

In fig.5, 6, 7 are the harmonic analyses of primary (supply) current for the 31st harmonics current, for different firing angle of transistors between 15^0 and 165^0, for different switching frequencies 8, 16 and 24 kHz.

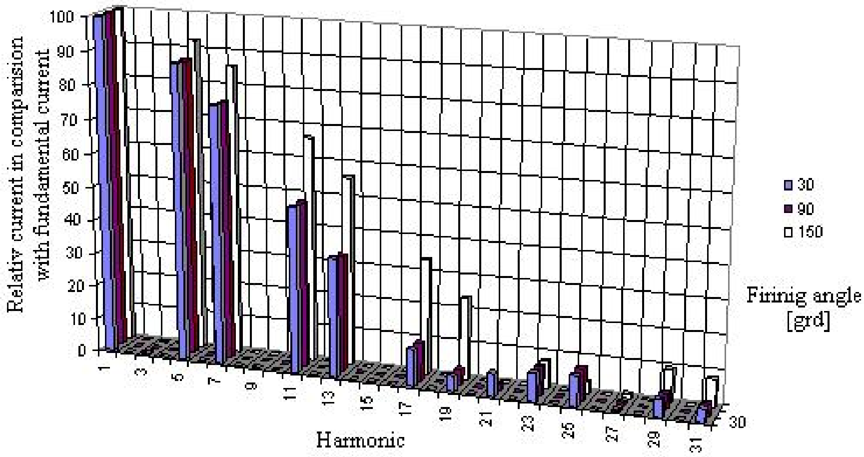

Fig.5. *Harmonic analyses of primary current (I_{supply}) at switching frequency by 8kHz*

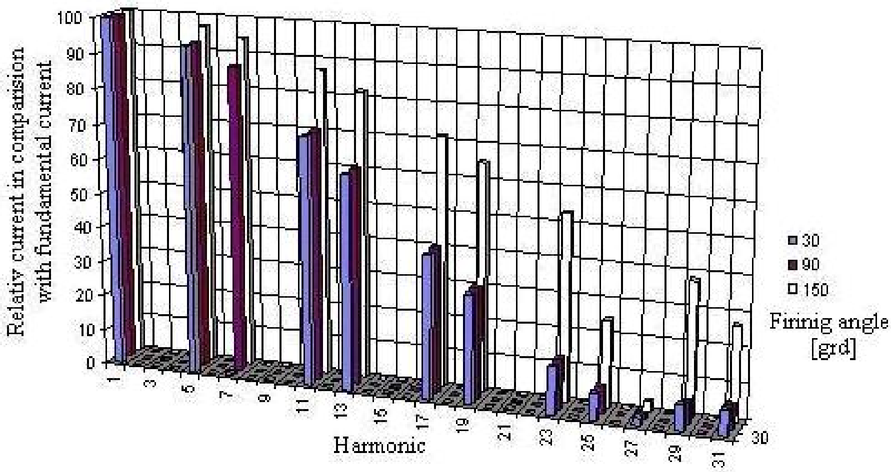

Fig.6. *Harmonic analyses of primary current (I_{supply}) at switching frequency by 16kHz*

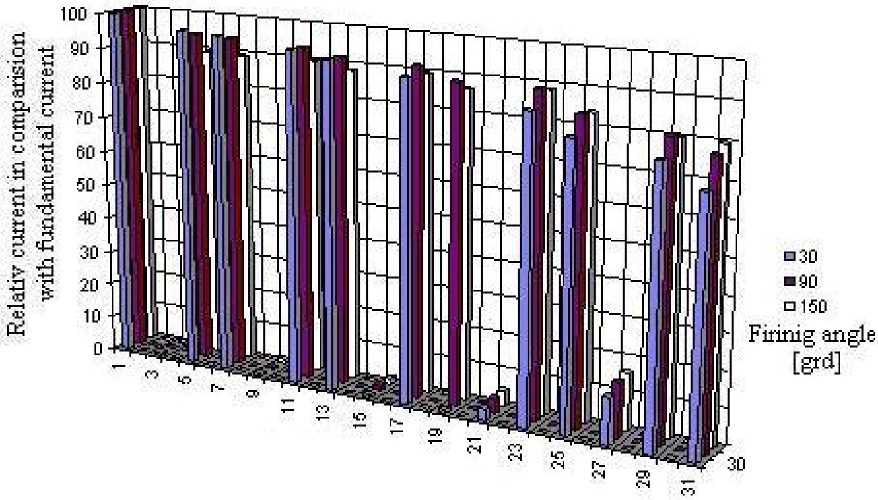

Fig.7. *Harmonic analyses of primary current (I_{supply}) at switching frequency by 24kHz*

In fig.8, 9 and 10 are present the total harmonic distorsions, the r.m.s. primary current, the first harmonic of primary current and the apparent power depending on the switching frequency.

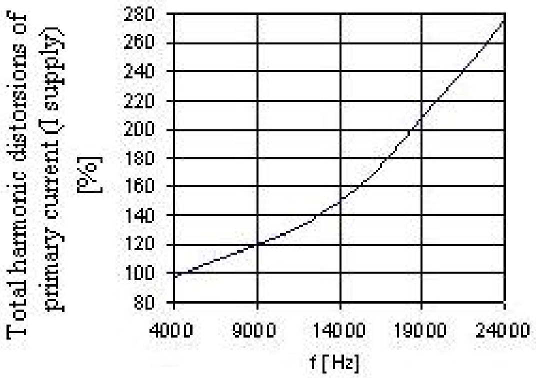

Fig.8. *The total harmonic distorsions the depending on switching frequency*

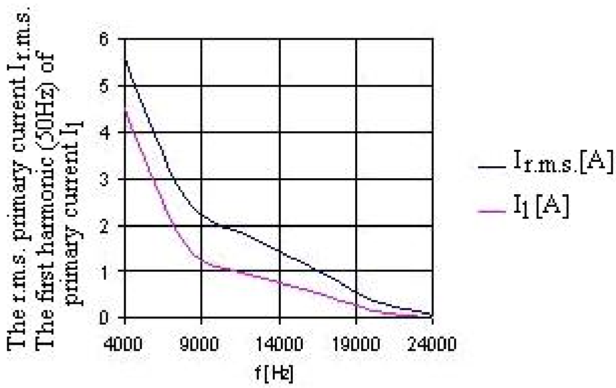

Fig.9. *The r.m.s. primary current and first harmonic of primary current depending on switching frequency*

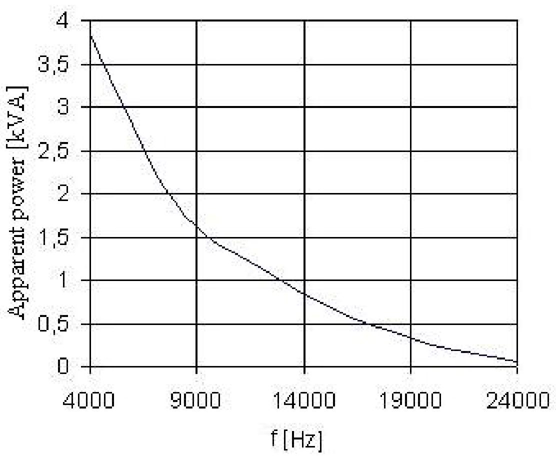

Fig.10. *The apparent power depending on switching frequency*

4.CONCLUSIONS

If its use the high frequency power supplies for plate-type electrostatic precipitator (ESP) sections, the secondary voltage (precipitator voltage) ripples slow down (fig.4) in comparision with traditional electrical power supplies (f=50Hz) [4]. The voltage control in every ESP sections may be done, without any difficult then in the case of traditional energization. From fig.5,6,7 result that the current harmonics grow up in the same time with switching frequency and the firing angle. The primary current has a lot of different harmonics and from this reason has not a sinusoidal form (fig.3). The bigger current harmonics are: 5, 7, 11, 13, 17, 19, 23, 25, 29, 31.

To diminish the harmonics amplitudes must be use passive or acive filter. Passive filter is not expensive, but it has a good function only in stationary conditions, that is not a behaviour of ESP sections. From this reason, a better filtration of primary current can be obtain with active filter, but the electrical installation for one ESP section is more expensive.

The total harmonic distorsions (fig.8) grow up and the r.m.s. primary current (fig.9) slows down in the same time with the rises of switching frequency. The apparent power (fig.10) slows down if the switching frequency rises.

The simulatuions from this paper show the posibility to use of high frequency power supplies for ESP sections, because the specify energy consumption and the gauge decrease, and the efficiency of ESP increase if it uses the performant automat voltage regulators.

5.REFERENCES

[1] Grass M. – *Fuzzy Logic – Optimising IGBT Inverter for Electrostatic Precipitators*, the 34th Annual Meeting, IEEE Industry Applications Conference, Phoenix, Arizona, U.S.A., 1999 (electronic support);

[2] Medlin A. – *Electrohydrodynamic Modelling of Fine Particle Collection in Electrostatic Precipitators*, doctorat thesis, School of Physics, University of New South Wales, Australia, 1998;

[3] Parker K.R. and other – *Applied Electrostatic Precipitation*, Chapman And Hall, London, England, 1997;

[4] Popa G.N., Popa I. - *Simulations of the plate-type electrostatic precipitators power supplies using PSCAD/EMTDC 3.0.8 software*, 6th International Conference on Acomplishments of Electrical and Mechanical Industries, pp.655-660, DEMI 2003, Banja-Luka, 2003;

[5] Prasad N.V.P.R. and other – *Automatic Control and Management of Electrostatic Precipitator,* IEEE Transactions on Industry Applications, vol. 35, no. 3, pp.561-567, may/june, 1999 ;

[6] Schmid H.J., Buggisch H. – *On the Modelling of Particle Transport in Electrostatic Precipitators*, the 7th ICESP, Kyongju, S.Korea, 1998 (electronic support).

ISIRR 2003

TECHNICAL REGULATION IN POWER QUALITY FIELD

Prof. Dr. Vladimir KATIĆ

UNIVERSITY OF NOVI SAD
FACULTY OF TECHNICAL SCIENCES
TRG D. OBRADOVIĆA 6, 21000 NOVI SAD
SERBIA & MONTENEGRO
E-mail: katav@uns.ns.ac.yu

ABSTRACT:
Electric power quality parameters and their border values are treated in the paper. Special attention is dedicated to standards and recommendations issued by International Electrotechnical Commission (IEC), which are usually used as a base for European Norms (EN). Experience from power quality research in Serbia will be also presented.

KEY WORDS:
Power quality, Harmonics, Voltage sags, Standards

1. INTRODUCTION

In the last few years, a high increase of electric energy consumption was noticed, together with wide introduction of power electronic converters in controlled electric drives and the other areas of industry. This resulted in deterioration of power quality and appearance of voltage sags and harmonic "pollution". At the same time, sophisticated, microprocessor controlled equipment, computers and tele-communication devices, sensitive to both voltage sags and harmonics type of disturbances, flooded all aspects of people every day life, business, commercial, industry, banking, government etc. The negative effects started to cause problems, mainly in industry, which lead to consumer complaints [1].

One of the methods for decreasing negative effects is establishing appropriate technical regulation – guidelines, recommendations, standards etc. The first documents were issued on national level in United Kingdom and former USSR back in 1967 and treated harmonics. After that many national and international organizations have discussed power quality parameters and issued different documents in order to explain the nature and effects of disturbances and to propose limits or border values. At the present moment, power quality issues are treated within much broader field of Electromagnetic Compatibility (EMC), which covers all kind of disturbances both of conducted and radiated nature.

The paper will present the present structure of international organizations, which deals with EMC and power quality in particular. Some of the experience from power quality research in Serbia and proposed technical regulative will be also presented.

2. ELECTROMAGNETIC DISTURBANCE PHENOMENA

EMC is defined as “the ability of an equipment or system to function satisfactory in its electromagnetic environment without introducing intolerable electromagnetic (EM) disturbances to anything in that environment” [2]. All disturbances are divided into four main categories:

- Conducted: Low frequency phenomena, High-frequency phenomena
- Radiated: Low frequency field phenomena, High-frequency field phenomena
- Electrostatic discharge (ESD)
- Electromagnetic pulses – High-altitude nuclear electromagnetic pulse (HEMP)

The parameters, which influence the quality of supply i.e. the electric power quality parameters, are treated as conducted EM disturbances.

3. CLASSIFICATION OF CONDUCTED EM DISTURBANCES PHENOMENA

Operation of a power system is always followed with large number of disturbances of different nature, duration, amplitude and spectral characteristics. A classification is presented in Table 1, where three main groups and 12 types of disturbances are distinguished [3]. Harmonics, flicker, voltage sags and interruptions have the most significant effects on operation of industry.

Table 1 – Classification of power quality parameters

Group	Type	Duration	Spectra	Amplitude
Deformation of transient nature	1. Impulses	< 200 μs	> 5 kHz	< 15 U
	2. Oscillations	< 50 ms	< 5 kHz	< 10 U
		< 20 μs	0.05-0.5 MHz	< 15 U
		< 5 μs	0.5-5MHz	< 15 U
Transient states deformation	3. Sag	0.01 - 0.6s 0.6 - 3 s 3 s - 1 min	50 Hz	0.1-0.9U
	4. Swell	0.01 - 0.6s	50 Hz	1.1-1.8U
	5. Outage	0.02-0.2s	/	0
	6. Under voltage	> 1 min	50 Hz	0.8-0.9U
	7. Over voltage	> 1 min	50 Hz	1.2-1.4U
	8. Interruptions	< 3 min	/	0
Steady state deformation	9. Harmonics	0.3 ms	0.15-5kHz	< 0.05 U
	10. Flicker		< 25 Hz	0.3-2.5U
	11. Dips & notches		0.2-0.3 kHz	0.1-0.9U
	12. Noise		> 5 kHz	0.9-1.1U

4. INTERNATIONAL REGULATIVE

Several international organizations deals with issuing technical regulative documentation in order to reach standard approach to EMC phenomena. Power quality parameters are treated by (in alphabetic order): CENELEC (Comite Europeen de Normalisation Electrotechnique), CIGRE (Conseil International des Grands Reseaux Electriques), CIRED (Congres International des Reseaux Electriques de Distribution), IEC (International Electrotechnical Commission), IEEEE (Institute of Electrical and Electronics Engineers) and UNIPEDE (Union Internationale des Producteurs et Distributeurs d'Energie Electrique),

CIGRE, CIRED and UNIPEDE are professional organizations, which issued technical regulative documents relative to member countries electric power systems [4,5,6]. These documents usually serve as basic references for preparation of CENELEC and IEC standards.

IEEE is also a professional organization, which issued guidelines, recommendations and standards targeted especially to North and South American countries [7].

CENELEC is founded in 1973. In line with the policy of the European Commission and with support from the EFTA (European Free Trade Association) Secretariat, CENELEC aims to prepare a single set of voluntary electrotechnical standards for Europe in order to support the achievement of the free market for goods and services inside Europe. European Standards are also prepared in response to specific requests from the European Commission and EFTA. A large number of co-operating partners give active support to the work of CENELEC by indicating priorities and by preparing draft specifications [8].

IEC is founded in 1906. It is the world organization that prepares and publishes international standards for all electrical, electronic and related technologies. The IEC's mission is to promote, through its members, international cooperation on all questions of electrotechnical standardization and related matters, such as the assessment of conformity to standards in the fields of electricity, electronics and related technologies. The IEC charter embraces all electrotechnologies including electronics, magnetics and electromagnetics, electroacoustics, telecommunication, and energy production and distribution, as well as associated general disciplines such as terminology and symbols, measurement and performance, dependability, design and development, safety and the environment. To further its mission, the Commission's objectives are to: meet the requirements of the global market efficiently; ensure primacy and maximum world-wide use of its standards and conformity assessment schemes; assess and improve the quality of products and services covered by its standards; establish the conditions for the interoperability of complex systems; increase the efficiency of industrial processes; contribute to the improvement of human health and safety; contribute to the protection of the environment [9].

5. IEC DOCUMENTS IN EMC FIELD

The first work in the EMC field can be traced back to when the International Special Committee on Radio Interference (CISPR, now part of the IEC) was established in 1934. But today the scope of EMC work has expanded to such an extent that the IEC organizes it among several committees. Many of these have working relationships or official liaisons with outside groups ranging from professional associations to national, regional and international organizations. The diagram on Fig. 1 outlines from an IEC perspective how these groups cooperate.

EMC-related standardization work is not limited to the IEC – indeed, numerous other organizations take part. Such groups usually deal with a large variety of technical problems, of, which EMC is only one. But clearly the greatest benefits to industry would derive if all the parties involved – worldwide – at least had access to identical Basic EMC standards.

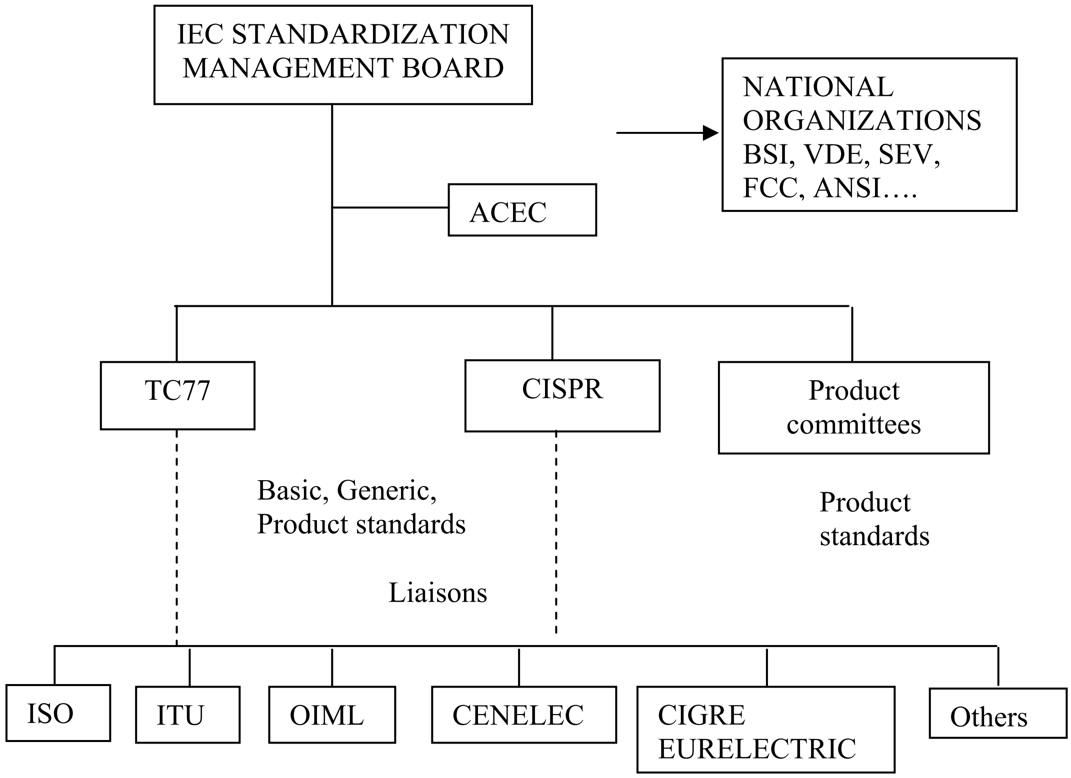

Fig. 1 - IEC and relation with other

The EMC area is covered by standards of 61000 series and this group of standards will be further discussed. Most of the IEC's EMC standards (IEC 61000) are in fact harmonized as European standards under the European Union's EMC Directive (EN 61000). They have the same numbers and titles.

6. STRUCTURE OF IEC 61000

All standards related to EMC field are divided into 3 categories:

a) **Basic standards** (gives description and definition of the phenomenon, detailed test and measurement methods, test instrumentation, basic test set up, specialized terminology, description and classification of the environment, etc.)

b) **Generic standards** (defines a set of precise EMC requirements, including limits, and indicate which standardized tests are applicable to those products intended to be used in a given environment)

c) **Product standards**, including product family standards and dedicated product standards (define specific EMC requirements, immunity and emission, and precise tests for the products within their scope).

The structure of the IEC 61000 series, large and considerably subdivided series of standards and technical reports, will consist of nine parts. Since the titles of Parts 7 and 8 are still open, the present structure is as follows:

Part 1: General: General considerations (introduction, fundamental principles, safety), Definitions, terminology

Part 2: Environment: Description of the environment, Classification of the environment, Compatibility levels

Part 3: Limits: Emission limits, Immunity limits (insofar as they do not fall under the responsibility of product committees)
Part 4: Testing and measurement techniques: Measurement techniques, Testing techniques
Part 5: Installation and mitigation guidelines: Installation guidelines Mitigation methods and devices
Part 6: Generic standards
Part 9: Miscellaneous

7. COMPATIBILITY LEVELS

The compatibility level is clearly a key quantity when it comes to setting limits. The IEC defines it as "the specified electromagnetic disturbance level used as a reference level for co-ordination in the setting of emission and immunity limits." By convention, the compatibility level is chosen so that there is only a small probability that it will be exceeded by the actual disturbance level. The probability distribution depends entirely on the method used for evaluating the levels (samples of time, location, intervals, etc.), but frequently the 95% probability level is defined as compatibility level. Table 2 shows compatibility levels of basic quantities, while harmonic levels are defined in Fig.2 for three distinguished classes of consumers.

Table 2 – Recommended compatibility voltage levels according to IEC 61000-2-4.

Disturbances	Class 1	Class 2	Class 3
Voltage variation *ΔUeff/Unom*	± 8%	± 10%	+10% do – 15%
Voltage sag *Ueff/Unom 100 [%]* *Δt (half periodes)*	10% do 100% 1	10% do 100% 1 - 300	10% do 100% 1 - 300
Interuptions [s]	None	Not applicable	≤ 60
Voltage unbalance Uneg/Upos	2%	2%	3%
Frequency tolerance *Δf/fnom*	± 1%	± 1%	± 2%

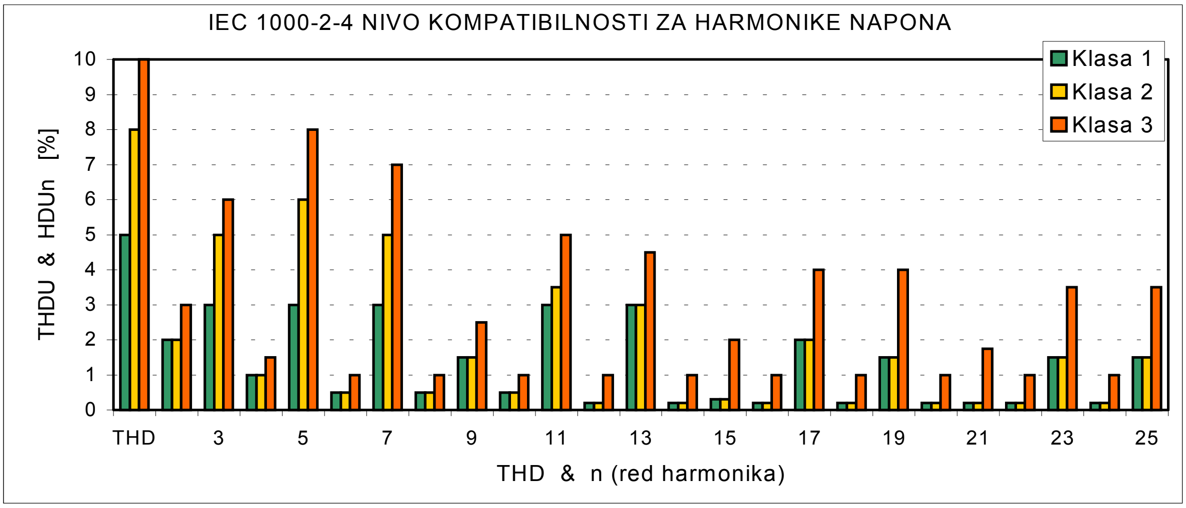

Fig. 2 – Voltage harmonics limits according to IEC 61000-2-4 [10].

8. EMC REGULATIVE IN SERBIA

At the moment, there are no power quality standards in Serbia, but for the basic quantities (voltage level, frequency and unbalance). After a long network harmonics survey, two sets of harmonics limits are proposed: lower limit (warning level) and upper limit (danger level), but they are not approved yed [11]. These levels are in accordance with IEC limits. Fig. 3 shows proposed harmonic border values for public distribution network (class 2).

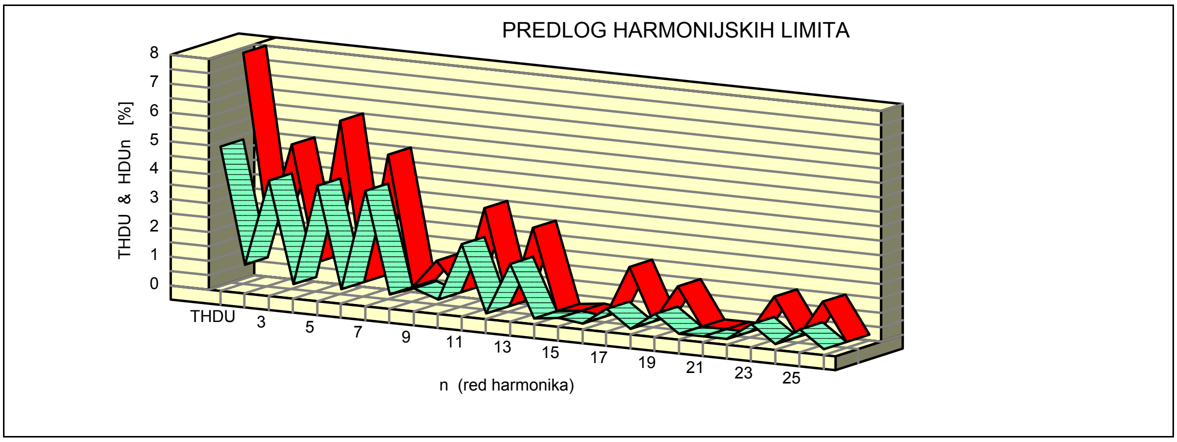

Fig. 3 – Proposed voltage harmonics levels in distribution network of Serbia [11].

9. CONCLUSION

Power quality and its compatibility levels are in focus of interest. The technical regulative is in constant development expanding globally (IEC standards). Electrical network in Serbia has to adapt it structure to the proposed limiting levels in order to be able to join to the common European grid.

10. REFERENCES

1. R.C. Dugan, M.F. McGranaghan, H.W. Beauty, *“Electric Power System Quality”*, McGraw-Hill, New York, 1996.
2. IEC 61000-1-1 (1992-05): *“Electromagnetic compatibility (EMC), Part 1: General - Section 1: Application and interpretation of fundamental definitions and terms”*, IEC Press, Geneve, 1992.
3. A.Robert, J.Marquet, "Assessing Voltage Quality With Relation to Harmonics, Flicker and Unbalance", CIGRE - 1992 Session, Paris, paper no. 36-203.
4. http://www.cigre.org
5. http://www.cired.be
6. http://www.unesco.org/uati/associations/associationseng/unipedeng.htm
7. http://www.ieee.org
8. http://www.cenelec.be; http://www.cenelec.org
9. http://www.iec.ch
10. IEC 61000-2-4 (1994-02): *“Electromagnetic Compatibility (EMC), Part 2: Environment - Section 4: Compatibility levels in industrial plants for low frequency conducted disturbances”*, International Standard, IEC Press, Geneve, 1994.
11. V.Katić, “Distribution network harmonics – research survey and experiences”, *Elektroprivreda*, Vol.54, No 3, Jul-Sep.2001, pp.72-79, *(in Serbian).*

A NUMERICAL ANALYSIS BY THE FINITE ELEMENT METHOD ABOUT THE WIRE ROPES LIFETIME CALCULATION

VÎLCEANU Lucia *, BABEU Tiberiu Dimitrie **

* Lecturer dr. eng., ENGINEERING FACULTY OF HUNEDOARA, ROMANIA,
e-mail: vilceanu63@yahoo.com
** Prof. dr. eng. Eur. eng., MECHANICAL ENGINEERING FACULTY OF TIMIŞOARA, ROMANIA, e – mail: tbabeu@mec.utt.ro

ABSTRACT

The paper presents a numerical analysis by the Finite Element Method regarding the deterioration of wire ropes subjected under variable traction loading. The FSTAR modulus, part of the COSMOS/M 2.5 software, and the PLM criterion for cumulative deterioration, has been used in order to perform the analysis. The specific and total cumulative deterioration coefficients for every loading range have been obtained after the program running.

KEYWORDS*: finite element method, cumulative deterioration, fatigue.*

1. Introduction

In order to perform a numerical analysis by the Finite Element Method regarding the wire deterioration in traction wire ropes, the FSTAR modulus, part of the Cosmos/M 2.5 software, has been used. The PLM criterion for cumulative deterioration has been considered as valid. The phenomenological definition of the deterioration process under a variable loading may be formulated as follows: the state of deterioration is considered as global state of the material, which for the initial lifetime is modified. If under a repeated loading until the crack appearance, the amplitude of cycles is non-continuous variable between the levels i = 1,…, q, the analytical expression of the PLM criterion for cumulative deterioration is:

$$\sum_{i=1}^{q} \frac{n_i}{N_i} = 1 \tag{1}$$

where: n_i – the number of loading cycles for the **i** level;
N_i - the number of loading cycles until the crack appearance (the life-time) for the **i** level.

The tests under a variable loading with single non-continuous amplitude between the σ_1 and σ_2 stress values, the succession of the loading cycles has an important effect. So, the PLM criterion became:

$$\frac{n_{11}}{N_1} + \frac{n_{22}}{N_2} = 1 \tag{2}$$

If the higher loading amplitude is applied at first ($\sigma_1 > \sigma_2$), the amount in relation (2) is less than **1**, respectively higher than **1** if the loading order is reversed.

The only logical opportunity to evaluate the safety of a machine part subjected under a variable loading consists in the introduction of the probabilistic methods: *the method of the guaranteed lifetime* **D.G** (safe-life) and *the method of the controlled deterioration* **D.C** (fail–life).

According to the **D.G** *method*, a metallic structure subjected under repeated loading, is designed for a low total or partial failure probability during the guaranteed working lifetime. When the guaranteed working lifetime is reached, the metallic element or structure must be substituted, even a perceptible deterioration may not be observed. A **D.G** designed structure is the traction chain where the working lifetime is imposed by the working lifetime of the weakest ring in the chain.

According to the **D.C** *method*, there is permitted to reach an enough low partial deterioration, which is easy to be observed and which has an enough low propagation velocity between two technical inspections, so that the loading capability of the structure (subjected under static and variable loading) will not be alterated. A classical example of a machine part, which has been designed according to the D.C conception, is represented by a wire rope composed of wires and strands. That is because when the fracture of a wire takes place, the loading capability is transferred to the other wires. The ending boundary wires, which have been fractured, represent a sign of the extension of the deterioration.

2. The lifetime calculation of wires by Finite Element Analysis

The data storage is obtained by using the NSTAR modulus, part of the Cosmos/M 2.5 software. The contact between two wires with the same diameter of 1,25 mm loaded with a pressing force of (3,6…327,5) N has been analyzed.

Nine working on loading cases have been studied for a wire rope. The loading cases have been accidentally considered both as number and amplitude of cycles. According to the same calculus model, it may be paired any number of cycles with any maximum stress.

The fatigue phenomenon induced by the maximum stress σ_{ymax}, which are not perpendicularly on the contact patch, has been simulated by accidental fatigue loading blocks (σ_{ymax} – number of cycles), see Fig. 1.

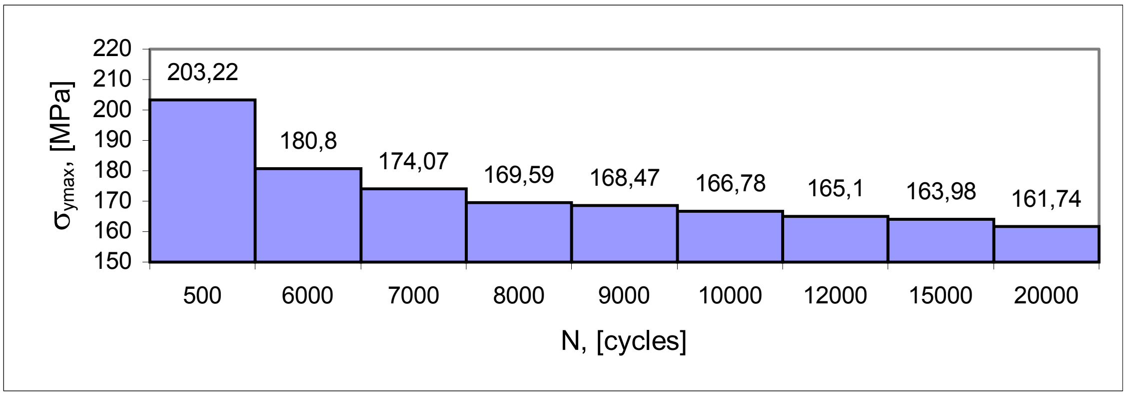

Fig.1 *Loading fatigue block σ_{ymax} – N*

The fatigue limit curve (Fig.2 – curve 1) for an alternative-symmetrical loading cycle of a non-torsion wire, which is blended on a roll with the diameter of 40 mm, has been plotted according to the experimental data [3] obtained on a fatigue contact compression test on the [NB] testing machine which belongs to the Laboratory of Strength of Materials from the Mechanical Engineering Faculty of Timisoara.

The stages to be followed to introduce the data and to use the software [5] are:

1) – The running of the Finite Element software for the contact between two wires with equal diameters of 1,25 mm, for the testing cases.

2) – The 9 testing loading steps and the associated number of cycles are entered.

3) – The central surface contact node (where the maximum stress $\sigma_{\mathbf{ymax}}$ is present) is prescribed.

4) – The fatigue limit curve (7 points on the curve 1, Fig.2, according to Table 1) is introduced. The curve followed an alternative-symmetrical loading cycle with a non-symmetry coefficient of $\mathbf{R_s = -1}$.

5) – The prescription for the results calculation is accurately defined.

6) – The software is running on according to the orders *Analysis* > *Fatigue* > *Run Fatigue Analysis*.

The particular values of the fatigue limit curve **Table 1**

N [cycles]	2000	3000	6000	20000	60000	200000	7000000
σ_{cmax} [N/mm^2]	3900	3550	3350	3100	3050	2948	2900

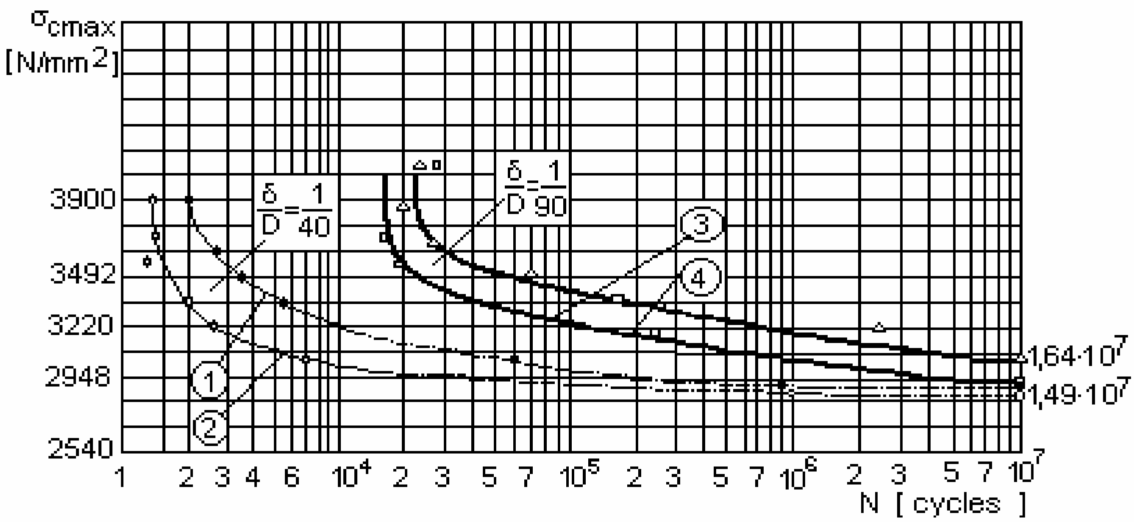

Fig.2 *The lifetime variation for the tested wires on the [NB] testing machine, in function of the contact compression stress*

3. Results and conclusions

The present calculus connects the stresses in wires, caused by the compression contact, with the lifetime of the traction wire ropes subjected to particular variable loading which have a specific nature for the working on of wire ropes.

After the software running on, the cumulative deterioration coefficients for every loading steps and the total cumulative deterioration coefficient have been obtained. The value of the total cumulative deterioration coefficient was of 6,75. A similar procedure has to be used in order to estimate the cumulative deterioration coefficient for any real loading cycle.

References:

[1] Babeu, T. – *The Basic Theory of Strength of Materials*, Mirton Publishing House, Timisoara, 1998.
[2] Ghita, E. – *Strength and working life-time of solid bodies in contact*, Mirton Publishing House, Timisoara, 2000.
[3] Vîlceanu, L. – *Contributions in the analysis of the influence of the local compresion effect about the working life-time of the component wires in a wire-rope*, Ph.D. Thesis, Defended at POLITEHNICA University of Timişoara, 2001.
[4] Zienkiewicz, O., C., Taylor R., L. – *La method des elements finis*, AFNOR Paris, 1991
[5] COSMOS/M 2.5, USER'S GUIDE, S.R.A.C., Santa Monica, Sept, 1999.

ISIRR 2003

THE ANALYTICAL STUDY ABOUT THE STATE OF STRESS FOR CONTACT BETWEEN THE STEEL ROPE'S WIRES

VÎLCEANU Lucia*, GHITA Eugen**

* lecturer dr. eng., Engineering Faculty of HUNEDOARA, ROMANIA
**conf.dr.eng., Mechanical Engineering Faculty of TIMIŞOARA, ROMANIA

Abstract

Examining the wires of an out-of work steel rope, they noticed that the local compression stress in between the wires had such high values that it produced an impression on the wire in the contact area. The contact stress appears between the wires of the same rope strand, of two adjacent rope strands and between the wires and the rope sheave.

The level of stress is function of the load, the geometry of the common contact surface and the Young's modulus. The practical observations are confirmed by the analytic calculations on the basis of Hertz's theory.

Keywords: local compression, contact stress, Hertz's theory.

1. Introduction

In order to perform a calculus at the contact between two rope's wires there is necessary to know the curvature radius and the contact forces both between wires and between a wire and the roll in contact. The distribution of forces on a bended wire around a roll is presented in Fig.1, where r is the curvature radius of the rope strand.

For the case of a wire rope composed from n_t rope strands, the average contact force on a wire has to be calculated with the formula

$$P_0 = \frac{4L\delta}{n_t D\ d} F \tag{1}$$

If a wire rope is wrapped up around a roll and is subjected to traction force F, then the interaction forces V and K actuate between the rope strands. The analytic relations in order to estimate the interaction forces are:

$$V = \frac{2\pi^2 (d - d_1)}{n_t L \sqrt{L^2 + \pi^2 (d - d_1)^2}} F \tag{2}$$

$$K = \frac{V}{2\cos\gamma} \tag{3}$$

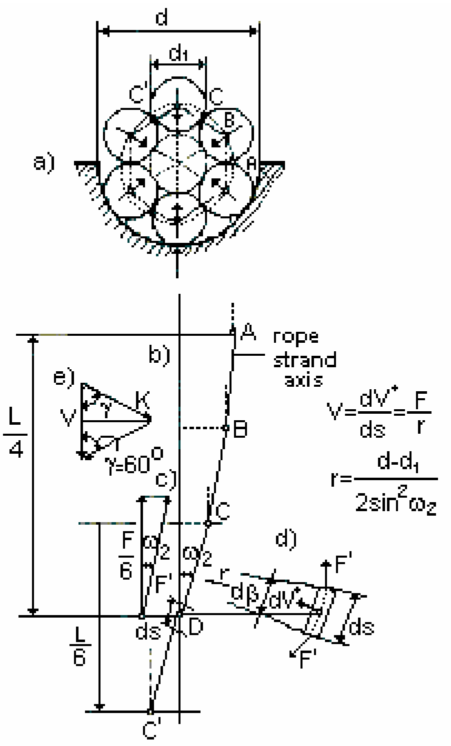

Fig.1. *Forces distribution on a bended wire around a roll*

The pressing force on the wires belonging to a rope strand when the wire rope is subjected to traction is:

$$P_{0s} = \frac{\sin\omega_1 \cdot tg\omega_1}{2n_t \sin\omega_2 \cos\gamma} \cdot \frac{\delta}{d - d_1} F \tag{4}$$

If the helix angles in a rope strand or a wire rope have the same value ($\omega_1 = \omega_2$), there will be obtained:

$$P_{0s} = \frac{\pi}{2n_t \cos\gamma} \cdot \frac{\delta}{L} F \tag{5}$$

For the characteristic case when $n_t = 6$ rope strands, $L = 7{,}5d$; $L' = 10d_1$; $\omega_1 = 15^0 40'$; $\omega_2 = 17^0 28'$; $\gamma = 60^0$; $d - d_1 = 2d/3$, according to (2), (3) and (5) the results will be:

$$V = K = \frac{1}{26{,}5d} F \quad \text{and} \quad P_{0s} = \frac{1}{15{,}9} \cdot \frac{\delta}{d} F \tag{5,a}$$

The interaction force between wires in the contact point or on the contact generatrix, for the case when the wire rope is wrapped on around a roll with the diameter D, will have the analytic expression:

$$P_0 = \frac{F \cdot \delta}{2n_t \sin\omega_1 \cdot \cos\gamma} \left[\frac{n_t - 1}{D} + \frac{\sin\omega_2 \cdot tg\omega_2}{d - d_1} \right] \tag{6}$$

For the usual values $n_t = 6$; $L = 7{,}5d$; $L' = 10d_1$; $\omega_1 = 15^0 40'$; $\omega_2 = 17^0 28'$; $d - d_1 = 2d/3$; $\gamma = 60^0$, there will be obtained

$$P_0 = F \cdot \delta \left[\frac{2{,}8}{D} + \frac{1}{15{,}9d} \right] \tag{6,a}$$

2. The calculus of the contact pressure

The Hertz's theory is used to calculate the maximum p_0, respectively the average contact pressure p_m, in the framework of the elastic range:

$$p_0 = -\frac{3 \cdot \sqrt[3]{P_0 \left(E \cdot \Sigma\rho\right)^2}}{4\pi(\eta\chi)} = -\frac{3P_0}{2\pi ab} \quad (7)$$

$$p_m = -\frac{\sqrt[3]{P_0 \left(E \cdot \Sigma\rho\right)^2}}{2\pi(\eta\chi)} \quad (8)$$

where: P_0 - the pressing force between the two bodies in contact, [N];

a, b – the half-axis of the elliptic contact patch, [mm];

E^* - the equivalent Young's modulus, $\frac{1}{E^*} = \frac{1}{2}\left(\frac{1}{E_1} + \frac{1}{E_2}\right)$ [MPa];

E_1, E_2 - the Young's modulus of the two bodies in contact, [MPa];

$\Sigma\rho$ - the amount of main curvatures of the surfaces in contact in the near vicinity of the contact point, [mm^{-1}] $\quad \Sigma\rho = \rho_{11} + \rho_{12} + \rho_{22} + \rho_{21} = \Sigma\frac{1}{R_i}$ (9)

The above-mentioned relationships may be adjusted (Fig.2) for the case of a wire belonging to a wire rope:

$$\rho_{11} = -\frac{1}{R_{11}}; \quad \rho_{12} = \frac{1}{R_{12}}; \quad \rho_{21} = \frac{1}{R_{21}}; \quad \rho_{22} = -\frac{1}{R_{22}},$$

where: R_{11} – the curvature radius of the deformed shape of the wire rope, [mm];

R_{12} – the nominal radius of the wire rope, [mm];

R_{21} – the radius of the take-up roller, [mm];

R_{22} – the guidance radius of the take-up roller, [mm].

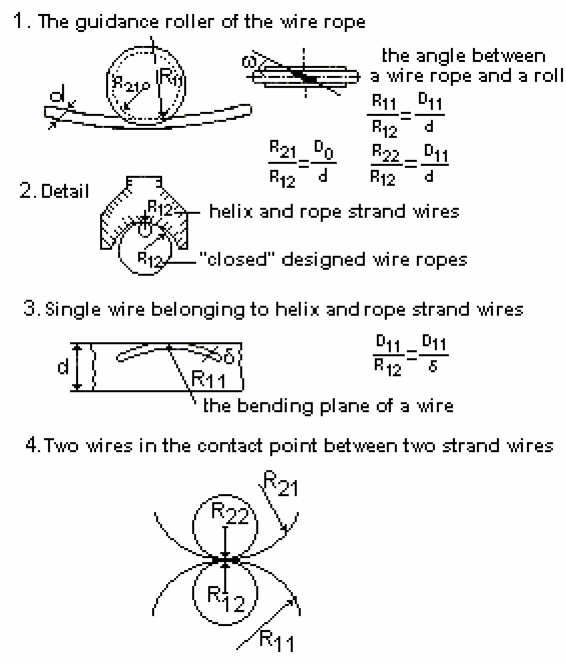

Fig.2. *The main curvature radius in the wire-wire, respectively wire-roll contact areas*

If the following notations are used: d – the diameter of the wire rope, [mm]; δ - the diameter of the wire, [mm]; D_{11} - the diameter of the deformed shape of the wire rope, [mm]; D_i – the diameter of the wire rope guidance, [mm]; D – the diameter of the wire rope take-up roller, [mm], the following mathematical relation will be obtained:

$$\Sigma\rho = 2\left[\frac{1}{D_{11}} + \frac{1}{\delta} + \frac{1}{D} + \frac{1}{D_i}\right] = \frac{2}{\delta}\left[1 + \frac{\delta}{D_{11}} + \frac{\delta}{D} + \frac{\delta}{D_i}\right] \tag{10}$$

The value ($\eta\chi$) is graphically obtained from the Fig.3, in function of the angle θ, where θ is defined by the relation

$$\cos\theta = \frac{\sqrt{(\rho_{11}-\rho_{12})^2 + 2(\rho_{11}-\rho_{12})(\rho_{21}-\rho_{22})\cos 2\omega + (\rho_{21}-\rho_{22})^2}}{\Sigma\rho} \tag{11}$$

In the relation (11) it was noticed ω, the angle between the axis of the wire rope or of the component wire and the symmetry plane of the roller (Fig.2).

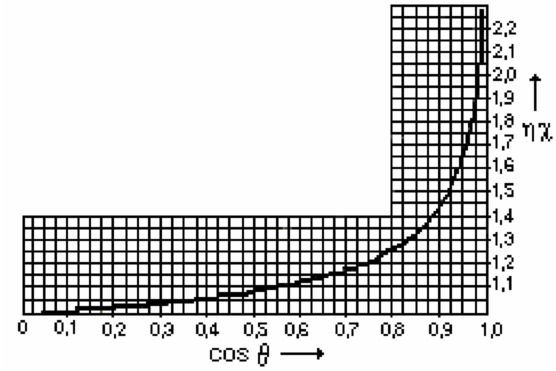

Fig.3. *The value ($\eta\chi$) in function of the angle* θ

For a general case, it will be obtained:

$$\cos\theta = \frac{\sqrt{\left(\frac{1}{D_{11}} - \frac{1}{\delta}\right)^2 + 2\left(\frac{1}{D_{11}} - \frac{1}{\delta}\right)\left(\frac{1}{D} - \frac{1}{D_i}\right)\cos 2\omega + \left(\frac{1}{D} - \frac{1}{D_i}\right)^2}}{\frac{1}{D_{11}} + \frac{1}{\delta} + \frac{1}{D} + \frac{1}{D_i}} \tag{12}$$

By using the notation

$$M = 1 + \frac{\delta}{D_{11}} + \frac{\delta}{D} + \frac{\delta}{D_i}, \tag{13}$$

for the case $\omega = 0$, the maximum pressure will became

$$p_0 = -\frac{0{,}38}{\eta\chi} \cdot \sqrt[3]{E^2} \cdot \sqrt[3]{M^2} \cdot \sqrt[3]{\frac{P_0}{\delta^2}} \tag{14}$$

Finally, the following relation will be obtained

$$p_0 = -k_3 \cdot \frac{\sqrt[3]{M^2}}{\eta\chi} \cdot \sqrt[3]{P_0} \tag{15}$$

For the external layer wires in contact with the guidance in the roll, the value of the coefficient k_3 is dependent by the character of the material of the guidance roll, in accordance with the Table 1, [3].

The value of the coefficient ***k_3*** **Table 1**

Material of the roll	Steel	Cast iron	Hard rubber	Lining	
				Leather	Wood
k_3	280	230	13	2,8	7

3. The analytic relations to calculate the contact pressure for the traction wire ropes composed by rope strands

By using the relations (7), (9), (11), adjusted for the same type of wire rope, the following relations to calculate the contact pressure will be obtained for different contact geometries:

a) The contact between the wires and the roll

a.1) – Cross knitted wire ropes (ω = 0)

$$p_0 = -\frac{280}{\eta\chi}\cdot\sqrt[3]{\left(1+\frac{\delta\sin^2\omega_1}{d_1}+\frac{\delta}{D}-\frac{\delta}{D_i}\right)^2}\cdot\sqrt[3]{\frac{P_0}{\delta^2}} \tag{16}$$

and

$$\cos\theta = \frac{1}{M}\left|1-\frac{\delta\sin^2\omega_1}{d_1}-\frac{\delta}{D}-\frac{\delta}{D_i}\right| \tag{17}$$

The usual values for the quantities between brackets are presented in Table 2.

The usual values for wire ropes **Table 2**

Wire ropes with six rope strands	d_1/δ	$d_1/\sin^2\omega_1\delta$		D_i/δ	D/δ	
		$L'=10d_1$	$L'=8d_1$		Roll	Puttee
7 wires in a rope	3	33	22	10...12		500...1000
19 wires in a rope	5	55	37	18...22	80…200	500...1000
37 wires in a rope	7	78	52	23...25	(100)*	500...1000

* - for parallel knitted wire ropes

a.2) - Parallel knitted wire ropes (ω = 27^0... 30^0)

The analytic expression of the pressure p_0 remain as in the mentioned above case, but the value of cos θ has a different one:

$$\cos\theta = \frac{1}{M}\sqrt{\left(1-\frac{\delta\sin^2\omega_1}{d_1}\right)^2 - 1{,}2\left(1-\frac{\delta\sin^2\omega_1}{d_1}\right)\left(\frac{\delta}{D}+\frac{\delta}{D_i}\right)+\left(\frac{\delta}{D}+\frac{\delta}{D_i}\right)^2} \tag{18}$$

The usual values for the quantities between brackets are found in the Table 2, and the values of the average contact force $\mathbf{P_0}$ has to be calculated according to the formula (1).

b) The contact between two component wires of a wire rope

For the both knitting methods (parallel, respectively in cross), the following mathematical relations for p_0 and cos θ will be obtained:

$$p_0 = -\frac{444}{\eta\chi}\cdot\sqrt[3]{\left(1+\frac{\delta\sin^2\omega_1}{d_1}\right)^2}\cdot\sqrt[3]{\frac{P_0}{\delta^2}} \tag{19}$$

and
$$\cos\theta = \left[\frac{1-\frac{\delta \sin^2\omega_1}{d_1}}{1+\frac{\delta \sin^2\omega_1}{d_1}}\right]\cos\omega \tag{20}$$

The interaction force P_0 in the formula (19) will be calculated according to the formula (6).

4. Conclusions

After the level of the normal stresses in the wire is calculated, the equivalent normal stress will be obtained according to one of the strength theories. The mathematical expressions of the main stresses in the contact patch between two bodies will be, [2]:

$\sigma_1 = \dfrac{2+\nu\frac{b}{a}}{\nu\left(1+\frac{b}{a}\right)}p_0$ - the longitudinal stress along the main axis of the contact ellipse,

$\sigma_2 = \dfrac{2\frac{b}{a}+\nu}{\nu\left(1+\frac{b}{a}\right)}p_0$ - the transversal stress along the secondary axis of the contact ellipse,

$\sigma_3 = -\dfrac{3P_0}{2\pi ab} = -p_0$ - the vertical stress along the normal direction on the contact patch.

In accordance with the shape modifying strength theory, the equivalent stress will be, [1]
$$\sigma_{echV} = \sqrt{\sigma_1^2+\sigma_2^2+\sigma_3^2-\sigma_1\sigma_2-\sigma_2\sigma_3-\sigma_3\sigma_1} \tag{21}$$

For the particular cases of wire ropes or even wires in contact, the maximum contact pressure p_0 is accompanied by the traction stress σ_t and the bending stress σ_i. The bending stress σ_I has a negative value because on the contact area between the wire rope and the roll, the bending became compression. So, the main stress along the wire is
$$\sigma_1 = \frac{2+\frac{b}{a}\nu}{\nu\left(1+\frac{b}{a}\right)}p_0 + (\sigma_t - \sigma_i) \tag{22}$$

The researches of A. Dumas [3] conduce to the value of the average accepted pressure $p_{0\max} = \frac{HBS}{2}$, where HBS is the hardness of the surface which has been estimated according to the Brinell's procedure, or $p_{o\max} \cong 2\sigma_r$, where σ_r is the ultimate strength of the wire material.

REFERENCES:

[1] Babeu, T. – The Basic Theory of Strength of Materials, Mirton Publishing House, Timisoara, 1998.

[2] Ghita, E. – Strength and working life-time of solid bodies in contact, Mirton Publishing House, Timisoara, 2000.

[3] Vîlceanu, L. – Contributions in the analysis of the influence of the local compresion effect about the working life-time of the component wires in a wire-rope, Ph.D. Thesis, Defended at POLITEHNICA University of Timişoara, 2001.

THE MEASUREMENTS OF CORONA SOUNDS FOR AN ELECTROSTATIC DISCHARGE SYSTEM

GABRIEL NICOLAE POPA[1], VIOREL TITIHĂZAN[2], IOSIF POPA[1]

[1] Faculty of Engineering Hunedoara, "Politehnica" University of Timişoara, Romania
[2] Faculty of Electrical Engineering, "Politehnica" University of Timişoara, Romania

Abstract:

The paper presents some measurements of Corona sounds for an electrostatic discharge system. The electrostatic discharge system it is a model with scale 1:5 for an area from a plate-type electrostatic precipitator section. The electrostatic discharge system has two electrodes: a discharge electrode (a piece from ISODYN B5 discharge wires with five pins) and a plane electrode. The distance between electrodes may be modify up to 50mm and the voltage up to 10kV. Using this electrostatic discharge system and a measuring system with data acquisition card (ADA 3100), may be study the Corona sounds from a plate-type electrostatic precipitator.

Keywords:
Corona, sounds, electrostatic, discharge, system, electrostatic precipitator

1.INTRODUCTION

In a plate-type electrostatic precipitator the dust particles are charged by electrones generated by negative Corona discharge. The Corona discharge depends on the electrical field strength and the shapes of discharge electrodes. The measurements of Corona sounds are often risky for an electronic equipment used in experiments. For a plate-type electrostatic precipitator the distance between the electrodes is up to 0,2 m and the maximum voltage is up to 50kV. The measurements of Corona sounds from a plate-type electrostatic precipitator are difficult to be done. From this reason, it is used an electrostatic discharge system with scale 1:5 for the measurements of Corona currents.

2.THE ELECTROSTATIC DISCHARGE SYSTEM AND THE MEASUREMENT DEVICES

In fig.1 is presented the electrostatic discharge system (EDS) using for experiments. In the left side is the discharge wire with five pins and in the right side is a plane electrode. The electrodes are mounted on electrical insulators (by 20kV).The discharge wires are fixed on textolit base and the plate electrode can be moved up to 50mm. Between the electrodes the voltage is continuous. If the supply of the discharge wire is with "-" polarity then the supply of the electrode is named negative Corona and if the discharge wire is with "+" polarity then the supply of the electrode is named positive Corona. For the plate-type electrostatic precipitators are used the negative Corona.

Fig.1. *Electrostatic discharge system*

The number of free electrons n[-] at the distance r[m] from the Corona negative is:

$$n = e^{\alpha \cdot r} \qquad (1)$$

where $\alpha[m^{-1}]$ is Townsend first coefficient of ionization. The discharge wire is bombarded with the positive ions that emits new electrons starting new avalanche. At higher voltages applied between electrodes appear the Trichel currents with frequency f_t. Between the frequency f_t [Hz] and the Corona currents i[A] is a linear function:

$$f_t = k_w \cdot i \qquad (2)$$

k_w[Hz/A] is a constant of proportionality. The coefficient k_w depends on pin diameter [1,3]. For the supply of electrostatic discharge system is used the circuit from fig.2.

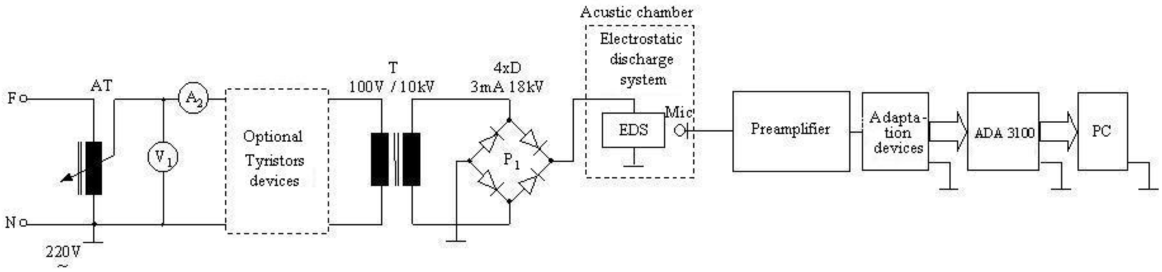

Fig.2. *Electrical circuit that is used to measure the Corona sounds*

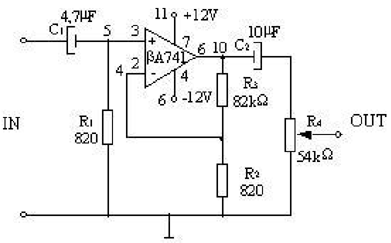

Fig.3. *Electrical circuit of preamplifier*

In fig.2 are used an autotransformer AT (0÷220V, 50Hz) to modify the voltage on electrode from electrostatic discharge system. Optional, is used a tyristors circuit for modify the voltage's shape and value. To obtain the Corona discharge is used the transformer T (100V/10kV) and the voltage is rectified with high voltage rectifier bridge P_1.

The Corona sounds from EDS is measured with a precision preamplifier (fig.3) that converts the sounds into voltages. To convert the signal into a voltage that may be measured with the data acquisition card (DAC) ADA 3100, is used an adaptation devices that assures the galvanic separation and convert the voltages. The DAC is connected to a personal computer PC that has a software (Signal View) for processing the signals [2,4]. The measuring sounds must not be disturb by the external perturbation. From this reason, the EDS was introduce into acustic chamber. The preamplifier has an amplification up to 100 that be modify from the resistor R_4.

3.THE MEASURING OF CORONA SOUNDS

In fig.2 is presented the positive Corona supply of electrostatic discharge system (+ on the discharge wire). If the bridge P_1 is connected with "-" on the discharge wire then it obtain the negative Corona.

To measuring the Corona sounds was used two cases:

- positive Corona discharge (+ on the discharge wire);
- negative Corona discharge (- on the discharge wire)

at different distances and voltages between the electrodes of EDS.

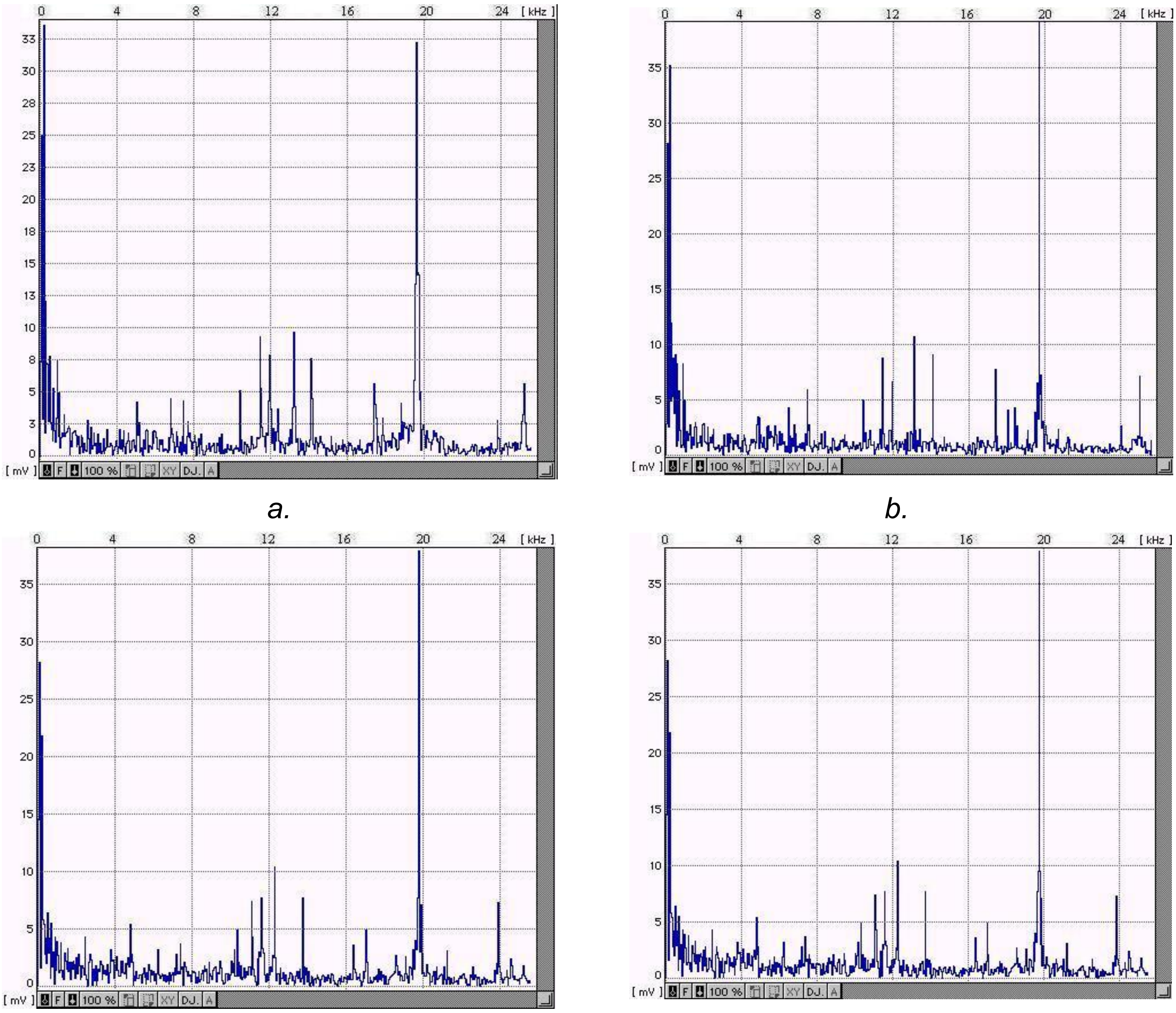

a. *b.* *c.* *d.*

Fig.4. *Harmonic analyses of Corona sounds at positive Corona (U^+) discharge: a. d=2cm, U^+=4kV; b. d=2cm, U^+=6kV; c. d=2cm, U^+=8kV; d. d=2cm, U^+=10kV*

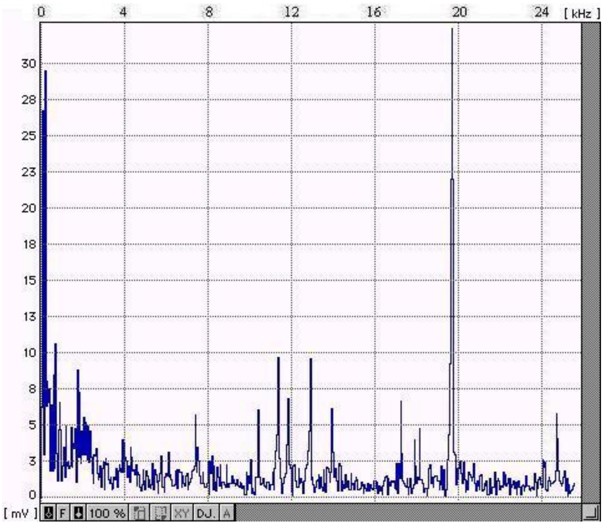

e.

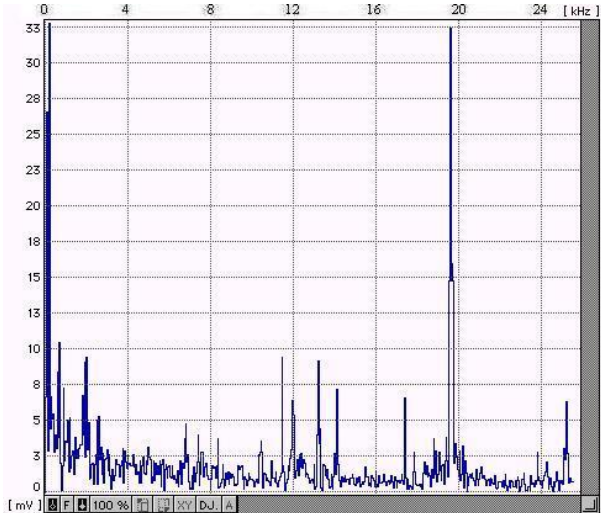

f.

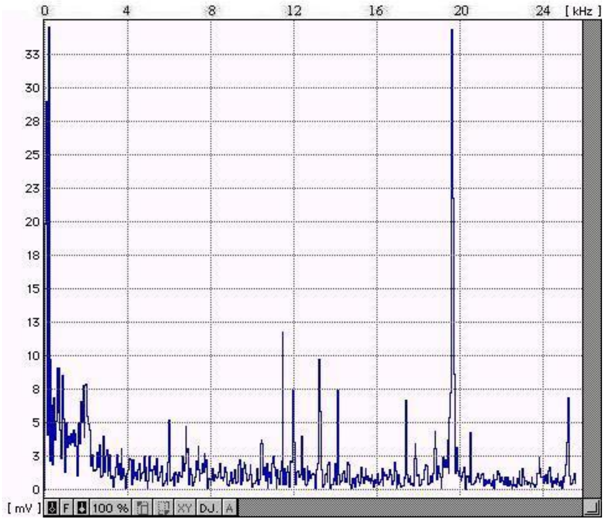

g.

Fig.4. *Harmonic analyses of Corona sounds at positive Corona (U^+) discharge:*
e. d=3cm, U^+=10kV; f. d=4cm, U^+=10kV; g. d=5cm, U^+=10kV

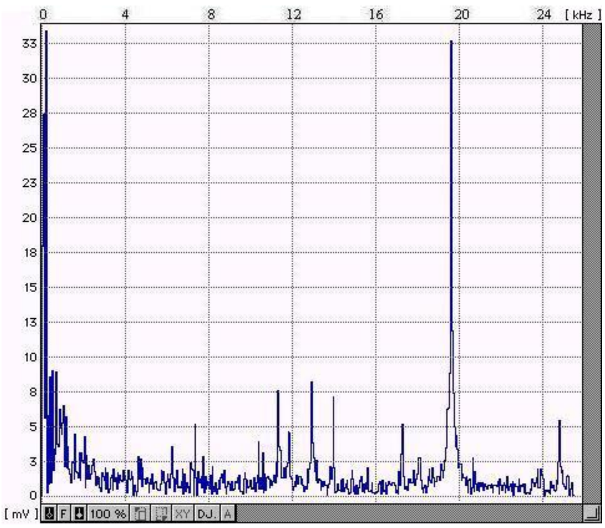

a.

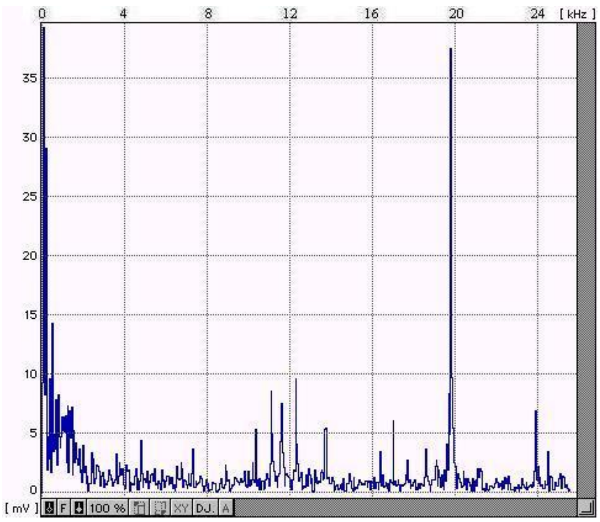

b.

Fig.5. *Harmonic analyses of Corona sounds at negative Corona (U^-) discharge:*
a. d=2cm, U^-=4kV; b. d=2cm, U^-=6kV

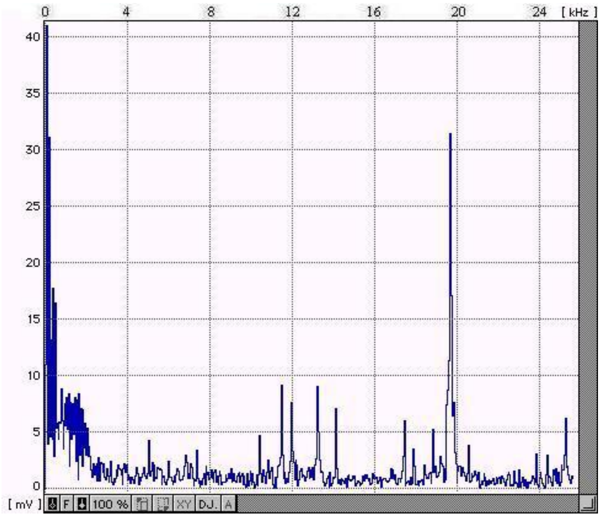

c.

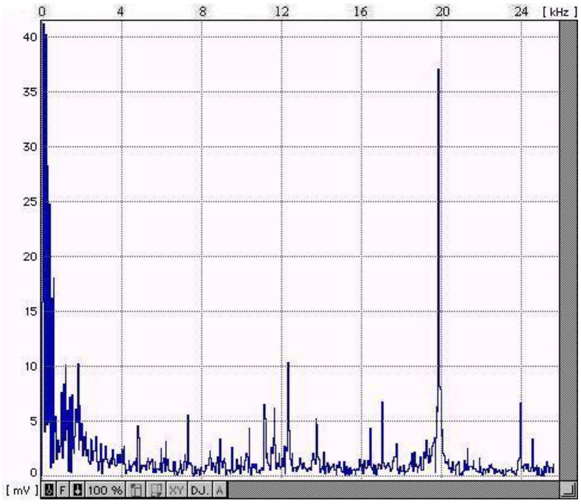

d.

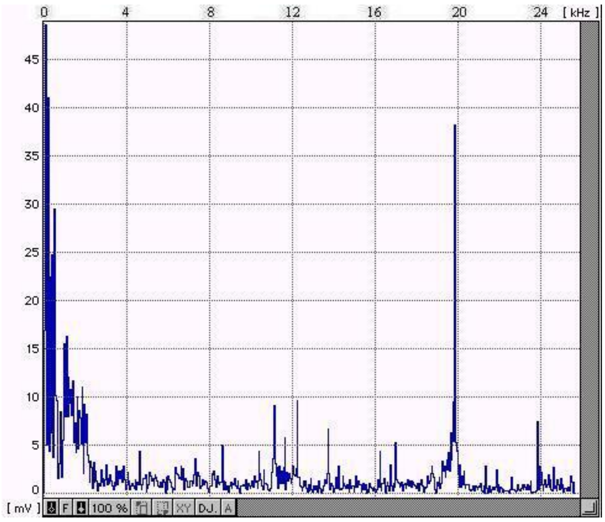

e.

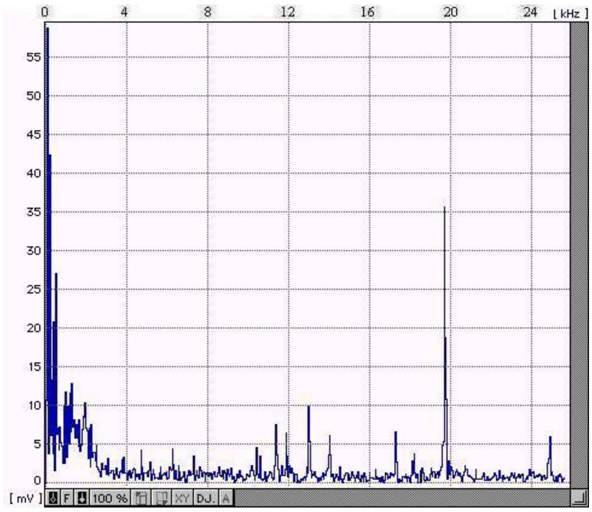

f.

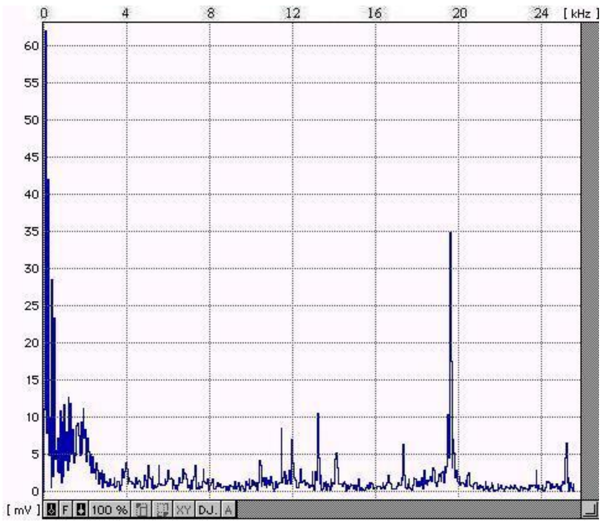

g.

Fig.5. *Harmonic analyses of Corona sounds at negative Corona (U^-) discharge: c. d=2cm, U^-=8kV; d. d=2cm, U^-=10kV; e. d=3cm, U^-=10kV; f. d=4cm, U^-=10kV; g. d=5cm, U^-=10kV*

In the case of positive supply at the distance by 1 cm and the voltage by 7kV, the electrical discharge appears, and in the case of negative supply at the distance by 1 cm and the voltage by 10kV, the electrical discharge does not appear.

4.CONCLUSIONS

In the case of positive Corona (fig.4), for the same distance between the electrodes (d=2 cm) the 19.5kHz harmonic grows up until become constant with the increase of voltage. If it is the same voltage (10kV), the 50Hz harmonic (fundamental) grows up with the distance between the electrodes and 19.5kHz harmonic slows down with the increase of distance between the electrodes.

The fundamental harmonic of the sound (50Hz), in the case of negative Corona (fig.5), in the same conditions, is bigger than in the case of positive Corona. The most important harmonic is that with frequency by 19.5kHz. The 19.5 kHz harmonic has the constant amplitude with the voltage increase, if it is the same distance between electrodes, the 19.5 kHz harmonic slows down. Other harmonics with bigger amplitude have the frequencies by 2kHz, 12kHz and 24kHz.

The 50Hz harmonic has a bigger value in the case of negative Corona, but the 19.5 kHz harmonic has a reverse behaviour. In the both situations, appear Trichel spectrums. The exponential increase and decrease, that are specify for Trichel spectrums, are the same in negative and positive Corona. The appear Trichel spectrums are more visible at 19.5kHz, 12kHz and 25kHz frequency. The harmonic amplitude, in the case of positive Corona are bigger than in the case of negative Corona.

5. REFERENCES

1. Kucerovsky Z., Greason W.D., Weigl A., *Corona Wind in a System with the Pin to Plane Discharge Geometry*, 34^{th} Annual Meeting, IEEE Industry Applications Conference, U.S.A., 1999;
2. Kucerovsky Z., Greason W.D., Doyle T., *Data Acquisition System for the Measurements of Corona Currents*, 33th Annual Meeting, IEEE Industry Applications Conference, U.S.A., 1998;
3. Seaver A.E., *Mobility and High Electric Fields*, IEEE Transactions on Industry Applications, vol.33, no.3, may/june, 1997;
4. ***, *ADA 3100 Manuals*, U.S.A., 1994.

ISIRR 2003

THEORETICAL RESEARCHES REGARDING THE DETERMINATION OF THE STRESSES WHICH APPEAR IN THE NOZZLES OF THE PEST AND DISEASES CONTROL THROUGH CHEMICAL MACHINERY USING COMPUTER PROGRAMME "COSMOS/M" WITH FINIT ELEMENT

BUNGESCU Sorin-Tiberiu[1]
BIRIŞ Sorin-Ştefan[2], VLĂDUŢ Valentin[3]

[1]U.S.A.M.V.B. Timişoara
[2]"Politehnica" University of Bucharest, [3]I.N.M.A. Bucharest

Abstract:

In speciality reference material from our country and in the countries with an advanced agriculture it hasn't appeared yet a calculation methodology with a view to projection's optimisation of these nozzles and on this line, the current paper, tries to bring a contribution in this field, benefiting by the advantages on which it presents the application of the analysis method with finite elements respectable programme of computer "COSMOS/M".

By means of "Finite Elements Method" (FEM) respectively of "COSMOS/M" programme it could be performed the stress state,s modelling in the nozzles, finally the author achieving one subprogramme of calculus. On the basis of this subprogramme, a complete study of the stress state was effected, using the "Finite Elements Method" (FEM).

Following the analysis with finite elements were calculated all the component parts of the stess tensor from the network's knots, as well as, from the centre of each finite element, for one working regime.

Keywords:
nozzle, Finite Elements Method, strength, stress, digitisation, the 5th theory of strength, COSMOS/M

1. INTRODUCTION

The methods of pest and diseases control of the agricultural crops through chemical way, by sprinkling, hold the biggest weight from the methods applied and utilized in crops protection.

It is estimated that the application of this method represents about 75% from the altogether of the ways and methods of control with pesticides in agriculture.

The application of the liquid pesticides by sprinkling it is achieved under the aspect of a very fine film or under the aspect of some extreme small drops. The fineness of the dispersion it is estimated by the size of the particles' (drops') diameter. The uniformity constitutes a distinct specific feature, considering that a dispersion is all the more uniform as the quantity of the particles with the same diameter is bigger.

The spraying of the solid chemical substances it is achieved by means of the nozzles. For the achievement of a suitable spraying of the chemical substances and implicitly of a quality uniformity of these it is imperious necessary that the nozzles to have a long tiredness in time. Also, the nozzles must be strength at the chemical action of the utilized substances at the pest and diseases control in agriculture.

Therefore, the study of the strength state out of the nuzzle represents a very important present problem, which leads to the achievement of some nozzles which resist in time at both tiredness and chemical action of the sprinkled substances.

2. THE MODELLING OF THE STRESS STATE FOR HARDY NOZZLE, USING THE PROGRAMME WITH FINIT ELEMENT "COSMOS/M"

Within the framework of the Strength of Materials Department from the Technical University Timişoara was studied the Hardy nozzles (figure 1), utilized at the sprinkling of the crops. The study followed the determination of the maximum stress zones, where can appear fissures or even tears during the working process, using the Finit Element Method and respectively the "COSMOS/M" programme. For the calculus of the strength state out of the Hardy nozzle it was achieved a calculus subprogramme.

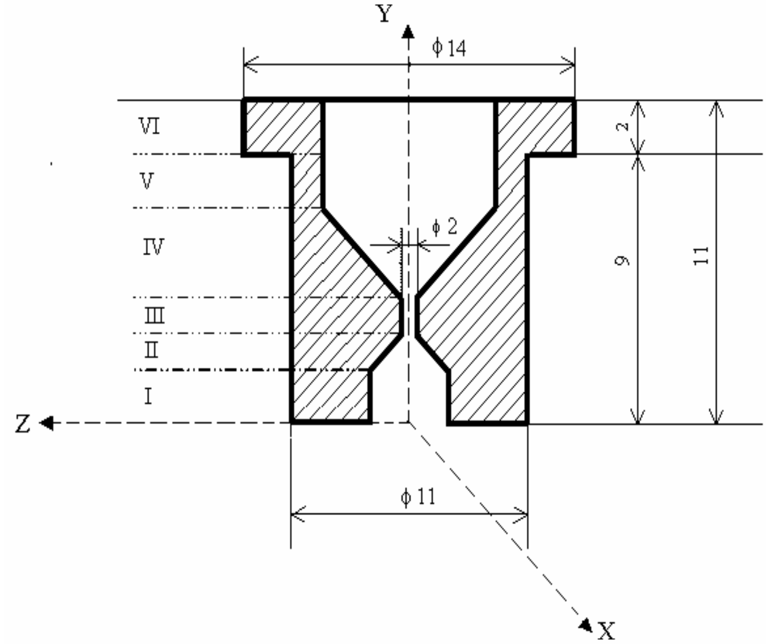

***Fig. 1.** Section through the studied Hardy nozzle.*

In order to achieve moulding as good as possible the nozzle was divided in six zones, conveniently selected.

The calculus was done for the most unpropitious case of loading that is when the sprinkling solution passes through the interior of the nozzle with a maximum pressure of 6 bar. This pressure was applied on the internal walls of the nozzle.

The digitisation of the nozzle it was done using isoparameter elements of thin plate type, with four knots on element and eight degrees of freedom on knots (figure 2). The net of finit elements used it was achieved by variable step, with a denser net in zones of passing from a larger diameter to a smaller diameter of the nozzle. For the knots in the fastening zone of the nozzle in the body of the nozzle and implicitly on the platform of the sprinkling machine were introduced bottomings for all those eight degrees of freedom.

In the fastening points were considered hampered the changes of place and turnings in all directions (ox, oy, oz) considering these points as being embedding points.

We introduced as well as real constants, associate to the selected elements group, the thickness of the nozzle, Poisson's ratio (for polyethylene ν = 0,26) and as well as material properties, the longitudinal resilience modulus($E = 14 \bullet 10^3$ MPa) and transversal resilience modulus.

There were determined σ_x, σ_y, σ_z and τ_{xy} stresses specific to the plane state of deformation, σ_1, σ_2 and σ_3 main stresses, as well as the equivalent stress in accordance to the 5th theory of strength (Von Mises), which it is calculated with the relation:

$$\sigma_{ech.} = \sqrt{\sigma_1^2 + \sigma_2^2 + \sigma_3^2 - \sigma_1\sigma_2 - \sigma_2\sigma_3 - \sigma_3\sigma_1} \qquad (1)$$

The stress state was also completed with a calculus of the change of place.

Figure 2 presents a sample of the obtained by using the achieved subprogramme and figure 3, 4, 5, represent the mode of accordance to the 5th theory of strength (Von Mises) in the case of Hardy nozzle.

```
*********************************************************************
*                    C  O  S  M  O  S  /  M
*                       VERSION:    1.60
*                        DISTRIBUTED BY:
*            STRUCTURAL  RESEARCH  AND  ANALYSIS  CORPORATION
*                    1661  LINCOLN  BLVD.  #200
*                  SANTA MONICA,   CALIFORNIA   90404
*                    TEL. NO.   (213)  452-2158
*                   COPYRIGHT  1988   S. R. A. C.
*********************************************************************
DATE:    5/05/2002    TIME:    0:12:39

TITLE : THE UTILIZATION OF THE "COSMOS/M" COMPUTER PROGRAMME AT THE DETERMINATION OF THE
STRESSES WHICH APPEAR IN THE NOZZLES FROM THE MACHINERY OF PEST AND DISEASES CONTROL THROUGH
CHEMICAL WAY IN THE EXPLOITATION PROCESS FROM AGRICULTURE

T O T A L   S Y S T E M   D A T A
NUMBER OF EQUATIONS . . . . . . . . . . . . . . .(NEQ)  =     3240
NUMBER OF MATRIX ELEMENTS . . . . . . . . . . . .(NWK)  =   860508
MAXIMUM HALF BANDWIDTH . . . . . . . . . . . . . (MK )  =     1536
MEAN HALF BANDWIDTH . . . . . . . . . . . . . . .(MM )  =      265
NUMBER OF ELEMENTS. . . . . . . . . . . . . . . .(NUME) =      760
NUMBER OF NODAL POINTS. . . . . . . . . . . . . .(NUMNP)=     1140
SIZE OF EACH BLOCK. . . . . . . . . . . . . . . .(MTBLK)=     8000
NUMBER OF BLOCKS. . . . . . . . . . . . . . . .  (NBLK) =      113
MAXIMUM DIAGONAL STIFFNESS MATRIX VALUE =   .476175E+04
MINIMUM DIAGONAL STIFFNESS MATRIX VALUE =   .274825E+03

S T R E S S   E V A L U A T I O N  FOR  S T A T I C  A N A L Y S I S

  STRESS OUTPUT FOR 3/D ELEMENT GROUP   1      CASE  NO.     1

 ELEMENT    OUTPUT
  NUMBER    NODE  SIGMA-X1  SIGMA-X2  SIGMA-X3   TAU-X12   TAU-X23   TAU-X13  VON MISES STRESS
       1
        CENTER    2.5000E-01 -2.6691E-03 -3.1385E-01 -3.5388E-03 -2.2014E-02 -9.3923E-02
5.1696E-01
             1    4.2813E-01  5.2146E-02 -3.0567E-01 -3.5020E-03 -2.1975E-02 -1.2204E-01
6.7090E-01
             2    4.7723E-01  5.2146E-02 -3.1211E-01 -3.5020E-03 -2.1975E-02 -1.3129E-01
7.2209E-01
```

Fig. 2. *Sample with the obtained results.*

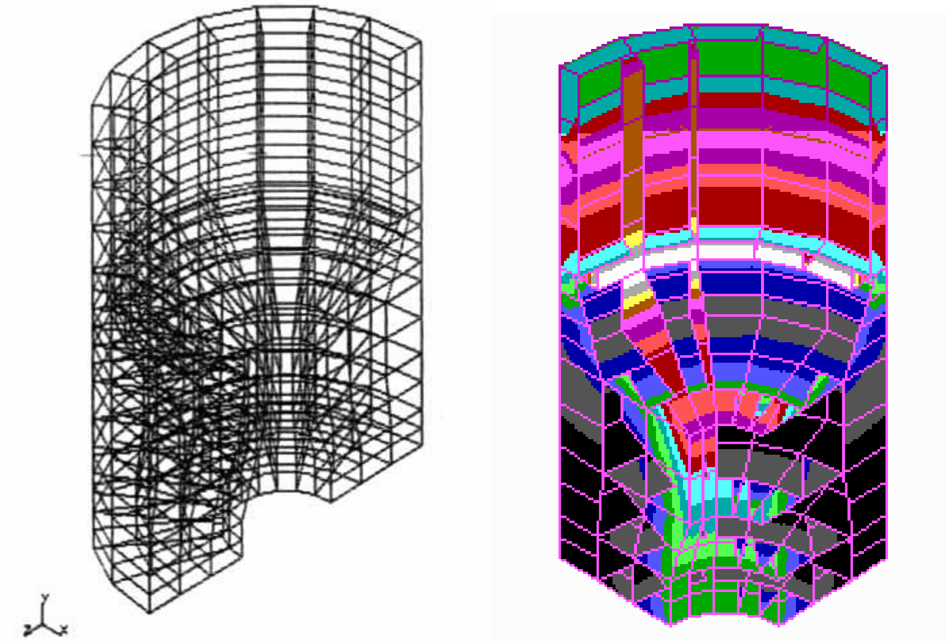

a) b)

Fig. 3. *a) The digitisation model of the Hardy nozzle; b) The distribution of the stresses in accordance to the 5*th *theory of strength (Von Mises)* $\sigma_{ech(5)}$ *for sectioned Hardy nozzle, established for the maximum pressure p = 6 bar.*

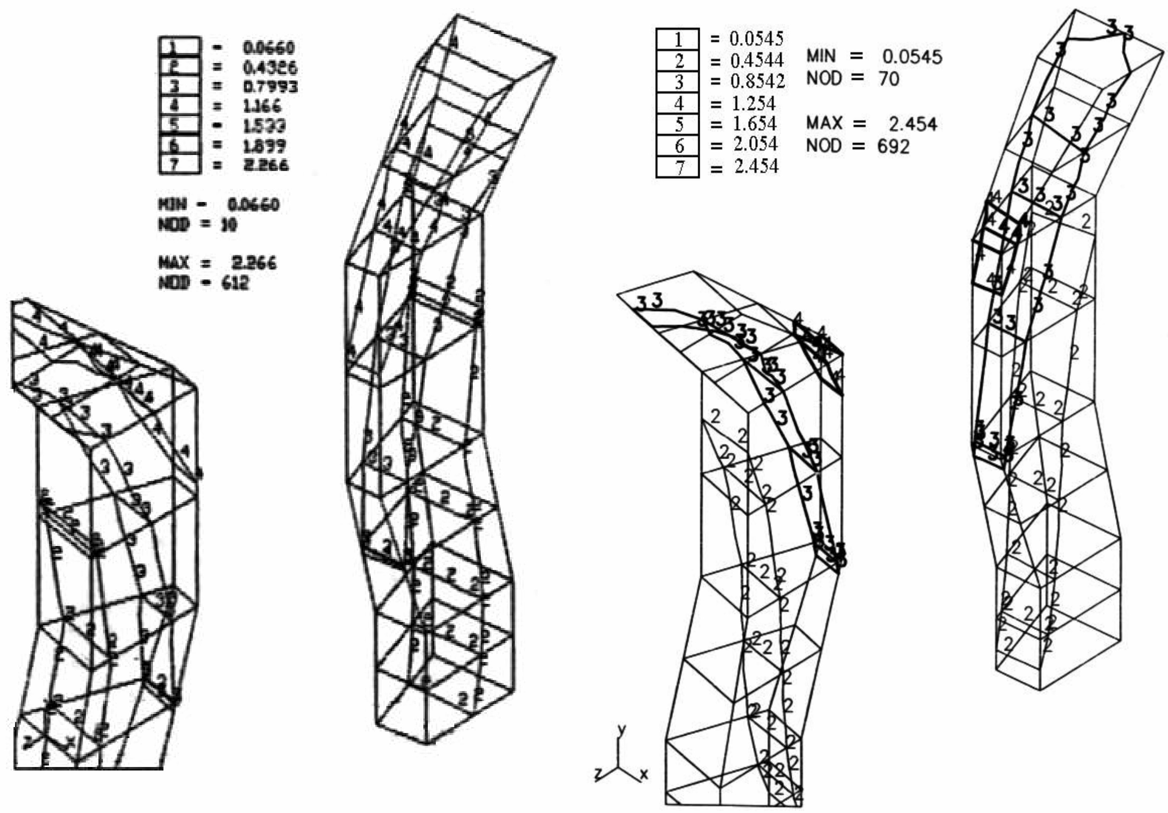

a) b)

Fig. 4. *a) The distribution of the stress* $\sigma_{ech.(5)}$ *in the concentration zones of the stresses, in the section 1, for a maximum pressure p = 6 bar; b) The distribution of the stress* $\sigma_{ech(5)}$ *in the concentration zones of the stresses, in the section 2, for a maximum pressure p = 6 bar.*

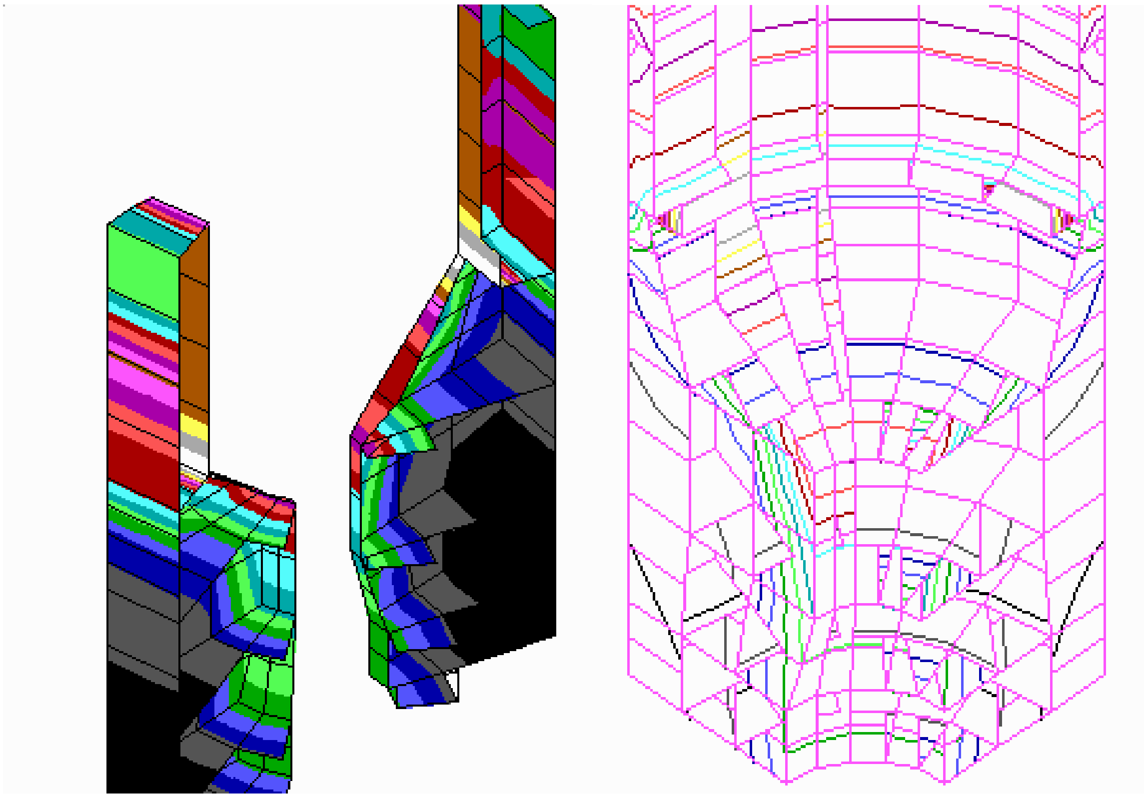

a) b)

Fig.5. *a) The distribution of the stress in accordance to the 5th theory of strength (Von Mises) $\sigma_{ech(5)}$, in a section of the nozzle, for the maximum pressure p = 6 bar; b) The distribution of the stress $\sigma_{ech(5)}$ for sectioned Hardy nozzle, in the zone in which it is actual achieved the spraying of the liquid, for a maximum pressure of 6 bar.*

3. CONCLUSIONS

1. The stage of the current development of the scientific and technical level permits the utilization of the Finit Element Method as a fundamental theoretical method of the determination of stresses distribution in the nozzles from the machinery of pest and diseases control through chemical way.
2. In the context of potential's capitalization offered by the COSMOS/M programme in this field, the modelling of the stresses field became a certainty.
3. The theoretical cognition of the stresses distribution is of an unchallenged utility in the evolution's estimate of this process, experimental praised in the ground.
4. The study effected on the Hardy nozzle praised the fact that this is solicited at tiredness in time, because of the pressure which acts on its internal walls.
5. The biggest strengths are manifest in the zones in which the internal diameter of the nozzle is reduced (the zones of influence from a bigger diameter to a smaller diameter), fact that leads to the conclusion these zones are considered concentrators of strength.
6. In order to learn some pertinent conclusions as concerns the determination of the strength at the nozzles of the sprinkled machinery is imperious necessary to be studied as many types of such nozzles as possible, because at present there is a very varied range in the world, and the materials are more and more performant (ceramics materials, composite materials).

4. REFERENCES

[1] **Blumenfeld, M.** – “Introduction in the finit element method”, Technical Publishing House, Bucharest, 1995;
[2] **Bungescu, S**. - "Studies and thorough researches on the improvements` evolution of the engineering and processes achieved by the machinery for sickness and pest control in agriculture", Dissertation, "Politehnica" University, Timişoara, 1996;
[3] **Bungescu, S.** - “The modelling of the stresses and deformations which appear in the most solicited mechanisms of the agricultural machinery, using "Finite Elements Method", respectively the COSMOS/M programme”, vol. XXXV, Scientifical Papers, Animal Science & Biotechnologies, Publishing House “Agroprint”, Timişoara, 2002, pages 288 – 293;
[4] **Bungescu, S.** – “The determination of the stresses’ distribution on the surface of the working mechanisms of the agricultural machineries benefiting by the performances of the finite element method (F.E.M.)”, IVth International Symposium “Young People and Multidisciplinary Research”, Publishing House “Sudura”, Timişoara, 2002, pages 28 – 37;
[5] **Dumitru, I.; Faur, N.** - " The Materials' Strength" (Theoretical basis in the Materials' Tiredness,Tear's Mechanic, Composite Materials and Numerical Methods), The multiplication center University "Politehnica" Timişoara, 1997;
[6] **Faur, N.; Dumitru, I.** - Finite difference and finite element in the Materials' Strength", Publishing House "Mirton ", Timişoara, 1997;
[7] **Stahli, W.** – “Machinery for the application of the phytosanitary treatments and foiled fertilizing of the vegetable crops”, Publishing House “AGROPRINT”, Timişoara, 2003;
[8] **Zienkiewicz, O.C; Taylor, R.L.** – “La methode des elements finis”, AFNOR, Paris, 1991;
[9] *** * * * - "COSMOS/M USER GUIDE",** Structural Research and Analysis Corporation, Santa Monica, California, 1990;

PHYSICAL AND MATHEMATICAL MODELLING OF THERMAL STRATIFICATION PHENOMENA IN STEEL LADLES

PUTAN Vasile

UNIVERSITY OF TIMISOARA, FACULTY OF ENGINEERING - HUNEDOARA

Abstract:
The paper is meant to present a physical hot-water model of industrial steel ladles. With this physical model, thermal stratification phenomena due to natural convection in steel ladles during the holding period before casting were investigated. By controlling the cooling intensity of the water model to correspond to the loss rate of steel ladles temperature distributions in the water model can simulate those in the steel ladles. Consequently, the temperature profile in the hot-water bath in the model can be used to deduce the thermal stratification phenomena in steel bath in the ladles.

Key words: *Steel ladle, natural convection, physical modelling, mathematical modelling, thermal stratification.*

1. INTRODUCTION

Due to inevitable heat losses, natural convection is a common phenomenon occurring in steel ladles during the holding period prior to casting. A typical consequence of this phenomenon is thermal stratification of the liquid steel bath. The thermal stratification phenomenon in steel ladles and its potential influence on temperature control during continuous casting are important in steelmaking. This is because the temperature of liquid steel coming from a thermally stratified melt bath held in the ladles, will have a direct impact on the temperature of steel melt held in the tundish.

The measurement of thermal stratification were made mostly on pilot-scale 6-7.5 tonne steel ladles by using instrumented refractory rods on which thermocouples were mounted at different heights or by installing thermocouples (with some penetration into the steel bath) at different levels on the ladle wall.

Based on the computational fluid dynamics (CFD) theory, several mathematical models have already been developed for simulating natural convection phenomena in steel ladles. The CFD models numerically solve the turbulent Navier-Stokes type partial differential equations describing the flow and heat transfer phenomena of interest, thus enabling the researchers to obtain flow patterns and temperature distribution inside the steel ladles.

An alternative approach that has the potential to achieve the same goal is physical modelling. Unlike the direct measurement of thermal stratification in steel ladles, physical models, established on the basis of the similitude theory, are normally easy to set-up, economic and efficient in implementation. In addition, the physical modelling results can also be used for verification of the mathematical modelling results.

2. EXPERIMENTAL

For the purpose of simulating fluid flow and heat transfer in steel ladles by means of the water model, a systematic analysis on the similarity between natural convection phenomena in steel ladles and in hot-water models has been carried out [5]. This similarity study suggested that water models with size scales in the range between 1/5 and 1/3 and using hot water of 45 ^{0}C or higher could be appropriate for modelling steel ladles with a promising similarity both in fluid flow and in heat transfer. Accordingly, in the present work, a 1/4-scale hot-water model has been established in the laboratory. The model is based on the mid-aged 107-tonne steel ladles. Fig. 1 illustrates this physical model set-up with (a) and (b) showing the sketches of inside arrangement.

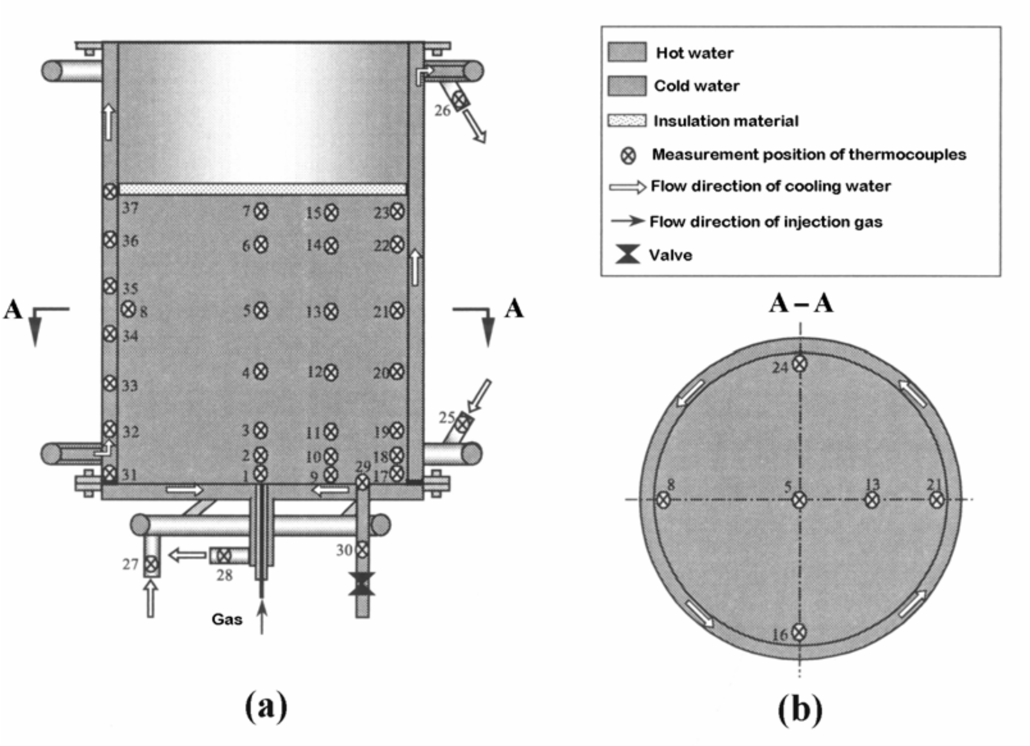

Fig.1. *Hot-water model set-up.*

The water model consist of two cooling chambers: the one is a cylindrical chamber for simulating ladle wall, and the other is a flat cooling chamber for simulating ladle bottom. The cooling chambers are made of 2 mm thick stainless steel sheet. Hot water is used as the liquid bath simulating liquid steel bath in ladles, while cold water with controllable temperatures is tangentially introduced into the cooling chambers in directions shows in Figs. 1a and 1b. T-type (cooper-constantan) thermocouples (TCs) were employed to get information from the water model. Figs. 1a and 1b also schematically illustrate the TC measurement position. 21 TCs were used for measuring the temperature profile in the water bath on a vertical plane bounded by sidewall and center axis. 7 TCs were used for measuring the temperature distribution in the side-cooling chamber under the level of the hot-water bath. 4 TCs were used for measuring temperatures of water inflows and outflows of the cooling chambers. In addition, for the purpose to check the symmetry of cooling intensity, 3 more TCs (No.8, No.16 and No.24) were used, together with TC No.21, to measure temperatures along the periphery of the hot-water bath, as shown in Fig. 1b. All the temperature signals were recorded into an data logger for post processing. To prevent heat loss from the top free surface of the water bath, the free surface was covered with a light porous plastic plate that can float on the surface. In order to homogenize the hot-water bath, if needed, pressurized air can be blown into the water bath via the tuyere located at the center of the bottom-cooling chamber.

3. RELATIONSHIP BETWEEN HEAT LOSS FLUXES OF WATER MODEL AND STEEL LADLE

One of the major aims of the present study is to explore the possibility of directly simulating thermal stratification phenomena in steel ladles by using the temperature information obtained from the hot-water model. This can be realized by scaling up, via certain similarity criteria, the water temperature distribution in the model into the steel temperature distribution in the prototype ladle. The criteria for such a scale-up can be derived from the similarity between natural convection phenomena in water models and in steel ladles [10], the key similarity criteria were found to be the following:

$$Fr_m = Fr_p \tag{1}$$

and

$$(\beta\Delta T)_m = (\beta\Delta T)_p \tag{2}$$

where: Fr – Froude number,[-];
β - thermal expansion coefficient, [1/K];
ΔT – difference of temperature from the initial temperature, [K];
m and p stand for the water model and the prototype steel ladle, respectively.

The above similarity criteria lead to a relationship between the heat loss flux of the water model and that of the prototype steel ladle as, [10]:

$$q_m = q_p \frac{\rho_m \cdot C_m \cdot \beta_p}{\rho_p \cdot C_p \cdot \beta_m} f_t \tag{3}$$

with

$$f_t = \frac{t_m}{t_p} = \sqrt{f_G} \tag{4}$$

where: q_m, q_p – heat flux to model and to prototype steel ladle, respectively, [W/m^2];
ρ_m, ρ_p – density of model and of prototype steel ladle, respectively, [kg/m^3];
C_m, C_p – thermal capacity of model and of prototype steel ladle, respectively, [J/kg K];
β_m, β_p – thermal expansion coefficient of model and of prototype steel ladle, respectively, [1/K];
t_m, t_p – time in model and in prototype steel ladle, respectively, [s];
f_t – time scale factor, f_t = 0,5;
f_G – geometry scale factor, for the present hot-water model f_G = 1/4 ;

Table 1. *Thermal-physical properties of steel, liquid steel and water.*

Property	Unit	Solid steel *	Liquid steel	Water
Temperature	^0C	< 400	1580	45
Density	kg/m^3	7900	6962,8	990,22
Thermal expansivity	$1/^0C$	-	0,00015	0,0004
Thermal conductivity	$W/m\cdot{}^0C$	15	27,9	0,637
Thermal capacity	$J/kg\cdot{}^0C$	500	787	4182
Viscosity	$Pa\cdot s$	-	0,006	0,00089

* Model shell material: ASTM 304 stainless steel

Introducing the thermal-physical properties of liquid steel and water given by Table 1 into eq. (10), after rearrangement, results in:

$$q_p = 7{,}0574\ q_m \tag{5}$$

Eqs. (4) and (5) are used in this work for scaling up the transient heat loss flux for water model to that for the steel ladle.

4. PREDICTION OF STEEL TEMPERATURES IN LADLE WITH USE OF WATER TEMPERATURES IN MODEL

The present work focused on using the temperature distribution in water model to directly predict the temperature distribution in steel ladles. The relation between the temperatures in the water model and the temperatures in the ladle is governed by Eq. (2), which can be further expressed as:

$$T_p = T_{0,p} - \frac{\beta_m}{\beta_p}\left(T_{0,m} - T_m\right) \tag{6}$$

where $T_{0,p}$ and $T_{0,m}$ are the initial temperatures of liquid steel and hot water, respectively. Eq. (6) is actually adopted in the present study for scaling up the water temperatures in the model to the steel temperatures in ladles.

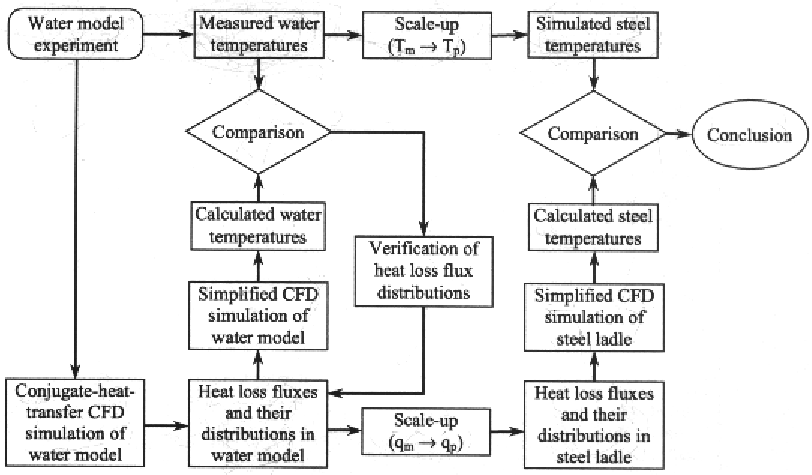

Fig. 2. *Flow chart showing a method for verification of using hot-water model to simulate thermal stratification in steel ladles.*

A method of verifying the feasibility of using the measured water temperatures in the model to directly predict the steel temperature in ladles has been developed in the present work, as shown in Fig. 2. This figure depicts how to establish consistent heat loss fluxes, obeying Eq. (5), for the water model and the steel ladle. Using the heat loss fluxes, scaled up, via Eq. (5), from those for the water model (predicted by the conjugate-heat-transfer CFD model) as thermal boundary conditions for the steel ladle, the steel temperatures can be predicted with the simplified CFD model and compared to the temperatures scaled up, via Eq. (6), from those measured in the water model experiment. This comparison will indicate the validity of using water model to deduce the extent of thermal stratification in steel ladles.

Following the flow chart given in Fig. 2, the same water model experimental case which was once simulated by the conjugate-heat-transfer CFD model, is further analyzed here. Fig. 3 illustrates the local heat fluxes from hot-water bath to cooling chambers at different times during cooling in this experimental case, predicted by the conjugate-heat-transfer CFD model. It is seen from Fig. 3a that the distribution of the heat flux along the height of the side-cooling chamber looks rather complicated. Apart from transient features, generally, larger heat loss fluxes exist in the lower section of the wall, while smaller loss fluxes occur in the upper section of the wall. Fig. 3b shows that during cooling (after the first 15 seconds) the heat flux from the hot-water bath to the bottom-cooling chamber appears to be nearly uniformly distributed along the radius of the chamber appears to be nearly uniformly distributed along the radius of the chamber, except for the center region.

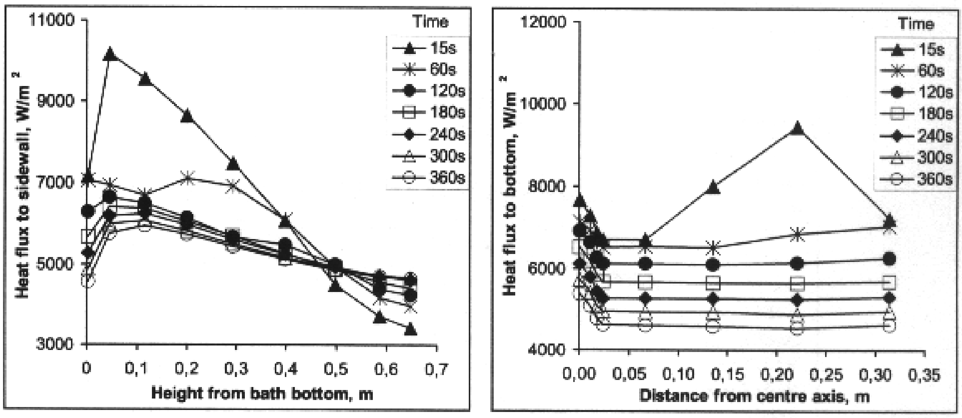

(a) Side-cooling chamber (b) Bottom-cooling chamber

Fig. 3. *Predicted distributions of heat fluxes from hot-water bath to cooling chambers.*

In order that the heat fluxes predicted by the conjugate-heat-transfer CFD model, as shown in Fig. 3, can be applied as thermal boundary conditions to the simplified CFD model, it is expected that these heat fluxes can be represented (approximated) with *simple equations*.

For the heat loss flux to the sidewall, according to Fig. 3a, it is assumed that the heat flux has a quadratic distribution along the height of sidewall and follows an exponential decay with time. Thus, trough quadratic and exponential curve fitting analyses, the heat loss flux and its distributions on the sidewall can be approximately by the following *simple equation*:

$$q_{s,m} = \left[1{,}2 + 0{,}2\left(\frac{h_m}{H_m}\right) - 0{,}9\left(\frac{h_m}{H_m}\right)^2\right]\left(1668{,}0 \cdot e^{-1.0374\cdot 10^{-2} t_m} + 5202{,}3\right) \qquad (7)$$

where: $q_{s,m}$ is the local heat flux to the sidewall of the water model;
H_m – the height of the hot-water bath;
h_m – the distance from the bottom of the hot-water bath ($0 \leq h_m \leq H_m$).

As for heat flux to the bottom of the water model, according to Fig. 3b, it is assumed that this heat flux is uniform at the model bottom and equal to the average heat flux that also follows an exponential decay with time,

$$q_{b,m} = 3987{,}1 \cdot e^{-3{,}3003 \cdot 10^{-3} t_m} + 3622{,}9 \tag{8}$$

where $q_{b.m}$ is the local heat flux to the bottom of the water model.

Now Eqs. (7) and (8) can be scaled up, via Eqs. (4) and (5), so that similar expression of heat loss fluxes to the sidewall and bottom of the prototype steel ladle can be derived as:

$$q_{s,p} = \left[1{,}2 + 0{,}2\left(\frac{h_p}{H_p}\right) - 0{,}9\left(\frac{h_p}{H_p}\right)^2\right]\left(11771{,}7 \cdot e^{-5{,}187 \cdot 10^{-2} t_p} + 36714{,}5\right) \tag{9}$$

and

$$q_{b,p} = 28138{,}4 \cdot e^{-1{,}6502 \cdot 10^{-3} t_p} + 25568{,}1 \tag{10}$$

where: $q_{s,p}$ and $q_{b,p}$ are, respectively, the local heat fluxes to the sidewall and bottom of the prototype steel ladle;
H_p – the height of the liquid steel bath;
h_p – the distance from the bottom of the liquid steel bath ($0 \leq h_p \leq H_p$).

Eqs. (7) through (10) are finally used as thermal boundary conditions for the simplified CFD model to simulate thermal stratification phenomena both in the water model and in the prototype steel ladle.

5. CONCLUSIONS

The present non-isothermal water model study has confirmed the validity of the dimensionless numbers Fr and $\beta\Delta T$ as key criteria governing the similarity between natural convection phenomena in hot-water models and in prototype steel ladles.

Establishing a non-isothermal water modelling system is useful for verification of CFD mathematical modelling results. In addition to mathematical methods, the hot-water model provides an alternative means of studying fluid flow and heat transfer phenomena in steel ladles.

REFERENCES:

[1] J. W. Hinka and T. W. Miller - Iron Steel Eng., 8 (1970), 123.
[2] K. O. Jonasson – PhD Thesis in ferrous metallurgy, (1970) MEFOS, Lulea, Sweden.
[3] C. E. Grip – Steelmaking Conference Proceedings, Vol.77, ISS, Chicago, USA, (1994), 103.
[4] O. J. Ilegbusi and J. Szekely – Transaction ISIJ, 27 (1987), 563.
[5] Yuhua Pan and Bo Bjorkman – Computational fluid dynamics analysis on the similarity between steel ladles and hot-water models regarding natural convection phenomena, ISIJ International, Vol. 42, No.1, 2001.

RELIABILITY STUDY OF A POWER ELECTRIC ENERGY

[1] Prof.dr.ing. GILLICH Nicoleta , [2] Ing. TICULA Eugen

[1] Universitatea „Eftimie Murgu" Reşiţa, Piaţa Traian Vuia, Nr.1-4, tel.0255210227, e-mail: n.gillich@uem.ro
[2] Electrica S.A. Reşiţa, Bd.Revoluţia din Decembrie, Nr.3, tel.0255212188, e-mail: ticula@cs.ro

***Abstract**:*

The paper treated the main aspects regarding the reliability of a power electric energy system from Electrica S.A.Reşiţa, with modern techniques for diagnosis and maintenance. It has been considered useful to treat the electric energy system with equivalent structural diagram method for reliability indicators calculus using the MathCAD medium.

***Key words**:*
Reliability indicators, power system, equivalent structural diagram

1. INTRODUCTION

The issue concerning reliability indicators of power electric energy system 110 kV from S.C. Electrica S.A. Reşiţa, is structured on two parts: references at power system reliability analyses and convenience of maintenance based on reliability indicators calculus.

The reliability models used in electric power systems give the information regarding the behavior of the systems at the work rhythm and the options concerning the optimum network configuration.

The complex configuration of the 110 kV network, covering the county Caraş-Severin, implied application of the equivalent method based on reliability equivalent structural diagram.

2. THEORETIC CONSIDERATIONS

The large number of network nods 220/110 kV and 110 kV/medium voltage (20, 6kV) give some basis conditions. The 220 kV bars of 220/110 kV nod Soceni was similar with national electric power system (SEN) because of double connection with: Porţile de Fier electric plant and local network from Timişoara, which give the maximum reliability.

The sense of energy flux through cascade nods begin from node 1 and the whole network contends 21 nods.

In the elaboration of reliability equivalent structural diagram for every nod it was very important to know the critical conditions for the consumers strongly conditioned by the quality of electric energy and the risks implied by the undesired failures.

Under this circumstance there are the following consumers: mining industry (Anina and Moldova-Nouă), metallurgical industry (Combinatul Siderurgic Reşiţa and Oţelul Roşu), important industrial complex: UCM Reşiţa, ICM Bocşa, ICM Caransebeş, IPL Balta Sărată, IM Topleţ, electric injection nods of electric railway (CFR Caransebeş, CFR Poarta, CFR Topleţ) and urbane zones with important consumers (hospitals, public institutions, theatres, etc.)

The reliability calculus was made based on reliability indicators: faulting rate λ_i and repairing rate μ_i on equivalents elements (series or parallel), given in the technical literature [3,4]. For λ and μ values was used the national normative regarding the maintenance equipment and installation (transformers, circuit breakers, separator, power line etc.) depending on voltage level. The notation for voltage level was as follow: 220kV noted with 1, 110kV noted with 2 and medium voltage (20, 6kV) noted with 3.

For each nod the calculus of equivalent reliability indicator was made with MathCAD medium, and can be modified for new configuration of networks.

3. CALCULUS EXAMPLE

A calculus example is given as follow and it show the results for electric station of Soceni 220/100 kV from Reşiţa (nod 1).

Station 220/110 kV Reşiţa nod 1

$\lambda L1 := 0.55 \cdot 10^{-6}$

$\mu L1 := 6.137 \cdot 10^{-2}$

$\mu I1 := 4.23 \cdot 10^{-2}$

$\lambda I1 := 4.26 \cdot 10^{-6}$

$\mu S1 := 9.68 \cdot 10^{-2}$

$\lambda S1 := 0.39 \cdot 10^{-6}$

$\mu B1 := 19.9 \cdot 10^{-2}$

$\lambda B1 := 1.47 \cdot 10^{-6}$

$\mu AT1 := 0.06 \cdot 10^{-2}$

$\lambda AT1 := 20 \cdot 10^{-6}$

$\mu B2 := 19.9 \cdot 10^{-2}$

$\lambda B2 := 1.47 \cdot 10^{-6}$

$\mu S2 := 4.64 \cdot 10^{-2}$

$\lambda S2 := 0.44 \cdot 10^{-6}$

$\mu L2 := 6.14 \cdot 10^{-2}$

$\lambda L2 := 1.47 \cdot 10^{-6}$

$\mu IO2 := 6.78 \cdot 10^{-2}$

$\lambda IO2 := 2.1 \cdot 10^{-6}$

$$\lambda a := \lambda B1 + 4.5\cdot\lambda S1$$

$$\lambda b := \lambda I1 + \lambda S1$$

$$\lambda a = 3.225 \cdot 10^{-6}$$

$$\lambda b = 4.65 \cdot 10^{-6}$$

$$\mu a := \frac{\lambda a}{\left(\frac{\lambda B1}{\mu B1}\right) + \left(\frac{4.5\cdot\lambda S1}{\mu S1}\right)}$$

$$\mu b := \frac{\lambda b}{\frac{\lambda I1}{\mu I1} + \left(\frac{\lambda S1}{\mu S1}\right)}$$

$$\mu a = 0.126385835566107$$

$$\mu b = 0.044396432443776$$

$$\lambda c := 9\cdot\lambda I1 + 18\cdot\lambda S1$$

$$\mu c := \frac{\lambda c}{\left(\frac{9\cdot\lambda I1}{\mu I1}\right) + \left(\frac{18\cdot\lambda S1}{\mu S1}\right)}$$

$$\lambda c = 4.536 \cdot 10^{-5}$$

$$\mu c = 0.046337553720344$$

$$\lambda A := 2\cdot\lambda a + \lambda b + \lambda c$$

$$\mu A := \frac{\lambda A}{\left(\frac{2\cdot\lambda a}{\mu a}\right) + \left(\frac{\lambda b}{\mu b}\right) + \left(\frac{\lambda c}{\mu c}\right)}$$

$$\lambda A = 5.646 \cdot 10^{-5}$$

$$\mu A = 0.049758698282387$$

$$\lambda d := \lambda AT1 + \lambda I1 + \lambda S1 + \lambda IO2 + 2.5\cdot\lambda S2$$

$$\lambda d = 2.785 \cdot 10^{-5}$$

$$\mu d := \frac{\lambda d}{\frac{\lambda AT1}{\mu AT1} + \left(\frac{\lambda I1}{\mu I1}\right) + \left(\frac{\lambda S1}{\mu S1}\right) + \frac{\lambda IO2}{\mu IO2} + \bigl(2}$$

$$\mu d = 8.318297533520635 \cdot 10^{-4}$$

$$\lambda e := \lambda IO2 + \lambda S2$$

$$\mu e := \frac{\lambda e}{\left(\frac{\lambda IO2}{\mu IO2}\right) + \left(\frac{\lambda S2}{\mu S2}\right)}$$

$$\lambda e = 2.54 \cdot 10^{-6}$$

$$\mu e = 0.062783933622478$$

$$\lambda f := \lambda B2 + 5.5\cdot\lambda S2$$

$$\mu f := \frac{\lambda f}{\frac{\lambda B2}{\mu B2} + \left(\frac{5.5\cdot\lambda S2}{\mu S2}\right)}$$

$$\lambda f = 3.89 \cdot 10^{-6}$$

$$\mu f = 0.065331917029837$$

$$\lambda g := \lambda B2 + 4\cdot\lambda S2$$

$$\mu g := \frac{\lambda g}{\frac{\lambda B2}{\mu B2} + \left(\frac{4\cdot\lambda S2}{\mu S2}\right)}$$

$$\lambda g = 3.23 \cdot 10^{-6}$$

$$\mu g = 0.071274155928574$$

$$\lambda h := \lambda B2 + 9.5\cdot\lambda S2$$

$$\mu h := \frac{\lambda h}{\frac{\lambda B2}{\mu B2} + \left(\frac{9.5\cdot\lambda S2}{\mu S2}\right)}$$

$$\lambda h = 5.65 \cdot 10^{-6}$$

$$\mu h = 0.057964685543116$$

$$\lambda i := 15\cdot\lambda IO2 + 37.5\cdot\lambda S2$$

$$\mu i := \frac{\lambda i}{\frac{15\cdot\lambda IO2}{\mu IO2} + \left(\frac{37.5\cdot\lambda S2}{\mu S2}\right)}$$

$$\lambda i = 4.8 \cdot 10^{-5}$$

$$\mu i = 0.058521939309383$$

$$\lambda B := \lambda d + \lambda f + \lambda g + \lambda e$$

$$\mu B := \frac{\lambda B}{\frac{\lambda d}{\mu d} + \left(\frac{\lambda f}{\mu f}\right) + \left(\frac{\lambda g}{\mu g}\right) + \left(\frac{\lambda e}{\mu e}\right)}$$

$$\lambda B = 3.751 \cdot 10^{-5}$$

$$\mu B = 1.115514986348169 \cdot 10^{-3}$$

$$\lambda Bd := \lambda B\cdot\frac{\lambda d\cdot(\mu B + \mu d)}{\mu B\cdot\mu d + \lambda B\cdot\mu d + \lambda d\cdot\mu B}$$

$$\mu Bd := \mu B + \mu d$$

$$\mu Bd = 1.947344739700232 \cdot 10^{-3}$$

$$\lambda Bd = 2.054459714754358 \cdot 10^{-6}$$

$$\lambda D := \lambda h + \lambda i$$

$$\mu D := \frac{\lambda D}{\frac{\lambda h}{\mu h} + \frac{\lambda i}{\mu i}}$$

$$\lambda D = 5.365 \cdot 10^{-5}$$

$$\mu D = 0.058462749425833$$

$$\lambda E1 := \lambda A + \lambda Bd + \lambda D$$

$$\mu E1 := \frac{\lambda E1}{\frac{\lambda A}{\mu A} + \frac{\lambda Bd}{\mu Bd} + \frac{\lambda D}{\mu D}}$$

$$\lambda E1 = 1.121644597147544 \cdot 10^{-4}$$

$$\mu E1 = 0.036096383963777$$

The notations from calculus example correspond to the reliability equivalent structural diagram given in figure 1, made in normal function regime of electric station.

The method replace the power system bars and the consumers in successive steps with more simple diagrams until one element noted E_1^1 respective E_2^1 (superior indices represented the nod number and the inferior indices the system number). The normal regime function of nod is reliability equivalent with series diagram of elements E_1^1 and E_2^1, respective element E^1.

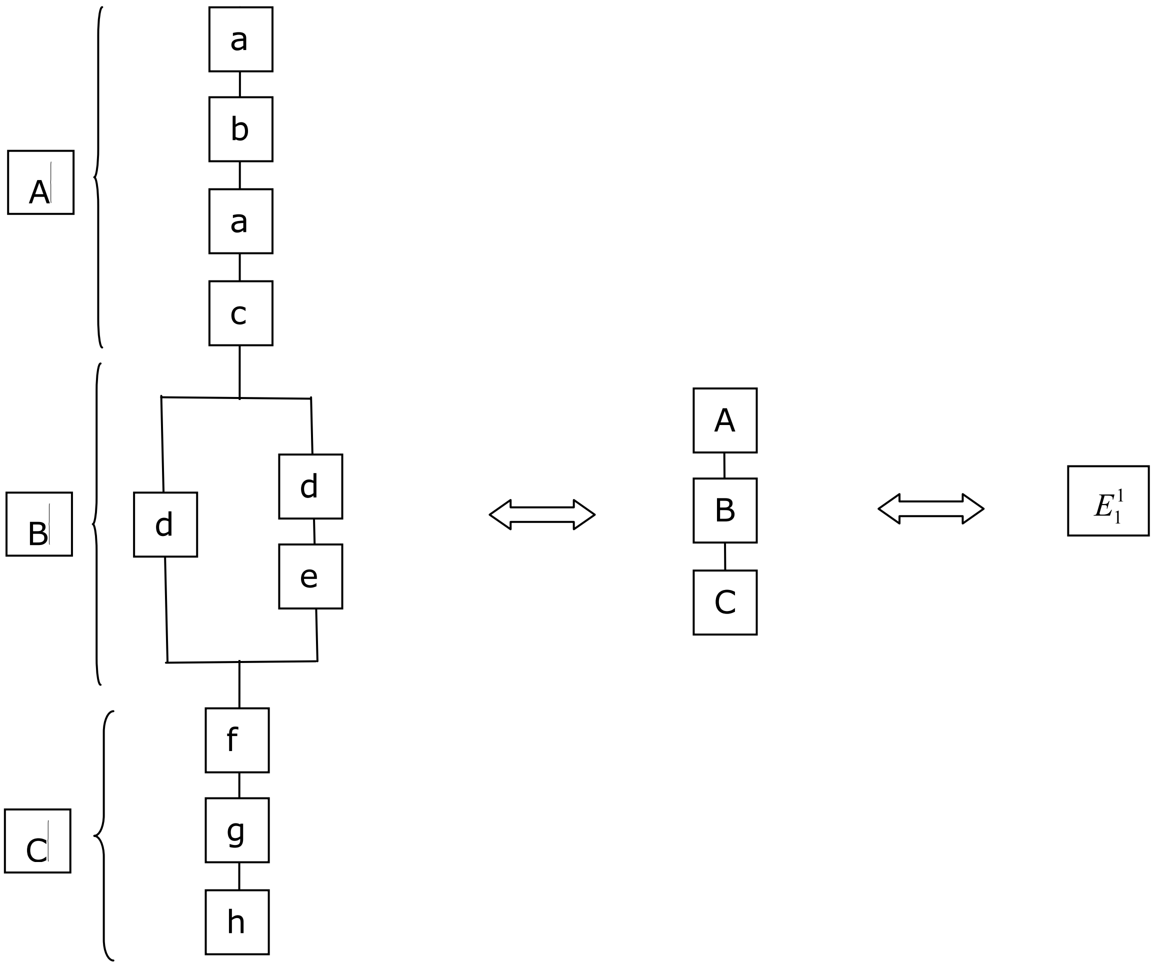

Fig.1.a.

Fig.1. *Equivalent calculus diagrams. a. System I; b. System II*

Based on calculated values for equivalent faulting rate λ_{Ei} and equivalent repairing rate μ_{Ei} (i=1, 21) for the 21 nods, was calculated the reliability indicators calculus: probability of function and failure, mean value of yearly time function and for ten years, respective of failure and medium number of failures on yearly time and on ten years time function.

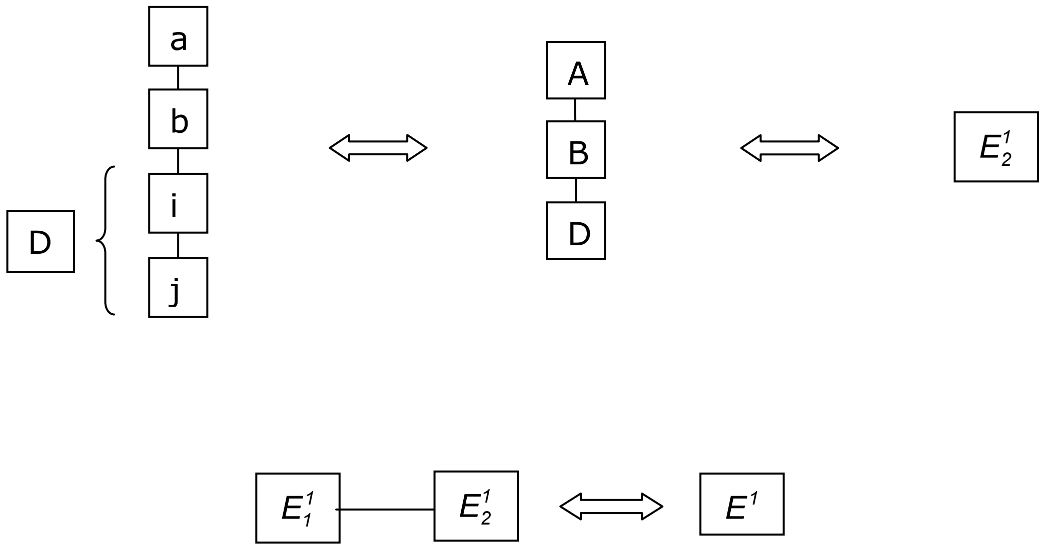

Fig.1.b.

It was also used the MathCAD medium and for Station Soceni 220/110kV, respective nod 1, for exemplification the results are given in table 1.

Table1.*Value of reliability indicators for nod 1*

Indicator	Value
Mean value of yearly time function (t =8760 h)	8,733x10^3 (h)
Mean value of function for ten years (t =8760 h)	8,733x10^4 (h)
Mean value of yearly time failure (t=87600h)	27,136 (h)
Mean value of failure for ten years (t=87600h)	271,362 (h)
Medium number of failures on yearly time function	0,98
Medium number of failures on ten years time function	9,795

4. CONCLUSIONS

The reliability indicators for actual network give for every nod the basis dates for the realistic assessment of electric power systems performances such as: quality and continuous delivering of energy, availability and functional flexibility. It is obvious that for “zero degree” consumers an own electric power sources is required.

The paper gives a dynamic model of reliability indicators calculus using the MATHCAD medium, which can be change for any new configuration of network or nods diagrams of power electric energy system 110 kV from S.C. Electrica S.A. county Caras-Severin.

5. BIBLIOGRAPHY

1. Gillich, N. – Producerea, transportul şi distribuţia energiei electrice, Editura AGIR, Bucureşti, 2003.
2. Gillich N. ş.a. - Analiza indicatorilor de fiabilitate în nodurile energetice ale sucursalei pentru estimarea parametrilor de calitate ai energiei electrice, Contract de cercetare, 2001.
3. Felea, I. – Ingineria fiabilităţii în electroenergetică, Editura Didactică şi Pedagogică, Bucureşti, 1996.
4. Velicescu, C., Oprea, L. – Fiabilitatea sistemelor energetice, Editura Politehnica, Timişoara, 1998

ABOUT THE WIND POTENTIAL FROM THE SOUTH BANAT AND A TECHNICAL SOLUTIION FOR USING IN INDIVIDUAL FARMS

Petru CHIONCEL*, Cristian CHIONCEL**

*Prof.univ.dr.ing. University "Eftimie Murgu" Reşiţa
**Prep.univ.ing. University "Eftimie Murgu" Reşiţa

Abstract:

Based on the wind average diagram from the south region of Banat, (Danubes 'clisura'), recorded during 2002, it is consider as possible to use that wind potential. Such, in a first phase, it propose a technical solution, applicable for individual farmhouses, for that place, respective a windgenerator group, command by a simple control scheme.

Keywords:

Wind installation, permanent magnet generator, automatic regulation scheme, and accumulator battery

1. **INTRODUCTION**

If the implementation of an extended wind park requires meteorological observation for a longer time period and a substantial investment effort, the creation of some windgenerator groups with a small power (<1kW) for the use of individual farms, can be considered as an easy beginning. That can have an immediate impact, which can wake peoples and autoritations interest for the renewable energy.

2. WINDPOTENTIAL IN SOUTH BANAT

The south Banat, respectively Danube's Clisura, it's a region characterized by meteorological phenomenon that can be principal expressed by a constantly wind direction (southwest) and an acceptable wind mean that allows the utilization of this energy (figure 1). We can observe in figure 1 the repartition of the mean month temperature during 2002 (figure 1.a), respectively the mean month wind speed in the same period (figure 1.b).

It's required specifying that this region has an easily access and, in winter, it's not affected by very less temperatures, massive snow falling, etc., like usual, in high mountain regions.

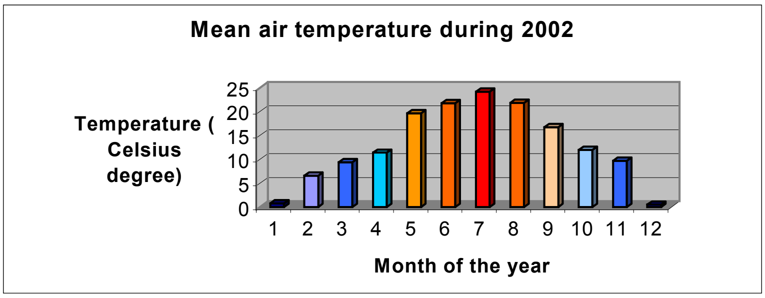

a.

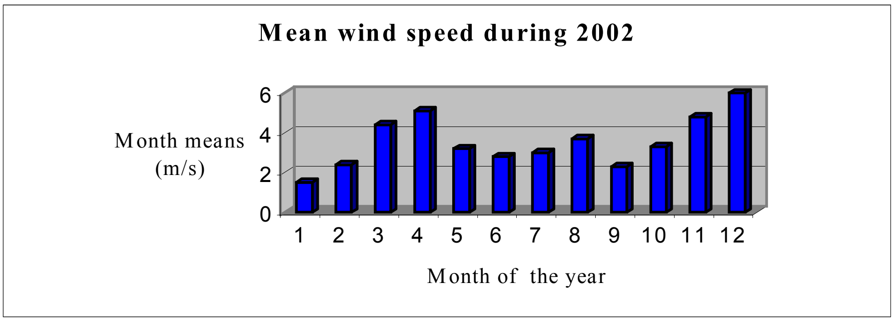

b.

Fig.1 *Nomograms a. temperature b. wind speed*

3. TECHNICAL SOLUTION OF A WINDGENERATOR FOR INDIVIDUAL FARMS

The electrical part of the windgenerator includes ensemble generator-transformer- rectifier-voltage regulator-accumulator and consumers, as presented in figure 2.

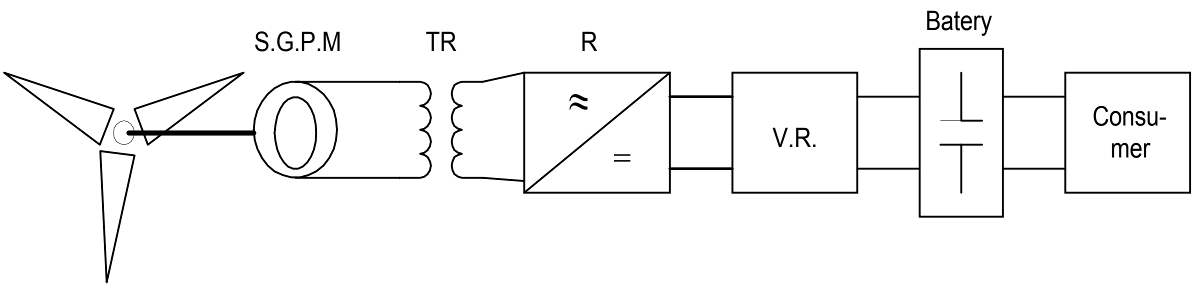

S.G.P.M.-Synchronous Generator with Permanent Magnet,
TR – Transformer, R – Rectifier, V.R. – Voltage Regulator

Fig.2 *Windgenerator ensemble*

The mono-phased synchronous generator with permanent magnet has the following main parameters: power~1kW, 220Va.c. voltage by an rotation speed of 100rpm which can increase to 250rpm, so that the voltage frequency is contained between 50Hz and 125Hz, depending on the wind speed. It is obviously, that once with the wind increasing, the produced power and voltage, by the permanent magnet generator, will grow, but this solicitation (electric and thermic) stay in acceptable limits.

For the good function of the generator in association with the rectifier and accumulator it's necessary that the loaded voltage and current should not exceed the maximum values determined by the battery capacity and temperature.

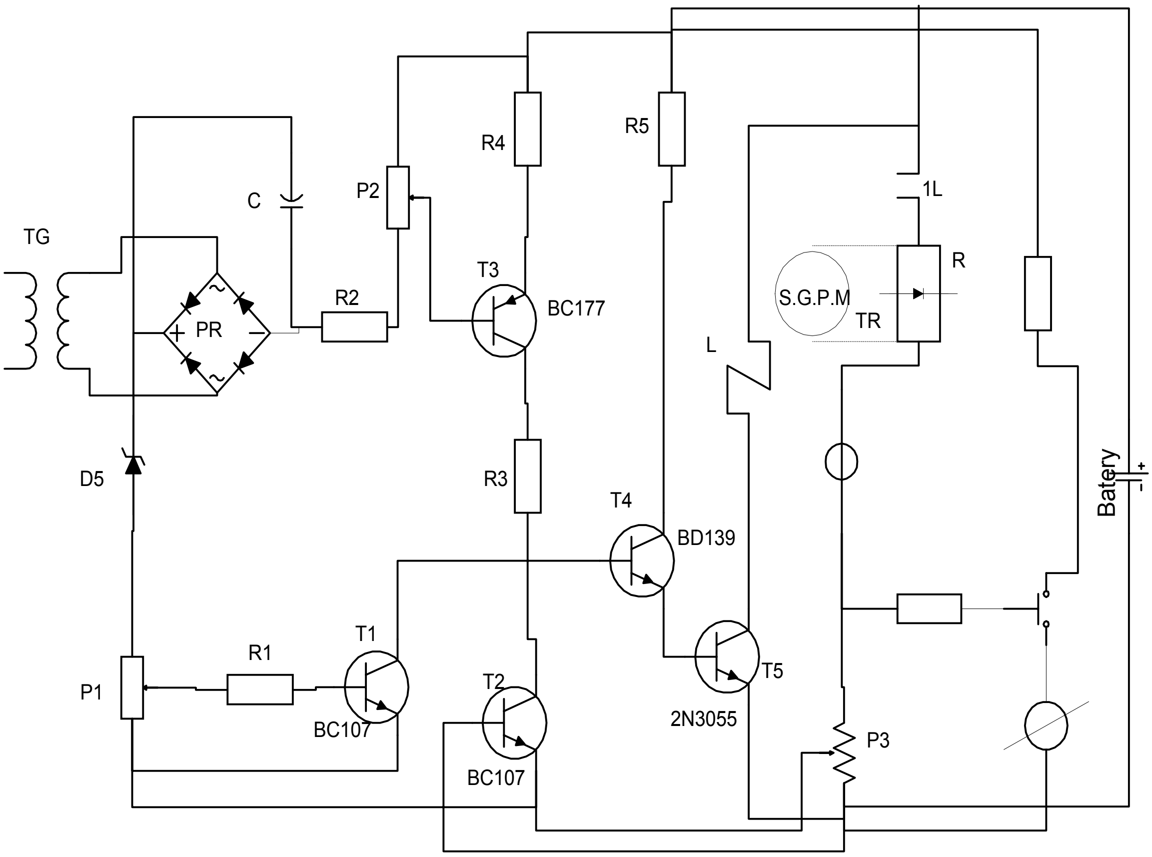

Fig.3 *Electric scheme of the windgenerator command*

Figure 3 presents a command scheme for the windgenerator, that carries out following functions:

- assures the generator connection just when his speed generates a higher voltage that the batteries;
- adjust the accumulator loaded current, indifferently on the primary energy source variation, the wind in our case
- regulates the maximum loaded voltage

The measurement element that controls the generator rotation speed is a taho-generator. He is couplet to the generator shaft, for example through a belt. If we follow the electrical scheme from figure 3, the function ascertains as: the taho-generators voltage TG polarizes the transistor T3. When this voltage crosses over a certain value, T3 enters in conduction, which imposes the entering in conduction of transistors T4 and T5 and allows the generator to be connected through the relay L contact 1L. If we assume that the wind speed falls, then the generators speed falls also and implicit the taho-generators too. This will reduce the voltage on the transistor base T3 and block transistor T5, consequently the generator will be disconnect through relay T.

The limitation loading function for the accumulator is carry out in this way: when the accumulators nominal voltage is overtaken, diode D5 opens and on the potentiometer terminal P1, appears a voltage that opens transistor T1, blocks transistor T4 and T5 and so the feeding contact 1L of the accumulator gets interrupted. Also, the potentiometer P3 is connected serial with the rectifier output, where, at his terminals, the voltage is proportional to the loaded current. When the loaded current overtakes a certain value, the transistor T2 gets open and T4 and T5 will be blocked, finally interrupting the accumulators feeding. For a better heat elimination, we notice that a radiator was connected on the T5 transistor; also, for the exact rapport of produced current and voltage, the electric scheme can be equipped with measurement instruments, as shown in figure 3.

The same command scheme can be also used for c.c. generator with derivation excitation, when the machine excitation is activated, just when his voltage is higher as the batteries.

4. CONCLUSION

The investigations of the energetic wind potential for favorable places like south of Banat (Danube 'clisura') and Banat Mountain (Semenic), needs an analyze and store a lot of meteorological parameters through a longer time period. For a the implementation of local applications, as the technical solution proposed in the paper, can be immediately started and depending of the obtained results and interest of users, can be spread on large scale.

5. BIBLIOGRAPHY

1. P.Chioncel <Conversia energiei, energii regenerabile>, Ed. Ef. Murgu Reşiţa, 2001

2. Ilie Gheorghe Mihăiescu <Automatizări în Gospodărie>, Ed. Teora, Bucureşti, 2002

USING OF KALMAN FILTRATION IN AUTOMATICS

Cristian CHIONCEL*

*Prep.univ.ing. University “Eftimie Murgu” Reşiţa

Abstract:

This paper presents the principals of Kalman filtration. For a better understanding of the Kalman filtration it is presented an analyses of the stochastic estimation of processes that are affected by noise and the relation of this to the Kalman filtering. The command signal for an automatic regulation system can be of a low power and affected by noise. For this particularly case it is presented a simulation program that calculates an estimation of the command signal, using the Kalman filtering.

Keywords:

Kalman filtration, stochastic estimation, ideal signal, noise, automation

1. INTRODUCTION

The filtration operation is met in an inevitable way in the signal treatment technique, because they have to go through the transmission channels, as some functional blocks, depending on the operation that has to be met of them.

To filtrate a signal x(t) through f(t), means to make the product:

$$x(t)\cdot f(t) \tag{1}$$

After the filtration, we want to know if the signal spectrum is influenced by this operation. If we apply the Plancherel theorem:

$$x_f(t) = x(t) \otimes f(t) \leftrightarrow X(j\nu)\cdot F(j\nu) \tag{2}$$

results from, that the spectrum of the filtered signal $x_f(t)$ is affected by the filtration operation.

In case that we consider the frequency representation, the filtration operation consist of blocking or allowed passing, totally or partial, of the spectrum lines through the cuadripol filter (figure 1).

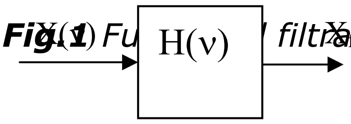

***Fig. 1** Functional filtration block*

Using the numerical signal process, in different application domains of filtration, the obtained results are more precisely, for example in signal identification. In averages that are not apriori known by the designer, the adaptive filters have a lot of applications. Adaptive filters are characterized by their possibility to modify the filter parameters, to optimize some characteristics, based on a recursive algorithm.

2. **STOCHASTIC ESTIMATION**

While there are many applications – specific approaches to "computing" (estimating) an unknown state from a set of process measurements, many of these methods do not inherently take into consideration the typically noisy nature of the measurements. This noise is typically statistical in nature, or can be effectively modeled as such, which leads to stochastic methods for addressing the problem.

Consider a dynamic process described by an n-th order difference equation of the form:

$$y_{i+1} = a_{0,i} y_i + \dots + a_{n-1,i} y_{i-n+1} + u_i, i \geq 0, \tag{3}$$

where $\{u_i\}$ is a zero-mean (statistically) white (spectrally) random noise process with autocorrelation

$$E(u_i, u_j) = R_u = Q_i \delta_{ij}, \tag{4}$$

and initial values $\{y_0, y_{-1}, \dots, y_{-n+1}\}$ are zero-mean random variables with a known nxn covariance matrix:

$$P_0 = E(y_{-j}, y_{-k}), j, k \in \{0, n-1\} \tag{5}$$

We consider that the noise is statistically independent from the process to be estimated. Under some other basic conditions, the difference equation (3) can be re-written as:

$$\vec{x}_{i+1} \equiv \begin{bmatrix} y_{i+1} \\ y_i \\ y_{i-1} \\ \dots \\ y_{i-n+2} \end{bmatrix} = \underbrace{\begin{bmatrix} a_0 & a_1 & \dots & a_{n-2} & a_{n-1} \\ 1 & 0 & \dots & 0 & 0 \\ 0 & 1 & \dots & 0 & 0 \\ \dots & \dots & \dots & \dots & \dots \\ 0 & 0 & \dots & 1 & 0 \end{bmatrix}}_{A} \underbrace{\begin{bmatrix} y_i \\ y_{i-1} \\ y_{i-2} \\ \dots \\ y_{i-n+1} \end{bmatrix}}_{\vec{x}_i} + \underbrace{\begin{bmatrix} 1 \\ 0 \\ 0 \\ \dots \\ 1 \end{bmatrix}}_{G} u_i \tag{6}$$

which leads, in that form, to the state-space model:

$$\vec{x}_{i+1} = A\vec{x}_i + Gu_i \tag{7}$$

$$\vec{y}_i = \begin{bmatrix}1 & 0 & \dots & 0\end{bmatrix}\vec{x}_i \tag{8}$$

or the more general form:

$$\vec{x}_{i+1} = A\vec{x}_i + Gu_i \tag{9}$$

$$\vec{y}_i = H_i\vec{x}_i \tag{10}$$

Equation (9) represent the way a new state $\vec{x}_{I+1}$ is modeled as a linear combination of both the previous sate $\vec{x}_i$, and some process noise u_i. Equation (10) describes the way the process measurements or observations $\vec{y}_i$ are derived from the internal state $\vec{x}_i$. These two equations are often referred to respectively as the process model and the measurement model, and they serve as the basis for all linear estimation methods, such as the Kalman filter.

3. THE KALMAN FILTER

Within the significant toolbox of mathematical tools that can be used for stochastic estimation from noisy measurements, is known as the Kalman filter.

The Kalman filter is essentially a set of mathematical equations that implements a predictor-corrector type estimator. That is a optimal operation in sense that it minimizes the estimated error covariance. The Kalman filter is frequently applied, especially in the domains of autonomous and assisted regulation.

The Kalman filter addresses the general problem of trying to estimate the state $x \in R^n$ of a discrete time controlled process that is governed by the linear stochastic difference equation:

$$x_k = Ax_{k-1} + Bu_k + w_{k-1} \tag{11}$$

with a measurement $z \in R^m$ *that is*

$$z_k = Hx_k + v_k \tag{12}$$

The random variables w_k and v_k represent the process and measurement noise. They are assumed to be independent of each other, white and with normal probability distributions.

The nxn matrix A in the difference equation (11) relates the state at the previous time step k-1 to the state at the current state k, in absence of the process noise.

It will be defined a value of x to be a priori state estimate at step k, $\hat{x}^{-}{}_{k} \in R^{n}$. This value gives us knowledge of the process prior step k, and $\hat{x}_k \in R^n$ defines a posteriori state estimate at step k given measurement z_k. We can then define a priori and a posteriori estimate errors as:

$$e_k^- \equiv x_k - \hat{x}_k^- \tag{13}$$

and

$$e_k = x_k - \hat{x}_k \tag{14}$$

The a priori estimate covariance is:

$$P_k^- = E\left[e_k^- e_k^T\right], \tag{15}$$

and the a posteriori estimate error covariance is:

$$P_k = E\left[e_k e_k^T\right]. \tag{16}$$

In deriving the equations for the Kalman filter, we begin with the goal of finding an equation that computes an a posteriori state estimate $\hat{x}_k$, as a linear combination of an a priori estimate $\hat{x}_k^-$ and a difference between an actual measurement z_k and a measurement prediction $H\hat{x}_k^-$, as shown below in equation. The justification for the next equation is given in the probabilistic origins of the filter.

$$\hat{x}_k = \hat{x}_k^- + K\left(z_k - H\hat{x}_k^-\right) \tag{17}$$

The difference $\left(z_k - H \cdot \hat{x}_k^-\right)$ in equation (17) is called the residual or the measurement innovation. The residual reflects the discrepancy between the predicted measurement $H \cdot \hat{x}_k^-$ and the actual measurement z_k. A residual of zero means that the two are in complete agreement.

The nxm matrix K in equation (17) is chosen to be the gain that minimizes the a posteriori error covariance equation (16).

The Kalman filter estimates a process by using a form of feedback control: the filter estimates the process state at some time and then obtains feedback in form of measurements. As such, the equation for the Kalman filter falls into two groups: time update equations and measurement equation. The time update equations are responsible for projecting forward (in time) the current state and error covariance estimates to obtain the a priori estimates for the next time step.

The measurement update equations are responsible for the feedback – i.e. for incorporating a new measurement into the a priori estimate to obtain an improved a posteriori estimate.

The specific equations for time and measurement update are presented in the following table:

Tabel 1

Discrete Kalman filter time update equations	*Discrete Kalman filter measurement update equations*
$\hat{x}_k^- = A \cdot \hat{x}_{k-1} + Bu_k$	$K_k = P_k^- H^T \left(HP_k^- H^T + R\right)^{-1}$
$P_k^- = AP_{k-1}A^T + Q$	$\hat{x}_k = \hat{x}_k^- + K_k\left(z_k - H\hat{x}_k^-\right)$
	$P_k = \left(1 - K_k H\right)P_k^-$

We notice how the time update equations project the state and covariance estimates forward from time step k-1 to step k.

After each time and measurement update pair the process is repeated with the previous a posteriori estimates used to project the new a priori estimates. This recursive nature is one of the most used features of the Kalman filter – it makes practical implementation of the filter more feasible then, for example, an implementation of a Wiener filter which is designed to operate on all the data directly for each estimate. The Kalman filter estimates the actual value depending on the previous measured values.

Figure 2 presents a complete picture of the operations effectuated by the filter, based on table 1:

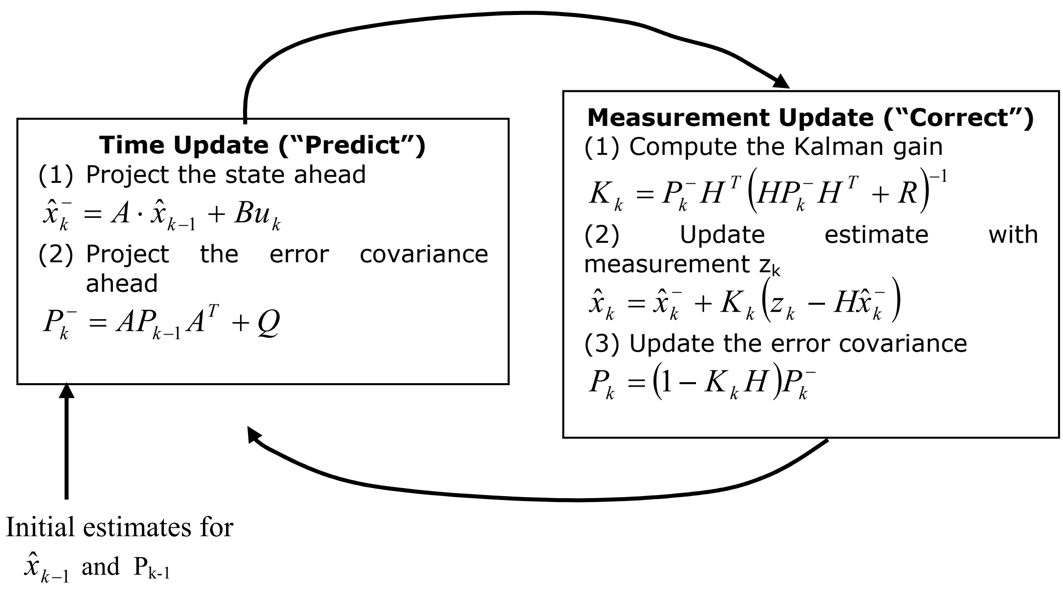

Fig.2 *Complete picture of the operation of the Kalman filter*

4. Parameter estimation of a control signal, affected by noise, for an automatic regulation system

One of the main reasons for a automatic regulation system to function in the correct direction for that it was implemented, it's necessary that the control signal parameters of the system shouldn't be changed by the specifically environment noises where it acts.

Through the implementation of the Kalman filter equation in MatLab, the user will have the possibility to modify a series of filter parameters, gain, number of iterations, the characteristics for the analyzed signal and that for the disturb signal.

The analyzed signal in that application is a step signal affected by an random, Gaussian white noise.

Figure 3 presents the obtained results throughout the simulation: the ideal signal form, not affected by noise (-), the disturber signal (--) and the estimate signal (0), obtained after the application of the predict correction Kalman filter algorithm.

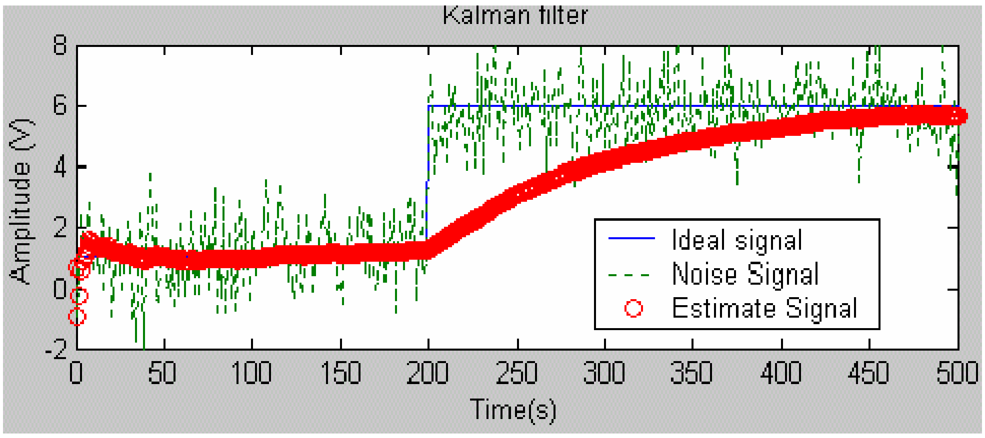

Fig.3 *Ideal signal, noise signal, estimate signal*

5. CONCLUSION

From the presented in this paper we can see an large applicability for the Kalman filter in the automation domain, under a large and fast extension of the digital leading devices in obtaining better general quality indicative.

6. BIBLIOGRAPHY

1. Greg Welch, Gary Bishop An Introduction to the Kalman Filter, Ed. Siggraph, Los Angeles, 2001
2. Ştefan Gârlaşu Prelucrarea în timp real a semnalelor fizice, Ed. Scrisul Românesc, Craiova, 1978
3. http://www.cs.unc.edu/~tracker/ref/s2001/kalman/
4. http://www.cs.unc.edu/~welch/kalman/

IMAGE PROCESSING AS A POSSIBILITY OF AUTOMATIC QUALITY CONTROL

[1]Elemér NAGY
[2]Margaret NAGY

[1]University of Szeged
[2]University of Szeged

***Abstract**:*
This poster displays the definition of the age of trees cut down. The objective is to be able to automatically detect the number of annual rings in the test image, approaching from a given centre to a particular point with a maximum detection error of two, despite the bias of the image, presuming that cracks in the cross-section of the rings total less than twenty degrees. We are aiming at making our algorithm profitable in business and education as well.

***Keywords**:*
Image processing, quality control, annual rings of trees

1. INTRODUCTION

Computer aided image processing has been steadily developing in the past thirty years. However, there is a long way to go. Despite the solutions available in the subdomains, the particular approach or software applicable on every field has not yet been found (Géza ÁLLÓ et al, 1993).

In our domestic economic situation an annual human work costs about one million HUF for the employer. If we accept the hypothesis that every application which is refund in five years can be considered economical, then to develop computer systems for a maximum of five million HUF is subservient in case it can substitute at least a man's work. This means a half year work for a good informatics specialist (including the expenditures of the use of technical means).

This poster displays the definition of the age of trees cut down, considering the fact that the issue of size measurement, wood type and wood defect detection has already been solved.

2. THE GOAL

Our subject is the definition of the age and quality of trees cut down with power saw; this definition and other wood features (like wood size, wood type and quality) would provide profitable information to the management of wood yards and foresting companies — if the information gained is with 90% accuracy.

By computer aided image procession, using a section of the woody stem, wood age can be defined. For trunk is accessible in trees cut down, it is practicable to examine annual rings (fig. 1). If the tree in question was not cut down in level but by wedging, the image to be processed should be properly transformed. Determining the actual age of a live, standing tree is also possible (e.g. by wood tomography), but this one is a rather expensive procedure.

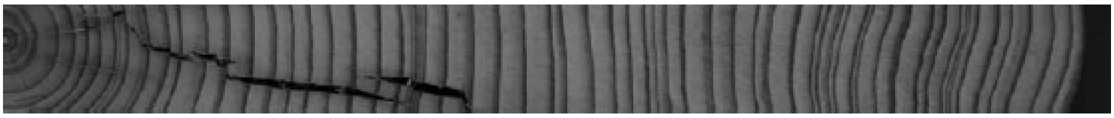

Fig.1. *The classic fair quality sample image to count annual rings. The image was converted to greyscale. To be analyzed easier the left side was cut.*

3. THE METHODS

For this reason, there seem to be four approaches to determine age:

- The isolation of annual rings from "the noise" by the methods of "weak artificial intelligence" and the definition of the number of rings.
- Image processing (filtering and colour transformation) to construct the binary image by filtering the noise to get an exclusive image of the annual rings and then counting the rings.
- Problem solving without complex approaches (e.g. finding the most pale-to-dark transitions forming a right angle to a line).
- The combination of these methods.

4. THE ANALYSIS OF METHODS

The first one of these approaches should be thrown out for the lack of time (seeming to be the most accurate approach, the first one needs a considerable investment). We had a go at the second approach first (contrast and brightness balancing, linear filtering with symmetric edge detection, threshold cutting and edge counting), but on the current level of implementation, this approach failed to be a robust one. The third approach worked fine.

5. THE DEGREE OF ROBUSTNESS

The mentioned robustness was measured by loading the available image with different noises (sharpening, smoothing, adjusting contrast and brightness, adding Gauss noise, adding salt and pepper) and then the available functions were tested on the image obtained. Unfortunately the method was only insensitive to sharpening (which is very rare in reality). With further corrections the system might have been able to register contrast and brightness alignment, but even with this it would not have been more efficient than the third method.

6. THE PRACTICAL PROCESS

In practice one should start with measuring the diameter of the tree and the relief of the surface with a suitable tool. Then based on the photo or another image that can be digitally processed, the image transposed to plane is generated with the background cut out (greyed uniformly with the grey given by the average of the pixels not to be cut out from the image). From the generated image it is possible to find the outline of the tree with simple methods, so the surface area can be easily calculated.

The next task is to locate the centre of the tree to count the annual rings from there (assuming that a centre-independent algorithm is used) (fig. 2). The weak artificial intelligence can be used for this – or according to KISS – the geometrical centre can be considered to be the centre of the tree.

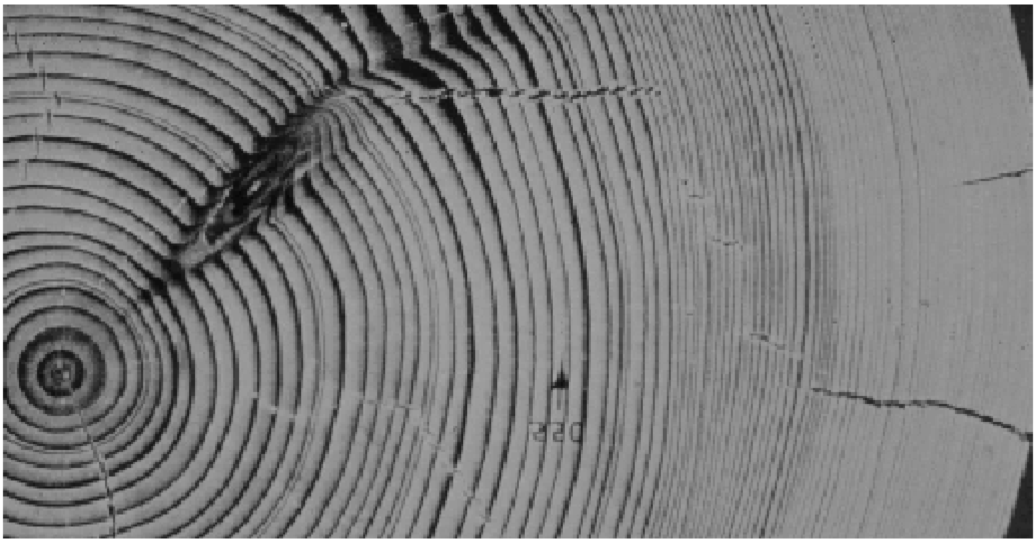

Fig.2. *Low resolution picture of a big trunk. With it the algorithm's sensitivity on thin annual rings can be well tested.*

The centre-independent algorithm is, for example, when an image cleared somehow of noise is cut through with dense lines along one side (for example by the average annual rings distance which comes directly from the resolution). Along these lines the annual rings can be counted and then the highest calculated can be considered the age of the tree (fig. 3).

By repeating the process on another perpendicular side (assuming sufficient calculating power) taking the minimum of the acquired results we can probably also eliminate the interference. This can only be realized if the lines which are near perpendicular to the slicing line are counted. Considering the deformity of the annual rings this came about 20 degrees. Cracks can appear only in two views in a gradient of 20 degrees while annual rings can be seen in all four views because of their shapes (fig. 4).

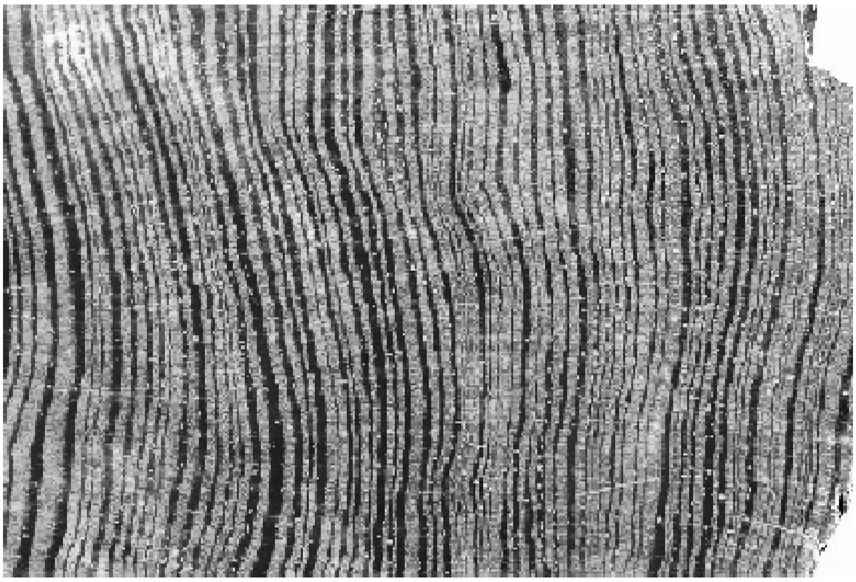

Fig.3. *A very bad resolution picture heavily loaded with noise. It was originally converted from orange-red colours. The image is practically useless without histogram alignment.*

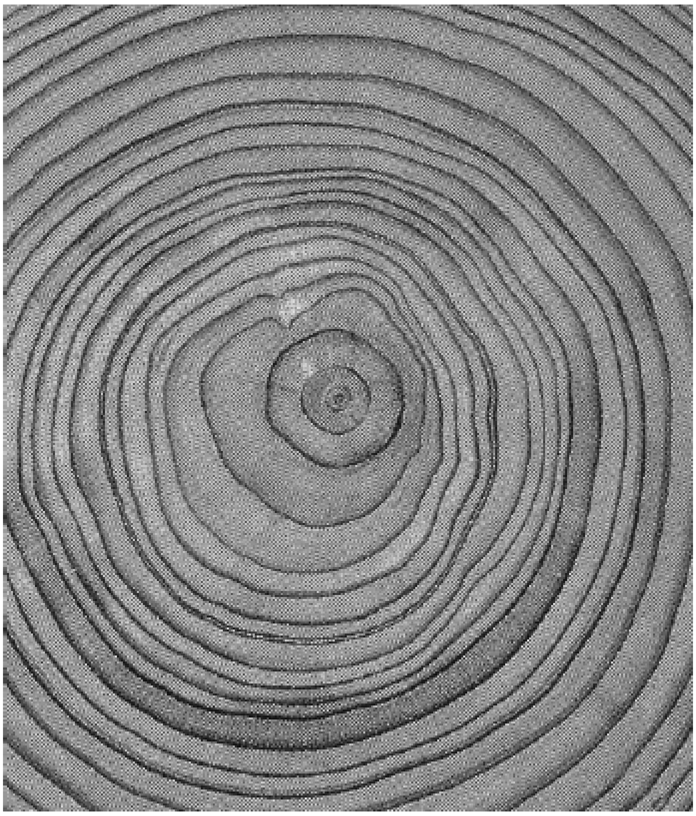

Fig.4. *A relatively high resolution image which has been heavily loaded with noise after using classic image compression and processing methods.*

Problems can occur in the case when there are at least four cracks on the tree which do not form a circle (a good weak artificial intelligence can handle this). The four cracks are at maximum 20 degree angles to four different axes. In this case however the wood possibly cannot be used.

Prepared for this case we can examine whether the annual rings are even or odd.

7. THE TOOLS

Considering that because of the trunk's size taking a photo in front of the suitable background is almost impossible, this possibility can be excluded. The size of the tree and the speed of processing practically exclude the possibility of mechanical scanning. So the technology to measure rebounding time of directional beam remains. The most appropriate tool – for the first approach – is the laser knife or the millimetre accurate sound radar.

In regard to sawdust an automatically cleaned industrial camera is suitable for the eventual target application which is capable of taking high resolution black and white photos. In the experimental and analysis phase an image also available on the Internet is used.

The suitable platform for the eventual target application seems to be the C/C++ language, for example under UNIX/Linux operating system. The freely accessible image programme running under Java Virtual Machine is the suitable platform of the experimental and analysis phases.

My advice for application refers to storing on hard disk and 24-pin dot-matrix printer because of the thrift and the reliability. The suitable output in the experimental and analysis phase seems to be a window created in Java.

8. THE OBJECTIVE

Now, the objective is to be able to automatically detect the number of annual rings in the test image, approaching from a given centre to a particular point, with a maximum of two detection errors despite the bias of the image, presuming that cracks in the cross-section of the rings are less than twenty degrees. Bias is simulated by sawdust and the noise of the CCTV camera. We are aiming at making our algorithm profitable in business and education as well.

9. THE ALGORITHM

The robustness of the applied KISS algorithm highly surpasses the classical image processing approach. The basic idea was given by the fact that if the dark stripes on the bright background can be counted in the filtered image, the darker stripes can also be counted on the brighter background in the original image. By aligning the brightness and contrast we can get an image where the annual rings grown in the winter is in the 0-25 scale of colours, while the summer part is in the 26-255 scale of colours.

The objective is to find as many as possible point triplets (A, B, C) along the line where it is true that points A and C are in the 26-255 scale of colours, point B is in the 0-26 scale of colours and there is a line through point B which is in a gradient of 20 degrees of AC line and eight from the ten closest points on the line are in the 0-25 scale of colours. From the possible ABC divisions we are looking for as many as possible divisions which do not overlap along a line, that is the AC distance has to be minimized.

Considering the alignment applied in the first step, the algorithm is immune to brightness and contrast offset (except for extreme over and under expose which does not occur in case of industrial cameras) and because of this it is more or less immune to the lighting so it can also be used in open air. This algorithm does not use (derivate) edge detection so some specific noise does not cause big errors during the image processing. As it does not use cutting after edge detection, no points are lost from the lines. It does not search for edges, thus it is resistant to blurring, moreover applying a median-filter in advance, it is also immune to salt and pepper type noise without detectable efficiency decay.

REFERENCES / BIBLIOGRAPHY

1. G Álló –J. Föglein – GY. CS. Hegedűs. - J. Szabó: Bevezetés a számítógépes képfeldolgozásba. BME Mérnöktovábbképző Intézet. Egyetemi jegyzet Javított kiadás. 1993
2. J. Berke, - GY. CS. Hegedűs - D. Kelemen - J. Szabó: Digitális képfeldolgozás és alkalmazásai. Keszthelyi Akadémia Alapítvány, ISBN 963 04 7466 2. 1996
3. Kobayashi Osamu: Jumoku-Nenrin (Tree Rings). http://village.infoweb.ne.jp/~fwga0159/trind-e.htm. 1993
4. W. Steven Conner, Robert A. Schowengerdt, Martin Munro, and Malcolm Hughes : Design of A Computer Vision-Based Tree Ring Analysis System. 1998. http://www.ece.arizona.edu/~dial/trees/base_files/background.html
5. http://www.ltrr.arizona.edu/dendrochronology.html. Laboratory of Tree-Ring Research. The University of Arizona. 2001

ISIRR 2003

PROGRAM BY CALCULATION THE REGIMES OF CHIP REMOVAL

Vasile George CIOATĂ, Imre Zsolt MIKLOS, Imre KISS

Faculty Engineering of Hunedoara

Abstract:

This paper presents an enlarged application in the Visual Basic programming and Access database, which are resolving some aspects regarding the practical side in the designing of technologies in the field mechanical workings through cutting. The users of this soft are free of a great volume of repetitive calculations and work for transposing the results in technical documentations (plans of operations, technological files, and so on).

Keywords:

application, technology, chip removal, technical documentation

1. INTRODUCTION

In the designing of technologies in the field mechanical working through cutting, the classical calculation of the cutting regime, is limited, because a lot of coefficient numbers, witch must be adopted. These coefficients depending of cutting tool (the material of the active part, the back rake, the main angle of incidence, the degree of wear an so on), and with the processed material (cutting workability, the state of material destined for the cutting process, an so on).

Because the cutting tools exist in a big variety, and, also the number of material destined for the cutting process is higher, the achievement of calculation programs, at witch coefficients automatically selected and adopted for the adequate cutting process guidance, is practically impossible to create. Also, the insert of this date, through the control keyboard, uses a long time, and in this case, the possible advantages of anyone calculation programmes, it may be possible to cancel being unefficient for any application.

From this reason, we created one of application program, witch try to resolve the practical size of the cutting range calculation. The users of this soft are free of repetitive calculations and work for transposing the results in technical documentation (plans of operation, operation sheet, and so on). The application program has be created on the model of the classical calculation mode of the cutting range. The phases of this program is the following:

- The material, destined for cutting, is choose; also, the type of the semi-finished product and the thermal treatment are chose, too;
- In function of this metallic material destined for cutting operation, is adopted the cutting tool from the existing list of tools; the durability of this cutting tool is adopted automatically;

- It is calculate the cutting depth, in function of the next cutting process, uses the classical formulas; the number of cutting phases it is introduced by the operators;
- The forward flow of the cutting process, is imposes by the program between an minimal and an maximal values, depending from the nature of process and the cutting depth;
- The cutting speed is a function of the materials witch is processed, the cutting tool, the depth of the operation and the forward flow of the cutting;
- The revolutions per minute is calculated in function of the material dimension and the minimal value indicated from the cutting speed; is adopted the value, witch is immediately lower at the revolutions per minute of the machine tool; the speed value will be recalculated, according to this value of revolutions per minute;
- The power of cutting is a function of the nature of the process, the depth, the cutting tool, and the materials nature; this value is compared with the value of the machine tool's power, and in the case of highly calculated power, the parameters of cutting will be modified;
- The time is calculated with the analytical formula, which take account the dimension of semi-finished product, the forward flow, the revolutions per minute and the numbers of the cutting phases;
- The values of cutting process, obtained in these phases of the programme, are transposes in the operational plans.

For resolving of this applications program, is used the Visual Basic programming, for the advantage, which is offered by this:

- Is very easy to learn – may be uses and understanding even the unspecialists;
- Is a visual programming language; the Windows type interface with the users can be easiness created;
- Is a language oriented on the objects and leading by the events; from each control's of the interface, is associated a code, formed on subroutines, each of these, being an adequate event;
- The program allowed many application which working with relational date (the recommended database of Microsoft for Visual Basic application is the Access database);
- A minimal hardware and software resources are necessary;
- At the base of this application stand the Microsoft Access database, which is content many table with technical characteristics of the machine tool, and the cutting tools, the durability of these, the representative forward flow for the cutting's nature, the cutting depth, power and speed of the process, depending of the material nature, and so on. The obtained results are cumulated and stoked in table, which is the source of technical operation (operational plans).

2. THE PROGRAM PRESENTATION AND MODE OF UTILIZATION

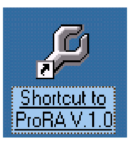

The application ProRA V.1.0 is executable, the this launch is done with a double click on the associate icon (or on shortcut). In figure 1 is presented the main window of application. The entering in this program is possible through the accessing of the ENTER>> button.

In figure 2 is presented the dialog box, which permitted to the operators the selection of the materials destined for the cutting process, from the existing list of materials in the program database. Also, is possibly to adopt the type of semi-finished materials (rolled material, forged, die forging or cast product) and the adequate heat treatment (hardening and tempering, hardening and lower annealing, normalizing). The displaying of the characteristics of these follows the select of the materials.

Through the ACCEPTA>> (ACCEPT) button, on pass at the next dialog box, presented in figure 3, which content the name of the test, the name of the choose mechanical operation, and, also the preferred machine tool.

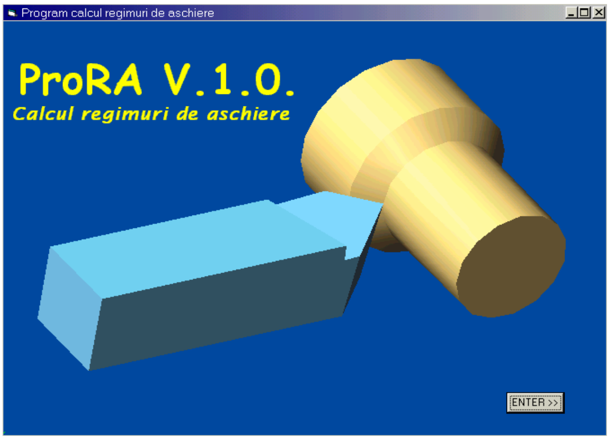

Figure 1. The Main Window of the ProRA program

Figure 2. The dialog Box for the Choose of Materials

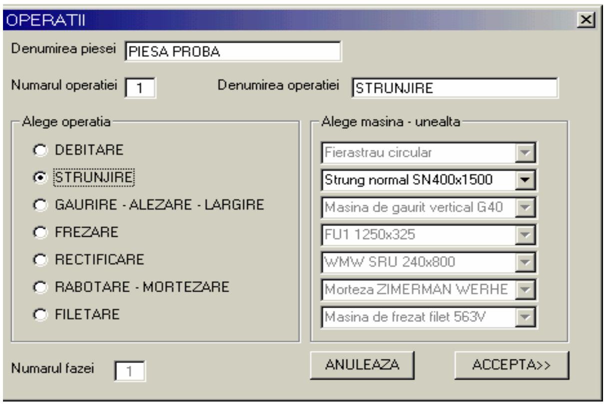

Figure 3. Dialog Box for the Choose of the Mechanical Operation

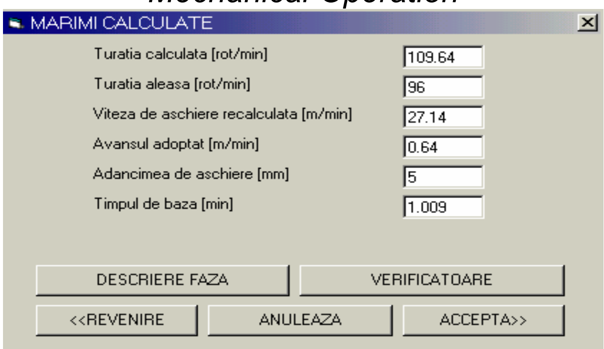

Figure 5. Window for the Calculate Values by the ProRA program

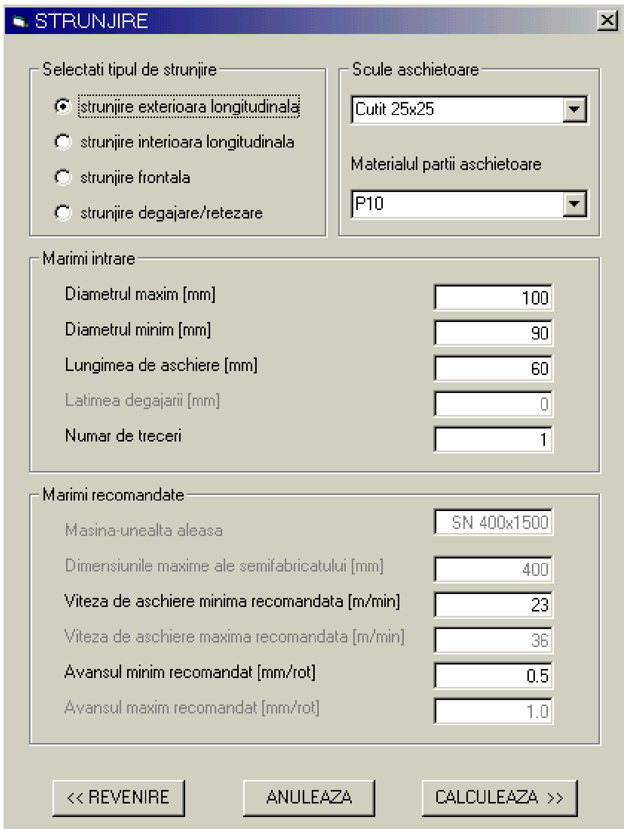

Figure 4. Window for turning operation

Through the choose of the machine tool, is selected also, the own characteristics and properties (the revolutions per minute, the overall dimension, the power of the adopted working machine, and so on).

Once with the choose operating mechanical process and adopted materials, the application program recommends automatically the adequate cutting range (the minimal and the maximal values of the cutting speed, the forward flows, and so on), which are presented in figure 3. In the dialog box it is enrollees the number (position) of the phase of the process. In the frame of operational plan.

Through the ACCEPTA>> (ACCEPT) button of menu of this dialog box, on pass at the next box, or through the <<REVENIRE, return at the primary slot.

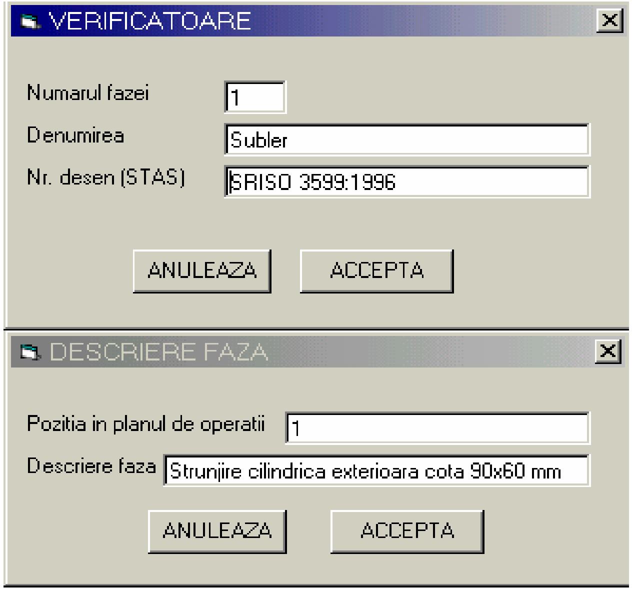

Figure 6. Windows for the Values Verify Option and Describe the Actual Phase

At the next – figure 4 – may be possible to choose the type of the adopted operation. It is introduces the primary dates, regarding the operation (the maximal and the minimal recommended values of diameters, the length of the cutting, the passing numbers, and so on). Both in this figure are presented the recommended values (MARIMI RECOMANDATE) for the adopted operation and the optimal characteristics of the cutting tool, especially the minimal cutting speed, the minimal forward flow, recommended by the program.

In figure 5 is presented the calculated date of the process , by the program, at which can be reach through the command CALCULEAZA (EXECUTE), contain in the dialog box, presented in figure 4. The values are showed in the operational plans and can be modifying in this steady of application program.

The two buttons in the figure 5 – DESCRIERE FAZA (DESCRIBE PHASE) and VERIFICATOARE – allowed the supplement of the adequate fields in the operational plan, can be called and will be appear the dialog box presented in figure 6.

The button ACCEPTA>> allowed entering in the next box of the application program, presented in figure 7. Through the SCHITA button is possible to insert the drawing of the respective operation. The drawing can be realized through the AutoCAD programme and insert in the operational plan form.

With the help of the TIPARIRE button can be possible to allow the printing of the operating plan (or the executive plan). Through the FAZA URMATOARE>> will be return to the operation phases of the program and will be resume the calculation for the next phases.

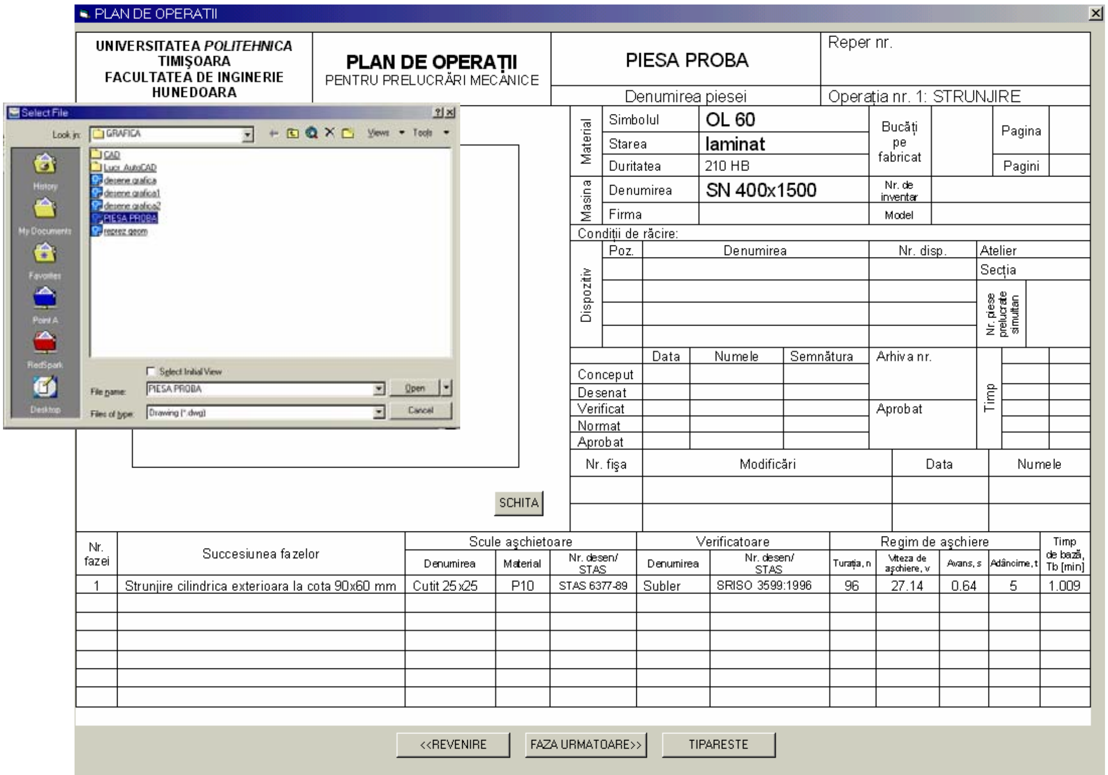

Figure 7 – Window for the Operational Plan

3. CONCLUSIONS

- The ProRA V.1.0 application program offered for the designers of the technology of processing through chip removal an efficient and comfortable alternative;
- This program can be uses in the case of some cutting process, through introduction an minimal numbers of technical date, by the keyboard of the personal computer, in logical succession and through proposal an convenient range of the operational plans and technological process;
- The interface is very sociable and friendly, being created upon as the know Microsoft Windows Application;
- The dialog box indicated in every steady, the next operation or the order of the application, which must be effectuated;
- The control of the program is very easy; every phase of this program allowed the introduction of the needed values, and the computer assured the adequate calculation;
- In this way, the time of calculation is reduces, and the precisions of date is considerable;
- The subjective errors will be eliminated, because the calculation is very exactly.

4. BIBLIOGRAPHY

1. *Heyman Mark, S. - Bazele VISUAL BASIC, Ed. Teora, Bucureşti, 1996*
2. *Pătruţ, B. - Aplicaţii în VISUAL BASIC, Ed. Teora, Bucureşti, 1999*
3. *MSDN Microsoft – Documentaţia pentru Visual Studio 6.0*
4. *Fînaru, L., Brava, I. – Visual Basic, primii paşi şi …următorii, Ed. Polirom, 2001*
5. *Epureanu, A., s.a. – Tehnologia construcţiei de maşini, Ed. Didactică şi Pedagogică, Bucureşti, 1983*
6. *Picoş, C., s.a. – Proiectarea tehnologiilor de prelucrare mecanică prin aşchiere, vol. 1 şi 2, Ed. Universitas, Chişinău, 1992*
7. *Vlase, A. s.a. – Tehnologii de prelucrare pe maşini de rectificat, Ed. Tehnică, Bucureşti, 1995*
8. *Vlase, A. s.a. – Tehnologii de prelucrare pe maşini de găurit, Ed. Tehnică, Bucureşti, 1994*
9. *Vlase, A. s.a. – Tehnologii de prelucrare pe maşini de frezat, Ed. Tehnică, Bucureşti, 1993*
10. *Vlase, A. s.a. – Regimuri de aşchiere, adaosuri de prelucrare şi norme tehnice de timp, vol. 1 şi 2, Ed. Tehnică, Bucureşti, 1985*

GEOGRAPHIC INFORMATION SYSTEM IN IRRIGATION SYSTEM MANAGEMENT

Pavel BENKA[1], Vladimir BULATOVIC[2]

[1]Faculty of Agriculture, NOVI SAD, SERBIA and MONTENEGRO
[2]Faculty of Technical Sciences, NOVI SAD, SERBIA and MONTENEGRO

ABSTRACT

This paper deals with the significance and potential application of Geographic Information System (GIS) for irrigation system management. In view of their actuality, spatial data contained in the GIS can be divided into two groups: long-term data, which do not change over a longer period of time (like topography) and the data of short-term character, related to rapidly changing parameters, like soil moisture. Possible ways of obtaining spatial data needed to form a GIS are considered. The importance of forming GIS as a step in applying principles of site-specific farming is pointed out.

Key words: *Geographic information system, irrigation, site-specific farming*

1. INTRODUCTION

Modern ways of production and production management require the availability of necessary information at a right time to allow planning and prompt decision making. Agricultural production should not be an exception in this respect. As agricultural production takes place on production plots – parts of land surface, and great deal of information important for production is related to the position of production plots, there appears a need for using Geographic Information System (GIS) for the purpose of manipulating such data.

According to some definitions GIS is described as a sort of digital map or chart of the surface area presented. However, GIS offers much more than can give us a map or topographic plan of a given area. Thanks to this system one can gather at one place more information about the phenomena occurring on the considered territory. The available pieces of information can be combined, updated and/or supplemented with new and actual ones, so that, in contrast to a geographic map, this is a dynamic system

GIS is a system consisting of various pieces of information about land that are spatially organized. The expression ‘spatially organized’ should be understood so that for each piece of data stored in the GIS one can find the place, i.e. the position of the object or phenomenon to which this data is related. This means that, in addition to providing answers to the questions such as *what*?, how?, *how much?,* one can get an answer to the question *where?*

GIS is organized so that it presents spatial units representing spatial objects or phenomena which are related to other pieces of information organized in the databases [1]. The basic spatial units of a GIS are:

- point
- line - polyline
- polygon

These basic units describe the space to which GIS is related.

Point is defined by a pair of coordinates (Y and X or λ and φ). By a point in the GIS we can present objects or phenomena that are of pointwise character, that is those that cover a very small area with respect to the area of the whole region considered.

Line is defined by two points (two pairs of coordinates) representing the beginning and the end of the line. Polyline is a series of continuously connected lines and is represented by an array of points standing for the beginning, breaking points and the end of the polyline. A polyline is not closed, i.e. it does not describe a figure of defined surface area. This spatial unit is related to the objects of linear type, which means of a defined length but negligible width, such as pipelines, canals for irrigation/drainage, etc.

Polygon is a figure described by a closed line. A polygon is represented by a series of points representing breaking points of the boundary line. By polygon we can represent surfaces such as agricultural plots, production sections of a plot, areas with the same type of soil or the same sort of crop, etc.

With the aid of these basic elements all data related to a particular parameter (e.g., amount of fertilizers used to treat the given area represented by a polygon) are spatially collocated. To achieve a better organization of these spatial elements they are organized in layers. In certain situations, particular layers can be excluded, i.e. make invisible, and thus we can combine the current presentation in the GIS.

2. GIS CONTENT FOR THE NEEDS OF AN IRRIGATION SYSTEM

The database contents should be determined in accordance with the functions that the GIS should offer in the irrigation system management.

Generally, the data that may be needed for the purpose of irrigation can be divided into two groups: long-term and short-term data. To the group of long-term data we can include the those data that do not change, at least in a shorter time period, while temporary data are those that are relatively frequently changed in the course of several hours, days, or weeks.

These long-term data make the basis of a GIS. Here we think of the presentation of the terrain on which the irrigation system is situated. This is related to the land surface characteristics, i.e. the terrain inclination as a factor important for irrigation because of the surface water runoff from the higher to the lower terrain. On the basis of the terrain topography it is possible to follow additionally the phenomena such as water erosion, i.e. the transport of surface soil layer from the inclined sections to depressions. Terrain topography in the GIS can be represented through a digital model of the terrain, i.e. by an array of points uniformly distributed over the whole surface area of the irrigation region. The density of particular points should be determined according to the terrain characteristics having in mind that it is necessary to register small inclinations of the terrain and microdepressions. Digital model of the terrain offers the possibility of obtaining isohypses for the cartographic presentation of the terrain on the basis of the necessary equidistances or obtaining a 3D plastic presentation.

The next layer of long-term data may be the cadastre plots presented by a series of polygons. To the polygons in the database should be related all those data that are standard in the soil cadastre, i.e. in the official register of real estates. It may happen that the area found in the GIS differs from the one in the official register because of the different data sources, so that in a separate field of the database we can also register in parallel this area (as the basis for taxation, etc.).

The objects existing on the territory of the irrigation system can be divided into several layers, depending of the function of particular objects. In dependence of their size they can be represented in the form of a polygon; in the case of covering a small area (fence, wall, etc.) the objects can be represented as a point or a line. The data related to these units would be those that describe the object more closely and some of its characteristics (e.g., pumping station data), and the like.

The most important layers encompassing the irrigation system objects would be those related to canals and water pipelines with all the necessary data about the capacity and other data, underground installations such as power cables and cables to control the irrigation equipment. Also, to this group belong the objects that may represent obstacles in the course of irrigation or land cultivation.

When the organization of agricultural production is concerned it is necessary to have the layer containing production units, which may not coincide with the cadastre plots. This layer can also vary, but in the course of one vegetation season it should be the same. This layer can serve as the base for preparing data that are related to the planning of agricultural production.

In parallel with the production units layer it is necessary to form also the layer containing the communication roads with and without pavement, for the purpose of planning transportation from the production area to the economic yard or storehouse.

The data that we termed as short-term ones are those data that are not of a long-lasting character, that is which are actual several hours, days, weeks. These data are useful while they are actual for decision making about the time of irrigation or amount of water, but can be used later on when analyzing the effects of particular activities or phenomena on the state of plants in the previous periods, for example in the preceding year.

For these data, new layers should be formed. They would contain the data about the current state of soil moisture, content of particular nutritive matter, the growth stage of plants currently grown on the considered section of the irrigation system area. As we deal with data that are periodically changed it is possible to update them through an automatic system, by reading the indication of the sensors placed at the representative points. In the case such system is lacking, especially if we monitor phenomena that change little in the course of several days, it is possible to collect data on the spot and enter them into the database manually. Automatic mode is certainly advantageous, not only because of instantaneous updating, but also because of eliminating possible errors due to human factor.

The values of particular parameters are related to the site on which the given quantity was measured, such as the site of taking soil sample for the purpose of determining its moisture content, nitrogen level, etc. Such site can be represented by a point. However, for the purpose of planning agricultural production on the basis of particular sites we often need the values that are related to the production sections, that is production plots. These values can be obtained by standard tools contained in the GIS software packages that provide the values between the measuring points by interpolation method, similar to drawing isohypses [3]. By further intersecting of the layer containing isolines with production areas appropriate data are obtained for each production unit.

One group of data that are not of lasting character, but which are very important are those concerning the production plot yields. These data allow the analysis of the effect of the measures applied on particular areas on crop yields and getting an insight into the future measures to be undertaken on these production units under particular crops. Contemporary combines have already the facilities for registering current yields that can be used for these purposes.

3. DATA SOURCES

As can be concluded from the above consideration, all pertinent data are defined in space via point coordinates, either of individual points or groups of points connected in a line, polyline or polygon. There are several ways to obtaining these coordinates.

Before beginning the positioning of the interesting points it is necessary to exactly establish the accuracy of positioning we need for data entering into the GIS database. It is necessary to start from the purpose and character of data. In some cases, when we deal with navigation of the agricultural machines in the course of operation on the plot, it is possible to tolerate a positioning error of only a few centimeters (e.g. inter-row cultivation). On the other hand, for pedological profile the accuracy of even several meters would be quite satisfactory as variations of soil properties have no strictly defined boundaries.

If the interesting points are determined with the accuracy at a level of a centimeter the coordinates of previous geodetic surveys (using adequate equipment), field survey using modern geodetic instruments or point recording with the aid of DGPS technology, can serve as source of data.

When the latter group of data is concerned the position of interesting points can be obtained by digitizing the existing plans and maps by manual GPS receivers, by treatment of aerophotogrammetric or satellite images at the appropriate scale or by classical geodetic survey on the terrain. When using the existing plans and maps and airplane or satellite survey it is necessary to bear in mind the correspondence of their contents to the current state on the terrain.

For the needs of establishing land cadastre, i.e. the official real estate register, the area of the Vojvodina province has been surveyed and cadastre plans were made. However, the survey has been carried out in different times and in different ways, so that the collected data are of different quality (accuracy, update, etc.). It is necessary to bear in mind the fact that in 1994 the state was such that on 528,385 ha, or 24.6% of Vojvodina area [2], the survey had been carried out 40 and more years ago, using the fathom system of measures. To the year 2002 there has been almost no attempts to update survey so that these data are still valid. The use of these data for the basis of making GIS may be quite problematic. Namely, there is only a graphic presentation of the terrain, that is the charts and not coordinates of particular points, so that the coordinates had to be obtained by digitizing such plans. As these plans are old, a question arises as to their updating, that is the degree to which they reflect the factual state on the terrain. However, even if we would accept these plans as updated, there would be still a problem of using them. Namely in the current state coordinate system use is made of the Gauss-Krieger projection whereas for the plans made in the fathom system use was made of stereographic projection, as well as the old way of surveying, so that the quality of these data is not high. On the other hand, in the Vojvodina regions for which there is a more recent survey in the metric system it is possible to obtain coordinates of all the points shown in the cadastre plans and thus form the basis for a GIS. Of course, a question has to be posed as to the update of the cadastre plans and their agreement with the factual state on the terrain.

4. GIS APPLICATION FOR IRRIGATION SYSTEMS

A geographic information system that contains specific data needed for organizing agricultural production involving an irrigation system allows a legible presentation of these data in the form of thematic maps. On the basis of them we can easier and in a more reliable way make decisions in the process of agricultural production and irrigation system management. By introducing the data on achieved yields on particular plots and intersecting these data with the conditions characterizing these plots (soil type, amounts of fertilizers, protective agents, moisture, water consumption for irrigation) it is possible to get a better insight into the effects of the applied measures.

If one wants to practice site-specific farming on production plots, formation of a GIS for these plots is an indispensable measure. Namely, the idea of site-specific farming is based on the fact that the conditions for agricultural production are not same over the whole production area. Because of that a large production area (several tens or hundreds of hectares) is to be divided into sections (e.g. 10*10 m) on which conditions for plant growing are uniform. For each of these sections of the large plot is separately determined the amounts of fertilizers, protective agents, water for irrigation, all in accordance with the conditions characteristic of that part of the area. To obtain these information it is necessary to store a large amount of data spatially distributed over the region considered. Manipulation of these data is carried out with the aid of some of GIS softwares. Through the appropriate queries the data needed are obtained from the database, which are then forwarded to the computers installed in the agricultural machines. With the aid of a GPS receiver it is possible to determine the instantaneous position of the sprinkler, fertilizer distributor or of the irrigation device, and on the basis of these data the necessary dose is read. In the opposite case, during the harvest, the GPS receivers read the combine position and an automatic device on the combine registers the current yield, which is later introduced into the database, providing thus a feedback, i.e. the information on the effect of the applied measures for each part of the plot.

If we want to navigate the agricultural machines on the plot in certain operation (sowing, inter-row cultivation, plant protection, harvest, etc.) it is necessary to determine the route according to the plot shape and plant rows. These data can be obtained with the aid of GIS software.

5. CONCLUSION

The application of GIS in irrigation of agricultural crops is a truly new approach to the planning of agricultural production involving an irrigation system. Using GIS, on the basis of data stored we can carry out the analysis of the situation and make decisions, first of all thanks to the possibility of different spatial presentation of data.

Recently, with the aim of more rational application and maximal effects of water, fertilizers, protective agents, etc., site-specific farming has been promoted. Since in this mode of farming larger areas are considered as a set of small areas with uniform conditions for agricultural production GIS is needed for storing and manipulating large amount of data about these areas, on the basis of which are determined optimal amounts of water for irrigation, i.e. fertilizers and protective agents for each individual area.

The database content should be determined in accordance with the functions to be fulfilled by GIS. Generally, the database content can be divided into long-term and short-term data. Short-term data are actual in a short period of time (hours, days) and can be activated later on for the purpose of analyzing plant development and effects of the measures applied.

Spatially defined data can be obtained in different ways, subject to their importance and required accuracy. They can be obtained directly in the field (GPS and geodetic survey), which is more accurate but more expensive, and use can be made of the existing charts and maps, photogrametric recording, satellite imaging, when the required precision of measurement is lower. It is necessary to have in mind the updating of data, i.e. how well they agree with the factual state on the terrain.

Acknowledgements: The work was undertaken as a part of the SOIL DETERIORATION, CONSERVATION AND UTILISATION AT LAND RECLAMATION SYSTEMS Research Projects No. 0419, under contract BTR.5.01.0419.B. It has been funded partially by the Ministry of Science, Technology and Development, Government of Serbia end "SRBIJAVODE" WATER AUTHORITY – Beograd (The River Danube Water Resource Center - Novi Sad).

6. REFERENCES / BIBLIOGRAPHY

[1.] Benka P., Tabakov J., Gostovic M.: Upravljanje zalivnim sistemom prema principima precizne poljoprivrede, Melioracija i poljoprivreda, pp. 156-160, Poljoprivredni fakultet, Novi Sad, 2002.

[2.] Damjanovic T., Benka P.: Prilog analizi stanja premera i uredjenja zemljista na teritoriji Vojvodine, Uredjenje, koriscenje i zastita voda Vojvodine, pp. 113-134, Poljoprivredni fakultet, Novi Sad, 1994.

[3.] Paul A. Lonlgey, Michael F. Goodchild, David J. Maguire, David W. Rhind: Geographic Information System and Science, John Wiley & Sons LTD, pp. 454, 2002.

ELECTRICAL SHAFT SCHEME WITH STATIC FREQUENCY CONVERTERS AND ASYNCHRONOUS MACHINES WITH SHORT CIRCUIT ROTOR

[1] DEACONU Sorin Ioan, [2] GHERMAN Petre Lucian

[1,2] Universitatea „Politehnica” Timişoara,
Facultatea de Inginerie Hunedoara

Summary:
This paper presents on original scheme for electrical shaft using asynchronous machines with the rotor winding in short circuit and static frequency converter.

***Key words**:*
electrical shaft asynchronous machine, static frequency converter.

1. INTRODUCTION

In the present state of the electrical shaft schemes is used asynchronous machines with winded rotor. Between the connected rotors take place a circulation of current when a lack of balance appears. For on important equalization torque of the speeds it is necessary to introduce resistances in the rotor winding which increase the losses.

2. THE METHOD PRINCIPLE

The paper proposed presents a scheme with two asynchronous motors with the rotor winding in short circuit each supplied by on static frequency converter. On of the converters is the master (SFC_1) and the other is the slave (SFC_2).

The master converter receive information about the speed reference the direction and the START/STOP controls. The slave converter receives the same information from the master converter through a optic fiber with a high speed. This way the broth converters impose the same output frequency which means same speeds for the both motors (AM_1; AM_2).

The static frequency converters can achieve internal regulators. The regulator is used in the slave converter to control the difference between the motors speed (fig. 2).

The speed of the motors is compared with the reference of speed imposed by the ruling converter. The slave converter is programmed that the error in the regulator output is null.

The figure 1 presents the principle scheme:

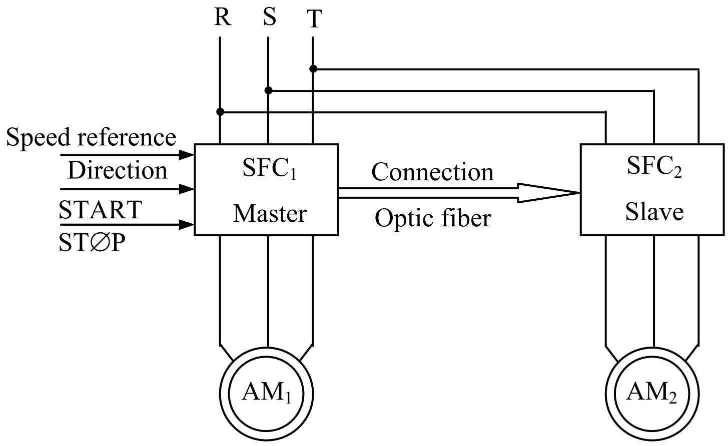

Fig. 1. *The principle scheme of the electrical shaft*

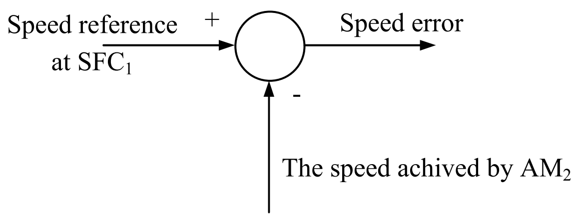

Fig. 2. *The scheme of the internal regulator of SFC_2*

3. EXPERIMENTAL RESULTS

This scheme is in use at a thermo power plant. The motors values are: P_N = 5,5 KW, n_N = 720 rpm, U_N = 380 V, I_N = 14 A.

The converters used are: ACS 800-01-0011-3 with, I_N =18,5 A, U_N = 400 V, I_{MAX} = 24 A, P_N = 7,5 KW.

The table 1 presents the measurement results with out the use of the internal regulator in SFC_2 at maximum load.

Table 1

n_1	rpm	100	300	450	600	750	900	1200	1350	1500
n_2	rpm	126	357	549	708	900	1098	1428	1607	1815
M_1	[%]	32	34	36	39	43	48	54	62	67
M_2	[%]	20	18	16	13	9	4	-2	-10	-15

It was established a difference between the speed imposed by SFC_1 and the speed achieved by AM_2. The torque of AM_2 decrease until the machine regenerating and an error come out. To resolve this problem in SFC_2 was created on internal regulator.

The results obtained are presented in table 2.

Table 2

n_1	rpm	100	300	450	600	750	900	1200	1350	1500
n_2	rpm	120	360	540	720	900	1080	1440	1620	1800
M_1	[%]	31	37	40	42	45	51	56	62	66
M_2	[%]	22	16	13	11	8	2	-3	-9	-13

Using the regulator the difference between n_1 and n_2 is 20%. After the verification of the mechanical part was established some differences between the motion wheels (different diameters) and the reference of speed for the SFC_2 was decreased with 20%. The results are shown in the table 3

Table 3

n_2	rpm	100	300	450	600	750	900	1200	1350	1500
n_2	rpm	100	300	450	600	750	900	1200	1350	1500
M_1	[%]	27	26	27	28	25	27	28	26	27
M_2	[%]	27	28	27	26	29	27	26	28	27

4. CONCLUSIONS

After the experimental attempts was established that the scheme is stout and flexible. Without the replacing of the mechanical parts it was succeeded to synchronize the speeds of the both motors.

5. REFERENCES

1. ***, ACS 800 Catalogue, Related tools and accessories
2. Kelemen, A., Imecs, M., Acționări electrice, Editura Didactică şi Pedagogică, Bucureşti, 1975

SCHEME FOR THE MODIFICATION OF THE ROTATION SPEED OF THE ROLLING DEVICES WITH STATIC FREQUENCY CONVERTERS

[1] DEACONU Sorin Ioan, [2] GHERMAN Petre Lucian

[1,2] Universitatea „Politehnica” Timişoara,
Facultatea de Inginerie Hunedoara

Summary:
This paper presents an original scheme for maintaining a steady wire stress in the rolling device using an ordinary asynchronous motor supplied by static frequency converter.

Key words:
Wire stress, rolling device, static frequency converter.

1. INTRODUCTION

The electric drives of the rolling devices are composed by special asynchronous machines with increased sliding. The mechanical characteristic of that motors allows to increase the sliding in the same time with the load torque increasing (at the increasing of the drum diameter).

Because of the increased sliding there are important losses and there is no exact correlation between the decreasing of the rotation speed in the same time with the increasing of the drum diameter and the maintaining of the strength and the linear speed of the rolled material.

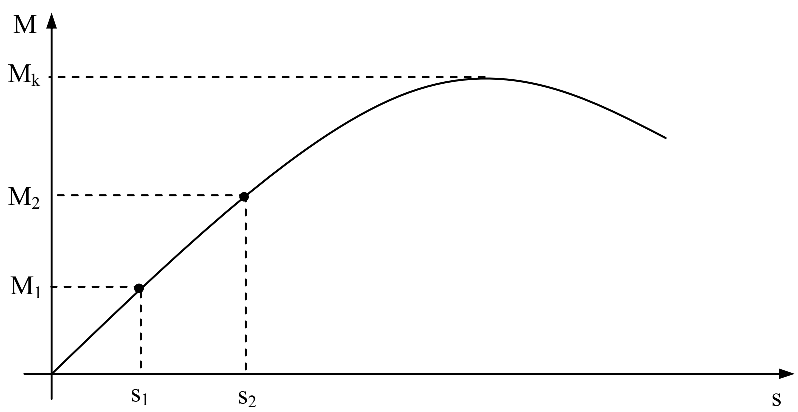

Fig. 1. *Mechanical characteristic of the asynchronous motor with increased sliding.*

This way the “consistency” of the reels decrease and the wire can unfold by the drum. If the motor was rewind the mechanical characteristic was modified and the differences which appears are more pronounced.

2. THE PRINCIPLE OF THE METHOD

The proposed scheme use a regular asynchronous motor supplied by an static frequency converter (SFC) which is controlled by a distance transducer following the reel diameter.

At the beginning the static frequency converter controls the motor with high speed and after that the speed decrease following a curve imposed by the distance traducer.

This way the linear speed and the wire strength are kept steady.

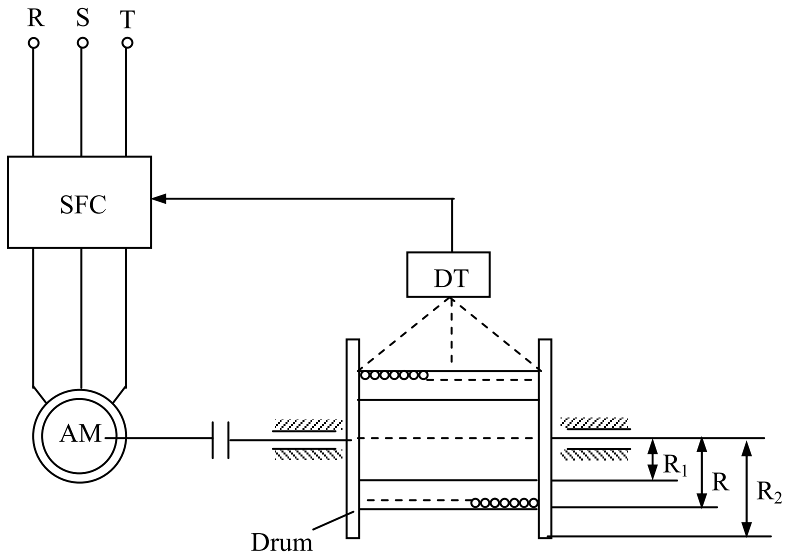

Figure 2. *The scheme with static frequency converter and distance transducer*

3. EXPERIMENTAL RESULTS

For the experiments was used a strength traducer to see the variation of the wire strength using the old scheme and the scheme with the static frequency converter.

The motors used has the following values: P_N = 2,2 KW, n_N =2920 rpm, I_N = 5,1 A. It was used a ACS 800-01-0004-3 static frequency converter with the rated values: U_N = 400 V, I_N = 5,4 A, I_{MAX} = 8,2 A, P_N = 2,2 KW.

The results of the measurements are presented in the tables 1 and 2.

Table 1.

F_R Old scheme	[N]	71	70,95	70,96	70,94	70,92	70,85	70,7	70,63	70,57	70,23	70,05
Drum diameter	[%]	0	10	20	30	40	50	60	70	80	90	100

Table 2.

F_R New scheme	[N]	71	71	71	71	71	71	71	71	71	71	71
Drum diameter	[%]	0	10	20	30	40	50	60	70	80	90	100

The linear speed has roughly V = 31 m/s. The strength of the wire in the old scheme is not steady, it's decreasing which lead to a low consistency reel and the possibility to un fold by the drum.

At the scheme with the static frequency converter (table 2) the strength in the wire remains steady at any speed.
(n_{max} = 2920 rpm, n_{min} = 975 rpm at R_1 = 0,1 m and R_2 = 0,3 m).

4. CONCLUSIONS

The scheme has a high endurance and precision and the quality of the obtained reels is steady.

The scheme could be adapted at different diameters and linear speeds by the corresponding setting of the static frequency converter.

5. REFERENCES

1. Kelemen, A., Imecs, M., Acționări electrice, Editura Didactică şi Pedagogică, Bucureşti, 1975
2. ***, ACS 800 Catalogue, Related tools and accessories

BUSINESS PROCESS AND EBXML - WEB SERVICES INTEGRATION PLATFORM, REQUIREMENTS, ARCHITECTURES, SECURITY

[1] Carmen RĂDUŢ, [2]Maria STĂNILOIU

[1] Conf. dr. ing., Universitatea "Constantin Brâncoveanu" – PITEŞTI
[2]Lect. drd. Universitatea "Constantin Brâncoveanu" – BRAILA

ABSTRACT

ebXML is a set of specifications that together enable a modular, yet complete electronic business framework. This session looks at various specifications that are being developed as part of the ebXML initiative and considers their relevance to designing an automated B2B collaboration. As part of designing the B2B collaboration, all the pieces in the puzzle are put together by using the modules that are part of ebXML.

Architecting a complex automated B2B collaboration involving multiple trading partners can be a very daunting job. This session presents the various steps involved in designing and implementing XML message-based collaboration layered on the ebXML framework. As part of implementing this architecture, various APIs for the JavaTM platform, available now and under development, will be utilized to access functionality presented by different layers.

This session offers you a look at a real-life business scenario with multiple layers, including the business process integration, partner profile management, registry/repository, and XML messaging. This session provides you with a detailed introduction to ebXML and the APIs for the Java platform available to implement this framework.

Keywords:
Business process and ebXML - architectures, web services

1. INTRODUCTION

The larger organizations have been engaged in defining and implementing their systems around EDI (Electronic Data Interchange). EDI has allowed for not only the capture of common data-interchange formats but it has also tackled the challenge of capturing those formats, i.e. messages, by defining the Business Processes in which they are used. EDI though, has proved to be expensive not only due to the high network infrastructure setup/running costs but also the high costs of System Integration. For the existing EDI Implementations out there, there is usually a dominant business entity that has tried to enforce proprietary integration approaches on all the other partners. As a result of this, several companies (especially smaller organizations) have gone about building their electronic businesses and collaboration with their trading partners in an ad-hoc manner. Listed below are some of the points:

- Define Common Business Transactions e.g. Sending a Purchase Order
- Define Common Data-Interchange Formats i.e. Messages in the context of the above Transactions
- Define a mechanism for listing your organization's capabilities and the business transactions that your organization can perform in a common Repository accessible to all other organizations. In short, an ability to describe your Company Profile.
- Define a mechanism to allow organizations to discover companies and lookup their profile.
- Define a mechanism that allows two organizations to negotiate on the business terms before they commence transactions.
- Define a common transport mechanism for exchanging messages between organizations
- Define the security and reliability framework

It is important to have a common standard in order to make the global electronic commerce a reality, and this is the vision of ebXML (electronic business XML).

1.1. About ebXML

ebXML is a global electronic business standard that is sponsored by UN/CEFACT (United Nations Center For Trade Facilitation And Electronic Business) and OASIS (Organization for the Advancement of Structural Information Standards).

The vision of ebXML[1] is to enable a global electronic marketplace where enterprises of any size and in any geographical location can meet and conduct business with each other through the exchange of XML-based messages.

---

[1] **ebXML terminology:**

- **Registry:** A central server that stores a variety of data necessary to make ebXML work. Amongst the information a Registry makes available in XML form are: Business Process & Information Meta Models, Core Library, Collaboration Protocol Profiles, and Business Library. Basically, when a business wants to start an ebXML relationship with another business, it queries a Registry in order to locate a suitable partner and to find information about requirements for dealing with that partner.
- **Business Processes:** Activities that a business can engage in (and for which it would generally want one or more partners). A Business Process is formally described by the Business Process Specification Schema (a W3C XML Schema and also a DTD), but may also be modeled in UML.
- **Collaboration Protocol Profile (CPP):** A profile filed with a Registry by a business wishing to engage in ebXML transactions. The CPP will specify some Business Processes of the business, as well as some Business Service Interfaces it supports.
- **Business Service Interface:** The ways that a business is able to carry out the transactions necessary in its Business Processes. The Business Service Interface also includes the kinds of Business Messages the business supports and the protocols over which these messages might travel.
- **Business Messages:** The actual information communicated as part of a business transaction. A message will contain multiple layers. At the outside layer, an actual communication protocol must be used (such as HTTP or SMTP). SOAP is an ebXML recommendation as an envelope for a message "payload." Other layers may deal with encryption or authentication.
- **Core Library:** A set of standard "parts" that may be used in larger ebXML elements. For example, Core Processes may be referenced by Business Processes. The Core Library is contributed by the ebXML initiative itself, while larger elements may be contributed by specific industries or businesses.
- **Collaboration Protocol Agreement (CPA):** In essence, a contract between two or more businesses that can be derived automatically from the CPPs of the respective companies. If a CPP says "I can do X," a CPA says "We will do X together."
- **Simple Object Access Protocol (SOAP):** A W3C protocol for exchange of information in a distributed environment endorsed by the ebXML initiative. Of interest for ebXML is SOAP's function as an envelope that defines a framework for describing what is in a message and how to process it.

In my opinion, ebXML will succeed in becoming universal by incorporating into the specifications more and more of what businesses do anyway as much as it will by actually getting businesses to do business differently. An illustration **(fig. 1, 2)** based on the ebXML Technical Architecture Specification will probably go a long way toward sorting out what ebXML means for business.

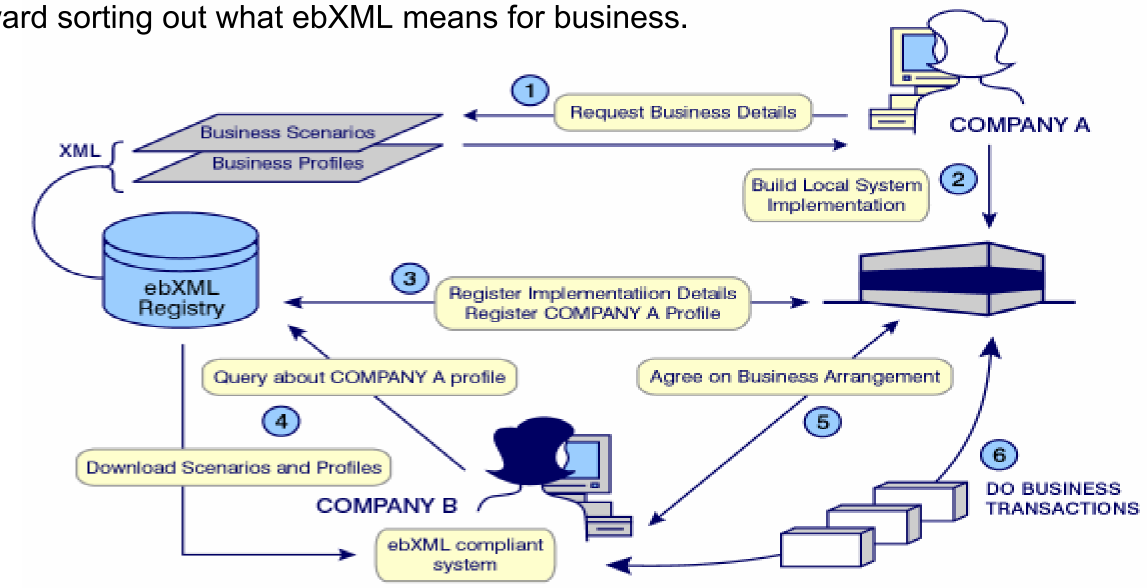

Fig. 1. *High-level overview of ebXML interaction between two companies*

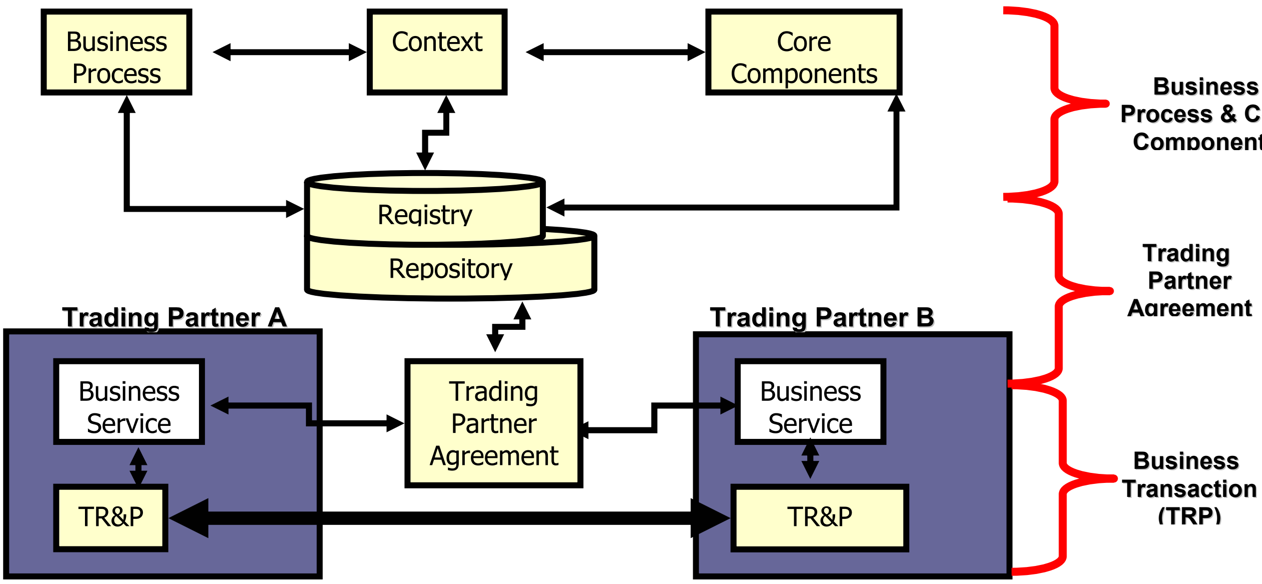

Fig. 2. *ebXML Overview*

ebXML thus defines a framework for global electronic business that will allow businesses to find each other and conduct business based on well-defined XML messages within the context of standard business processes which are governed by standard or mutually-negotiated partner agreement. The ebXML standard addresses each of the above points, as we shall see in the next section. We shall now take a look at how a business would get itself ready to perform business transactions with other organizations, based on the ebXML Standard. Shown below are 3 key phases in the order in which they are supposed to be executed towards meeting that goal:

Implementation Phase **(fig. 3.)**, Discovery of Partner Information and Negotiation Phase **(fig. 4.)**, Transaction Phase **(fig. 5.).**

In the next diagram **(fig. 3.)**, the first thing to note is the ebXML Repository. This repository contains industry defined Business Processes and Scenarios that are commonly applicable to most business transactions. Companies can choose to extend these processes and add scenarios of their own. The repository also contains profiles for businesses that have already registered themselves for performing ebXML transactions with other trading partners. For an example Organization A, which is interested in doing electronic business as per the ebXML standard, consists of 3 steps as shown in the diagram above: Request Information, Implement ebXML System, Publish Business Profile

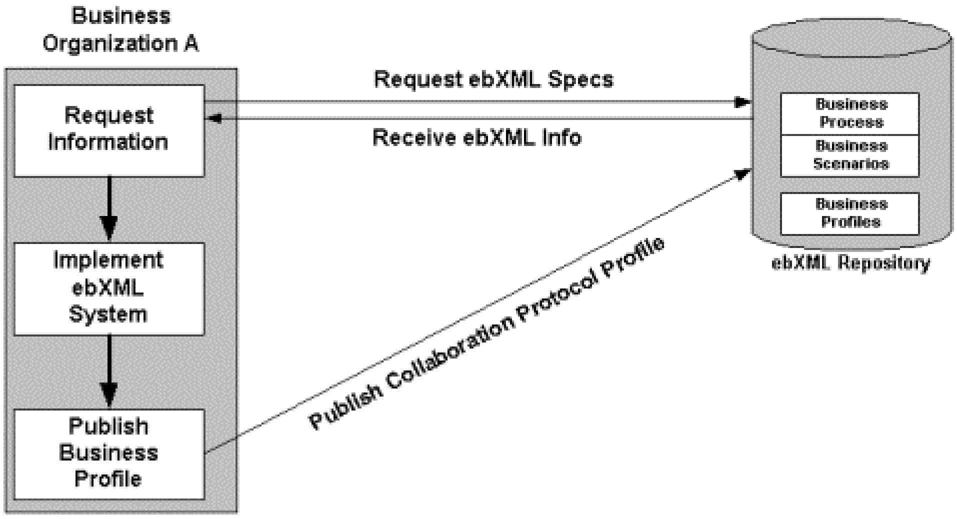

Fig. 3. *Implementation Phase*

The first step towards that is to request the ebXML Specs (Business Processes, Business Scenarios) and understand them. Once the organization has taken a look at the specs, it decides which business processes it would like to implement, following which it needs to implement a system in-house based on those standards. It could either build a new system or build on top of an existing legacy system. The whole idea is to expose a system that understands and talks ebXML. There are several choices available today in the form of third-party applications that can just take and assemble together an ebXML System. Once the system is built, the organization is ready to conduct business with other organizations. To facilitate that, it needs to publish its profile known as a Collaboration Protocol Profile (CPP) to the ebXML Repository for other organizations to discover. A CPP thus enables any organization to describe its profile i.e. which business processes it supports, its roles in that process, the messages exchanged, the transport mechanism for the messages. Once the CPP is published to the ebXML Repository, it will allow other organizations to access it and learn about the capabilities of Organization A. At any time, Organization A is free to access its own profile, review and make changes as necessary.

We see in the next phase **(fig. 4.),** how Organization A readied itself for electronic business on the ebXML standard by first implementing the ebXML System in-house and then publishing its profile, which described its capabilities to the ebXML Repository. In this phase, we shall look at how Organization A does electronic business with a partner Organization B. As our Organization A has published its profile, Organization B has done the same. So the first step that Organization A does is to retrieve Organization B's profile information from the ebXML Repository. Once it has the profile, it is in a better position to understand Organization B's capabilities i.e. whether it supports the business processes that it is interested in, the messages to be exchanged, transport mechanisms, security and reliability of the process, etc. In the real world, businesses always negotiate terms and implement business contracts before conducting any business. ebXML is no different in that regard. So, the next step for Organization A is to send over a business contract called a Collaborative Partner Agreement (CPA), in ebXML, to Organization B. The CPA will be a reflection of the profile (CPP) of both the organizations. Both the organizations can now collaborate on the CPA and refine it to meet the business needs of both the organizations. Finally, both parties accept the agreement.

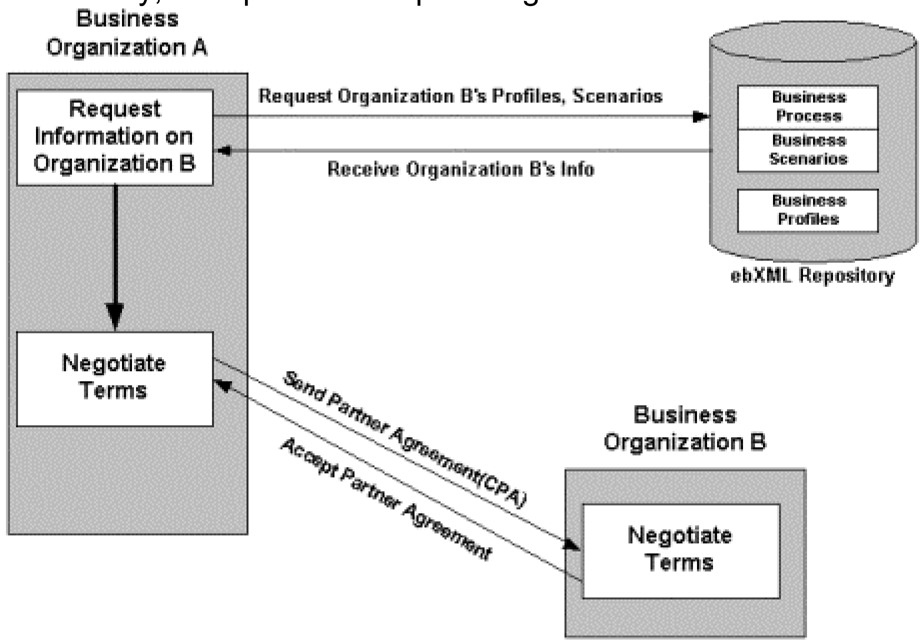

Fig. 4. *Discovery of Partner Information and Negotiation Phase*

During this phase, it is very likely that key personnel from both organizations will meet in person and make assessments before committing to an eBusiness relationship.

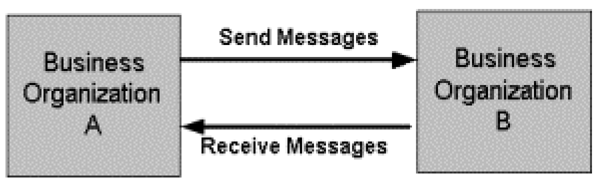

Fig. 5. *Transaction Phase*

We are now ready to conduct transactions **(fig. 5.)** . A CPA was accepted in the previous phase and the transactions can be conducted in a pre-defined fashion where each business organization plays a pre-determined role in the transaction. The transactions consist of ebXML messages, which are sent over the standard ebXML Messaging Service.

1. 2. ebXML as Web Services Framework

As e-business continues to develop, various technologies associated with computing underlie its evolution. Currently, the Java™ programming language and platform, the Extensible Markup Language, and transcoding are emerging as major technologies for performing e-business functions. In this overview essay, trends in these technologies are described, indicating how they will lead to future Web services.

In this overview, I would like to describe four major trends that I see coming along for the emerging e-business technologies of the Java** programming language, Extensible Markup Language (XML), and transcoding:

1. Continued integration of Java and XML into robust middleware such as the IBM WebSphere* software platform
2. Continued and accelerated standardization of Java and XML technologies for infrastructure and industries
3. Use of transcoding and XML technologies to support a much wider range of clients of every description, both synchronous and asynchronous
4. The move from tightly coupled applications to loosely coupled Web services

The Evolution of Integration is present in **fig. 6**:

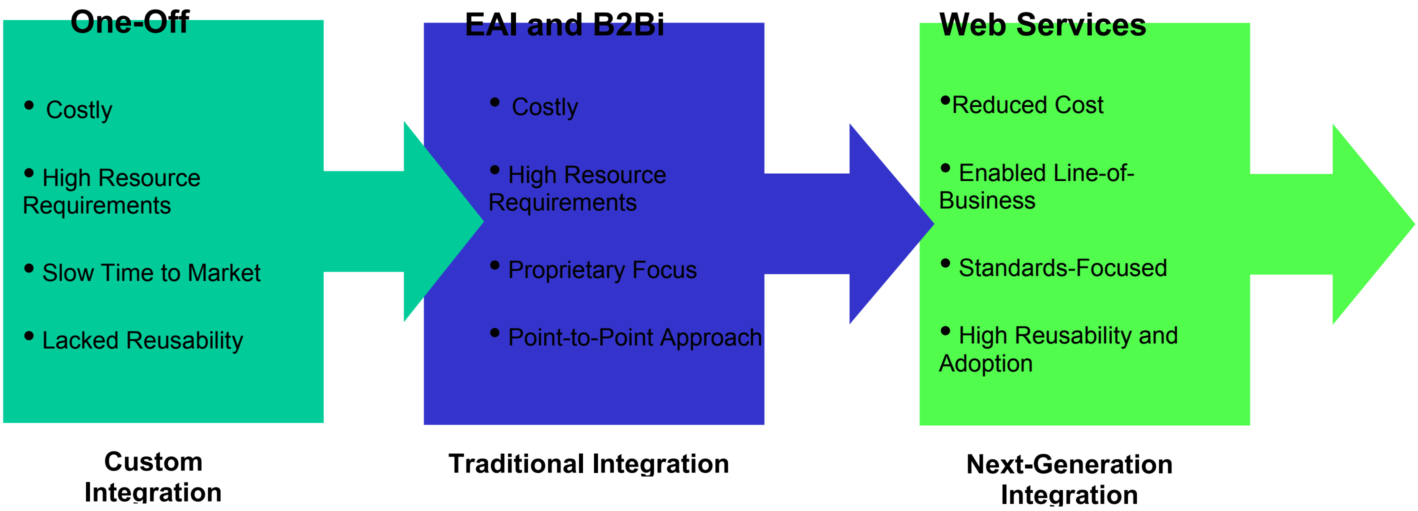

***Fig. 6.** The Evolution of Integration*

•Web services are the future of the Web because:
–Direct access to applications, programs and databases
–Browsers not required

•Web services are loosely defined as:
–Based on SOAP, WSDL, and UDDI
–An Internet address that maps XML documents to programs
–Web access to software-based services
–Anything that exposes programs to the Web!

Types of Web Services are:

•Simple: RPC based –Supports synchronous exchanges
•Compound: Aggregated “Simple” WS
•Complex: Conversational/Message-based
–Supports loosely coupled asynchronous exchanges
–Required for Enterprise Web Services
–Requires Enterprise QoS

Simple Web Services:

•Typically stateless
•Appears as an URI to the client application.

•The interaction centers around a service-specific interface
•Tightly coupled and synchronous, meaning response without request context is meaningless

Complex Web Services:

•Loosely coupled and document-driven
•Client invokes a message-based Web Service by sending it an entire document, such as a purchase order, rather than a discrete set of parameters
•The Web Service accepts the entire document, processes it, and may or may not return a result message
•Promotes a looser coupling between requestor and provider

A web service is a software application or component identified by a URI, whose interfaces and binding are capable of being described by standard XML vocabularies and that supports direct interactions with other software applications or components through the exchange of information that is expressed in terms of an XML Infoset via Internet-based protocols .

1.3. Security in ebXML Messaging

Elements of Security are:

- **P**rivacy –Protect against information being disclosed or revealed to any entity not authorized to have that information
- **A**uthentication –Authenticate the claimed identity of the originator of a data item
- **A**uthorization –Protect against the threat that unknown entities enter into a system and ensures that an entity performs only authorized actions within the system
- **I**ntegrity –Protect against the threat that the value of a data item might be changed in a way that is inconsistent with the recognized security policy
- **N**on-repudiation –Protect against one party to a transaction or communication later falsely denying that the transaction or communication occurred

Security can be applied to: Transports (SSL, IPSEC), Messages (S/MIME, PGP), Systems

2. CONCLUSION

In this article we have seen what ebXML is all about. The article also highlights the different phases involved in getting an organization to conduct electronic business based on the ebXML Standard. We have all heard of and how businesses are trying to understand Web Services to achieve more dynamic and inter-operable applications between themselves and their trading partners. Several such organizations are now at an intriguing phase of their life where they are trying to understand how best to be a player within a global standard like ebXML.

The approval of ebXML specifications is moving along at a fairly rapid pace (certainly for a standards organization). The draft specifications were approved as version 2.5 recommendation in June, 2003. I suspect that it will take another year or two to shake out all of the issues and details for such an ambitious vision. It appears, however, that ebXML is on the way to widespread use a few years down the road. Now is the time, therefore, for businesses to begin a serious consideration of their own ebXML implementation plans.

“ebXML is our only chance this decade to establish an international e-commerce standard.”

3. REFERENCES

- Clark, Jim; u.a.: ebXML Business Process Specification Schema Version 1.01. UN/CEFACT und OASIS, 2001, p. 230
- Eric Chiu, "ebXML Simplified – A Guide to the New Standard for Global E-Commerce", 2002, p. 265
- Alan Kotok & David R.R. Webber, "ebXML", September 2001, p. 330
- Commerce Extensible Markup Language (cXML) Users Guide, Version 1.2, Ariba Inc., 2001.
- XML Common Business Library (xCBL) Element and Datatype Structure Reference, Version 3.0, Commerce One, Inc., 2001.
- Open Catalog Interface (OCI), Release 2.0 B, SAP AG, 2000.
- Extensible Markup Language (XML), 1.0, World Wide Web Consortium, 1998.
- Collaboration-Protocol Profile and Agreement Specification, Version 1.0, UN/CEFACT and OASIS, 2001.
- ebXML Business Process Specification Schema, Version 1.01, UN/CEFACT and OASIS, 2001.
- Web Services Description Language (WSDL) 1.1 Specification, World Wide Web Consortium, http://www.w3.org/TR/wsdl (2001).
- Common Object Request Broker Architecture (CORBA), Object Management Group (OMG), http://www.omg.org/.
- Universal Description, Discovery, and Integration (UDDI) Programmer's API Specification,Version2.0,UDDI.org,http://www.uddi.org/pubs/ProgrammersAPI-V2.00- Open-20010608.pdf (2001).
- Universal Description, Discovery, and Integration (UDDI) Technical White Paper, UDDI.org, http://www.uddi.org (2000).
- Open Applications Group (OAG), http://www.openapplications.org/.
- OASIS/ebXML Registry Services Specification v2.5. Committee Approved Specification. Produced by the OASIS/ebXML Registry Technical Committee. June 2003. 189 pages.
- OASIS/ebXML Registry Information Model v2.5. Committee Approved Specification. Produced by the OASIS/ebXML Registry Technical Committee. June 2003. 94 pages.
- OASIS/ebXML Registry Services Specification v2.5 [source]
- OASIS/ebXML Registry Information Model v2.5 [source]
- OASIS/ebXML Registry Technical Committee website.
- "... the OASIS ebXML Registry Services Specification 2.4 and the OASIS ebXML Registry Information Model Specification 2.4 have been approved by the TC as TC approved specs.
- "OASIS ebXML Registry Technical Committee Releases Approved Version 2.0 RIM/RS Specifications." News story 2001-12-12.
- "Electronic Business XML Initiative (ebXML)" - Main reference page.
- http://www-3.ibm.com/software/webservers/commerce/wc_be/.
- http://www-3.ibm.com/software/webservers/commerce/wcs_me/.
- www.ebxml.org/specs/ebMS.pdf
- www.w3c.org/TR/SOAP-attachments
- www.w3c.org/2000/xp/Group
- www.oasis-open.org/committees/ebxml-msg
- www.ws-i.org (NOT www.wsi.org)

THE INFLUENCE OF THE ELEMENTS C, Cr AND Mo UPON THE HARDNESS OF THE BIMETALLIC CASTED IRON PIG MILLING ROLLS

Gabriela MIHUŢ, Isidor PREJBAN, Ştefan MAKSAY

University "Politechnica" Timisoara, Faculty of Engineering - Hunedoara

Abstract

The bimetallic hard-crusted iron rolls casting, for decrease of the hardness and the wear resistance destine the hard iron, alloyed with Cr and Mo. This paper suggests a mathematical shaping of the influence of the main alloy elements upon the mechanical features of this iron type, for 50 industrial batch, resulting the average values and average square aberration of the variables HSh, Cr and Mo, the equations of the hyper surface in the four dimensional space, they appealed to the successive replacement of each independent variable with the average value, resulting the equations that belong to the tree dimensional space, which are graphically represented and easy to interpret by technologists. Knowing the level curbs allows the correlations of the values of the two independent variables so that the hardness value (HSh) can be obtain in the requested boundaries.

Keywords

bimetallic milling rolls, alloy elements, hardness, wear resistance

1. INTRODUCTION

Technical conditions imposed to the milling rolls are very different and often contradictory. Thus, raised hardness from the crust correlated with mechanical resistance and raised high temperature, as well as with the raiser resilience of the alloys from the middle and journals, are enough difficult to obtain. For this reasons, the realization of the rolling mills is complexes enough, being necessary the obtaining mechanical-physical properties different in diverses points of the one and the same cast piece. Because the properties of each cast piece from de steel and pig irons are determined by the microstructure which is formed during the solidification and cooling of this, the base criterion, which determine the physical and mechanical properties of the milling rolls, is this structure.

In cast milling rolls from the pig iron are found all the carbon-iron alloys structures. One of the base factor which determine the given structure of the rolls is the chemical composition of the alloy and his speed cooling besides of the iron and the usually elements: carbon, silicon, manganese, phosphor, sulphur there are found also: chromium, cerium, nickel, calcium, molybdenum, copper, magnesium and aluminum. For the whiten degree correction of the liquid pig iron, purposed to crusting rolls with white crust, are utilized at large action of the tellurium. Besides of those previous showed, in any alloy for the milling rolls there also found gases: oxygen (almost entirely on shape of oxides), hydrogen and nitrogen. The exposed elements exert up to the alloy a carburide or graphiting action (figure 1) [1].

Chromium is one of the most established active elements of carburides. His contain in the very different types of pig iron rolls various in 0,15 … 1,5% limits, and some of the specials types rolls in 12 … 25% limits. In fated alloys to rolls cast, chromium builds established carburides, increase the hardness and the depth of the whit crust, in the conditions favorizing the development and the depth of the passing area, mitigating by these mechanical characteristics and the thermic resistance of the rolls. Therefore at the manufacture of whit crust rolls, for flatting mill, which work at heat, it isn't use chromium alloyment his content limiting to 0,2% maximum.

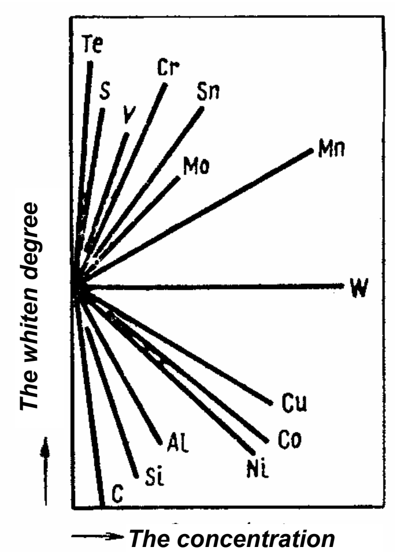

Fig.1. The carburide action of chemical elements over the alloyments fated to the rolls

The manufacture of the bimetallic milling rolls with high hardness used to flatting mill influence of chromium it is used in the major measure. For the increasing of the cruxes and journal, this rolls are washed with gray pig iron. As a consequence, the chromium content from the rolls axis area it dwindles until 0,3%.

It is useful of reminding the property of alloy white crust rolls with chromium: near bay the chromium carburides and the complexe carburides of chromium and iron, in whit crust it is appear, gnarled graphite microscopic dissociating, which provocate, after the rolls burnish, the appearance of the mat nuance of the work surface (indefinite structure) the presence of graphite nodule dwindles some way the rolls hard crust hardness.

In alloyed high bimetallic rolls, of different types, the content of chromium may various in: 0,5 … 0,8% large limits to the hardness of the hard crust of 70 … 85 HSh; 1,2 ... 1,5% to the crust with indefinite structure and harnesses of 75 ... 88 HSh.

Chromium capacity to maintain the hardness during the entire section of the piece has a big importance in the rolls manufacture case for profile, where it is request a little fall of the hardness for the gauges depth accomplished by mechanical processing.

The rolls for profile are as a rule, alloy with chromium in 0,6 … 1,5 % limits, indifferent of their type. In this cases, usually it is adding also nickel, of which content is with 0,2 … 0,3% upper from the chromium content. A such report between chromium and nickel assurance the equality of the hardness by the rolls area and dwindles, in the same time, of their fragility.

Chromium in Fgn formed established carburide, but her influence in this case it is amplified because the establishing action of the magnesium. Therefore, the chromium content in rolls of white pig iron in which with all content upper of silicium, in comparison with the rolls from alloyed lamellar graphite with chromium and nickel, it must not pass over the value of 0.4%.

For the increasing of the resistance to usance of the profile roll, although of the plate rolls, this it if manufacture from pig iron with 14…18%Cr. The hardness of this milling rolls is of the 400 HB on plate, but she is lower, in big measure, on the hard crust depth. In the structure of this rolls are founding 20 … 30% eutectide carburides of the type $(FeCr)_7O_3$, which by their discontinues structure in net shape, assure those a big resistance to wear (see figure 1) [1].

Alloyed high rolls manufacture with chromium with bimetallic structure it is achieved in abroad by centrifugal casting. Achieved rolls bay this procedure presented in harnesser upper serviceability.

The molybdenum belongs the carburides elements group but her influence it is evince only to the contents over 0,6 % Mo. To the lower contents 0,6% Mo in reports kept conditions from structural elements, it is obtain thick structure with fine granulation on the entire section of the rolls, event in the hard rust, and also in her center, also in journals trifles. In this way it is obtain the resistance increase at usuance and at height temperatures of the hard crust, of the mechanical resistance and the dur5abulity in harnesser of the rolls resistance. Even to the low content of molybdenum, this dissolving in perrlite-ferrite, provokes the increasing of the base metallic mass resistance and, as consequence, of the total resistance of the rolls. The content over 0,4% Mo, dispersion metallic mass of base increase in a visible way.

In alloyed height bimetallic rolls with the contents over 3,8%Ni and 0,8%Cr, in hard crust appear frugal contents of silicon and height in chromium, can not stop the graphite process from alloyed pig iron with nickel in a long time maintaining conditions of pieces in temperature plane 900 … 950^{o}C. Linked with the reduction the carbon content in the austenite arias, being in the neighborhood of the graphite, the iron uncompose it is deploy faster. The presence of an enough quantity of molybdenum induce the stopping of this uncomposing. Because of this, the rolls with alloyed lamellar graphite with chromium, nickel and molybdenum are distinguished by higher hardness and, as a result, they have a higher resistance to usance.

At the contents of 1%Mo, when it is develop her carburide action, the depth of the crossing area on the entire section of the roll. Therefore, at the rolls for table rolling, the content of molybdenum is limit at 0,3 … 0,6%. The rolls casting with molybdenum under 0,25%, it is not reasonable, because it not conduct to the visible improvement of their structure.

The pig iron alloyment for rolls casting wit molybdenum, which it is solidifing with frugal speeds, it is needful the assurance of some frugal contents of phosphor (under 0,15%), because the formation of the complexes eutectoids of molybdenum and phosphor it is followed by the molybdenum diffusion from the base metallic mass, fact which increases the roll alloyment with molybdenum. In the fast solidification case of the whit area (so as this take place at the casting in chill, mold) eutectoid of Mo-P it not succeed to form and, therefore the properties influence of molybdenum in crust it is maintain even to the raiser contents of phosphor.

The adding molybdenum in pig iron for rolls presents one of the safe method of increasing of the resistance to usance and high temperature, also the all-out resistance of those [1] .

2. THE RESULTS OF THE EXPERIMENTS

In this paper we suggest a mathematical shaping of the influence of the main alloy elements over the mechanical characteristics of this type iron pigs, resulting the average values and average square aberration of the variables HSh, Cr and Mo, the equations of the hyper surface in the four dimensional space.

For the statistical and mathematical analysis, there were used 50 industrial batches.

The average values and the average square aberration of the variables are:

C	3.2152	0.049
Cr	1.4484	0.23358
Mo	0.2946	0.039152
HSh	69.58	3.8808

Next, there are shown the results of the multidimensional processing of experimental data. For that purpose, we searched for a method of molding the dependent variables depending on the independent variables x, y, z:

$$u = c_1 \cdot x^2 + c_2 \cdot y^2 + c_3 \cdot z^2 + c_4 \cdot x \cdot y + c_5 \cdot y \cdot z + c_6 \cdot z \cdot x + c_7 \cdot x + c_8 \cdot y + c_9 \cdot z + c_{10} \quad (1)$$

The optimal form of molding, studied on a sample of 50 batches is given by the equations:

$$HSh = -13.72 \cdot C^2 - 8.297 \cdot Cr^2 + 428.9 \cdot Mo^2 - 101.2 \cdot C \cdot Cr - 12.59 \cdot Cr \cdot Mo - 41.07 \cdot Mo \cdot C + 252.9 \cdot C + 359.7 \cdot Cr - 110.7 \cdot Mo - 594.7, \quad (2)$$

where the correlation coefficients are:

$$r = 0.38141835933719, \quad (3)$$

and the aberrations from the regression surface are:

$$s = 3.58739648457368. \quad (4)$$

These surfaces from the four dimensional space allow a saddle point, having the following co-ordinates:

$$C_ş = 3.271$$
$$Cr_ş = 1.487$$
$$Mo_ş = 0.3075$$
$$HSh_ş = 69.23 \quad (5)$$

3. CONCLUSIONS

The chemical, physical and mechanical properties of alloyed reach pig iron are induced, in first place, by their chemical composition (nature and content of alloy elements) and the way of thermal manufacture, but the big importance is the casting and elaboration method, so as to obtain a pure pig iron regarding of the gases content (oxygen, hydrogen, nitrogen) and nonmetallic inclusions, wit chemical homogeneous and advanced structural.

The hard pig iron, alloyed with Cr, Ni and Mo, it is fated to casting the bimetallic rolls crust, in purpose of their hardness in creasing and of the usuance resistance.

In the technological field, the behavior of these hyper surfaces in the vicinity of the saddle point, or of the point where three independent variables take their average value, can be studied only tabular, which means that the independent variables are attributed values on spheres concentric to the studied point.

Because these surfaces cannot be represented in the three-dimensional space, the independent variables were successively replaced with their average values. This is how the following equations were obtained.

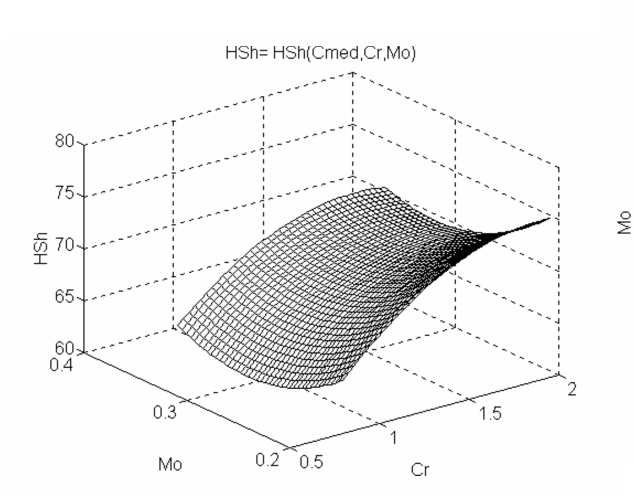

Fig.2. The surface
HSh = HSh(C_{med}, Cr, Mo)

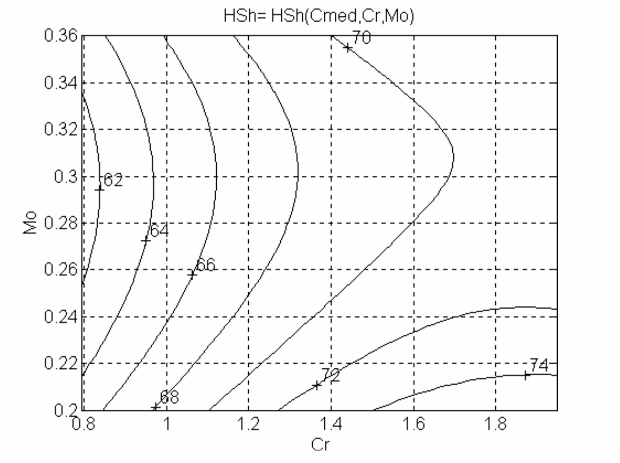

Fig.3. The level curves of distribution
HSh = HSh(C_{med}, Cr, Mo)

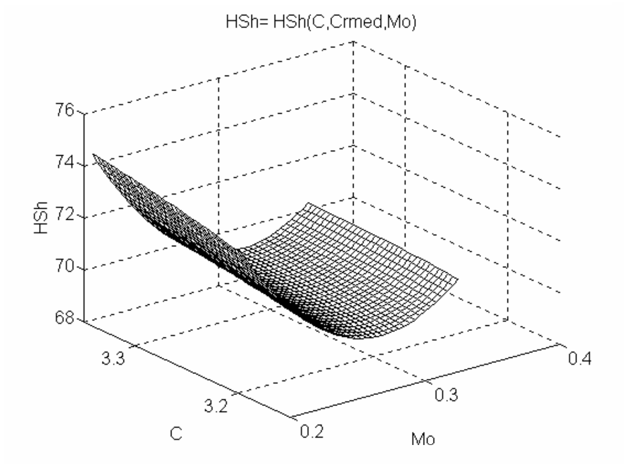

Fig.4. The surface
HSh = HSh(C, Cr_{med}, Mo)

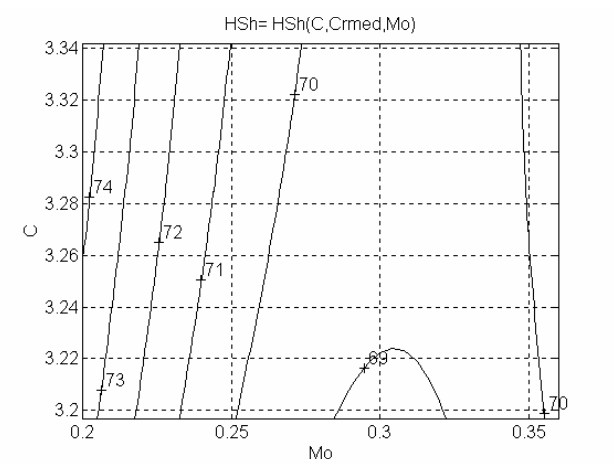

Fig.5. The level curves of distribution
HSh = HSh(C, Cr_{med}, Mo)

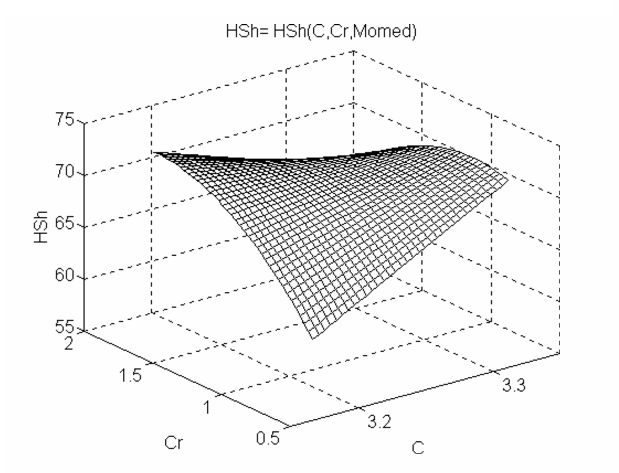

Fig.6. The surface
HSh = HSh(C, Cr, Mo_{med})

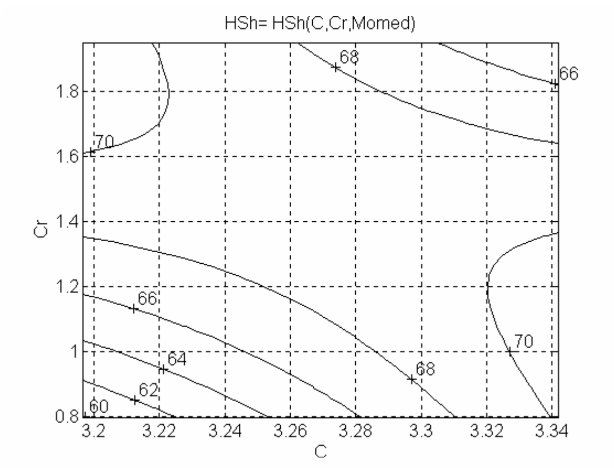

Fig.7. The level curves of distribution
HSh = HSh(C, Cr, Mo_{med})

$$HSh(C_{med}) = -8.297 \cdot Cr^2 + 428.9 \cdot Mo^2 - 12.59 \cdot Cr \cdot Mo + 34.17 \cdot Cr - 242.7 \cdot Mo + 76.57 \quad (6)$$
$$HSh(Cr_{med}) = 428.9 \cdot Mo^2 - 13.72 \cdot C^2 - 41.07 \cdot Mo \cdot C - 128.9 \cdot Mo + 106.2 \cdot C - 91.12 \quad (7)$$

$$HSh(Mo_{med}) = -13.72 \cdot C^2 - 8.297 \cdot Cr^2 - 101.2 \cdot C \cdot Cr + 240.8 \cdot C + 356 \cdot Cr - 590.1 \quad (8)$$

These surfaces, belonging to the three-dimensional space, can be represented and, therefore, interpreted by technologists. The surfaces are represented in figures 2, 4 and 6. For a more correct quantitative analysis, in figures 3, 5 and 7 there were represented the corresponding level lines, resulting the following conclusions: in the case of C = C_{med}, the hardness HSh allows a maximum for Mo of minimum value and Cr = 2%, and a minimum for Mo = 0,3% and Cr of minimum value; in the case of Cr = Cr_{med} it can be observed a maximum values in the maintained area of Mo = 0,22% and C = 3,35%, the minimum value being touched for Mo = 0,31% and for the minimum values of the carbon; in the case of Mo = Mo_{med} the surface allows a minimum point for Cr of maximum value and C =3,22%, therefore has a great importance because they offer stability to the process in the vicinity of this point, stability that should be either preferred or avoided. In our case, it is preferred.

Knowing these level curves allows the correlation of the values of the twos independent variables so that HSh can be obtained in between the requested limits.

BIBLIOGRAPHY

1. Budaghianț, N.A. – Casting Milling Rolls, The Technical Publishing House, Bucharest, 1986.
2. Maksay, Şt. - Special Mathematics, vol. I-II, „Politehnica” Publishing House, Timisoara, 2001.
3. Taloy, F. - The Optimization of the Metallurgical Process, E.D.P., Bucharest, 1982
4. Todoran, I. - The Mathematical Analysis of the Experimental Data, The Academy Publishing House, Bucharest, 1976

THE INFLUENCE OF THE ELEMENTS C, Ni AND Mo UPON THE HARDNESS OF THE BIMETALLIC CASTED IRON PIG MILLING ROLLS

Gabriela MIHUȚ, Ion SPOREA

The Polytechnic University of Timişoara, The Faculty of Engineering of Hunedoara

Abstract

The bimetallic hard-crusted iron rolls casting, for decrease of the hardness and the wear resistance destine the hard iron, alloyed with Ni and Mo. This paper suggests a mathematical shaping of the influence of the main alloy elements upon the mechanical features of this iron type, for 50 industrial batch, resulting the average values and average square aberration of the variables HSh, Ni and Mo, the equations of the hyper surface in the four dimensional space, they appealed to the successive replacement of each independent variable with the average value, resulting the equations that belong to the tree dimensional space, which are graphically represented and easy to interpret by technologists. Knowing the level curbs allows the correlations of the values of the two independent variables so that the hardness value (HSh) can be obtain in the requested boundaries.

Keywords

bimetallic milling rolls, alloy elements, hardness, wear resistance

1. Introduction

Technical conditions imposed to the milling rolls are very different and often contradictory. Thus, raised hardness from the crust correlated with mechanical resistance and raised high temperature, as well as with the raiser resilience of the alloys from the middle and journals, are enough difficult to obtain. For this reasons, the realization of the rolling mills is complexes enough, being necessary the obtaining mechanical-physical properties different in diverse points of the one and the same casted piece. Because the properties of each casted piece from de steel and pig irons are determined by the microstructure which is formed during the solidification and cooling of this, the base criterion, which determine the physical and mechanical properties of the milling rolls, is this structure.

In casted milling rolls from the pig iron are found all the carbon-iron alloys structures. One of the base factor which determine the given structure of the rolls is the chemical composition of the alloy and his speed cooling besides of the iron and the usually elements: carbon, silicon, manganese, phosphor, sulphur there are found also: chromium, cerium, nickel, calcium, molybdenum, copper, magnesium and aluminum. For the whiten degree correction of the liquid pig iron, purposed to crusting rolls with white crust, are utilized at large action of the tellurium. Besides of those previous showed, in any alloy for the milling rolls there also found gases: oxygen (almost entirely on shape of oxides), hydrogen and nitrogen. The exposed elements exert up to the alloy a carburide or graphiting action (figure 1) [1].

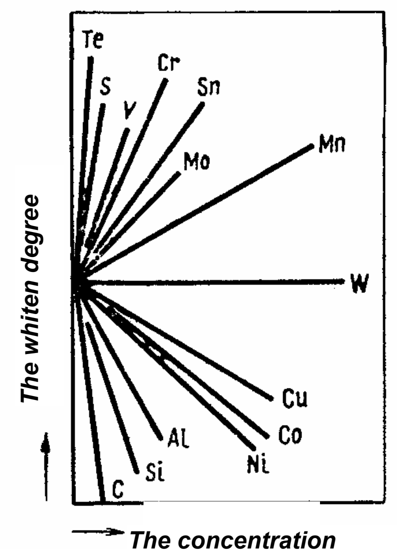

Fig.1. The carburide action of chemical elements over the alloyments fated to the rolls

Nickel. From the point of view of nickel influence in liquid pig iron, this belongs to the graphite elements groups, but this influence of his, it is not taken in deeming in the rolls casting manufacture. In this last case it is more important the fact that the nickel, having a unlimited solubility in pig iron, allows the improvement of properties series of harnesser of casted piece: brings the extension ferrite resistance from perrlite, magnify the mechanical resistance and at the pig iron rolls. Her bases property consists in the fact that, in certainness limits, exact brought, magnify the base metallic volume mass hardness, as a result of dwindle of critique point of eutectoids transformation.

Because this property, even in piece so unwieldy how there are the rolling mill rolls, in usual conditions cooling, it may obtain, not only the hard crust, but on their entire section, the entire gamut of transition structure of (depending on the nickel content), from fine lamellar perlite, until the martensite with are of uncomposed austenite and, as consequence, conformably to this, a harnesses large gamut 68 … 88 HSh. Martensite structure of base metallic mass it is brought by the content over 3,4 … 3,6%Ni, for small rolls and over 3,8%Ni, for the big one.

The extension of nickel content over 4,5% brings the appearance in rolls structure a some important quantity of residual austenite. This fact provokes the increase of resistance properties of the hard crust and in the same time, a somehow a lower of her hardness. The study of this rolls shows that the work surface hardness, during rolling process, may even increase as a result of transformation martenasite-austenite of residual austenite. It seems that, it is possible the deploy of the one and the same transformation at law temperature processing of the rolls [1].

The nickel it is used to the rolls manufacture for profiles of all types. Almost all this rolls it is cast in alloyed pig iron with chromium and nickel. The nickel neutralize the carburide influence of chromium and the resistance increase obtained on the nickel, it is double at the report Ni/Cr 2 : 1.

The molybdenum belongs the carburides elements group but her influence it is evince only to the contents over 0,6 % Mo. To the lower contents 0,6% Mo in reports kept conditions from structural elements, it is obtain thick structure with fine granulation on the entire section of the rolls, event in the hard rust, and also in her center, also in journals trifles. In this way it is obtain the resistance increase at usuance and at height temperatures of the hard crust, of the mechanical resistance and the dur5abulity in harnesser of the rolls resistance. Even to the low content of molybdenum, this dissolving in perrlite-ferrite, provokes the increasing of the base metallic mass resistance and, as consequence, of the total resistance of the rolls. The content over 0,4% Mo, dispersion metallic mass of base increase in a visible way.

In alloyed height bimetallic rolls with the contents over 3,8%Ni and 0,8%Cr, in hard crust appear frugal contents of silicon and height in chromium, can not stop the graphite process from alloyed pig iron with nickel in a long time maintaining conditions of pieces in temperature plane 900 … 950^{o}C. Linked with the reduction the carbon content in the austenite arias, being in the neighborhood of the graphite, the iron uncompose it is deploy faster. The presence of an enough quantity of molybdenum induce the stopping of this uncomposing. Because of this, the rolls with alloyed lamellar graphite with chromium, nickel and molybdenum are distinguished by higher hardness and, as a result, they have a higher resistance to usance.

At the contents of 1%Mo, when it is develop her carburide action, the depth of the crossing area on the entire section of the roll. Therefore, at the rolls for table rolling, the content of molybdenum is limit at 0,3 … 0,6%. The rolls casting with molybdenum under 0,25%, it is not reasonable, because it not conduct to the visible improvement of their structure.

The pig iron alloyment for rolls casting wit molybdenum, which it is solidifing with frugal speeds, it is needful the assurance of some frugal contents of phosphor (under 0,15%), because the formation of the complexes eutectoids of molybdenum and phosphor it is followed by the molybdenum diffusion from the base metallic mass, fact which increases the roll alloyment with molybdenum. In the fast solidification case of the whit area (so as this take place at the casting in chill, mold) eutectoid of Mo-P it not succeed to form and, therefore the properties influence of molybdenum in crust it is maintain even to the raiser contents of phosphor.

The adding molybdenum in pig iron for rolls presents one of the safe method of increasing of the resistance to usance and high temperature, also the all-out resistance of those [1] .

2. The results of the experiments

In this paper we suggest a mathematical shaping of the influence of the main alloy elements over the mechanical characteristics of this type iron pigs, resulting the average values and average square aberration of the variables HSh, Cr and Mo, the equations of the hyper surface in the four dimensional space.

For the statistical and mathematical analysis, there were used 50 industrial batches.

The average values and the average square aberration of the variables are:

C	3.2152	0.049
Ni	2.6278	0.53185
Mo	0.2946	0.039152
HSh	69.58	3.8808

Next, there are shown the results of the multidimensional processing of experimental data. For that purpose, we searched for a method of molding the dependent variables depending on the independent variables x, y, z:

$$u = c_1 \cdot x^2 + c_2 \cdot y^2 + c_3 \cdot z^2 + c_4 \cdot x \cdot y + c_5 \cdot y \cdot z + c_6 \cdot z \cdot x + c_7 \cdot x + c_8 \cdot y + c_9 \cdot z + c_{10} \qquad (1)$$

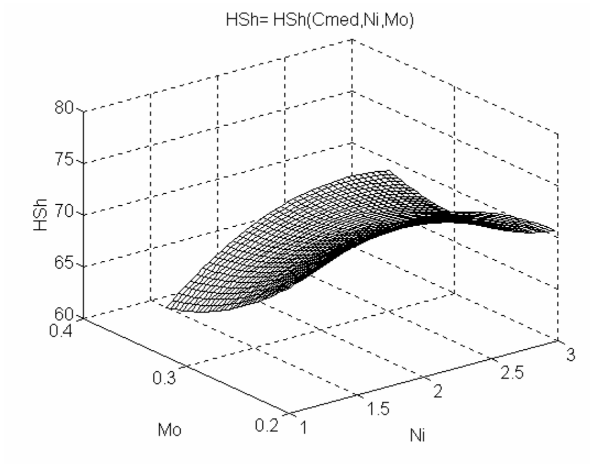

Fig.2. The surface
HSh = HSh(C_{med}, Ni, Mo)

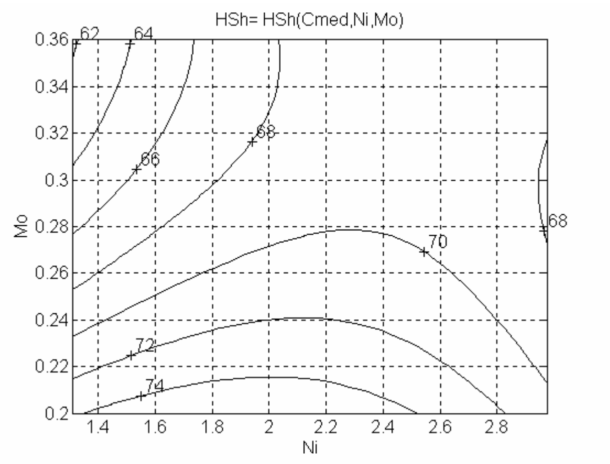

Fig.3. The level curves of distribution
HSh = HSh(C_{med}, Ni, Mo)

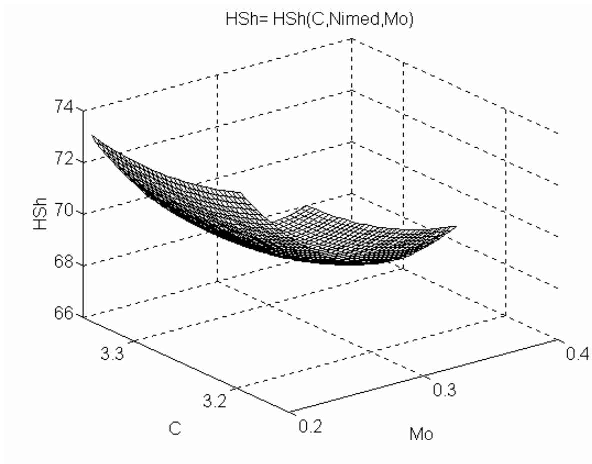

Fig.4. The surface
HSh = HSh(C, Ni_{med}, Mo)

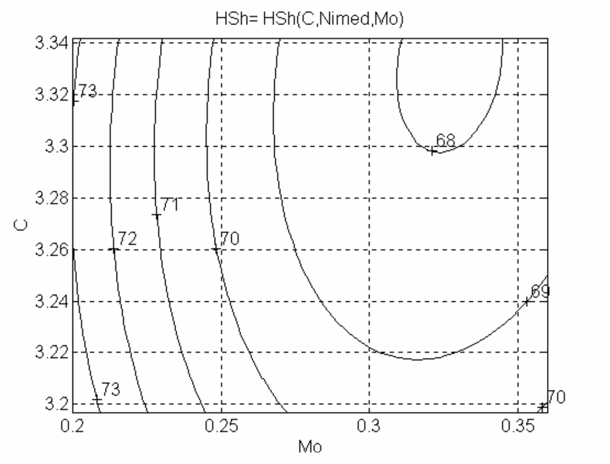

Fig.5. The level curves of distribution
HSh = HSh(C, Ni_{med}, Mo)

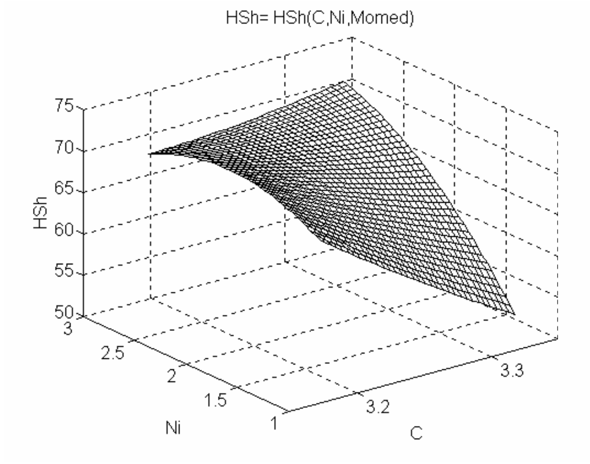

Fig.6. The surface
HSh = HSh(C, Ni, Mo_{med})

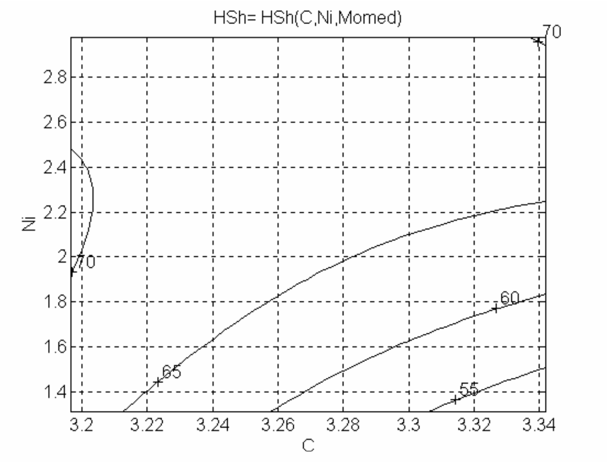

Fig.7. The level curves of distribution
HSh = HSh(C, Ni, Mo_{med})

The optimal form of molding, studied on a sample of 50 batches is given by the equations:

$$HSh = 85.68 \cdot C^2 - 4.378 \cdot Ni^2 + 324.2 \cdot Mo^2 + 73.41 \cdot C \cdot Ni + 39.36 \cdot Ni \cdot Mo - 60.47 \cdot Mo \cdot C - 744.2 \cdot C - 227 \cdot Ni - 113.8 \cdot Mo + 1615, \quad (2)$$

where the correlation coefficients are:

$$r = 0.44722511771627 , \quad (3)$$

and the aberrations from the regression surface are:

$$s = 3.47104664168859 . \quad (4)$$

These surfaces from the four dimensional space allow a saddle point, having the following co-ordinates:

$$C_ş = 3.258$$
$$Ni_ş = 2.788$$
$$Mo_ş = 0.3103$$
$$HSh_ş = 68.5 \quad (5)$$

3. Conclusions

The chemical, physical and mechanical properties of alloyed reach pig iron are induced, in first place, by their chemical composition (nature and content of alloy elements) and the way of thermic manufacture, but the big importance is the casting and elaboration method, so as to obtain a pure pig iron regarding of the gases content (oxygen, hydrogen, nitrogen) and nonmetallic inclusions, wit chemical homogeneous and advanced structural.

The hard pig iron, alloyed with Cr, Ni and Mo, it is fated to casting the bimetallic rolls crust, in purpose of their hardness in creasing and of the usuance resistance.

In the technological field, the behavior of these hyper surfaces in the vicinity of the saddle point, or of the point where three independent variables take their average value, can be studied only tabular, which means that the independent variables are attributed values on spheres concentric to the studied point.

Because these surfaces cannot be represented in the three-dimensional space, the independent variables were successively replaced with their average values. This is how the following equations were obtained.

$$HSh(C_{med}) = - 4.378 \cdot Ni^2 + 324.2 \cdot Mo^2 + 39.36 \cdot Ni \cdot Mo + 9.052 \cdot Ni - 308.3 \cdot Mo + 107.8 \quad (6)$$

$$HSh(Ni_{med}) = 324.2 \cdot Mo^2 + 85.68 \cdot C^2 - 60.47 \cdot Mo \cdot C - 10.42 \cdot Mo - 551.3 \cdot C + 988.2 \quad (7)$$

$$HSh(Mo_{med}) = 85.68 \cdot C^2 - 4.378 \cdot Ni^2 + 73.41 \cdot C \cdot Ni - 762 \cdot C - 215.4 \cdot Ni + 1609 \quad (8)$$

These surfaces, belonging to the three-dimensional space, can be represented and, therefore, interpreted by technologists. The surfaces are represented in figures 2, 4 and 6. For a more correct quantitative analysis, in figures 3, 5 and 7 there were represented the corresponding level lines, resulting the following conclusions: in the case of $C = C_{med}$, the hardness HSh allows a maximum for Ni of maximum value and Mo = 0,2% and a minimum for Mo of maximum value and Ni = 1,5%; in the case of $Mo = Mo_{med}$ it can be observed a maximum values in the Ni arya of the maximum value and C = 3,35%, the minimum value being touched for Ni of minimum value and for C = 3,35%; in the case of Ni = Ni_{med} the surface allows a minimum point for Mo = 0,325% and C =3,33%, therefore has a great importance because they offer stability to the process in the vicinity of this point, stability that should be either preferred or avoided. In our case, it is preferred.

Knowing these level curves allows the correlation of the values of the twos independent variables so that HSh can be obtained in between the requested limits.

BIBLIOGRAPHY

1. Budaghianț, N.A. – Casting Milling Rolls, The Technical Publishing House, Bucharest, 1986.
2. Maksay, Şt. - Special Mathematics, vol. I-II, „Politehnica” Publishing House, Timisoara, 2001.
3. Taloy, F. - The Optimization of the Metallurgical Process, E.D.P., Bucharest, 1982
4. Todoran, I. - The Mathematical Analysis of the Experimental Data, The Academy Publishing House, Bucharest, 1976

ANALYSIS OF THE LATERAL EFFORTS IN ASYMMETRICAL LONGITUDINAL ROLLING

Lect. Eng. Vasile ALEXA, Dr. Es Sc

University "Politehnica" - Timişoara
Engineering Faculty - Hunedoara

ABSTRACT

This paper presents the variation module of lateral effort according to the difference between the working diameter of the rolls and the working direction of the side efforts in the case of asymmetrical longitudinal rolling.

At the same time it contains an analysis of the peculiarities that are transmitted in the rolling process.

KEYWORDS
efforts, lateral, rolling, asymmetrical

1. INTRODUCTION

Any well managed operation of rolling needs a precise determination of the force factors. It is a complicated problem, to solve it means knowing the basic rules of process of plastically deformation of metallic materials, generally, and also to know the physical and mechanical characteristics of the mentioned materials.

One knows that the efforts applied to a metallic material during its plastic deformation are conditioned not only by its properties, but also by stress status applied to it.

The metal material deformed between the rollers of rolling mill suffer high compression stress due to the action of the rollers, and it also bears tangential surface tensions because of the friction between the rollers and the metal material.

In spite of the great number of theoretical and experimental works regarding the classic operation of mechanical deformation between equal diameter rollers, there are not enough clarified many issues regarding the physical and mechanical nature of the transformations that appear in the metallic material during its plastic deformation.

In the Romanian and international theory of rolling it is usually analysed the plastic deformation between rollers of equal diameters, even if this operation it is first an abstractisation compared to the real conditions of the rolling, for there is actually a certain difference between the diameters of the work rollers, and sometimes the rolling mill is made having unequal diameter rollers.

2. RESEARCH METHODICS

The research for this theme purpose have been made on a 170mm reversing two-high rolling mill, created and installed in the no conventional technologies and plastic deformation laboratory of the Engineering Faculty from Hunedoara.

An experimental installation formed of: special construction rollers, bearings, punctiform captors for lamination pressure, lamination forces captors and lateral pressure captors it was created for research in condition of technological similitude symmetrical and asymmetrical process.

In figure 1 it is presented in overview the mentioned installation, with the way force captors are assembled in order to determine the lateral efforts in the longitudinal asymmetrical lamination but also to show the author’s contribution regarding method of experimentation.

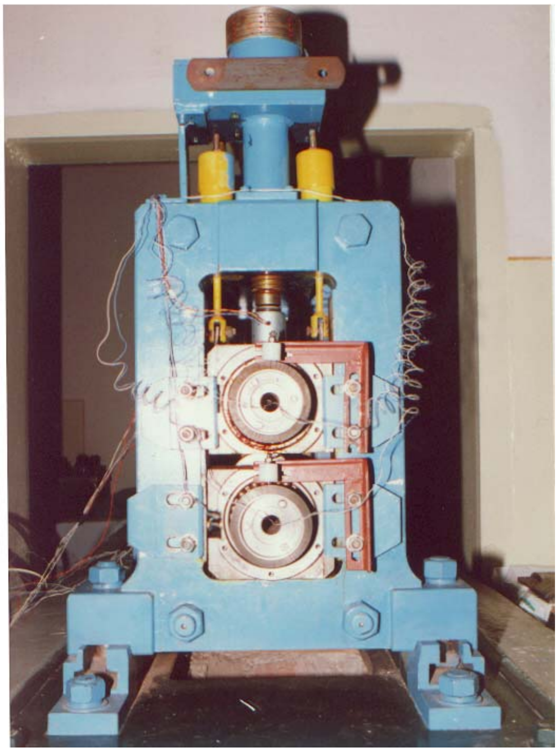

Fig.1. *Montages punctifom captors for recording the lateral efforts*

The bearing holders of the inferior roller were modified for recording the lateral efforts so that the respective captors could be installed incorporated perpendicularity on the bearing’ s axis.

On the surface of captors were stuck tensometric stamps bound in deck, stamps that modify their dimension under the action of the effort to be measured. These dimensional modifications of tensiometer stamps are generating variations of their electric resistance, that are proportional to the deformation efforts and the measuring of the forces is limited to the measuring of these resistance variations.

Usually, the tensiometer stamps of a forces captor are bound in deck. The deck has on a diagonal it is measured a electrical signal – proportional of the applied effort – and for recording of the measured values this signal is recorded by an oscillograph.

The oscillograph is a the type N-700, having 14 channels, the impulses on recorded are a scale of 120 mm width, heaving 4 cm/s moving speed of the paper band.

Through experimentations between rollers of equal diameters we where convinced that galvanometers conectated to the electric scheme of captors from inferior bearing holders for the seizing of the appearance of lateral efforts, these galvanometer give on the paper band of the oscilograph line of zero.

In the place of segments for the symmetrical process, with $\frac{D_s}{D_i} = \frac{170}{170}[mm]$, we installed segments for asymmetrical process, with $\frac{D_s}{D_i} = \frac{140}{200}[mm]$. With respective punctiform captors repeating the experimentations for variant of lamination between rollers of unequal diameter.

This time, according to the characteristic oscillogram they noticed big enough lateral efforts having a value that vary depending on the thickness of the samples and on the applied reduction.

The respective values, obtained from the processing oscillograms recorded and presented in the form of curves X=f(ε) in figure 2 which a matter of fact represent only parables with the peak at the beginning axis of coordinates and which are growing in the same time with the thickness of the laminate sample and of the decrease degree.

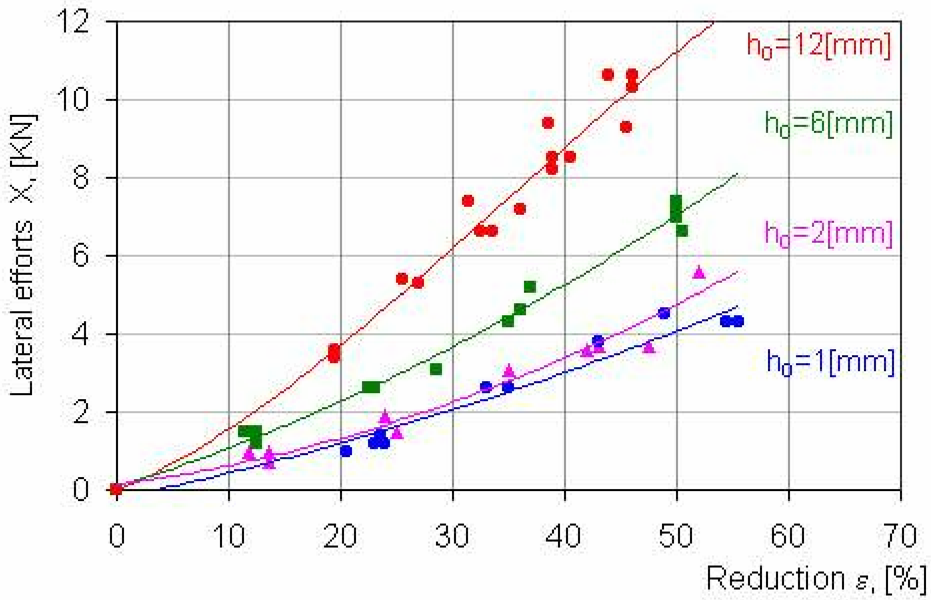

Fig.2. *Dependency lateral efforts of decrease, to the lamination samples from aluminum of different thickness, between operates rollers of unequal diameters*

$$\left(\frac{D_s}{D_i} = \frac{140}{200} mm\right)$$

It is obvious that the samples lamination of same thickness between rollers of unequal diameters, the value of lateral efforts grows with growing of the differences between work diameter rollers.

The explanation of this phenomenon consist in continue increasing of the "φ" angle in the same time with the growing at the "*a*" arm (see figure 3). This may be described as differerence among "a_s "and "a_j".

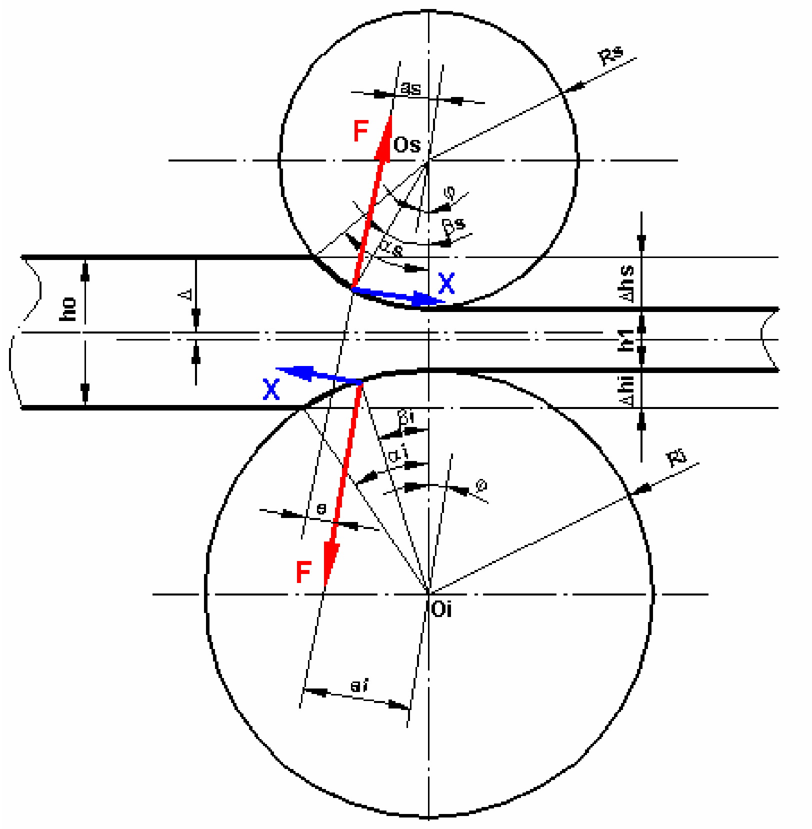

Fig.3. *The resultance arms of pressure (a_s and a_i) and direction of lateral efforts(X), to lamination between unequal diameters in operated roller.*

The value of lateral efforts which appear to the lamination between rollers operated by unequal diameters it is modified by the curve factor of the roller's segments and the different periphery speed factor.

It can be noticed the influential factors of peripheral different speed, which on chart it is represented by the discrepancies between the curves $X=f(\varepsilon)$ for same laminate thickness by analyzing both the dependencies $X=f(\varepsilon)$ obtained for the lamination between rollers of unequal diameters when both rollers are operating and the variant when the superior roller of less diameter is in operating (fig.5).

The lateral efforts, which appear in the lamination between roller operating by unequal diameters, these efforts are equal on the side of the superior roller (less) on inferior roller (bigger).

The experimentations effectuated confirm the rightness of the schemes of actioning of the forces proposed by the specialty literature.

To clarify the direction of operation of the lateral efforts great numbers of samples were laminate.

Captors for the lateral efforts recorded the presence efforts of only in the cases when captors took over the action against the senses of lamination.

On experimental way it was clarified that lateral efforts from smaller diameter roller (superior) are headed on direction of lamination, and from bigger diameter roller (inferior) the efforts are headed against the lamination direction.

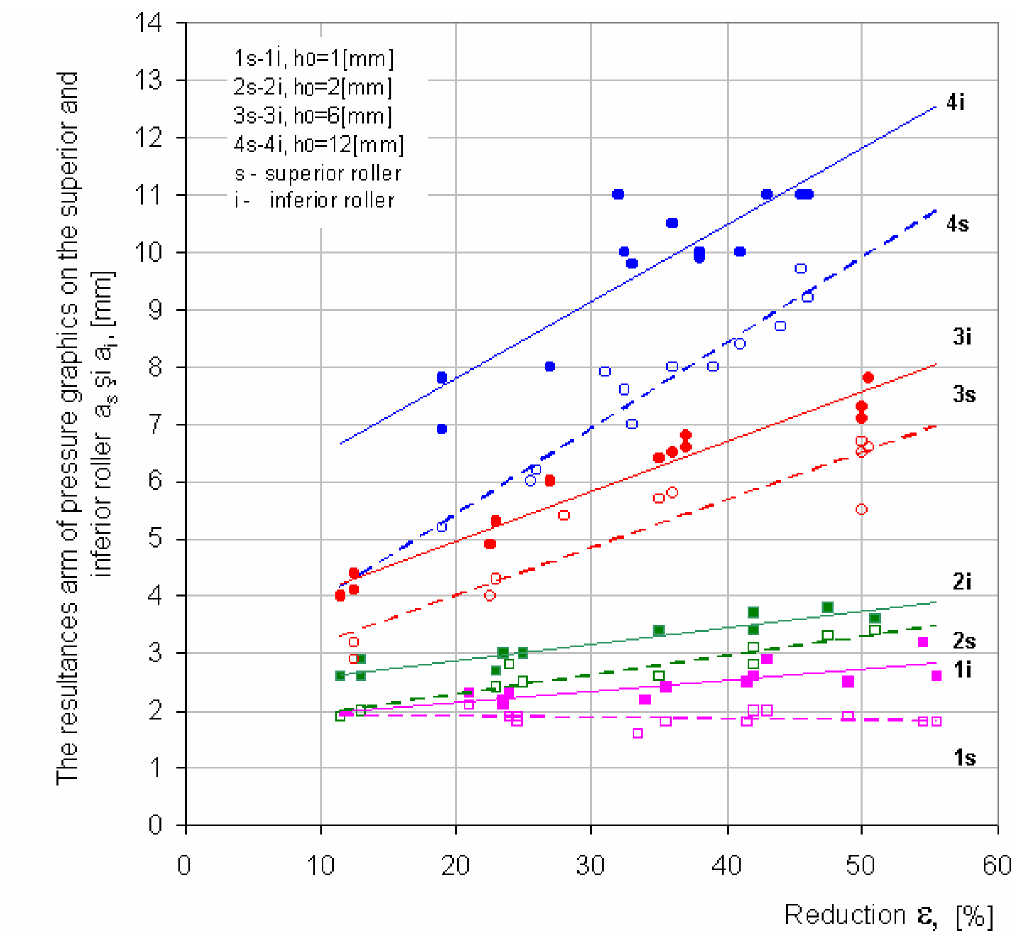

Fig.4 *The dependence of the resultance arm of pressure graphics on the superior and inferior roller, reduction function, in aluminum laminate samples of different thickness between rollers of unequal diameters* $\frac{D_s}{D_i} = \frac{140}{200}$

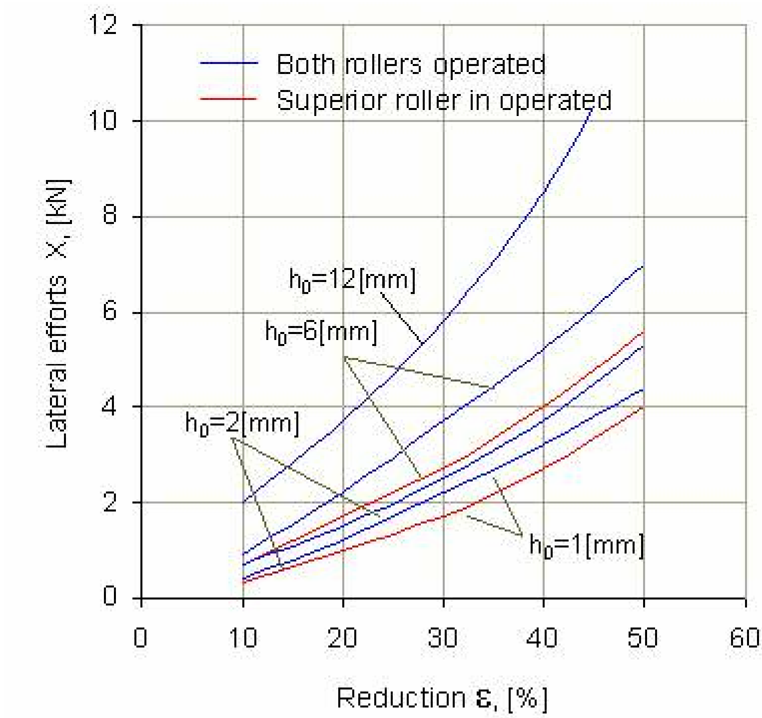

Fig.5. *The dependence of the resultance arm of pressure graphics on the superior and inferior roller, reduction function, in aluminum laminate samples of different thickness between rollers of unequal diameters* $\frac{D_s}{D_i} = \frac{140}{200}$

3. CONCLUSION

- the lateral efforts, who appear to the lamination between operates rollers of unequal diameters, is favorizate to the differences factor of curvature because the rollers have unequal diameters and the factor of peripheral speed is different.
- the lateral efforts influence favorably about allocation pressure on the surfaces of contact, action in analogous to mode the adhibition previous drawing the posterior and anterior. This influence is intensified along with breed the thickness samples laminate reduced relatively.
- he established as size lateral efforts result to lamination, when one of the rollers is inaction, he don't depends on the difference among the diameters of thing, because in this variant the which factor look the peripheral different speed, absent ones.

4. BIBLIOGRAPHY

1. Litovcenko, N.V – *"Profiles Calibrate and Rolling Mills"*, Metallurgical Editors, 1990, Moscow;
2. Ilca, I., Alexa, V. – *"Influence of the metallic material no uniformity upon the force parameters in the rolling process"*, in: Scientific Bulletin - UPT, tom 44 no. 1/1999, pg. 345-348.
3. Ilca, I., Alexa, V. – *"Theoretic consideration on the rolling kinematics with rolls unequal diameters",* in: Scientific Bulletin - UPT, tom 44 no. 1/1999, pg. 349-354.

THE INFLUENCE OF TEMPERING TEMPERATURE AND TESTING ON STRENGHTNESS CHARACTERISTICS OF SOME ALLOYED STEELS FOR MACHINE CONSTRUCTIONS

Isidor PREJBAN

Politehnica University of Timisoara, Faculty of Engineering of Hunedoara

Abstract

In the present work is studied the high temperature behave of the steels of high resistance from the class Cr-Mo-V. It was shown that under the high temperature effect, the ultimate tensile strength value, which is producing a certain degree of plastic deformation of the steel, is in general, lower then the determined value at open air temperature. From the tested samples these temperatures the broken pieces have been taken for measuring the hardness after tempering -at different temperatures- representing graphic their variation according to the testing temperatures (20° C, 300°C, 500°C) for cooling area at tempering.

Keywords

alloyed steels, the thermal treated, mechanical characteristics

1. INTRODUCTION

The mechanical characteristics values of steels are depending as well on the time period of the tests at high temperatures, as for, in accordance with the duration of the load application; there are two groups of tests, as follows:

a) Short time duration tests, in which the heated sample is, tested same as at the usual temperature. In the case of the present work the tests has been done at short time duration.
b) Long time duration tests, in which the heated sample is charged with a constant or variable load for establishing the combined influence of high temperature and long time duration of the tests on resistance characteristics and deformation of the steel.

Industrial work area for rolled steel products, which have to resist at high temperatures, is up to 450 – 500° C, so is useful to study the mechanical characteristics variations in this area.

In case of low alloyed and alloyed steels, in case when it was used silicon – calcium as deoxidized, it was noticed an increasing of the yield point Rp 0,2 and of the elongation A5, and in the mean time a sensitive decreasing of the tensile strength Rm.

As well, at the deoxidized steels and with silicon-calcium, is noticed an increasing of the breaking energy values and minimizing of the dispersion for all mechanical characteristics.

Taking in consideration that from the steel 15VMoCr14X are produced components for undercarriage of the planes, which during operation are subjected to high and low temperatures, these has to keep their admitted properties in between –75°C up to +500°C.

For this, tensile tests were made at high temperatures and the results are shown in Table 1 for the Rp 0,2 characteristics.

The graphic representation of data from Table 1 is shown in Fig. 1.

Table 1.

Tempering temperature, °C	Test temperature, °C				
	100	200	300	400	500
550	98,7 95,8 97,2	89,7 85,6 87,4	89,7 87,4 85,6	79,1 85,3 82,2	74,1 75,3 74,8
	97,2	87,5	87,5	82,2	74,7
580	93,7 105,2 99,6	86,9 94,8 91,6	86,0 92,2 93,1	85,2 86,0 85,7	79,1 74,2 72,0
	99,5	91,1	90,4	85,6	78,1
610	106,7 101,0 103,8	98,3 94,9 96,7	95,4 92,0 93,3	87,5 88,4 87,9	79,1 80,4 79,8
	108,8	96,6	93,6	87,6	79,7
625	108,3 101,7 105,0	101,3 99,3 96,2	95,0 96,3 97,8	93,0 83,1 88,1	78,6 81,8 79,3
	105,0	98,9	96,3	88,1	79,9
640	103,2 101,6 102,4	93,1 97,1 95,0	89,2 94,1 91,4	98,2 83,2 86,4	83,2 75,1 79,5
	102,4	95,1	91,6	89,3	79,6
670	93,1 86,9 90,0	85,8 83,6 84,0	84,1 80,2 82,0	79,0 73,4 76,2	70,0 67,4 69,2
	90,0	84,4	82,1	76,2	68,8
700	82,1 80,0 80,3	79,4 74,4 76,6	72,6 73,4 72,5	63,0 67,9 65,9	60,1 64,2 62,0
	80,8	76,8	73,1	65,6	68,1

Guiding limit values which, has to be fulfilled by the steel 15VmoCr14X, are show in Table 2, and the graphic representation in Fig. 2.

Table 2.

Mechanical characteristic, daN/mm²	Temperature, °C					
	100	200	300	400	500	600
$Rp_{0,2}$	86,4	80,9	79	75	68	52
Rm	106	93	90	88	84	60

From the samples tested, at high temperature, the broken pieces have been taken and it was measured the hardness after tempering temperatures, tests temperatures for the tempering cooling in free air and the values are given in Table 3.

Graphic representation of the hardness variation according to tempering temperature and test temperatures for tempering in free air is shown in Fig. 3.

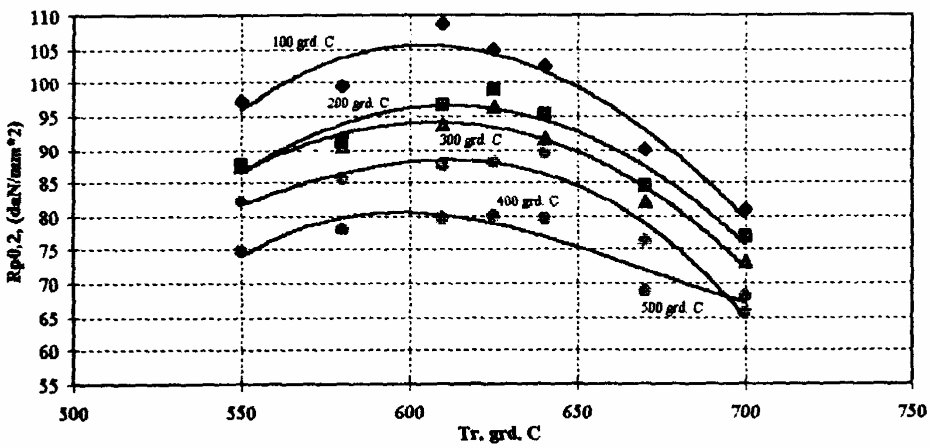

Fig. 1. The variation of the technical yield point with tempering temperature and test temperature.

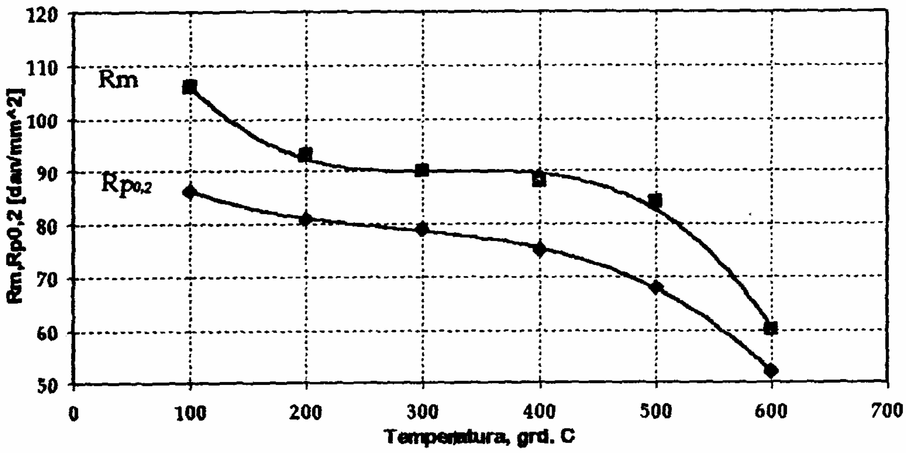

Fig. 2. The variation of the mechanical characteristics Rm and Rp 0,2 with tempering temperature.

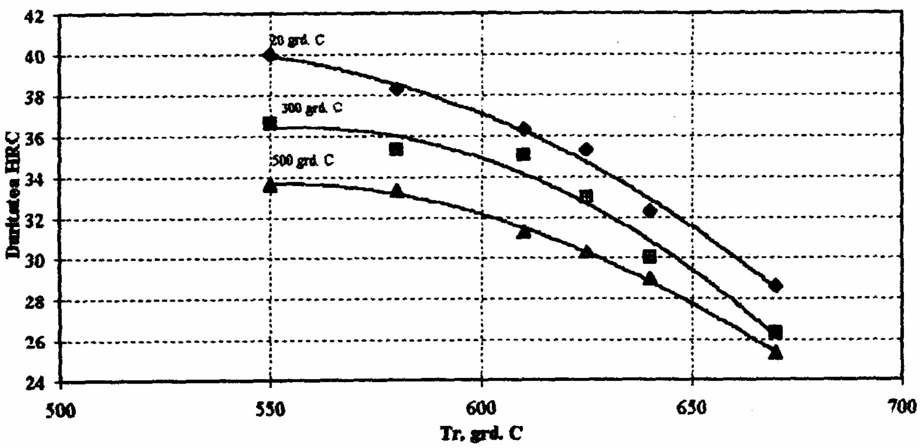

Fig. 3. the variation of the hardness with tempering and test temperature.

Table 3.

Tempering temperature, °C	Test temperature, °C and hardness HRC					
	20		300		500	
550	40 39 40	40 40 40	39 37 37	39 35 36	33 34 34	32 35 34
	39,6	40	37,6	36,6	33,6	33,6
580	38 39 40	38 39 38	36 35 35	37 34 35	34 32 32	32 31 31
	39	38,3	35,3	35,3	32,3	31,3
610	38 37 36	37 36 36	35 33 34	35 34 35	31 32 31	32 31 31
	37	36,3	34	35	31,3	31,3
625	37 33 34	36 35 35	35 33 33	34 32 33	31 29 30	31 30 30
	34,6	35,3	33,6	33	30	30,3
640	30 32 34	32 33 33	30 30 31	29 31 30	29 29 28	29 30 28
	32	32,6	30,3	30	28,6	29
670	28 29 28	29 29 28	28 27 26	25 28 26	24 25 24	25 27 24
	28,3	28,6	27	26,3	24,3	25,3

BIBLIOGRAPHY

1. *Mantea, S., Dulămiță, T. – Teoria şi practica tratamentelor termice, Ed. Tehnică, 1966*
2. *Rău, A. – Incluziuni nemetalice în oțeluri, Ed. Tehnică, 1973, Bucureşti*
3. *George, E., Dieter, Fr. – Metalurgie mecanică (tr. limba engleză), Ed. Tehnică, 1970*
4. *Schumann, I. – Metalurgie fizică, Ed. Tehnică, Bucureşti, 1926*
5. *Nădăşan, S., ş.a. – Încercări şi analize de metale, Ed. Tehnică, Bucureşti, 1965*
6. *Cheşa, I., ş.a. – Alegerea şi utilizarea oțelurilor, Ed. Tehnică, Bucureşti, 1984*

SIMULATIONS OF THE REACTIVE POWER COMPENSATION SYSTEM FUNCTIONING OF THE ALTERNATIVE CURRENT MACHINE WITH VARIABLE LEAD USING PSCAD-EMTDC PROGRAM

Caius PĂNOIU, Manuela PĂNOIU, Corina CUNŢAN

Technical University of Timişoara, Engineering Faculty of Hunedoara

Abstract

This paper present the simulation results on reactive power compensation system, which is used on a A.C. machine with variable leads. To demonstrate the efficiency of the reactive power compensation system the simulations were be made in two circumstances: with and without the reactive power compensation system. The simulations were be made using the PSCAD-EMTDC simulation program.

Keywords

Reactive power compensation system, A.C.machine.

1. INTRODUCTION

The three phased systems was projected and realized to functioning under balanced conditions. In these cases all the components, such as generators, transformers and leads have identical parameters on each phase, and voltages and currents three phased systems are symmetric in any section. If one of these elements became nonsymmetrical, the functioning of the whole installation became unbalanced.

The most unfavorable consequence of the unbalanced voltage consist in circulation of supplementary current components which lead to supplementary looses of voltage, parasitical couple on a.c. machine, a growing frazzle, etc.

Another unfavorable consequence consists in reactive power appearance, due to nonzero phase between direct components of currents and voltages.

On a.c. machine the negative effects consist especially in reactive power circulation in three-phased system, which is as higher as the power machine is higher.

This paper present the simulation results of the a.c. machine functioning with variable lead, analyzing three-phased power and the possibility to compensate the reactive power using capacitors battery.

2. THE EQUIVALENT ELECTRIC SCHEME OF THE A.C. MACHINE

To simulate the functioning of the a.c. machine we consider an electric system, which is composed by a three-phased a.c. machine supplied from a three-phase inverter. Because the a.c. machine is a high power machine, the parameters value was chosen as it follows:

$$U_N = 6\ \mathrm{KV} \tag{1}$$

$$P_N = 6\ \mathrm{MW} \tag{2}$$

$$\mathrm{COS}\varphi_N = 0{,}9 \tag{3}$$

$$\eta_N = 0{,}95 \tag{4}$$

With this parameters value it can be computed next electrical parameters value:

$$P = \frac{\mathbf{P_N}}{\eta_{\mathbf{N}}} = 5{,}26\ \mathrm{MW} \tag{5}$$

$$U_f = \frac{\mathbf{U_{nl}}}{\sqrt{\mathbf{3}}} = 4{,}8\ \mathrm{KV} \tag{6}$$

$$I_f = \frac{\mathbf{P}}{\mathbf{3} \cdot \mathbf{U_f} \cdot \mathbf{cos}\,\varphi} = \mathbf{398{,}39}\ \mathrm{A} \tag{7}$$

The a.c. machine has the Y stator connection wrapping, whose mono-phase electrical scheme is presented in figure 1.

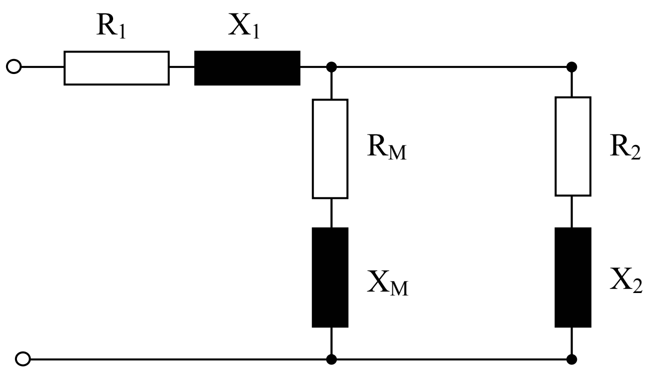

Fig. 1. *Mono-phase electrical scheme.*

Relations (8) – (13) give the parameter values from figure 1.

In relation (13), *s* parameter represents the slide between stator and rotor fields.

$$R_1 = 1\ \text{m}\Omega \tag{8}$$

$$X_1 = 10\ \text{m}\Omega \tag{9}$$

$$R_M = 1\ \Omega \tag{10}$$

$$X_M = 10\ \Omega \tag{11}$$

$$X_2 = X_1 = \mathbf{10m}\Omega \tag{12}$$

$$R_2 = \frac{\mathbf{R_1}}{\mathbf{s}} \tag{13}$$

Considering that electrical scheme from figure 1 can be approximate by the three-phased simplified electrical scheme from figure 2, is obvious

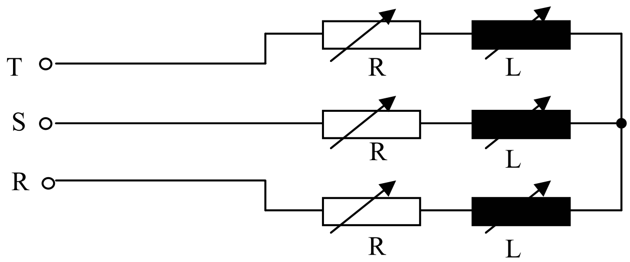

Fig. 2. *The three-phase simplified electrical scheme.*

that electrical parameter values depend on the *s* parameter.

3. THE ELECTRIC SCHEME OF THE THREE-PHASED INVERTER

The a.c. machine supply is assured from a three-phased inverter whose electrical scheme is presented in figure 3.

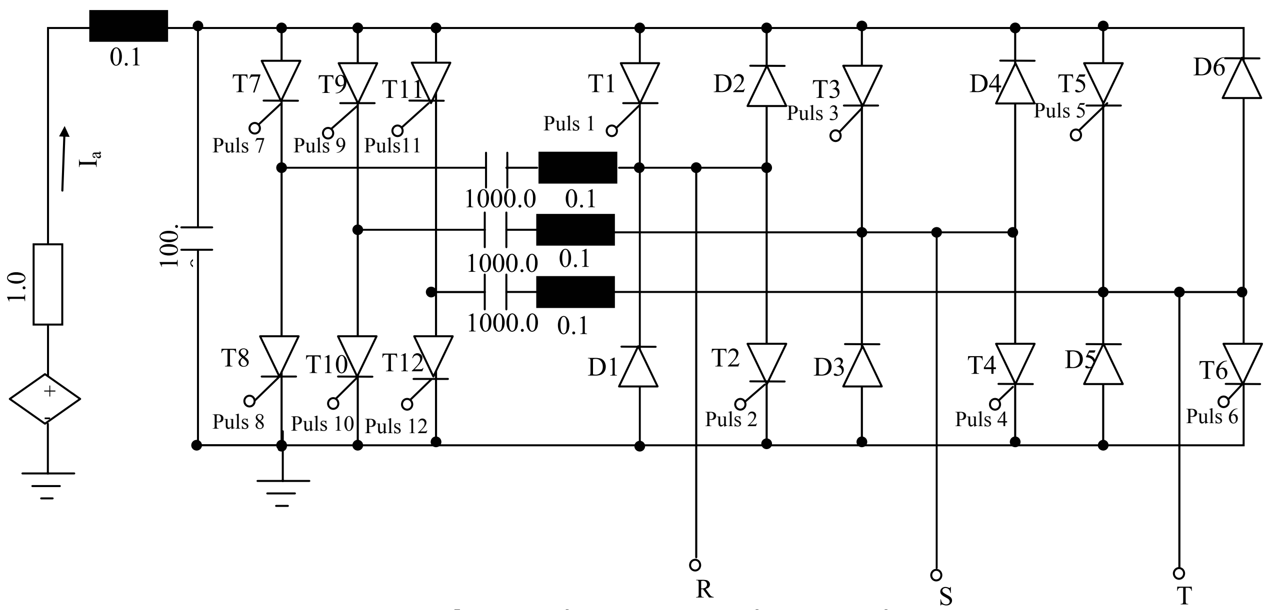

Fig. 3*. The inverter electric scheme.*

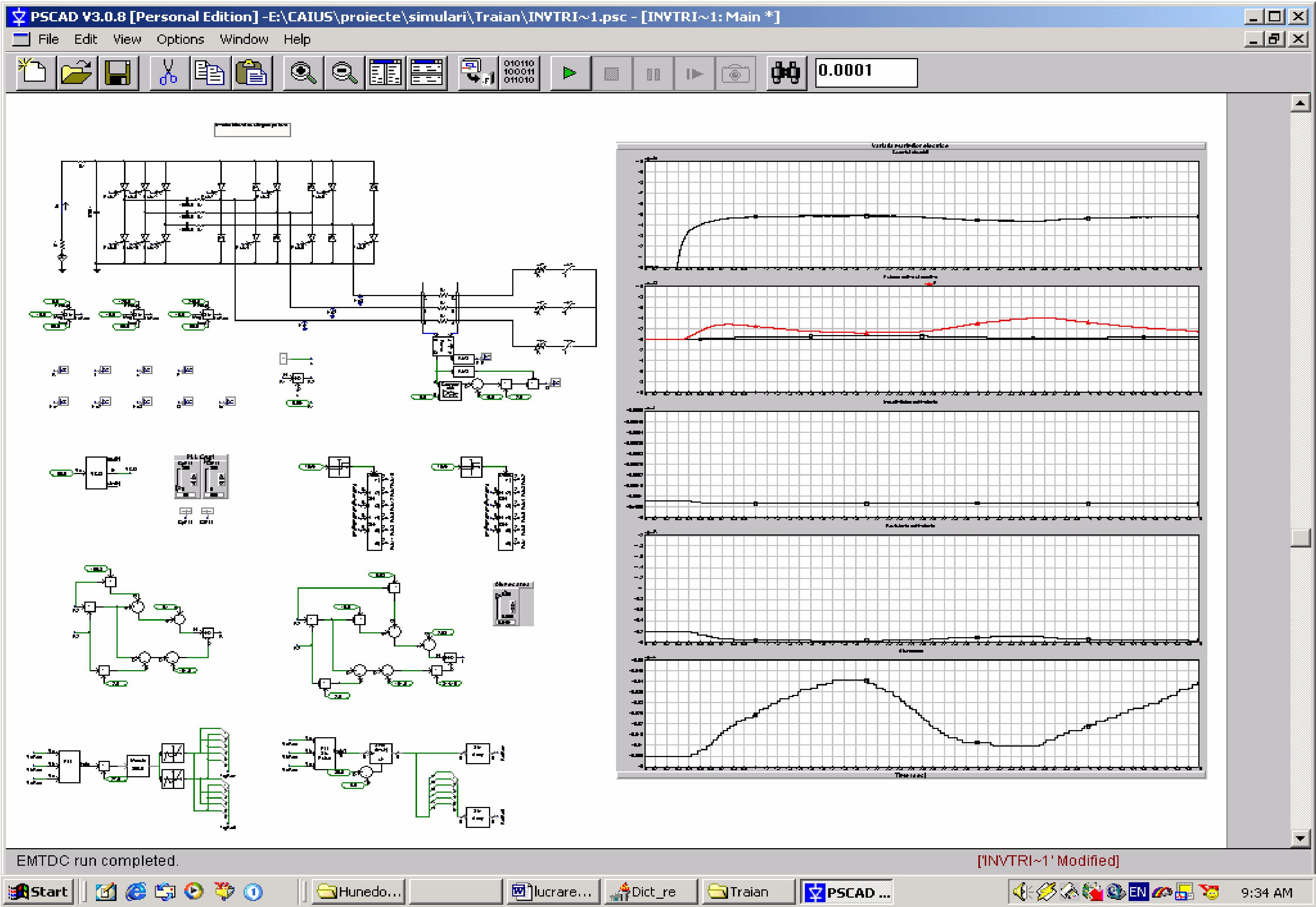

Fig. 4. Simulation rezults without reactive power compensation system.

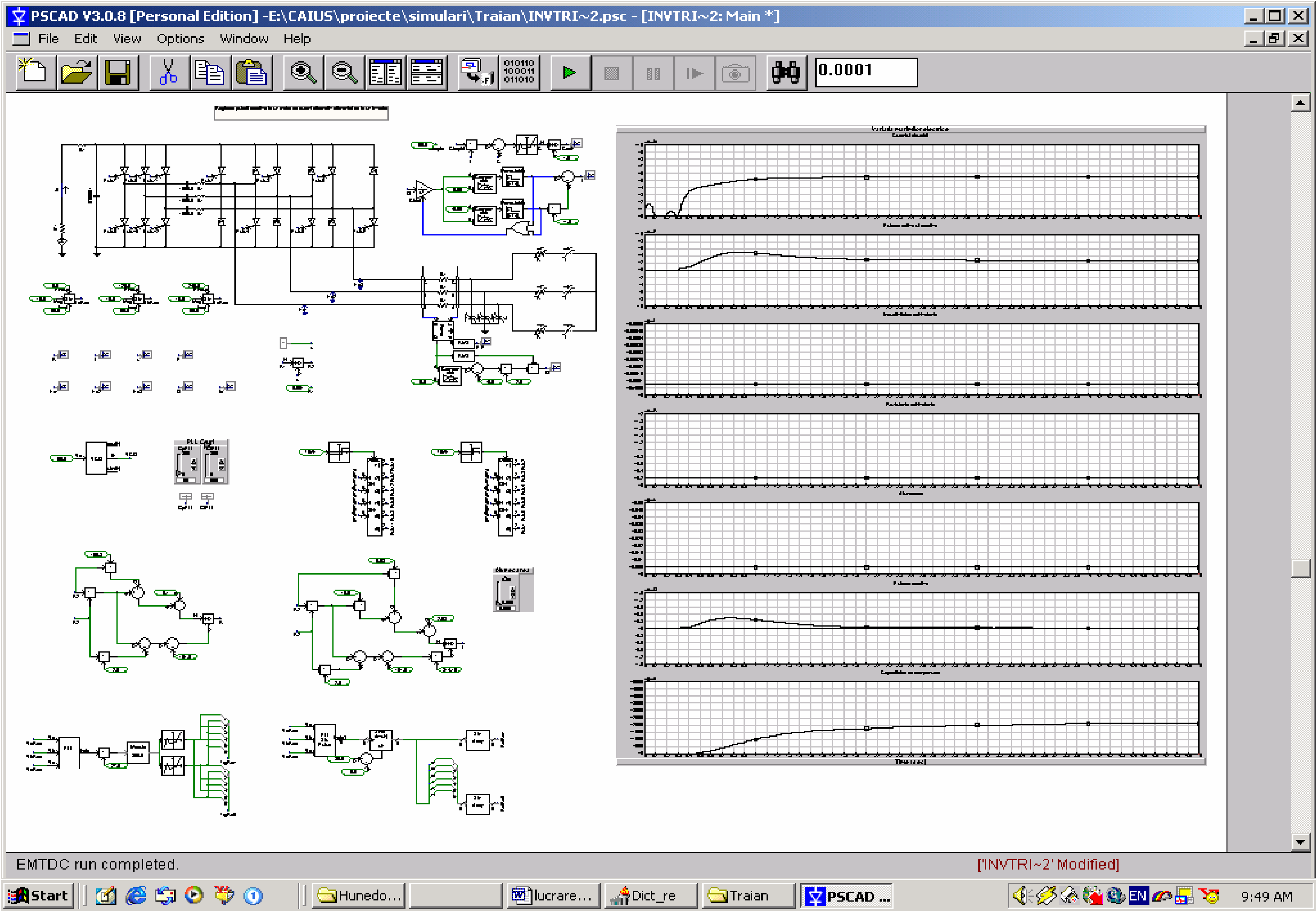

Fig.5. *Simulation rezults with reactive power compensation system.*

4. THE REACTIVE POWER COMPENSATION ALGORITHM

The results using PSCAD-EMTDC simulation program are shown in figure 4. It can be see that the reactive power values depend on *s* parameter.

To realize the reactive power compensation process was used a reactive power compensation installation, composed from condenser battery. Considering that Q is the reactive power values introduce by a compensation step the control algorithm is:

- If the reactive power value is in –Q to +Q domain the reactive power step compensation does not change;
- If the reactive power value is greater then +Q the next reactive power step compensation will be used;
- If the reactive power value is lower then –Q the previous reactive power step compensation will be used.

The simulation results are presented in figure 5. It can be see that the reactive power is control by the compensation system such as the final reactive power tends to zero value.

5. CONCLUSIONS

The simulations realized by the authors was concerned in two directions. The first consist in verifying by simulation that the values reactive power compensation installation permit to obtain the wanted values of the reactive power step.

The second direction demonstrate that it can be implemented a reactive power control algorithm.

6. REFERENCES

[1]. Varadan, S., Makram, E.B., Girgis, A.A., *A New Time Domain Voltage Source Model for an Arc Furnace using EMPT*, IEEE Transactions on Power Delivery, vol. 11, No. 3, pg. 1685-1691, July 1996.

[2]. *Montanari, G.C., Loggini, M., Cavallini, A., Pitti, L., Zaminelli, D.,* Arc-Furnace model for the Study of Flicker Compensation in Electrical Networks*, IEEE Transactions on Power Delivery, vol. 9, No. 4, pg. 2026-2036, October 1994.*

[3]. *Golovanov, N., Şora, I.*, Electrotermie şi electrotehnologii*, vol I, Editura Tehnică Bucureşti, 1997.*

THE FILLING-OUT OF COMBUSTIBLE FLUIDS ONBOARD SECIFIED SHIPS

Gheorghe SAMOILESCU, Alina BARBU,
Mircea CONSTANTINESCU, Vergil GRADINARU

"Mircea cel Batran" Naval Academy – Constanta, ROMANIA

ABSTRACT:

Loading filling out and unloading operations of oil products can result in electric storage that can be turned into electric discharges.

This paper focuses on the conditions to be taken into account for the crew, ship and environment safety, in the case of combustible fluids onboard specialized ships considering the plusical and chemical phenomena that acher. Specific measures against electric discharges can be taken if the occurrence and evolution of electric load in the lines and compartments of the ship are known. An analysis is made on the methods of electric loading of oil products, the role of the water in the oil emulsion, the role of inversion, the need for the implementation of normsand recommendations within the Romanian Ship Register. Based on the charts showing combustible fluids loading during the transportation, through lines according to electrical resistivity, tables are drawn for the differences in limit potential for cargo and ship safety. The analysis of production and storage mechanisms of electric loads within lines as well as the determination of load sensity evolution allow for an analysis of safety conditions of navigation on the seas, oceans and in the harbors of the world.

KEYWORDS: *electrostatic load; combustible liquid; flowing current; diffusion; migration; connection of electric load*

1. INTRODUCTION

When flowing through pipes, combustible liquids get charged with electricity. When electric load appear their value is determined by a process of setting up a double electric layer, which represents a spatial distribution of electric of electric loads on the contact surface of the liquid phase with the wall of the specific pipe.

The equations which govern the distribution of electric loads in the case of flowing combustible liquids of low conductivity enable us to make a compression between experimental results and theoretical results, in order to ensure a better understanding of the phenomenon of electrostatic charging.

Static electricity present a risk of fire and explosion during loading, unloading, decantation and storage of oil products is due to the impurities which are deposited.

Where the oil liquid comes in contact with the wall of the delivery pipe, Wan der Waals and Coulomb resulting forces can be channeled towards the interior or the exterior of the pipe depending on the sign of the load on the product to be carried. The production of electric loads when liquids move about can be explained on the grounds of a specific feature of the separation boundary between the liquid and the solid phase [1]. The maximum depth at which the loading particles may penetrate from one surface to the other in order to obtain a measurable separation of loads is $5\cdot10^{-10}$ m for the electrons and $25\cdot10^{-10}$ m for the ions [2] [3].

Any displacement of the liquid trigger a shipping of fixed loads as opposed to free ones within the double electric stratum, creating thereby an electric current and the possibility to accumulate electric at both ends of the tract. Therefore, the combustible liquid which flow through pipes gather the loads non-absorbed by the walls of the pipes and conveys them as a spatial load in the storage area.

The appearance of electrostatic discharge depends on the composition of the combustible substances, the percentage of generation and relaxation of the electric load, the gradients, the outcoming potential, the volatility and inflammability of component substances within the oil product, the minimum ignition energy of mixtures.

Both the electric charging and the electric conductivity of a combustible product are due to the presence of ions. The accumulation of electric loads is dangerous because it is achieved by means of an increase in the intensity of the electric field. In the case of oil liquids which have an electric risistivity greater than $10^7 \div 10^8 \Omega\cdot m$ when passing trough pipes, the electric lead increases conversely proportional through the section of the pipe and directly proportional to the flowing speed, the rugosity of the interior surface of the pipes and its length.

2. GENERAL EQUATIONS WHEN CARRYING LIQUIDS THROUGH PIPES

In conformity with the researches which have been made in hydrodynamics, due to the ions of opposite signs, which take part in the laminar movement as well as in a turbulent movement, the thickness of the double electric stratum is [4]

$$\delta = \sqrt{\frac{RT\cdot\varepsilon_0\cdot\varepsilon_r}{2C\cdot F^2\cdot z^2}} \tag{1}$$

where: R- universal constant of gases
F-Faraday number
C-concentration of ions
Z-ion valence
T-absolute temperature
$\varepsilon = \varepsilon_0\cdot\varepsilon_r$ - electric permitivity

In conformity with Stern's models, the double stratum is made up of two different liquid strats: the compact stratum, close to the wall and the diffuse stratum, who's thickness is proportional to the square root of liquid resistivity.

The equation which govern the diffuse stratum are:

a) conservation equation

$$div\,\bar{j} + \frac{\partial\rho^*}{\partial t} - \beta\frac{\partial\sigma^*}{\partial t} = 0$$

$$div\,\bar{j} + \frac{\partial\sigma^*}{\partial t} - \frac{\partial\rho^*}{\partial t} = 0 \tag{2}$$

b) Poirson's equation

$$\Delta\Psi = -\frac{1}{\varepsilon}\left(\rho^* - \beta\sigma^*\right) \tag{3}$$

c) equation of electric current density

$$\vec{j} = -D_0 grad\vec{d}\rho + \frac{e_0 z D_0}{KT}\cdot\sigma^*\cdot grad\vec{d}\Psi + \left(\rho^* - \beta\sigma^*\right)\vec{v}$$
$$\vec{j}^* = -D_0 grad\vec{d}\sigma^* - \frac{e_0 z D_0}{KT}\cdot\rho^* grad\vec{d}\Psi + \left(\sigma^* - \beta\rho^*\right)\vec{v} \tag{4}$$

with:

$$\sigma^* = \sigma\frac{KT}{e_0 z D_0} \quad ; \quad \beta = \frac{D_C - D_A}{D_C + D_A}$$
$$\rho^* = \rho + \beta\sigma\frac{KT}{e_0 z D_0} \quad ; \quad \rho = \frac{X\cdot v\cdot\Delta_0\cdot L}{\frac{\Pi d^2}{4}} \tag{5}$$
$$D_0 = \frac{2D_C\cdot D_A}{D_C + D_A}$$

ρ - volume density of the electric load
σ - electric conductivity
e_0 - electric load
$D_C D_A$ -cationic and anionic diffusion coefficients
D_0 -average diffusion coefficient
j, j^* -total and conjugated current densities
K- Baltzman coefficient
z- valence
Ψ -electric potential
v-transportation speed
Δ_0 -relative rugosity of the walls
X- F.c.t
C- concentration of molecules
t- time to move the fluid
$A_C = \frac{\Pi d^2}{4}$ - area of the transversal section of the conveyance pipe.

Differential equation which conducts the density of the electric load when a combustible fluid flows is:

$$\frac{\partial q}{\partial t} + v\nabla q + \frac{\sigma_0}{\varepsilon}q - D\nabla^2 a = 0 \tag{6}$$

In this equation we notice that the contribution brought by each and every term to the quantity of loads $\left(\frac{\partial q}{\partial t}\right)$, to the density of loads due to the convection $v\nabla q$, to the electric migration of the load $\left(\frac{\sigma_0}{\varepsilon}q\right)$ and the diffusion of the load $\left(D\nabla^2 q\right)$. The expression of admissible speed for pumping inflammable liquids through pipes is:

$$v_{\lim}^{1,875} = \frac{1}{8} \cdot \frac{2 \cdot 10^{7} \cdot \varepsilon_{rg} \cdot \nu^{0,875} \cdot n \cdot F}{\chi \cdot \tau_{l} \cdot \varepsilon_{rl} \cdot R \cdot TS_{C}^{0,25}\left(1 - \frac{C_{P}}{C_{0}}\right)} \cdot \frac{S}{d_{C}^{0,875}} \tag{7}$$

where:

υ-cinematic viscosity of the liquid

n- 0,5 - transportation number of ions

$S_C = \frac{P_e}{R_e}$ – Schmidt's number; P_e - Pechet's number

R_e - Reynold's number

C_P -ion concentration of the pipe wall

C_0 -ion concentration in the volume of liquid

d_C -pipe diameter

χ -coefficient depending on the nature of load carriers and the degree of the wetness of the pipe walls

$\tau_l = \frac{\varepsilon_0 \cdot \varepsilon_{rl}}{\gamma} \Big/ \left(1 - \frac{\alpha}{2}\right)$ -relaxation time of the liquid

$\alpha = \frac{\varepsilon_{rg} \cdot h_f}{\varepsilon_{rg} \cdot h_f + \varepsilon_{rl} \cdot h_g}$ -feeling coefficient of cargo compartment

ε_{rl} -relative permitivity of the liquid phase

Admissible pumping speed of oil products through pipes of 1,23 .... 5 m/s depends on their positioning onboard ship. In the case of orizontal pipes, this speed is at least two times greater than that of a vertical pipe, table no. 1.

***Table 1.** - Admissible flowing speed of some hydrocarbonic products*

Hydrocarbonic product	Resistivity	Flowing speed for the bottom pipe (m/s)	Flowing speed for the surface pipe (m/s)	Contents in impurities (g/m3)
air fuel	48	6.62	2.8	
Gasoline 98	58	8	4	
Gasoline 95	60	8.4	4.2	
Special fuel	46	15	5	
Benzene	60	3,6	1.3	40
Dietil bezene	60	1.64	0.48	50-70
Isopropylbenzene	6	5.2	0.72	70-100
Xylen	8.5	6.7	1.4	40
Toluen	8.6	6.8	1.5	40
cyclohexane	460	2	1.2	40

3. Mathematic formulation of the theory of spatial load when hydrocarbonic fluids flow.

As a result of studying fundamental processes, which generate the production of electric loads when transporting oil products, we tried to approximate the nature of the balance existing between the migration ant the convection of the loads on and near the surface of separation. In order to make possible a solution for the partial differential equations written above, we developed a problem in which, knowing the section of a pipe with given dimensions, the problem becomes bidimensional due to the simetry following the cylindrical coordinate φ (fig. 2.) [5-8]

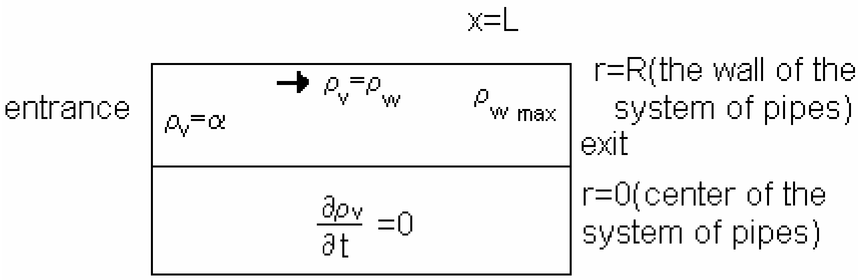

Fig. 2

Limiting conditions are those in the figure an the numerical boundary is chosen in order to completely ignore the flux and the load due to the term $v\nabla\rho_v$ and the boundary load remains unaffected both by the flow of liquid (the load is static) and by the load accumulation in the lower part of the system of pipes.

The equations which govern the density of the load are solved using the numerical method of finite differences. The flow is supposed to be linearly and the speed profile is given by the relation:

$$v = 2v_m\left(1-\frac{r^2}{R^2}\right)\widehat{a}_x \tag{8}$$

where: v_m-medium speed of the fluid
R- internal radius of the system of pipes
$\widehat{a}_x$-the speed vector of Ox axis (the module of which is 1)

The equation (5) becomes:

$$\frac{\partial\rho_v}{\partial t}+2v_m\left(1-\frac{r^2}{R^2}\right)\frac{\partial\rho_v}{\partial x}+\frac{\sigma_0}{\varepsilon}\cdot\rho_v-D\left(\frac{\partial^2\rho_v}{\partial r^2}+\frac{1}{r}\frac{\partial\rho_v}{\partial r}\right)-D\frac{\partial^2\rho_v}{\partial r^2}=0 \tag{9}$$

The low density is approximated on a matrix in time and space and the differential solution is written as follows:

$$\rho^n_{v,jk}=\rho_v\left(j\Delta x,k\Delta r,n\Delta t\right) \tag{10}$$

where: j;k;n - whole values
$\nabla x,\nabla r,\nabla t$ - levels (steps) of the matrix $\nabla x=0\div L;\nabla r=0\div R$

Depending on the notations, the explicit methods of finite differences in accordance with the equation (10) is written:

$$\left(1+\frac{\Delta t}{\varepsilon}\sigma_0\right)\rho^{n+1}_{v;j,k}=\rho^n_{v;j,k}-2v_m\left(1-\frac{r^2}{R^2}\right)\frac{\Delta t}{\Delta x}\left(\rho^n_{v;j,k}\rho^n_{v;j-1,k}\right)+\frac{D\Delta t}{(\Delta r)^2}\left(\rho^n_{v;j,k+1}-2\rho^n_{v;j,k}+\rho^n_{v;j,k+1}\right)+$$

$$+\frac{D\Delta t}{2\rho_{jk}\Delta r}\left(\rho^n_{v;j,k+1}-\rho^n_{v;j,k-1}\right)+\frac{D\Delta t}{(\Delta r)^2}\left(\rho^n_{v;j+1,k}-2\rho^n_{v;j,k}+\rho^n_{v;j-1,k}\right)$$

where: $\rho_{jk}=k\Delta r$

$$\left.\begin{array}{l}\dfrac{D\Delta t}{(\Delta n)^2}\langle\dfrac{1}{2}\\[2ex]\dfrac{D\Delta t}{(\Delta x)^2}\langle\dfrac{1}{2}\end{array}\right\}$$ conditions (of sufficiency) due to the terms of diffusion

$2v_m\dfrac{\Delta t}{\Delta x}\langle 1$ condition (of sufficiency) due to the term of convection

Limiting conditions are numerically approximated as follows:

- the density of volume of the load where entering the system of tubes is considered to be equal to naught.

$$\rho_{v;0k}^{n}=\rho_v\left(0,k\nabla r,n\nabla t\right)$$

- the density of volume of the load on the wall of the system of pipes is considered to be equal to the unity.

$$\rho_{v;jk}^{n}=\rho_v\left(j\Delta x,k_{\max}\Delta r,n\Delta t\right)$$

Newmann's boundary condition in the center of the system of pipes is imposed by establishing the relation:

$$\rho_v;j,-1=\rho_v\left(j\Delta x,-\Delta r,n\Delta t\right)$$

Whenever it is required in the scheme. The same condition is imposed when we determine the contribution due to the term of diffusion, that is:

$$\rho_{v;jmsx+1,k}^{n}=\rho_v\left(\left(j_{\max}+1\right)\Delta x,k\Delta r,n\Delta t\right)=\rho_{v;j\max-1,k}^{n}=\rho_v\left(\left(j_{\max}-1\right)x,k\Delta r,n\Delta t\right)$$

4. CONCLUSIONS

Active measures can be taken against the disturbing effects that cause electrostatic discharges in order to prevent the phenomenon of electrostatic charging or passive measures, which constitute proper protection methods.

Norms and recommendations to R.N.R. (Romanian Classification Society) have been settled against electrostatic discharges:

- all pipes user for oil products and inert gas must be earthed to the ship's hull and intervals of 10 m at the most.
- between intermediate flanges there must be an electrical convection to allow the electric load to drain into the ground.
- the initial rate of transport must not exceed 1 m/s until the longitudinal measurements of the cargo compartment haven't been fully covered so as to minimize the mixture with the remaining water and to reduce spraying and the electrical charged fog
- entering the residual tanks of the systems of pipes must be done so as to avoid turbulence and the production of hydrocarbures or emulsion with water

5. REFERENCES:

1. *Samoilescu Gheorghe - "Contributii la diminuarea influentei nociva fenomenelor electrostatice din navele petroliere", teza de doctorat, Universitatea Politehnica Bucuresti 1998*
2. *Samoilescu Gheorghe - "Fenomene electrostatice la navele petroliere", Editura Zeda&Muntenia, Constanta, 2000*

3. *Tanaescu, F.T. - "Charged particle trajectories in electrostatic fields", Journal of Electrostatic, vol. 23, 1989*
4. *Murgulescu, G., Radovici, O.M. - "Introducere in chimie fazica" Editura Academiei, vol IV, Bucuresti 1986*
5. *Inculet, I.I. - "Electric charges and explosion hazards", Ontario, Canada, 1993*
6. *Bailey, A.G. - "Electrostatic hazards during liquid transport and spraying", Handbook of Electrostatic Processes, 1995*
7. *Mastubara, Y. - "Effect of fill pipe on transient decay of surface potential in a cylindrical vessel containing charged liquid", I.E.E.E Transaction on Industry Applications, vol. 30, no. 1, 1994*
8. ** * * Journal of Electrostatic, no. 36, 1996*

THE POTENTISTATICAL METHOD USED FOR PURCHASING THE CORROSION BEHAVIOR OF THE WC COATINGS DEPOSITED BY PLASMA SPRAYING

M. L. BENEA

"Politehnica" University of Timisoara, Engineering Faculty of Hunedoara

ABSTRACT

The method used for purchasing the corrosion behavior of the WC coatings deposited by plasma spraying, on a martensitic stainless steel substrate consists in measuring the electrochemical potential of the coating, respectively that of the substrate, immersed in NaCl solution as corrosive agent. The mathematical processing of the obtained experimental results in Matlab allowed us to make some correlations between the electrochemical potential difference, concentration and temperature of the NaCl solution, the result being the 2^{nd} degree correlation surface, to make a comparison the experimental and the theoretical results and the behavement of the surface R2 around the medium point.

KEYWORDS

WC coatings, plasma deposition, corrosion resistance, potentiostatic method.

1. INTRODUCTION

The WC-Co coatings are designed to protect machines parts (roll cylinders, turbine shuffles, parts of diesel engines) during the combined wear and chemical corrosion stress [1, 2, 3].

The studied coatings within the framework of the present paper have been deposited by Air Plasma Spraying, on a martensitic stainless steel substrate using a Metco 73 spraying powder [4,5].

In order to purchase the corrosion behavior of these coatings, in literature there are mentioned the 0.1 M NaOH, 0.1 M H_2SO_4 and also NaCl solutions [6].

As corrosive agents there have been used NaCl solutions of different concentration, at different temperatures.

The protective action of the coating has been appreciated by measuring the electrochemical potentials of the substrate respectively of the coating, both immersed in the NaCl solution. The higher the electrochemical potential of the coating is, in comparison to that of the substrate, the better the protective action of the coating is being considered [7,8].

2. EXPERIMENTAL PART

The substrate is the martensitic stainless steel Z12CNDV12. Before being coated, the surface of the substrate has been prepared by sanding with corundum powder.

The coatings have been using a Metco 7MB equipment. The powder used is Metco 73, with 83 % WC and 17 % Co and particle size between 10 and 45 μm.

The coating thickness is 0.1 mm.

The corrosion resistance is determined by the potentiostatic method. The couple made of the coating (WC-Co) and substrate has been immersed in NaCl solutions having concentrations between 1 and 15 %, at temperatures between 20 and 48°C. In each case has been determined the electrochemical potential of the coating and substrate, using as reference electrode the calomel electrode.

The corrosion resistance has been tested using the installation shown in figure 1.

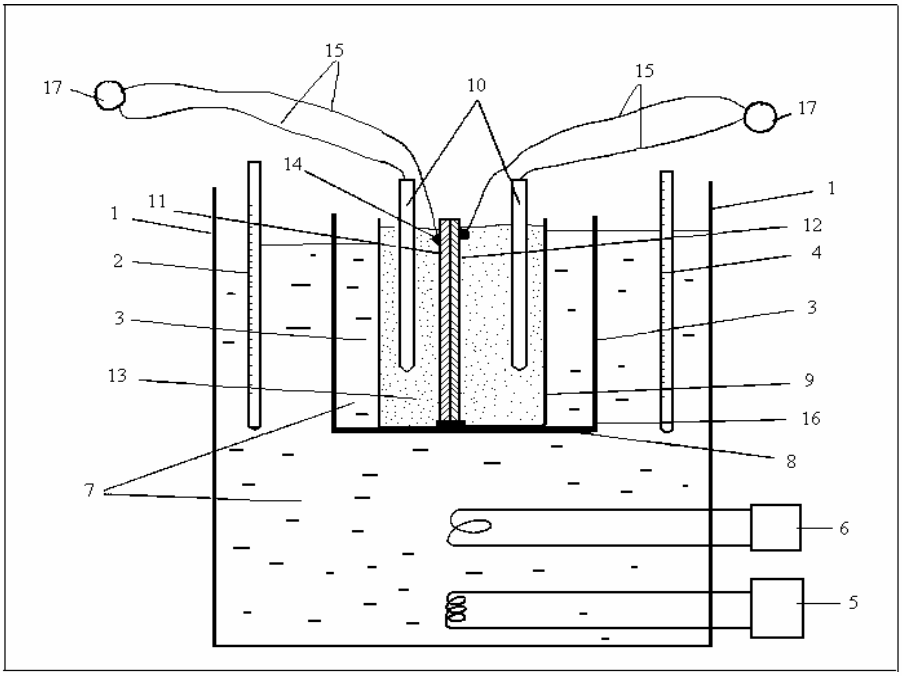

Fig. 1. *The assembly made for the determination of the corrosion resistance. 1-Thermostate; 2-Measurement thermometer; 3-Fixing device of the support; 4-Contact thermometer; 5-Heater; 6-Water recycling pump; 7-Water; 8-Support; 9-Berzelius glass; 10-Reference (calomel) electrodes; 1-Coating; 12-Metallic substrate; 13-Electrolite (NaCl solution); 14-Contact; 15-Conductors; 16-Silicon (adhesive for sealing); 17-Milivoltmeter*

3. RESULTS AND DISCUSSION

The results of the experimental determinations are shown in the table1.

Table 1 *- The values of the electrochemical potential differences [mV] between the coating and the substrate, when varying the temperature and the concentration of the NaCl solution.*

C [%]	The electrochemical potential difference [mV] for different temperatures of the NaCl solution [°C]														
	20	22	24	26	28	30	32	34	36	38	40	42	44	46	48
1	253	250	248	245	240	245	237	235	233	225	225	225	225	227	227
2	225	215	209	205	198	199	195	194	192	191	190	188	190	198	191
3	210	200	195	190	180	175	174	180	172	171	170	170	172	172	173
4	195	179	168	170	159	159	157	155	152	154	149	152	152	154	155
5	190	176	161	150	142	144	143	142	141	141	140	140	141	142	142
6	185	160	152	150	141	142	135	134	133	132	132	133	133	135	137
7	184	181	165	151	140	135	134	132	132	131	130	131	132	132	133
8	183	165	150	143	140	137	133	132	132	131	131	132	133	134	134
9	184	160	155	145	142	138	137	140	133	132	132	133	135	136	136
10	183	160	160	143	140	135	134	133	132	131	131	132	133	135	137
11	183	177	168	157	150	143	142	140	137	135	132	132	133	137	140
12	183	170	159	155	140	137	135	135	133	133	131	132	132	137	140
13	183	172	165	151	145	142	139	138	140	134	133	135	138	139	140
14	183	170	160	153	150	148	142	139	136	135	135	137	140	139	140
15	180	168	157	150	145	143	140	137	136	135	135	137	139	140	142

The experimental results were processed in Matlab, obtained correlation surface of the 2nd degree (fig.2) as well as level lines of the corresponding correlation surfaces (fig.3).

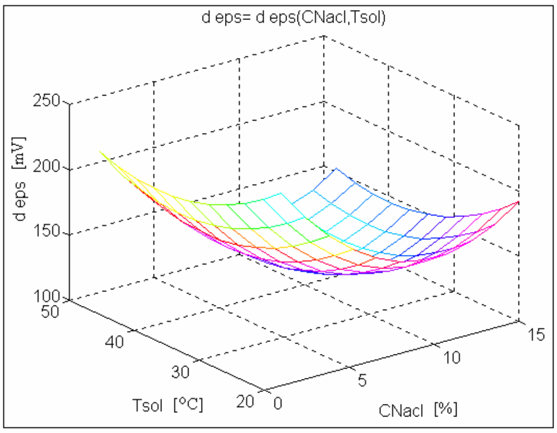

Fig. 2. *2nd degree correlation surface*

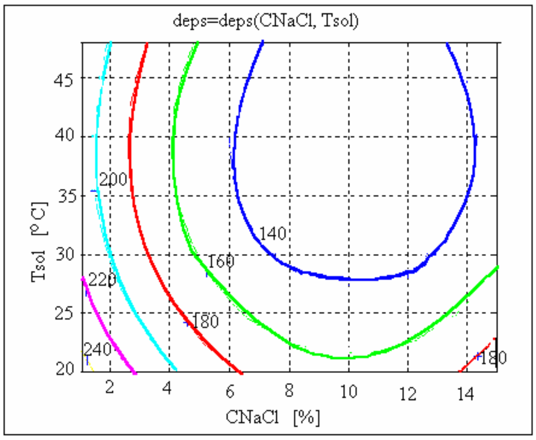

Fig. 3. *The level lines of the 2nd degree correlation surface.*

On the x axis is has been represented the concentration of the NaCl solution (CNaCl) in %. On the y axis has been represented the temperature of the NaCl solution (Tsol), in °C. u represents the electrochemical potential difference (d eps) between the coating made of Metco 73 powder and the martensitic stainless steel Z12CNDV12.

The deviations of the regression surfaces are being calculated with relation (1):

$$deviation2 = \sqrt{\frac{1}{225}\sum_{i=1}^{225}\left(u_i - c_{21}\cdot x_i^{\,2} - c_{22}\cdot x_i\cdot y_i - c_{23}\cdot y_i^{\,2} - c_{24}\cdot x_i - c_{25}\cdot y_i - c_{26}\right)^2} \quad (1)$$

where c_{21}, c_{22}, c_{23}, c_{24}, c_{25}, c_{26} are the coefficients in the equation of the 2nd degree correlation surface:

$$u = c_{21}\cdot x^2 + c_{22}\cdot x\cdot y + c_{23}\cdot y^2 + c_{24}\cdot x + c_{25}\cdot y + c_{26}$$

The values of these coefficients are:
c_{21}=1; c_{22}= -0,01; c_{23}=0,11; c_{24}= -19,7; c_{25}= -8,9; c_{26} = 399,27 [9,10]

so that the ecuation (2) for the correlation surfaces may be now written:

$$u = x^2 - 0.01\cdot x\cdot y + 0.11\cdot y^2 - 19.7\cdot x - 8.9\cdot y + 399.27 \quad (2)$$

A comparison between the experimental data and the theoretical results is made in table 2.

Table 2. *The comparison of the experimental data with the theoretical ones*

Current number	C NaCl (%)	T sol (ºC)	The deviation of the experimental values from the theoretical ones, for the 2nd degree correlation surface eq.
1	1	20	5.321
2	3	20	-5.567
3	5	20	-1.479
4	7	20	8.585
5	9	20	16.63
6	11	20	15.64
7	13	20	7.633
8	15	20	-11.4
9	1	28	19.82
10	3	28	-7.814
11	5	28	-21.47
12	7	28	-7.144
13	9	28	3.154
14	11	28	11.43
15	13	28	-1.321
16	15	28	-17.1
17	1	36	25.65
18	3	36	-2.716
19	5	36	-9.111
20	7	36	-1.53
21	9	36	8.027
22	11	36	12.56
23	13	36	8.069
24	15	36	-11.45
25	1	48	11.43
26	3	48	-9.549
27	5	48	-15.56
28	7	48	-7.587
29	9	48	4.358
30	11	48	9.278
31	13	48	2.175

The first column contains the current number, the second column – NaCl solution concentration in %, and the third column – the temperature of the NaCl solution, in °C.

The forth column shows the deviation of the experimental results from those theoretical given by the 2nd degree correlation surface equation, deviation calculated according to the relation:

$$u_i - c_{21} \cdot x_i^2 - c_{22} \cdot x_i \cdot y_i - c_{23} \cdot y_i^2 - c_{24} \cdot x_i - c_{24} \cdot y_i - c_{26}$$

The medium values calculated are:

$$x_m = 8{,}000; \quad y_m = 34{,}000; \quad u_m = 157{,}5.$$

Table 3 shows the behavament of the surface R2 around the medium point.

Table 3. The behavament of the surface R2 around the medium point

Current number	Values for:		
	x	y	u
1.	8,500	34,000	128,4
2.	8,353	34,353	128,5
3.	8,000	34,500	129,7
4.	7,646	34,535	131,5
5.	7,500	34,000	132,7
6.	7,646	33,646	132,39
7.	8,000	33,500	130,9
8.	8,353	33,646	129,4
9.	9,000	34,000	127,1
10.	8,707	34,707	127,0
11.	8,000	35,000	129,2
12.	7,293	34,707	133,0
13.	7,000	34,000	135,5
14.	7,293	33,292	134,7
15.	8,000	33,000	131,7

4. CONCLUSIONS

- The paper presents an original method to purchase the corrosion behavior of the WC coatings deposited by plasma spraying, on a martensitic stainless steel substrate; the method is based on measuring the electrochemical potential of the coating, respectively that of the substrate, immersed in NaCl solution (corrosive agent), related to a reference calomel electrod.
- The values of the potential differences between the coating and the substrate are decreasing when raising the temperature and the concentration of the NaCl solution, which shows a decrease of the protection provided by the coating.
- The mathematical processing of the obtained experimental results in Matlab allowed us to make some correlation between

the electrochemical potential difference, concentration and temperature of the NaCl solution, the result being the 2nd degree correlation surface.

- Comparing the experimental data with the theoretical ones there resulted the deviations shown in table 2.
- The behavament of the surface R2 around the medium point shown in table 3.

5.REFERENCES

1. S. Kasai, A. Yanogisawa, A. Ichihara, Y. Shimoyama, K. Ochiai, H. Onishi - Proceedings, 1th Plasma –Technik- Symposium, Vol. I, Lucerne/Switzerland, May, 205, (1988).
2. R. W. Smith, Z. Z. Mutasim – Journal of Thermal Spray Technology, ASM International, 57 (1992).
3. I. Kvernes, E. Lugscheider, O. Norholm, Proceedings - 1th Plasma – Technik- Symposium, Vol. 3, Lucerne/Switzerland, May, 41, (1988).
4. A. Scrivani, R. Groppetti, U. Bardi, A. Lavacchi, F. Niccolai, G. Rizzi – A Comparative Study On HVOF, Vacuum Plasma Spray and Air Plasma Spray for CoNiCrAlY alloy deposition, document placed on line on June 2001*, http://www.unifi.it/unifi/surfchem/solid/ bardi/tbcs/mcraly/CoNiCrAlYart12jun01.html*
5. *** Commission On Engineering And Technical Systems, National Research Council – Coatings For High-Temperature Structural Materials: trends And Opportunities, National Academy Press, Washington D. C. (1996).
6. D. Toma, W. Brandl, G. Mărginean – Wear and Corrosion Behavior of Thermally Sprayed Cermet Coatings-Surface and Coatings Technology, 138 (2001).
7. M. L. Benea, Ş. Maksay, 6th International Symposium Interdisciplinary Regional Research Hungary-Romania-Yugoslavia, Novi Sad, oct. (2002).
8. M. L. Benea, Ş. Maksay, Analele Facultăţii de Inginerie din Hunedoara, Tomul IV, Fascicola 1, 129, (2002).
9. M.L.Benea, S.Maksay, R.I.Lazau, D.Becherescu, Using the potentiostatic method in order to purchase the corrosion behavior of the WC coatings deposited by plasma spraying, part I, Materials engineering, vol.14,nr.2, pp 127-140.
10. M.L.Benea, S.Maksay, R.I.Lazau, D.Becherescu, Using the potentiostatic method in order to purchase the corrosion behavior of the WC coatings deposited by plasma spraying, part II, Materials engineering, vol.14, nr.2, pp 141-155.

THERMAL SHOCK BEHAVIOR OF THE COATS DEPOSITED BY PLASMA SPRAYING OF THE Al_2O_3

M.L. BENEA

"Politehnica" University of Timisoara, Engineering Faculty of Hunedoara

ABSTRACT

For the coats made by using the Al_2O_3 powder (type Metco 101) on a martesitic stainless steel substrate, the thermal shock testing conditions consist in: fast heating to 800°C (or 500°C) (10s) and water cooling without maintaining to maximum temperature.

After 22 cycles to a maximum temperature of 800°C we noticed the appearance of a pattern fine cracks, which is developed along the next 20 cycles but with no scorching.

For a maximum temperature of the 500°C of the thermal shock, after 205 cycles we not observed the appearance of the scorches on the coats surface.

KEYWORDS

Thermal shock, Al_2O_3 coatings, plasma deposition

1. INTRODUCTION

Compared to other coating methods, plasma spraying is unique in that the high temperatures (~ 10.000 K) and specific energy densities achieved in thermal gas plasmas enable the melting of any material which has a stable molten phase. Plasma spraying of materials such as ceramics and non-metallic, which have high melting points, has there fore become well established as a commercial process. Such coatings are increasingly used in aerospace, automobile, textile, medical, printing and electrical industries to impart proprieties such as corrosion resistance, thermal resistance, wear resistance, etc [1,2].

This paper describes the results of tests conducted to determine the thermal shock behavior of the coats deposited by plasma spraying of the Al_2O_3.

2. EXPERIMENTAL PART

2.1. Experimental conditions at the Al_2O_3 coatings spraying in plasma

The substrate is the martensitic stainless steel Z12CNDV12.

The powder used is Metco 101, with 97% Al_2O_3 and 2% TiO_2 and particle size between 30 and 75 μm.

The coatings have been made using a plasma generator GPPR-400 equipment.

There have been working using the following parameters:

- intensity of the current at the generator: 500 A;
- voltage: 70 V;
- spraying distance: 50 mm;
- plasma gas flow: 36,6 l/h;
- coating thickness: 0,3 mm.

2.2. Thermal shock testing

For the coats made by using Metco 101 powder on a martensitic stainless steel substrate, the thermal shock testing consist in: fast heating to 800°C or 500°C (10 s) and water cooling (600°C/s) without maintaining to maximum temperature.

3. RESULTS AND DISCUSION

Some results of the experimental determination are shown in table1.

Table 1. Results of the thermal shock determination

Cod sample	The number of thermal cycles	The maximum temperature cycle [°C]	Cooling medium	Observation
19	50	800	water	The appearance of scorches
21	62	800	water	The appearance of scorches
29	65	800	water	The appearance of scorches
Medium		59		
35	205	500	water	No cracks, No scorches

Figure 1 shows some images for the the coats made using Metco 101 powder, in a different moments of the determination.

After 22 cycles to a maximum temperature of 800°C, we noticed the appearance of the pattern fine cracks, which is developed along the next 20 cycles but with no scorching.

For a maximum temperature of the thermal shock of 500°C, after 205 cycles we not observed the scorches appearance on the coats surface.

4. CONCLUSIONS

- for a maximum temperature of the thermal shock of 800°C, after 22 cycles, it is observed the appearance of a fine cracks;
- along the next 20 cycles to a maximum temperature of the thermal shock of 800°C, a pattern fine cracks is developed but with no scorching;
- after 205 cycles for a maximum temperature of the thermal shock of 500°C, we not observed the scorches appearance on the coats surface;
- the coats deposited by plasma spraying of the Metco 101 showed a good thermal shock resistance.

Figure 1. Images for the coats made by using the Metco 101 powder at the thermal shock

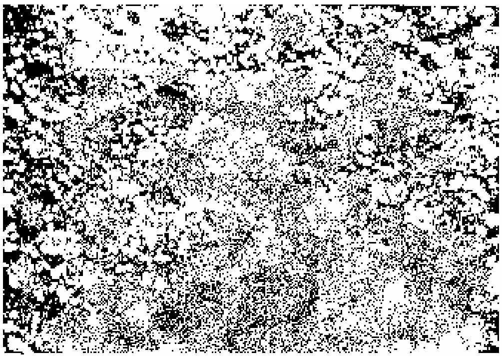

Sample 21, 70x, Initial state

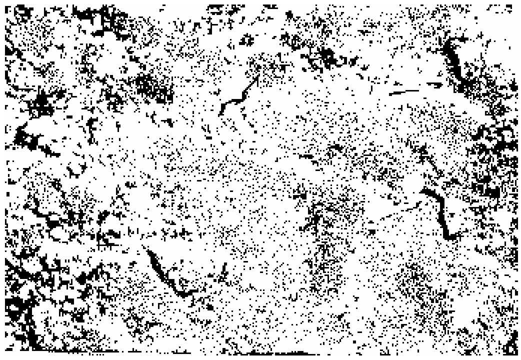

Sample 21, 70x, 800^{0}C/water/ 22 cycles.

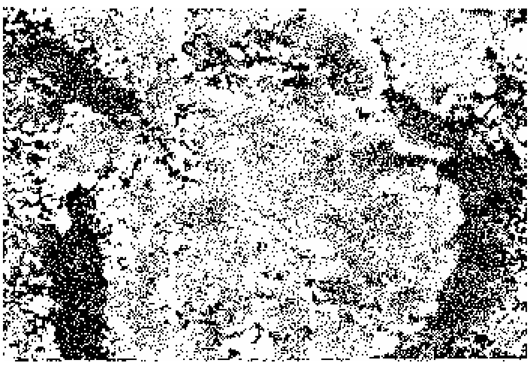

Sample 21,70x, 800^{0}C/ water/ 66 cycles

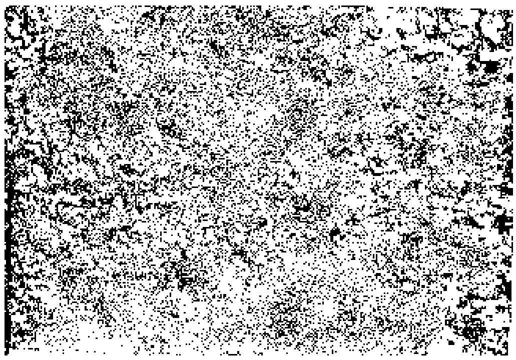

Sample 29, 70x, initial state

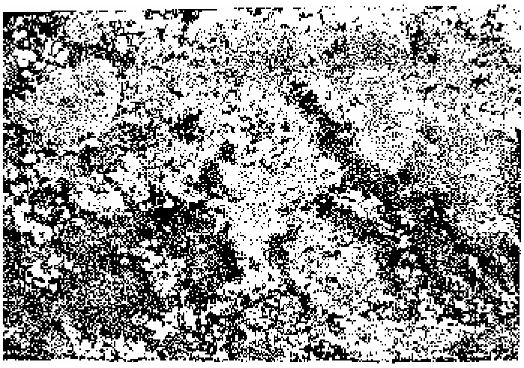

Sample 29,70x , 800^0C/water/ 22 cycles Crack

Sample 29, 70x, 800^0C/water/44 cycles Cracks

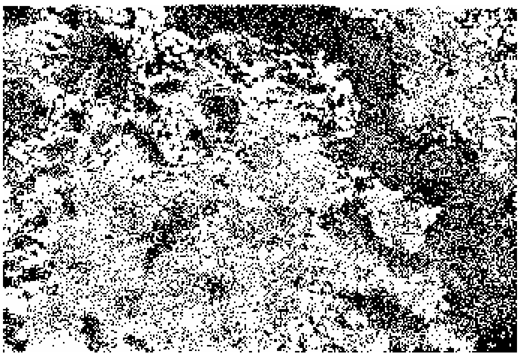

Sample 29, 70x, 800^0C/water/ 44 cycles cycles Cracks

Sample 35, 70x, 500^0C/ water/ 104 Means cracks

Sample 29,70x,800°C/water/44 cycles Cracks

Sample 35, 70x, 500°C/water/182 cicluri Network fine cracks

5. REFERENCES

[1] Nicoll, A.R., "Protective Coatings and their Processing – Thermal spray", Plasma Technik AG,Wohlen, Switzerland, Publ.No.86002E.

[2] Calosso, W.F., Nicoll, A.R., "Process requirements for plasma sprayed coatings for internal combustion engine components", Proc. Energy – Surface Technology Conerence and Exhibition, ASME,1987.

[3] Benea, M.L.: "Contribuţii teoretice şi experimentale asupra acoperirilor ceramice superrefractare realizate în jet de plasmă", Teză de doctorat, Timişoara, 2003

THE OBTAINING OF DUCTILE IRONS ELABORATED IN ELECTRIC ARC FURNACES

PETRE Doina Elena, JOSAN Ana

Engineering Faculty of Hunedoara

ABSTRACT

The present paper presents a series of experiments concerning the concocting of irons destined to the modification in electric arc furnaces, with bazic wall lining. The chosen modifier is a classical one, based on Fe, Si, and Mg.

It will be presented the chemical compositions of irons that are subject to modification, the parameters of the modification process, and also the results (the final composition of ductile irons, the characteristics of the graphite and of the matrix, gases contents).

The conclusions can be used for the making up of a modifying technology, on an industrial scale. This is similar with the experimenting technology.

Keywords
Modification, ductile iron, graphite, magnesium.

1. FOREWORD

It is known that at the concocting of ductile irons, the electric arc furnaces are being used only at the making up of superior quality irons. When a low quality raw materials is used, the electric arc furnace oven with bazic wall lining is the only aggregate that allows the de-sulfuration and de-phosphoration processes.

The following experiments were made in an electric arc furnace with bazic wall lining, with a 5 tones capacity, which was set on a steel casting platform. The resulting irons are destined to the nodulizing modification of the graphite.

2. EXPERIMENTS

The materials from the oven were chosen so that they would satisfy low percentage of sulphurus and other anti-modifier elements and in the same time high percentage of carbon in order to limit the carburating process.

The weighted 4700-5500 kg, and the was made from 85-90 % new and old cast iron and from 10-15 % old iron.

Depending on the ingredients of the raw materials, the chemical composition of the resulting cast irons was the following (table 1)

Table 1. *Chemical composition of the resulting cast irons*

Nr. crt.	Chemical composition, %							S_C	η_{Mg}, %
	C	Si	Mn	P	S_i	S_f	Mg_{rez}		
1	3,68	1,56	0,66	0,110	0,030	0,004	0,048	0,98	25
2	3,72	1,73	0,70	0,110	0,022	0,002	0,043	1,01	12
3	3,60	1,92	0,68	0,110	0,020	0,013	0,005	0,98	-
4	3,64	1,87	0,92	0,127	0,021	0,019	-	0,99	-
5	3,80	2,03	0,79	0,120	0,025	0,008	0,063	1,05	38
6	3,70	1,34	0,76	0,095	0,021	0,011	0,059	0,96	28
7	3,72	1,80	0,75	0,130	0,033	0,010	0,037	1,01	23
8	3,60	1,94	0,79	0,150	0,030	0,010	0,080	0,99	40
9	3,66	1,66	0,78	0,140	0,023	0,009	0,031	0,98	21
10	3,73	1,95	0,68	0,113	0,022	0,011	0,048	1,02	28

For the modification it was chosen the pot modifying technology together with the help of the modifying bell. The modifier quantity was calculated taking into account the sulphurus percentage from the resulting cast irons as well as the parameters of the modifying process. The relationship is the following:

$$Q_{mod} = \frac{0{,}76(S - 0{,}10) + Mg_{rez} + t.10^{--3}}{\eta.\frac{Mg_{prealiaj}}{100}}.\left(\frac{T}{1450}\right)^2.G \tag{1}$$

where: Qmod – the alloy quantity needed for modification;

S – the sulphurus percentage in iron exposed to the modification, %

Mg_{rez} – the proposed magnesium in iron, %

t – the time required to maintain iron in, after modification, min

η– the assimilation efficiency of the magnesium

$Mg_{prealiaj}$ – the quantity of magnesium in prealloy,

T – modification temperature, ^oC

G- the quantity of modified iron, kg

The prealloy used had the following chemical composition:

Mg = 10-15 %; Si = 40-45%; Ca=max 1%, Fe= rest

The chemical composition of molted irons before modification was:

C = 3,15 – 3,70%; Si = 1,34 – 1,92 %; Mn = 0,68 – 0,80 %; P = 0,095 – 0,110 %; S = 0,020 – 0,030 %; S_c = 0,98 – 1,05.

The rezidual elements in ductile iron are presented in table 2:

Table 2. *Rezidual elements in cast irons*

Nr. crt.	Chemical composition, ppm								
	Cr	Ni	Mo	Co	Ti	V	Cu	Pb	As
1	11	414	163	113	443	81	164	183	108
2	88	310	17	113	198	26	178	45	44
3	58	484	29	123	221	29	219	8	71
4	9	251	76	76	139	37	125	63	52
5	125	461	96	188	215	79	77	194	113
6	96	284	22	104	147	24	163	44	40
7	100	293	8	105	152	25	168	36	42
8	98	288	-	55	157	25	166	31	41
9	12	440	189	112	299	90	201	210	119

The sequence of the modification operations of cast iron was the following:

1. Molted iron, elaborated in the 5 tone furnace was melted in the 8 tone modification pot, after which the transportation of this on the casting platform was executed;
2. In the modification area the molted iron was cleaned of the formed slag and the temperature was measured;
3. After closing the modification pot-bell, the actual modification was undertaken. The reaction during modification was strong due to the high temperature of the iron. The modification time was 3-4 minutes;
4. After cleaning the pot of the slag formed during the modification, the casting was executed. The stop time between modification and casting process was 6-8 minutes and the duration of modification was 1-2 minutes.

***Table 3**. The parametres of the modification process*

Nr. crt.	Temperatures, ^oC		Durations, min				Prealloy		$Q_{iron,}$ to
	Modifing	Casting	modif	stat	cast	total	Tipe	Quantity	
1	1370	1300	3	7	2	12	FeSiCaMg	100	5,0
2	1300	1250	2	8	1	11	FeSiCaMg	100	5,0
3	1260	1200	2	6	1	9	FeSiCaMg	75	4,8
4	1270	1190	2	7	1	10	FeSiCaMg	85	5,0
5	1300	1240	3	7	2	12	FeSiCaMg	80	5,0
6	1340	1280	2	8	1	11	FeSiCaMg	85	4,5
7	1330	1260	2	6	2	10	FeSiCaMg	75	5,2
8	1350	1260	2	6	2	10	FeSiCaMg	80	5,0
9	1360	1310	3	7	1	11	FeSiCaMg	80	4,9
10	1350	1280	3	7	1	11	FeSiCaMg	75	45,0

The total duration to maintain the molted status did not go over 12 minutes (see table 3). The cast pieces out of the modified irons (ingots respectively) were exposed to a heat treatment for detention, according to the following pattern:

- heating from 150 to 650 ^oC with a speed of 100^oC/h, for 5 hours
- maintain at 650 ^oC for 4 hours
- cool from 650 ^oC to 300 ^oC with a speed of 100 ^oC/h
- free cooling from 300 ^oC to the environmental temperature

The microstructures and mechanical properties are shown in tables 4 and 5.

***Table 4.** Microstructure of the ductile irons*

Nr. crt.	Mg_{rez}, %	Heat treating	Microstructure			
			Graphite	Surface ocupated by graphite, %	Diameter of graphite, μm	Matrix
1	0,049	Detension	Nodular + vermicular graphite	10,91	75	Ferrite
2	0,043	Detension	Nodular graphite	9,52	60	Ferrite
3	0,005	Detension	Flake graphite	14,50	-	Ferrite
4	-	-	Flake graphite	11,91	-	Ferrite
5	0,063	Detension	Nodular graphite	7,71	70	Ferrite
6	0,059	Detension	Nodular graphite	10,09	75	Ferrite+ pearlite
7	0,037	Detension	Nodular graphite	13,02	90	Ferrite+ pearlite
8	0,080	Detension	Nodular and vermicular graphite	11,44	62	Ferrite+ pearlite
9	0,031	Detension	Nodular and flake graphite	6,52	70	Ferrite+ pearlite
10	0,048	Detension	Nodular, vermicular and flake graphite	11,84	70	Ferrite+ pearlite

4. CONCLUSIONS:

- The elaboration of cast irons for modification in electric arc furnaces is possible especially due to the fact that the process for elaboration can be led much easier, resulting in less quantities of sulphurus, the main restrictive element in the composition of chemical composition, as well as other hampering elements (P, O, H, N).
- the temperatures at the moment of evacuation from the furnace can be more easily framed within the limits indicated by the specialized readings in modification process
- Due to the less quantities of hampering elements within the composition, the quantities of pre-alloy unmodifying required to ensure the modification effect of the graphite are smaller.
- The duration of the modification effect is longer and the graphite nodulizing is more secure
- The proportion of nodular graphite is bigger than in the case of ductile irons obtained in other types of furnaces, and all the characteristics of the graphite (size, distribution) are better than the previously mentioned process
- The proposed technology can be applied for the elaboration of ductile irons in electric arc furnaces of any size.

REFERENCES

1. Cartis, I. — Tratamente termice, Editura Facla, Cluj, 1982
2. Sofroni, L. — Elaborarea si turnarea aliajelor, Editura didactica si pedagogica, Bucuresti, 1975
3. Sofroni, L., Stefanescu, D.M., Vincentz, G. — Fonta cu grafit nodular, Editura tehnica Bucuresti, 1978

POSSIBILITIES OF IMPROVEMENT OF RESISTANCE CHARACTERISTICS OF STEELS THROUGH COLD PLASTIC DEFORMATION

PETRE Doina Elena

Engineering Faculty of Hunedoara

Abstract

The application of a pressing along the generatrix for some steel laminates for general use, with diameters between 6-16 mm, leads to ensuring an important improvement of resistance characteristics, especially the flow limit.

Key words
concrete iron, pressing, generatrix, flow limit

1. FOREWORD

The following paper shows the results obtained through the application of the mentioned procedure as well as the optimum domain of chemical composition and deformation degrees, in order to get an optimum correlation between the resistance and plastic characteristics of steels.

Steels which are the main objective of the presented study, are part of the following categories:

- round wire of laminated steel (STAS 563-89)
- concrete steel laminated in heat (STAS 438/1-80)

With chemical composition of the following types:

- steels for general use for construction (STAS 500/2-80 less type OL70)
- quality carbon steels for heat treatments aimed at machines manufacture (STAS 880-88)
- concrete laminated steel at heat type OB37 with periodical or smooth / fine profile (STAS 438/1-80)

2. EXPERIMENTS

Out of all groups of mentioned steels, the following research was undertaken on steel for general use and concrete iron as well as steels similar to the mentioned ones.

The utilization characteristics of these steels, and especially flow limit (apparent Re_H or technical $Rp_{0,2}$) and tenacity, are influenced by a complex of factors including the chemical composition and deoxidation practices used for elaboration, the regime of temperatures and the deformation degree in lamination, the width of the products.

Regarding the mechanical characteristics of the presented products in the above table, the following mentions must be made:

a. the contain of carbon through influencing the pearlite/ferrite proportion and the contain of manganese through the alloying effect of ferrite, are the main controlling factors to reach the guaranteed resistance characteristics. The structure modifications that ensure the improvement of resistance characteristics have adverse effect on plastic characteristics
b. the majority of products of generals use steel are delivered in hot deformation status. Once the width of the product increases – as an effect of temperature increase at the end of lamination and decrease of cooling speed, at the same chemical composition, the wider products have less resistance characteristics than thiner products.

I chose the concrete irons as a first application of the studied procedure because:

- they are the steels with a contain of carbon within the limits of the theoretical interval;
- on of the compulsory characteristics at the reception of these steels isfloe limit, on which the pressing by generatrix has an absolute influence;
- they are not very pretentious form a dimensional point of view;
- can substantially increase sales value if delivered with higher resistance characteristics;
- the require restrictions for chemical composition, more precisely the limitation of contains of alloying elements (calculus relations for CE), and thus the value of resistance characteristics cannot be influenced through alloying.

For the research regarding the influence of plastic deformation at cold through the application of force on generators over the resistance characteristics of carbon not-alloyed steels, we used wire samples 6 mm diameter, with lengths between 500 and 1500mm. the wire was taken for the heart of wire order to avoid the results be influenced by the way of cooling of wire (eventually not uniform) and in order to ensure very similar conditions at trials.

The samples taken on plastic deformation at cold and determination of characteristics, were used as such, without any preliminary pre-work, in order to reproduce very accurately and application of this process directly on industrial products.

After the cold deformation on generatrix, some samples were taken out from each charge in order to determine the mechanical characteristics. The samples were debited to 150mm, according to the prescriptions.

The steel charge that were used for quasi-industrial trials have carbon contains between the limits 0,07-0,22%. The chemical composition of the studies charges is shown in table 3.

Table 3 *Chemical compositions of experimental charges*

Charge	Chemical composition, %								
	C	Mn	Si	S	P	Cr	Ni	Cu	Al
1.A	0,07	0,32	0,01	0,030	0,016	0,06	0,07	0,07	-
2.A	0,11	0,50	0,01	0,045	0,020	0,08	0,06	0,12	-
3.A	0,09	0,53	0,01	0,028	0,016	0,06	0,09	0,12	-
4.A	0,07	0,34	0,01	0,030	0,018	0,10	0,10	0,15	-
5.A	0,14	0,53	0,22	0,030	0,017	0,06	0,06	0,09	0,007
6.A	0,09	0,37	0,22	0,043	0,015	0,08	0,06	0,09	0,006
7.A	0,08	0,46	0,01	0,040	0,016	0,07	0,10	0,10	-

Six samples were taken out of eachcharge, out of which one is the etalon sample (E) and the others (1,2,3,4,5) were exposed to cold deformation on generatrix with different deformation degrees.

The deformation degree was determined using the following relation:

$$\varepsilon = \frac{d_0 \quad d}{d_0} \quad 100 \qquad (1)$$

in which e represents the degree of deformation, %

Do – the initial diameter of the sample, mm

D – the final diameter of the sample, mm

Each sample was marked with 2 signs at a distance of 100mm of each other, each signed being done at 25 mm from the end of the sample

The samples were exposed to trials of traction till break. The trials were done on an universal trial machine of traction, with a force interval between 0-2500 daN.

The study undertaken before, using a deformation through pressing on generatrix for steel products with diameters between 6 and 8 mm, showed the fact that it is possible to obtain a significant growth of resistance characteristics and especially flow limit (proportion $Rp_{0,2}/R_m$=0,70-0,98) when relatively small degrees of deformation are applied (table 2).

Table 2. *Mechanical characteristics of deforming samples*

Nr. crt.	Sample	ε,%	Mechanical characteristics				Increase $R_{p0,2}$,%	Increase R_m,%	$R_m/R_{p0,2}$	$R_{p0,2}/R_m$
			Z, %	A, %	$R_{p0,2}$, N/mm^2	R_m, N/mm^2				
1.A	E.1A	-	74,68	23,3	265	353	-	-	1,33	0,75
	1.1 A	4,92	68,68	20,5	310	385	16,98	8,96	1,24	0,80
	2.1 A	18,03	60,89	14,4	440	455	66,03	25,76	1,03	0,96
	3.1 A	26,23	64,69	15,8	482	493	81,88	39,20	1,02	0,97
	4.1 A	29,51	65,60	14,8	507	520	91,32	46,76	1,02	0,98
	5.1 A	34,43	56,54	10,7	528	537	99,24	51,52	1,01	0,99

The aim was to experiment the same procedure on industrial products with bigger diameters.

In order to do this, samples were taken from steels out of the current production, from steel charges with different chemical compositions and different dimensions of the laminated products.

The samples had lengths between 500-1500 mm. the samples used for trials were collected so that the results of the application of deformation not to be influenced by the cooling way and in order to ensure initial conditions as similar as possible.

The samples exposed to plastic cold deformations and determinations of characteristics were used as such, without any preliminary influence, in order to obtain a very accurate reproduction of this procedure directly on industrial products.

After cold deformation on generatrix, from each charge, some samples were taken in order to determine the mechanical characteristics. Samples were debited at 150mm , according to the prescriptions.

The steel charges that were used for the second set of trials have carbon contains between the limits 0.07-0.22%.

After an analysis of the presented data, it comes out that like in the case of wider industrial products, the effect of plastic deformation by pressing on generatrix shows especially on flow limit, that registers the higher growth rates till deformation degrees of aprox. 30%, after which the growth rate of, flow limit decreases.

The conclusions that can be drowned from the analysis of the presented data, are:

- the plastic deformation process at cold by pressing on generatrix applied to industrial products of wire with medium diameter between 6-8 mm and laminated products with width between 12-25 mm, made of steels with less carbon contain, are applied without any difficulty, steels presenting a weak resistance to deformation
- the influence on resistance characteristics is very strong starting even from low deformation degrees (aprox. 12%)
- the growth rate of resistance characteristics is high , till deformation degree of cca. 30%, after which the continuing application of deformation on generators does not lead anymore to high growth of resistance.
- the biggest influence is on floe limit, that registers substantial increases, reaching values similar to those of resistance to breaking for the same type of steels.
- the proportion $Rp_{0,2}/R_m$ increases very much, which constitutes a criteria for determination of steel quality for concrete, which reaches values of cca. 0.99.

In order to set up the technological conditions of the plastic deformation by pressing on generatrix, the data obtained from the experiment in the lab and industrial trials was studied. The analysis of data was based on statistical-mathematical methods, using specific calculus programs.

In order to obtain the correlation between the technological factors that influence the plastic deformation, more precisely the chemical composition of steel and the deformation degree applied, the MATLAB program was used.

We considered 48 sets of data that include the chemical composition of steel, the value of the proportion C/Mn, the value of the reduction degree, applied, as well as determined values flow limit, resistance to breaking, and the calculated value for the proportion $Rp_{0,2}/R_m$.

For each correlation the medium values of the parameters, the correlation coefficient, standard exception from the regression area, and the values of the stationary point (minimum, maximum or medium) are presented.

In the following lines, based on the analyzed data, the variation areas obtained and the diagrams of level curves, one can set the technological conditions, respectively the chemical composition and deformation degree which leads to the best correlation with the mechanical characteristics of resistance of the deformed products.

During the experiments it was observed that the substantial influence of the deformation by pression on generatrix process is on flow limit, that registers very high growth at relatively low deformation degrees. Therefore, in the following lines we present the variation areas of flow limit $Rp_{0,2}$, as well as the variations of the proportion $Rp_{0,2}/R_m$, function of independent parameters mentioned before.

The analyzed data are;

- independent parameter Rp0,2
- independent parameters C, C/Mn, Є.

The variation limits of the variables are:

$C_{min} = 0{,}07\% - C_{max} = 0{,}22\ \%$; $(C/Mn)_{min} = 0{,}17 - (C/Mn)_{max} = 0{,}35$;

$\varepsilon_{min} = 0 - \varepsilon_{max} = 38\%$; $R_{p0,2min} = 255 - R_{p0,2max} = 623$

The equation of the hiper-surface of regression is:

$$R_{p0,2} = 5064 * C^2 - 5295 * (C/Mn)^2 - 0{,}1725 * \varepsilon^2 - 5595 * C * C/Mn \\ - 1{,}945 * C/Mn * \varepsilon + 5{,}866 * \varepsilon * C + 3274 * C + 3606 * C/Mn + 13{,}75 * \varepsilon \quad (2)$$

To correlation coefficient for this hypersurface is r=0,98, standard exemption from the regression surface is s=21,13, and the coordinated of the maximum point are; C = 0,2319; C/Mn = 0,2103; ε = 42,62; $R_{p0,2}$ = 649,5.

Due to the fact that these hypersurfaces cannot be represented in a tridimensional space, I chose the successive replacement of an independent variable with its medium value, getting to surfaces that can be represented in the tridimensional space and can be interpreted from the technological point of view.

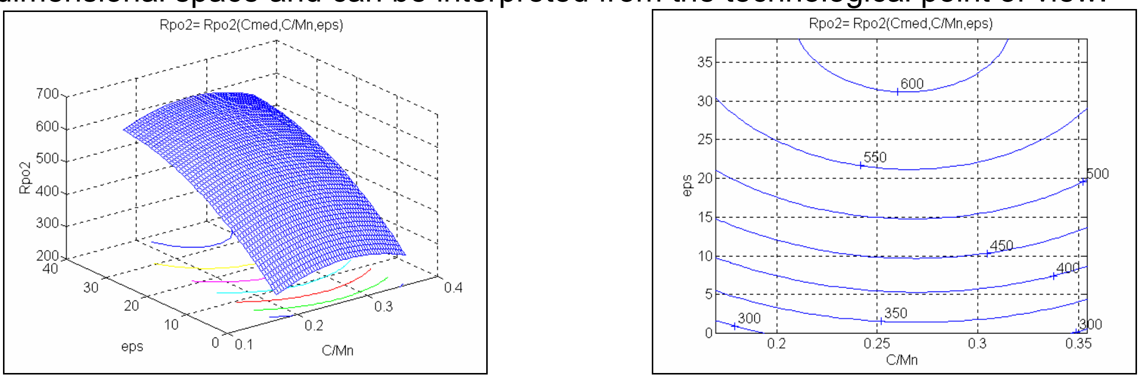

Figure 1. *The $R_{p0,2} = R_{p0,2}(C_{med}, C/Mn, \varepsilon)$ distribution and level curves*

Therefore, we obtain the surfaces that are the object of the following study. Associated to the surfaces we have the level curves for each value of the presented characteristics. Based on these analyses, one can set the maximum level of deformation by pressing on generatrix, that can ensure simultaneously with the increase of resistance of steels and a convenient behavior while processed.

The influence of chemical composition and degree of deformation over the flow limit is highlighted through the regression surface represented by the equation:

$$R_{p0,2} = - 5295 * (C/Mn)^2 – 0,1725 * \varepsilon^2 – 1,945 * C/Mn * \varepsilon + 2858 * C/Mn + 14,54 * \varepsilon - 55,1 \quad (\text{for } C = C_{med}) \qquad (2)$$

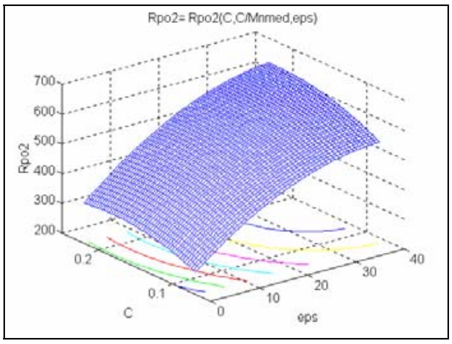

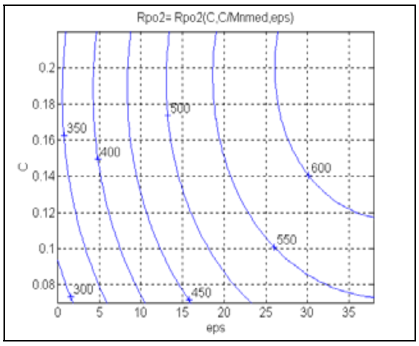

Figure 2. *The $R_{p0,2} = R_{p0,2}(C, C/Mn_{med}, \varepsilon)$ distribution and level curves*

The dependency between the value of flow limit, value C/Mn and the degree of reduction if a constant carbon contain and equal with the medium level on charge is considered, presented by figures 1.a and 1.b is the normal one, technological, in the sense that its value increases continuously with the increase of C/Mn and E, on one hand due to the hardness effect of the two elements and on the other, due to hardness induced by the increasing reduction degrees.

CONCLUSIONS

The undertaken analysis through mathematical methods of the obtained data, under the conditions of a plastic deformation at cold on generators, with deformation by pressing on generatrix degrees varying between 2- 40%, highlights the fact that in order to obtain increase of resistance, which would not affect the behavior during processing of steels, one must consider a series of measures such as:

- the carbon contain must be kept under 0,25%, and Mn contain must be kept at the technological limit necessary for carbon not-alloyed steels, respectively under 0,8%.
- the proportion C/Mn must be kept within the interval 0,2-0.3, so that the value of the flow limit and the proportion $Rp_{0,2}/R_m$ can be maintained within the technologically admitted limits.
- the data shown before highlight the fact that the described process cam be applied without any problems directly on industrial products, without a preliminary preparation, getting to important increases of the resistance characteristics.

REFERENCES

1. Petre Doina Elena — Metode de crestere a capacitatii de rezistenta a laminatelor din otel prin modificari microstructurale - Teza de doctorat, Timisoara 2002
2. Dieter, E.G. — Metalurgie mecanica, Editura tehnica, Bucuresti, 1970
3. Cazimirovici, E. — Teoria deformarii plastice, Editura didactica si pedagogica, Bucuresti 1977

THE SOLVING OF A NON-LINEAR PROBLEM OF THERMAL TRANSFER BY A PARTICULAR ANALYTICAL METHOD

Sorin RAŢIU, Imre KISS, Diana BALAN

University of Timisoara, Faculty of Engineering – Hunedoara

ABSTRACT

This paper deals with the distribution of temperature in an ingot heated inside a pit furnace. In order to determine the non-stationary thermal field we resorted to a linear discreeting of the thermo-physical parameters along time intervals. For each interval we considered a polynomial interpretation of temperature, imposing besides the connection conditions we also considered the checking of the Galerkin integral.

The analytical results we obtained were compared to the experimental measurements given in the reference literature, which lead to satisfactory approximations.

KEYWORDS:

ingot, non-stationary thermal field, pit furnace

1. INTRODUCTION

The cracking of alloy steel ingots during heating up, is caused by the thermal stress, whose value reaches the temperature limit before the core temperature exceeds the elasticity limit (500 – 550 ^{o}C). The choice of the proper hot working technology for these steel grades is first dependant on the heating conditions, decided upon according to their technological characteristics. The choice of the optimal heating pattern is most often done according to practical experience.

This paper is meant to introduce an analytical method enabling a most accurate estimation of the temperature field decided upon for the heating up of these ingots, thereby allowing considerations on the magnitude and distribution of thermal stress resulting from the heating process.

The method we suggest is a direct one and represents a powerful instrument for the study of linear and non-linear problems in mechanics and physics. As a result of this direct method we obtained an approximate analytical solution to the equation under consideration. In many cases, practical engineering considers such an analytical solution, even if approximate, preferable to the "exact", numeric one. Finding a solution to the equation of thermal conduction is usually associated to major difficulties, particularly because of its non-linearity (material properties that are dependent on temperature) and also because of the limit conditions related to the radiation phenomenon. In this study we focused on the non-linear problems caused by the temperature variation of the material properties.

The method we have introduced consists in sequentially turning thermal coefficients linear, in order to simplify the main equation. As a result of this approach, instead of having one non-linear differential equation with partial derivatives, we have an equivalent set of linear differential equations. In the case under consideration, this method gives satisfactory results for a wide range of temperatures

The authors consider that the problems related to the radiation conditions still persist (and they will be a topic of high interest for many researches) but, by this approach at least, and for certain temperature ranges, the results are acceptable.

The temperature values obtained by means of the method we introduced will be compared to the magnitudes obtained experimentally in Romania by Prof. Ilca Ioan Dr. es Sc. [1].

2. THE MATHEMATICAL MODEL

In order to derive the mathematical method appropriate to the ingot-heating phenomenon we have to take a few hypotheses into consideration. From the physical point of view, we are dealing with a rigid, isotropic body (the ingot), inside which a non-stationary phenomenon of thermal conduction takes place. From the geometrical standpoint, the ingot can be assimilated to a parallelepiped with a square basis and an infinite height.

Because of the cross-sectional symmetry and of the relative position of the ingot inside the pit-furnace (see fig. 1), the behavior of the system under consideration can be described by means of a parabolic differential equation simulating a mono-directional conduction phenomenon, and also with the help of an initial limit (frontier) condition given below [2]:

$$\rho(T)\cdot c_p(T)\cdot\frac{\partial T}{\partial t}(y,t)=\frac{\partial}{\partial y}\left[\lambda(T)\cdot\frac{\partial T}{\partial y}(y,t)\right] \tag{1}$$

$$T(y,0)=T_0 \tag{2}$$

$$\lambda(T)\cdot\frac{\partial T}{\partial y}(0,t)=\varepsilon\cdot\sigma_0\cdot\left[T_f^4(t)-T^4(0,t)\right]+\alpha\cdot\left[T_f(t)-T(0,t)\right]=q_1(t) \tag{3}$$

$$\lambda(T)\cdot\frac{\partial T}{\partial y}(L,t)=\varepsilon\cdot\sigma_0\cdot\left[T_f^4(t)-T^4(L,t)\right]+\alpha\cdot\left[T_f(t)-T(L,t)\right]=q_2(t) \tag{4}$$

where: $T = T(y,t)$ is the temperature distribution in the ingot cross section, dependant on width y and time t. The ingot lateral is marked L; ρ is the specific mass, c_p is the specific heat, and λ represents the thermal conductivity of the steel under consideration, all of them depending on temperature. Moreover, ε is the emission factor of the ingot surface and $\sigma_0 = 5{,}67\cdot 10^{-8}$ W/(m$^2\cdot$K^4) is the radiation constant of the perfectly black body, or the Stefan - Boltzmann constant. The initial temperature of the ingot is T_0=293K, and the temperature inside the pit furnace is marked $T_f(t)$. Finally, α [W/(m$^2\cdot$K)] represents the mean coefficient of convection heat transfer at the surface of the ingot.

We looked for a solution to equation (1), of the form:

$$T(y,t)=a_1(t)+b(t)\cdot y+c(t)\cdot y^2 \tag{5}$$

Coefficients b(t) and c(t) are to be determined by setting such conditions so as solution (5) observe equations (3) and (4):

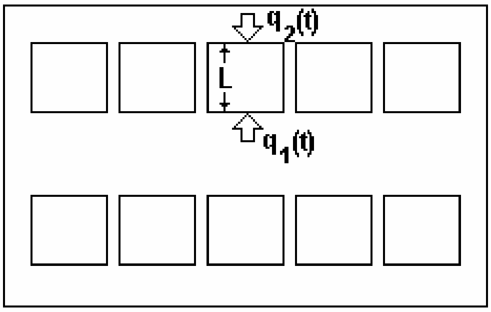

***Fig.1**. Ingot positioning inside the pit furnace*

$$b(t) = \frac{q_1(t)}{\lambda(T)} \tag{6}$$

$$c(t) = \frac{q_2(t) - q_1(t)}{2 \cdot L \cdot \lambda(T)} \tag{7}$$

From (5), (6) and (7) it results

$$T(y,t) = a_1(t) + \frac{q_1(t)}{\lambda(T)} \cdot y + \frac{q_2(t) - q_1(t)}{2 \cdot L \cdot \lambda(T)} \cdot y^2 \tag{8}$$

In order to facilitate the solving of the problem, we resorted to a simplifying hypothesis, which consists in considering the thermo-physical parameters as constant along certain time intervals whose span and number shall be chosen later in a convenient way. So, if we suppose λ = ct., c_p = ct., and ρ = ct. along the intervals, we have:

$$T(y,t) = \frac{1}{\lambda} \cdot \left[\lambda \cdot a_1(t) + q_1(t) \cdot y + \frac{q_2(t) - q_1(t)}{2 \cdot L} \cdot y^2 \right] \tag{9}$$

We note: $\lambda \cdot a_1(t) = a(t)$ and by deriving the expression (9) with respect to time we obtain:

$$\frac{\partial T}{\partial t}(y,t) = \frac{1}{\lambda} \cdot \left[a'(t) + q'_1(t) \cdot y + \frac{q'_2(t) - q'_1(t)}{2 \cdot L} \cdot y^2 \right] \tag{10}$$

We then derive the same expression (9) with respect to y and we have:

$$\lambda \cdot \frac{\partial T}{\partial y}(y,t) = q_1(t) + \frac{q_2(t) - q_1(t)}{L} \cdot y \tag{11}$$

$$\frac{\partial}{\partial y}\left[\lambda \cdot \frac{\partial T}{\partial y}(y,t) \right] = \frac{q_2(t) - q_1(t)}{L} \tag{12}$$

In order to find the expression of a(t) we impose the checking condition for Galerkin integral:

$$\int_0^L \left\{ \rho(T) \cdot c_p(T) \cdot \frac{\partial T}{\partial t}(y,t) - \frac{\partial}{\partial y}\left[\lambda(T) \cdot \frac{\partial T}{\partial y}(y,t) \right] \right\} \delta T dy = 0 \tag{13}$$

But as λ, c_p and ρ are constant along the time intervals, considering (10) and (12) Galerkin integral becomes:

$$\delta T \cdot \int_0^L \left\{ \frac{\rho \cdot c_p}{\lambda} \cdot \left[a'(t) + q'_1(t) \cdot y + \frac{q'_2(t) - q'_1(t)}{2 \cdot L} \cdot y^2 \right] - \frac{q_2(t) - q_1(t)}{L} \right\} dy = 0 \tag{14}$$

In order that expression (14) be true irrespective of the values taken by δT the Galerkin integral has to be null, which means:

$$\frac{\rho \cdot c_p}{\lambda} \cdot \left[a'(t) \cdot L + q'_1(t) \cdot \frac{L^2}{2} + \frac{q'_2(t) - q'_1(t)}{2 \cdot L} \cdot \frac{L^3}{3} \right] - \frac{q_2(t) - q_1(t)}{L} \cdot L = 0 \tag{15}$$

and

$$a'(t) = \frac{\lambda \cdot [q_2(t) - q_1(t)]}{\rho \cdot c_p \cdot L} - q'_1(t) \cdot \frac{L}{2} - \frac{q'_2(t) - q'_1(t)}{6} \cdot L \tag{16}$$

The integral of relation (16) with respect to time is:

$$a(t) = \frac{\lambda}{\rho \cdot c_p \cdot L} \cdot \int [q_2(t) - q_1(t)] dt - \frac{L}{2} \cdot q_1(t) - \frac{L}{6} \cdot [q_2(t) - q_1(t)] + C \tag{17}$$

In order to determine the heat fluxes $q_1(t)$ and $q_2(t)$ we considered a variation of the temperature in the main pit furnace with respect to time, $T_f(t)$, as given in figure 2, and the variations T(0,t) respectively T(L,t) were considered linear variations.

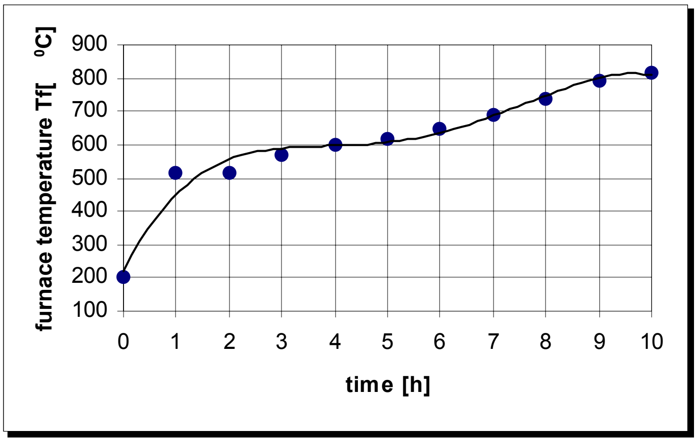

Fig.2. *The time variation of temperature inside the pit furnace*

If we mark:

$$\int q_1(t) dt = g_1(t)\,; \quad \int q_2(t) dt = g_2(t) \tag{18}$$

and we introduce (17) in (9) we obtain the final expression for the approximate temperature distribution in the ingot cross section (for a certain time interval):

$$T(y,t) = \frac{q_2(t) - q_1(t)}{\lambda} \cdot \left(\frac{y^2}{2 \cdot L} - \frac{L}{6} \right) + \frac{g_2(t) - g_1(t)}{\rho \cdot c_p \cdot L} + \frac{q_1(t)}{\lambda} \cdot \left(y - \frac{L}{2} \right) + \frac{C}{\lambda} \tag{19}$$

As we have already mentioned, in order that hypothesis: λ = ct., c_p = ct., and ρ = ct. (along intervals) be as plausible as possible, we have to consider the time interval divided into several shorter intervals. These intervals have been chosen so as the modifications of the thermo-physical property values along each should be insignificant. As a result of such hypotheses, the integration constant of (19) shall be modified for each interval. Anyway, it is obvious that the temperature (of a point on the ingot cross-section) at the end of one time interval is identical to the temperature at the beginning of the next time interval:

$$T_{n+1}(y, n\Delta t) = T_n(y, n\Delta t) \tag{20}$$

where n = 0,1,2… represents the number of the time interval, and Δt is the width of this time interval. Combining (19) and (20) we obtain the formula for the determination of the temperature function along the interval under consideration (n+1):

$$T_{n+1}(y,t) = T_n(y,n\Delta t) + \frac{1}{\lambda_{n+1}}\left[q_2(t) - q_2(n\Delta t) + q_1(n\Delta t) - q_1(t)\right]\left(\frac{y^2}{2L} - \frac{L}{6}\right) +$$
$$+ \frac{1}{\rho_{n+1}\cdot c_{p_{n+1}}\cdot L}\left[g_2(t) - g_2(n\Delta t) + g_1(n\Delta t) - g_1(t)\right] + \frac{1}{\lambda_{n+1}}\left[q_1(t) - q_1(n\Delta t)\right]\left(y - \frac{L}{2}\right) \quad (21)$$

The total heating time is 10 hours. This interval has been divided into 10 equal parts, so that Δt = 1 hour. The real variations of thermal conductivity λ and specific heat c_p are given in figures 3 respectively 4. The value of the specific mass is considered to be constant along the entire heating span and equal to ρ=7800Kg/m^3.

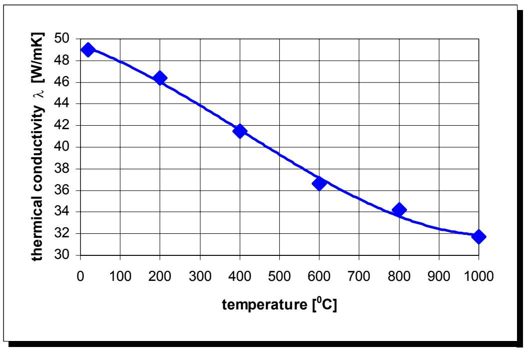

Fig.3. The real variation of thermal conductivity with respect to temperature

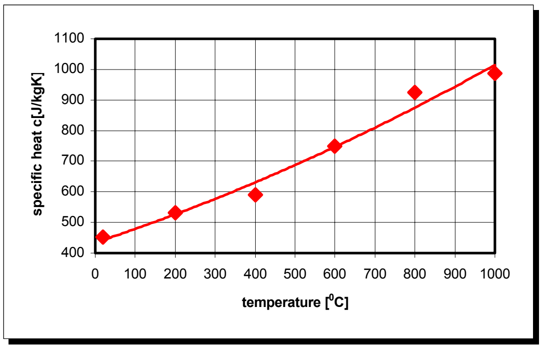

Fig.4. The real variation of specific heat with respect to temperature

3. RESULTS

We hereinafter give the values we obtained by means of the method for the temperatures of points on the ingot surface (y = 0) and inside it (y = L/2). These values are compared to the temperature obtained by experimental measurements, at industrial scale.

4. CONCLUSIONS

The analytically determined temperature values on the ingot surface overlap with the experimental ones by an error that differs according to the time interval of the heating up. This can be noticed in figure 5.

The reason these differences appear is determined by the way in which the heat transfer conditions have been determined, i.e. by convection and radiation, between the burned gases and the surface of the ingot. The choice of a global heat exchange coefficient α, with a constant average value all along the heating time of the ingot surface, makes the model under consideration be closer to reality for the temperature range corresponding to a mean value of α, i.e. in the medial zone of the total heating interval (400 – 600 ^{0}C), as can be noticed in figure 5.

The analytically obtained values of temperatures in the ingot core differ relatively much from the experimental ones, particularly in the first part of the heating time. This can be noticed in figure 6.

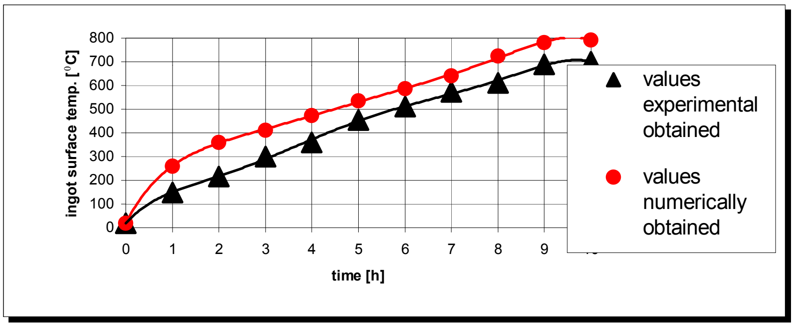

***Fig.5**. Temperatures of points belonging to the ingot cross-section for which y = 0 (outer surface)*

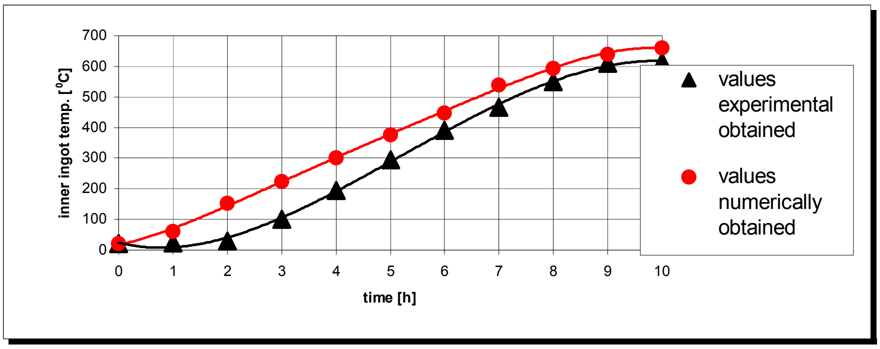

***Fig.6.** Temperatures of points belonging to the ingot cross-section for which y = L/2 (ingot core)*

The explanation of these errors resides in the fact that on establishing the thermo-physical properties of the material, the temperature variables (thermal conductivity λ and specific heat c), we could only use some of their values, corresponding to the last heating time intervals. In order to cover the temperature interval corresponding to the entire heating time, we extrapolated the existent values and drew approximate variation curves for these magnitudes (see figures 3. and 4.). It is obvious that the precision of these curves is less than acceptable particularly in the area of low temperatures, and this is why the values calculated for temperatures in the core area of the ingot are subject to errors.

The explanation given above is based on the fact that inside the ingot, the heat transfer from hot areas to colder areas is done exclusively by thermal conduction, a phenomenon that is directly influenced by the thermo-physical properties of the material inside which they take place.

Finally, the errors can also be blamed, of course, on the way of constructing the mathematical model that describes the phenomenon, as well as on the method of solving it.

We can therefore conclude that the analytical model under consideration is capable of furnishing its user relatively exact results with respect to the evolution of the temperature field inside a field of analysis, provided the initial data be closest to the practical ones, and that the limit conditions, initial or spatial, be least simplified, so that the numeric model emulate as minutely as possible the real phenomenon.

REFERENCES / BIBLIOGRAPHY

1. *I, Ilca,., ş.a. - Contribuţii la studiul încălzirii lingourilor în cuptoare industriale, Revista Metalurgia, nr.10, 1982, p.521;*
2. *Zoran D., Jeličić, ş.a. - Use of Galerkin's Method on Heat Transfer Problem For the Reheat Furnace, 5-th International Symposium of Interdisciplinary Regional Research, Szeged, 4-6 oct. 2001;*
3. *Minkowycz, W.J., ş.a. - Advances in Numerical Heat Transfer, Volume I, Taylor & Francis, 1996*

EDUCATIONAL SOFTWARE FOR PREZENTATION AND IMPLEMENTATION DATA STRUCTURES AS ORIENTED GRAPHS

Manuela PANOIU, Caius PĂNOIU

Technical University of Timişoara, Engineering Faculty of Hunedoara

Abstract

The informative society needs important changes in educational programs. The informational techniques needs a reconsideration of the learning process, of the programs, manuals structures, a reconsideration of the methods and organization forms of the didactic activities, taking into account the computer assisted instruction and self instruction. This paper presents a software package, which can be used as educational software. The oriented graphs, which have applicability in many fields, are presented. The paper presents a graphical interface written in Java, and also the classes, which modeled the data structure

Keywords

Educational software, informational techniques, oriented graphs.

1. INTRODUCTION

In the condition of informatics society whose principal source in the social–economic development is to produce and consumption the information, the complex and fast knowledge of the reality for rational, opportune, effective decisions is a desideratum which generate the necessity to form some superior level habituation in information manage for the whole population.

The use of the computers, which are machines which model and manipulate the information, and software programs in the initial and continuous forming is directly related with some habituation ask for young population and generally to the all people, for integration in the society and yours future profession.

The computers and their programs offer to the users powerful capabilities for the information manipulation:

- Image and text visualize on the screen which can be manipulate later;
- Memory storage of an important quantity of information, his accessing and selection of a part of them;
- Possibility to realize a great volume of computation;
- Possibility of equipment control and fast decisions;
- Computer based training.

This facilities offer to the microcomputers higher educational capabilities versus other technologies used in education and provide learning controlled based on many parameters: intellectual aptitude, level of knowledge, abilities, rhythm of work.

2. COMPUTER BASED TRAINING AS A DIDACTIC METHOD

The informatics society makes sensitive modification in education programs. In this scope, the school must prepare programmers, maintenance technicians, etc.

In the same time it is necessary that the teacher make ready to use the computer in education process.

These informational techniques impose to reorganize the contents of the education process, of the programs, course books and manuals, to reconsider the methods and organization forms of didactic activities, which follow to be center on individualization of the teaching process.

As a method of the informational didactic, the computer-based training is based on the programmed teaching.

B. F. Skinner was promulgating the linear programming idea: division of the content in small steps and his successive presentation, followed by the self-control.

N. Crowder work out a new programming type: the branch programming which is characterized by: division of the content in small steps, his successive presentation according to the student needs and corrective feedback, use of author language.

The programmed teaching consist in information presentation in small units, logic structured, units that compose a program, the teaching program.

The user will have possibility that after each sequence to have a knowledge about the measure of understanding the give information. The programmed teaching method organize the didactic action applying the cybernetic principles to the teaching-learning-evaluating activities level, considering like a complex and dynamic system, composed as an elements ensemble and inter-relations and develop his personal principles valid on the strategic level in any cybernetic organization form of teaching.

On the other hand, programmed teaching assume some principles which the teaching program must respect:

- The small steps principle consists in progressive penetration, from simple to complex, in a subject content which logic divided in simple units series lead to minimal knowledge, which later will form an ensemble. This principle regards the subject division in contents/information units that give to user the chance to succeed in his teaching activities;
- The principle of personal rhythm of study regard mannerism observance and capitalization of each user of the program which will be able to make the sequences of knowledge learning or control, in a personal rhythm appropriate to his psycho-intellectual development, without time limits. The user can progress in the program only if he accomplished the respective sequence requirement;

- The active participation principle, or active behavior, regard user effort trend into selection, understanding and applying the necessary information in elaboration of a correct answer. On each step the user is liable to an active participation to resolve the step job;

- The inverse connection principle, regard positive or negative inputs of user competence, refer to the success or breakdown in task performed;

- The immediate and directly control of the task work precision with the possibility to progression to the next sequence, in case of success;

- The success principle, which presume that the succeed percentage of experimental programs must be approximate 90%.

- The repetition principle, based to the fact that the programs are based on return to the users initial knowledge.

The combined programming interposes the linear and branch sequence according to teaching necessities.

After linear and branch programming the computer aided generative teaching has appear, where the exercises are gradually present, with different difficulty steps and answers on the students questions.

The expert system consists of self-teaching training programs, tutorial strategies, and the usage of natural language, mixed initiative and some complex representation of knowledge usage.

The simulation is a training computer programs onset characterized by the fact that the computer is like a lab witch contains typical interactive graphical programs.

The computer based programmed teaching realize learning process with a inputs flow – the command, an executive controlled system, an output flux – control and a control system functions which correct measure establish.

In such a system have tree stages of teacher perceive: teaching, evaluating and the feedback loop closing, the computer being present in all of tree stages.

3. THE COMPUTER BASED TEACHING ADVANTAGES

Based on W. Feuerzeig it is very possible that computer based teaching to produce students thinking modifications such as:

- Thinking disciplined increases, of mental precisions operation and their expression, of is precise need;

- Some general concepts early forming, such as: formal procedures, the variables, transform functions, hypothetic-deductive reasoning;

- Simplification of heuristic methods application in any kind problems solve, such as cause-effect analyze.

The intelligent tutorial programs being flexible and with capacity of each student word analyzes with explanations and motivates answer on questions, has human tutor nearly and therefore are in teaching individualization proposed.

Between computer-based training advantages it can be enumerate some phenomena animate simulation, states, etc respective problem situation possibility.

The compute based training assure:

- The instructive individualization process;
- Pass through teaching-evaluating sequences in user personal rhythm;
- Eliminate the delays in instructive process;
- Some "drudgery" teacher release, which in classic lesson was perforce to accomplish;
- Changing the relation between teacher and student, conducting to the modification wanted by the young student, to be treated not as a subject which only accept the information, but as an equal teacher partner in the own formation act.

4. PRACTICAL STUDY

From desire of improve the instructive educational process, using modern teaching methods, was realized an courseware on "Data structures" discipline, where the subject "oriented graphs" was especially developed.

The oriented graphs are data structures, which have a very large applicability, such as towns map, communications in a group of persons, electricity, etc.

This application presents the simulation part of oriented graphs. The simulation use the computer instruction program, which is characterized by the fact that computer is considered a laboratory which contain typical programs of interactive graphics. This action is a graphical representation of an oriented graph.

It can be realized the step by step interactive construction of a graph, visualization of the constructed graph, saving the constructed graph in a file or loading from a file the graph.

This application is realized in Java language. It was implemented the next classes of objects: "Node" class, "Branch" class, "Graph" class, "Draw" class and "Menu" class, which is main starting application class. From Java collection classes was used java.io, java.awt and javax.swing.

The most important facilities offered by this application are presented as follow. In figure 1 is present the creation and drawing of a new graph. It can be observe that in the bottom of the window the user have information referring to the way of constructing of a node, branch and the possibility to move a node.

After the end of graph construction, the user can act the "Terminare" button to can start another operations, or he can delete the constructed graphs to start another. This application offer also the possibility to save the constructed graphs, to continue the edit on an old graph or finish the work, as is presented in figure 2. Another possibility is to scan a deep or weight graph and show the kind of branches, as is presented in figure 3.

It can be see that the user can choose the start scan button, and using "Step" button can vizualize in step by step way which are the next nodes. On bottom of the window are presented all the operations and the draw on grafical window present in black colour the scaned graphs and in yellow colour the not scaned part.

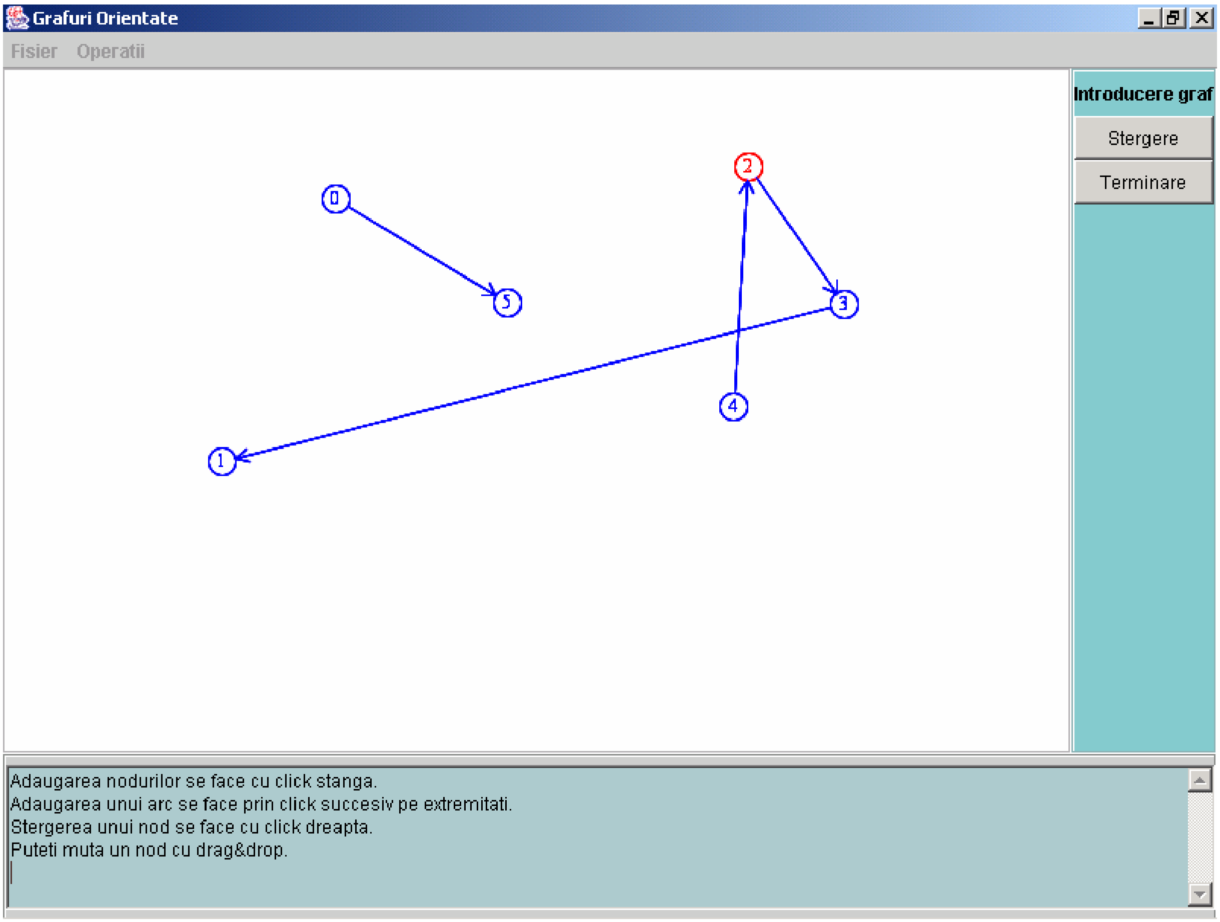

Fig. 1. *The construction of an oriented graph.*

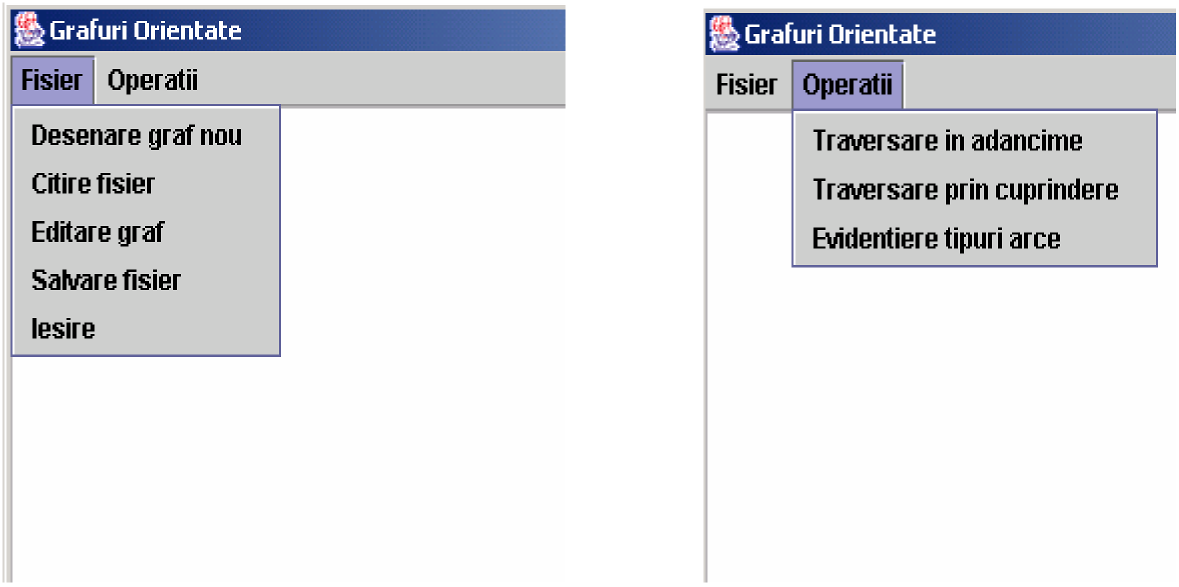

Fig. 2. *Offered facilities applications by user menu.*

5. CONCLUSIONS

On this application, authors take into consideration the condition which must accomplish a courseware, being make necessary steps. So, in eleboration and utilization of this application must take into consideration next criteria:

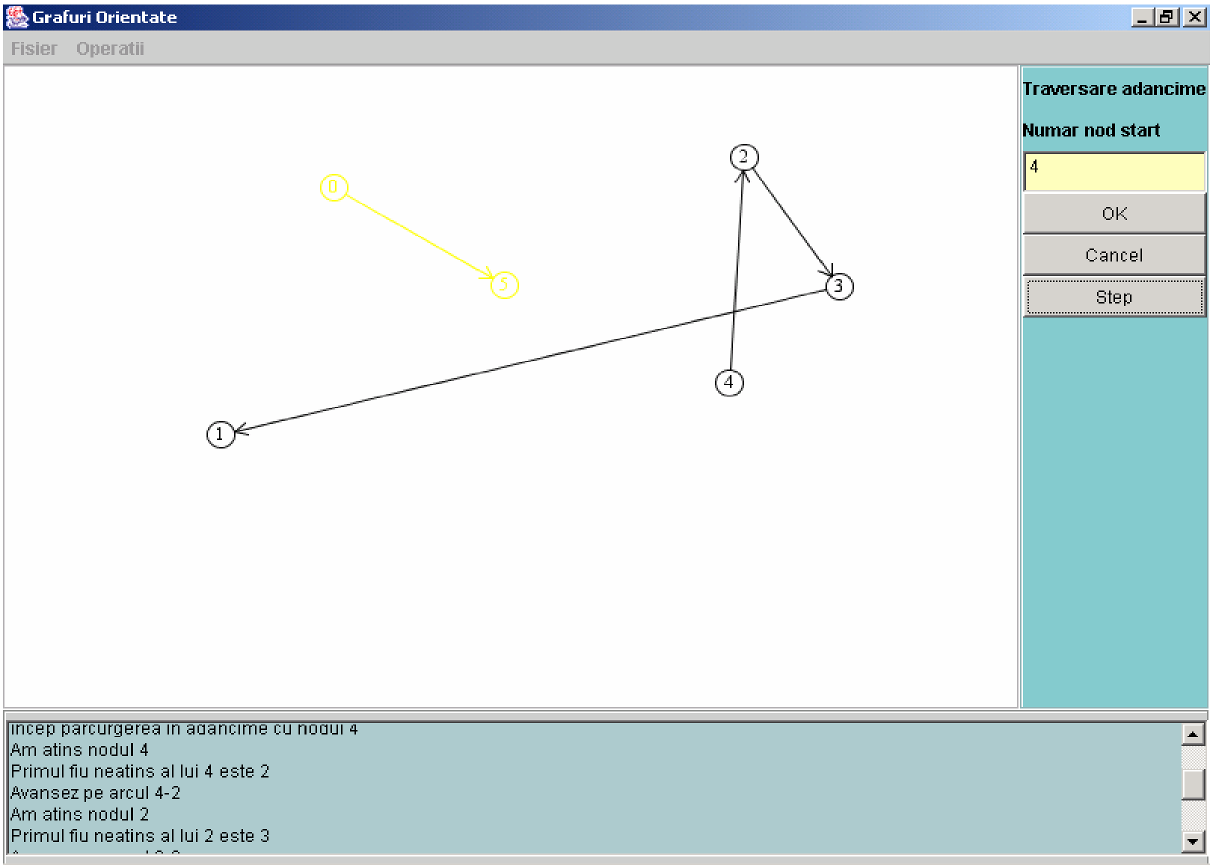

Fig. 3. *The deep oriented graph scan.*

- To follow up the curriculum for a specific domain;

- To accomplish some teaching and learning strategy. In this kind of selfinstruction and evaluation program it must find basic notions and reprezentation and scaning notions. Animation and grafical modelation must represent the graphical construction way and also scaning of them;

- To exist the possibility to use parametrized variable, in conditions in which users have the posibility to input the variables value;

- To prezent a method in which the user can be informed about how can use graphical module, i.e. a interaction user-computer exist.

The prezented application accomplish this criteria, and for this we consider that is a good example of how an educational software must be realized.

6. REFERENCES

[1]. Laura Lemay, Rogers Cadenhead, Java 2 fără professor în 21 zile, Editura Teora, Bucureşti 2001.
[2]. Mark C. Chan, Steven W. Griffith, Antony F. Iasi, Java 1001 secrete pentru programatori, Editura Teora, Bucureşti 2001.
[3]. Mitchell Waite, Robert Lafore, Structuri de date şi algoritmi în Java, Editura Teora, Bucureşti, 2001.
[4]. Eugen Rotariu, Limbajul Java - Publicații Web, Computer Press Agora SRL.

NOGOOD ELIMINATION IN THE ALGORITHMS DISTRIBUTED WITHIN THE DCSP MODELING (DISTRIBUTED CONSTRAINT SATISFACTION PROBLEM)

MUSCALAGIU Ionel, ABRUDEAN Cristian

The University „Politehnica” din Timisoara,
The Faculty of Engineering of Hunedoara, ROMANIA

ABSTRACT

One of the characteristics of the algorithms of asynchronous search is that of the appearance of the “nogood” values while searching for the solution. The number of the recordings of nogood messages determines the exponential complexity of the algorithm in the unfavorable case in the first place. As a consequence, we have the fact that the calculus time and the askings for the hardware resources grow much faster than the dimension of the problem. Doubtlessly in the practical applications, in which we use slow means communications such as Internet, the algorithms become inefficient because of the large number of the developed nogood values and their necessity for communications during the searching. In this article we will study the effect of their elimination or diminution. We will demonstrate that is a connection between the quantity of nogood values and the efficiency of the asynchronous searching algorithms.

Keywords
Artificial intelligence, distributed programming, constraints, agents.

1. INTRODUCTION

According to the IT literature the backtracking algorithm distributed in an asynchronous way- ABT, existing for the DCSP model, is considered the first complete algorithm for the asynchronous search. It is the first complete algorithm asynchronous, distributed and competitor, in which the agents the agents can roll up in a competitive and asynchronous way, published Yokoo and al. in [8]. This algorithm is based on sending nogood messages among agents for doing an intelligent backtracking and to assure the complexity of the algorithm. The nogood messages are lists of joined values at distinct variables in which there are inconsistent among some variables.

The appearance of the nogood values has as an effect the introduction of some new constraints. Although the nogood list indicates the cause of the failure and its incorporation as a new constraint will teach the agents not to repeat the same mistake, it is expected that during the course of the algorithm the nogood values to be as few as possible, because they have as an effect the increasing of the execution time (because of the fact that new messages are sent, etc.)

The number of the recordings of nogood messages determines the exponential complexity of the algorithm in the first place. As a consequence, in the practical applications, in which slow means of communications are used, such as Internet, the algorithm becomes totally inefficient because of the large number of the nogood values that must be communicated during the search.

As the nogoods are in fact a way of constraints dynamic generated while searching, which is some situations rise in an explosive way, we have to study the effect of their elimination or diminution.

In this context, during the last years a lot of studies were done and they ended in results based on the fact that this algorithm of reference can be modified in an algorithm with a polynomial space of searching. As a fact there are studies from [3], [4], [9], [6], which created some algorithms efficiently distributed. There is about the algorithms DIBT-Distributed Backtracking, AAS-Asynchronous Search with Aggregations, DisDB-Distributed Dynamic Backtracking. We will demonstrate further how these algorithms are in fact (in some sort) variants ABT with the reductions or elimination of nogood messages. At the other extreme there is AWCS- Asynchronous weak- Commitment Search [9], which records all the nogood values, algorithm which is however much more efficient than ABT because of the dynamical order. The idea of permitting the agents to be able to modify a wrong decision by a dynamical change of the agent priority order, proved beneficial in case of AWCS.

We will demonstrate that there is a connection between the quantity of nogood values and the efficiently of the asynchronous searching algorithms. For example, the asynchronous search with (AAS) units or the backtracking distributed (DIBT) is efficient algorithms because they eliminate a part of the nogood values.

2. THE FRAMEWORK

In order to do this analysis of the impact of the nogood values, in this paragraph we will present some notions known from the IT literature relative to the DCSP modeling and ABT algorithm.

Definition 1.-CSP model. The model based on constraints CSP-Constraint Satisfaction Problem, existing for centralized architectures, consists in:

-n variables X_1, X_2. X_n, whose values are taken from finite, discrete domains D_1, D_2, …., D_n, respectively .

-a set of constraints on their values.

The solution of a CSP suppose to find an association of values to all the variables so that all the constraints to be fulfilled.

Definition 1.-The DCSP model. A problem of satisfying the distributed constraints (DCSP) is a CSP, in which the variables and constraints are distributed among autonomous agents that communicate by transmitting, messages.

In this algorithm, each agent instantiates its variables in a competitive way and sends the value to the agents with which is directly connected, using direct communication channels which function according to the FIFO principle. It is also considered a global statically order among the agents, in which the A_i agent has a smaller priority than A_j, if i>j. In this way A_j can impose the first the favorite values.

Definition 2.- the assignment. It is called assignment for the variable X_i a pair (X_i,v), where v is a value from the X_i domain.

Definition 3. - the list agent_view. The list agent_view of an agent A_i is a set with the newest assignments received by the A_i agent for distinctive variables.

Definition 4.- the nogood list. The Nogood list is a set of assignments for distinctive variables for which looseness was found.

The ABT algorithm uses 3 types of messages:

- the OK message, which contains an assignment variable –value, is sent by an agent to the estimate in order to see if the value is good.
- the nogood message which contains a list (called nogood) with the assignments for the looseness, it is being sent in case in which the estimator agent found an unfulfilled constraint.
- the add- link message, sent to announce the necessity to create a new direct link, owing to a nogood appearance.

Each agent receives a lot of values from the agents it is being connected to through links, these values forming agent_view. If the OK?, message is received the estimator agent adds the variable the value in the list of values and checks if the new pair is consistent with the others. If an assignment that is not consistent is found, the agent tries to change this value so that to be consistent with the values from the agent_view list. It is possible that the agent not to find any good combination for some pairs in the list (such a set is nogood), than the values assigned for other agents can be changed. In this situation, it is said that the agent caused a backtrack, it having to send a nogood message to one of the agents.

3. THE REDUCTION OF *NOGOOD* IN AWCS CASE.

The AWCS algorithm is a hybrid algorithm obtained by the combination of ABT algorithm with WCS algorithm, which exists for CSP. It can be considered as being an improved ABT variant, but not necessarily by reducing the nogood values, but by changing the priority order. It deliberately follows to record all the nogood values (which are fewer) to ensure the completeness of the algorithm, but also the avoidance of some unstable situations.

The authors show in [9] that this new algorithm can be built by the dynamical change of the priority order. The AWCS algorithm uses, like ABT, the two types of *ok* and *nogood* messages, with the same significance. There is a major difference in the way you treat the ok message. In case of receiving the ok message, if the agent can't find a value to its variable that should be consistent with the values of the variables that have a greater priority, the agent not only creates and sends the nogood message, but also increases the priority in order to be maximum among the neighbors.

We have to emphasize that the AWCS algorithm also requires the recording of each nogood list to assure the completeness of the algorithm, giving the impression of an exponential space inefficient in the real environment. However the experiments show a bigger efficiency towards the ABT algorithm. According to the experimental results, the AWCS algorithm, especially for problems of a larger dimension, proved to be very efficient. More than that the algorithm could give an answer to certain instance in an acceptable period of time, matter that the basically ABT algorithm hadn't succeeded.

In conclusion, AWCS is efficient and complete because of the recording of all the nogoods (which are much fewer), but suffer after the explosion of the appearance of nogoods. So, the costs owed to the checking of the constraints can become expensive because an agent in AWCS can create nogoods for all its neighbours. A last idea, linked by the practice, is to limitate the number of nogood recordings at a fixed value, sacrificing the completeness, but getting fast results.

4. IN ELIMINATION OF NOGOOD IN CASE OF ASYNCHRONOUS SEARCH WITH AGGREGATIONS.

Silaghi suggests, in [6], two techniques the ensurance of a polynomial space in case of asynchronous search: the tagging of assignments and retransmission of the messages.

These two techniques are the beginning of the creation of three variants that reduce or eliminate completely the nogood values:

- **AAS-2:** is based on the complete recording of nogood list, similar to the Yokoo's asynchronous backtracking algorithm (ABT).
- **AAS-1:** proceeds similar to the dynamic backtracking variant in [1]. The nogoods that depend on the assignment of the modified variables, being obtained a space of polynomial complexity.
- **AAS-0**: it is a modified variant of AAS-1 with the fewest nogood recordings. AAS-0 is an algorithm, which ties the entire nogood list, kept by every agent of AAS1 in just one nogood using more of relaxation presented in [6].

The tagging of assignments is done by introducing a local counter, which is incremented by every agent every time when a new instance is chosen and the current value labels each generated assignment. This labeling assures an order of sending the messages. Silaghi presents in [7] an algorithm named ABT_p got through modifying the ABT algorithm by adding the previous labeling. This demonstrates much more direct the link between the elimination of nogood values and the polynomial space.

The retransmission of the messages is a second solution of nogood suggested by Silaghi for the elimination of nogood values from ABT. It consists in retransmitting the suggestions after every change of a view. The agents that have a smaller priority and received once again deduce a nogood for these values. Silaghi presents in [7] an algorithm named ABT_r obtained by modifying the ABT algorithm through adding the techniques of retransmitting the messages getting an algorithm with a polynomial space. This second technique requires transmitting much more messages, being much more expensive. It is applied in AAS-0 after the nogood values are eliminated.

The algorithms AAS0, AAS1, AAS2 were estimated using long snapshots of messages and constraints. The AAS2 algorithm supplies better results than the ABT algorithm. It is remarked the fact that, in case that there is no solution, the AAS2 algorithm supplies constantly better solutions than ABT and can reduce the long snapshots of messages and the number of nogoods on an average with 50 %.

As a conclusion, the use of the sets technique offers an improvement of the efficiency for searching for the solution, conversely proportional to the quantity of nogood recorded.

5. THE ELIMINATION OF NOGOOD IN DIBT CASE

Another algorithm of asynchronous search is DIBT published in [4] and [3. this is a variant of algorithm which does not requires for add-link messages eliminating almost entirely the recording of nogood values.

The variant of DIBT, has as a starting base the classical algorithm of backtracking, the centralized case. If the ABT uses schemes of learning, this algorithm eliminates the schemes of learning, such as the recording of the nogood.

The elimination of the nogood messages is done using few techniques of improving the backjumping based on the graph of constraints. In fact, this method is based most of it on relative techniques of backjumping. In the first place, the centralized variant of backjumping used the graph of constraints to determine the origin of the failure. The DIBT algorithm uses this idea also. The second idea is that of preserving the previous work through the fact that when getting a message, first it is checked if the current value satisfies the constraints with the transmitter agent, before trying another value form its domain. This idea reduces the effort of calculation because if there isn't any change, neither its children are announced. The third idea consists in using a so named repair technique. At the beginning the entire system initializes the variables simultaneously. While rolling the algorithm, the agents revise their values according to their environment. So, the system starts with global instances of the variables and then executes local reparation of different parts of the instance, but simultaneously.

The assessment of this method, comparatively with the ABT method was done solving aleator DCSP problems getting better results. It must be mentioned the fact that the elimination of add-link messages is favorable for problems that have the graph of constraints very dense, but has as an effect the engendering of some useless connections which the ok messages produces and throttle the network.

We also have to specify the fact that the first DIBT variant, published in [4], had some difficulties as far as the finding of the solution is concerned. To eliminate these difficulties and assure the completeness of the algorithm, in [3] the author extends the algorithm, adding in advance some ABT connections. Unfortunately, in [10], it is shown that this algorithm is incomplete (with all these extensions). As a conclusion, we notice the complete elimination of the additional ABT connections and of nogood values is not possible 100 %.

6. EXPERIMENTAL RESULTS

In the previous paragraph we saw diverse estimations of the algorithm distributed for search, comparatively with the ABT algorithm, results obtained from IT literature and from our own estimations. We will present our own experimental results for the estimation of the quantity of nogood recorded and used by the presented techniques. In order to make such estimation, we implemented these techniques in NetLogo 1.3, a distributed environment, done in Java, using a special language named NetLogo (see [10]).

These four techniques were used in order to make estimation to a classical problem (distributed variant) the problem of the n queens. The number of nogood values was countered. The obtained results are visualized in figure 1.

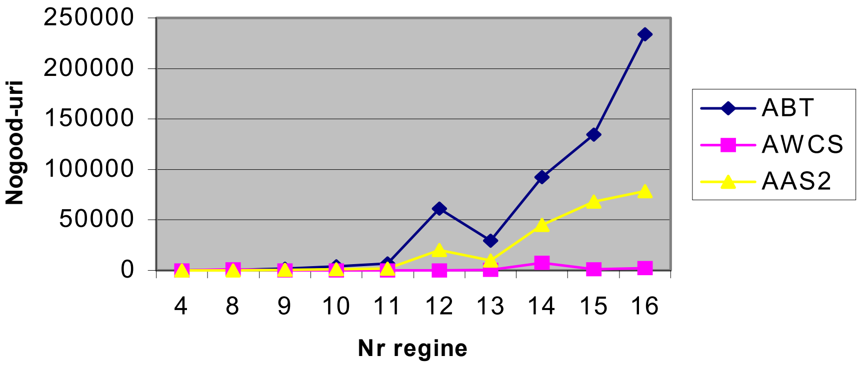

Figure 1. The Evaluation of the efficiency after the number of the nogood

Studying the effect of elimination or reducing the nogood, we notice that there is a connection between the quantity of nogood and efficiency of the asynchronous search algorithm.

The main feature of the ABT algorithm is the way in which the backtracking is processed (deadend) to assure the completeness while searching and that is the appearance of the nogood. It is the main problem of the ABT algorithm that leads to the exponential complexity of the algorithm.

The AWCS algorithm uses a dynamic order that can be changed while searching. However, to assure the completeness, the nogood can't be eliminated and so the algorithm has a space of exponential complexity, but very efficient.

The AAS algorithm constantly supplies better solution than ABT and can reduce the number of nogoods recorded on an average with 50 %. As a conclusion, the use of the aggregation technique offers an improvement of the efficiency for finding the solution, conversely proportional with the quantity of nogood stocked.

The DIBT algorithm tries to keep the distributed structure of the network as much as possible. It is built hierarchy of the agents using a method called Distributed Agents Ordering (DisAO), without adding other new connections neither before, nor during other the search). DIBT doesn't have to record the nogood. Unfortunately, the completeness is not guaranteed any more by adding some additional connections.

8. BIBLIOGRPHY

[1] Christian Bessière, Arnold Maestre, Pedro Meseguer. *Distributed Dynamic Backtracking*. In Proceedings of the CP Workshop on DCSP, Singapore, 2000.

[2] M. Ginsberg. *Dynamic backtracking.* Journal of A.I Research 1:25-46, 1993.

[3] Hamadi Y. – Traitement des problemes de satisfaction de constraintes distributes. PhD theisis, Universitatea Motpellier II, 1999.

[4] Hamadi Y., Bessiere C., Quinqueton J. *Backtracking in Distributed Constraint Networks*. In Proceedings of the 13^{th}, ECAI , Brighton, UK, 1998, pag. 219-223.

[6] Marius Călin Silaghi, D. Sam-Haroud, B. Faltings. *Asynchronous Search with Aggregations*. In Proceedings AAAI'00, pages 917-922, Austin, Texas, 2000.

[7] Marius Călin Silaghi . *Asynchronously Solving Distributed Problems With Privacy Requirements.* PhD theisis, Lausanne , EPFL 2002, Elvetia.

[8] Yokoo M., E.H. Durfee, T. Ishida, K. Kuwabara - *Distributed constraint satisfaction for formalizing distributed problem solving.* In ICDCS, 614{621). 1992.

[9] Yokoo M., E.H. Durfee, T. Ishida , K. Kuwabara - *The distributed constraint satisfaction problem : formalization and algorithms* . IEEE, 1998 .
[10] Yokoo Makoto . Private communication, 2000.
[11] http://ccl.northwestern.edu/netlogo/

ON THE COMPLETENESS OF THE ALGORITHMS DISTRIBUTED WITHIN THE DCSP MODELING (DISTRIBUTED CONSTRAINT SATISFACTION PROBLEM)

MUSCALAGIU Ionel, PĂNOIU Manuela, OSACI Mihaela

The University „Politehnica” din Timisoara,
The Faculty of Engineering of Hunedoara, ROMANIA

Abstract

One of the basic characteristics to be met by any acceptable algorithm is its completeness. The problem makes more sense within the DCSP distributed framework, where the agents act concurrently and asynchronously, each agent being in the position of making decisions that influence the decisions of the other agents. In this article we will analyze the completeness of some algorithms distributed asynchronously, to be found in the reference literature: the classic backtracking algorithm distributed asynchronously (Asynchronous Backtracking), its improved variant (Asynchronous Weak–Commitment Search) and Hamadi's distributed backtracking algorithm (Distributed Backtracking). We will point out to the fact that the first two are complete algorithms, unlike the third, for which the completeness has not been demonstrated yet.

Keywords

Artificial intelligence, distributed programming, constraints, agents.

1. INTRODUCTION

One of the basic characteristics to be met by any acceptable algorithm is its completeness. It consists in knowing whether the algorithm has an end, i.e. whether it does not lead to an infinite loop, without giving an answer. In other words, we are interested in finding out whether the algorithm, for a certain instance, can lead to an answer, either affirmative (i.e. to find a solution) or negative (pointing out that there is no solution).

This characteristic is very important for any algorithm. The problem makes sense particularly in the case of the distributed framework, as, for instance, in the situation of agent modeling, if one agent keeps on changing its values and never reaches a stable condition, the algorithm will enter a loop. Things become even more complex in the distributed context, where agents act concurrently and asynchronously, each agent being in the position of making decisions that influence the decisions of the other agents.

In this chapter we will analyze the completeness of the most important asynchronous distributed algorithms . We will introduce the way in which each DCSP technique ensures the completeness of the algorithm.

We are talking about Yokoo's classical asynchronously distributed backtracking algorithm (AB–Asynchronous Backtracking), (AWCS-Asynchronous Weak–Commitment Search) published in [6] and about Hamadi's distributed backtracking algorithm (DIBT - Distributed Backtracking) [2,3] . For the first two, the authors have demonstrated their completeness, whereas for the third one, there is no such demonstration.

2. THE FRAMEWORK.

In order to carry out the completeness analysis, we will introduce in this paragraph a few notions that are to be found in the reference literature in relation to DCSP modeling [5] .

Definition 1.- CSP model. The model based on constraints CSP-Constraint Satisfaction Problem, existent for centralized architectures, consists in:

- *n* variables $x_1, x_2, \dots, x_n$, which can take finite values, within several finite, discrete domains $D_1, D_2, \dots, D_n$.
- a set of constraints among these variables .

Solving a CSP supposes finding an association of values for all variables so that all constraints be met (realized).

Definition 2.- DCSP model. One problem of meeting the distributed constraints (DCSP) is a CSP, in which the variables and the constraints are distributed among autonomous agents that communicate by message exchange.

3. COMPLETENESS IN CASE OF ABT ALGORITHM

The first algorithm we are going to analyze from the point of view of its completeness is Yokoo's classical backtracking algorithm. In this algorithm, every agent instantiates its variable concurrently and sends its value to the agents it is directly connected to, further waiting for the messages to be answered. This behavior, in which each agent keeps changing the value, leads to the question whether the algorithm has an end, i.e. if it does not end up in a loop. For example, a looping instance is the one where x_1 obliges x_2 to change its value, the changing of x_2 causing the value of x_3, to change and x_3 determining the change of x_1. Such situations can arise in the case of applying an asynchronous algorithm.

In [5, 6], the authors suggest one way of eliminating the loops in a network of constraints, based on a technique using a unique identifier, technique used for avoiding dead ends in systems with distributed databases. This technique consists in using a relationship of complete order among the knots. If a knot has a unique identifier, one can define a priority order of the agents by using the alphabetical order of the respective identifiers (the alphabetically preceding agent having a higher priority). If a link is directed by means of this priority order (from the agent having a higher priority to the one having a lower priority), then no loop can appear in the network. This means that for each constraint, the lower priority agent will be the estimator and the higher priority agent will OK the message of the estimator.

The authors of the algorithm demonstrate in [5,6] that the algorithm is complete. They point out that if there is a solution, the algorithm leads to a stable solution where all the values of the variables meet all the constraints and all the agents are in wait of messages. Also, if there is no solution, they point out that the algorithm reveals this situation and closes.

4. THE COMPLETENESS OF THE AWCS ALGORITHM - ASYNCHRONOUS WEAK–COMMITMENT SEARCH

The next algorithm to be analyzed is the asynchronous search algorithm, in its improved variant. We have seen in the previous paragraph that the completeness problem was solved for the basic algorithm (the asynchronous algorithm), which this new algorithm is derived from.

The AWCS algorithm is a hybrid one, obtained by combining the ABT algorithm with the WCS one, existent for CSP, within centralized architectures. It can be considered as an improved variant of ABT, due to the priority change. It purposely aims at stocking all the nogood values in order to ensure the completeness of the algorithm, but also to avoid instable situations.

In [6] the authors show that this new algorithm can be built by a dynamic change of the priority order.

The AWCS algorithm uses, as ABT, the two types of messages, OK? and nogood, with the same signification. There is a major difference in dealing with the OK? message. In case of receiving it, if the agent cannot find a value for its variable to be consistent with the values of higher priority variables, it no longer generates and sends the nogood message, but increases the priority, in order to maximize it with respect to the neighbors.

By means of the rules mentioned above, when a backtracking arises, the priority order will be changed in such a way that the agent having higher priority before the backtracking should meet the constraints of the agent generating the backtracking and having now a higher priority value. Moreover, in the asynchronous backtracking algorithm, the agents are trying to avoid situations labeled as nogood. Yet, because of the delays that might arise on message transmittal, the view agent set of an agent can occasionally be a superset of the values previously found as nogood. In order to avoid the effects of unstable situations and of those where useless changes of priority value were operated, each agent keeps a record of the nogood situations reported. When the *agent view* list is identical to the *nogood* one, the agent will not change the priority value, but will wait for the next message.

As to the problem of its completeness, we have noticed that it was raised and solved for the basic algorithm (the asynchronous algorithm) out of which this one is derived. When can blocking situations arise? The priority of values is changed if and only if a non-solution is found. But the number of nogood value combinations is finite (even if large), the value priority cannot be changed at infinitum. Therefore, according to the authors of the algorithm, after a certain, surely finite, period of time, the priority of values is bound to be stable. In [6], the authors show that the situation mentioned above cannot arise in the situation in which value priority is stable.

We have to point out that the AWCS algorithm itself needs record keeping of each nogood list, in order to ensure the completeness of the algorithm, giving the impression of an inefficient exponential space in real media. Yet, the experiments show its greater efficiency, as compared to the ABT algorithm.

Therefore, AWCS is efficient and complete by record keeping of all nogoods (whose number is smaller), but suffers if there is an outburst in the appearance of nogood values. Thus, the costs of constraint checking can be rather high, as in AWCS, an agent can generate nogoods for all its neighbors. One last idea, related to practice, is to limit the number of nogood recordings to a fixed value, sacrificing the completeness, but leading to more rapid results.

5. COMPLETENESS IN THE CASE OF DISTRIBUTED BACKTRACKING.

Another algorithm for asynchronous search is the **Distributed Backtracking**, published in [2, 3]. This is a variant of algorithm that does not imply add-link-type messages and eliminates completely the record keeping of nogood values.

The variant of distributed backtracking (DIBT- Distributed Backtracking) is based on the classical backtracking algorithm, the centralized case. If the ABT asynchronous algorithm uses learning schemata, this one eliminates them.

This is a synchronous algorithm, but it needs a certain order for the agents applying the backtracking schema, in order to ensure the completeness of the algorithm. Hence, a partial order among the agents is to be sought, in order to be used at initiating the variables and which will be further extended to a total order with the aim of guiding the backtracking steps. As there are no restrictions regarding the order to be used, we will be able to decide upon the use of a certain order, which best fits the topology of the constraint graph. This fact results in the restriction of the search space and of the number of exchanged messages. The author defines in [3] a generic method, named DAO, in order to determine the order of the distributed variables. This order, as well as the lexicographic order in ABT, is vital for ensuring completeness.

In [3] is introduced a demonstration schema for the correctness of the algorithm. The author points out to a few elements meant to ensure the demonstration of the correctness of the algorithm, but they are unfortunately not enough. We are going to analyze them further on. The author says that irrespective of the heuristic used for the order of variables, the oriented graph induced by set Γ in algorithm DAO, has no circuit. Thus, the backtrack step (respectively the instantiating one) from one agent cannot lead to the receiving of *bt* - type messages (respectively *infoVal*) from one of the children (respectively parents). During the backtrack step, it is only the remaining values that are tested for consistency, while during *infoVal* message receiving, the agent reconsiders its entire initial domain. Based on this observation, associated to the fact that message transmittal is done in finite time and also on the correctness of the detection of algorithm ending from **[LC85],** the author concludes that it is correct.

Unfortunately, while this algorithm is efficient from the point of view of memory, it fails some valid situations, being unable to find the solution. For instance, for the network with 5 agents given in figure 1, the algorithm is incomplete.

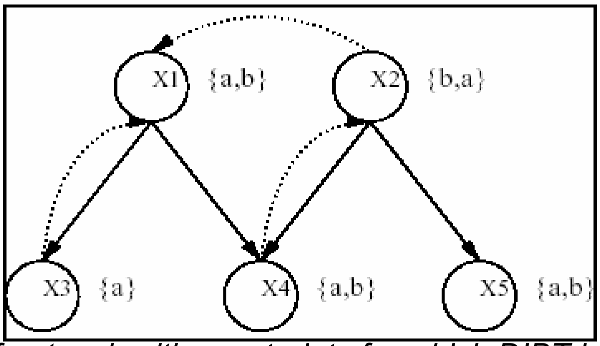

Fig.1. *Example of network with constraints for which DIBT is not complete.*

The links among variables represent constraints of inequality type. The domains are formed of values a, b, as it can be seen in figure 1. DIBT can run in the following way:

- x_1 and x_2 select a, respectively b and inform their children (see fig. 1.).
- x_3 has no other choice than value a so that a backtrack is generated to x_1 while x_4 performs a backtrack to x_2 because of the value conflicts.
- x_1 and x_2 select b, respectively a and inform their children.
- x_4 performs a backtrack to x_2 whose domain is empty, then a backtrack to x_1 follows, leading to inconsistency.

This way of running of algorithm DIBT leads to the impossibility of finding a solution, although it exists (a,a,b,b,b). One cause of the fail is that x_2 ignores the behavior of x_1 and does not reset its domain when x_1 changes its value from a into b.

In order to eliminate these difficulties and ensure the completeness of the algorithm, in [2] the author extends sets Γ^+ and Γ^-, named the sets of children and parents, in order to be sure that the *InfoVal()* message will reset all the relevant domains, and the *btSet()* message will beable to identify, for all backtracks, the guilty ones, adding in advance a few ABT-type links.

Unfortunately, in [7], Yokoo shows that this algorithm is incomplete. This is due to the fact that when it checks if a nogood value is old, algorithm DIBT takes into consideration its own values only, neglecting the values in the parent sets. This can lead to false deductions, such as the unification of several nogood values from different contexts. One example of such behavior is given in figure 2.

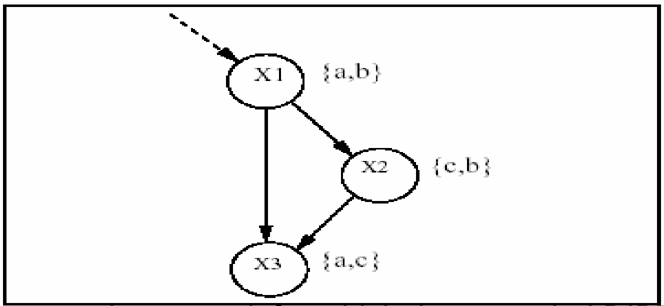

Fig.2. *Example of constraint network for which the extended DIBT is not complete.*

We consider, as in the previous example, the existence of inequality constraints among the link knots. DIBT can run in the following way :

- x_1 selects value a and informs its children (notice x_2 and x_3), x_2 selects value c and informs its child (x_3). In exchange, x_3 has an empty domain, having nothing left to choose. Therefore, it performs a backtrack to x_2 with value nogood (x_1=a and x_2 =c) .(**P1**)
- in the meantime, x_1 is bound to change its value because of the messages coming from the parents, eliminating value a. x_1 selects value b and informs its children, making x_2 eliminate value b from its domain. (**P2**)
- the message sent by x_3 to step 1 now reaches x_2. Unfortunately, this nogood is old in the context of the agents (x_1 no longer has value a but b), but because local values are not checked again, it is processed. Therefore, is make to backtrack with value nogood (x_1=b). (**P3**)
- now, the domain of x_1 is empty, x_1 also performing backtrack. And thus, not finding any solution (x_1=a, x_2 =b şi x_3=c). (**P4**)

In [1] a patch is suggested for fixing this bug. It consists in checking once again the incoming nogood messages, within the new context: each agent must be sure that the incoming and outgoing item of information is consistent with its local view. As a conclusion, we notice that the complete wipe out of the ABT-type additional links and of the nogood values is not 100% possible. Yet, the algorithm DIBT a needed to add a few ABT-type links and some nogood values, in order to ensure completeness (according to the elements mentioned above).

6. CONCLUSIONS

Each of the three techniques presented above is based on certain elements meant to ensure the completeness of the algorithm.

The ABT algorithm ensures completeness by means of a technique based on a unique identifier, technique used to avoid the dead ends in systems with distributed databases. This technique consists in using a relationship of total order among the knots. If a knot has a unique identifier, a priority order can be defined among the agents by using an alphabetical order of those identifiers (the alphabetically preceding agent has a higher priority with respect to the other agent).

The AWCS algorithm needs the record keeping of nogood lists in order to ensure the completeness of the algorithm. The main problem consists in changing the priority of agents. But value priority is changed if and only if one nogood is found. But, the number of nogood value combinations is finite (even if large), value priority cannot be changed at infinitum. Therefore, according to the authors of the algorithm, after a certain time, which is surely finite, value priority will be stable.

The DIBT algorithm needs no add-link-type messages, eliminating completely the record keeping of nogood values and uses a method of ensuring order among the agents applying the backtracking schema, meant to ensure the completeness of the algorithm. Unfortunately, in [7], Yokoo shows that this algorithm is incomplete. This is due to the fact that when verifying if a nogood value is old, algorithm DIBT takes into calculation only its values, ignoring the values in the parents' set.

As a conclusion, we notice that the complete wipe out of ABT-type additional links and nogood values is not 100% possible. Nevertheless, algorithm DIBT needed some extra ABT-type add-links and some nogood values in order to be able to ensure completeness in the situation given in [7].

7. BIBLIOGRPHY

[1] Christian Bessière, Arnold Maestre, Pedro Meseguer. *Distributed Dynamic Backtracking*.In Proceedings of the CP'00 Workshop on DCSP, Singapore,2000.

[2] Hamadi Y. – Traitement des problemes de satisfaction de constraintes distributes. PhD theisis, Universitatea Motpellier II, 1999.

[3] Hamadi Y., Bessiere C., Quinqueton J. *Backtracking in Distributed Constraint Networks*. In Proceedings of the 13th, ECAI , Brighton, UK, 1998, pag. 219-223.

[4] L. Lamport K. M. Chandy. *'Distributed snapshots: Determining global states of distributed systems'*, TOCS, 3(1), 63–75, 1985.

[5] Yokoo M., E.H. Durfee, T. Ishida, K. Kuwabara - *Distributed constraint satisfaction for formalizing distributed problem solving.* In ICDCS, 614{621). June 1992.

[6] Yokoo M., E.H. Durfee, T. Ishida , K. Kuwabara - *The distributed constraint satisfaction problem : formalization and algorithms* . IEEE 10 (5), 1998 .

[7] Yokoo Makoto . Private communication, 2000.

ISIRR 2003

THE INFLUENCE OF THE THERMAL TREATED SEMI-FINISHED PRODUCTS THICKNESS ON THE TECHNOLOGICAL AND OPERATIONAL CHRACTERISTICS

Isidor PREJBAN, Stefan MAKSAY

Polytechnic University of Timisoara, Faculty of Engineering of Hunedoara

Abstract

The present paper analyzes the influence of the thickness of the thermal treated semi-finished products on the mechanical characteristics of the heat-treatable and case-hardening steels. The thermal treatments that consist of repeated heating and cooling performed under well-ascertained conditions have the highest influence on the steel structure, respectively on their properties.

The steel grades that were chosen for study are OLC45, 40BCr10 and 17MoCrNi14, and the samples for the mechanical tests had dimensions between Ø15mm and Ø60mm.

As a result of the experimental data processing, it was found out that the values of the mechanical characteristics $Rp_{0,2}$ and Rm decrease and the values of the characteristics A_5, Z and KCU increase together with the increasing of the diameter of the thermal treated sample.

Keywords

the thermal treated, mechanical characteristics, semi-finished products thickness

1. INTRODUCTION

The various scopes the steels are used in and the conditions under which the steels work have led to the necessity to ensure properties having the values of the mechanical, physical and chemical characteristics as high as possible. The structure of the steels depends on the treatments the steel was subject to during its subsequent processing (thermal-mechanical treatments, thermal or thermal-chemical treatments). If these treatments were wrongly performed or applied, the steel having the suitable chemical composition, but the defective structure, can show unsuitable properties.

Thermal treatments consisting in heating and cooling performed under well-ascertained conditions have the highest influence on the steel, respectively on its properties.

In order to study the influence of the thickness of the thermal treated specimen on the mechanical characteristics of the heat-treatable and case-hardening steels, three representative steel grades were chosen: OLC45, 40BCr10 and 17MoCrNi14. Two samples per each heat for each steel grade out of fifteen heats, rolled out of □100 mm billet were sampled. Out of a sample per each heat and out of each material there were machined specimens having the dimensions Ø60 mm, and out of the second batch there were machined the other specimens at Ø40 mm and Ø25 mm for the heat-treatable steels, respectively Ø40 mm and Ø15 mm for the case-hardening steels, according to Table 2.

The sampling for the tensile and toughness tests was performed according to Figure 1 and each sample was marked. After sampling, the specimens were metal-cut at the required dimensions.

The thermal treatment conditions applied are shown in Table 1. After performing the thermal treatment, the specimens having different thickness were machined in gauged sample for the tensile and impact bending (toughness) tests.

Thermal treatment conditions applied to the steels Table 1.

Steel grade	Quenching	Cooling agent	Heating time	Annealing	Cooling agent	Heating time
OLC45	850°C	oil	35′	620°C	air	60′
40BCr10	850°C	oil	35′	550 °C	water	60′
17MoCN14	850°C	oil	40′	180 °C	air	120′

Figure 1 shows the schematic representation of the way of sampling the specimens out of the semi-finished products of the three steel grades, and Table 2 shows the number of specimens sampled on each dimension.

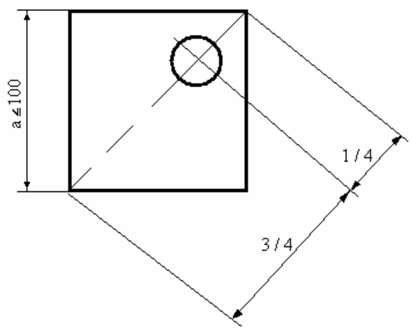

Figure 1. Way of sampling the specimens for the tensile and toughness test

Table 2

Steel grade	Specimen dimension and number of pieces				
	Ø60 mm	Ø40 mm	Ø30 mm	Ø25 mm	Ø15 mm
OLC45	15	20	-	21	-
40BCr10	15	20	-	27	-
17MoCN14	15	-	30	-	27

The results of these tests are centralized as a table, and based on the results achieved experimentally for the same mechanical characteristic, a high dispersion of the values for the same steel grade at the three specimen dimensions that were subjected to the same thermal treatment, has been obtained. This fact shows that the thermal treatment applied under the same conditions has an influence on the mechanical characteristics.

The variation diagrams of the mechanical characteristics were drawn depending on the dimensions of the treated specimens shown in Table 3, where $\overline{Rp_{0,2}}$, $\overline{Rm}$, $\overline{A_5}$, $\overline{Z}$, $\overline{KCU}$ 300/2 represent the arithmetic mean of the mechanical characteristics for each typo-dimension of the studied specimens.

Table 3

Steel grade	Dimension	Arithmetic mean of the values of the mechanical characteristics on each typo-dimension of the studied specimens				
		$\overline{Rp_{0,2}}$ daN/mm^2	$\overline{Rm}$ daN/mm^2	$\overline{A_5}$ daN/mm^2	$\overline{Z}$ daN/mm^2	$\overline{KCU\ 300/2}$ daN/mm^2
OLC45	Ø60	48,266	79,533	20,2	50,6	7,733
	Ø40	50,25	81,7	19,05	49,25	7,02
	Ø25	52,857	84,428	17,958	45,523	6,466
40BCr10	Ø60	73,866	93,8	17,533	60,133	12,106
	Ø40	81,9	99,6	16,25	58,15	11,9
	Ø25	91,851	102,814	14,074	56,407	9,581
17MoCrNi14	Ø60	61,266	86,533	19,066	60,4	17,226
	Ø30	76,933	97,366	15,966	58,066	14,066
	Ø15	93,592	102,259	14,222	54,777	12,348

Figure 2 shows the variation of the $Rp_{0,2}$ characteristic depending on the specimen dimension. It can be noticed that if the dimension of the thermal treated specimen increases, the value of the $Rp_{0,2}$ decreases.

Figure 3 shows the variation of the mechanical characteristic Rm depending on the dimension of the thermal treated specimen. It can be noticed that the value of the maximum tensile load Rm decreases together with the increasing of the dimension of the thermal treated specimen.

Figure 4 shows the variation of the specific elongation A_5 in % depending on the diameter of the thermal treated specimen. For OLC45 the A_5 value is higher than the minimum value specified by the norm. For the steel grades 40BCr10 and 17MoCrN14, the A_5 values are higher than those specified by the norms and it increases together with the increasing of the specimen diameter.

Figure 5 shows the variation of the contraction Z depending on the specimen diameter, where there have been recorded higher values than those specified by the norms for all the analyzed steel grades. The values of the contraction Z recorded for OLC45 are much under the values corresponding to the steel grades 40BCr10 and 17MoCrNi14, the last two being close enough. They increase together with the increasing of the diameter of the thermal treated specimen.

Figure 6 shows the variation of the toughness KCU 300/2 depending on the diameter of the thermal treated specimen. The toughness increases together with the increasing of the specimen diameter. The recorded values of the toughness are higher than those specified in the norms, for all the analyzed steel grades.

It can be summarized that the values of the mechanical characteristics $Rp_{0,2}$ and Rm decrease and the values of the characteristics A_5, Z and KCU increase together with the increasing of the diameter of the thermal treated specimen.

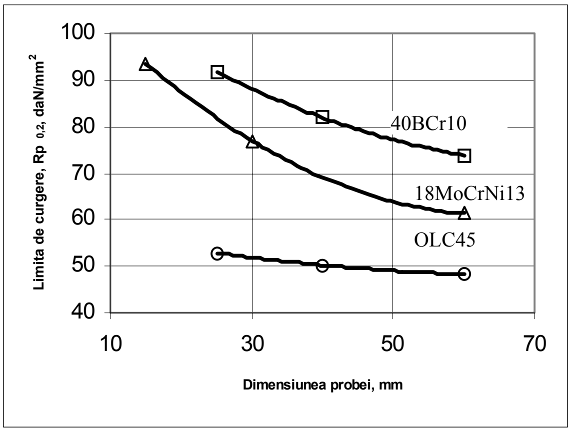

Figure 2.Variation of the characteristic $Rp_{0,2}$ depending on the specimen dimension

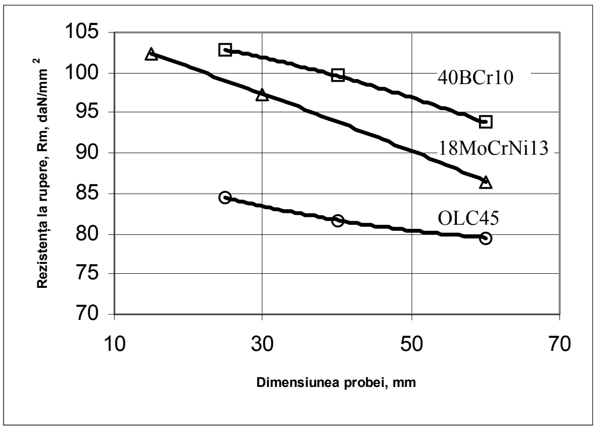

Figure 3.Variation of the characteristic Rm depending on the specimen dimension

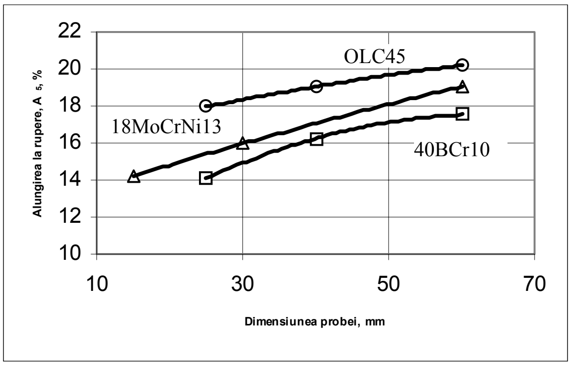

Figure 4.Variation of the A_5 characteristic depending on the specimen dimension

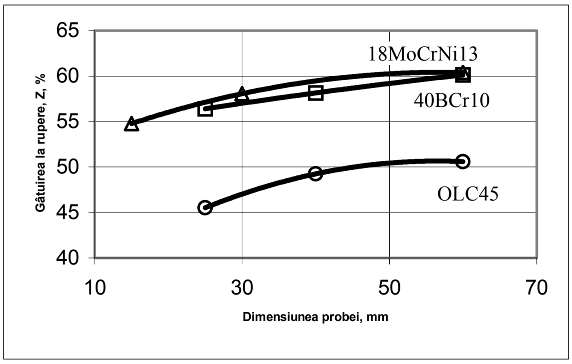

Figure 5.Variation of the characteristic Z depending on the specimen dimension

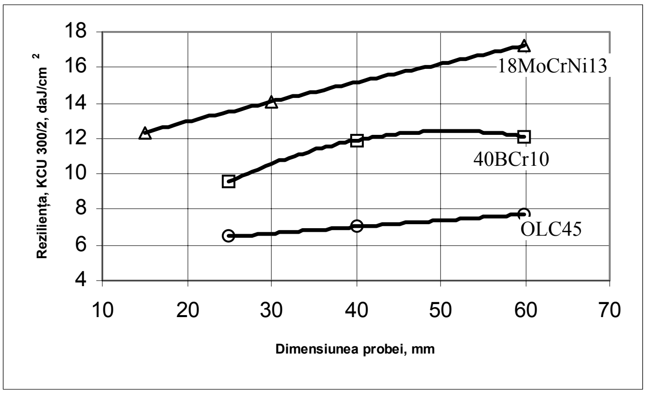

Figure 6.Variation of the characteristic KCU300/2 depending on the specimen dimension

BIBLIOGRAPHY

1. *Cheşa, I., ş.a. – Alegerea şi utilizarea oţelurilor, Ed. Tehnică, Bucureşti, 1984*
2. *Vermeşan, G. – Tratamente termice, Îndrumător, Ed. Dacia, Cluj-Napoca, 1987*
3. *Mitelea, I., ş.a. – Studiul metalelor – Îndreptar ethnic, Ed. Facla, Timişoara, 1987*
4. *Popescu, N., ş.a. – Tratamente termice şi prelucrari la cald, E.D.P., Bucureşti, 1983*
5. *Dulamiţă, T., ş.a. – Tratamente termice şi termochimic4e, E.D.P., Bucureşti, 1982*
6. **** STAS 8580-74 ; STAS 880-88 ; STAS 7324-75 ; SR EN 10002/1,2,3,4,5*

ISIRR 2003

RESEARCHES CONCERNING DEPHOSPHORIZATION PROCESS AT ELECTRIC FURNACE EBT

HEPUŢ Teodor, SOCALICI Ana Virginia, PUŢAN Vasile, POPA Erika Monica

[1] University "Politehnica" – Timisoara, Faculty of Engineering - Hunedoara

ABSTRACT

This paper shows the results of researches concerning the steel dephosphorization processed in electric furnace EBT at steel shop no 2, SC Siderurgica Hunedoara.

During researches it was recorded the phosphor content at each fabrication stage and the technological parameters. Processing the results it was obtain a series of correlations between the dephosphorization ratio and the technological parameters, presented both graphical and analytical.

Knowledge of these correlations allow in the given stage limitation of final phosphor content at max 250ppm.

KEY WORDS:

electric furnace, EBT, steel, phosphor content, dephosphorization process

1. INTRODUCTION

The reduction content of phosphor content from steel it was and will remain a concern of steel makers, indifferent of steel processing method.

In Romanian steel industry are operating four main producers of electric steel for long products (sections, bars, wire rod etc). All this steel makers have steelshoops equipped with EBT electric furnaces (I.S. Campia Turzii, C.O.S. Targoviste, S.C. "Siderurgica" S.A. Hunedoara and C.S. Resita), at Hunedoara and Targoviste being continuous steel cast plants. On an other side a steelshop modernised in 1996-1998 is for the moment closed (Siderca Calarasi).

Share electric steel has major increase since EBT furnace was introduced. The technological aims that were predominant for the specialists from steelshops, starting from the commissioning of these new furnaces have been to regulate the tapping targets for [C], [P], temperature and the technological way.

The present paper shows the results of steel dephosphorization made Siderurgica Hunedoara.

2. EXPERIMENTS AND RESULTS

Specialised in the fabrication of a varied range of long products and facing to the customers requirements concerning for putting into operation band exploitation, the Siderurgica Hunedoara steelshop started a policy to limit the content of residual elements, including the P concentration for which, in a first stage it was established a maximum target of 200 ppm.

The main technological approaches were oriented to:

- control of the metallic charge quality;
- control of the quality and quantity of admixtures (lime, fluorite and dolomite;
- slag conditions in the electric furnace EBT ;
- practice to use some iron-alloys for alloying and correction in ladle (at tapping and LF) witch known and limited P concentration;
- technologically justified limitation of refining time.

The technological results presented here were obtained for a number of 40 experimental heats carried out in EBT furnace from Otelaria Electrica no.2, Siderurgica Hunedoara.

From the point of P concentration in steel, recorded in different stages of the technological, recorded in different stages of the technological process, the results performed during the trials for the 40 heats are presented in the frequency diagrams from figure 1, 2 and 3. The results recorded according to the moment: melting, start LF and final (cast sample) are emphasising the performances obtained, that means:

- at melting end in EBT furnace we succeeded to reach a P concentration, in a percent of 85%, under the limit of 100ppm;
- at the starting moment of LF treatment, due to the inherent rephosphorisation in ladle with the slag and alloying additions, the P concentration increased, the level of setting under the limit of 100ppm decreasing up to 73% but succeeding a setting in a percent of 97 %under the final aim that we had in mind, of max. 250 ppm;
- as concerns the final P concentration in steel (casting sample), the final aim of 250 ppm was reached in 95% of the heats.

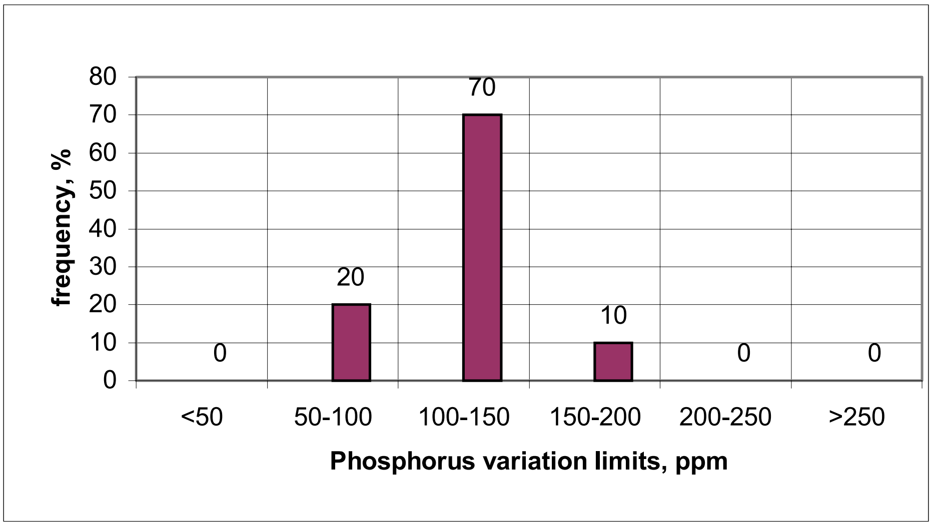

Fig. 1. *Variation limits of phosphor content at melting*

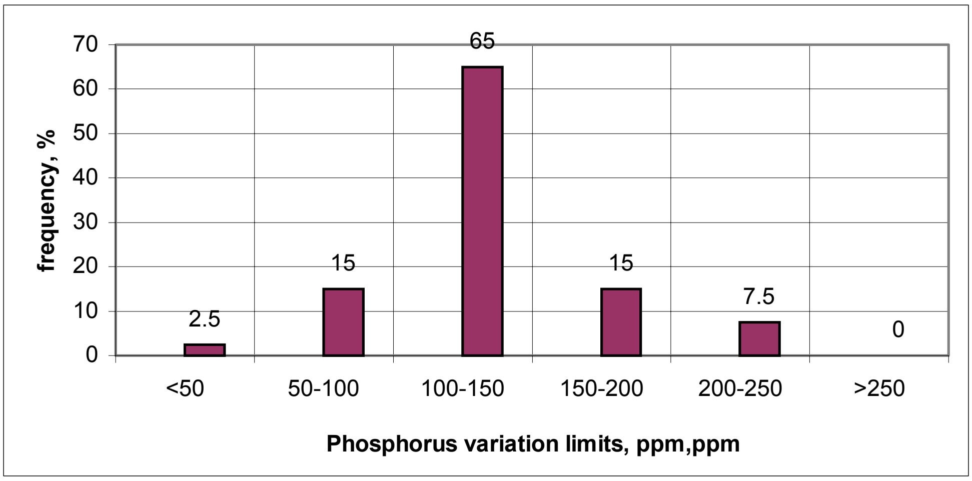

Fig.2. *Variation limits of phosphor content at start of LF treatment*

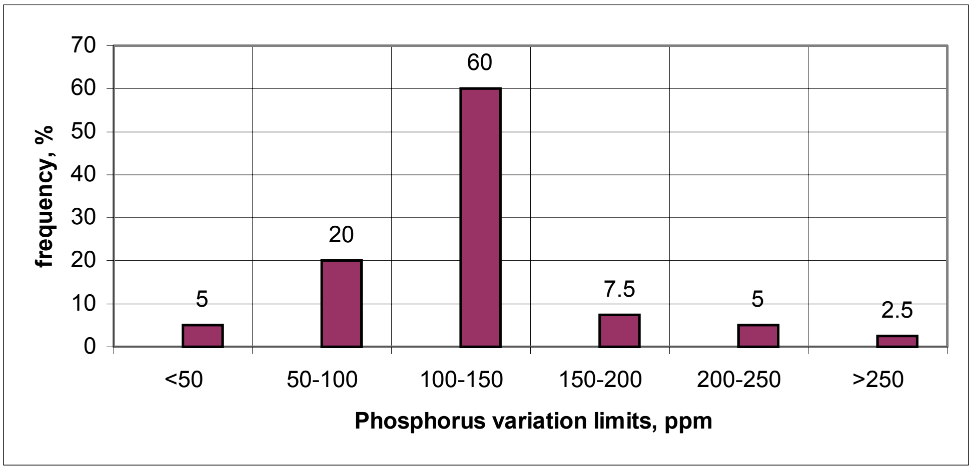

Fig.3. *Variation limits of phosphor content at casting*

- at melting end in EBT furnace we succeeded to reach a P concentration, in a percent of 85%, under the limit of 100ppm;
- at the starting moment of LF treatment, due to the inherent rephosphorisation in ladle with the slag and alloying additions, the P concentration increased, the level of setting under the limit of 100ppm decreasing up to 73% but succeeding a setting in a percent of 97 %under the final aim that we had in mind, of max.250 ppm;
- as concerns the final P concentration in steel (casting sample), the final aim of 250 ppm was reached in 95% of the heats.
- synthetically speaking, having in mind that the lower value of P concentration at melting end was of 60ppm, and the higher at final was of 260 ppm it results that that succeeded to control the rephosphorisation process as well on the whole, limiting it by 40% as in the most sensible stage, technologically speaking , which follows the tapping where4 the rephosphorisation was limited at about 24%;
- the trials emphasised once more that the start condition, meaning the melting end concentration is very important for the phosphorus control in steel making process, as well technologically as economically.
- the slag quality at melting end was characterised by the variation of parameters mentioned in table 1.

Table 1. Quality indicators for slag at melting end

Quality indicators	Slag composition, %				$I_B = CaO/SiO_2$
	CaO	$FeO_{Echiv.}$	MgO	Al_2O_3	
Minim value	21,82	20,86	4,21	2,76	1,36
Maxim value	39,73	38,97	15,64	6,54	5,21
Average value	30,22	32,88	8,98	4,82	2,63

Processing the obtained dates using EXCEL program it results the following technological aspects:

- From the point of view of the slag composition we worked in a kinetic conditions favourable as a rule, determined by the concentrations of the major compounds (CaO, FeO, Al_2O_3, MgO), in the same time favourable for a higher fluidity;
- The relative high (FeO) concentration, reaching 38,97%, was in many cases higher than (CaO) concentration, determining the bordering of CaO/FeO ratio in limits closed to one (0,85-1,25);
- The relationship between the distribution ratio $L_P = (P_2O_5)/[P]$ and the (CaO), (MgO), (Al_2O_3) concentration emphasis in accordance to figures 4,5 and 6 the following:
  a. the (CaO) concentration reached the optimum in the in the range 30-35%, which statistically corresponded to a lime consumption of 30-32kg/t;
  b. in the recorded range, the (Al_2O_3) concentration kept a favourable trend, preserving the fluidisation ability;
  c. as we expected, the growth of dephosphorisation performance, in our trials especially over the limit of 8%. So, we must to review the melting conditions in order to limit it concentration;

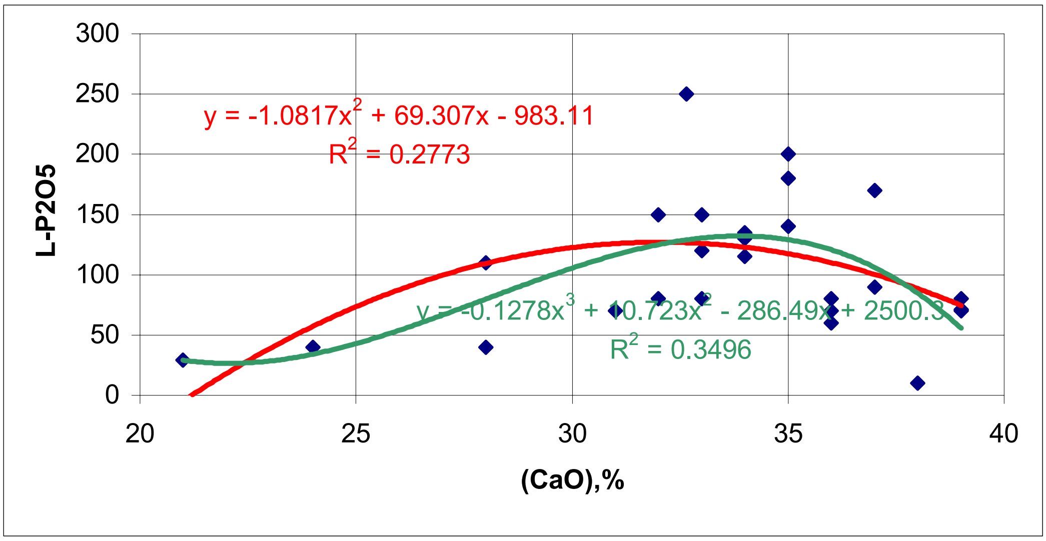

Fig.4. *Correlation between dephosphorization ratio and content of CaO from slag*

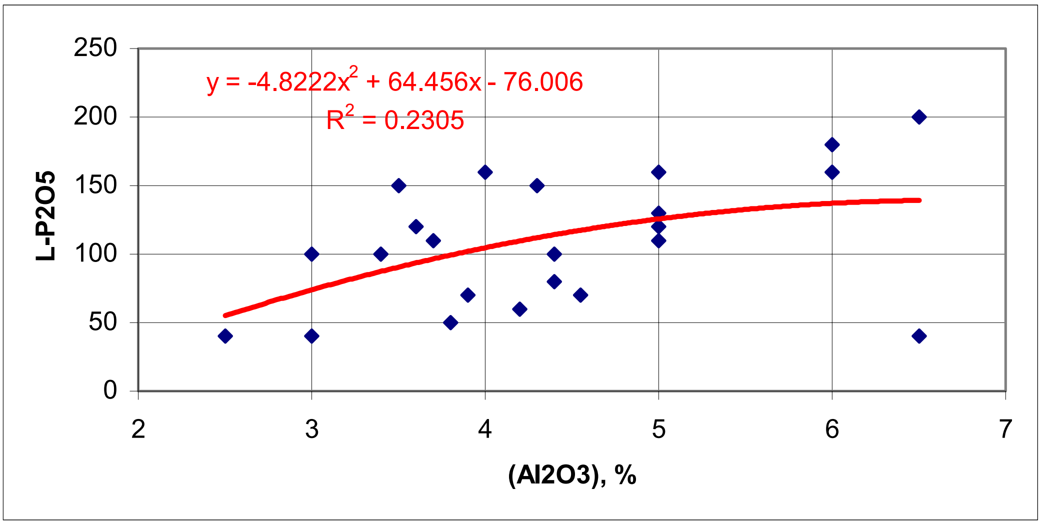

Fig.5. *Correlation between dephosphorization ratio and content of* ***Al_2O_3*** *from slag*

- As concerns the (FeO) concentration and the slag basicity index, two of the main technological parameters which determine the dephosphorisation performance during melting, we must to have in view that they are conditioning also the foaming process and as these in the electric furnace. The relations hip between L_P and (FeO) determined for our trials and high lighted in figure 7 emphasises an optimum in the range 25-35% (FeO). In the same time, diagram from figure 8 shows that the best performance was recorded for I_B =2-3.

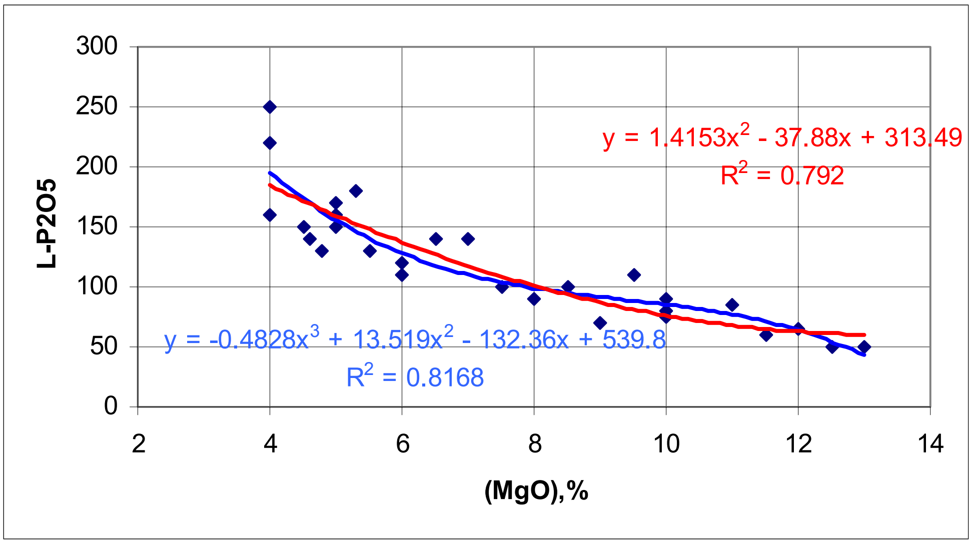

Fig.6. *Correlation between dephosphorization ratio and content of MgO from slag*

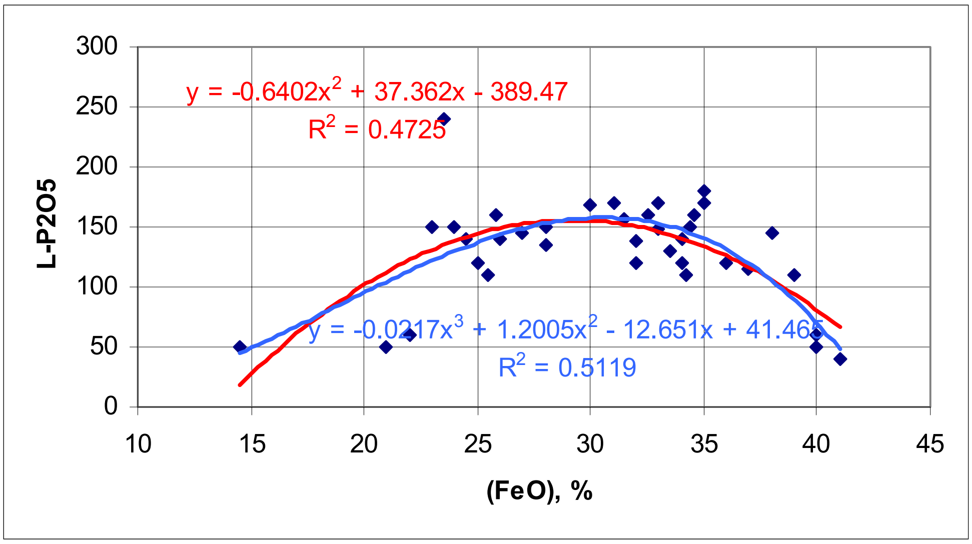

Fig.7. *Correlation between dephosphorization ratio and content of FeO from slag*

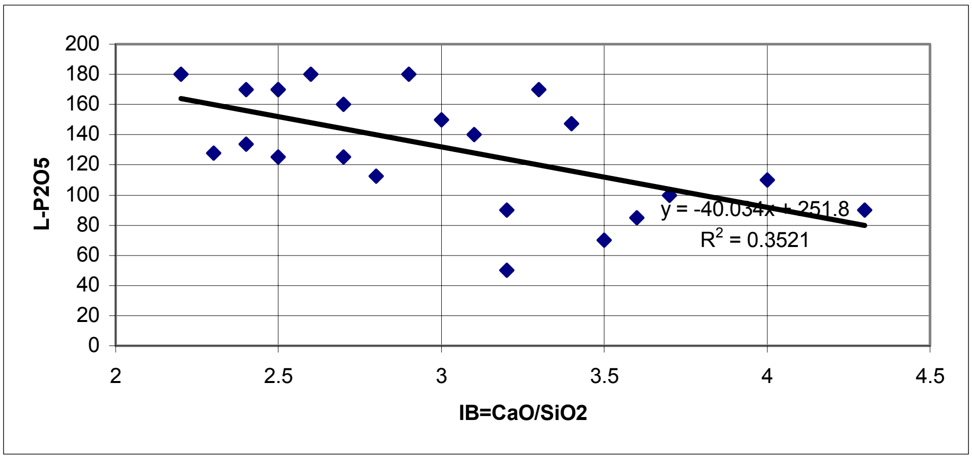

Fig.8. *Correlation between dephosphorization ratio and I_B from slag*

3. CONCLUSIONS

- the ultimate technological factors proved to be control of metallic charge and the slag quality (chemical composition, quantity and temperature);
- the P concentration at the melting end in decisive to reach the final purpose, the concentration under the threshold of 150 ppm in this stage being the stronger technological solution;
- dephosphorization process in EBT furnace fallow in good conditions, that is proof by the dephosphorization output value (average value is 60% on entire process and 70% at melting).
- the results of mathematical processing using EXCEL program are useful both for research and practical purposes.
- an extension of dates processing using MATLAB program it will fallow to the obtaining of some complex relation between dephosphorization ratio and different technological factors.

4. BIBLIOGRAPHY/REFERENCES

1. RAU AL., TRIPSA I.: "Metalurgia oţelului", Editura Didactica si Pedagogica, Bucuresti, 1973;

2. * * * - "Instructiunui tehnologice pentru elaborarea otelului in cuptoare electrice EBT", S.C. SIDERURGICA S.A. Hunedoara, 2002;

3. "Results Obtained by the Technological Dephosphorisation Practice in EBT Electric Furnace" – Practical Guide.

CONSIDERATIONS UPON THE MOTION OF THE POROUS MATERIALS WITH ELASTIC SKELETON

Vasile BACRIA

"Politechnica" University of Timişoara

Abstract

The porous materials are used in the attenuation of the sound waves.

In the paper are established the differential equations of motion for porous materials with metallic skeleton.

We obtain relations that allow the determination of porous material impedances and the absorption coefficients of sound for different porous materials applied on the acoustic screens.

Keywords: *motion, porous materials, elastic skeleton.*

1. THE EQUATIONS OF MOTION

Let us consider a porous material with cylindrical open pores having radius equal to R*,* placed parallel on the length of the material. The air friction force with viscosity ν at laminar flowing through an element of the material with transversal section 1 cm^2 and thickness dx*,* according to Poiseuille law, is

$$P_f = \sigma_P \cdot v_P \cdot h \cdot dx \tag{1}$$

where

$$\sigma_P = \frac{8 \cdot \nu}{R^2} \tag{2}$$

is the resistance of the air in the pores of the material, $v_P = \frac{Q}{h \cdot t}$ - the linear speed of the air on the length of the pore's axle, Q – the flow of the air through the pores, t – the time necessary for passing air and h – the porosity.

The expression *(1)* of friction force of the air from the walls of the pores is also available for non uniform and non cylindrical pores and non laminar or oscillating flowing of the air, but the air resistance is not expressed anymore through the simple formula *(2).*

Let us consider a material with parallel pores of different diameters situated under the angle θ as to the normal at the surface of the material from which we isolate an element 1 cm^2 in section and dx in thickness.

In order to ease the following deductions, suppose that all the pores came together; the projection of their surface on the plan perpendicular to the normal equals h (fig. 1).

By replacing a few parallel pores with the equivalent pore we are influencing the value of the friction force. This force is the one given by the formulas *(1)* and *(2)*. The inertness forces against (on) the element and the air contained in it did not change.

Suppose that on the surface of the isolated element of the skeleton and of the air, there are operating the sonorous pressure p_s and p_a. On the unit of the surface of the material will operate the forces $p_1 = p_s(1-h)$ and $p_2 = p_a \cdot h$

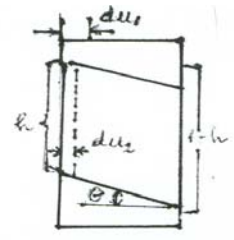

Fig 1.

We shall use the following notations: ρ_1 for the density of the skeleton of the material and v_1 for its speed in direction of the normal at the surface of the material; in that case, the inertness force corresponding to the element of the skeleton is $\rho_1 \cdot dX \cdot \frac{\partial v_1}{\partial t}$.

The air also takes part in two motions: one portable with an acceleration equal with the acceleration of the skeleton $\frac{\partial v_1}{\partial t}$ and a relative motion with relative acceleration $\frac{\partial v_p}{\partial t} = \frac{1}{\cos\theta} \cdot \frac{\partial (v_2 - v_1)}{\partial t}$ where v_p is the linear speed of the air on the length of the axis of the pore in its relative motion, and v_2 represents the linear speed of the air on the direction of the normal at the surface of the element. The inertness forces corresponding to the air are equal to $\rho_2 \cdot dx \cdot \frac{\partial v_1}{\partial t}$ and $\rho_2 \cdot \frac{dx}{\cos\theta} \cdot \frac{(v_2 - v_1)}{\partial t}$ where $\rho_2 = p \cdot h$ is the mass of the air contained in the unit of the volume and ρ represent the density of the air in the atmosphere.

During the air motion in the pore also appears an interaction force between the air and the skeleton with the normal component P_n and the tangential one P_f.

Also on the volume cut from the skeleton operate the force T perpendicular on the ox axis in perpendicular direction on the normal, due to the deformation of the material (fig. 2).

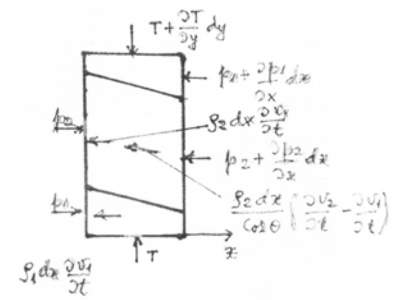

Fig. 2

In the same way we may consider separately the section of the skeleton of the volume element cut and the air contained in this volume which operate on it (fig. 3 and 4).

Projecting the forces which operate on the volume element cut from the porous material on ox axis (fig. 2) after making the reduction and simplifications necessary, we obtain

$$-\frac{\partial p_1}{\partial x}-\frac{\partial p_2}{\partial x}=\rho_1\cdot\frac{\partial v_1}{\partial t}+\rho_2\cdot\frac{\partial v_2}{\partial t} \qquad (3)$$

Furthermore, by projecting on the axle of the posre the forces which operate on the air, situated in the volume element cut from the element (fig. 4) and using the expression *(1)* where $v_p=\frac{v_2-v_1}{\cos\theta}$ results

$$-\frac{\partial p_2}{\partial x}=\rho_2\cdot\frac{\partial v_2}{\partial t}+\rho_2\cdot(\varepsilon-1)\cdot\left(\frac{\partial v_2}{\partial t}-\frac{\partial v_1}{\partial t}\right)+\sigma\cdot h^2\cdot(v_2-v_1) \qquad (4)$$

where $\varepsilon=\frac{1}{\cos^2\theta}$ is the structure factor and $\sigma=\sigma_p\cdot\frac{\varepsilon}{h}$ represents the resistance of the material faced up by the air which is different from the one established in the expression *(2)*. If the pores are not parallel and have a chaotic orientation, the structure factor has a more complex formula.

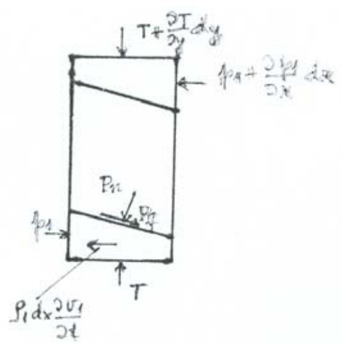

Fig. 3

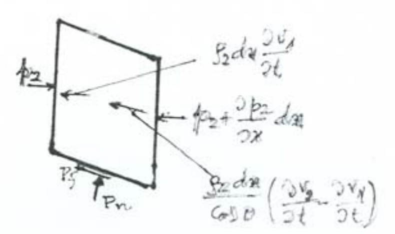

Fig. 4

The equation obtained can receive a symmetrical formula if we introduce the expression of $\frac{\partial p_2}{\partial x}$ from the equation *(4)* in the equation *(3)*

$$-\frac{\partial p_1}{\partial x} = \rho_1 \cdot \frac{\partial v_1}{\partial t} + \rho_2 \cdot (\varepsilon - 1) \cdot \left(\frac{\partial v_1}{\partial t} - \frac{\partial v_2}{\partial t} \right) + \sigma \cdot h^2 \cdot (v_1 - v_2) \tag{5}$$

Two of the expressions *(3)-(5)* are the motion equations for porous materials with elastic skeleton.

These equations are universal because they are valid for stationary process and also for non stationary ones. For instance, if we consider $\frac{\partial}{\partial t} = i \cdot \varpi$ (for harmonic oscillation) the expressions *(4)-(5)* appear in the motion equation obtained by Zwikker, Kosten [4] and L. Beranek [1].

Beranek introduces in the equation *(1)* an additional term that estimates the damages at the friction in skeleton; the damages at the friction in the air are not take considered.

We can estimate easier the damages of the friction in the skeleton and in air through the complex modules of elasticity.

2. THE CONTINUITY EQUATIONS

Next, we will establish the continuity equations. For the porous material skeleton, based on Hooke's law, we may write $-p_1 = E_1 \cdot (\varepsilon_1 + \varepsilon_1^{'})$. Here $E_1 = E_s \cdot (1 + i \cdot \eta_s)$ is the complex module of elasticity E_s and η_s is the dynamic module of elasticity and the coefficient of the damage of the skeleton; ε_1 - the deformation of the skeleton in the direction of the ox axis; $\varepsilon_1^{'}$ - the supplementary deformation on the same axis determined by the air pressure.

For the various porous materials (glass wool, mineral wool, polymer etc.) due to the fact that the elasticity module of the air is a lot less significant than the elasticity module of the material used to produce the skeleton of the porous materials we may consider $\varepsilon_1 >> \varepsilon_1^{'}$. Subsequently, $-p_1 = \varepsilon_1$ and by differencing this equality in function of time we obtain

$$-\frac{\partial p_1}{\partial t} = E_1 \cdot \frac{\partial v_1}{\partial x} \tag{6}$$

We can obtain the continuity equation for the air from the equation of status for the polytrophic process PV^n = const., where P and V represent the pressure and the volume, and n – the polytrophic index. From the equation of status we obtain the increase of pressure $-\Delta P = P \cdot n \cdot \frac{\Delta V}{V}$ where ΔV is the increase of the volume.

The increase of ΔP pressure equals the increase of sonorous pressure ΔP_a $\Delta P = \Delta P_a = \frac{\Delta P_2}{h}$.

Multiplying the air pressure by the polytrophic index leads to the complex module of air elasticity $P \cdot n = E_2 = E_a \cdot (1 + i \cdot \eta_a)$, where E_a and η_a are the dynamic module of elasticity and the damage coefficient for air. These relations lead to $-\Delta P_2 = E_2 \cdot h \cdot \frac{\Delta V}{V}$.

In the isolated element of the volume, the initial volume of air (fig. 1) is V = hdx.

If we consider that at the modification of the hydrostatic pressure the skeleton volume does not change in the initial conditions because the elasticity module of the air is much less significant than the elasticity module of the material, used to make the skeleton, then at the compression of the skeleton to the value Δu_1 and the air to the value Δu_2, the air volume in the element adjusts to the value $\Delta V = h \cdot \Delta u_2 + (1-h) \cdot \Delta u_1$.

Replacing the values of volumes V and ΔV in expression of Δp_2, after dividing with Δt and effecting the limit for $\Delta t \to 0$ we obtain

$$-\frac{\partial p_2}{\partial t} = h \cdot E_2 \cdot \frac{\partial v_2}{\partial x} + (1-h) \cdot E_2 \cdot \frac{\partial v_1}{\partial x} \tag{7}$$

where $v_{1,2} = \frac{\partial u_{1,2}}{\partial t}$.

The expressions *(6)* and *(7)* represent the continuity equations for some porous materials (glass wool, mineral wool, polymer etc.). For other materials these equations are not so accurate,

3. THE INTEGRATION OF MOTION EQUATION

We will solve the equations *(4)*-*(7)* for the harmonic vibrations $\left(\frac{\partial}{\partial t} = i \cdot \varpi \right)$.

Introducing the expression *(6)* in formula *(5)* and the expression *(7)* in formula *(4)* we obtain a system of two equations

$$\frac{\partial^2 v_2}{\partial x^2} = \left[\frac{E_1}{h \cdot E_2} \cdot \frac{\rho_2 \cdot \varpi^2 - i \cdot \varpi \cdot s}{i \cdot \varpi \cdot s} - \frac{1-h}{h} \right] \cdot \frac{\partial^2 v_1}{\partial x^2} + \left[\frac{(\rho_1 \varpi^2 - i \cdot \varpi \cdot s)(\rho_2 \varpi^2 - i \cdot \varpi \cdot s) + \varpi^2 \cdot s^2}{i \cdot \varpi \cdot s \cdot h \cdot E_2} \right] \cdot v_1 \tag{8}$$

$$v_2 = -\frac{E_1}{i \cdot \varpi \cdot s} \cdot \frac{\partial^2 v_1}{\partial x^2} - \frac{\rho_1 \cdot \varpi^2 - i \cdot \varpi \cdot s}{i \cdot \varpi \cdot s} \cdot v_1 \tag{9}$$

where $s = i \cdot \varpi \cdot \rho_2 \cdot (\varepsilon - 1) + \sigma \cdot h^2$ is the coefficient which characterizes the link between the vibrations of the skeleton and of the air.

If we eliminate v_2 from the expression *(8)* and *(9)*, we obtain the equation

$$\frac{\partial^4 v_1}{\partial x} + A \cdot \frac{\partial^2 v_1}{\partial x^2} + B \cdot v_1 = 0 \tag{10}$$

where

$$A = \frac{\rho_1 \varpi^2}{E_1} - \frac{i \cdot \varpi \cdot s}{h \cdot E_1} + \frac{\rho_2 \cdot \varpi^2}{h \cdot E_2} - \frac{i \cdot \varpi \cdot s}{h \cdot E_2} \tag{11}$$

$$B = \frac{\rho_1 \varpi^2}{E_1} \cdot \frac{\rho_2 \cdot \varpi^2}{h \cdot E_2} - \frac{\rho_1 \cdot \varpi^2}{E_1} \cdot \frac{i \cdot \varpi \cdot s}{h \cdot E_2} - \frac{\rho_2 \cdot \varpi^2}{h \cdot E_2} \cdot \frac{i \cdot \varpi \cdot s}{E_1} \tag{12}$$

The solution of the equation *(10)* is

$$\varpi_1 = i \cdot \varpi \cdot \left(C_1 e^{\gamma_1 \cdot x} + C_2 e^{-\gamma_1 \cdot x} + C_3 e^{\gamma_2 \cdot x} + C_4 e^{-\gamma_2 \cdot x} \right) \cdot e^{i \cdot \varpi \cdot t} \tag{13}$$

where

$$\gamma_{1,2} = \sqrt{-\frac{A}{2} \mp \sqrt{\frac{A^2}{4} - B}} \tag{14}$$

From the continuity equation *(6)* as well as from the solution *(13)* we obtain

$$p_1 = E_1 \left(-\gamma_1 \cdot C_1 e^{\gamma_1 \cdot x} + \gamma_1 \cdot C_2 e^{-\gamma_1 \cdot x} - \gamma_2 \cdot C_3 e^{\gamma_2 \cdot x} + \gamma_2 \cdot C_4 e^{-\gamma_2 \cdot x} \right) \cdot e^{i \cdot \varpi \cdot t} \tag{15}$$

From the expression *(9)* and *(13)* results

$$v_2 = \left(C_1 a_1 e^{\gamma_1 \cdot x} + C_2 a_1 e^{-\gamma_1 \cdot x} + C_3 a_2 e^{\gamma_2 \cdot x} + C_4 a_2 e^{-\gamma_2 \cdot x} \right) \cdot i \cdot \varpi \cdot e^{i \cdot \varpi \cdot t} \tag{16}$$

Finally from the continuity equation *(7)* and the expressions *(13)* and *(16)* we obtain

$$p_2 = E_2 \left(-\gamma_1 \cdot b_1 \cdot C_1 e^{\gamma_1 \cdot x} + \gamma_1 \cdot b_1 \cdot C_2 e^{-\gamma_1 \cdot x} - \gamma_2 \cdot b_2 \cdot C_3 e^{\gamma_2 \cdot x} + \gamma_2 \cdot b_2 \cdot C_4 e^{-\gamma_2 \cdot x} \right) \cdot e^{i \cdot \varpi \cdot t} \tag{17}$$

where

$$\begin{aligned} b_1 &= a_1 \cdot h + (1 - h) & \qquad b_2 &= a_2 \cdot h + (1 - h) \\ a_1 &= 1 - \frac{E_1 \cdot \gamma_1^2 + \rho_1 \cdot \varpi^2}{i \cdot \varpi \cdot s} & \qquad a_2 &= 1 - \frac{E_1 \cdot \gamma_2^2 + \rho_1 \cdot \varpi^2}{i \cdot \varpi \cdot s} \end{aligned} \tag{18}$$

From the expressions *(13)-(17)* we observe that in the porous material with elastic skeleton, two waves propagate simultaneously with constants γ_1 and γ_2. These waves are coupled and they propagate in the game time in the skeleton as well as in the air.

The relations *(13), (15), (16)* and *(17)* allow the determination of porous materials impedances and absorption coefficients of sound for different porous materials applied on acoustic screens.

REFERENCES:

[1] BERANEK L., *Acoustical properties of homogeneous isotropic rigid tiles and flexible blankets,* J. A. S. A., Nr.4, 1947, Vo1.19.

[2] BREHOVSKIH A. M., *Volnî v sloistîh sredah,* Izd. “Nauka”, Moskva, 1973.

[3] BACRIA V., *Considerations upon acoustic screens with intermediary*

porous layer. Seventh International Congress on Sound and Vibrations, 4-7 July 2000, Garmisch–Partenkirchen, Germany pages 30313034.

[4] ZWIKKER C., KOSTEN C.W., *Sound absorbing materials,* New-York – London, 1949.

[5] BACRIA V., *Consideration upon the reverberation time. Proceedings of the ninth Symposium of mathematics and its applications.* November 1–4, 2001, Timişoara pages 227-232.

ISIRR 2003

DIGITAL INTERFACE BOARD WITH FOUR 8-BYTE OUTPUT PORTS

[1] TIRIAN Gelu Ovidiu

[1] University "POLITEHNICA" TIMISOARA,
Faculty of Engineering HUNEDOARA

Summary:

This work presents a digital interface board with four 8-byte output ports to be connected to the ISA bus of the computer. The 4 ports can be addressable anywhere in the address space of the port by using the 3 jumpers.

Key words: *digital interface, output ports.*

1. INTRODUCTION

The digital interface board with four 8-byte output ports has been created in didactic scope.

The output ports have a 25 mA stream capability (in either HIGH or LOW state). The four output ports are implemented by four 74373 circuits (8-byte Bus Driver with HZ and LATCH capability).

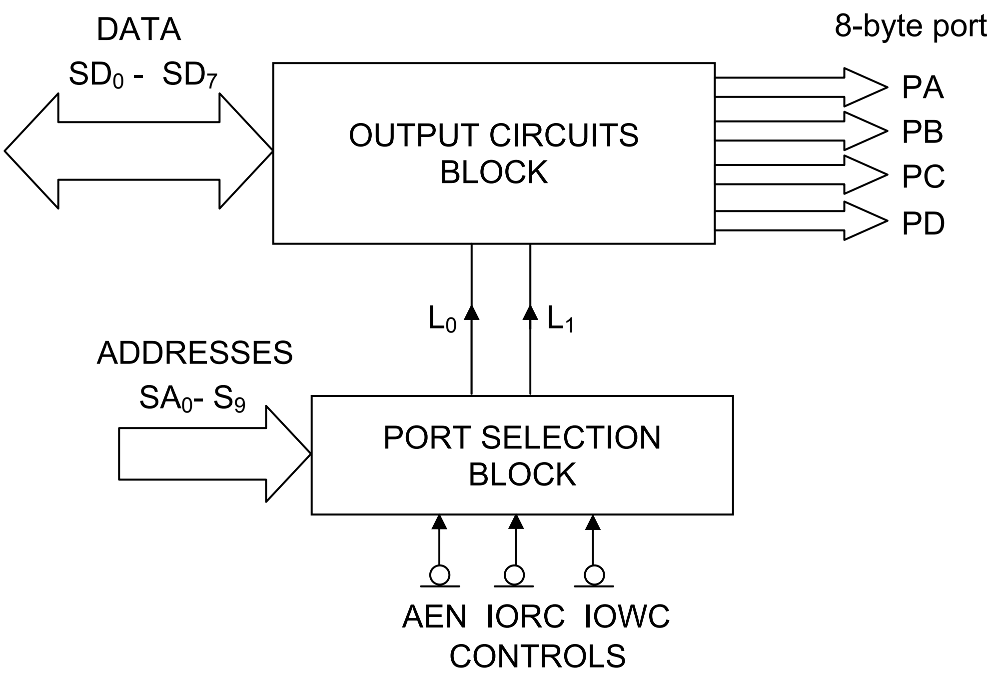

Fig. 1. *The block diagram*

The block diagram of the board is described in Fig. 1 and contains the selector block implemented by 4 BCD decimal decoders, as well as the input circuits block that has 4 output circuits.

These two blocks are connected to the address, data and control buses, as follows:

a) The input circuits block to the data buses (SD_0- SD_7)
b) The port selection block to the address buses (SA_0- SA_9) and to the control buses (AEN, IORC, IOWC).

2. THE SYNTHESIS OF THE DECODER

The decoders can be defined as demultiplexer circuits for which the input is at logic level 1 I= 1 (+V). In this case, according to the Boolean operation that describes the action of the DEMUX, the circuit becomes a code identifier. This is realized because each output will identify one of the input operations. Therefore, the decoders can be represented as a block diagram like in Fig. 2.

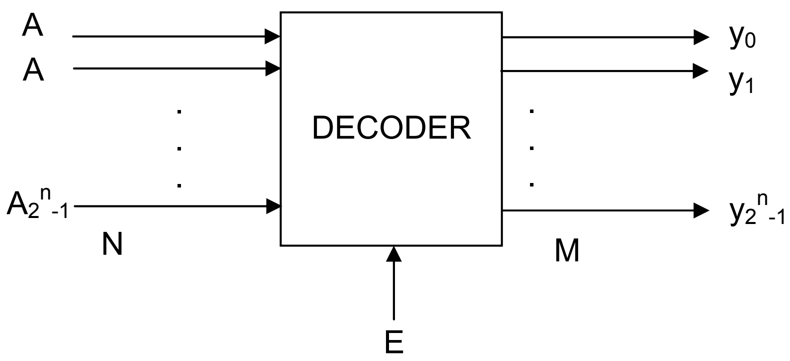

Fig. 2. *The block diagram*

Let N be the binary number expressed by the input combination and M the binary number expressed by the output combination. Thus, it can be written:

$M= 2^N$

As one can notice, the expression obtained is an inverse function of the function realized by the decoder, for which the encoding outputs were obtained as $M= \log_2 N$.

The decoders can also be found as an M.S.I. circuit, implemented in TTL (with the active outputs on 0) and CMOS (with the active outputs on 1) technology.

Generally, these integrate circuits are 4-byte decoders.

The binary-decimal decoder

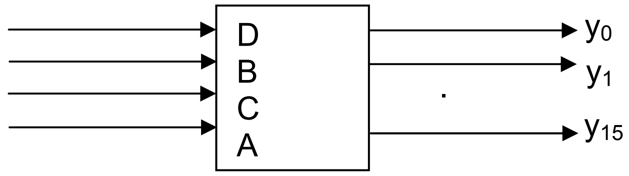

Fig. 3 *The block diagram*

Related to the principle of working, the decoders can be:

- binary
- BCD
- BCD- 7 segments

The working of the circuit can be briefly described in the truth table (Table 1):

Table 1

No.	D	C	B	A	Active outputs	Active outputs
0	0	0	0	0	y_0	y_0
1	0	0	0	1	y_1	y_1
2	0	0	1	0	y_2	y_2
3	0	0	1	1	y_3	y_3
4	0	1	0	0	y_4	y_4
5	0	1	0	1	y_5	y_5
6	0	1	1	0	y_6	y_6
7	0	1	1	1	y_7	y_7
8	1	0	0	0	y_8	y_8
9	1	0	0	1	y_9	y_9
10	1	0	1	0	y_{10}	-
11	1	0	1	1	y_{11}	-
12	1	1	0	0	y_{12}	-
13	1	1	0	1	y_{13}	-
14	1	1	1	0	y_{14}	-
15	1	1	1	1	y_{15}	-

The decoder can identify by its outputs any combination of inputs. The binary-decimal decoders can be used for the implementation of logical functions, but they can especially be found in the memory circuits, for the selection of the cells addressed at a certain time. They can also be used for the selection of the memory circuits and input-output circuits within the systems with µP.

The decoding was carried out by means of 4 decoders. The four binary-decimal decoders (ic1-ic4) achieve a complete decoding of the address space reserved to the ports, using the SA9-SA0 and AEN, IORC, IOWC signals (table 2).

Table 2

	SP1			SP2			SP3						
AEN	SA 9	SA8	SA7	SA6	SA5	SA4	SA3	SA2	SA1	SA0	IOWC	IORC	DESCRIPTION
1	X	X	X	X	X	X	X	X	X	X	X	X	-
0	X	X	X	X	X	X	X	X	X	X	X	X	-
										0	0	1	PA
										1	0	1	PB
										0	1	0	PC
										1	1	0	PD
										X	1	1	IMPOSSIBLE
	0 – 34			0 – Fh			0 - Fh						

In order to assign the port addresses, 340h- 341h for example, the JP1- JP3 jumpers must be set as it follows:

JP1	JP2	JP3
$X \longrightarrow 6$	$Y \longrightarrow 3$	$Z \longrightarrow 0$

3. CONCLUSIONS

This work carried out the study of the board that will be connected to the ISA bus of the computer. This board was built and its functioning was tested by means of a program that represents a four non-multiplexed display-cell decimal counter.

4. REFERENCES

1. *Poantă, A., Sisteme cu microprocesor, Note de curs*

2. *Lupu Stăncescu, Microprocesoare. Circuite. Proiectare, Editura Militară, Bucureşti, 1986*

STUDY OF MACHINE DYNAMICS PHENOMENA WITH JAVA APPLETS

PhD. Gillich Gilbert-Rainer[1]
PhD. Nadia Potoceanu[2]
PhD. Constantin Marta[2]

[1]Universitatea „Eftimie Murgu" Reşiţa
[2]Universitatea „Eftimie Murgu" Reşiţa

Abstract:

The work presents a modern instrument for learning and understanding physical phenomena, implicit special phenomena witch appears in the study of "Machine dynamics", using Java applets. This kind of programs is preferred, because Java is free, is good supported by various browsers and is very flexible.

Keywords:
Java, applets, machine dynamics, learning tools

1. INTRODUCTION

The Java language was developed at Sun Microsystems in December 1990 as part of the Green project, a small research effort into consumer electronics. Researchers were working on a programming language for smart appliances. The language was named Oak in honor of a tree Gosling could see out his office window. It was renamed in 1995 Java in honor of the lawyers who found out about another product called Oak and didn't want to go out on a limb. It was an inventive toy for the World Wide Web that had the potential to be much more. The word "potential" is an unusual compliment, because it comes with an expiration date. Sooner or later, potential must be realized or new words such as "letdown," "waste," and "major disappointment to your mother and I" are used in its place. Now in its fourth major release, Java appears to have lived up to the expectations that accompanied its arrival. More than two million people have learned the language and are using it in various domains. First used to create simple programs on World Wide Web pages, Java can be found today in a lot of, yesterday unusual, places. Java is now present in each of the following places and many more:

- Web servers
- Relational databases
- Mainframe computers
- Telephones
- Orbiting telescopes
- Personal digital assistants
- Credit card-sized "smartcards"

An interesting field of appliance is the educational system. This because Java is:

- small - Programs load reasonably quickly on a Web page
- secure - Safeguards protect against programs that cause damage, whether accidental or intentional
- portable - Owners of Windows, Macintosh, Linux, and other operating systems can run the same program in their Web browsers without modification
- free - …

Java is an object oriented programming language. He creates two kinds of programs: applications and applets. An applet is a piece of software code that runs under the control of a web browser, as distinct from the application which requires an interpreter. Applets are commonly used to enhance the interactivity of a web page, and deliver client-side content. Applets run in their own frame, and can display graphics, accept input from GUI components, and even open network connections. Due the potential security risks associated with running applets from external and potentially malicious sources, most web browsers limit file access, and impose additional restrictions on applets.

2. STUDY OF MACHINE DYNAMICS WITH JAVA SUPPORT

The study of physical phenomena, mechanics make not a difference, request good and divers laboratory equipment. It is very hard or not possible to have this in all our schools or universities. So Java applets can successful substitute the laboratory equipment, or to complete it.

In my experience in teaching Machine dynamics I use to work with applets. Located in html files in a browser like Internet explorer it has the advantage to combine the possibilities of both. This are: the capability to present hypertext with the theoretical presentation, the possibility to link the student to appropriate or similar pages, the interactivity and visualization. So, introducing new dates the student can observe the influence in the system, he/she can call information about the subject from other places (internet or local network), can print the results and so on.

Next is presented an example linked to wave superposition, an important phenomena in Machine dynamics. The applet can be used to illustrate phenomena in both dispersive and non-dispersive media. For non-dispersive media, the user must enforce

$$| w_1/k_1| = |w_2/k_2| \quad (1)$$

when specifying input values.

In the laboratory the student opens the html site and can see the following image (***Fig 1***).

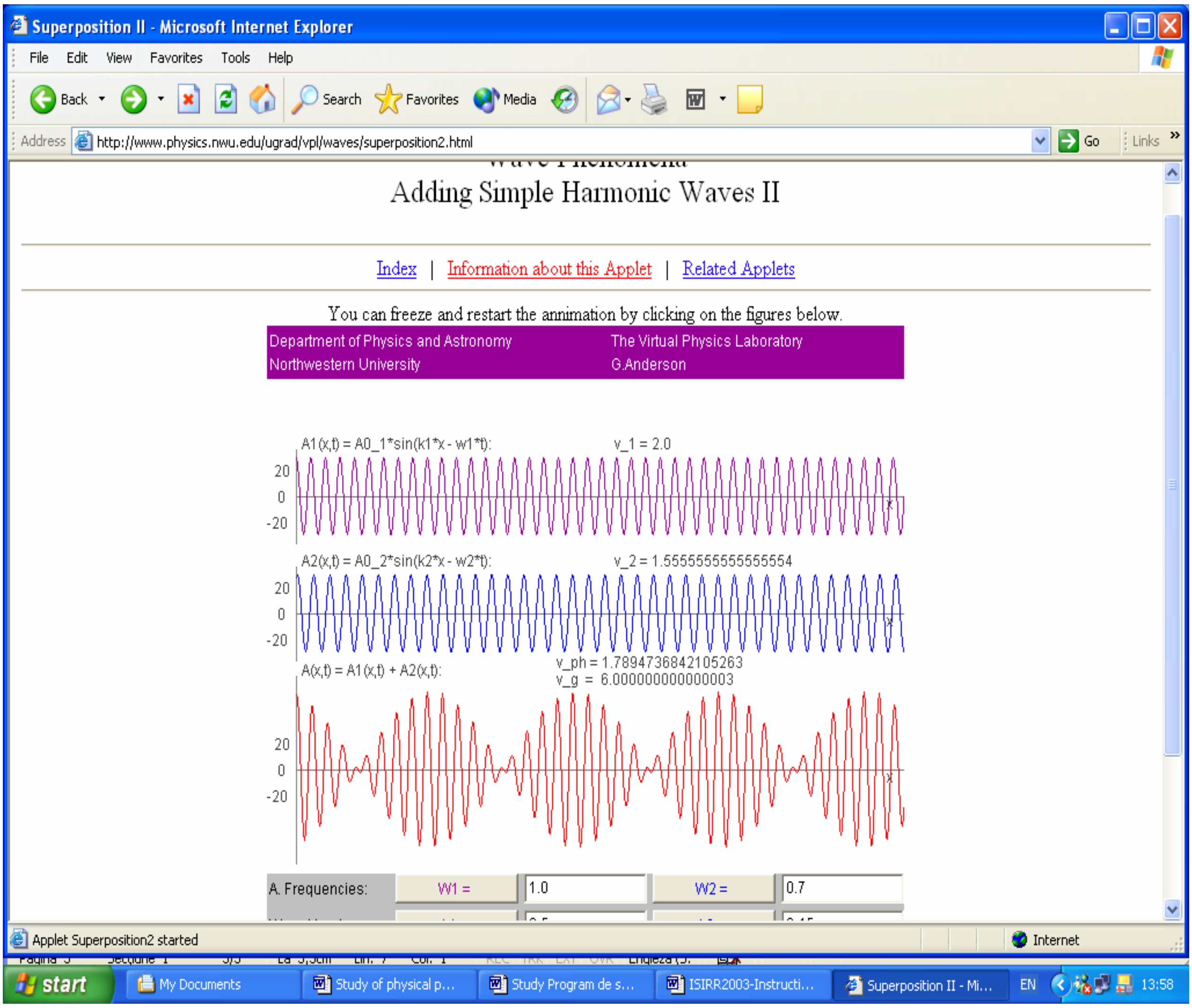

Fig. 1 *Adding simple harmonic waves*

The student can see what happens in case of wave superposition. Now, he/she can look in the theoretical background of the problem with a simple link. A dvi., postscript or pdf document is available. In the new window appears ***Fig. 2***. for the pdf version. This permit a revue of the in courses learned elements, useful to understand the illustrated phenomena. With help of theoretical knowledge the students calculate the new waves equation, and then compare it with the applets result. Parameters of the both waves (amplitudes, frequencies and phases) can be modified.

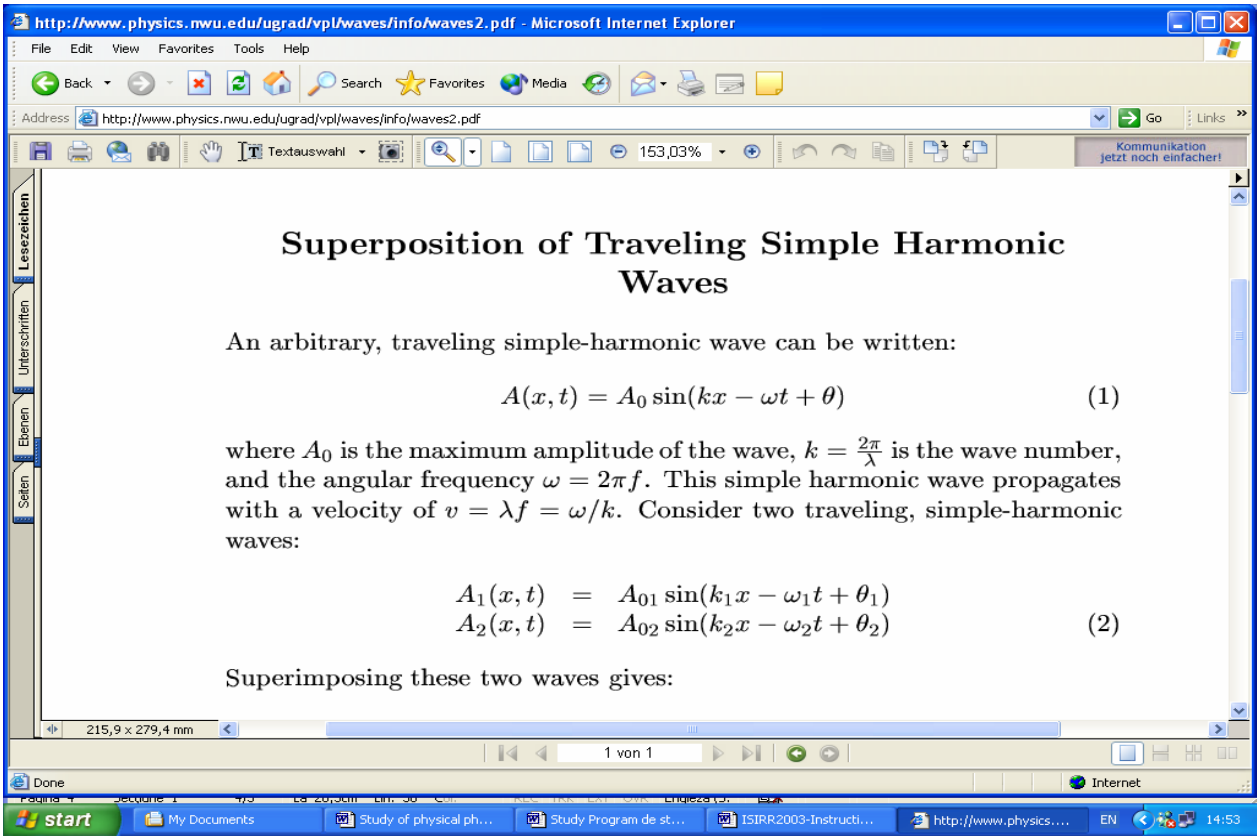

***Fig. 2** Theoretical background of the applet*

It can be evidenced a various number of phenomena, like beats, resonance or amplitude modulation.

Examples of applets are presented in the following pictures, where beats (***Fig. 3***) and resonance (***Fig. 4***) are studied.

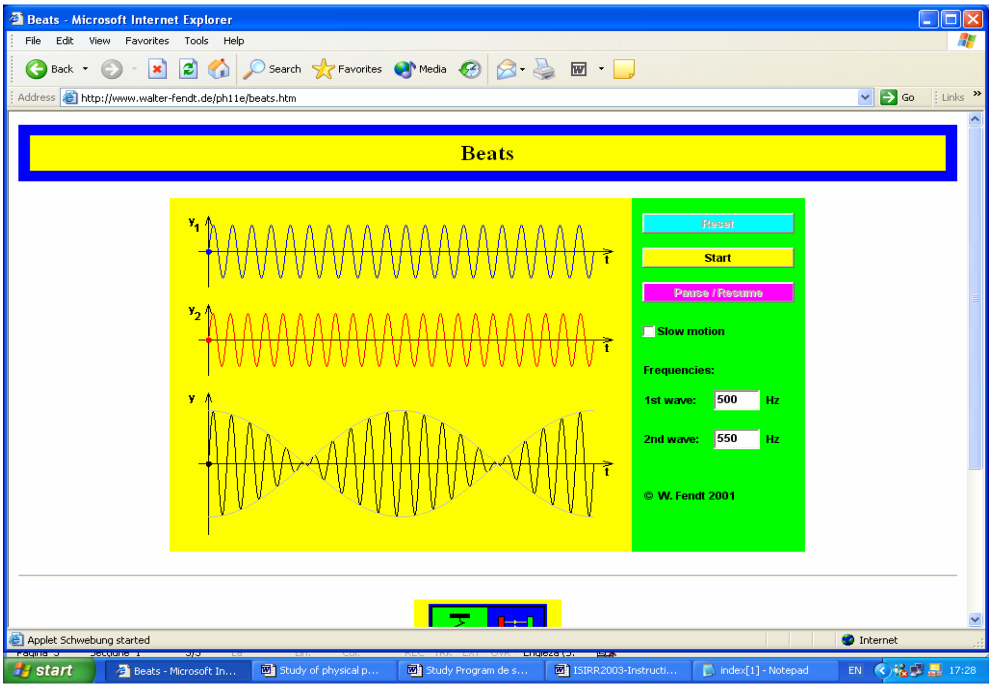

***Fig. 3** Beats phenomena modeled with Java applet*

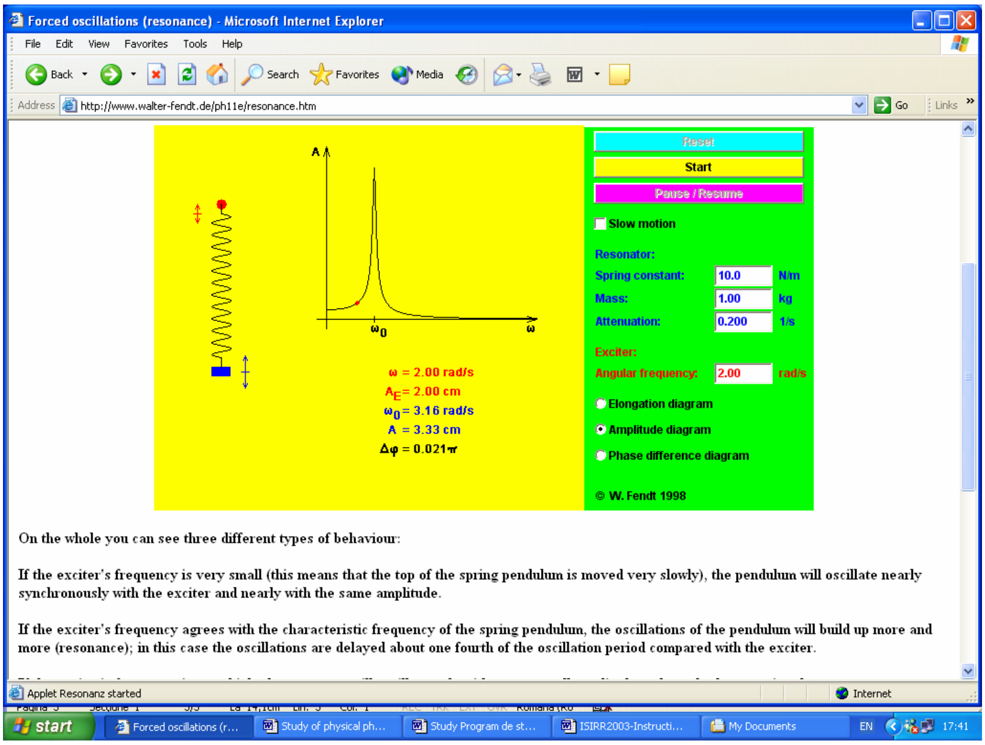

Fig. 4 *Resonance phenomena modeled with Java applet*

In these two applets the students can change the entering parameters - like frequency, mass, spring constant, attenuation - and so they can see the transformation in the studied system. The programs allow also designing diagrams for elongation, amplitude and phasing difference.

3. CONCLUSIONS

Java is a simple object orientated language, useful in educational process; it allows a lot of application. The dimension, high security, portability and in special because it's free make Java an interesting tool for teachers in the teaching process. Students like to work with applets because the interactivity transforms the educational process in a game. So, Java is a kindly tool more and more used in education.

4. BIBLIOGRAPHY

[1] Lemay L., Cadenhead R. - Teach Yourself Java 2 in 21 Days, SAMS Publishing, 1999

[2] Lalani S., Jamsa K. – Biblioteca programatorului Java, Ed. ALL Educational, Bucureşti, 1997

[3] Manger J. – Netscape Navigator, Ed. Teora, Bucureşti, 1998

[4] *** - Web pages

INDUSTRIAL STUDY UPON THE BASIC CHEMICAL COMPOSITION OF THE NODULAR CAST IRON ROLLS

[1] Imre KISS; [1] Vasile CIOATA; [1] Vasile ALEXA; [1] Maria SCURTU

[1] "POLITEHNICA" UNIVERSITY – TIMISOARA,
FACULTY of ENGINEERING – HUNEDOARA, ROMANIA

ABSTRACT

In our foundries, specialised in the cast iron rolls, in spite of trying the most accurate guidance of the iron melting processes, of the outside treatments melting aggregate, of the moulding and drying of moulds (the so-called casting process), of the cooling and the directional solidification of the castings in the moulds, as well as of the rapping, cleaning and the subsequent processing of the rolls, the performance factor remains relatively low.

This paper presents some considerations upon the mechanical properties, especially the hardness of the iron rolls, assured by the chemical composition and tries to draw some conclusions upon the optimal composition of this irons destined for rolls casting. Also, the paper presents the results of some researches regarding the chemical composition of the irons (with nodular graphite) destined for casting semihard rolls. It is presented, in graphical form, the influence of each chemical element, from the composition of these irons on the hardness, measured on the crust and the necks. Also, the hardness variation graphic is presented, with the carbon equivalent value.

KEYWORDS:
nodular semihard cast iron rolls, basic elements, hardness

1. INTRODUCTIVE NOTES AND PRESENTATION

The technical conditions, which are imposed to the cast iron rolls in the exploitation period, are very different and often contradictory. The obtaining of various physical and mechanical properties in the different points of the same foundry product meets difficult technological problems in the industrial condition. This supposes us to know many technological factors, which lead to this deformation equipment.

The rolls must present high exploitation qualities, which are determined from the hardness, resistance and high temperature stability.

These qualities assure the high resistance at the wear in dried friction conditions, as well as the stability at unexpected temperature variations in the rolling operation, resistance at the thermal fatigue (because the rolls are heated at the contact of the laminate), high resistance at the thermal shock stress, as well as the bending strain. Also, the rolls must assure the clamping of materials, as well as the high quality of laminate surface.

The rolls must present high hardness at the crust of rolls and lower in the care and the neck's, adequate with mechanical resistance and in the high work temperature. If in the crust, the hardness is guarantied by the quantities of cementite in the structure of irons, the core of rolls must be content graphite, to assure this property.

One of the parameters, which are determined the structure of the irons destined for rolls casting, its is the chemical composition. If we do not respect this composition, which guaranties the exploitation properties of the each roll in the stand of rolling mill, leads to rejection. First, the hardness achievement of the crust of rolls, fixed strictly by the standards for each type in part, is conditioned by the achievement of the structure of iron (which contains pearlite, cementite and graphite). This structure is a result of the correct chemical composition, which is respected at elaboration, and the modification treatment of the graphite nodularity, in the case of irons with nodular graphite.

In our foundries, specialised in the cast iron rolls, in spite of trying the most accurate guidance of the iron melting processes, of the outside treatments melting aggregate, of the moulding and drying of moulds, the so-called casting process, of the cooling and the directional solidification of the castings in the moulds, as well as of the rapping, cleaning and the subsequent processing of the rolls, the performance factor remains relatively low.

The industrial analysis included charges of rolls from different hardness classes (semihard, hard), with definite and indefinite crust, in simplex or duplex cast processes. The main defects, which appear in the weight or on the surface of the rolls, are presented in their great variety on the figure 1, in graphical form.

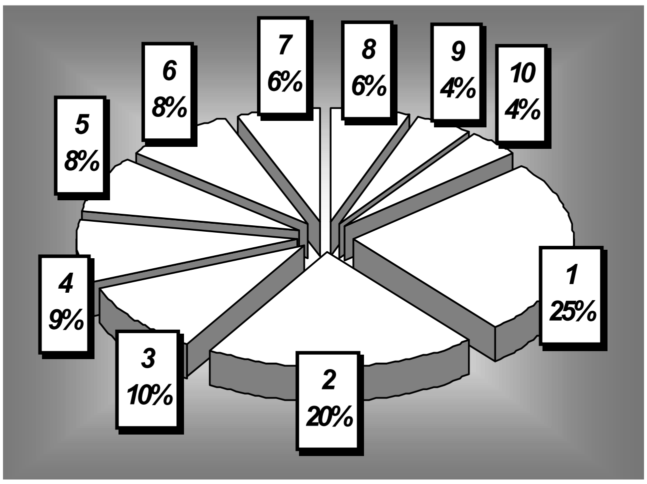

Figure 1.
The Repartition of the Cast Iron Rolls Rejection Forms
1. pockets (pipes);
2. cracks (longitudinal or transverse, at heat or at cold);
3. insufficient or extended depth of the roll's hard crust;
4. inadequate hardness at the necks and the body of roll;
5. inclusions and adherences;
6. shrinkages and porosities;
7. inadequate chemical composition;
8. texture defects;
9. inadequate base size;
10. other defects

From the total quantity of rejects, the pockets in the mass of the castings cause more than 25% and the causes for the presence of the pockets are various. The cracks (longitudinal or transverse) represent almost 20% from the total mass of rejects. Avoiding the occurrence of cracks is an extremely complex task, which requires an adequate respect of the rolls production technologies, especially in the preparation of the chill for casting.

Another group of defects, which lead to rejection, consists of inadequate depths of the hard crust of the rolls. These defects may consist of insufficient thickness of the crust, or of excessive thickness, instead of the specified ones by their subsequent destination. The uneven thickness on the height of the crust, on the rolling face, leads to rejection, too.

The rejected rolls quantity, caused by the inadequate hardness of the crust (the rolling surface), as well as of the necks and the core of rolls, is approximately 9% from the total reject forms. The insufficient or extended depth of the roll's hard or semihard crust is caused by the other 10% from the reject forms. In 6% of the situations, the rejection is caused by structural and texture defects.

2. TECHNICAL AREA OF ANALYSES

This study analyses iron rolls cast in the simplex procedure, in combined forms (iron chill, for the crust and moulding sand, for the necks of the rolls). The research included rolls from the semihard class, with hardness, between 33…59 Shore units (219…347 Brinell units) for the 0 and 1 hardness class, measured on the crust, respectively 59…75 Shore units (347…550 Brinell units), for the class 2 of hardness.

This study is required because of the numerous defects, which cause rejection, since the phase of elaboration of these irons, destined to cast rolls. According to the previous presentation, it results that one of the most important reject categories is due to the inadequate hardness of the rolls. The recommended hardness of these, on the crust, as well as on the necks and in the core of rolls, fixed by the standards, is presented in *table 1*. The recommended chemical composition for the semihard class rolls, cast from lamellar graphite iron (type FS) and nodular graphite iron (type FNS) is presented in *table 2*.

Table 1. *The Recommended Hardness of the Semihard Cast Iron Rolls*

Analysed Roll Types	*Class of Hardness*	***Recommended Hardness for these Rolls***			
		on the Crust (Surface) of Rolls		*on the Core and the Neck's of Rolls*	
		[Shore Hardness]	*[Brinell Hardness]*	*[Shore Hardness]*	*[Brinell Hardness]*
FNS	*0*	*33…42*	*218…286*	*30…40*	*195…271*
FNS	*1*	*43…59*	*294…347*	*30…40*	*195…271*
FS	*2*	*59…68*	*420…491*	*35…45*	*218…309*
FNS	*2*	*69…75*	*499…550*	*35…45*	*218…309*

Table 2. *The Recommended Chemical Composition of the Semihard Cast Iron Rolls*

Types of Rolls	Chemical Composition, [%]								
	C	Si	Mn	P	S	Ni	Cr	Mo	Mg
FS	2,9... 3,6	0,3... 1,2	max 0,6	max 0,15	max 0,1	max 0,6	max 0,5	0,3... 0,5	-
FNS	3,0... 3,5	1,2... 2,5	0,1... 0,7	max 0,15	max 0,02	1,5... 2,5	max 0,8	0,3... 0,5	0,02... 0,04

The chemical composition include both the basic elements (*C, Si, Mn, S, P*), and the alloying elements (*Cr, Ni, Mo*), as well as the magnesium content (in the case of nodular irons). In special cases, these irons can contain up to 0,15…0,2% vanadium. Also, in the case of elaboration of irons with nodular graphite, destined to casting rolls (type *FNS*), a higher content of phosphorus is accepted, because this chemical element participates at the hardening of the rolling surface of the rolls.

3. RESULTS OF ANALYSES

The research includes semihard cast rolls, from nodular graphite irons (type FNS), hardness class 1 and 2, with the semihard crust of 40…150 mm depth. The lot of analysed rolls is representative for the semihard category, the chemical composition and the measured hardness of that is presented in table 3. The hardness checking, both on the two necks of the rolls, and on the rolling surface, are made in equidistant points of the manufactured surfaces, according to the standard stipulation. The measured values of the hardnesses are presented in table 3.

The value of the equivalent carbon, calculated by the formula *I*, is recommended to be maximum 4,3%, for castings with the heavy thickness (in this case of rolls). Also, for the equivalent carbon value calculation, the formula *II* is accepted, too.

$$C_{ech} = C + 0,3\ (Si + P) - 0,03\ Mn + 0,4\ S + 0,07\ Ni + 0,05\ Cr\ [\%] \qquad (I.)$$

$$C_{ech} = C + 0,33\ Si + 0,1\ Ni\ [\%] \qquad (II.)$$

Table 3. *The Chemical Composition and the Measured Hardness of the Semihard Cast Iron Rolls*

Chemical Composition [%]					C_{ech} [%]	**Hardness** [Brinell units]	
C	**Si**	**Mn**	**P**	**S**		on the Necks	on the Crust
3,22…3,42	1,72…2,19	0,62…0,79	0,13…0,165	0,011…0,024	3,952 - 4,219	219…276	282…352
Ni	**Cr**	**Mo**	**Mg**				
1,49…2,22	0,36…0,72	0,18…0,28	0,021…0,029				

The main basic element of the irons composition is the carbon, which is influenced, both on the hardness, and on the strength of rolls. In this case of the semihard iron rolls, this chemical element varies between 3,0…3,5%, that assures the recommended hardness of the crust

(220…420 Brinell units) and of the core and of the necks (220…300 Brinell units). The chemical composition, analysed after the elaboration period, in the case of carbon content (3,22…3,42%), fits in the established values, while the hardness is between 219…276 Brinell units, measured on the different points of necks, respectively between 222…352 Brinell units (*table 3*).

The silicon percentage in these irons, destined to rolls casting, is in close dependence with the carbon content. With the growth of silicon and carbon content in the chemical composition of these irons, the semihard crust's thickness is narrowed, due to the growth of the graphite's quantity.

The separate effect of each of them is stronger when one of the elements is in a smaller or a larger proportion accordingly. But their action is similar. The silicon has influence upon the refinement of graphite, being one of the elements that have graphitesing effect and favours the presence of graphite in the core of rolls.

The hardness variation by the carbon and silicon content, on the crust and the necks, is presented in *figure 2*, respectively in *figure 3*. The chemical composition showed that the silicon varied between the values of 1,64…2,19%, which are accepted by the FNS types cast iron rolls standard (1,2…2,5%). *Figure 3* remarks the hardness diminution with the silicon content growth in the composition of these irons, the variation being similar with a carbon variation.

At a lower limit of manganese content, this element has a strong anti-graphitesing effect. Above the 0,7% in the manganese content of irons, the carbides are stabilised and the hardness is increasing. Above 1,0%, the manganese acts like alloying element, stabilises the cementite, and implicitly hardens the irons. The hardness variation with this chemical element is presented graphically in *figure 4*.

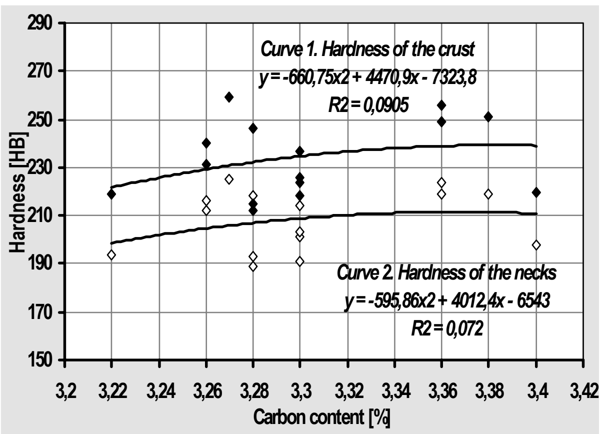

Figure 2.
The Hardness Dependence with the Carbon Content at the Semihard Cast Iron Rolls

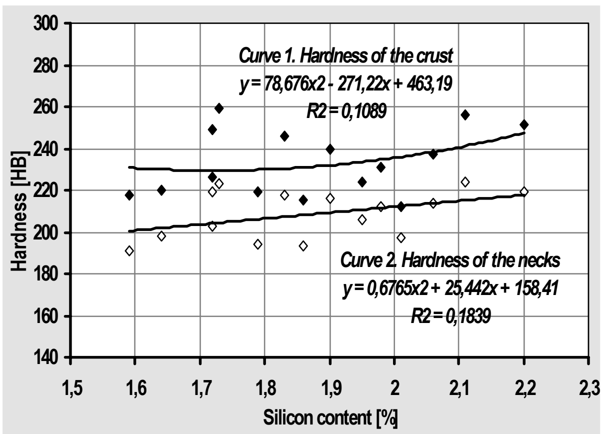

Figure 3.
The Hardness Dependence with the Silicon Content at the Semihard Cast Iron Rolls

The sulphur in these irons is recommended to be in minimal quantities, because this element has an unfavourable effect upon the mechanical properties; the hardness, as well as the strength decreases while the sulphur content grows. Also, the content of sulphur in the chemical composition affects the graphite nodularity, in case of nodular graphite irons, so there is a need to reduce it to the minimum. In this condition, the sulphur contents are strictly imposed and are recommended to be at maximum 0,02 %.

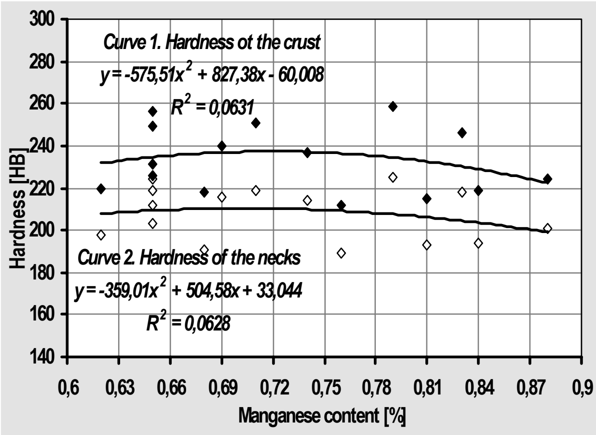

Figure 4.
The Hardness Dependence with the Manganese Content at the Semihard Cast Iron Rolls

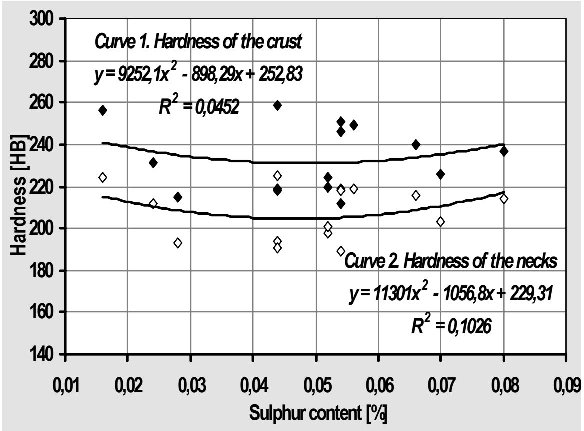

Figure 5.
The Hardness Dependence with the Sulphur Content at the Semihard Cast Iron Rolls

The graphical representation of hardness (*figure 5*) presents the optimal value of the hardness, on the crust and in the core of these rolls, for the analysed chemical composition. The graphic is made according to this data, and presents the hardness dependence with the sulphur content. In the conditions of the sulphur content limitation to the standard values, this element cannot prejudice the structure of the irons. Above this value, the sulphur has a negative value upon the irons' mechanical properties.

Figure 6.
The Hardness Dependence with the Phosphorus Content at the Semihard Cast Iron Rolls

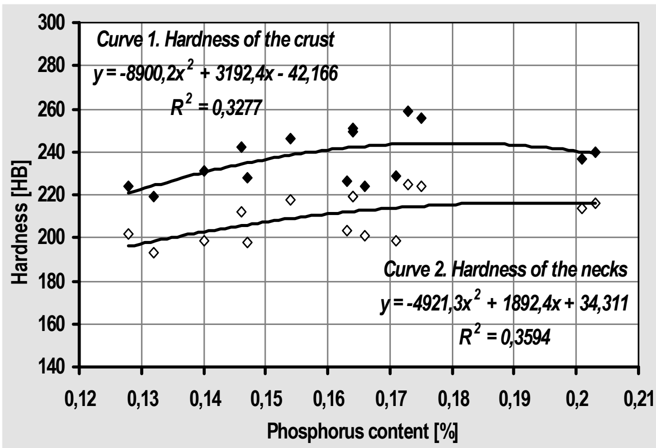

In the case of semihard rolls, the phosphorus content is limited to a maximum of 0,2…0,3%. Because this chemical element shapes tough compounds, needed in the rolling surface, the phosphorus does not affect, if limited in the recommended intervals. The increase of hardness can be observed in the graphic of *figure 6*, together with the growth in the chemical composition of phosphorus percentage.

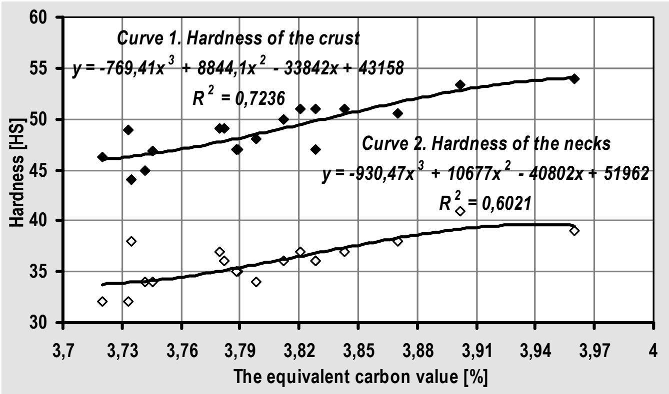

Figure 7.
The Hardness Dependence (on the Necks and on the Semihard Crust of Rolls) with the Value of Equivalent Carbon

Figure 7. presents the hardness variation both on the crust and on the necks and in the core of the rolls according the equivalent carbon values, calculated for the each chemical composition in part. A smooth increase of the hardness is to be noticed at higher values of the equivalent carbon and also a concentration of the marks for hardnesses at values of approximately 3,7…3,8%. Having in view the considerable stress during the workings of the rolls, high mechanical properties (resistance to wear, resistance to abrasion, resistance to thermal shock, hardness on the rolling surface and in the core and on the necks, etc.) are imposed on them. Consequently the equivalent carbon content diminishes from 4,2% (its value stands between 3,8 ÷ 4,0%), as the irons are hypoeutectic.

4. CONCLUSIONS

- in the processing phase of the irons, the hardness is adjusted through the quality of the metallic charge and of the addition materials, as well as through a proper leading of the melting and of the processing; An optimal proportion between the silicon and the manganese contents is needed both from the basic metallic charges and from the ferro-alloy addition (FeSi, FeMn, SiMn);
- the optimal values of the chemical composition in the main elements (C, Si, Mn, S, P) of this irons destined to the cast of the semihard rolls are to be found on the diagrams on figures 3…7. According to them the optimal values in the concentration of each main element can be noticed, values that can assure the adequate hardness on different areas of the rolls; a special importance is needed to be given to the sulphur from this irons, as it can effect the nodularity;
- for a narrower semihard or hard crust on the rolling surface of the rolls, a supplementary addition of FeSi is made, which released the silicon, thus segregating supplementary quantities of graphite in the crust area and narrowing the crust; For crusts of increased depth a supplementary addition of carbides is made to heighten the quantity of the tough formation cementite;
- the main chemical composition must be correlated with further addition of alloying elements, respecting the adequate proportions between nickel and silicon, chrome and nickel, molybdenum and phosphorus, sulphur and magnesium, besides an optimal ratio of carbon and silicon.

5. BIBLIOGRAPHY/REFERENCES

1. BUDAGHIANŢ, N.A., KARSSKI, V.E. - *Cast Iron Rolls,* Editura Tehnică, Bucureşti, 1984.
2. DIETER, G.E.: *Mechanical Metallurgy,* Editura Tehnică, Bucureşti, 1970
3. PIWOWARSKI, E.: *High Quality Irons,* Editura Tehnică, Bucureşti, 1967
4. SOFRONI, L., RIPOŞAN, I.: *Iron Casting*, Editura Tehnică, Bucureşti, 1985
5. SOFRONI, L., STEFANESCU, D.M.: *Special Irons*, Editura Tehnică, Bucureşti, 1974
6. SOFRONI, L., STEFANESCU, D.M.: *Inoculate Irons with High Properties*, Editura Tehnică, Bucureşti, 1971
7. SOFRONI, L., STEFANESCU, D.M.: *Irons with Nodular Graphite*, Editura Tehnică, Bucureşti, 1974
8. RIPOŞAN, I.: *Nodular Graphite Iron for the Cast Iron Rolls*, in: Buletin of University Politehnica Bucureşti, 1980/3
9. SOFRONI,L., RIPOŞAN, I.: *Contribution for the Improvement of the Cast Iron Rolls Quality,* in: Metalurgia, 1983/10
10. KISS, I.: *Considerations upon the Reject Forms of the Cast Iron Rolls,* at Scientific Conference, Bucureşti, 2000
11. KISS, I.: *The Hardness of Cast Iron Rolls with Indefinite Structure,* in: Symposium, Petroşani, 2001
12. KISS I., HEPUŢ T.: *Mechanical properties of the cast iron rolls, assured by the chemical composition*, Buletinul Ştiinţific al Universităţii Politehnica Timişoara – Mechanics series, 2002
13. KISS I., HEPUŢ T.: *The hardness of the cast iron rolls, assured by the alloy elements and the modification treatment of the graphite nodularity*, Buletinul Ştiinţific al Universităţii Politehnica Timişoara – Mecanics series, 2002
14. KISS I., RATIU S., VILCEANU L, ALEXA V.: *Particularităţi ale proprietăţilor mecanice la cilindri de laminor turnaţi din fonte cu grafit nodular*, Simpozion International Universitaria ROPET, Petroşani, 2002
15. A. JOSAN, D. PETRE, I. KISS.: *Studies and researches on the influence of chemical composition of cast rolls made of hypereutectic steel, on their hardness in exploitation*, Scientific Conference Research and Development of Mechanical Elements and Systems JAHORINA – IRMES, Sarajevo, Bosnia & Herzegovina, 2002
16. KISS I.; RAŢIU S.; NICA GH.: *Some considerations regarding the mechanical properties of the cast iron rolls, assured by the chemical composition and the modification treatment of the graphite nodularity (I)*, Scientific Conference Research and Development of Mechanical Elements and Systems JAHORINA – IRMES, Sarajevo, Bosnia & Herzegovina, 2002
17. KISS I.; JOSAN A; CIOATĂ V.: *Some considerations regarding the mechanical properties of the cast iron rolls, assured by the chemical composition and the modification treatment of the graphite nodularity (II)*, Scientific Conference Research and Development of Mechanical Elements and Systems JAHORINA – IRMES, Sarajevo, Bosnia & Herzegovina, 2002
18. KISS I., HEPUŢ T., RAŢIU S.: *The Hardness Of The Cast Iron Rolls, Assured by the Alloyed Elements and the Modification Treatment of the Graphite Nodularity*, in: "MASINSTVO" – Journal of Mechanical Engineering, No.1 / 2003, Zenica, Bosnia & Herzegovina
19. KISS I.: *The Mechanical Properties of the Semihard Cast Iron Rolls Assured by the Basic Elements*, in: "MASINSTVO" – Journal of Mechanical Engineering, No.4 / 2003, Zenica, Bosnia & Herzegovina

ALLOYED ELEMENTS FOR THE NODULAR CAST IRON SEMIHARD ROLLS

[1] Imre KISS; [1] Sorin RATIU; [1] Ana JOSAN; [1] Maria SCURTU

[1] "POLITEHNICA" UNIVERSITY – TIMISOARA,
FACULTY of ENGINEERING – HUNEDOARA, ROMANIA

ABSTRACT

The technical conditions, which are imposed to the cast iron rolls in the exploitation period, are very different and often contradictory. The obtaining of various physical and mechanical properties in the different points of the same foundry product meets difficult technological problems in the industrial condition. This supposes us to know many technological factors, which lead to this deformation equipment.

The rolls must present high hardness at the crust of rolls and lower hardness in the core and on the necks, adequate with the mechanical resistance and in the high work temperatures. If in the crust the hardness is assured by the quantities of cementite from the structure of the irons, the core of the rolls must contain graphite to assure these properties.

One of the parameters, which determine the structure of the irons destined for rolls casting, is the chemical composition. If we not respect this composition, which guaranties the exploitation properties of the each roll in the stand of rolling mill, it will lead to rejection. Also, the inadequate treatment with magnesium for obtaining the nodular graphite's iron can produce one of the important forms of rejection in the case of cast iron rolls. This paper presents an analysis of the main factors in the practical conditions of the foundry, factors that have influences on the durability of the magnesium treatment and on the later inoculation effect on irons destined to cast rolls, and presents also some graphical addenda.

KEYWORDS: *nodular semihard cast iron rolls, alloyed elements, hardness*

1.INTRODUCTION

Ductile iron belongs to the family of cast graphitic irons, which possess high strength, ductility and resistance to thermal shock. Its strength, toughness and ductility duplicate many grades of steel and far exceed those of standard grey irons. Yet it possesses the advantages of design flexibility and low cost casting procedures similar to grey iron. The difference between ductile iron and grey iron is in the graphite formation.

The nodular graphite cast iron is considered as one of the most versatile roll materials nowadays. A small proportion of magnesium added to the melt as nickel-magnesium or alternative alloy, or as pure magnesium produces it. In the nodular graphite's iron roll, the free carbon takes the shape of spheroids or nodules, thereby eliminating the notch effect of flake graphite and improving upon the mechanical properties of the cast iron. Nodular graphite cast iron rolls are so superior in wear resistance to that of cast steel rolls that they are specially adapted for roughing and intermediate plate mills and rod or bar mill roughers. As a result of the spherical form of the graphite, these iron rolls are much stronger than rolls of the clear-chill type and the gradual fall in hardness is an added advantage. As such, these rolls are particularly suitable for strip mills, also bar billet mills, and are being increasingly used for other applications.

The improved mechanical properties increase its resistance to breakage from physical load, or mechanical and thermal shock far above that of grey iron. The corrosion resistance of ductile iron is equal or superior to grey cast iron and to cast steel in many corrosives. Its wear resistance is comparable to some of the best grades of steel and superior to grey irons in heavy load or impact load situations. Because it can be cast with the same low cost procedures used for grey iron it is considerably less expensive than cast steel and only moderately more expensive than grey iron.

The nodular cast iron rolls are characterised by the nodular shaped graphite in the microstructure. Through adjusting the alloy elements of nickel, chrome and molybdenum and heat treatment technique, the different type of rolls of popular nodular graphite cast iron. Large scale alloyed nodular graphite cast iron, pearlitic nodular graphite cast iron and acicular nodular graphite cast iron can be manufactured. All these types of rolls have high strength, excellent thermal properties and resistance to accidents and there is very little hardness drop in the surface work layer.

These type of material may be used to produce large scale rolls in double pouring process, the barrel of rolls has high hardness while the neck has high toughness, so these type of rolls exhibit the properties of high thermal stability and resistance to wear. As the characteristics of any casting are influenced by the microstruture that is formed during the solidification in the casting form, and under the influence of the cooling speed, the main criteria, which determines the mechanical properties of the rolls is the structure. All structural components can be found in cast iron rolls, each of the components having its own well-determined hardness. One of the parameters, which are determined the structure of the irons destined for rolls casting, its is the chemical composition. If we do not respect this composition, which are guarantied the exploitation properties of the each roll in the stand of rolling mill, leads to rejection of this.

All FNS type rolls are alloyed especially with chrome, nickel and molybdenum, in different percentages. The irons destined to these cast rolls belong to the class of low alloyed irons, with reduced content of these elements. The technological instructions firmly state the elements required to rise the quality of rolls. In this case, the contents of these elements stand between large limits. Also, the contents of these alloying elements can be reduced due to the strong effect of the magnesium from the nodulising agent, upon the structure and the form of the graphite.

3. RESULTS OF ANALYSES

In the case of the semihard cast iron rolls, the chrome has a less important influence than in the case of hard and extrahard rolls, as in their case the chrome proves to be the most efficient alloying element to regulate the crust depth. The semihard rolls have chrome content, which is preserved at low limits (a maximum of 0,6%), although this content still assures the necessary hardness on the rolling surface and in the core the rolls. According to the practical values, the graphic from figure 1 has been made, presenting the hardness variation with the chrome content of these irons. An increase of the hardness is to notice, together with a growth of the chrome content.

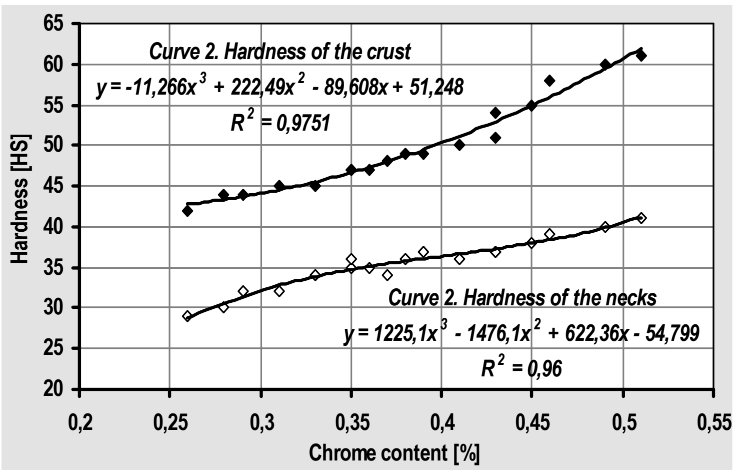

Figure 1. *The Hardness Dependence with the Chrome Content at the Semihard Iron Rolls*

The nickel addition leads to the improvement of the mechanical properties (resistance at wear, resistance at thermal shock, hardness and upon the workability of the cast rolls). If we do not allow this element to increase the graphitisation degrees and the white solidification in the peripherical area of the rolling surface, this content will be considerably reduced. Accordingly, the silicon content of the irons is modified, as this element replaces nickel.

Also, the nickel content is in close accordance with the chrome content of the irons, to favour the formation of the perlitical structure, without the massive and rough carbides. These two elements are added simultaneously, because the addition of chrome compensates the graphitising effect of the nickel. The proportion between the nickel and the chrome is situated between 2 ÷ 4. Figure 2 presents the optimal value of the hardness both on the crust and in the core of rolls, for the obtained contents of nickel. The variation is almost linear, maximum hardness being obtained at a higher limit of the recommended nickel.

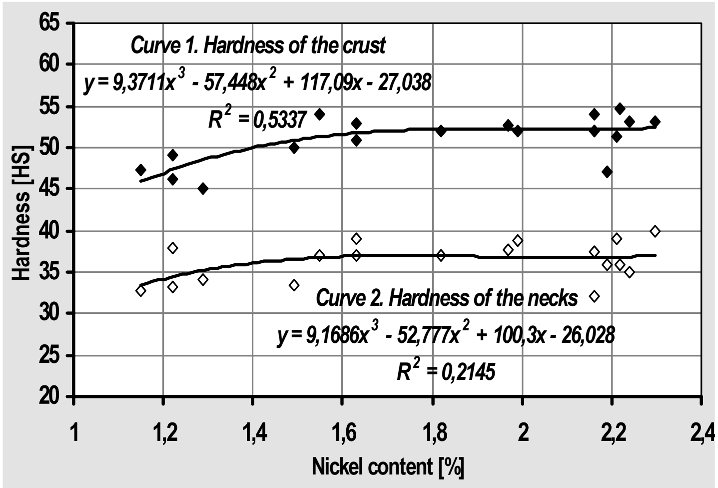

Figure 2.
The Hardness Dependence by the Nickel Content at the Semihard Iron Rolls

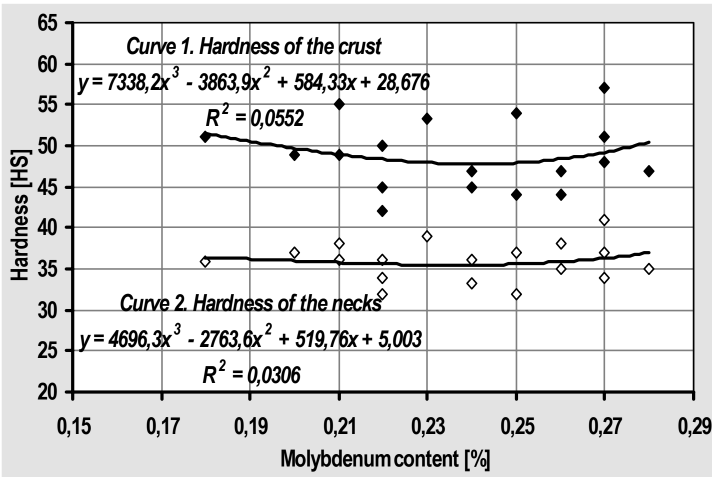

Figure 3.
The Hardness Dependence by the Molybdenum Content at the Semihard Iron Rolls

The molybdenum is a carburigenous element, but this effect is relevant only at percentage above 0,6%. Below this value, fine structures are obtained on the entire section, also an increase of the wear resistance and to high temperature stabilities, as well as a considerable mechanical resistance.

The molybdenum addition in the irons composition, increases both the resistance at the thermal shock and the fatigue resistance.

In the molybdenum alloyed irons, contents beyond a percentage of 0,15 %, are not recommended, because a portion of the molybdenum is lost through the combination with the phosphorus, and the molybdenum loses a part of its alloying element function.

In the case of semihard rolls, the content of phosphorus does not pass this limit, and is imposed by standards to 0,1…0,3%. The analysed nodular graphite irons present a molybdenum content, which varies between 0,18…0,28 %.

To illustrate this composition interval and for the measured hardness on the rolls' area, the graphic of figure 3 has been made. Although the marks seem dispersed, it is easy to notice the growth of hardness as the content of molybdenum increases in this interval.

Magnesium plays a special part, as it is the element with which the ladle inoculation has been made, either by itself or as a master alloy. The graphite's nodularity in the irons destined to cast rolls (type FNS) assures higher mechanical properties, by eliminating a series of the inconveniences that are to be found at the rolls cast from irons with lamellar graphite. This aspect, concerning the nodularity of the graphite and the inoculation treatment with magnesium, is dealt with a special attention in this study.

4. CONCLUSIONS

- the optimal values of the alloying elements in this irons (chrome, nickel and molybdenum) are to be found on the diagrams of figures 1…3. Thus the optimal additions can be determined in these elements to assure the proper hardnesses;
- an optimal proportion between the silicon and chrome contents is to be respected, the contents originating both from the main charge and from the ferro-alloy additions (FeSi, FeCr);
- a delayed FeCr addition determines the presence of non-uniformities on the semihard crust, due to the incomplete disolvation of the chrome in the metallic mass, which usually is homogenous;
- the smooth decrease of hardness and its maintaining on the depth is performed through optimal carbon contents, and exactly determined proportions between the elements;
- the non-uniformity of the hardness of the crust is due to shape deformations, which cause hard marks on the surface of the rolls, disturbing further mechanical manufacturing;
- the non-uniformity of the crust can be technologically imposed, just as in the case of the passing area;
- the macrostructure is not imposed (except for the nodular graphite irons, where a spherical shape of the graphite is required), conditioned by the adequate quantities of cementite in the crust and graphite in the core and on the necks.
- the process of de-modification (the magnesium losses effect) can be counteracted through a post-modification of the irons, treated by strong inoculate agents or through a second addition, before the casting.

5. BIBLIOGRAPHY/REFERENCES

1. BUDAGHIANŢ, N.A., KARSSKI, V.E. - *Cast Iron Rolls,* Editura Tehnică, Bucureşti, 1984.
2. DIETER, G.E.: *Mechanical Metallurgy,* Editura Tehnică, Bucureşti, 1970
3. PIWOWARSKI, E.: *High Quality Irons,* Editura Tehnică, Bucureşti, 1967
4. SOFRONI, L., RIPOŞAN, I.: *Iron Casting*, Editura Tehnică, Bucureşti, 1985
5. SOFRONI, L., STEFANESCU, D.M.: *Special Irons*, Editura Tehnică, Bucureşti, 1974
6. SOFRONI, L., STEFANESCU, D.M.: *Inoculate Irons with High Properties*, Editura Tehnică, Bucureşti, 1971
7. SOFRONI, L., STEFANESCU, D.M.: *Irons with Nodular Graphite*, Editura Tehnică, Bucureşti, 1974
8. RIPOŞAN, I.: *Nodular Graphite Iron for the Cast Iron Rolls*, in: Buletin of University Politehnica Bucureşti, 1980/3
9. SOFRONI,L., RIPOŞAN, I.: Contribution for the Improvement of the Cast *Iron Rolls Quality,* in: Metalurgia, 1983/10
10. KISS, I.: *Considerations upon the Reject Forms of the Cast Iron Rolls,* at Scientific Conference, Bucureşti, 2000
11. KISS, I.: *The Hardness of Cast Iron Rolls with Indefinite Structure,* in: Symposium, Petroşani, 2001
12. KISS I., HEPUŢ T.: *Mechanical properties of the cast iron rolls, assured by the chemical composition*, Buletinul Ştiinţific al Universităţii Politehnica Timişoara – Mecanics series, 2002
13. KISS I., HEPUŢ T.: *The hardness of the cast iron rolls, assured by the alloy elements and the modification treatment of the graphite nodularity*, Buletinul Ştiinţific al Universităţii Politehnica Timişoara – Mecanics series, 2002
14. KISS I., RAŢIU S., VÎLCEANU L, ALEXA V.: *Particularităţi ale proprietăţilor mecanice la cilindri de laminor turnaţi din fonte cu grafit nodular*, Simpozion International Universitaria ROPET, Petroşani, 2002
15. A. JOSAN, D. PETRE, I. KISS.: *Studies and researches on the influence of chemical composition of cast rolls made of hypereutectic steel, on their hardness in exploatation*, Scientific Conference Research and Development of Mechanical Elements and Systems Jahorina – IRMES, Sarajevo, Bosnia & Hertegovina, 2002
16. KISS I.; RAŢIU S.; NICA GH.: *Some considerations regarding the mechanical properties of the cast iron rolls, assured by the chemical composition and the modification treatment of the graphite nodularity (I)*, Scientific Conference Research and Development of Mechanical Elements and Systems Jahorina – IRMES, Sarajevo, Bosnia & Hertegovina, 2002
17. KISS I.; JOSAN A; CIOATĂ V.: *Some considerations regarding the mechanical properties of the cast iron rolls, assured by the chemical composition and the modification treatment of the graphite nodularity (II)*, Scientific Conference Research and Development of Mechanical Elements and Systems Jahorina – IRMES, Sarajevo, Bosnia & Hertegovina, 2002
18. KISS I., HEPUŢ T., RAŢIU S.: *The Hardness Of The Cast Iron Rolls, Assured by the Alloyed Elements and the Modification Treatment of the Graphite Nodularity*, in: "MASINSTVO" – Journal of Mechanichal Engineering, No.1 / 2003, Zenica, Bosnia & Hertegovina
19. KISS I.: *The Mechanical Properties of the Semihard Cast Iron Rolls Assured by the Basic Elements*, in: "MASINSTVO" – Journal of Mechanichal Engineering, No.4 / 2003, Zenica, Bosnia & Hertegovina

NOBLE METAL AND SEMICONDUCTOR NANOPARTICLES STABILIZED IN LAYER STRUCTURED MATERIALS

Imre DÉKÁNY, Szilvia PAPP,
Rita PATAKFALVI, László KÖRÖSI

DEPARTMENT OF COLLOID CHEMIST AND NANOSTRUCTURED MATERIAL RESEARCH GROUP OF HUNGARIAN ACADEMY OF SCIENCES,
UNIVERSITY OF SZEGED,
Aradi vt. t. 1, SZEGED, H-6720, HUNGARY.
e-mail: i.dekany@chem.u-szeged.hu

In layer structured materials, such as montmorillonite, kaolinite, graphite oxide and layer double hydroxides can be regarded as a nanophase reactor, in which size-quantized semiconductor and noble metal particles can be prepared. Particle growth is sterically hindered in the interlamellar space between neighbouring lamellae, which favors the formation of monodispersed particles.

This layer structured self-assembled materials can be used for the fixation of surfactant- or polymer-stabilized nanoparticles. These particles adsorb on the surface of the support with their protecting layers allowing the preparation of semiconductor and noble metal nanocomposites by this method. These synthesis strategies were successfully applied for the preparation and intercalation of Pd and Ag metal and ZnO, SnO_2, semiconductor nanoparticles in layer-structured materials. The properties of these composites have been investigated by optical measurements (band-gap energies), X-ray diffraction, small angle X-ray scattering, atomic force and transmission electron microscopy.

In the last few years research of semiconductor nanoparticles for photooxidation experiments are in the centre of the interest. Layer-by-layer self-assembled nanofilms were prepared from aqueous suspensions of semiconductor nanoparticles and various clay mineral suspensions onto glass surface. Spectrophotometric, XRD, and photocatalytic experiments were performed on self-assembled layered nanofilms. In the course of these experiments ZnO/clay, SnO_2/clay, ZnO/layer double hydroxide (LDH) as talcite sandwiches were prepared. The photodegradation efficiencies of semiconductor/layer silicate nanocomposites were compared to a reference of the bulk microcrystalline material. It was found that the efficiency of nanostructured material was 2-3 times greater than that of reference materials.

DIAGNOSTIC TEST OF FOOD INDUSTRY MACHINES

Endre FORGÁCS, László SZERI

UNIVERSITY OF SZEGED
COLLEGE FACULTY OF FOOD ENGINEERING

SUMMARY

Resonance phenomena of an already employed, supposedly constructional faulty plucking machine are examined in our work. The bearings supports of the machines tend to break because of heavy dynamical overstrain.

The equipment can be described as dynamically totally instable due to faulty construction. We can solve this problem using the results of resonance diagnostics analysis. Resonance was detected, and then it was eliminated. We have put into practice the simplest solution in a test drive system, in which we measured the resonance spectrum. The results verified our assumptions.

Resonance can be stopped, thus dynamical bearing force of the parts of the drive system is decreased too. The lifetime of bearing houses significantly increases, resulting in a quick return of reconstruction costs.

ISIRR 2003

COMPUTERIZED SYSTEM FOR A MORE FLUID CROSS-BORDER RAILROAD TRAFFIC

[1] DEMIAN Doru, [2] RUSU Nicolae, [3] ANGHEL Stela,
[4] FÜLE Antal, [5] TAKÁCS Imre

[1] CN.C.F. „CFR" S.A. – Timişoara
[2], [3] The University „Politehnica" Timişoara,
Faculty of Engineering of Hunedoara
[4], MÁV – Széged – Hungary, [5] MÁV – Békéscsaba - Hungary

SUMMARY*: The paper introduces a computerized system of global communication and railroad traffic coordination, created by the authors for the area Curtici (Romania) – Bekescsaba (Hungary), which is on course of implementation and that can further be extended to other cross-border areas.*

KEY WORDS*: railroad transport, making fluid, cross-border*

1. INTRODUCTION

Railroad transportation shows, in general, several advantages with respect to other types of transportation, but it can face competition only by a continuous update and adaptation to the market requirements. Due to the major dangers which travelers could be exposed to and to the important damage in case of technical fails, the railroad authorities imposed highly exigent internal technical norms, both with respect to equipment safety in exploitation and in the compartment of coordination and management of train circulation.

Both the technical level of such equipment and the internal regulations differ quite a lot from one county to another, according to their general level of development, traditions, military strategies, network density, etc. This aspect generates important problems in border areas, where national networks come into junction, which leads to the necessity of having a permanent communication between the authorities of the two countries, and where there is need for correlation of traffic parameters, safety measures, etc. All these suppose special efforts and responsibilities (with an international character), which are boosted by traffic growth and the increase in quality requirements. Linguistic difficulties are not to be neglected when it comes to operative communications between parties, one misinterpreted message being likely to cause bad accidents.

At present, considering European integration and the increase in commercial and personal exchanges, all the problems mentioned above have grown keener and can be solved by means of information technology.

The paper introduces a system of global communication and train coordination created by the authors for the area Curtici (Romania) – Bekescsaba (Hungary), which is on course of implementation and that can further be extended to other cross-border areas.

2. SYSTEM DESCRIPTION

The block diagram of the system of information management and transfer between CFR – MÁV in the area mentioned above is given in fig.1.

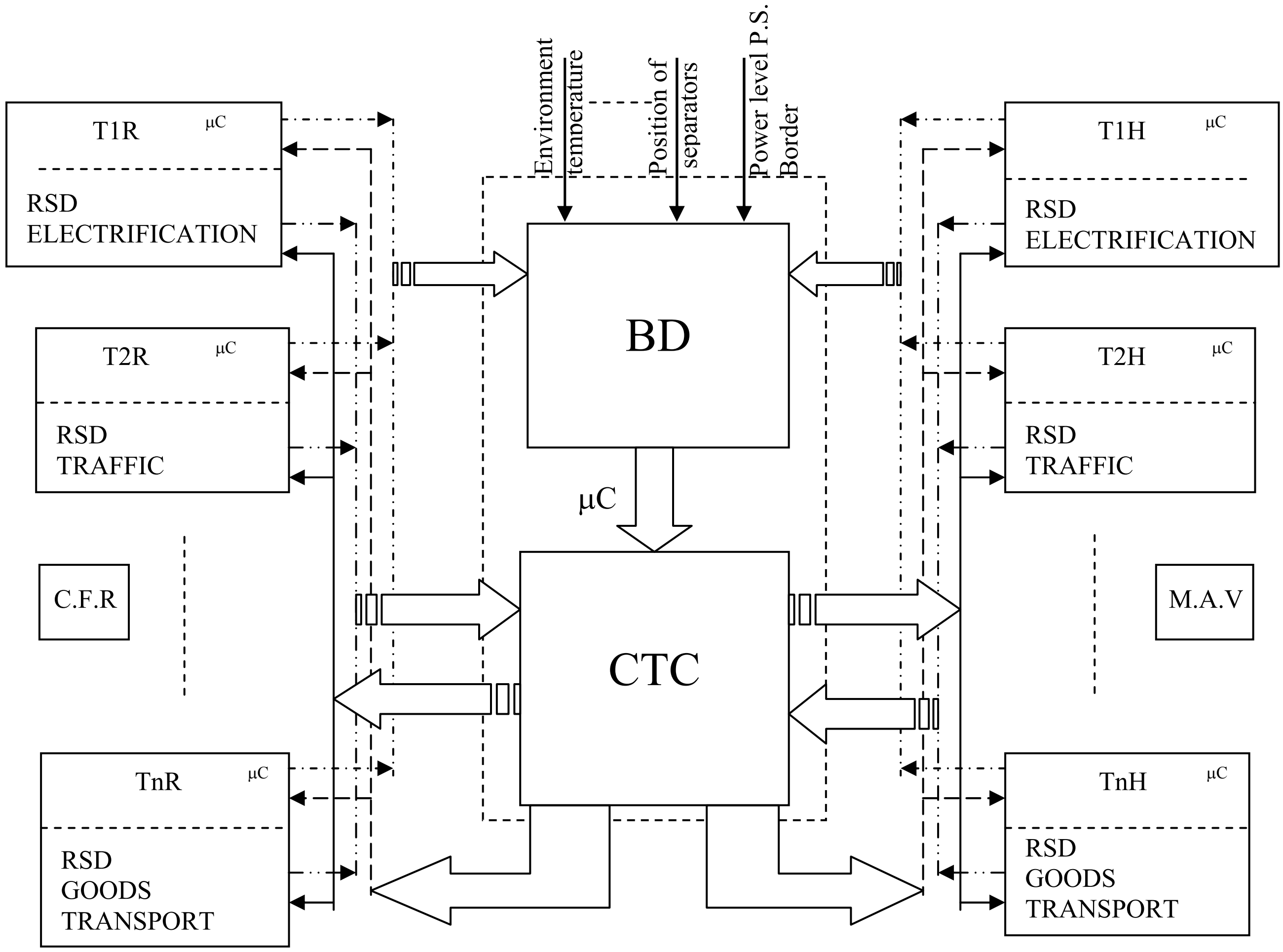

Fig.1

The basic targets are:

- the permanent bilateral access to a common database, permanently updated, allowing both parties to have a correct overview of the situation with respect to momentary traffic possibilities and restrictions on each side;
- the bilateral transfer of information by means of a software capable of translating messages (without any erroneous interpretations) and allowing the fluent and operative conversations between the partners. This procedure eliminates the actual negative situations such as: slow and imprecise correspondence or dealings; mutual requests, impossible to meet, but made out of lack of knowledge with respect to the actual state of the partner; uncertainties and mistiming in solving special cases or failures, etc.

The significations of notations in fig.1 are:

TkR - **T**erminal no. **k** **R**omania
TkH - **T**erminal no. **k** **H**ungariy
DRS - **D**estination **R**ailroad **S**pecific **Department**
DB - **D**ata**b**ase
CTC - **C**ommunication **T**ranslator **C**entral

- information input line (text , image) from the terminals to the DB
- information input line form the DB
- message broadcast line
- message reception line
- DB information input line (using the interface of parameter measurement, state detection, etc.)
- information transfer line from the DB to the CTC allowing communication adequate to the solicitant.

The database (DB) contains partitions for each compartment of railroad activity, and they can be accessed according to the respective compartment, by the specific terminals in view of updating or consulting. The DB also receives state information about certain equipment or on the magnitude of some parameters, by means of the data acquisition interface, directly connected to the railroad apparatuses in the area.

The Communication Translation Central (CTC) translates the text messages stored in the DB and offers them on request in case of real time conversation between partners, in each situation the information being communicated in the language of the recipient.

Each TkR sau TkH terminal is capable of communicating with:

- DB in order to input text or image information corresponding to the compartment of railroad activity to which it is destined (electrification, traffic, etc.);
- DB through the CTC in order to collect information exclusively from the compartment of railroad traffic it is destined to ;
- terminal k (pre-assigned correspondent) from the other railroad administration for the transfer of messages (broadcast, reception).

Terminals (TkR TkH) can be interconnected only according to the assignment (k) of railroad compartment, i.e. they can access for modification or collection of data only the DB partition assigned to them. The possibility of sending over data directly to the partner, i.e. through the DB, has been created in order to maintain a clear and actual situation of the configuration in the area for each compartment, without bothering the partner with information that is not absolutely necessary. For the information that is needed immediately, for emergency situations or for special clarifications we created the possibility of direct communication through real time appeals and messages.

From the physical point of view, the terminals are μC running software that is adequate to the application in the railroad compartment to which it is destined, and the DB, CTC and the interface for external signals are hardware-software components of a μC that manages communications.

In fig.2 we presented an aspect from the hall where the respective application has been implemented, application that is specific to the railroad energetic dispatcher.

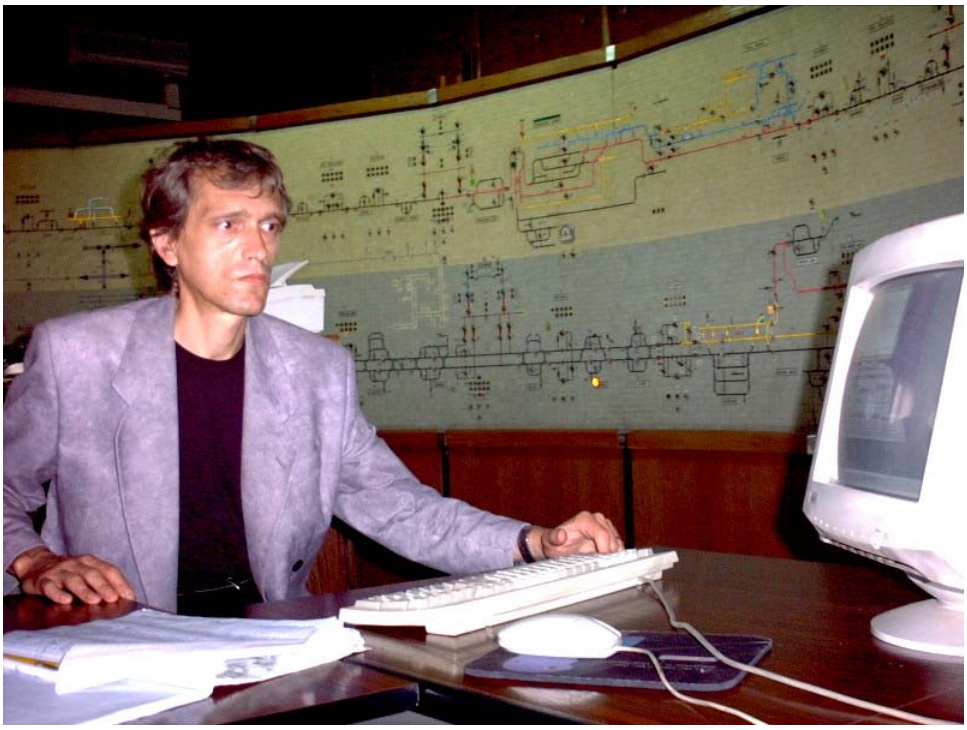

Fig.2

3. CONCLUSIONS

The paper introduces a complex system meant to ease railroad traffic in the cross-border area in the area Curtici (Romania) – Bekescsaba (Hungary), which can also be used in other border points. This system ensures optimal performances with respect to traffic safety and an increased operational character in the activity of traffic coordination.

The system has been created by the authors and represents a fruitful collaboration between the experts of several fields of activity from Romania and Hungary. At present, the stage of implementation is as follows :

- The project under question is in an advanced stage, two of its applications being already functional: the former, for the electrification compartment, where the solutions have been tested and which constituted the application prototype, respectively, the latter, for the traffic compartment, based on the former, with the corresponding modifications;
- at present, it is also in an advanced stage the procedure of interconnection to the equipment of telemechanics and remote railroad energetic signaling for the border PS;
- we envisage to create a procedure of data transmission for energetic remote management;
- during the period of using the equipment already set into function, we brought a series of improvements, among which the possibility of μC registering and the off-line analysis of conversations.

4. BIBLIOGRAPHY

1. The CFR and MÁV internal norms

ISIRR 2003

THE USING OF COMPUTING TECHNOLOGY IN ACQUISITION AND INTERPRETATION OF MECHANICAL CONSTRUCTION VIBRATIONS

Ioan RUJA, Ştefan SZABO, Ion VELA

University "Eftimie Murgu" Reşiţa

Abstract

This paper wants to present an instalation to generate mechanical vibrations with variable parameters to treat mechanical constructions. The treatment with such vibrations is ment to equalize the internal tensions. The recording of the parametrs is made with computers trough LabVIEW software.

Keywords

Vibrations, detensioning, virtual instruments

1. INTRODUCTION

This paper wants to present some results obtained by the authors in the field of mechanical constructions tension releaf using vibrations. Are shown elements of system modelling, mathematical system solving, and different recordings of techical parameters measured during treatment with the vibration generation equipment.

2. THEORETICAL APROACH AND MODELLING

Figure 1 shows the main component of the forced vibration generation equipment. The parts of the instalation are: 1 – main body, 2 – DC electric motor, 3 – Rectifier bridge with controlled output voltage, 4 – construction undergoing tension relief, 5 – elastic material.

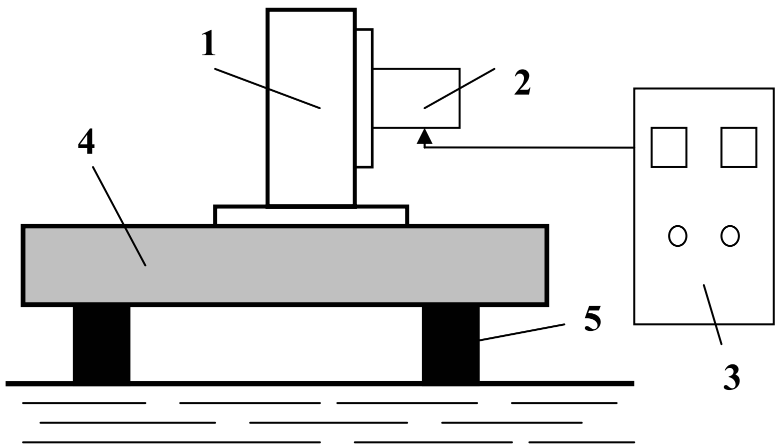

Figure 1. *View of the instalation*

It has been considered that the vibratory system can be modelled and described by an one freedom degree system similar to the one presented in figure 2.

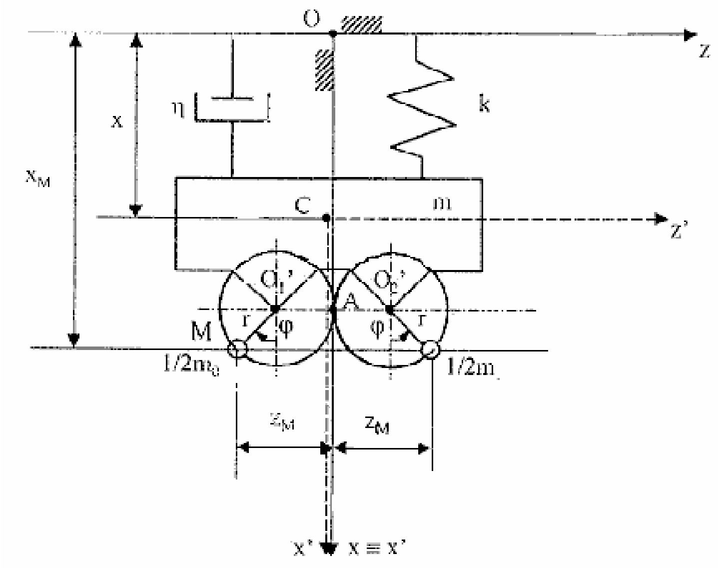

Figure 2. *Phisical model of the vibratory system*

in which m_0 is the mass of the excentric bodys situated at r distance from spinning center, ω is the angular speed of the rotating masses, K id the system elasticity conssidered as constant, ξ is flow coefficient considered nonlinear.

Ozy is an fixed reference point at which is reffered the total mass $m=m_a+m_p$ and the excentrical mass m_0. m_a is the mass of vibratory system and m_p is the mass of the construction undergoing treatment.

O'z'y' is an mobil referential system with axis paralel to the first and the center in O' in the gravity center of the mass m.

Elastic force can be modelled like:

$F(\dot{x}) = b\dot{x}, (b = ct)$ - liniar

$F(\dot{x}) = c\dot{x} + d\dot{x}^3$ - nonliniar (1)

By applying to the system from figure 2 the second degree Lagrange equations, using the coordonetes x and φ it can be obtained the following:

$$\begin{cases} (m+m_0)\dfrac{d^2x}{dt^2} + b\dfrac{dx}{dt} + Kx = \omega_0 r\omega^2\cos(\omega t) \\ -m_0 r\dfrac{d^{2r}}{dt^2}\sin(\omega t) + \omega_0 gr\sin(\omega t) = Q_\varphi \end{cases} \quad (2)$$

For ω=constant, in case of stationary movement, Q_φ represents the generalized force coresponding to the shaft force of the vibratory element .

The solution of the first equation is as follows:

$$x(t) = X\cos(\omega t - \xi) \quad (3)$$

in which

$$X = \frac{\lambda r \omega^2}{\sqrt{(\omega_n^2 - \omega^2)^2 + 4\xi^2\omega^2}} \; ; \; tg\xi = \frac{2\xi\omega}{\omega_n^2\omega^2} \; ; \; \omega_n^2 = \frac{k}{m + m_0}$$

$$\xi = \frac{b}{2(m - m_0)} \; ; \; \lambda = \frac{m_0}{m + m_0} \tag{4}$$

where: ξ is the amortisment constant, ωn is the self pulsation of the system,
X is the amplitude of the movement and γ is the offset between movement and perturbatory force.

$$F(t) = \omega_0 r \omega^2 \cos(\omega t)$$

Movement resonance is obtained if

$$\frac{d\omega}{dt} = 0 \text{ or } \omega_{rez} = \frac{\omega_n^2}{\sqrt{\omega_n^2 - 2\xi^2}} > \omega_n \tag{5}$$

in case of resonance the amplitude of the movement is:

$$X_{\max} = \frac{\lambda r \omega_n^2}{2\xi\sqrt{\omega_n^2 - \xi^2}} \tag{6}$$

The medium power necessary to maintain the oscilations is:

$$P_m = \frac{(m_0 r)^2 \xi}{(m + m_0)} \frac{\omega^6}{(\omega_n^2 - \omega^2) + 4\xi^2\omega^2} \tag{7}$$

By taking account of the presented model particularities, in course of experimentations it was used the following technique:

- The construction undergoing stress relief im mounted on rubber feet to isolate it from the ground.
- The excentricity of the vibratory mass is in concordance to the mass of the treated object.
- The vibratory equipment is firmly placed on the treatment undergoing construction.

3. EXPERIMENTAL RESULTS

Both the forced vibration generator and the measurement equipment was concieved and phisicaly constructed by the authors. Recordings were made on stres relief tests to mechanical constructions with masses between 600 and 1200 kg.

The data acquisition system used for making the measurement is based on the graphical programming language LabVIEW which make possible the real time aquiring and processing of signals.

The measured parameters are:

- Shaft speed of the electrical motor n [rot/min]
- Electrical motor current I[A]
- Vibtation x [mm]

The tension equalizing procedure was repeated at least 3 times on each object .

The results obtained are shown in figures 3, 4 and 5.

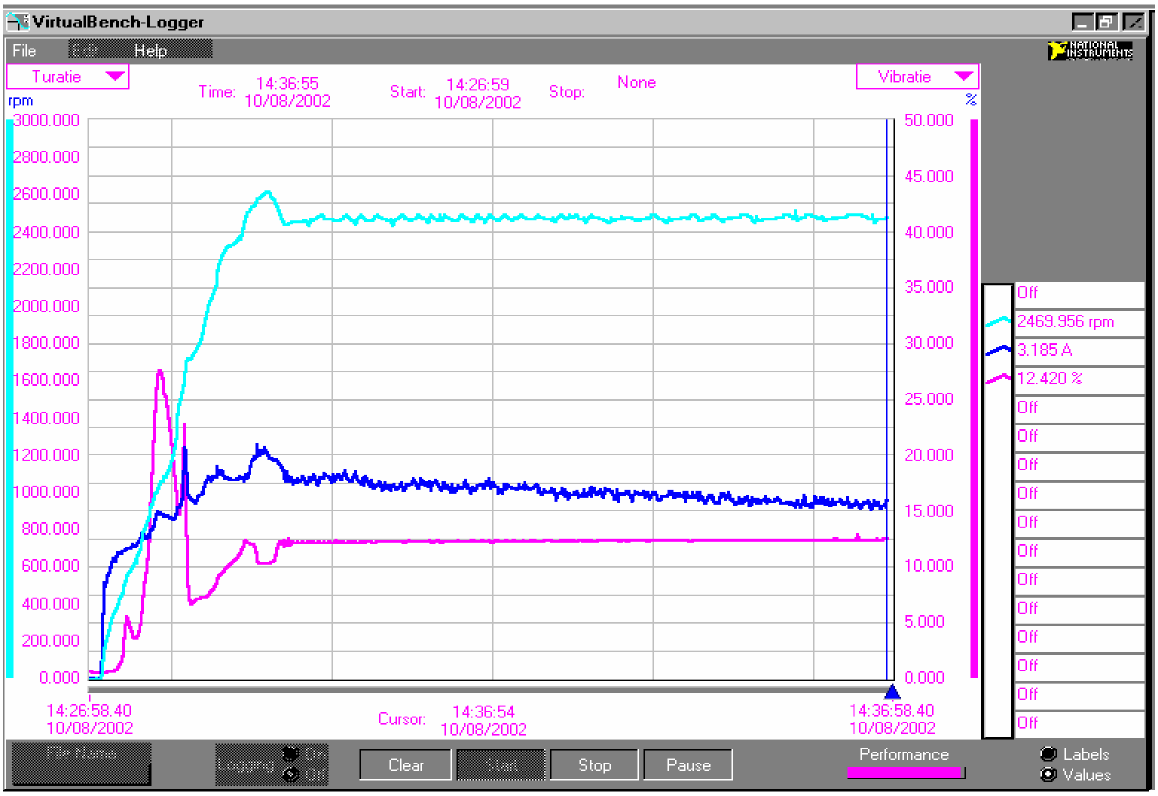

Figure 3. *Recording made at testing a beam.*

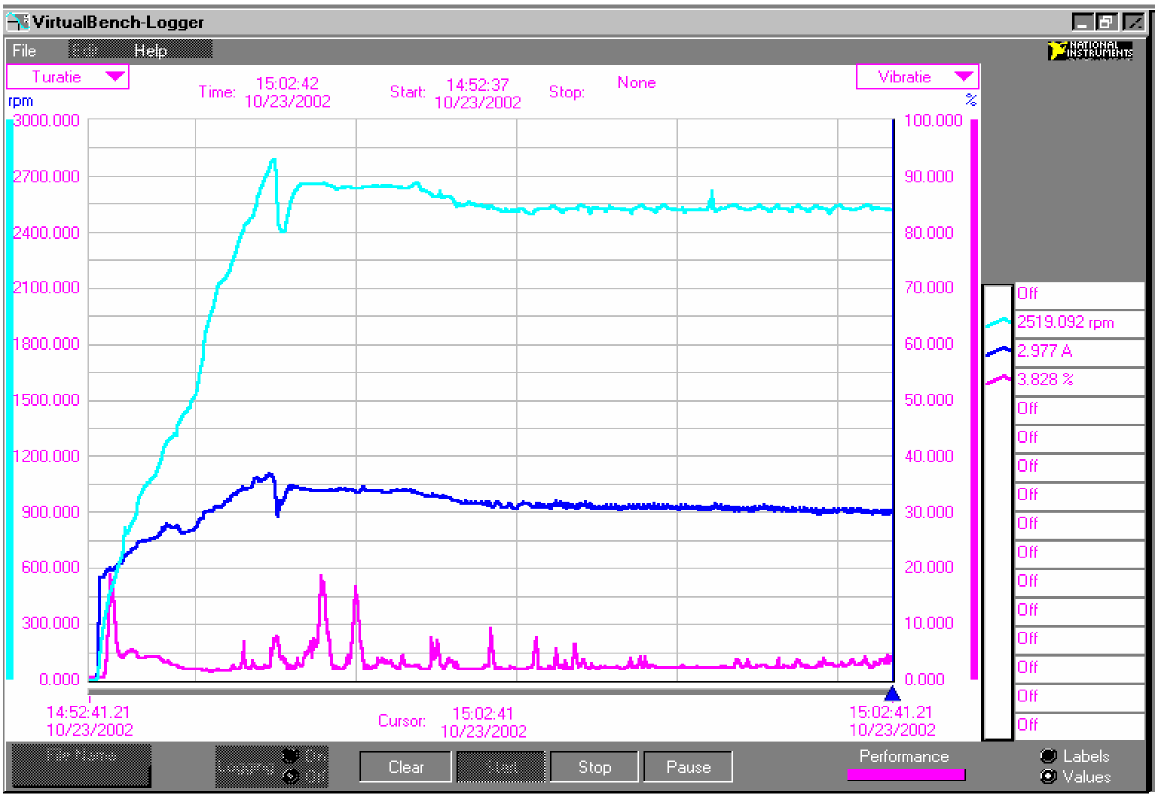

Figure 4. *Parameter recording from a holder.*

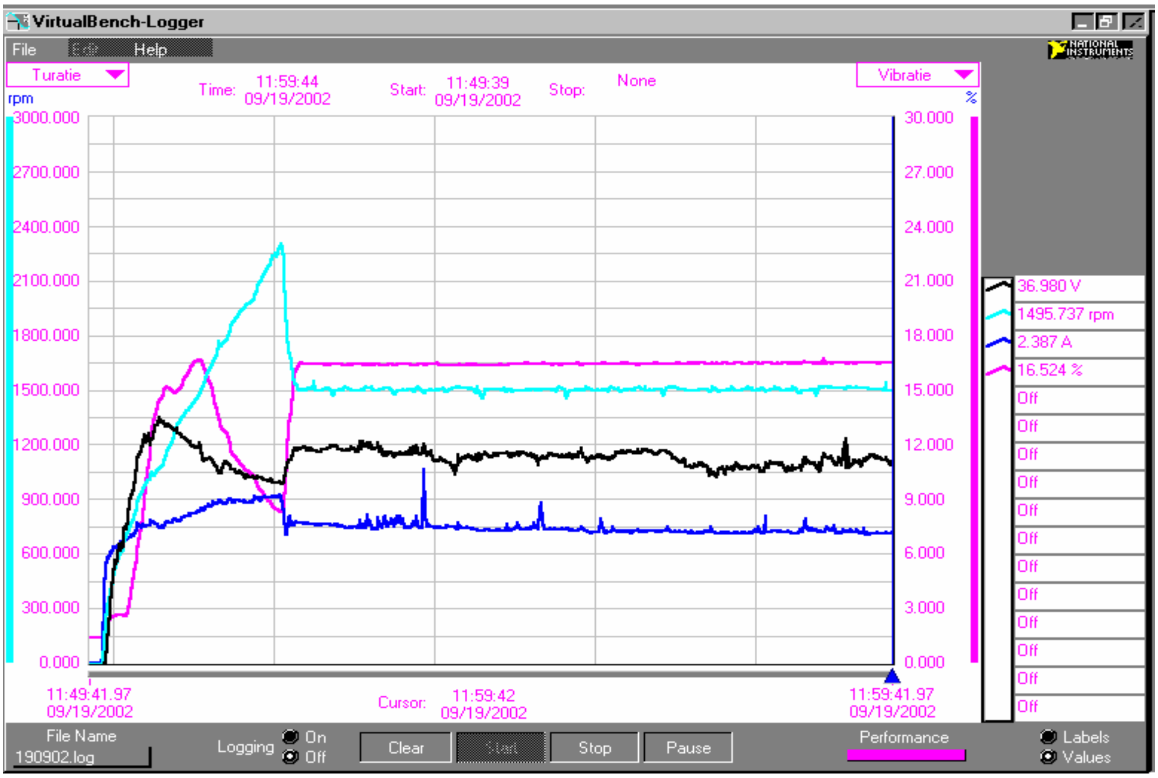

Figure 5. *Stres relief on a welded structure*

4. CONCLUSIONS

The following conclusions were drawn after analizing the experimental results:

- This technique for equalising internal stress is usefull for cast or welded constructions of any sizes.
- The technique is easily applicable if all the necessary equipment is available .
- The method can be used in non-metalical objects.
- The good results obtained can be extended with reaserch about deformation and tension repartition inside the objects

5. REFERENCES

[1] Iosif Ţăpaşu – Mecanică analitică şi vibrații. Teorie şi probleme, Editura Tehnică, Bucureşti, 1998

[2] Polidor Bratu – Vibrațiile sistemelor elastice. Editura Tehnică, Bucureşti, 2000

[3] Ioan Ruja – Tehnica Reglării Automate. Actualități în teorie şi aplicații, Editura Eftimie Murgu Reşița, 1997

[4] George Vermeşan – Introducere în ingineria suprafețelor, Cluj Napoca, 2000